University of Glasgow

Molecular Evolution of Outer Membrane Proteins and Characterisation of Temperate Bacteriophages of *Pasteurella multocida* Strains from Different Host Species

A thesis submitted to the University of Glasgow for the degree of Doctor of Philosophy

Rezheen Fatah Abdulrahman

(BVSc., MVSc.)

October 2016

Institute of Infection, Immunity and Inflammation
College of Medical, Veterinary and Life Sciences
University of Glasgow

Declaration

I hereby declare that the work presented in this thesis is the result of my own work. No Part of this thesis has been presented for any other degree. This is the record of my work carried out by myself, except where otherwise cited or acknowledged. The research for this thesis was performed in the University of Glasgow between November 2012 and October 2016.

Rezheen Fatah Abdulrahman

October 2016

Acknowledgement

I would like to express my deepest and sincerest appreciation to my supervisor Dr. Robert Davies for his endless guidance, supervision, support and encouragement over last few years. His supervision taught me logical thinking in both laboratory and data analysis. I would like to thanks Dr. Daniel Walker for the help and advice he offered throughout my PhD.

I would like to express my sincerest gratitude to Prof. Jose R Penades who provided me support in bacteriophage analyses. I am very grateful for his kind help, guidance and encouragement throughout my study. Special thanks to the members of his group especially Dr. Nuria Quiles, Alfred Fillol, Maan Al-Naqeeb and Ibrahim Alotibi for their help and support. I would like to thank my assessors Prof. Olwyn Byron and Dr. Andrew Roe for their helpful advice for my project over the years.

Sincerest thanks to the members of my group, both past and present, for their endless support, guidance and encouragement and being there for me throughout this PhD journey. Thank you Dr. Michael Ormsby, Miss Erin Sutherland, Miss Nurshahira Sulaiman, Miss Claire Jones, Dr. Edward Grahame, Dr. Nicky O'Boyle and Dr. Daniel Cozens. Thanks for the friendship and continuously enjoying my Biryani!. I will surely treasure all the memories we had together.

Thank you Dr. Alastair Gardiner, Dr. James Connolly, Miss Síle Johnson, Miss Heather Hulme, Miss Caitlin Jukes, Miss Catriona Thompson; Dr. Khedidja Mosbahi, Mrs Liyana Azmi and all members of the level 2 GBRC for the help, support and friendship. You are all amazing people; thank you and all the best.

I would like to thank Dr. Graham Hamilton at Glasgow Polyomics for his useful advice for genome analyses in this study. I would also like to thank Dr. Taya Forde at the Institute of Biodiversity for helping me with core genome analyses. I would like to acknowledge Mrs Margaret Mullin for electron microscopy and Ms Julie Galbraith at Glasgow Polyomics for running genomic samples.

I sincerely thank my family for their endless love, support, encouragement in every way in my life even though we were thousands of miles apart. Without them, I could not have come this far. Special thanks to my friend Miss Shameeran Ismael for being so supportive during my study.

I owe my deepest thanks to my sister and brother, Jihan Hassan and Omran Ali for their enduring support, endless love and for accepting me as one of their family. There are not words to express how grateful I am to you. Thank you for everything.

Finally, I would like to thank my financial sponsor, the Ministry of higher Education and scientific Research/Kurdistan/Iraq, for providing me with an opportunity to pursue my PhD study.

Dedication

This four year PhD study is dedicated to the wishes and memories of my beloved father, Fatah Abdulrahman.

Presentations

1. Abdulrahman, R. F., and Davies, R. L. **Characterisation of temperate bacteriophages of *Pasteurella multocida*. Poster presentation** at the Young Microbiologist Symposium (YMS), 2nd – 3rd June 2014, Dundee, United Kingdom.

2. Abdulrahman, R. F., and Davies, R. L. **Characterisation of temperate bacteriophages of *Pasteurella multocida* strains from different host species. Poster presentation** at the Bacteriophages 2015, 27th – 29th Jan. 2015, London, United Kingdom.

3. Abdulrahman, R. F., Penadés, J. R., and Davies, R. L. **Characterisation of temperate bacteriophages of *Pasteurella multocida* strains from different host species. Poster presentation** at the Viruses of microbes, 18th – 22nd July 2016, Liverpool, United Kingdom.

Summary

Pasteurella multocida is a Gram-negative commensal bacterium which resides in the upper respiratory tract of mammals and birds. The organism is responsible for a variety of economically important diseases in a wide range of domestic animal species. It causes fowl cholera of poultry, haemorrhagic septicaemia of cattle and water buffalo, atrophic rhinitis of pigs, and pneumonia of cattle, sheep and pigs. In the present study, *P. multocida* isolates were selected based on an established framework of evolutionary relationships among 123 isolates of *P. multocida* based on the concatenated partial sequences (3990 bp) of seven housekeeping enzyme genes (Davies *et al.*, unpublished; http://pubmlst.org/pmultocida_multihost). The isolates were recovered from different host species (cattle, sheep, pigs and poultry) and were associated with different diseases. The isolates represented various capsular serotypes, outer membrane protein (OMP)-types, 16S rRNA types, and sequence types.

Phylogenetic trees based on the concatenated partial sequences (3990 bp) of the seven housekeeping enzyme genes, complete sequences (22,371 bp) of fifteen housekeeping enzyme genes and the core genome were almost identical in their topographies. The trees represented eight major groups or clusters of isolates and these clusters could also be defined, to varying degrees, by the host species of origin and/or disease syndrome. The pattern of clustering of isolates associated with different host species also demonstrated that transmission of *P. multocida* has occurred between different host species. Such host-switching could play an important role in generating diversity within *P. multocida*. Comparative nucleotide sequence analysis of genes encoding the predicted outer membrane proteins of different functions was carried out in 40 isolates of *P. multocida* to investigate nucleotide diversity and to assess the roles horizontal DNA transfer and recombination in the evolution and diversification of *P. multocida*. Comparative nucleotide sequence analysis provided clear evidence that horizontal DNA transfer and recombination (both intragenic and assortative) have occurred within the genes encoding *P. multocida* OMPs. However, it was also demonstrated that this varied from gene-to-gene.

Four functional groups of OMPs were predicted based on the prediction analyses and these functions include outer membrane biogenesis and integrity (12

proteins), transport and receptor (25 proteins), adherence (7 proteins) and enzymatic activity (9 proteins). Thirty five OMPs were analysed in this study in detail. The results showed limited levels of nucleotide and amino acid sequence variation was found within the genes encoding selected proteins with the exception of OmpA and OmpH1. However, there was evidence of gene exchange (assortative recombination) between isolates from different host species and divergent genetic lineages. High levels of nucleotide and amino acid sequence variation was found within two major surface-exposed proteins, OmpA and OmpH1. The results indicated that the *ompA* and *ompH1* genes have undergone extensive horizontal DNA transfer, intragenic and assortative recombination. Variation in OmpA and OmpH1 occurred predominantly in the surface-exposed loop regions. There was strong evidence that natural selection is driving diversification of the hypervariable extracellular loop regions in both proteins. The diversity and molecular evolutionary relationships of *ompA* were further investigated in a larger selection of 74 *P. multocida* isolates. Sequence analysis of the 26 different *ompA*-type alleles revealed that the *P. multocida ompA* gene has undergone multiple horizontal gene transfer and recombination events because complex mosaic structures were found between *ompA* alleles.

The diversity of temperate bacteriophages was examined in 47 *P. multocida* isolates. Phage particles were induced with mitomycin C and characterised morphologically by transmission electron microscopy (TEM). The phage particles were morphologically diverse and represented both the *Siphoviridae* and *Myoviridae* families. Both *Siphoviridae* and *Myoviridae* phage types were induced in certain isolates indicating that a single host may harbour multiple prophages. Moreover, phage DNA was successfully isolated from 18 *P. multocida* isolates. Bacteriophage DNA from isolates PM86, PM172, PM486, PM934 and PM954 showed the presence of two bands of different molecular size. Although these phages had a distinct *Myoviridae*-type morphology, they possessed an unusually small capsid as identified by TEM. Taken together, these results suggest the presence of phage-inducible chromosomal islands (PICIs), in these *P. multocida* strains. To date, PICIs have not been described in *P. multocida*. Genetic diversity of temperate bacteriophages was assessed by restriction endonuclease (RE) analysis and 10 different RE types (A to J) were identified. Plaque assay appeared to be

less sensitive than TEM for detection of temperate bacteriophages. Only 11 (38%) *P. multocida* phages produced signs of infection against indicator strains.

Nucleotide sequence analysis of phage genomic DNA from the same isolates demonstrated that both λ-like and Mu-like phages are induced in the same isolates of *P. multocida*. The results also showed that more than one λ-like and Mu-like phage is induced in the majority of isolates. Annotation of the sequenced phages resulted in five different Mu-like phages, one phage-inducible chromosomal island and seven λ-like phages. Further bacterial genome analyses identified additional intact prophages within the genomes of 40 isolates. From one to five intact prophages and prophage-like elements were identified within the genomes of *P. multocida* strains. The annotated phage genomes were analysed since phages are known to carry virulence factors, including genes encoding OMPs and various toxins, and also mediate horizontal DNA transfer. Nucleotide sequence analysis of λ-like phage genomes induced in toxigenic porcine isolates, PM684 and PM848 of capsular types A and D, demonstrated the presence of the *toxA* gene which encodes the *P. multocida* toxin (PMT). Moreover, genomic analysis identified additional intact λ-like prophages containing *toxA* within the bacterial genomes of the porcine toxigenic isolates PM918, PM926, PM40 and PM696 as well as in ovine isolates of capsular type D. No genes encoding OMPs were found to be carried by any of the bacteriophages. Overall, it was concluded that strains of *P. multocida* recovered from different host species carry a diverse range of bacteriophages. The presence of two bands of different molecular size of phage DNA from isolates PM86, PM172, PM486, PM934 and PM954; together with the identification of small capsids by TEM, suggest that these elements represent PICIs. Interestingly, Southern blot hybridisation of phage DNA in these isolates confirmed induction of both Mu-like phages and PICIs for the first time in *P. multocida*.

This study represents the first comparative genomic analysis of the genes encoding the outer membrane proteome of *P. multocida*; it also represents the first detailed characterisation of the temperate bacteriophage content of a large number of *P. multocida* isolates recovered from different host species (cattle, sheep, pigs and poultry) and various disease syndromes. The study has, for the first time, identified PICIs in *P. multocida*.

Table of Contents

List of Tables

List of Figures

Abbreviations

Φ	Phage
λ	Lambda phage
°C	Degrees Celsius
µg	Microgram
µl	Microlitre
µm	Micrometre
ABC	ATP-binding cassette
AR	Atrophic rhinitis
BAM	ß-barrel assembly machinery
attB	Bacterial attachment site
attP	Phage attachment site
BHIA	Brain Heart Infusion agar
BHIB	Brain Heart Infusion Broth
bio	Biotin
bp	Base pair (s)
$CaCl_2$	Calcium chloride
Cos	Cohesive ends
dH_2O	Distilled water
DNAse	Deoxyribonuclease
dNTP	Deoxynucleotide triphosphate
et al.	*et alios* (and others)
F	Forward
FC	Fowl cholera
Fig.	Figure
gal	Galactose
h	Hour(s)
HS	Haemorrhagic septicaemia
HGT	Horizontal gene transfer
HV	Hypervariable
ICTV	International Committee for the Taxonomy for Viruses
IHF	Integration Host Factor
IM	Inner membrane
int	Integrase
kb	Kilo base pairs
Da	Dalton

Lol	Lipoprotein localisation machinery
LP	phospholipids
LPS	Lipopolysaccharide
M	Molar
MEGA	Molecular Evolution and Genetic Analysis
min	Minute(s)
$MgCl_2$	Magnesium chloride
$MgSO_4$	Magnesium sulphate
mg	Milligram
min	Minute(s)
ml	Millilitre(s)
MLEE	Multilocus enzyme electrophoresis
MLST	Multi-locus sequence typing
mM	Millimolar
ND	Not determined
Nacl	Sodium chloride
NCBI	National Centre for Biotechnology Information
ng	Nanogram (s)
OD_{600}	Optical density at 600 nm
OM	Outer membrane
OMP	Outer membrane protein (s)
ORF	Open reading frame
PEG	Polyethylene glycol
PHAST	PHAge Search Tool
PICI	Phage-inducible chromosomal island
pmol	Picomole
PM	*P. multocida*
PMλ	*P. multocida* λ-like phage
PMMu	*P. multocida* Mu-like phage
PMT	P. *multocida* toxin
PL	Lipoproteins
R	Reverse
RAST	Rapid Annotation using Subsystem Technology
RE	Restriction endonuclease
RecA	Recombinase A
RNAse	Ribonuclease
rpm	Revolutions per minute

rRNA	Ribosomal RNA
s	Second(s)
spp.	Species
rRNA	Ribosomal RNA
SDS	Sodium dodecyl sulphate
ST	Sequence type (s)
TEM	Transmission electron microscopy
UV	Ultraviolet
V	Voltage
v/v	Volume per volume
w/v	Weight per volume
x g	Centrifugal force

Chapter 1 Introduction

1.1 Family *Pasteurellaceae*

The *Pasteurellaceae* are facultative anaerobic, Gram-negatives which belong to the order *Pasteurellales* within the class *Gammaproteobacteria* (Fig. 1.1) (Naushad *et al.*, 2015). They represent a heterogeneous group of pathogenic and commensal bacteria. The family comprises 19 recognised genera, and some of these include pathogens that are responsible for causing disease in humans and a wide range of animal species (Christensen & Bisgaard, 2008; Kuhnert & Christensen, 2008; Muhldorfer *et al.*, 2014; Naushad *et al.*, 2015).

1.2 The genus *Pasteurella*

The genus *Pasteurella* of the family *Pasteurellaceae* includes species that are commensal in the mucosal layer of lower genital and upper respiratory tract of birds and mammals (Fig. 1.1). The genus *Pasteurella* is also responsible for causing a wide range of economically important diseases in birds and mammals worldwide. The taxonomy of *Pasteurella* has been reviewed (Christensen & Bisgaard, 2006; Dziva *et al.*, 2008). Both DNA-DNA hybridisation and phenotypic characterisation have been used in the classification and nomenclature of the genus *Pasteurella* (Christensen & Bisgaard, 2006; Dziva *et al.*, 2008). 16S rRNA sequence comparison and rRNA-DNA hybridisation have been used to study the phylogeny of the genus (De Ley *et al.*, 1990; Dewhirst *et al.*, 1992; Kuhnert *et al.*, 2000). The genus comprises nine species, namely *Pasteurella multocida*, *Pasteurella dagmatis*, *Pasteurella gallinarum*, *Pasteurella avium*, *Pasteurella volantium*, *Pasteurella stomatis*, *Pasteurella langaa*, *Pasteurella canis* and *Pasteurella anatis* (Christensen & Bisgaard, 2006). Two additional unnamed *Pasteurella* species, *Pasteurella* species *A* and species *B* were also designated (Christensen & Bisgaard, 2006). However, it has recently been suggested that *Pasteurella* species *B* be classified as *Pasteurella oralis* sp. nov based on analysis of both phylogenetic and phenotypic data (Christensen *et al.*, 2012). This genus is differentiated from other genera of the *Pasteurellaceae* by the lack of ß-haemolysis, positive reaction to D-fructose, D-mannose, D-galactose and sucrose fermentation, and lack of ability to ferment glycosides and D-melibiose (Christensen & Bisgaard, 2006).

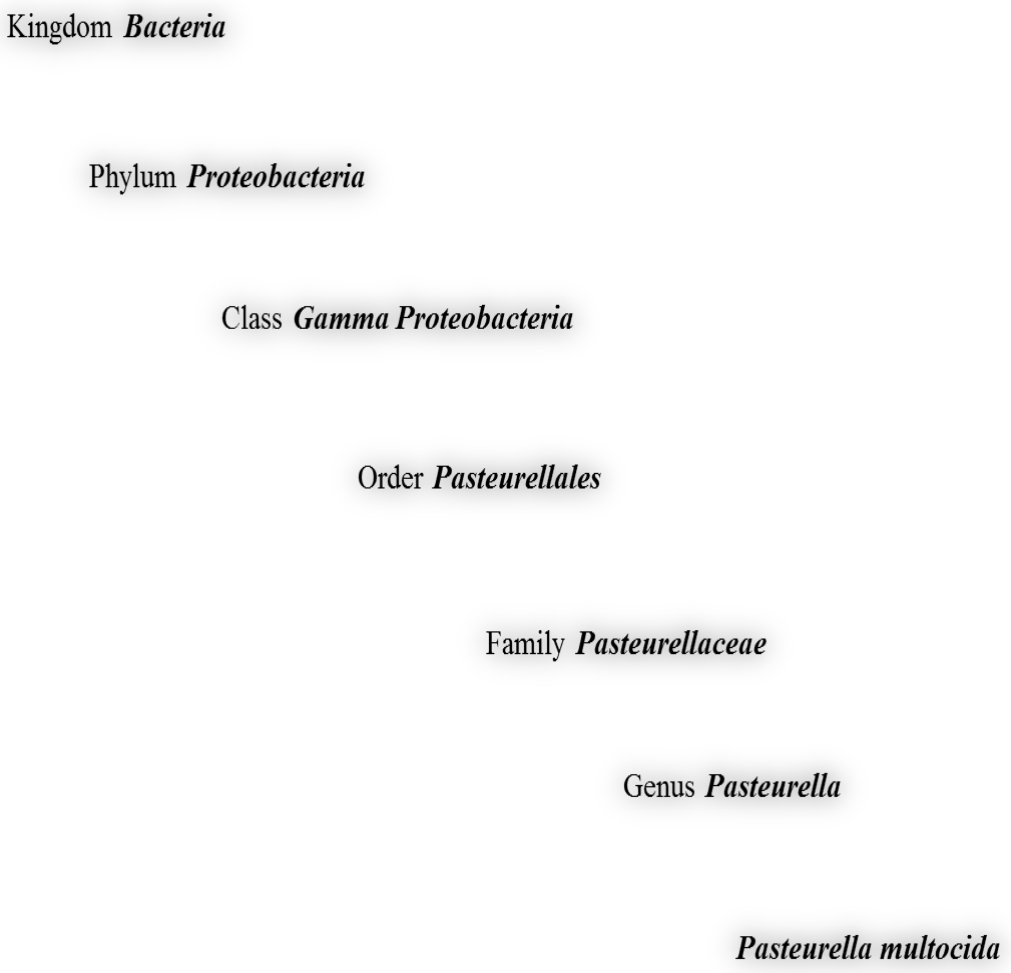

Fig. 1.1 Taxonomy of *P. multocida*
Adapted from (Christensen & Bisgaard, 2008).

1.3 *Pasteurella multocida*

In 1881, Louis Pasteur first identified *P. multocida* as the causative agent of fowl cholera in birds (Harper *et al.*, 2006; Wilkie *et al.*, 2012). *Pasteurella multocida* represents a diverse group of Gram-negative bacteria that are commensal in the upper respiratory and lower genital tracts of a variety of healthy mammals and birds (Rimler & Rhoades, 1989). The bacterium is widely distributed throughout the world and causes a broad range of primary and secondary infections in a wide range of animal species, especially many of which are economically significant (Rimler & Rhoades, 1989; Wilkie *et al.*, 2012).

The species *P. multocida* has traditionally been subdivided into three subspecies: *multocida*, *gallicida*, and *septica* (Mutters *et al.*, 1985). However, a fourth subspecies named *tigris* has also been described, this was isolated from the infected wound of a child resulting from a tiger bite (Capitini *et al.*, 2002). *Pasteurella multocida* can be distinguished from other *Pasteurella species* by positive reactions to ornithine decarboxylase, indole and mannitol fermentation, but it is unable to ferment maltose and dextrin (Christensen & Bisgaard, 2006).

1.3.1 Morphology and cultural characteristics

Pasteurella multocida is a Gram-negative coccobacillus which occurs singly, in pairs and sometimes as filaments or chains. It measures 0.2-04 × 0.6-2.5 μm, is non-motile, facultative anaerobic and displays bipolar staining with Giemsa or Wright's stain (Rimler & Rhoades, 1989). *Pasteurella multocida* can grow routinely on nutrient agar, brain heart infusion agar (BHIA) and blood agar (BHIA containing 5% sheep's blood) (Dziva *et al.*, 2008). The colonies are usually about 0.2-2.0 mm in diameter (Christensen & Bisgaard, 2006) and usually appear after 18-24 h of growth at 35-37°C (Rimler & Rhoades, 1989). On blood agar plates, the colonies are non-haemolytic, round, and grey in colour. Mucoid or non-mucoid colonies may grow on culture media with a typical sweetish smell due to the formation of indole by the bacterium (Dziva *et al.*, 2008). It has been shown that colony morphology of *P. multocida* is host related. For instance, mucoid colonies are typically recovered or cultured from pneumonic lesions in cattle, pigs and rabbits while non-mucoid colonies are mostly obtained from poultry (Dziva *et al.*, 2008).

Mucoid colonies are large, discreet, convex, circular, moist, viscous with mucous-like consistency; Mucoid colonies consist of hyaluronic acid in the capsule and show a yellowish-green, bluish-green or pearl-like iridescence. Rough colonies are occasionally encountered which consist of non-capsulated filamentous cells. Non-capsulated cells are grey, blue, and greyish-blue without iridescence (Rimler & Rhoades, 1989). Mucoid colonies are normally associated with all serogroup A and some serogroup D strains; strains that produce watery mucoid colonies are from serogroup A. A pearl-like iridescence is displayed by colonies of serogroups A, D and F strains, but watery mucoid colonies of serogroup A appear grey. However, serogroup B and E strains usually display bluish-green or yellowish iridescence in oblique transmitted light (Rimler & Rhoades, 1989).

1.4 Phenotypic and genotypic characterisation and classification

A number of phenotypic and genotypic methods are used to characterise *P. multocida* for different purposes such as classification, assessment of diversity, and for epidemiological and pathogenesis studies.

1.4.1 Phenotypic characterisation

1.4.1.1 Biotyping

Pasteurella multocida is differentiated into subgroups or biotypes according to biochemical reactions such as dulcitol and D-sorbitol fermentation. *Pasteurella multocida* subsp. *multocida* ferments sorbitol but not dulcitol; *P. multocida* subsp. *septica* ferments neither sorbitol or dulcitol; *P. multocida* subsp. *gallicida* ferments both sorbitol and dulcitol (Mutters *et al.*, 1985). A study by Kuhnert *et al.*, (2000) using 16S rRNA sequencing showed that only two of six *P. multocida* supsp. *septica* isolates gave negative reactions to sorbitol. The results indicate that subgrouping of *P. multocida* subsp. using sorbitol and dulcitol fermentation do not reflect the genetic relationships of strains correctly. Similarly, a study of the genetic diversity among *P. multocida* strains of avian, bovine, ovine and porcine origin by comparative sequence analysis of the 16S rRNA gene , (Davies, 2004), revealed that dulcitol and sorbitol fermentation are inaccurate indicators of genetic relatedness among *P. multocida* isolates.

1.4.1.2 Serotyping

Pasteurella multocida can be grouped serologically based on lipopolysaccharide (somatic antigens) 1-16 and capsular antigens A, B, D, E and F (Rimler & Rhoades, 1989; St. Michael *et al.*, 2009). The Nomioka and Heddleston systems have been used for the somatic typing of *P. multocida*. Eleven serotypes are recognised by the Nomioka system using tube agglutination, and 16 serotypes are identified by the Heddleston system based on gel diffusion precipitation test. Capsular typing system uses passive haemagglutination of erythrocytes sensitized by capsular antigen. Five serogroups (A, B, D, E and F) are recognised in the Carter system (Rimler & Rhoades, 1989). Fowl cholera is most commonly caused by serogroup A although serogroup D (non-toxigenic strains) also causes disease in birds (Rimler & Rhoades, 1989). In pigs, atrophic rhinitis (AR) is caused by toxigenic capsular type D strains and it also caused by type A strains (Chanter & Rutter, 1989; Davies, 2004; Kloos *et al.*, 2015; Orth & Aktories, 2010). Capsular types A and D are also associated with pneumonia in pigs (Chanter & Rutter, 1989; Davies, 2004). Serogroup A isolates are one of the most prominent causative agents of bovine respiratory diseases (Frank, 1989), whereas Serogroups B and E are the causative agents of haemorrhagic septicaemia in cattle and water buffaloes in tropical regions of Africa and Asia (Carter & De Alwis, 1989). Catry *et al.* (2005) have isolated serogroup F stains from calves predominantly from a fatal case of fibrinous peritonitis in calves. Similarly, serogroup F was also isolated from sheep (Davies *et al.*, 2003a).

1.4.1.3 Bacteriophage typing

Bacteriophages (or phages) are viruses that infect bacteria. The ability of phages to infect a particular bacterium is primarily dependent on whether or not the bacteriophage can attach to specific receptors or attachment sites (Lindbergl, 1973). Phage typing has been used in epidemiological investigations involving a wide range of both Gram-negative and Gram-positive bacteria including *P. multocida* (Fussing *et al.*, 1999; Nielsen & Rosdahl, 1990). This is the only phage typing method that has been developed for typing toxigenic and non-toxigenic *P. multocida* strains (Nielsen & Rosdahl, 1990). Phage typing is based on differences in the ability of a panel of different phages to lyse, or not lyse, bacterial strains (Nielsen & Rosdahl, 1990). It has been suggested that this

system in *P. multocida* could be useful (1) in epidemiological studies of the spread of the bacterium within and between herds, (2) to identify sources of infection in pig herds previously free of toxigenic *P. multocida* and (3) as a typing system in infections caused by non-toxigenic *P. multocida* in other mammalian and avian species (Nielsen & Rosdahl, 1990). Fussing *et al.* (1999) used a phage-typing system for epidemiological studies of porcine toxigenic strains causing atrophic rhinitis. An epidemic strain was identified from cases of disease involving six herds (Fussing *et al.*, 1999).

1.4.2 Genotyping characterisation

A variety of genotypes approaches have been established for characterising *P. multocida* reviewed by (Blackall & Miflin, 2000). These include restriction endonuclease analysis (REA), ribotyping, pulsed field gel electrophoresis (PFGE), extragenetic palindromic- PCR (REP-PCR) and multilocus enzyme electrophoresis (MLEE). A multi-locus sequence typing (MLST) scheme has been created for assessing genetic relatedness among various bacterial species and it was initially found to be effective in studying the phylogeny of bacteria based on the sequence of seven housekeeping genes (Maiden *et al.*, 1998).

1.4.2.1 Multi-locus sequence typing (MLST)

Multi-locus sequence typing is a sequence-based approach used for bacteria typing that uses the sequence of seven housekeeping gene fragments (Maiden *et al.*, 1998; Spratt, 1999; Urwin & Maiden, 2003). The genes encode basic metabolic functions that provide enough discrimination for typing of bacteria without undergoing diversifying selection among bacterial isolates (Maiden, 2006). In 1998, it was first proposed as a portable approach for the identification of clones within populations of pathogenic microorganisms (Maiden *et al.*, 1998). Strains are differentiated based on comparing the sequences of the housekeeping gene fragments (Maiden *et al.*, 1998; Spratt, 1999; Feil *et al.*, 2000; Jolley *et al.*, 2004). MLST was developed from multilocus enzyme electrophoresis (Spratt, 1999) and provides a high degree of discrimination since DNA sequencing assigns alleles directly at multiple housekeeping genes. In MLEE, alleles are assigned indirectly through the electrophoretic mobility of the encoded proteins, which may reflect similar sequences (Spratt, 1999). MLST

schemes have been created for the study of the molecular evolution of a wide range of Gram-positive and Gram-negative bacteria. One of the key advantages of this approach is that sequence data are portable electronically and this allows typing of bacteria via the internet (Spratt, 1999; Urwin & Maiden, 2003). The MLST database currently includes 85 species of bacteria available at http://www.pubmlst.org (Inouye *et al.*, 2012). Another benefit is that nucleotide sequence data are more efficient for bacterial typing since they are generic and can be easily compared among the laboratories (Maiden, 2006). As a consequence, MLST data can be used to investigate evolutionary correlations among bacteria and are more efficient for global epidemiological studies (Spratt, 1999; Urwin & Maiden, 2003). MLST has been established for a large number of bacterial species including *Clostridium* species (Jacobson *et al.*, 2009; Lemée *et al.*, 2005; Macdonald *et al.*, 2011), *Campylobacter* species (de Haan *et al.*, 2010; Miller *et al.*, 2006), *E. coli* (Reid *et al.*, 2000; Turner *et al.*, 2006); *Streptococcus* species (Birtles *et al.*, 2004; Chalker *et al.*, 2012); *Staphylococcus* species (Li *et al.*, 2009), *Neisseria* species (Ch'ng *et al.*, 2011), *Yersinia* species (Bastardo *et al.*, 2012; Hall *et al.*, 2015; Laukkanen-Ninios *et al.*, 2011), and *Haemophilus* species (Mullins *et al.*, 2013; Olvera *et al.*, 2006).

Multi locus sequence typing has been established to study the molecular evolution and population structure of *P. multocida* using the seven housekeeping enzymes adk, est, gdh, mdh, pgi, pmi and zwf. MLST has been used for single host of *P. multocida* (Cardoso-Toset *et al.*, 2013; Hotchkiss *et al.*, 2011b; Moustafa *et al.*, 2013; Petersen *et al.*, 2014; Subaaharan *et al.*, 2010; Silva *et al.*, 2012; García-Alvarez *et al.*, 2015) and has also been developed for multiple hosts of *P. multocida* (Davies *et al.*, unpublished; http://pubmlst.org/pmultocida_multihost).

1.5 Diseases associated with *P. multocida*

Pasteurella multocida represents a diverse group of Gram-negative bacteria that are commensals in the upper respiratory tract and lower genital tract of a variety of mammals and birds (Rimler & Rhoades, 1989). *Pasteurella multocida* is responsible for causing disease primarily in animals but may occasionally cause disease in humans, usually the results of cat or dog bites (Table 1.1). *Pasteurella multocida* is responsible for causing a number of specific and economically

important diseases either as the primary or secondary causative agent in a wide range of animal species. These diseases can be grouped into two categories. First, diseases in which the *P. multocida* is the primary cause and has the principle role in the disease process (Wilkie *et al.*, 2012). These diseases include fowl cholera in poultry (Rimler & Rhoades, 1989; Saif, 2008; Mohamed *et al.*, 2012), haemorrhagic septicaemia in cattle and water buffaloes (Carter & De Alwis, 1989), atrophic rhinitis of pigs (Chanter & Rutter, 1989; Kloos *et al.*, 2015; Orth & Aktories, 2010) and snuffles of rabbits (Manning *et al.*, 1989) (Table 1.1). Secondly, there are diseases in which *P. multocida* makes a major contribution, although it requires other, poorly understood factors for the condition to develop. This group includes lower respiratory tract infections of ungulates and sporadic septicaemias that involve different capsular types (Wilkie *et al.*, 2012).

In humans, *P. multocida* is also responsible for non-specific disease syndromes (Frederiksen, 1989; Wilkie *et al.*, 2012). Human infections with *P. multocida* mostly occur following dog and cat bites or scratches (Frederiksen, 1989; Freshwater, 2008; Oehler *et al.*, 2009). *Pasteurella multocida* is a common commensal of the feline oral cavity with a 90% carriage rate. About 50 % of dogs are carriers of *P. multocida* especially in the nares and oral cavity (Manning *et al.*, 1989). Between 20-80% and 3-18% of cat and dog bite wounds, respectively become infected, (Freshwater, 2008).

1.6 Virulence factors

1.6.1 Capsule

The capsule in a wide range of Gram-negative bacteria, including *P. multocida* is involved in pathogenesis, acting as a virulence factor (Boyce & Adler, 2000). Polysaccharide capsules lie outside the outer membrane and constitute major components of the cell surface in a wide range of bacteria (Boyce & Adler, 2000; Roberts, 1996).

Table 1.1 Disease caused by *Pasteurella multocida*.

Disease	Species	Capsular type	Virulence factor
Enzootic pneumonia	Cattle, sheep, pigs	A, D,F	Not determined , Secondary infection with other bacteria, virus and mycoplasma
Atrophic rhinitis	Pigs	A, D	*P. multocida* toxin (PMT)
Fowl cholera	Chickens, turkeys, ducks and wild birds	A, B, D and F	Capsule, LPS, iron acquisition protein, fimbriae, filamentous haemagglutinin, sialic acid uptake
Haemorrhagic septicaemia	Cattle and water buffaloes	B, E	Capsule, fimbriae, filamentous haemagglutinin
Snuffles	Rabbits	A, D	Not determined

In *P. multocida,* the antigenicity of the capsule is used to determine the serogroup (Carter, 1955). Five serogroup A, B, D, E, and F, have been identified (Carter, 1955). Some serogroups are responsible for causing a particular disease. For example, serogroup A strains cause fowl cholera in poultry, serogroup D strain cause atrophic rhinitis in pigs and serogroups B and E cause haemorrhagic septicaemia in cattle and water buffaloes (Adlam & Rutter, 1989; Mohamed *et al.*, 2012; Wilkie *et al.*, 2012). The presence of a capsule in *P. multocida* enhances its ability to invade and multiply within its host (Furian *et al.*, 2014). Functions include to determine access of molecules to the cell membrane, adherence, antiphagocytic activity, interaction with the host complement system (Roberts, 1996; Boyce *et al.*, 2000). It has also been shown that the polysaccharide capsule is involved in virulence of the bacterium; encapsulated *P. multocida* strains are more resistant to phagocytosis and the bactericidal activity of complement (Boyce *et al.*, 2000). The complete nucleotide sequence of the A and B capsule biosynthetic loci have been determined (Boyce *et al.*, 2000; Chung *et al.*, 1998). The serogroup B consists of 15 ORFs and the serogroup A locus consists of 11 ORFs. The serogroup B locus contains the genes that are involved in transport and biosynthesis of polysaccharide (Boyce *et al.*, 2000).

1.6.2 Lipopolysaccharide (LPS)

Lipopolysaccharide also termed endotoxin, is the major cell wall component in almost all Gram-negative bacteria and is a representative pathogen-associated molecular pattern (PAMP) that allows mammalian cells to recognise bacterial invasion and trigger innate immune responses (Matsuura, 2013). Generally in Gram–negative bacteria, the LPS consists of three distinct regions: a hydrophobic membrane-anchor portion known as the lipid A domain; a core-polysaccharide region; and an O-antigen (Alexander & Rietschel, 2001; Knirel & Valvano, 2011; Matsuura, 2013). However, in *P. multocida* the LPS does not contain an O-antigen. In that respect, the LPS is similar to the LPS or lipooligosaccharide (LOS) expressed by other mucosal pathogenic bacteria such as *Neisseria spp*. and *Haemophilus influenzae* (Harper *et al.*, 2006). Lipopolysaccharide is present either as smooth type which comprises of lipid A, core and side chain or rough type which lacks O-chain but contains lipid A and the core (Rakhuba *et al.*, 2010).

Lipopolysaccharide has been used to classify *P. multocida* into 16 Heddleston serovars (somatic serotypes 1-16) (Rimler & Rhoades, 1989). Variation in LPS or LOS structure of *P. multocida* typically occurs in the outer core oligosaccharide regions (Harper *et al.*, 2007). Lipopolysaccharide is considered as a virulence determinant in *P. multocida* and a major antigen responsible for host protective immunity (Harper *et al.*, 2004; Harper *et al.*, 2007). The LPS structures of the following Heddleston type serovars, 1, 2, 3, 4, 5, 8, 9, 10, 11, 12, 13, 14 and 15, and that of the genome-sequenced serovar 3 strain PM70, have been characterised (Harper *et al.*, 2011; Harper *et al.*, 2012; Harper *et al.*, 2013a, b; Harper *et al.*, 2014; St Michael *et al.*, 2005; St. Michael *et al.*, 2009). A number of Heddleston type strains share a common LPS outer core biosynthesis locus but differ in LPS structure due to mutations in the LPS genes.(Harper *et al.*, 2014). *P. multocida* LPS plays a role in the activation of neutrophils and in promoting their transmigration through endothelial cells to the sites of inflammation (Galdiero *et al.*, 2000). Horadagoda *et al.* (2002) demonstrated that endotoxin plays a major role in developing the clinical symptoms of HS when buffalo are injected intravenously with LPS from B:2 strains. Chicken embryos and mice are both very susceptible to *P. multocida* LPS, whereas turkey poults are relatively resistant (Harper *et al.*, 2004; Harper *et al.*, 2006; Harper *et al.*, 2007).

1.6.3 Adhesins

Type 4 fimbriae or pili are long, filamentous appendages which have been identified in many species of Gram-negative bacteria (Adler *et al.*, 1999; Dabo *et al.*, 2007; Harper *et al.*, 2006; Ruffolo *et al.*, 1997). Type 4 fimbriae are involved in the pathogenicity of Gram-negative bacteria by acting as a ligand that mediates adherence, attachment and colonisation of bacteria to host tissue (Adler *et al.*, 1999; Dabo *et al.*, 2007; Harper *et al.*, 2006; Ruffolo *et al.*, 1997). Like other Gram-negative bacteria, the colonisation of host surfaces by *P. multocida* is mediated by adhesins such as pili or fimbriae (Ruffolo *et al.*, 1997). In *P. multocida,* type IV fimbriae consist of repeated fimbrial subunit protein, PftA, which has a molecular mass of 15.2 kDa (Adler *et al.*, 1999). Under microaerophilic conditions, *P. multocida* of capsular types A, B and D form bundles of type IV fimbriae which are highly expressed (Ruffolo *et al.*, 1997). The *P. multocida* genome contains several genes that encode proteins similar to fimbriae or fibrils in other bacteria. These include *ptfA*, *fimA*, *flpA1* and *flpA2*

as well as homologs of *Bordetella pertussis* filamentous hemagglutinin (*pfhaB1* and *pfhaB2*) and *Haemophilus influenzae* surface fibril (*hsf1* and *hsf2*) (Dabo *et al.*, 2007; Harper *et al.*, 2006). It has been found that *pftA*, *fimA* and *hsf2* are present in all pathogenic isolates of *P. multocida* and this indicates the role of these genes in the virulence of *P. multocida* isolated from different host species (Sellyei *et al.*, 2010; Tang *et al.*, 2009). Polymorphism of *pftA* has also used for epidemiological studies in avian *P. multocida* strains (Sellyei *et al.*, 2010).

1.6.4 *Pasteurella multocida* toxin (PMT)

Pasteurella multocida toxin is also known as the dermonecrotic toxin. *Pasteurella multocida* toxin is produced by toxigenic strains of *P. multocida*, mainly capsular type D strains that cause atrophic rhinitis in pigs (Chanter & Rutter, 1989; Horiguchi, 2012; Kloos *et al.*, 2015; Orth & Aktories, 2010). However, strains of type A can also possess *Pasteurella multocida* toxin and cause the disease (Chanter & Rutter, 1989; Davies, 2004). Progressive atrophic rhinitis is mainly due to production of the 143-kDa toxin which is encoded by the *toxA* gene (Nagai *et al.*, 1994). *Pasteurella multocida* toxin stimulates diverse cellular signal transduction pathways by activating heterotrimeric G proteins (Orth & Aktories, 2010). Kloos *et al.* (2015) found that PMT activates the serine/threonine kinase mammalian target of rapamycin (mTOR) in fibroblasts. Activation of mTOR signalling plays a central role in the formation of osteoclasts. On the molecular level, PMT-induced activation of the mTOR leads to down regulation of PDCD4, a known repressor of AP-1 complex, culminating in the activation of c-Jun, an essential transcription factor for triggering osteoclastogenesis. Pullinger *et al.* (2004) demonstrated that PMT that acts as a potent mitogen. Sequence analysis of DNA flanking *toxA* showed homology to bacteriophage tail protein genes and a bacteriophage antirepressor, suggesting that the *toxA* gene resides within bacteriophages (Pullinger *et al.*, 2004). It has been suggested that induction of temperate bacteriophages could possibly enhance the release of PMT from the bacterial cells (Pullinger *et al.*, 2004).

1.6.5 Outer membrane proteins (OMPs)

Several OMPs of *P. multocida* are considered to have roles as virulence factors and are involved in bacterial adaptation to specific host niches, colonisation,

invasion, and iron uptake. OMPs provide protective immunity against *P. multocida* infection and have been used to develop vaccines. Some OMPs are also involved in protein export and multidrug resistant and *in vivo* survival of *P. multocida* (Dabo *et al.*, 2003; Dabo *et al.*, 2008; Hatfaludi *et al.*, 2010; Luo *et al.*, 1997; Lin *et al.*, 2002; Okay *et al.*, 2012; Piddock, 2006; Prasannavadhana *et al.*, 2014; Tan *et al.*, 2010; Wu *et al.*, 2007). The heat modifiable protein, OmpA, is surface-exposed and expressed *in vivo* (Carpenter *et al.*, 2007; Dabo *et a*l., 1997; 2003; 2008). OmpA is multifunctional protein; it is involved in the maintenance of outer membrane integrity and cell shape (Hatfaludi *et al.*, 2010; Sonntag *et al.*, 1978), serves as a receptor for several bacteriophages (Datta *et al.*, 1977; Morona *et al.*, 1985; Parent *et al.*, 2014; Porcek & Parent, 2015; van Alphen *et al.*, 1977), and plays a role in conjugation (Klimke *et al.*, 2005; Skurray *et al.*, 1974; van Alphen *et al.*, 1977), biofilm formation (Orme *et al.*, 2006) and adherence to host tissue (Dabo *et al.*, 2003; Hill *et al.*, 2001; Torres & Kaper, 2003). The porin protein OmpH is an antigenic surface-exposed protein that is also a vaccine candidate (Dabo *et al.*, 2007; Garrido *et al.*, 2008; Luo *et al.*, 1997; Okay *et al.*, 2012; Tan *et al.*, 2010). PlpE is an immunogenic lipoprotein that confers cross protection against *P. multocida* (Okay *et al.*, 2012; Wu *et al.*, 2007). Tad (tight adherence) transport system proteins such TadD, RcpA and RcpB provide the machinery that is required for the assembly of adhesive Flp pili which can be essential for biofilm formation and colonisation (Hatfaludi *et al.*, 2010). Furthermore, some other proteins allow *P. multocida* to survive *in vivo*. For example, haem receptors (HasR), transferrin receptors (TbpA) and haemoglobin receptors (HgbA, HgbB and HemR) are involved in iron-uptake (Hatfaludi *et al.*, 2010). In *P. multocida*, the TolC protein is a component of both type I secretion systems and efflux pumps and is involved in protein export and multidrug resistant (Hatfaludi *et al.*, 2010).

1.7 The structure of Gram-negative bacterial cell envelope

The cell envelope in Gram-negative bacteria is a complex structure, which consists of multi-layered components that protect bacteria from an aggressive and unpredictable environment (Silhavy *et al.*, 2010). The structure of the Gram-negative bacteria cell envelope is shown in Fig. 1.2. It consists of two membranes, the cytoplasmic or inner membrane (IM) and the outer membrane

(OM). The two membranes are separated by the periplasm which contains a thin peptidoglycan layer (Chatterjee and Chaudhuri, 2012; Tommassen, 2010). Although both membranes are phospholipid bilayers, they are very different in their overall structure and composition, due to variation in their functions and surrounding environments (Ruiz *et al.*, 2006).

1.7.1 Inner membrane

The inner membrane is a symmetrical bilayer consisting of phospholipids, mainly phosphatidylethanolamine (70-80%), phosphatidylglycerol and cardiolipin, equally distributed among the inner and outer leaflet (Fig. 1.2) (Koebnik *et al.*, 2000). Proteins present in the inner membranes include integral proteins and lipoproteins and these proteins are crucial for many cellular functions (Facey & Kuhn, 2010). Integral inner membrane proteins span the membrane in the form of hydrophobic α-helices (Bos *et al.*, 2007; Ruiz *et al.*, 2006). Lipoproteins attach to the membrane within the periplasmic space via an N-terminal N-acyl-diacylglycerylcysteine (Bos *et al.*, 2007; Ruiz *et al.*, 2006). Inner membrane proteins are involved in many cellular processes including energy transduction, protein translocation, transport across the membrane and lipid biosynthesis (Facey & Kuhn, 2010; Ruiz *et al.*, 2006).

1.7.2 Periplasm

The periplasm of Gram-negative bacteria is a highly viscous environment that comprises ~10% of cell volume. It contains soluble proteins that serve various cellular functions, and it also contains enzymes that are involved in the formation of disulphide bonds. The periplasm contains a peptidoglycan layer which serves as an extracytoplasmic cytoskeleton that contributes to cell shape and prevents cell lysis (Fig. 1.2) (Ruiz *et al.*, 2006).

1.7.3 Outer membrane

The outer membrane is the external layer of the Gram-negative bacterial cell envelope and protects bacteria against harsh environments (Koebnik *et al.*, 2000). The OM serves as a permeability barrier that prevents the entry of toxic molecules into the cell such toxins, antibiotics and detergents, allowing survival

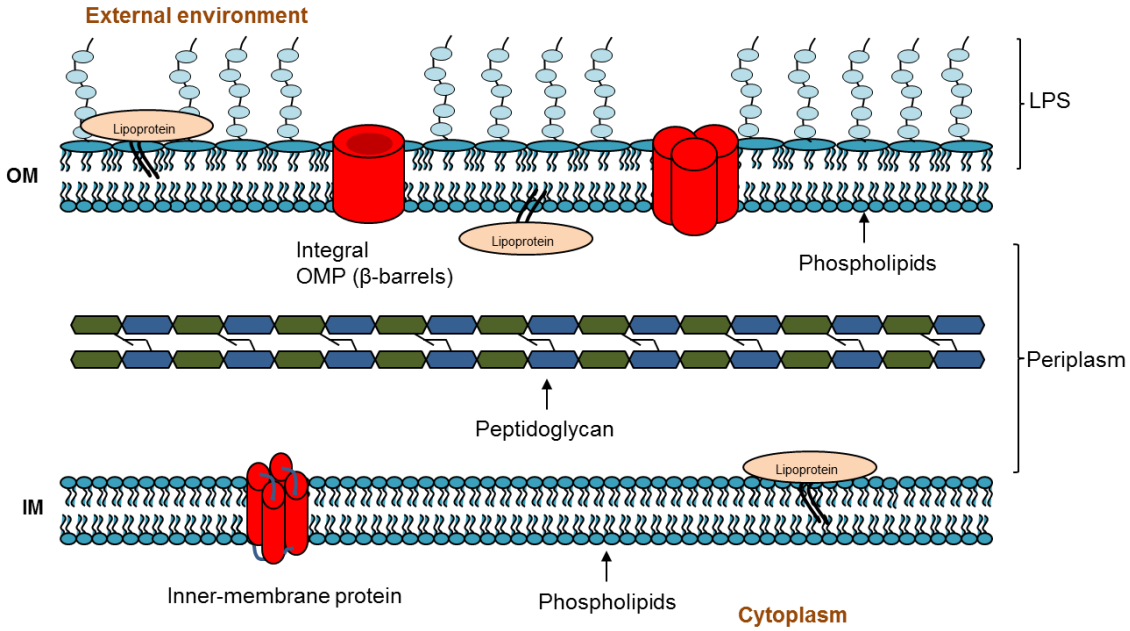

Fig. 1.2 Structure of cell envelope of Gram-negative bacteria.

The cell envelope consists of two membrane layers, the outer membrane (OM) and inner membrane (IM). These two membranes are separated by the periplasmic space. The OM possesses two types of proteins: integral outer membrane proteins, which spam the membrane and have a β-barrel structure, and lipoproteins that are anchored to the inner or outer leaflet of the outer membrane. Unlike the IM, the OM is highly asymmetric; consists of phospholipids in the inner leaflet and LPS in the outer leaflet. Lipopolysaccharide consists of lipid A, core oligosaccharide and an O-antigen polysaccharide. The IM is a symmetrical bilayer consisting of phospholipids and inner membrane proteins. Inner membrane proteins can be integral proteins or lipoproteins. Integral inner membrane proteins span the membrane in the form of hydrophopic α-helices, whereas lipoproteins attach to the membrane within the periplasmic space via an N-terminal N-acyl-diacylglycerylcyseine.

in different environments (Hatfaludi *et al.*, 2010; Ruiz *et al.*, 2006; Tommassen, 2010; Polissi & Sperandeo, 2014). The OM serves as the anchor for surface components such as pili and has also other functions such as channels that allow transport of molecules (Ruiz *et al.*, 2006). Unlike the IM, the OM is highly asymmetric; consists of phospholipids in the inner leaflet and LPS in the outer leaflet. Lipopolysaccharide consists of lipid A, core oligosaccharide and an O-antigen polysaccharide. In addition to phospholipid and LPS, the OM possesses two types of proteins: integral outer membrane proteins, which span the membrane and have a ß-barrel structure, and lipoproteins that are anchored to the inner or outer leaflet of the OM (Fig. 1.2) (Koebnik *et al.*, 2000). About 50% of the outer membrane mass consists of OMPs either integral OMPs or lipoproteins (Koebnik *et al.*, 2000).

1.7.4 Outer membrane biogenesis

Details of OM biogenesis in Gram-negative bacteria have been described in various reviews (Costerton *et al.,* 1974; Bos & Tommassen, 2004; Bos *et al.*, 2007; Ruiz *et al.*, 2006; Rollauer *et al.*, 2015; Silhavy *et al.*, 2010; Tommassen, 2010; Polissi & Sperandeo, 2014; Walther *et al.*, 2009). Integral OMPs and lipoproteins are synthesised in the cytoplasm as precursors with an N-terminal signal sequence that allow them to be transported across the inner membrane via the Sec system (SecYEG translocon) (Fig. 1.3) (Du Plessis *et al.*, 2011; Lycklama a Nijeholt & Driessen, 2012; Polissi & Sperandeo, 2014; Ruiz *et al.*, 2006; Rollauer *et al.*, 2015).

The assembly of ß-barrel OM proteins requires a conserved protein complex called the ß-barrel assembly machinery (BAM) (Fig. 1.3). The BAM complex is composed of the ß -barrel protein, BamA (Omp85 or YaeT), and four lipoproteins, BamB/C/D/E. Periplasmic chaperones, SurA, Skp, and DegP, are involved in the formation of the folded ß-barrel structure (Gessmann *et al.*, 2014; Okuda & Tokuda, 2011; Rollauer *et al.*, 2015). The majority of lipoproteins are transported and delivered to the OM assembly sites by specific lipoprotein localisation machinery (Lol) which consists of five proteins; LolA, B, C, D and E (Fig. 1.3). LolCDE constitutes an ATP-binding cassette (ABC), whereas LolA is the periplasmic chaperone and LolB is the OMP receptor which acts as the site for the insertion of lipoprotein to the outer membrane (Okuda & Tokuda, 2011).

Both LPS and phospholipids are flipped to the outer leaflet of the inner membrane after their synthesis at the inner leaflet of the inner membrane (Fig. 1.3) (Bos *et al.*, 2007; Ruiz *et al.*, 2006). The translocation of LPS and phospholipids is mediated by an ABC transporter called MsbA (Fig. 1.3). However, translocation of phospholipids could be carried out by helical transmembrane domains (Ruiz *et al.*, 2006). In addition to MsbA others ABC proteins are required for the transport of the LPS to the cell surface including LptB (ABC protein), LptA (periplasmic protein), RlpB (OM-attached lipoprotein) and Imp (integral OMP) (Bos *et al.*, 2007). The LPS is delivered to the periplasmic chaperone LptA by interaction of ABC transporter LptB with YrbK. It is transferred from LptA to the periplasmic domain of Imp, which has a structure similar to LptA. Alternatively, LPS transport may take place at contact sites between the two membranes. YrbK, LptA, LptB, and an unknown transmembrane domain, may function in the formation of these contact sites(Bos & Tommassen, 2004; Bos *et al.*, 2007). Finally, Imp and RlpB are required to transfer LPS to the cell surface, possibly by acting as a flippase complex (Bos & Tommassen, 2004; Bos *et al.*, 2007).

1.7.5 Outer membrane proteins

In Gram-negative bacteria, approximately 50% of OM mass is composed of protein, either in the form of integral membrane proteins or lipoproteins (Koebnik *et al.*, 2000). Two to three percent of the genes in Gram-negative bacterial genomes encode ß-barrels (Wimley, 2003). Outer membrane proteins serve essential cellular functions, including: nutrient uptake, cell signalling and waste export; they also act as virulence factors in pathogenic bacteria (Rollauer *et al.*, 2015). In *E. coli*, OMPs have been categorised into six different groups based on their function: (1) general porins, (2) passive transporters, (3) active transporters, (4) enzymes, (5) defensive proteins and (6) structural proteins (Tamm *et al.*, 2004). Like other Gram-negative bacteria, the OM of *P. multocida* exhibits a wide range of OMPs. Likewise, in *P. multocida,* OMPs of have been grouped into six different functional categories: (1) structural proteins, (2) transport proteins, (3) binding proteins, (4) adhesins, (5) protein assembly machines, and (6) membrane-associated enzymes (Hatfaludi *et al.*, 2010).

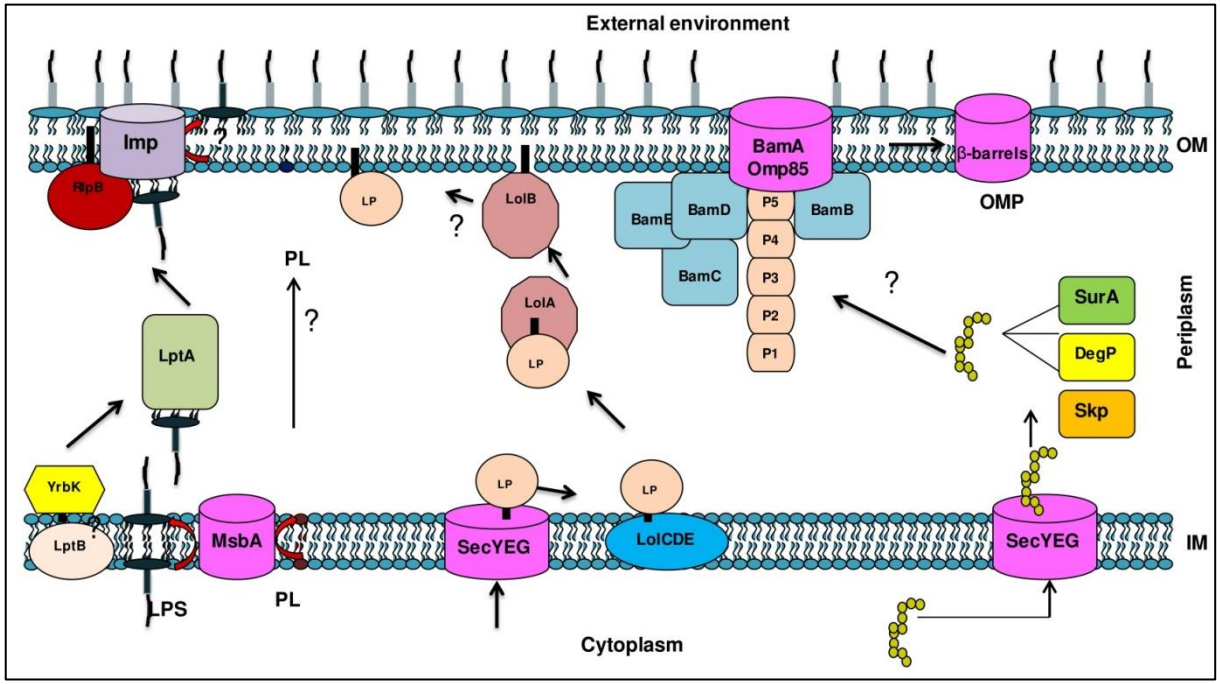

Fig. 1.3 Outer membrane biogenesis in Gram-negative bacteria.

Integral OMPs and lipoproteins are synthesised in the cytoplasm while LPS and phospholipids are synthesised at the inner leaflet of the IM. These components are transported across the IM by different mechanisms. However, the mechanism of OMP passage through periplasm and assembly of lipoproteins and LPS to the outer membrane remains unclear. The figure is adapted from Ruiz *et al.* (2006); Walther *et al.* (2009).

1.7.5.1 Structural proteins

Structural proteins include OmpA and Lpp (Braun's lipoprotein). OmpA is the heat modifiable protein, an integral component of the outer membrane of Gram-negative bacteria and is highly conserved (Beher *et al.*, 1980). It is present at about 100,000 copies per cell (Confer & Ayalew, 2013; Koebnik *et al.*, 2000). The OmpA protein is a multifunctional protein; it is involved in the maintenance of outer membrane integrity and cell shape (Sonntag *et al.*, 1978; Hatfaludi *et al.*, 2010). The 35-kDa OmpA protein has been well studied and characterised in *E. coli* and is composed of a 19 kDa (177 residues) transmembrane domain and a 16 kDa globular C-terminal domain (Arora *et al.*, 2001; Confer & Ayalew, 2013; Pautsch & Schulz, 1998; Pautsch & Schulz, 2000). Nuclear magnetic resonance (NMR) spectroscopy and X-ray crystallography were used to solve the crystal structure of the transmembrane domain of OmpA (Arora *et al.*, 2001; Pautsch & Schulz, 1998; Pautsch & Schulz, 2000). This structure consists of eight antiparallel ß-barrel stranded and four flexible, mobile surface exposed loops (Arora *et al.*, 2001; Confer & Ayalew, 2013; Davies & Lee, 2004; Pautsch & Schulz, 1998; Pautsch & Schulz, 2000; Smith *et al.*, 2007). OmpA serves as a receptor for several bacteriophages (Datta *et al.*, 1977; Morona *et al.*, 1985; Parent *et al.*, 2014; Porcek & Parent, 2015; van Alphen *et al.*, 1977), and plays a role in conjugation (Klimke *et al.*, 2005; Skurray *et al.*, 1974; van Alphen *et al.*, 1977), biofilm formation (Orme *et al.*, 2006) and adherence to host tissue (Dabo *et al.*, 2003; Hill *et al.*, 2001; Torres & Kaper, 2003). Braun's lipoprotein is involved in the OM integrity through its interaction with peptidoglycan (Kovacs-Simon *et al.*, 2011). In *P. multocida*, peptidoglycan-associated lipoproteins, PCP and P6-like protein (Omp16) also act as structural proteins (Hatfaludi *et al.*, 2010).

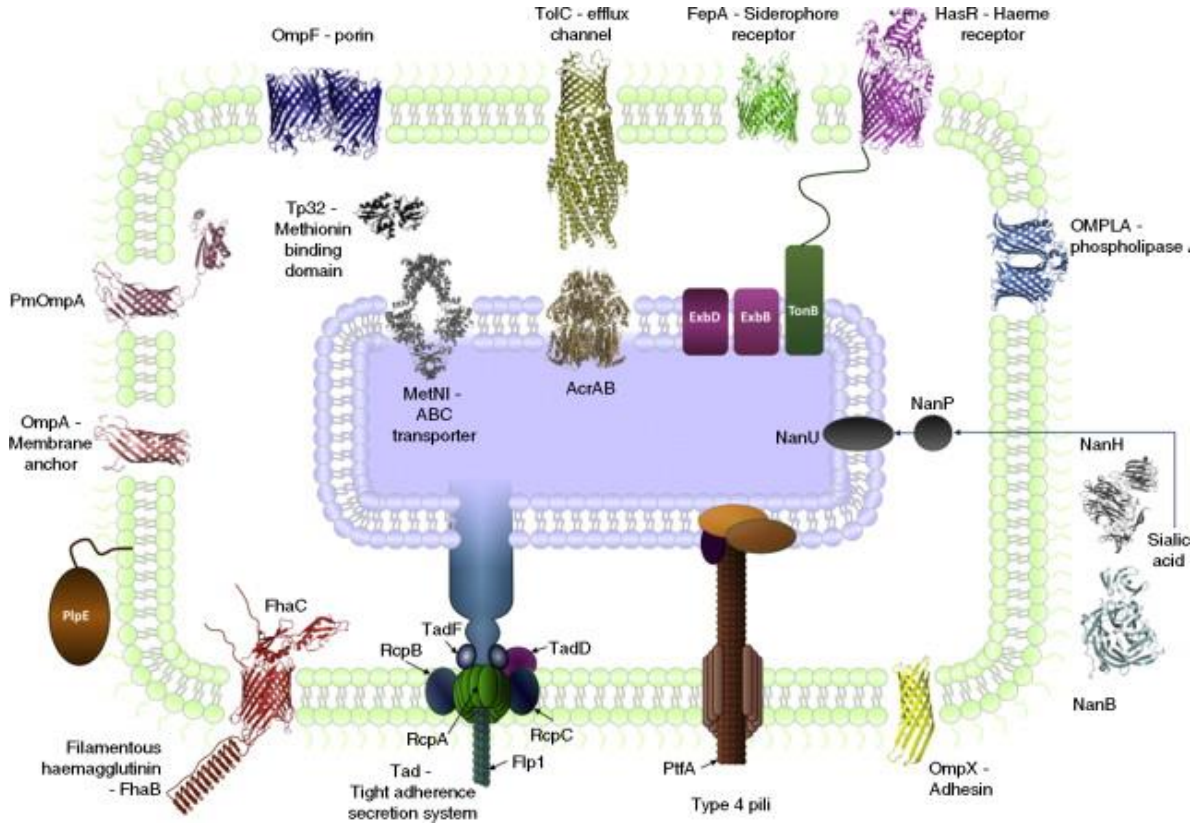

Fig. 1.4 The OM and OM-associated proteins of *P. multocida.*

In *P. multocida*, OMPs of have been grouped into six different functional categories*: (1) structural proteins, (2) transport proteins, (3) binding proteins, (4) Adhesins (5)* protein assembly machines, and (6) membrane-associated enzymes*.* Adapted from Hatfaludi *et al*. (2010)

1.7.5.2 Transport and receptor proteins

Transport proteins include non-specific porins and energy-dependent transport-efflux proteins (Fig. 1.4) (Hatfaludi *et al.*, 2010).

Porins are highly conserved major OMPs that serve as a channel for passive diffusion of hydrophilic substances of low molecular weight (Lee *et al.*, 2007). Two classes of porins are recognised, general porins and substrate-specific porins (Koebnik *et al.*, 2000). General porins are homotrimers that span the outer membrane, in each monomer, 16 ß-strands span the outer membrane (Koebnik *et al.*, 2000). OmpH is the major porin in the OM of *P. multocida* and is a major antigenic and surface-exposed OMP (Dabo *et al.*, 2007; Garrido *et al.*, 2008; Luo *et al.*, 1997; Okay *et al.*, 2012; Tan *et al.*, 2010). However, OmpC, OmpF, and PhoE are the major porins present in the OM of *E.coli* (Tamm *et al.*, 2004). OmpC and OmpF are regulated by osmotic pressure whereas, PhoE is expressed under phosphate-limited growth conditions (Tamm *et al.*, 2004). The crystal structures of OmpF and PhoE have been determined by X-ray crystallography and these structures revealed that porins form homotrimers in the OM (Koebnik *et al.*, 2000). Each subunit consists of a 16-stranded antiparallel ß-barrel structure containing a pore (Cowan *et al.*, 1992). On the basis of diffusion rates of organic molecules, the OmpC channel appears to be slightly smaller than the OmpF channel (Nikaido, 2003). These porins are not selective for their substrate and allow for passage of molecules smaller than ~600 Da (Tamm *et al.*, 2004).

Unlike general porins, substrate-specific porins act as a channel with specificity for certain substances (Koebnik *et al.*, 2000). Examples of substrate-specific porins are the maltoporin LamB of *E. coli* and the maltoporin ScrY of *Salmonella typhimurium* (Koebnik *et al.*, 2000). The crystal structures of both have been elucidated, and each are homotrimers with each subunit consisting of an 18-stranded antiparallel ß-barrel (Koebnik *et al.*, 2000). The maltoporin LamB channel allows diffusion of maltose and maltodextrin, whereas the ScrY channel permits rapid diffusion of glucose, fructose, arabinose, maltose, lactose, raffinose, maltodextrin, and sucrose (Nikaido, 2003). Energy-dependent transport-efflux proteins include TolC which is a core component of both the type I secretion system and efflux pumps (Fig. 1.4) (Hatfaludi *et al.*, 2010).

In Gram-negative bacteria, iron sources are transported into the bacterial cell via specific uptake pathways, which include a TonB-dependent outer membrane receptor, a periplasmic binding protein (PBP), and an inner membrane ATP-binding cassette (ABC) transporter. The outer membrane of Gram-negative bacteria lacks ATP to provide energy for transport as the result consequently, energy is derived from the proton motive force of the cytoplasmic membrane via three proteins, TonB, ExbB, and ExbD (Krewulak & Vogel, 2008). TonB is a 26-kDa protein consisting of three domains: a N-terminal domain 32-residue transmembrane domain; a central domain (residues 33–100) which is located in the periplasm; and carboxy-terminal domain (residues 103–239). ExbB is a 26-kDa cytoplasmic membrane protein consisting of three transmembrane domains. ExbD is a 17-kDa protein that has only one transmembrane domain and a periplasmic domain of about 90 amino acids (Krewulak & Vogel, 2008). Siderophore receptors are involved in the removal of iron from host iron-binding glycoproteins. The iron-siderophore complex is bound by a receptor on the bacterial cell surface and the iron is transported into the cell (Hatfaludi *et al.*, 2010). The crystal structures of the following siderophore binding proteins have been solved: FhuA (ferric-ferrichrome), FepA (ferric enterobatin), FecA (ferric-citrate), and BtuB (vitamin B12) from *E. coli* and FpvA (ferric-pyoverdine) from *Pseudomonas aeruginosa* (Hoegy *et al.*, 2005). These proteins consist of a C-terminal ß-barrel domain and an N-terminal cork domain that fills the barrel interior (Hoegy *et al.*, 2005).

Transferrin and lactoferrin receptors have a molecular mass of 80 kDa, and are too large to pass through the bacterial outer membrane (Hatfaludi *et al.*, 2010). Transferrin receptors usually consist of two binding proteins, TbpA and TbpB (Hatfaludi *et al.*, 2010). TbpA is an integral membrane protein that is predicted to have large surface loops that bind to transferrin (Hatfaludi *et al.*, 2010). TbpB is a 65 to 85 kDa protein that is attached to the OM with an N-terminal lipid anchor. TbpB acts as an initial binding site for iron-saturated transferrin facilitating subsequent binding to TbpA (Hatfaludi *et al.*, 2010). Bovine strains of *P. multocida* have only the TbpA protein (Hatfaludi *et al.*, 2010). Haemoglobin receptors include HgbA of *H. influenzae*, HemR of *Y. enterocolitica* (Hatfaludi *et al.*, 2010) and HmbR of *N. meningitides* (Evans *et al.*, 2010). Multiple

haemoglobin binding proteins, HgbA, HgbB, HemR, HasR PlpB-MetQ and PlpE have been predicted in *P. multocida* (Fig. 1.4) (Hatfaludi *et al.*, 2010).

1.7.5.3 Adhesins

Adhesins are involved in host attachment and colonisation (Hatfaludi *et al.*, 2010). Adhesins are produced by many Gram-negative bacteria and include OmpX of *E. coli*, Hap, Hia/Hsf, HMW1/2, haemoagglutinating pili of *H. influenzae* and ptfA (type 4 fimbriae), putative fibronectin-binding protein (ComE1-PM1665) and filamentous heamagglutinin proteins in *P .multocida* (Hatfaludi *et al.*, 2010). Tad locus represents an ancient and major subtype of type II secretion (Tomich *et al.*, 2007). The tad genes encode the machinery that is required for the assembly of adhesive Flp (fimbrial low-molecular-weight protein) pili, which can essential for biofilm formation and colonisation (Hatfaludi *et al.*, 2010).

1.7.5.4 Enzymatic activity

Some of the OMPs of Gram-negative bacteria have enzymatic activity. Membrane-associated enzymes include phospholipase A, sialidase, neuraminidases (NanH and NanB), GlpQ and protease (Fig. 1.4) (Hatfaludi *et al.*, 2010; Mccarter *et al.*, 2004). The function of OmpLA is predicted to be the hydrolysis of phospholipids present on the external surfaces of the OM, although it's enzymatic function remains unclear (Koebnik *et al.*, 2000). Phospholipase A (OmpLA) is an OM phospholipase of *E. coli* and involves the release of colicin. It also participates in the virulence of other Gram-negative bacteria such as *Campylobacter* and *Helicobacter* strains. OmpLA was the first OM enzyme whose three dimensional structure was solved (Koebnik *et al.*, 2000). It has been demonstrated that sialidase contributes to the virulence of certain pathogens that inhabit and invade mucosal surfaces (Hatfaludi *et al.*, 2010). GlpQ is a lipoprotein but not surface exposed; it has been found in Gram-negative bacteria such *E. coli* and *P. multocida* (Hatfaludi *et al.*, 2010).

1.7.5.5 Protein assembly machinery

Include the BAM complex for transmembrane proteins folding and insertion, the Lol complex for lipoproteins insertion and the LPS insertion proteins (Hatfaludi *et al.*, 2010). Details are described in section 1.7.4.

1.7.5.6 Other proteins and hypothetical proteins

Other proteins that are surface-exposed play an important roles in immunity, such as lipoprotein E (PlpE) of *M. haemolytica* which is highly immunogenic in cattle (Hatfaludi *et al.*, 2010). Similarly, PlpE of *P. multocida* is a surface-exposed and immunogenic OMP in *P. multocida* (Okay *et al.*, 2012; Wu *et al.*, 2007). Various other hypothetical proteins have been predicted. However, their functions have not been demonstrated *in vivo*.

1.8 Bacteriophages

Bacteriophages are a diverse group of viruses that infect bacteria. They were first discovered by Frederick Twort (1915) in England and Felix d'Herelle (1917) at the Pasteur Institute in France (Ackermann, 2003). Felix d'Herelle coined the term "bacteriophage" which means "bacterial eater" (Ackermann, 2003). Bacteriophages are so called because they cause the complete lysis of susceptible bacterial cultures (Orlova, 2012). They are also referred as "phage" (Michael *et al.*, 2003). Bacteriophages are found in almost every environment on Earth, including soil, sediment, water, and associated with both living and dead plants and animals (Elbreki *et al.*, 2014; Orlova, 2012). Bacteriophages are diverse in their morphology but all are composed of nucleic acid encapsulated by a protein coat called a capsid. The phage genome can be double- or single-stranded DNA or RNA (Elbreki *et al.*, 2014; Kutter & Alexander, 2005). Bacteriophage capsids also vary in their forms, ranging from hexagon-like structures to filaments to a highly complex structures consisting of a head and a tail (Elbreki *et al.*, 2014).

1.8.1 Classification and taxonomy of bacteriophages

Phages are obligate intracellular parasites that multiply inside bacteria by hijacking the host biosynthetic machinery system (Cuervo & Carrascosa, 2012;

Kutter & Alexander, 2005; Michael *et al.*, 2003). It has been shown that phages are extremely diverse; and they are probably the most abundant of viruses (Cuervo & Carrascosa, 2012; Hendrix, 2002). Like other microorganisms, phages have been classified based on various criteria. However, there is still a debate about the current classification system for bacteriophages. Historically, the International Committee on Taxonomy of Viruses (ICTV) classified phages into 17 families according to their morphology (Ackermann, 2003; Ackermann, 2007). The ICTV taxonomy has faced criticism because this system is only based on morphology by transmission electron microscopy and does not take in to consideration the genetic relatedness of bacteriophages determined from sequence data (Lawrence *et al.*, 2002; Nelson, 2004). Comparative analyses of phage genomes demonstrate three main features. First, bacteriophages have a very high degree of genetic diversity, suggesting early evolutionary origins. Secondly, the genome architectures have mosaic structures, reflecting an unusually high degree of horizontal genetic exchange in their evolution. Thirdly, phage genomes contain a very high proportion of novel genetic sequences of unknown function and likely represent the largest reservoir of unexplored genes (Hatfull, 2008; Hatfull & Hendrix, 2012). For example, *Streptococcus pyogenes*, whole genome sequencing have identified the presence of six prophages, none of which are recognised by the ICTV (Nelson, 2004). The reason is that some phages exist as lysogenic prophages that are unable to produce a mature virion (Nelson, 2004). In another example, *Salmonella* P22 phage was originally assigned to the *Podoviridae* family based on the presence of a short tail as visualised by TEM. However, it has subsequently been shown that P22 is genetically similar to the long-tailed lambda phages of the *Siphoviridae* family (Byl & Kropinski, 2000, Nelson, 2004). A new system has been established for phage classification and taxonomy. For instance, phage proteome trees have been described by Rohwer & Edwards (2002). This system is based on the overall sequence similarity of predicted proteins from 105 complete phage genome sequences (Rohwer & Edwards, 2002). Although taxonomy results were compatible with the ICTV system, it has been argued that viral species definition and classification are not meaningful due to the presence of excessive gene transfer (Lawrence *et al.*, 2002).

According to their nature of nucleic acid, bacteriophages are currently classified into double or single-stranded DNA (dsDNA, ssDNA) or double or single-stranded RNA (dsRNA or ssRNA) (Fig. 1.5) (Ackermann, 2003; Brüssow & Hendrix, 2002). Based on virion morphology bacteriophages are classified into tailed, polyhedral, filamentous and pleomorphic types (Fig. 1.5) (Ackermann, 2003; Ackermann, 2007; Ackermann, 2011). Since 1959, the morphologies of at least, 5,568 phages have been examined by electron microscopy (Ackermann, 2007). Filamentous, polyhedral and pleomorphic phages were represent only 3.7% of these (208 viruses) (Fig. 1.5) (Ackermann, 2007). The vast majority of the phages (~96%) represent tailed (dsDNA) phages (Ackermann, 2007). Tailed phages belong to the order Caudovirales; they possesses many common properties in terms of morphology and replication (Ackermann, 2001). These phages represent the largest and probably oldest virus group and are characterised by diversification in their fine structure, physiology and DNA composition (Ackermann, 2001; Ackermann, 2003). According to tail morphology, they are grouped into three families: 60% of the phages are *Siphoviridae*, with long, non-contractile, flexible tails; 25% are *Myoviridae*, with contractile tails; and, 15% are *Podoviridae* with short tails (Fig. 1.5) (Ackermann, 2003; Ackermann, 2009; Murphy *et al.*, 2012).

Phages can be classified as lytic (virulent) and temperate bacteriophage based on their ability to lyse or lysogenize host bacterial cells. Lytic and temperate phages are both highly diverse (Casjens, 2003; Michael *et al.*, 2003; Orlova, 2012) and further details are provided in section 1.8.2. Four additional types of prophage have been characterised which are referred to as non-inducible phages or prophage-like entities (Casjens, 2003). Details are provided in section 1.8.2.3.

1.8.2 Lytic (virulent) and temperate (lysogenic) bacteriophages

1.8.2.1 Lytic (virulent) bacteriophage

Lytic phages lyse or kill their hosts after infection. In contrast to temperate phages, lytic phages are associated with most of the phage family groups and the best-studied lytic phages are the T-series bacteriophages (T1 to T7) (Birge, 2006; Michael *et al.*, 2003; Murphy *et al.*, 2012). Lytic phages after initial phage attachment and entry, redirect host cell metabolism toward the production of

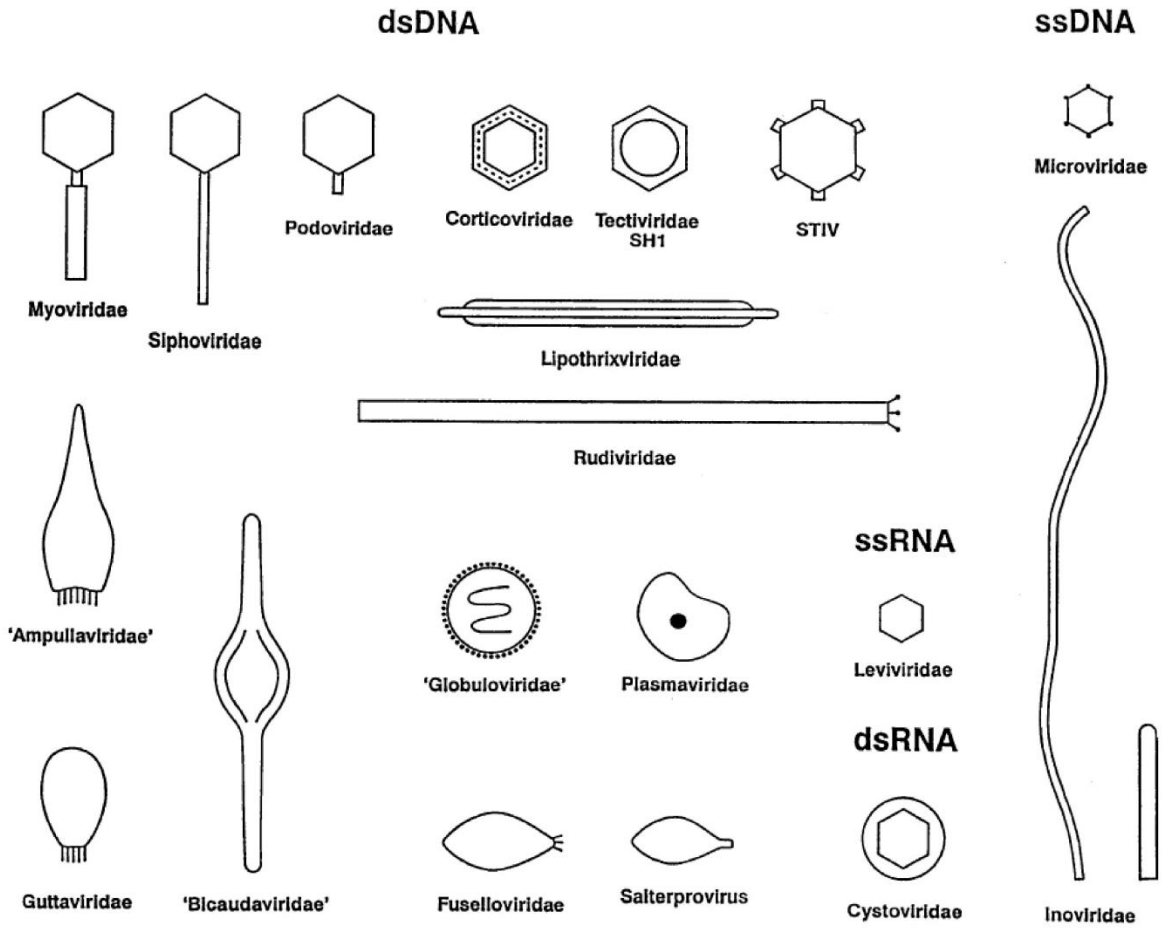

Fig. 1.5 Schematic representation of bacteriophage classification based on morphology and nucleic acid type

The classification is adapted from (Ackermann, 2007)**.**

new progeny, which are released upon cell death within several minutes to hours after the initial attachment (Fig. 1.6) (Elbreki *et al.*, 2014). Lytic phage infection produces clear plaques on bacterial lawns (Elbreki *et al.*, 2014). An example of a well studies lytic phage is the T4 phage. Phage T4 is a dsDNA phage belonging to the *Myoviridae* family. T4 infects *E.coli*, and is among the largest phages being 200 nm long and 80-100 nm wide (Michael *et al.*, 2003; Orlova, 2012). T4 phage consists of a head (or capsid) and a complex tail (Fig. 1.7). The head is an elongated icosahedral capsid, measuring 110×80 nm (Murphy *et al.*, 2012). The tail consists of a sheath, a connecting neck and collar, a complex base plate, six short spikes and six long fibres which help to bind to the surface of the target bacterial cell (Elbreki *et al.*, 2014; Michael *et al.*, 2003; Murphy *et al.*, 2012; Orlova, 2012). The structure of T4 phage is presented as Fig. 1.7.

1.8.2.2 Temperate bacteriophage

In contrast to lytic phages, temperate bacteriophages generally do not kill or lyse their hosts. These phages remain in a lysogenic state as a prophages (Bobay *et al.*, 2013; Birge, 2006; Casjens, 2003). In other words, their genomes become incorporated into and replicate along, with the genome of their bacterial hosts (lysogen) by a process known as lysogeny (Fig. 1.6) (Birge, 2006; Elbreki *et al.*, 2014; Michael *et al.*, 2003). However, under certain circumstances, lysogenic bacteriophages can switch from the lysogenic state and convert to a vegetative state that produces lytic infection (Fig. 1.6) (Birge, 2006; Elbreki *et al.*, 2014; Salmond & Fineran, 2015). Temperate phages are mostly dsDNA tailed phages (Caudovirales) of the *Siphoviridae, Myoviridae* and *Podoviridae* families, although some are members of the family *Inoviridae* (ssDNA phages) (Murphy *et al.*, 2012). Lysogenic ***Siphoviridae*** phages include the enterobacterial lambda (λ-like) phages, the *Bacillus* phage SPβ and the *Mycobacterium* phage L5. Lysogenic ***Myoviridae*** phages include Mu-like, P1-like and P2-like. Morphologies and properties of selected temperate phage are shown in Fig. 1.8 & Table 1.2. Morphologically, *Myoviridae* phages are characterised by possessing long, thick (80–455×16–20 nm) contractile tails. The heads and tails of *Myoviridae* phages are assembled in separate pathways (Murphy *et al.*, 2012).

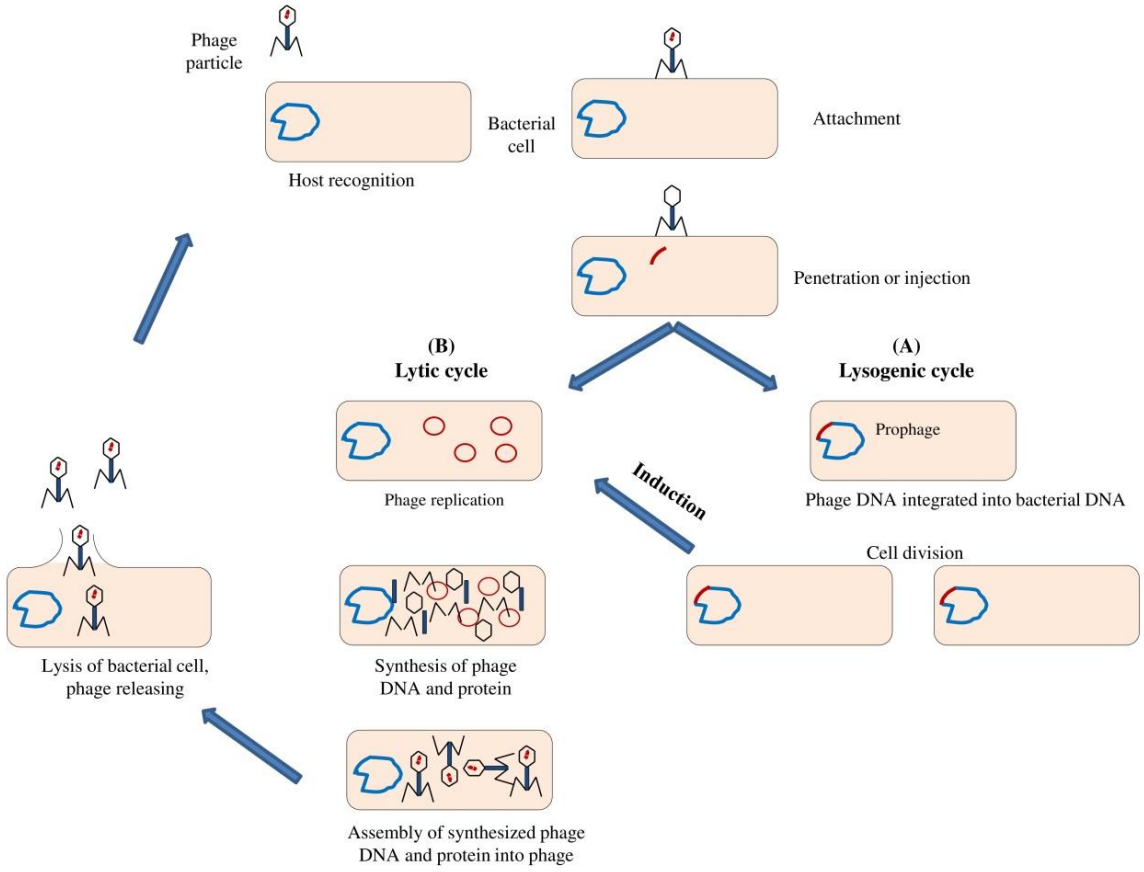

Fig. 1.6 Lytic and lysogenic life cycle of bacteriophage.

The phage particle first binds with its attachment binding receptor to the host-cell surface and then injects its genome into the host cells. The phage can subsequently enter either the lysogenic (A) or lytic cycle (B). (A) Lysogenic cycle; the phage DNA is integrated into the host DNA (lysogenization). (B) Lytic cycle; the virus replicates and new mature particles are release from the host cell by lysis. The new progeny are then free to infect other host cells with the appropriate receptor on the host cell surface. The lysogenic cell can enter the lytic cycle by a process called induction.

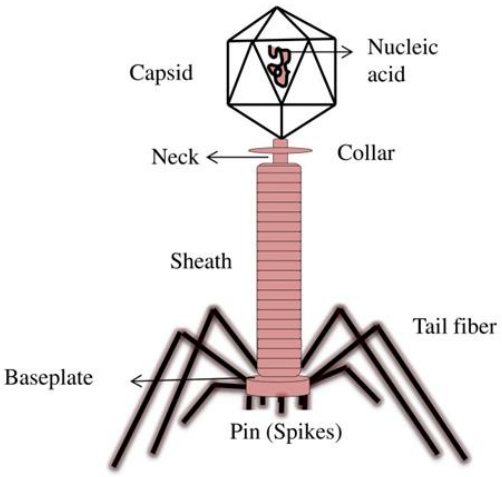

Fig. 1.7 Typical enterobacterial T4 phage

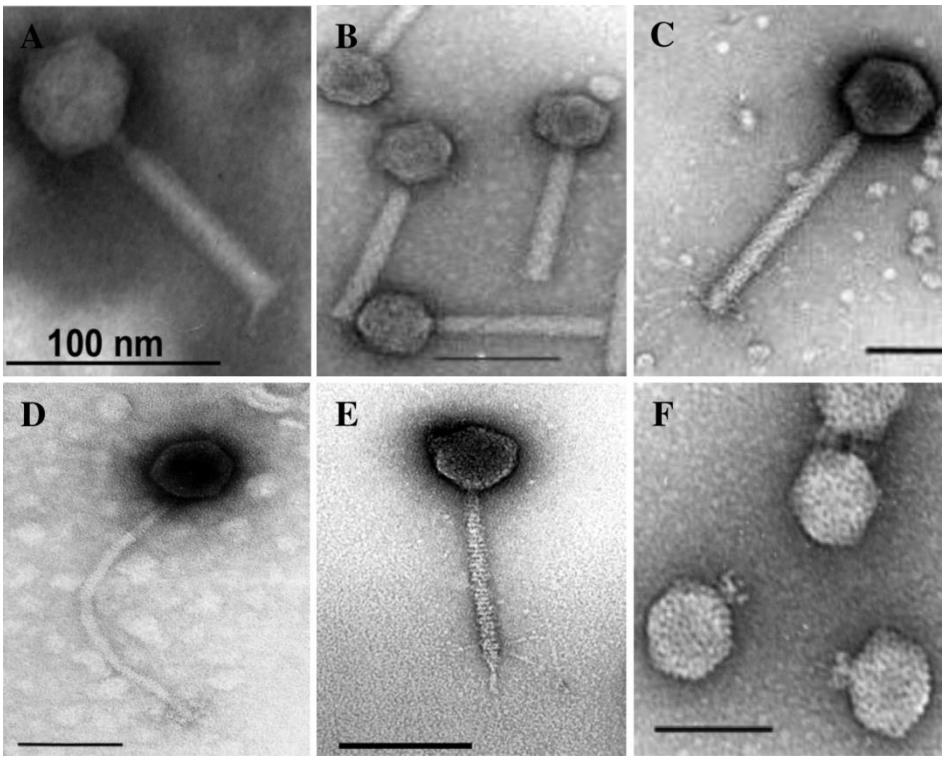

Fig. 1.8 Electron micrograph of negatively stained temperate bacteriophages.

Shigella flexneri Mu-like phage (**A**) (Jakhetia & Verma, 2015), Enterobacteria phage P2 (**B**) http://www.virology.net/Big_Virology/BVDNAmyo.html and phage P1 (**C**) of the *Myoviridae* family www.thebacteriophages.org; Bacillus phage SPβ (**D**) (Murphy *et al.*, 2012) and Enterobacteria phage λ (**E**) of the *Siphoviridea* family (Murphy *et al.*, 2012); phage P22 (**F**) of the *Podoviridae* family (Murphy *et al.*, 2012).

Table 1.2 Physical properties and characteristics of temperate bacteriophages.

Phage	Family	Host	Morphology		Genome size (kb)	Integration sites
			Head	Tail		
Phage λ	*Siphoviridae*	*E. coli*	Icosahedral, 60 nm	Flexible, non-contractile, long, 4 long terminal fibres, 150×8 nm	48.5	Integrates at specific sites
P1-like	*Myoviridae*	*E. coli, Shigella, Serratia*	Icosahedral, 87 nm	Contractile, long, tails have base plates and 6 long fibres, 226×18 nm	97	Use plasmid as integration sites
P2-like	*Myoviridae*	*E. coli, Shigella, Serratia*	Icosahedral, 57 nm	Contractile, tails have base plates, collar and 6 long fibres, 135×18 nm,	33.8	Integration site is chromosome (specific sites recombination)
Mu-like	*Myoviridae*	*E. coli*	Icosahedral, 56 nm	Contractile, Tails have base plates and 6 long fibres, 120×18 nm,	42	Integrates at host chromosome (transposition)
Phage P22	*Podoviridae*	*Salmonella*	Icosahedral, 65 nm	Short, 18 nm, 6 spikes	43	Integrates at specific sites

Myoviridae phages also seem to be more sensitive to freezing and thawing as well as to osmotic shock (Murphy *et al.*, 2012). Lysogenic ***Podoviridae*** phages have short, non-contractile tails about 20×8 nm in length. The phage P22 is an example of the *Podoviridae* (Fig. 1.8 & Table 1.2) (Murphy *et al.*, 2012). ***Inoviridae*** phages are filamentous and about 7 nm in diameter. The genomes of *Inoviridae* phages are able to integrate into bacterial genomes, although they are not stable (Murphy *et al.*, 2012).

1.8.2.3 Additional prophage types

Recently, there has been a rapid increase in the number of published bacterial genome nucleotide sequences. Comparative genomics analysis of bacterial genomes have revealed the pervasiveness of prophages in most bacterial genomes (Fortier & Sekulovic, 2013) and they represent 10 to 20% of the bacterial genome (Casjens, 2003). Genomes analysis allows non-inducible prophages to be studies (Casjens, 2003). In addition to fully-functional prophages, four additional types of prophage-like entities have been characterised; these include defective and satellite prophages, bacteriocin-like phages, and gene transfer agents (Casjens, 2003).

Defective (or cryptic) **phages** are prophages that are they are unable to be induced and enter the lytic phase and are in a state of mutational decay. Although defective phages may still harbour functional genes, they are unable to program the full phage replication cycle (Casjens, 2003). Examples of defective phages include Rac, e14, DLP12 and QIN in *E. coli* and PBSX and SKIN in *Bacillus subtilis* (Casjens, 2003).

Satellite phages are functional phages that do not carry their own virion structural protein genes. They are characterised by having a chromosome that is designed to be encapsidated by the virion proteins of other specific phages (Casjens, 2003). A well-studied example is the satellite phage P4. Although phage P4 carries genes involved in replicating its own DNA, P4 is able to use the helper phage P2 to produce the coat proteins required for encapsidation (Casjens, 2003).

Bacteriocin-like phages are produced by some bacteria which are similar to the phage tails and are able to kill bacteria. Two bacteriocins of *P. aeruginosa* PAO1 have been well characterised, namely, type F and R bacteriocins that are similar to λ-like tails and P2-like phage tails, respectively (Casjens, 2003).

Finally, gene transfer agents are tailed phage-like particles that encapsidate random fragments of the bacterial genome. Because the majority of the particles do not carry genes, these particles cannot propagate as viruses (Casjens, 2003). However, these virion-like particles can deliver their DNA into another bacterium of the same species where the DNA can be incorporated into the chromosome by homologous recombination (Casjens, 2003). For example, a gene transfer agent is encoded by a cluster of genes on the *Rhodobacter capsulatus* chromosome (Casjens, 2003).

1.8.3 Life cycle of bacteriophages

Phages can use either the lysogenic or lytic pathway (Birge, 2006; Salmond & Fineran, 2015). In either case, the ability of phages to infect a particular bacterium is primarily dependent on whether or not the bacteriophage can attach to specific receptors on the cell surface (Lindbergl, 1973; Parent *et al.*, 2014). A successful infection is initiated by successful attachment (adsorption) of the bacteriophage with the cell-surface receptors, penetration of the phage nucleic acid into the bacterial cell, synthesis of nucleic acid and proteins, assembly and packaging of virions and, finally, lysis of the bacterial cell and release of new mature virus particles (Lindbergl, 1973; Michael *et al.*, 2003; Rakhuba *et al.*, 2010). These steps are described in further detail below.

1.8.3.1 Adsorption

Adsorption is the first step in the interaction between phage and host cell (Fig. 1.6) (Lindbergl, 1973; Michael *et al.*, 2003; Rakhuba *et al.*, 2010). Attachment is enhanced by the ability of the phage to recognise specific binding or attachment sites on the bacterial cell surface known as receptors (Lindbergl, 1973; Michael *et al.*, 2003; Rakhuba *et al.*, 2010). Receptors include OMPs such as OmpA and porins, LPS, pili, flagella and capsule (Jakhetia & Verma, 2015; Jin *et al.*, 2015; Lindbergl, 1973; Parent *et al.*, 2014; Porcek & Parent, 2015; Rakhuba *et al.*,

2010). In encapsulated Gram-negative bacteria, bacteriophages use different mechanisms to infect bacteria and reach the bacterial cell surface because capsule may block the access of bacteriophages to their receptor localised in the cell wall (Lindbergl, 1973; Rakhuba *et al.*, 2010). To infect the bacterial cells, phage induce an enzyme called capsular depolymerases that cause degradation of capsular layer and reach the bacterial cell wall (Lindbergl, 1973). Phage cannot attach to a host cell in the absence of a receptor. However, infection may occur either by mutation of the virus or sometimes the phage can attach to more than one target (Michael *et al.*, 2003).

1.8.3.2 Penetration

Penetration usually follows adsorption (Fig. 1.6). Penetration involves the injection of phage DNA into the bacterial cell (Michael *et al.*, 2003). The mechanism of DNA injection varies among different phages. In contractile tail phages, the DNA is injected into the bacterial cell through the hollow core of the phage tail (Parija, 2009). Penetration through the cell wall is enhanced by the enzyme lysozyme which is present in the tail core; this produces a hole in the bacterial cell wall (Parija, 2009). The phage DNA passes through the central core of the tail into the bacterial cytoplasm. The empty phage particles (head and tail) that remain on the bacterial cell surface are called a ghost (Parija, 2009).

1.8.3.3 Replication, packaging and release

Replication and packaging usually begins after the phage DNA is injected into the host cell. In lytic (virulent) phage, once DNA is injected into the host cell the host biosynthetic machinery is redirected replication and assembly of phage particles. This process allows the reproduction of both nucleic acid and protein and leads to new phage assembly and their release from the bacteria by cell lysis (Fig. 1.6) (Michael *et al.*, 2003). Temperate bacteriophage uses different mechanisms for replication and assembly depending on whether they enter the lytic or lysogenic cycle (Birge, 2006; Dale, 1999). In phages λ and P2 the DNA is linear and circularised by pairing of complementary cohesive ends (Birge, 2006; Dale, 1999), whereas in phage P22 and P1, the DNA is circularised by site-specific recombination of terminally redundant ends (Birge, 2006; Dale, 1999). Temperate phage may enter the lysogenic or the lytic cycle depending on the

conditions inside the bacterium (Rogers, 2012). Further details are described in section 1.8.4.

1.8.4 Control and regulation of the lysogenic and lytic pathways in temperate bacteriophages

The mechanisms of the lytic-lysogenic switch have been studied in detail in phage lambda of *E.coli* (bacteriophage λ). Details of the mechanisms that regulate and control both the lytic and lysogenic pathways have been reviewed (Birge, 2006; Dale, 1999; Dodd *et al.*, 2005; Michael *et al.*, 2003; Oppenheim *et al.*, 2005; Rogers, 2012; Waldor & Friedman, 2005). The CI and Cro regulator determine the lysogenic and lytic phase of temperate bacteriophages, respectively (Oppenheim *et al.*, 2005).

1.8.4.1 The lysogenic cycle

Generally after infection of the host cell with temperate bacteriophage, the phage enters the lysogenic pathway in which the phage DNA is integrated into the host chromosome because the lysogenic genes are expressed. However, under certain circumstance the bacteriophages enter the lytic phase, in which the mature phage particles are released by host lysis (Waldor & Friedman, 2005). To establish lysogenic pathways early after infection the phage must control the production of late protein by the rapid synthesis of a large amount of lambda repressor called *cI* (Fig. 1.9) and integrate into the host chromosome (Fig. 1.10).

The cI gene encodes lambda repressor protein that acts to switch off the lytic pathway. The cI gene is expressed from a promotor called P_E (Birge, 2006; Dale, 1999; Michael *et al.*, 2003). CII is an activator protein that stimulates the transcription of the *cI* gene from P_E. CII is highly sensitive to degradation by host protease. A phage-encoded protein called CIII stabilises the CII protein pathway (Birge, 2006; Dale, 1999; Michael *et al.*, 2003). CI represses the P_L and P_R and it stimulates the synthesis P_M (Fig. 1.9). The repressor protein binds to O_L and O_R and this will prevent the synthesis of N and Cro. N is an anti-repressor protein which is necessary for the anti-termination that allows the transcription of P_L and P_R (delayed early genes) (Fig. 1.9).

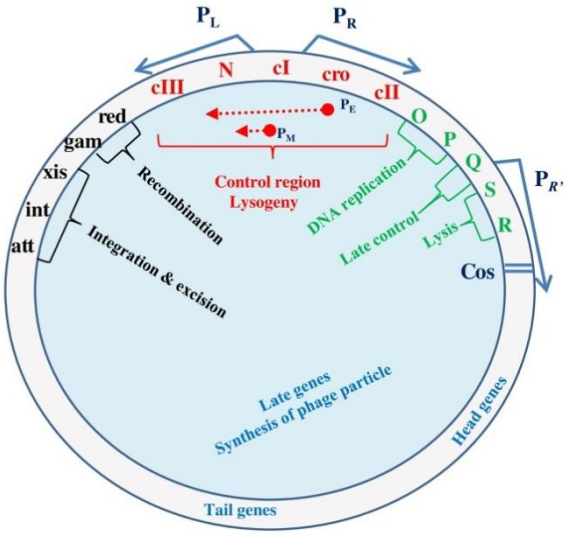

Fig. 1.9 Genetic map of bacteriophage λ.

The genes are designated by letters; *att*, attachment site for the phage to host chromosome; *cI*, repressor protein; P_L, promoter left; P_R, promotor right; *cro*, gene for second repressor; N, anti-terminator. Transcript needed for the lytic cycle is designated by the blue arrow while red arrow represents the transcript involved only in lysogenic cycle.

If the lysogenic pathway is followed, Integration always occurs at site-specific recombination between two DNA recognition sequences, the bacterial attachment site, *attB,* and the phage attachment site, *attP* (Fig. 1.10) (Groth & Calos, 2004). The host chromosome attachment site (*attB*) is located between the *gal* (galactose) and *bio* (biotin biosynthesis) genes (Michael *et al.*, 2003). Both *attB* and *attP* have 15 bp core region of homology. Recombination between *attP* and *attB* is mediated by a gene encoding integrase (*int*) and the integration host factor (IHF) (Dale, 1999; Rogers, 2012). The integrase gene (product of phage λ) enhances the recognition of *attP*, whereas IHF is a host protein that helps to cut, align and ligate the phage DNA into the bacterium chromosome (Rogers, 2012). The integrated phage DNA is replicated as part of the host chromosome using the bacterial replication machinery as the Cro repressor continues to repress the genes that control the lytic pathway (Dale, 1999; Rogers, 2012). Furthermore, some phage, such as Mu-like phages do not use site specific attachment sites but integrate randomly into the host chromosome via transposition (Feiner *et al.*, 2015; Jakhetia & Verma, 2015; Morgan *et al.*, 2002). The mechanisms of site-specific recombination have been reviewed by Craig, 1988; Grindley *et al.*, 2006; Sadowski, 1986. Under stress conditions, the lysogenic pathway breaks down and a protein called Xis is produced. The ***xis***

gene triggers the excision of the phage chromosome from the host chromosome by interacting with integrase (Fig. 1.10). The lysogenic phage can be switched to the lytic phase by a process called induction using different physical stimuli and chemical mutagens. These treatments cause damage to a host DNA and this activates host defence mechanism called the SOS response. The SOS response is explained in more detail in section 1.8.5.

1.8.4.2 Lytic cycle

The genetic map of phage lambda (bacteriophage λ) is shown in Fig. 1.9. The genes are arranged based on their function; early genes control replication, the control region and early transcription, whereas late genes are responsible for the synthesis of the head, tail and production mature phage particle (Dale,1999). When the lytic pathway is activated, transcription initiates at two early major promoters P_L and P_R which are the major leftwards and rightward promoters, respectively (Fig. 1.9). Transcription and translation of both promoters leads to the expression of N and Cro. The N protein is an anti-terminator that interacts with RNA sites that allow transcription of delayed early genes such as O, P, and Q, that are involved in DNA replication (Dale, 1999). Replication is initiated when the O and P proteins are produced in sufficient amounts during delayed early mRNA synthesis. The Q protein is an anti-terminator that acts under the control of the N protein. The Q protein allows transcription of late genes, those located between Q and S. The Q protein results in transcription of late mRNA that lead to formation of late structural proteins such as phage capsid protein, tail protein, those protein that involved in cell lysis, phage packaging, maturation, and release. Once the phage DNA is packaged into the capsid, the phage particles begin to assemble; the phage capsid and tail are assembled separately (Fig. 1.9) (Dale, 1999). Eventually, the mature particles are released from the host cell by cell lysis. The release of phage particles from the host cell occurs by the action of some phage-coded proteins such as holin which opens the host cell envelope to release the mature phage particles (Krupovič & Bamford, 2008).

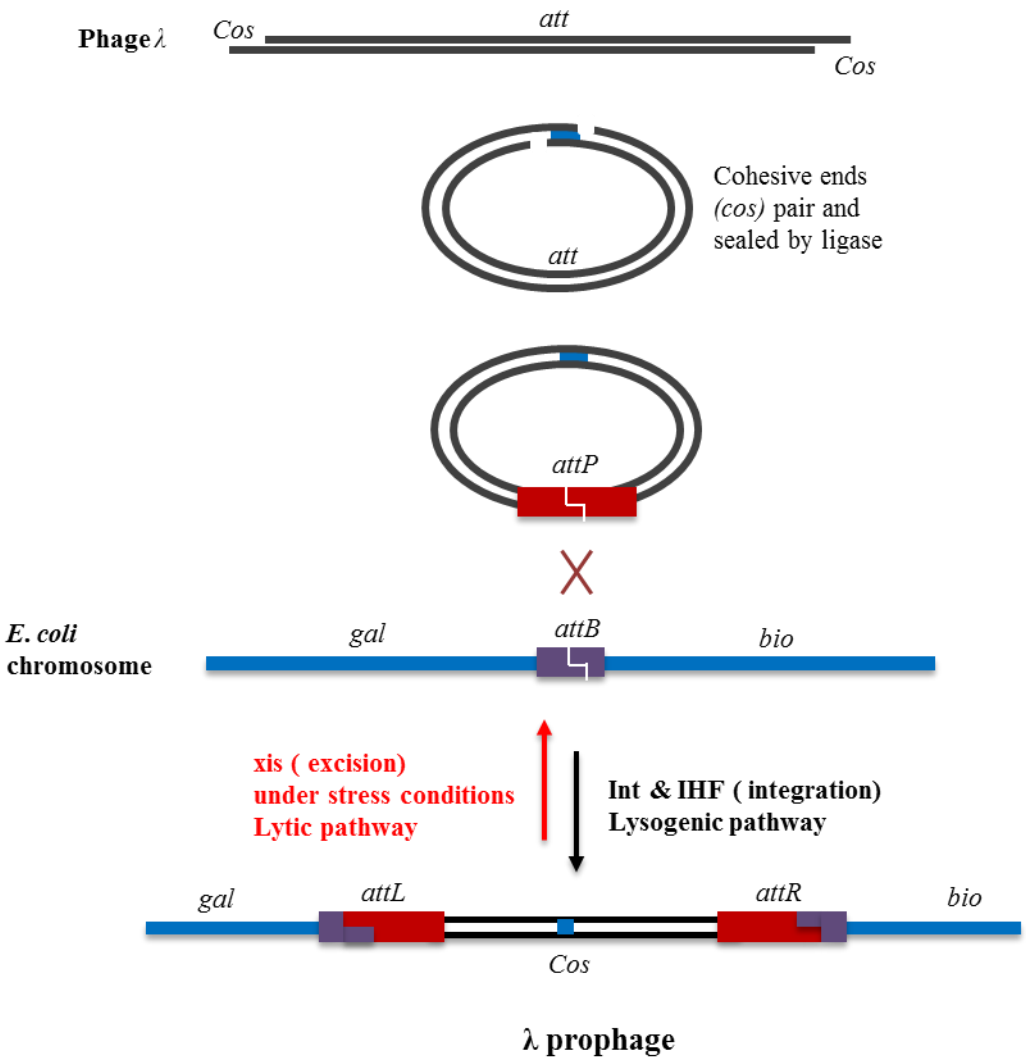

Fig. 1.10 Integration and excision of λ DNA

The λ phage chromosome is injected into a host such as *E. coli* as linear dsDNA and the circularisation of the phage chromosome occurs via its cohesive ends (Cos). The λ chromosome integrates into the host chromosome near to *gal* and *bio* genetic loci. Integration occurs at site-specific homologues regions between two DNA recognition sequences, the bacterial attachment site, *attB*, and the phage attachment site, *attP*. Integration is mediated by integrases produced by phage and integration host factor by the bacterium. The phage DNA is then called prophage. However, under stress condition the lysogenic pathway breaks down and a protein called Xis is produced. The *xis* gene triggers the excision of phage chromosome from the host chromosome to begin the lytic pathway.

1.8.5 Induction of lysogenic prophage

Lysogenic bacteriophages are very stable and replicate along with the bacterium chromosome. They persist in a dormant state by repression of the lytic genes. However, they can irreversibly switch to the lytic cycle, producing phage particles when they are expose to DNA-damaging agents (Feiner *et al.*, 2015; Oppenheim *et al.*, 2005). Different physical stimuli and chemical treatments have been used to convert the prophage to the vegetative state. These include ultraviolet (UV) light (Kuhn *et al.*, 1987; Richards *et al.*, 1985; Shinagawa *et al.*, 1977), heat treatment (Armentrout & Rutberg, 1971), X-ray (Shinagawa *et al.*, 1977) and exposure to antibiotics including enrofloxacin (Ingrey *et al.*, 2003), ciprofloxacin (Strauch *et al.*, 2004; Ubeda *et al.*, 2009), norfloxacin (Nale *et al.*, 2012). However, the most popular chemical treatment used to induce phages in both Gram-negative and Gram-positive bacteria is mitomycin C (Campoy *et al.*, 2006a; Davies & Lee, 2006; Goerke *et al.*, 2006; Nielsen & Rosdahl, 1990; Niu *et al.*, 2013; Pullinger *et al.*, 2004; Shinagawa *et al.*, 1977; Shin *et al.*, 2014; Ubeda *et al.*, 2009; Urban-Chmiel *et al.*, 2015; Williams *et al.*, 2002). The exposure of prophages to the DNA-damaging agent causes the activation of a multifunctional cellular response, termed the SOS response (Crowl *et al.*, 1981). Details of the SOS response have been described in various reviews (Crowl *et al.*, 1981; Campoy *et al.*, 2006b; Galkin *et al.*, 2009; Miller *et al.*, 2004; Michel, 2005; Ubeda *et al.*, 2009; Walker, 1984). The regulation of the SOS response is controlled by two key proteins, LexA and RecA (Michel, 2005). The LexA protein functions as a repressor for a set of about 43 genes including *recA* and *lexA* that are involved in the SOS response (Galkin *et al.*, 2009). The RecA protein is an inducer of the SOS response. It is an essential enzyme in homologous recombination and is involved in many cellular functions in bacteria (Michel, 2005; Ubeda *et al.*, 2009).

The SOS response is initiated when RecA is activated by an inducing single in the form of a single-stranded DNA (Galkin *et al.*, 2009). The activated RecA causes auto-cleavage of LexA allowing SOS gene expression (Galkin *et al.*, 2009). In bacteriophage λ, lysogeny is under the control of CI as a lambda repressor protein. However, activation of the SOS response elicits switching of the lysogenic cycle to the lytic cycle because the activated RecA results in the inactivation of CI protein as a repressor. Auto-cleavage of the CI protein is due

to its structural similarity to the LexA protein (Crowl *et al.*, 1981; Campoy *et al.*, 2006b; Galkin *et al.*, 2009; Michel, 2005). However, sometimes induction or release of mature particles occurs by random DNA damage in the a very small proportion of lysogens in the absence of the above stressors (Oppenheim *et al.*, 2005). This type of induction is known as spontaneous or basal induction (Dale, 1999; Oppenheim *et al.*, 2005; Waldor & Friedman, 2005). In spontaneous induction, the induced cells enter the lytic phase and become non-lysogenic (Oppenheim *et al.*, 2005). The expression of the lytic genes under the stressful conditions using DNA damaging agents (induction) can promote the excision of the phage genome, followed by DNA replication, assembly of phage particles, DNA packaging, and release of the new progenies through bacterial cell lysis (Feiner *et al.*, 2015).

1.8.6 Bacteriophage and bacterial evolution

1.8.6.1 Prophages and bacterial genomics

Bacterial genome nucleotide sequences are being completed very rapidly. Comparative genomics analysis of bacterial genomes have revealed that prophages are common in bacterial genomes (Canchaya *et al.*, 2003; Casjens, 2003; Fortier & Sekulovic, 2013). Studies have shown that prophages are one of the main sources of genetic diversity and strain variation associated with the virulence of many bacterial pathogens including *E. coli* (Ohnishi *et al.*, 2001; Weinbauer & Rassoulzadegan, 2004), *S. enterica* (Cooke *et al.*, 2007), *S. aureus* (Rahimi *et al.*, 2012); and *S. pyogenes* (Aziz *et al.*, 2005). In *E. coli* strain O157 Sakai, bacteriophages were shown to be major contributors to the genetic diversity of the species due to the acquisition of new DNA though transduction (Weinbauer & Rassoulzadegan, 2004). The genome of *E. coli* strain O157 Sakai contains 18 prophages and prophage-like elements accounting for approximately 50% of site-specific genomic DNA sequences, suggesting that phages contribute to the emergence of new strains (Weinbauer & Rassoulzadegan, 2004). Temperate bacteriophages, especially bacteriophage-encoded virulence genes, have also been demonstrated to contribute to bacterial pathogenesis (Boyd & Brüssow, 2002; Boyd, 2012; Penades *et al.*, 2015). Bacteriophage-encoded virulence determinants can transform their host from a commensal to a pathogen or virulent strain by a process known as lysogenic conversion (Allison,

2007; Boyd & Brüssow, 2002; Boyd, 2012; Veses-Garcia *et al.*, 2015). In lysogenic conversion bacteriophage-encoded virulence genes provide mechanisms that enable attachment, invasion, survival and damage to the host and/ or host cells bacterial cell (Boyd & Brüssow, 2002; Boyd, 2012). Temperate bacteriophages can increase the bacterial host fitness under certain condition such as virulence, antibiotic resistance and biofilm formation and some prophages can provide bacteria with regularity switches and protect the bacteria against these infections (Bobay *et al.*, 2014).

1.8.6.2 Phages as agents of horizontal gene transfer (lateral gene transfer)

A major driving force in the emergence and evolution of pathogenic bacteria is horizontal gene transfer (HGT) and acquisition of virulence factors (Boyd & Brüssow, 2002). Virulence factors could be encoded on mobile and integrative genetic elements such as plasmids, bacteriophages, conjugative transposons, integrons, insertion sequences and pathogenicity islands (Boyd, 2012; Kelly *et al.*, 2009). These elements contribute substantially to the genetic diversity of many bacterial species (Masignani *et al.*, 2001). In pathogenic bacteria some of these elements involve the exchange of genetic material coding for virulence. Therefore, this mechanism may increase the fitness of bacteria through acquisition of virulence determinants (Masignani *et al.*, 2001). The exchange of genetic material and dissemination of virulence genes is mediated by HGT. The acquisition of new DNA sequence through HGT is mediated by conjugation, transduction or transformation (Kelly *et al.*, 2009).

Bacteriophages play a crucial role in the dissemination of genes and the promotion of genetic diversity within bacterial populations. Such horizontal transfer of DNA leads to the emergence of new pathogenic strains through the dissemination of genes encoding virulence factors such as toxins, adhesins and agressins (Saunders *et al.*, 2001). Phage-mediated transfer of genes from one host to another can be mediated either by generalized or specialised transduction (Canchaya *et al.*, 2003; Saunders *et al.*, 2001). Generalized transduction is common among many bacteriophages. The phage DNA is normally packaged after the phage heads are completed. However, sometimes errors happen and the DNA fragments of the bacterial genome are packaged instead of the phage DNA (Brüssow *et al.*, 2004). Up on infection, the foreign bacterial DNA

is injected into the bacterium and the injected foreign bacterial DNA can be integrated into the host genome by homologous recombination (Brüssow *et al.*, 2004). Transducing phages have been found in many bacterial species. For instance, in *Salmonella spp*. (Schicklmaier & Schmieger, 1995; Schicklmaier *et al.*, 1998), *E. coli* (Schicklmaier *et al.*, 1998), *Vibrio cholerae* (Hava & Camilli, 2001), *L. monocytogenes* (Hodgson, 2000), *Staphylococcus spp*. (Uchiyama *et al.*, 2014) and *S. coelicolor* (Burke *et al.*, 2001). Specialised transduction can happen when a small segment of bacterial DNA is packaged with the phage DNA during the excision of the phage from the host chromosome. The small bacterial DNA segment and phage DNA can be integrated into the host genome after infection by site specific recombination (Birge, 2006). Phages can transfer genes that are not necessary for bacteriophage persistence and are generally recognised by their ability to convert the host bacteria to new phenotypes. This phenomenon is known as phage conversion (Saunders *et al.*, 2001). Lysogenic conversion has the ability to convert bacterial strains to virulent or pathogenic strains (Boyd & Brüssow, 2002) when the converting gene encodes for virulence determinants (Saunders *et al.*, 2001). In lysogenic conversion, the phage encode factors that increase the fitness and survival of the bacterial host (Feiner *et al.*, 2015).

A variety of toxins expressed by pathogenic bacteria are phage-encoded virulence factors. Examples of well-studied phage-encoded toxins include diphtheria toxin, botulinum toxin, exfoliative toxin, shiga-like toxin, cytotoxin and cholera toxin (Boyd, 2012; Brüssow *et al.*, 2004; Cheetham & Katz, 1995; Saunders *et al.*, 2001). Details of phage-encoded virulence genes and their role in the evolution of bacterial pathogens have been reviewed (Boyd, 2012; Brüssow *et al.*, 2004; Cheetham & Katz, 1995; Feiner *et al.*, 2015; Saunders *et al.*, 2001). It has been suggested that these toxin genes were acquired by transduction because in most cases they located near to bacteriophage attachment sites (*attB*) (Cheetham & Katz, 1995). In addition to toxins, other virulence genes may be carried by bacteriophages including the *oac* genes which encode a lipopolysaccharide O-antigen acetylase in *S. flexneri,* gene for capsule production by *S. pneumoniae* (Cheetham & Katz, 1995) and SpoE effector proteins of *S. enterica*. Furthermore, phages encode genes involved in adhesion, colonisation, immune system evasion, serum resistance and surface-exposed antigens (Boyd, 2012; Cheetham & Katz, 1995; Feiner *et al.*, 2015; Masignani *et*

al., 2001; Saunders *et al.*, 2001). Examples of phage-encoded virulence factors are shown in Table 1.3. The presence of these genes in the phage genomes suggests that there is an evolutionary advantage for the bacteriophages to carry such genes, perhaps due to enhanced replication of bacteria carrying these virulence determinants (Cheetham & Katz, 1995).

Comparative genomics demonstrated that the chromosomes from bacteria and their viruses (bacteriophages) are coevolving. This process is most evident for bacterial pathogens where the majority contain prophages or phage remnants integrated into the bacterial DNA. Many prophages from bacterial pathogens encode virulence factors. Two situations can be distinguished: V. *cholerae*, shiga toxin-producing *E. coli*, *C. diphtheriae*, and *C. botulinum* depend on a specific prophage-encoded toxin for causing a specific disease, whereas *S. aureus*, *S. pyogenes*, and *S. typhimurium* harbour a multitude of prophages and each phage-encoded virulence or fitness factor makes an incremental contribution to the fitness of the lysogen (Brüssow *et al.*, 2004). These prophages behave like "swarms" of related prophages. Prophage diversification seems to be fuelled by the frequent transfer of phage material by recombination with superinfecting phages, resident prophages, or occasional acquisition of other mobile DNA elements or bacterial chromosomal genes (Brüssow *et al.*, 2004). Prophages also contribute to the diversification of the bacterial genome architecture. In many cases, they actually represent a large fraction of the strain-specific DNA sequences. In addition, they can serve as anchoring points for genome inversions (Brüssow *et al.*, 2004).

Table 1.3 Phage-encoded bacterial virulence factors.

Phage	Bacterial host	Gene	Function	Reference
Lambda	*E. coli*	*lom*	Cell attachment	(Barondess & Beckwith, 1990)
Lambda	*E. coli*	*bor*	Cellular survival	(Barondess & Beckwith, 1990)
Lambda	*E. coli*	*eib*	Cellular survival	(Sandt *et al.*, 2002)
SopEphi	*Salmonella enterica*	*sopE*	Effector protein	(Mirold *et al.*, 1999)
Gifsy-1	*S. enterica*	*gipA*	Invasion	(Figueroa-Bossi *et al.*, 2001)
Fels-1	*S. enterica*	*nanH*	Neuraminidase	(Figueroa-Bossi *et al.*, 2001)
P22	*S. enterica*	*gtr*	Glucosylation antigenicity	(Allison & Verma, 2000)
Sf6	*Shigella flexneri*	*oac*	O-antigen acetylase	(Clark *et al.*, 1991)
Stx-phage	*Shigella dysenteriae*	*Stx1,2*	Shiga toxin	(Strockbine *et al.*, 1988)
Mu-like phage	*Neisseria meningitidis*	*OMP*	Antigenicity	(Masignani *et al.*, 2001)
ϕCTX	*Pseudomonas aeruginosa*	*ctx*	Cytotoxin	(Nakayama *et al.*, 1999)
CTXϕ	*Vibrio cholerae*	*ctxAB*	Cytotoxin	(Waldor & Mekalanos, 1996)
phage C1	*Clostridium botulinum*	*C1*	Botulium toxin	(Barksdale & Arden, 1974)
ß-phage	*Corynebacterium diphtheriae*	*tox*	Diphtheria toxin	(Freeman, 1951)
ϕETA	*Staphylococcus aureus*	*eta*	Exfoliative toxin A	(Yamaguchi *et al.*, 2000)
T12	*Streptococcus pyogenes*	*speA*	Toxin type A	(Weeks & Ferretti, 1984)

1.9 Research objectives

Very little is known about the diversity and molecular evolution of genes encoding OMPs in *P. multocida* with respect to the underlying species phylogeny. Therefore, the initial objective of this study was to investigate the phylogenetic relationships of 40 representative *P. multocida* isolates based on variation within fifteen housekeeping enzyme genes and on the core genome. This was compared with a framework of evolutionary relationships among 123 isolates of *P. multocida* based on the concatenated partial sequences (3990 bp) of seven housekeeping enzyme genes (Davies *et al.*, unpublished; http://pubmlst.org/pmultocida_multihost). Subsequently, comparative nucleotide sequence analysis of genes encoding OMPs was performed to assess the extent of horizontal DNA transfer and recombinational exchange and to better understand potential mechanisms of host adaptation. The molecular evolution of the genes encoding various OMPs was assessed in relation to the underlying evolutionary relationships of the strains based on the phylogenies obtained from the housekeeping genes and core genomes. In this way, the roles of horizontal DNA transfer and recombination in the evolution of the *P. multocida* OMP were assessed.

A further goal of this study was to investigate the diversity and molecular evolutionary relationships of *ompA* in a larger selection of *P. multocida* isolates from different host species. Specifically, the aim was to assess the roles of horizontal gene transfer, recombinational exchange and host-switching of isolates in the evolution of the *ompA* gene. An additional aim was to determine the action of natural selection on amino acid diversity in OmpA. To achieve these aims, the *ompA* gene was sequenced from 74 *P. multocida* strains representing various host species, disease syndromes, capsular types, OMP types and sequence types. The molecular evolution of the *ompA* gene was assessed in relation to the underlying relationships of the strains based on MLST.

Since bacteriophages are known to play important roles in bacterial evolution, another goal of the study was to identify and characterise temperate bacteriophages among 47 *P. multocida* isolates representing multiple host species, disease types, capsular serotypes, OMP-types and sequence types. Mitomycin C was used to induce temperate phages in *P. multocida* and these

were characterised by transmission electron microscopy (TEM), host range and restriction endonuclease analysis.

To further assess the roles of bacteriophages in the evolution and pathogenesis of *P. multocida,* the complete genomes of 18 induced phages were examined. In addition, complete genome sequences were obtained for 40 *P. multocida* isolates and their phage content assessed. Comparative genomic sequence analysis was used to identify and classify the temperate bacteriophages within these *P. multocida* isolates. In particular, these phages were analysed to determine whether they encode any virulence genes, especially genes encoding OMPs and toxins.

Chapter 2 Diversity and molecular evolutionary relationships OMPs of *P. multocida* isolates from different host species

2.1 Introduction

Pasteurella multocida represents a diverse group of Gram-negative bacteria that are commensals in the upper respiratory and lower genital tracts of a variety of mammals and birds (Rimler & Rhoades, 1989). Outer membrane proteins of Gram-negative bacteria have diverse functions and are directly involved in the interaction with various environments encountered by pathogenic bacteria (Lin *et al.*, 2002) and allowing them to adapt to different host niches (Lin *et al.*, 2002; Ruiz *et al.*, 2006). As in other Gram-negative bacteria, different functional groups of OMPs have been identified in *P. multocida* (E-komon *et al.*, 2012; Hatfaludi *et al.*, 2010). These functions include outer membrane biogenesis and integrity, nonspecific porin activity and energy-dependent transport, adherence, membrane associated enzymatic activity and uncharacterised functions (E-komon *et al.*, 2012; Hatfaludi *et al.*, 2010). Various virulence factors are associated with disease in *P. multocida*. These factors include OMPs, LPS, capsule, fimbriae, exotoxins, siderophores, and extracellular enzymes (Harper *et al.*, 2006; Wilkie *et al.*, 2012).

Horizontal DNA transfer and recombination involving small DNA segments (intragenic) or entire genes (assortative), together with random mutation are recognised as major determinants in the evolution and diversification of bacteria (Castillo-ramirez *et al.*, 2012; Chaguza *et al.*, 2015; Croucher *et al.*, 2013; Feil *et al.*, 1999; Hanage *et al.*, 2009; Li *et al.*, 1994; Kelly *et al.*, 2009; Ochman *et al.*, 2000; Smith *et al.*, 1990). Horizontal DNA transfer and recombination are involved in the diversification of various virulence factors including outer membrane proteins (Bart *et al.*, 1999; Davies & Lee, 2004; Evans *et al.*, 2010; Ford, 2001), transferrin iron up-take systems (Lee & Davies, 2011), leukotoxin (Davies *et al.*, 2001; 2002), aureolysin gene (Sabat *et al.*, 2008), flagellar antigens (Li *et al.*, 1994; Smith *et al.*, 1990), lipopolysaccharide (D'Souza *et al.*, 2005; Reeves, 1993; Reeves *et al.*, 2013) and capsular polysaccharide (Coffey *et al.*, 1998; Wyres *et al.*, 2013). Bacteria show various levels of host specificity

and is thought to be the result of multiple molecular interaction between pathogens and their hosts (Pan *et al.*, 2014). Several surface-exposed proteins have been observed to have a role in eliciting host specific infection in several pathogenic bacteria (Pan *et al.*, 2014). These include immunoglobulin A1 (IgA1) protease, type IV pili, complement factor H binding proteins (FHBP), gonococcal porin, transferrin-binding proteins and lactoferrin-binding proteins of *Neisseria*; the metallo-type IgA1 protease of S. *pneumoniae;* and the avian-specific AC/I pili and lamb-specific K99 from septicemic *E. coli* strains (Pan *et al.*, 2014). Many OMPs are surface-exposed and may experience high selection pressure and undergo frequent genetic variation and exhibit high levels of diversity. Horizontal gene transfer of exogenous DNA can result in recombination of either related or unrelated DNA segments (Chaguza *et al.*, 2015). Homologous recombination occurs in the core genome, a subset of genes that are shared and conserved across all members of the species (Chaguza *et al.*, 2015; Forde *et al.*, 2016). Various mechanisms may contribute to the recombinational exchanges in bacteria and these processes are transformation, transduction (bacteriophage) and conjugation (Chaguza *et al.*, 2015). Many bacteria are naturally competent and able to transport foreign DNA into their cytoplasm across the cell envelope (Mell & Redfield, 2014).

However, very little is known about the genetic diversity of genes encoding OMPs in *P. multocida*. Therefore, the main aim of this part of the study was firstly to investigate the phylogenetic relationships of 40 representative *P. multocida* isolates based on variation within fifteen housekeeping enzyme genes. Subsequently, comparative sequence analysis of genes encoding OMPs was performed to assess the extent of horizontal DNA transfer and recombinational exchange and to better understand potential mechanisms of host adaptation. A framework of evolutionary relationships among 123 isolates of *P. multocida* based on the concatenated sequences (3990 bp) of seven housekeeping enzyme genes (Davies *et al.,* unpublished; http://pubmlst.org/pmultocida_multihost) was established and this was supplemented with phylogenetic analysis of *P. multocida* isolates based on core genomes. The molecular evolution of the genes encoding various OMPs was assessed in relation to the underlying relationships of the strains based on MLST and core genes. In this way, the roles of horizontal

DNA transfer and recombination in the evolution of the *P. multocida* OMP were assessed.

2.2 Materials and methods

2.2.1 Bacterial isolates

Forty *P. multocida* isolates were selected to investigate the diversity and molecular evolutionary relationships of *P. multocida* by next-generation genome sequencing. The isolates were associated with different diseases in different host species (cattle, sheep, pigs and poultry) and have been investigated in previous studies (Davies *et al.*, 2003a; b; c; Davies, 2004; Davies *et al.*, 2004). The strains represented various capsular serotypes, outer membrane protein types, 16S rRNA types, and sequence types (Davies *et al.*, unpublished; http://pubmlst.org/pmultocida_multihost). The MLST scheme has been updated with permission of Dr. Robert L. Davies. The properties of the isolates are listed in Fig. 2.1 & Table 2.1.

2.2.2 Bacterial growth conditions

2.2.2.1 Media for bacterial growth

Bacterial cultures were routinely cultured on blood agar (BHIA containing 5% (v/v) defibrinated sheep's blood [E & O Laboratories Limited]) or in brain heart infusion broth (BHIB; Oxoid) at 37°C. BHIB was used for the preparation of overnight broth cultures. All media were sterilised by autoclaving at 120°C for 15 min.

Table 2.1 Properties of 40 *P. multocida* isolates selected for (next-generation) genome sequencing.

Isolate [a]	ST	MLST group [b]	Host species	Clinical symptoms	Isolation site	Geographical origin	Capsular type	OMP-type [c]	16S rRNA type	*toxA*
PM316	1	A	Bovine	Pneumonia	Lung	Penrith	A	1.1	3	ND
PM564	1	A	Bovine	Pneumonia	Lung	Thirsk	A	2.1	3	ND
PM344	3	A	Bovine	Pneumonia	Lung	Shrewsbury	A	3.1	1	ND
PM632	4	A	Bovine	Pneumonia	Lung	Winchester	A	4.1	1	ND [d]
PM666	3	A	Porcine	Pneumonia	Lung	Sutton Bonington	A	2.1	1	-
PM116	3	A	Porcine	Pleuropneumonia	Lung	Sutton Bonington	A	3.1	1	-
PM966	16	B	Ovine	Pneumonia	Lung	Winchester	A	1.1	1	-
PM382	13	B	Porcine	Respiratory problems	Lung	Winchester	A	4.1	2	-
PM2	17	C	Ovine	Severe peritonitis	ND	Penrith	F	2.1	4	-
PM246	25	C	Avian	Septicaemia	Viscera	Bury St. Edmunds	F	2.2	2	ND
PM994	12	C	Ovine	Pneumonia	Lung	Penrith	F	1.1	2	ND
PM148	12	C	Avian	Eye infection	Eye	Thirsk	F	2.2	2	-
PM86	15	D	Avian	Fowl cholera	Pleura	Winchester	A	3.1	1	-
PM934	15	D	Porcine	Pneumonia	Lung	Bristol	A	5.1	1	-
PM954	15	D	Porcine	Pneumonia	Lung	Winchester	A	5.1	1	ND
PM486	9	D	Bovine	Pneumonia	Lung abscess	Bristol	A	9.1	1	ND
PM490	ND	ND	Bovine	Recurrent mastitis	Milk	Reading	A	9.1	ND	ND
PM172	26	D	Avian	Septicaemia	Lung	Starcross	A	3.1	ND	ND
PM302	6	E	Bovine	Rhinitis + others	Nasal swab	Sutton Bonington	A	5.3	ND	ND
PM144	21	E	Avian	Septicaemia	Lung/liver	Thirsk	A	1.1	2	ND
PM402	5	E	Bovine	Pneumonia	Lung	Newcastle	A	5.1	1	ND
PM122	ND	ND	Ovine	Pneumonia	Lung	Sutton Bonnington	D	3.1	ND	+
PM964	18	E	Ovine	Pneumonia	Lung	Winchester	D	3.1	ND	+
PM982	18	E	Ovine	Pneumonia	Lung	Carmarthen	D	3.1	1	+
PM986	18	E	Ovine	Pneumonia	Lung	Luddington	D	3.1	1	+
PM988	ND	ND	Ovine	Pasteurellosis	Lung	Winchester	D	3.1	ND	+
PM54	10	F	Porcine	Pneumonia	Lung	Shrewsbury	A	1.1	1	-
PM734	10	F	Porcine	Pneumonia	Lung	Cambridge VIC	A	1.1	2	-

Table 2.1 (continued)

Isolate [a]	ST	MLST group [b]	Host species	Clinical symptoms	Isolation site	Geographical origin	Capsular type	OMP-type [c]	16S rRNA type	*toxA*
PM850	10	F	Porcine	Pneumonia	Lung	Bury St Edmunds	A	1.1	2	-
PM200	10	F	Avian	Pneumonia	Lung	Bristol	A	1.2	ND	ND
PM336	7	F	Bovine	Pneumonia	Lung	Sutton Bonington	A	6.1	2	ND
PM684	11	G	Porcine	Suspect snouts	Nasal swab	Cambridge VIC	A	6.1	2	+
PM918	11	G	Porcine	Pneumonia	Lung	Shrewsbury	A	6.1	ND	+
PM926	ND	ND	Porcine	Pneumonia	Lung	Bury St Edmunds	A	6.1	ND	+
PM40	ND	ND	Porcine	-	-	NCTC	A	6.2	2	+
PM848	11	G	Porcine	Pneumonia	Lung	Starcross	D	4.1	ND	+
PM696	11	G	Porcine	Toxin Assay	Nasal swab	Cambridge VIC	D	6.1	ND	+
PM714	11	G	Porcine	Pneumonia	Lung	Thirsk	D	6.1	5	-
PM226	11	G	Avian	Pneumonia/death	Lesion	Sutton Bonington	D	13.1	ND	ND
PM82	32	H	Avian	Swollen heads3	Peritoneal	Bury St Edmunds	A	7.1	19	-

[a] isolates are arranged by order of MLST group (column 3) (Fig. 2.1); [b] ST= sequence type (Davies *et al*., unpublished http://pubmlst.org/pmultocida_multihost/); [c] OMP types for bovine, ovine, porcine and avian isolates are not equivalent, i.e. bovine OMP-type 1.1 is not as same as porcine OMP-type 1.1, etc. (Davies *et al.*, 2003a; b; c; Davies, 2004; Davies *et al.*, 2004); [d] ND: not determined.

2.2.2.2 Bacterial storage and growth conditions

P. multocida isolates were preserved in 1 ml of 50% (v/v) glycerol in BHIB at -80°C for long term storage. Fifteen microliters of thawed stock suspensions were streaked onto blood agar plates and incubated at 37°C overnight.

2.2.2.3 Preparation of broth starter cultures

Liquid cultures were prepared by inoculating 3 to 4 well-isolated colonies from overnight culture plates into 10 ml of volumes of BHIB in Universals and incubating at 37°C with shaking at 120 rpm.

2.2.3 Genome sequencing

2.2.3.1 Preparation of bacterial DNA for genomic sequencing

DNA was extracted using the PurElute Bacterial Genomic Kit (Edgebio; 85171). Bacteria in 5 ml of an overnight culture were harvested by centrifugation at 4,000 x g for 5 min at 4°C. The supernatants were discarded and the bacterial pellet resuspended in 2 ml of sterile PBS and centrifuged at 13,000 x g for 1 min at 4°C. Four hundred microlitres of spheroplast buffer were added and the sample vortexed at high speed for 10 s to resuspend the pellet. The samples were incubated at 37°C for 10 min in a water bath. One hundred microlitres of Lysis solution 1 were added and mixed by vortexing for 10 s. One hundred microlitres of Lysis solution 2 were added and mixed by vortexing for a further 10 s. The samples were incubated at 65°C for 5 min in a water bath. One hundred microlitres of extraction buffer were added and the samples were vortexed vigorously for 10 s and centrifuged at 13,000 x g for 3 min at 4°C. The supernatants were transferred to a clean Eppendorf tube and 100 µl of Advamax 2 beads added. The samples were inverted ten times to mix and the beads were pelleted by centrifugation. The supernatants were transferred to clean Eppendorfs, an equal volume of isopropanol was added, and the samples were inverted ten times to mix. The DNA was pelleted by centrifugation at 13,000 x g for 3 min at 4°C and the supernatants were carefully removed. The DNA was washed by adding 750 µl of 70% ethanol, inverted two to three times, and centrifuged at 13,000 x g for 3 min at 4°C. The supernatants were removed and

the samples left to air dry for 30 min. Finally, the DNA was resuspended in 100 µl nuclease free water and stored at -20°C.

2.2.3.2 Whole genome sequencing

DNA sequencing (whole genome and phage genome) was carried out by Glasgow polyomics using the Illumina Mi-Seq platform, employing 300 bp paired-end sequencing. The reads were trimmed of Illumina adapter sequences and low quality bases, then de novo assembled and scaffolded using the CLC Genomics Workbench (v7.5.1, Qiagen). Assembled scaffolds were annotated using the Rapid Annotation using Subsystem Technology (RAST) resource (Aziz *et al.*, 2008; Overbeek *et al.*, 2014).

2.2.4 Genome analysis

2.2.4.1 Nucleotide and amino acid sequence analysis of housekeeping enzyme genes and OMPs of *P. multocida*

Template sequences for housekeeping enzymes and predicted OMPs were obtained from the NCBI reference genome PM70. The template sequences were used to analyse 40 sequenced *P. multocida* genomes. An internal BLAST database was generated in CLC genomic workbench (v7, Qiagen) and used to extract sequences of both housekeeping enzymes and OMPs. A Microsoft word document (Microsoft, 2010) was used to format the sequences obtained for each housekeeping enzyme and OMP. The formatted files were then used to carry out phylogenetic and evolutionary analyses in MEGA (Molecular Evolution and Genetic Analysis, V4;Tamura *et al.*, 2007).

Phylogenetic and evolutionary analyses were conducted with MEGA in conjunction with alignment programs written by T. S. Whittam (Michigan State University). These programs included AAseq, RealigX, Psfind and Happlot. The sequences were firstly converted to amino acid sequences using AAseq and the amino acid sequences were aligned using ClustalX (v2.0.12). The nucleotide sequences were then aligned based on the amino acid alignment using RealigX. RealigX generates an output (.meg) file which serves as an input for MEGA. MEGA was used to generate Neighbour-Joining phylogenetic trees using the Jukes-Canter correction model and also to determine sequence variation (nucleotide

and amino acid polymorphisim). Boot-strap (500 replications) analysis, substitution rates and pairwise difference calculations were also conducted in MEGA. The Psfind and Happlot programs were used to represent polymorphic nucleotide sites graphically and to help identify recombination events. The output file from Happlot served as an input file to Micrographic Designer (MicrografX, Inc).

2.2.4.2 Secondary structure analysis

Secondary structure prediction was performed with the Psipred secondary structure prediction method (http://bioinf.cs.ucl.ac.uk/psipred/) and PRED-TMBB (http://bioinformatics.biol.uoa.gr/PRED-TMBB/). The *ompA* gene sequences of *P. multocida* were aligned and compared with the proposed secondary structure of OmpA of the closely related species *Mannheimia haemolytica* (Davies & Lee, 2004). The domains were identified in MEGA and the d_S and d_N ratios were calculated using the Nei-Goojbori (number of difference) and boot-strap (500 replications).

2.2.4.3 Phylogeny of *P. multocida* based on 15 housekeeping genes

The nucleotide sequences of 15 housekeeping enzyme genes were obtained from the NCBI *P. multocida* strain PM70 (reference strain). The properties of the 15 housekeeping enzyme genes are listed in Table 2.2. These genes were selected based on previous MLST studies used for *P. multocida* (Davies *et al.*, 2004; García-Alvarez *et al.*, 2015; Hotchkiss *et al.*, 2011; Moustafa *et al.*, 2013; Varga *et al.*, 2013), *N. meningitidis* (Birtles *et al.*, 2005), *H. parasuis* (Olvera *et al.*, 2006), *Y. pseudotuberculosis* (Ch'ng *et al.*, 2011), *Y. ruckeri* (Bastardo *et al.*, 2012) and *Pasteurellaceae* (Kuhnert & Korczak, 2006; Naushad *et al.*, 2015). Nucleotide sequences were obtained from the housekeeping genes of the 40 genomes of *P. multocida* using CLC genomics 'internal BLAST' tool. The fifteen sequences of each isolate were concatenated using CLC genomics 'join sequence' tool, and resulted in a sequence of 22,371 nucleotides. The sequences were analysed as described above (section 2.2.4.1).

Table 2.2 Properties of 15 housekeeping genes used to construct phylogeny of *P. multocida.*

Gene	Name	Size (bp)	Position (start-stop)	Direction	Species /Publication
adk	Adenylate kinase (nucleotide biosynthesis),)	645	323720-324364	Complement	*P. multocida*/Davies *et al.*, 2004
aroA	3-phosphoshikimate 1-carboxyvinyltransferase (amino acid biosynthesis)	1323	988954-990276	Forward	*P. multocida*/Davies *et al.*, 2004
aroE	Shikimate 5-dehydrogenase	810	1463132-1463941	Forward	*N. meningitides*/Birtles *et al.*, 2005
atpD	F1-ATPase_beta	1374	1685352-1686725	Forward	*H. parasuis*/Olvera *et al.*, 2006
deoD	Purine nucleoside phosphorylase (nucleotide biosynthesis)	717	1485823-1486539	Complement	*P. multocida*/Davies *et al.*, 2004
est	Triacylglycerol_lipase_like	2040	102920-104959	Forward	*P. multocida*/Moustafa *et al.*, 2013
gyrB	DNA gyrase subunit B	2421	1668610-1671030	Complement	*Y. pseudotuberculosis*/Ch'ng *et al.*, 2011
mdh	Malate dehydrogenase (energy metabolism; the TCA cycle))	936	634091-635026	Forward	*P. multocida*/Davies *et al.*, 2004
pgi	Phosphoglucose isomerase (energy metabolism; glycolysis)	1650	488453-490102	Forward	*P. multocida*/Davies *et al.*, 2004; García-Alvarez *et al.*, 2015
pmi	Mannose-6-phosphate isomerase, class I	1203	978551-979753	Complement	*P. multocida*/Hotchkiss *et al.*, 2011
recA	Recombinase A	1065	2047013-2048077	Complement	*Y. ruckeri*/Bastardo *et al.*, 2012
recN	DNA repair	1677	385501-387177	Complement	*Pasteurellaceae*/Naushad *et al.*, 2015
rpoA	DNA-directed RNA polymerase subunit alpha	990	1585273-1586262	Complement	*Pasteurellaceae*/Kuhnert & Korczak, 2006
rpoB	DNA-directed RNA polymerase subunit beta	4029	1956592-960620	Complement	*P. multocida*/Varga *et al.*, 2013
***zwf*/g6pd**	Glucose-6-phosphate dehydrogenase	1491	1751723-1753213	Forward	*P. multocida*/Davies *et al.*, 2004; Hotchkiss *et al.*, 2011

2.2.4.4 Phylogeny of *P. multocida* based on the core genome

The program Parsnp was used to generate a core genome alignment of the 40 *P. multocida* isolates (Treangen *et al.*, 2014). The core nucleotide alignment was used as the input file for Gubbins (Croucher *et al.*, 2015). Gubbins is best suited for detecting recombination in closely-related isolates and was run using default settings within the publicly available virtual machine. Tree output by Gubbins was based on the SNP sites determined to be outside of recombinant segments. The tree was visualised in FigTree (v1.4.2).

2.3 Results

2.3.1 Phylogeny of *P. multocida* based on 7 housekeeping genes

Multilocus sequence analysis has been used to determine the genetic relationships of 123 *P. multocida* isolates associated with different diseases in different host species (cattle, sheep, pigs and poultry). The strains represented various capsular serotypes, outer membrane protein types and 16S rRNA types (Davies *et al.*, unpublished; http://pubmlst.org/pmultocida_multihost). Seven housekeeping enzyme genes were selected based on their widespread locations around the chromosomes and these were *adk*, *aroA*, *deoD*, *gdhA*, *g6pd*, *mdh* and *pgi* (Table 2.2). Internal fragments approximately 500-600 bp in length were sequenced. The MLST scheme is based on comparative nucleotide sequence analysis of fragments from the seven housekeeping enzyme genes. Concatenated sequences are 3990 bp in length (Fig. 2.1). Preliminary details of the scheme were previously published in a study of evolutionary relationships among 35 bovine isolates of *P. multocida* (Davies *et al.*, 2004). The tree represented eight different clusters or groups which were designated, A to H as in Fig. 2.1.

Cluster A (bovine pneumonia cluster) included the majority of the bovine pneumonia isolates of capsular A (OMP-types 1 to 4 and also OMP-type 8.1 and STs 1 to 4) and certain porcine pneumonia isolates of capsular type A, OMP-type 2 and 3 and ST 3 (Fig. 2.1). Cluster B included ovine isolates of capsular type A (OMP-type 1 and ST 16) and haemorrhagic septicaemia isolates of capsular type B and E (STs 44, 45 and 46). Cluster C (avian/ovine F cluster) was associated with avian, bovine, ovine and porcine isolates of capsular type F. However, cluster C also contained porcine isolates of capsular type A (Fig. 2.1). Cluster D (avian/bovine/porcine cluster) included avian, bovine and porcine isolates of capsular type A (Fig. 2.1). Cluster E included avian, bovine, ovine and porcine isolates, isolates with the same capsular type, OMPs and STs clustered together. For examples, ovine D cluster was associated with ovine capsular type D, OMP-type 3 and ST 18, 19 and 20 (Fig. 2.1). Cluster F (porcine pneumonia cluster) was associated with majority of porcine pneumonia isolates and certain avian isolates of capsular type A OMP-type 1 and ST 10.

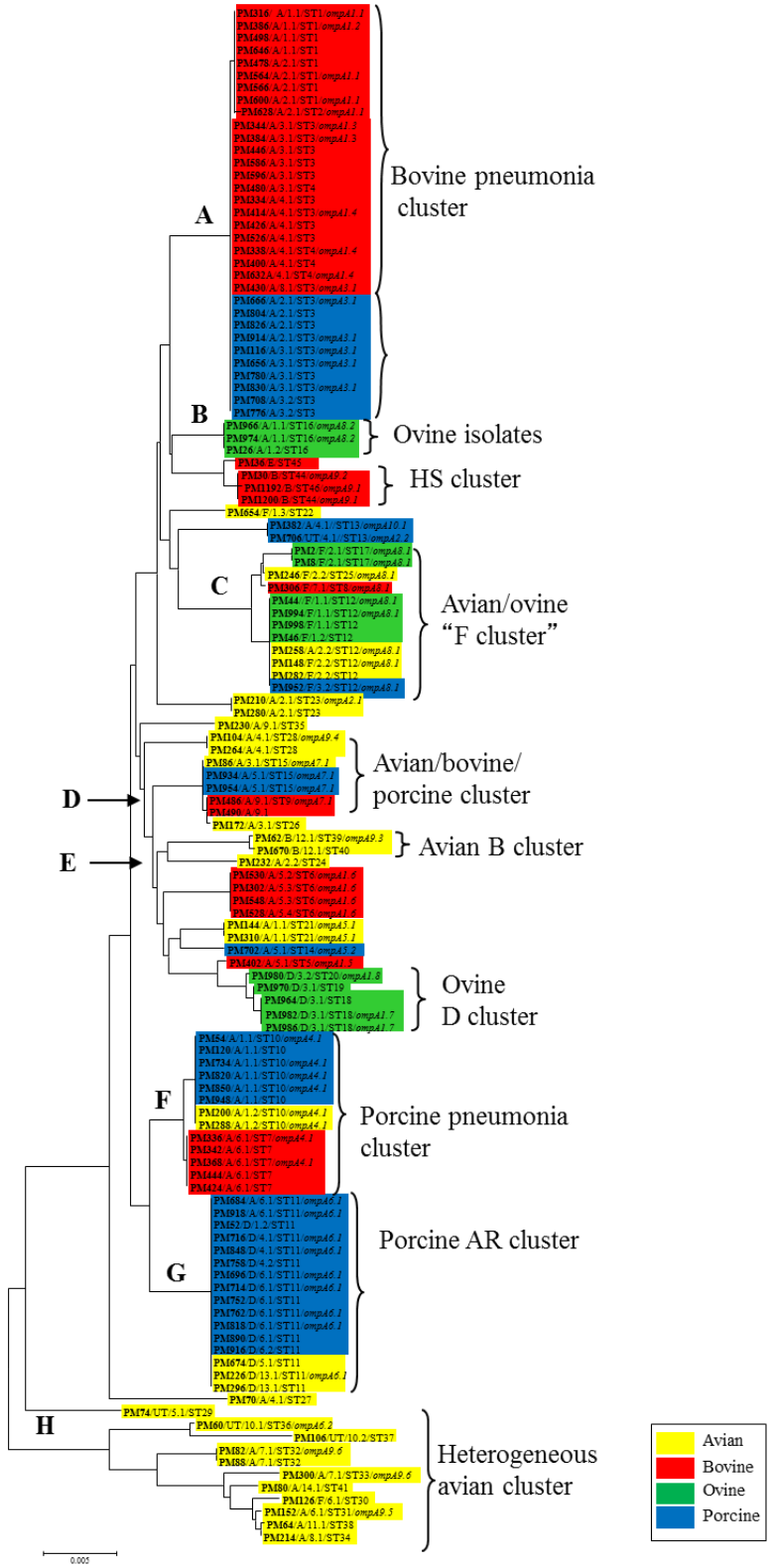

Fig. 2.1 Multi locus sequence typing (MLST) scheme of *P. multocida* isolates.

Neighbour-Joining tree representing the genetic relationships of *P. multocida* strains based on the concatenated sequences (3990 bp) of seven housekeeping enzyme genes from 123 isolates of *P. multocida* of avian, bovine, ovine and porcine origin **(http://pubmlst.org/pmultocida_multihost/).** Isolate designation, capsular type, OMP type, ST type and *ompA* alleles (where appropriate) are provided for each isolate (e.g. PM316/A/1.1/ST1/*ompA1.1*). The *ompA* alleles were obtained in this study. The MLST scheme has been updated with permission of Dr. Robert L. Davies.

Cluster F also included bovine isolates of capsular type A, OMP-type 6 and ST 7 (Fig. 2.1). Cluster G (porcine AR cluster) was associated with majority of porcine isolates associated with atrophic rhinitis in pigs (capsular type A and D, OMP-types 4 and 6) and certain avian isolates of capsular type D (OMP-types 5 and 13). Isolates within this cluster all are of ST 11. Finally, cluster H was associated with heterogeneous avian isolates of different OMP-types and STs (Fig. 2.1).

The tree revealed that the strains of the same OMP-type and ST have identical nucleotide sequences over the 3990 bp and they were clustered together. However, a few exceptions were found among the 123 isolates (Fig. 2.1). The phylogenetic relatedness based on seven housekeeping enzyme genes showed evidence of strain associations with different hosts and diseases. The cluster of isolates associated with different host species could possibly be due to the transmission of *P. multocida* from one host to another and this could possibly play an important role in generating diversity within *P. multocida*.

2.3.2 Phylogeny of *P. multocida* based on 15 housekeeping genes

The phylogenetic relatedness of the 40 *P. multocida* isolates was determined using the concatenated sequences of 15 housekeeping enzymes. The functions and other details of these genes are presented in Table 2.2. The genes were carefully selected based on their widespread locations around the chromosome (Fig. 2.2). Genes in very close proximity were avoided because they may have been affected by the some recombination event(s). The fifteen sequences of each isolate were concatenated; the concatenated sequences were 22,371 nucleotides in length and encoded 7457 amino acids. There were 1084 polymorphic nucleotide sites (4.8%) in the 40 concatenated sequences and pairwise differences ranged from 1 to 542 nucleotide sites. A minimum-evolution tree representing the phylogenetic relationships of the 40 *P. multocida* isolates was constructed from the concatenated sequences of fifteen housekeeping enzyme genes (Fig. 2.3). Notably, the phylogenetic relationships of the *P. multocida* isolates was very similar to the phylogenetic relatedness based on the concatenated partial sequences of seven housekeeping enzyme loci, i.e. the MLST tree (Fig. 2.1).

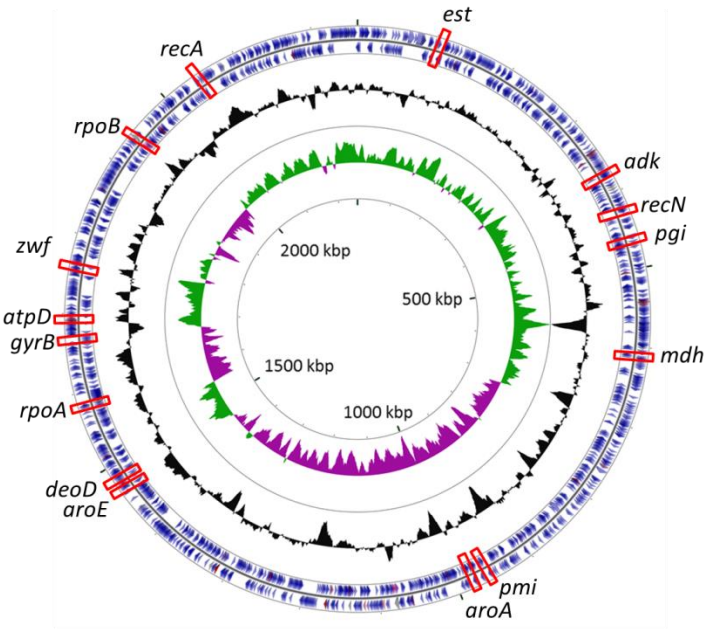

Fig. 2.2 Positions of housekeeping genes in the closed genome of *P. multocida* strain PM70.

The locations of the fifteen selected housekeeping enzyme within the closed *P. multocida* genome of strain PM70 (GenBank: NC_002663) are shown. The properties of the fifteen housekeeping enzyme are listed in **Table 2.2**. The circular genome was created using CGView Server software (V 1.0) (Grant & Stothard, 2008).

The tree represented eight major groups or clusters, A to H (Fig. 2.3). Cluster A was associated with the majority of bovine pneumonia isolates, PM316, PM564, PM334, PM632 of capsular type A (OMP-types 1.1 to 4.1 and STs 1, 3 and 4) and certain porcine pneumonia isolates PM666 and PM116 of capsular type A, OMP-types 2.1 and 3.1 and ST 3 (Fig. 2.3). Cluster A was classified as major bovine pneumonia cluster. There were 35 (0.5%) polymorphic nucleotide sites among the group A sequences and pairwise differences ranged from 0 to 32 nucleotide sites (0.0 to 0.2%). Group B included only three isolates, ovine isolate PM966 (capsular type A, OMP 1.1 and ST 16), porcine isolate PM382 (capsular type A, OMP 4.1 and ST 13) and bovine isolate PM490 (capsular type A and OMP 9.1). Isolates PM382 has previously been shown to be closely related to avian and ovine capsular type F isolates (MLST group C) (Fig. 2.3). There were 341 (1.5%) polymorphic nucleotide sites among the group C sequences and pairwise differences ranged from 218 to 242 nucleotide sites (0.9 to 1.1%).

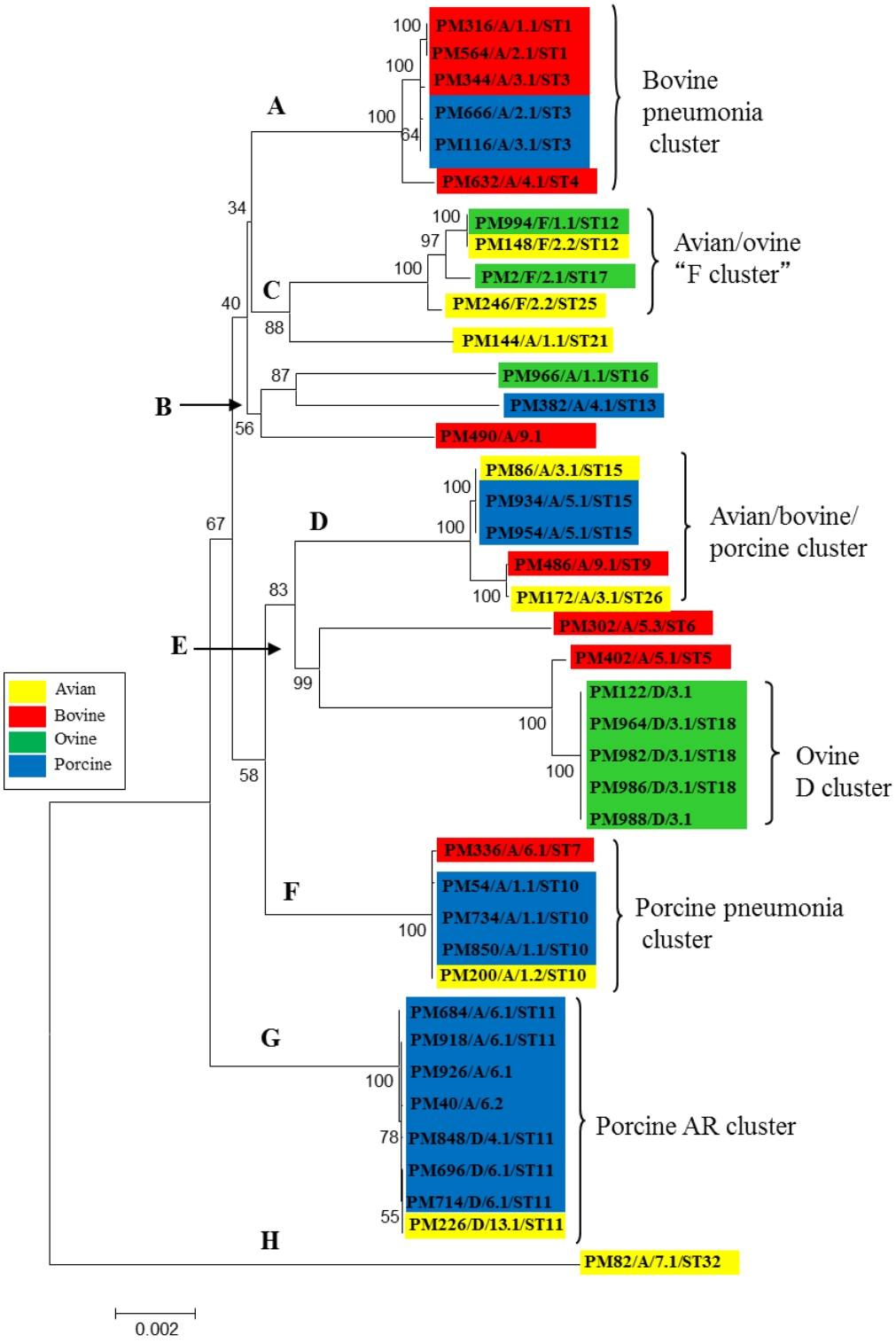

Fig. 2.3 Neighbour-Joining tree representing the phylogenetic relationships of 40 *P. multocida* strains based on the concatenated sequences of fifteen housekeeping enzyme genes.

The concatenated sequence of 15 housekeeping genes represented 22,371 bp and 7457 amino acids. The phylogenetic tree was constructed with Jukes-Cantor correction for nucleotide substitutions. Isolate designation, capsular type, OMP type and ST type are provided for each isolate (e.g. PM316/A/1.1/ST1).

Group C was associated with avian and ovine isolates of capsular type F including PM994, PM148, PM2 and PM246 (OMPs 1.1, 2.1 and 2.2 and STs 12, 17 and 25) and also included avian isolate PM144 (capsular type A, OMP 1.1, ST 21 and MLST E). There were 209 (1.0%) polymorphic nucleotide sites among the group B sequences and pairwise differences ranged from 0 to 180 nucleotide sites (0.0 to 0.8%) (Fig. 2.3). Group D included isolates PM86 (avian), PM934 and PM954 (porcine), PM486 (bovine) and PM172 (avian) (MLST group D). These isolates were of capsular type A, OMP-types 3.1, 5.1 and 9.1 and STs 15, 19 and 26. There were 24 (0.1%) polymorphic nucleotide sites among the group D sequences and pairwise differences ranged from 0 to 24 nucleotide sites (0.0 to 0.1%). Cluster E was associated with ovine capsular type D isolates PM122, PM964, PM982, PM986 and PM988 (OMP 3.1 and ST 18 and MLST group E) as well as the bovine isolates PM402 (capsular type A, OMP-type 5.1 and ST 5) and PM302 (capsular type A, OMP 5.3, ST 6 and MLST group E) (Fig. 2.3). There were 281 (1.2%) polymorphic nucleotide sites among the group E sequences and pairwise differences ranged from 0 to 274 nucleotide sites (0.0 to 1.2%).

Cluster F included isolates that represented the majority of isolates responsible for porcine pneumonia, PM54, PM734, PM850 (capsular type A, OMP-type 1.1 and ST 10). This group also included the avian isolate PM200 (capsular type A, OMPs 1.2 and 1.2 and ST 10) and bovine isolate PM336 (capsular type A, OMP 6.1 and ST 7) (Fig. 2.3). These isolates differed at only 3 polymorphic nucleotide sites. Cluster G included isolates that were associated with majority of porcine AR isolates PM684, PM918, PM926, PM40, PM848 and PM714. These were of capsular type A and D, OMP 4.1, 6.1 and 6.2 and ST 11. This group also included avian isolate PM226 (capsular type D, OMP 13.1 and ST 11) (Fig. 2.3). The *P. multocida* isolates within this group differed at only 4 polymorphic nucleotide sites. Cluster H was highly divergent from the other groups and included the avian isolate PM82 (capsular type A, OMP 7.1 and ST 32) (Fig. 2.3). Pairwise differences between PM82 and the other isolates ranged from 487 to 536 nucleotide sites (2.3 to 2.4%). Both the phylogenetic relatedness based on seven and fifteen housekeeping enzyme genes showed evidence of strain associations with specific hosts and diseases. The cluster of isolates associated with different host species could possibly be due to the transmission of *P. multocida* from one host to

another and this could possibly play an important role in generating diversity within the *P. multocida*.

2.3.3 Phylogeny of *P. multocida* based on core genome alignment

The core genome alignment generated using Parsnp comprised 1,705,798 bp, representing 75% of the reference genome, PM70 (GenBank: NC_002663). A minimum-evolution tree representing the phylogenetic relationships of the 40 *P. multocida* based on their core genomes is shown in Fig. 2.4. The phylogenetic relationships of *P. multocida* based on their core genomes was identical to that based on the concatenated sequences of seven and fifteen housekeeping enzyme loci (Fig. 2.1 & Fig. 2.3). The tree represented eight major groups or clusters which are designated A to H as in Fig. 2.4 .

Cluster A was associated with the majority of bovine pneumonia isolates, PM316, PM564, PM334, PM632 of capsular type A (OMP-types 1.1 to 4.1 and STs 1, 3 and 4) and certain porcine pneumonia isolates PM666 and PM116 of capsular type A, OMP-types 2.1 and 3.1 and ST 3 (Fig. 2.4). Group B included only three isolates, ovine isolate PM966 (capsular type A, OMP 1.1 and ST 16), porcine isolate PM382 (capsular type A, OMP 4.1 and ST 13) and bovine isolate PM490 (capsular type A and OMP 9.1). Isolates PM382 has previously been shown to be closely related to avian and ovine capsular type F isolates (MLST group C) (Fig. 2.4). Group C was associated with avian and ovine isolates of capsular type F including PM994, PM148, PM2 and PM246 (OMPs 1.1, 2.1 and 2.2 and STs 12, 17 and 25) and also included avian isolate PM144 (capsular type A, OMP 1.1, ST 21 and MLST E) (Fig. 2.4). Group D included isolates PM86 (avian), PM934 and PM954 (porcine), PM486 (bovine) and PM172 (avian) (MLST group D). These isolates were of capsular type A, OMP-types 3.1, 5.1 and 9.1 and STs 15, 19 and 26. Cluster E was associated with ovine capsular type D isolates PM122, PM964, PM982, PM986 and PM988 (OMP 3.1 and ST 18 and MLST group E) as well as the bovine isolates PM402 (capsular type A, OMP-type 5.1 and ST 5) and PM302 (capsular type A, OMP 5.3, ST 6 and MLST group E) (Fig. 2.4). Cluster F included isolates that represented the majority of isolates responsible for porcine pneumonia, PM54, PM734, PM850 (capsular type A, OMP-type 1.1 and ST 10). This group also included the avian isolate PM200 (capsular type A, OMPs 1.2 and 1.2 and ST 10) and bovine isolate PM336 (capsular type A, OMP 6.1 and ST 7) (Fig. 2.3).

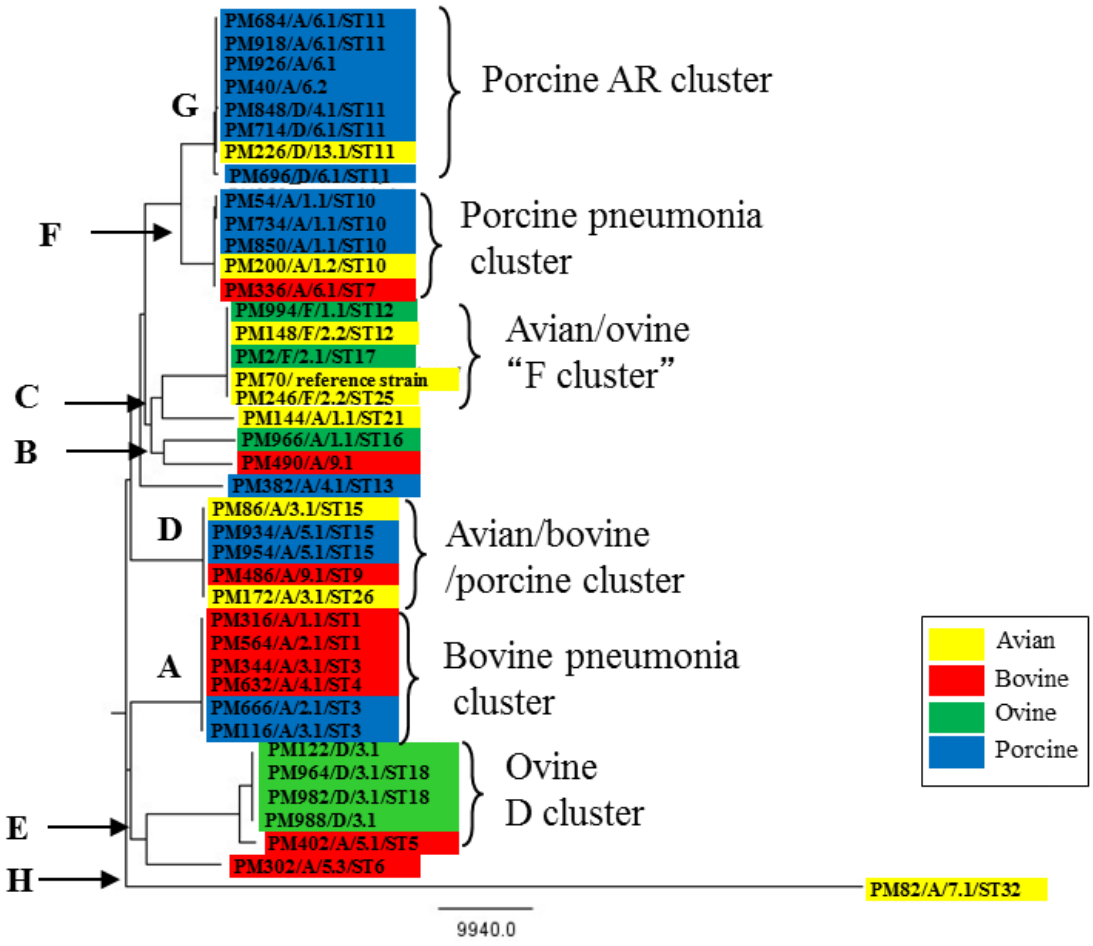

Fig. 2.4 Neighbour-Joining tree representing the phylogenetic relationships of 40 *P. multocida* strains based on the core genome alignments.

Isolate designation, capsular type, OMP type and ST type are provided for each isolate (e.g. PM316/A/1.1/ST1).

Cluster G included isolates that were associated with majority of porcine AR isolates PM684, PM918, PM926, PM40, PM848 and PM714. These were of capsular type A and D, OMP 4.1, 6.1 and 6.2 and ST 11. This group also included avian isolate PM226 (capsular type D, OMP 13.1 and ST 11) (Fig. 2.4). Cluster H was highly divergent from the other groups and included the avian isolate PM82 (capsular type A, OMP 7.1 and ST 32) (Fig. 2.4). The phylogenetic relatedness based on seven and fifteen housekeeping enzyme genes and core genome showed a correlation between phylogenetic cluster and association with specific hosts and disease types. The cluster of isolates associated with different host species could possibly be due to the transmission of *P. multocida* from one host to another and this could possibly play an important role in generating diversity within the *P. multocida*.

2.3.4 Comparative sequence analysis of genes encoding OMPs

Previously in our group, the functions of the 98 OMPs were confidently predicted from the avian genome based on the prediction analyses (Table 2.3) (E-komon *et al.*, 2012). These functions include outer membrane biogenesis and integrity (12 proteins), transport and receptor (25 proteins), adherence (7 proteins) and enzymatic activity (9 proteins). Forty one proteins have unknown function, although 17 were named and 27 of these were lipoproteins.

2.3.4.1 Comparative sequence analysis of genes encoding proteins involved in OM biogenesis and integrity

Nucleotide sequences were obtained in all 40 genomes (Table 2.4). Examination of nucleotide and amino acid variation in MEGA revealed that the majority of the proteins exhibited relatively low nucleotide and amino acid variation except *ompA* and *mipA* (Table 2.4). However, Neighbour-Joining phylogenetic trees showed evidence for recombination events among the genes. Therefore, four different proteins were selected and analysed in detail; these proteins were MltB, NlpB, OmpA and MipA (Table 2.4). The Neighbour-Joining phylogenetic trees for the remaining proteins were constructed and are shown in Appendices, Fig. 8.1.

Table 2.3 Functional classification of the 98 confidently predicted OMPs from the avian *P. multocida* genome.

Protein	Protein function
Outer membrane biogenesis and integrity	
LolB	Chaperone and protein transport activity
MltB	Cell wall catabolic process
NlpB	Insertion of OMPs
RlpB	LPS assembly
LppB/NlpD	Cell wall catabolic process & proteolysis
SmpA	Maintaining envelope integrity and ß-OMP assembly
OmpA	Outer membrane integrity
MipA/OmpV	MlrA-interacting protein
LptD/Imp/OstA	LPS assembly/response to organic substance
Oma87	Outer membrane biogenesis & surface antigen
MltC	Cell wall catabolic process
Pal/OmpP6	Envelope integrity/link outer membrane to peptidoglycan
Transport and receptor	
OmpW	Transport small hydrophobic molecules
TonB-dependent receptor	Receptor & transport activities
TonB-dependent receptor	Receptor and transport activities
TonB-dependent receptor	Receptor r and transport activities
ComL	DNA uptake/outer membrane biogenesis
PlpB/MetQ	Amino acid transport
FadL	Transport hydrophobic compounds
OM hemin receptor	Haem receptor & transporter activities
HgbA	Haemoglobin receptor & iron transport
HgbB	Haemoglobin receptor & iron transport
HgbB	Haemoglobin receptor & iron transport
HasR	Haem receptor & transporter activities
HmbR	Haemoglobin receptor and iron transport
PfhR	Haemoglobin receptor & iron transport
TonB-dependent receptor	Receptor and transport activities
OmpH1	Porin/iron transport activity
OmpH2	Porin/iron transport activity
OmpH3	Porin iron transport activity
LspB_1	Two-partner secretion/secretion of filamentous hemagglutinin
LspB_2	Two-partner secretion/secretion of filamentous hemagglutinin
IbeB	Lipid binding & transport activity
HemR	Haem receptor and transport activity
Outer membrane efflux TolC	Protein secretion/transporter activity
Wza	Capsular polysaccharide transport
HexD	Capsular polysaccharide transport
Adherence	
ComE/PilQ	Pilus assembly/protein secretion
RcpA	Protein secretion/Flp pilus biogenesis
RcpC	Tight adherence & fibril production
TadD	Protein secretion/biding/assembly & transport of Flp pili
Hsf_1	Adherence
Hsf_2	Adherence
Opa	Porin activity/adherence
Enzymatic activity	
NlpP-like protein	Metalloendopeptidase activity
Lipoprotein NlpC/P60	Cell-wall peptidase
Peptidase M48B family protein	Metalloendopeptidase activity/zinc ion binding
Lipoprotein E/OmpP4	Acid phosphatase activity/utilization of NAD, NADP
NanB	Exo-alpha-sialidase/produces free sialic acid as energy & carbon sources
NanH	Exo-alpha-sialidase/produces free sialic acid as energy & carbon sources
EstA	Lipid metabolism/hydrolase activity, acts on ester bond
Phospholipase A/OmpLA	Lipid metabolic process/maintain asymmetry of the OM
GlpQ	Glycerol metabolic process/lipid metabolic process

Table 2.3 (continued)

Protein	Protein function
Other functions	
Mod_2	DNA binding/N-methyltransferase activity
Virulence factor SrfB	Unknown
RlpA-like protein	Unknown
Skp/Outer membrane p25	Unknown
Conserved hypothetical protein	Unknown
Hypothetical protein	Unknown
Hypothetical protein	Unknown
OmpL41/YtfN-like protein	Bacterial morphogenesis
Mce/PqiB	Unknown
YccT	Unknown
Conserved hypothetical protein	Unknown
Hypothetical protein	Unknown
Slp	Starvation-inducible lipoprotein
VacJ	Promoting spread of bacteria through tissues
PlpE	Unknown
PlpP	Unknown
HlpB	Unknown
HlpB	Unknown
PilW/PilF	Unknown
LppA	Unknown
Lipoprotein	Unknown
Lipoprotein	Unknown
Lipoprotein	Unknown
Lipoprotein	Unknown
Lipoprotein	Unknown
Lipoprotein	Unknown
Lipoprotein	Unknown
Lipoprotein	Unknown
Lipoprotein	Unknown
Lipoprotein	Unknown
Hypothetical protein	Unknown
Hypothetical protein	Unknown
Hypothetical protein	Unknown
Outer membrane autotranspoter	Unknown
Omp85 family protein/ YtfM	Unknown
Conserved hypothetical protein	Unknown
Hypothetical protein	Unknown
Plp4	Unknown
Lpp/Pcp	Unknown
Lipoprotein	Unknown
Hypothetical protein	Unknown
PlpE	Unknown
Lipoprotein	Unknown
LppC	Unknown
Lipoprotein	Unknown
Mod_2	DNA binding/N-methyltransferase activity
Virulence factor SrfB	Unknown
RlpA-like protein	Unknown
Skp/Outer membrane p25	Unknown
Conserved hypothetical protein	Unknown
Hypothetical protein	Unknown
Hypothetical protein	Unknown
OmpL41/YtfN-like protein	Bacterial morphogenesis

Table 2.4 Properties of 12 OMPs/ genes of *P. multocida* involved in outer membrane biogenesis and integrity.

Gene	Protein function	Total no. of strains	Gene size		Polymorphic sites		Sequence diversity (%)	
			No. of nucleotides	No. of amino acids	No. of nucleotides	No. of amino acids	Nucleotides	Amino acids
lolB	Chaperone and protein transport activity	40	615	205	28	10	5	5
mltB[a]	Cell wall catabolic process	40	1092	364	95	22	9	6
nlpB[a]	Insertion of OMPs	40	1011	337	46	10	5	3
rlpB	LPS assembly	40	501	167	16	6	3	4
lppB/nlpD	Cell wall catabolic process & proteolysis	40	1413	471	101	21	7	4
smpA	Maintaining envelope integrity and ß-OMP assembly	40	411	137	7	2	2	1
ompA[a]	Outer membrane integrity	40	1074	358	281	77	26	21
mipA/ompV[a]	MlrA-interacting protein	40	771	257	103	45	13	18
lptD/imp/ostA	LPS assembly/response to organic substance	40	2361	787	82	20	3	3
oma87	Outer membrane biogenesis & surface antigen	40	2373	791	151	27	6	3
mltC	Cell wall catabolic process	40	1074	358	39	6	4	2
pal/ompP6	Envelope integrity/link outer membrane to peptidoglycan	40	450	150	10	3	2	2

[a]= gene/proteins analysed in further detail

2.3.4.2 Outer membrane protein MltB

This protein is involved in cell wall catabolic processes. The gene encoding MltB (*mltB*) was found in all 40 genomes. The complete sequence of *mltB* is 1092 nucleotides and the encoded protein is 364 amino acids in length (Table 2.4). Total nucleotide variation among all sequences was 9% (95 polymorphic nucleotide sites) and the amino acid variation was 6% (22 variable inferred amino acid sites) (Table 2.4). The *mltB* Neighbour-Joining phylogenetic tree identified three different lineages, I, II and III and 12 different alleles (*mltB1.1*- to *mltB5.2*-types). The *mltB* phylogeny was not in agreement with the phylogeny of *P. multocida* based on the concatenated sequences of seven and fifteen housekeeping enzyme genes and on the core genome (Fig. 2.1, Fig. 2.3 & Fig. 2.4). Lineage I included *mltB1-*, *mltB2-* and *mltB3*-allele types and was associated with isolates from different genetic origins. Lineage II included only *mltB4.1*-allele type and was associated exclusively with isolates of the porcine pneumonia and AR clusters. The *mltB* gene tree shows clear evidence of assortative recombination of the *mltB* gene between the porcine pneumonia and AR clusters because the two clusters possess an identical *mltB* gene. Lineage III was divergent from lineages I and II and was represented by two different alleles, *mltB5.1*- and *mltB5.2*-type associated with isolates of the avian/ovine serotype F cluster (Fig. 2.5).

The aligned nucleotides sequences of *mltB1.1*- to *mltB5.2*- are shown in Fig. 2.6. The *P. multocida mltB5.1*- and *mltB5.2*-type alleles were divergent from the others. Visual inspection of the nucleotide sequences of the *mltB* alleles showed the *mltB5.1* and *mltB5.2*-type alleles are almost identical and differed from each other at only 11 nucleotides. However, these alleles were highly divergent, differing from the other alleles at 67 to 80 nucleotide sites. Visual inspection of the nucleotide sequences also showed intragenic recombination within the *mltB* gene. Allele *mltB4.1* shared an identical recombinant segment (green, nucleotides 5 to 381) with the corresponding region of *mltB2.4*- and *mltB4.1*-type alleles (Fig. 2.6). Allele *mltB2.4* shared an identical recombinant segment (yellow, nucleotides 600 to 626) with the corresponding region of *mltB5.1*- and *mltB52*-type alleles (Fig. 2.6). Pairwise difference in nucleotide and amino acid sequences among the *mltB* alleles ranged from 2 to 80 (0.2 to 7.3%) nucleotide sites and 1 to 19 (0.0 to 5.2%) amino acids positions (Fig. 2.6).

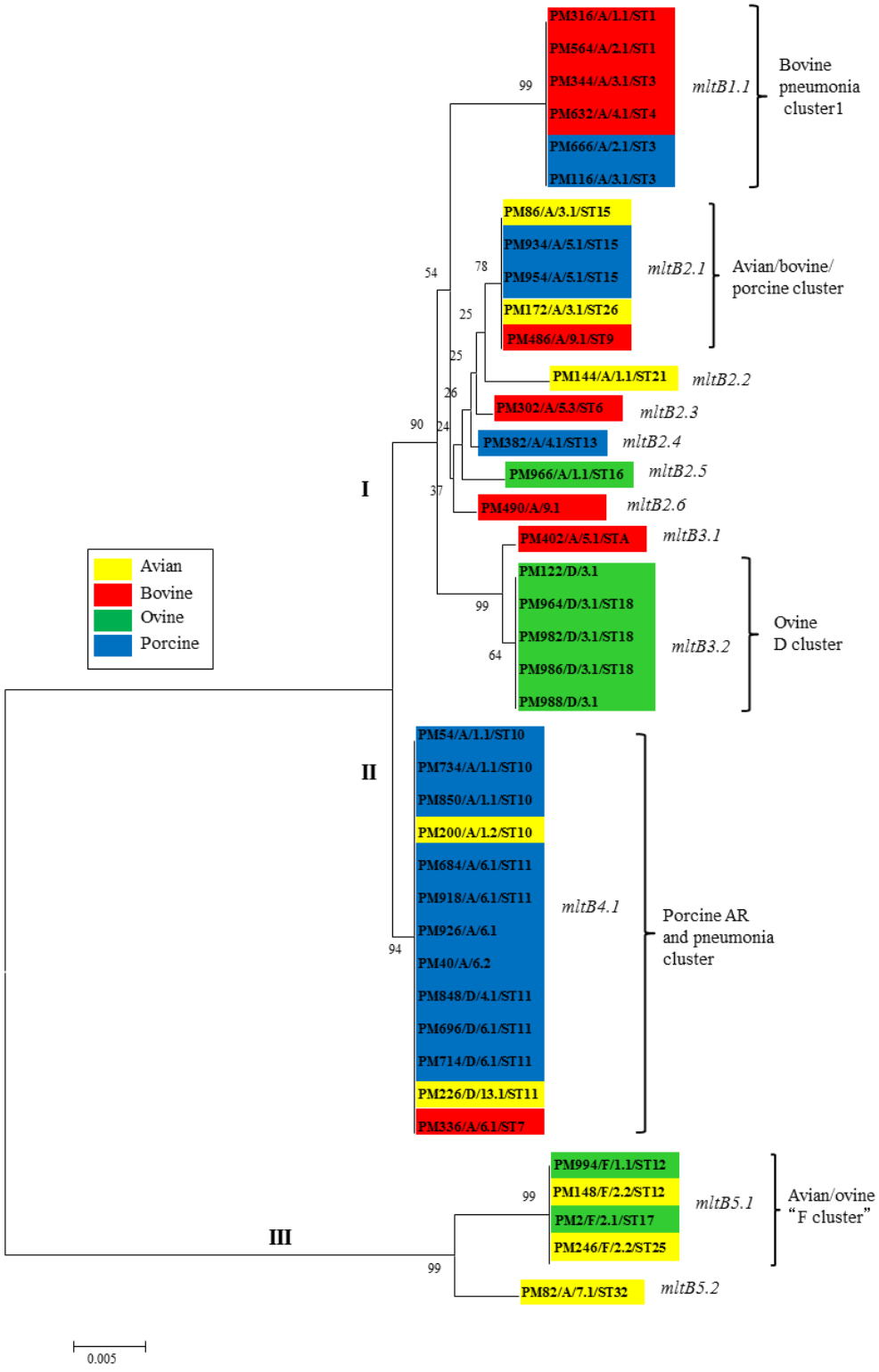

Fig. 2.5 Neighbour-Joining tree representing the phylogenetic relationships of *mltB* alleles in 40 *P. multocida* strains.

The phylogenetic tree was constructed with Jukes-Cantor correction for nucleotide substitutions and the bootstraps values (500 replications). Isolate designation, capsular type, OMP type and ST type are provided for each isolate (e.g. PM316/A/1.1/ST1). Allele designations are shown to the right (*mltB1.1,* etc.).

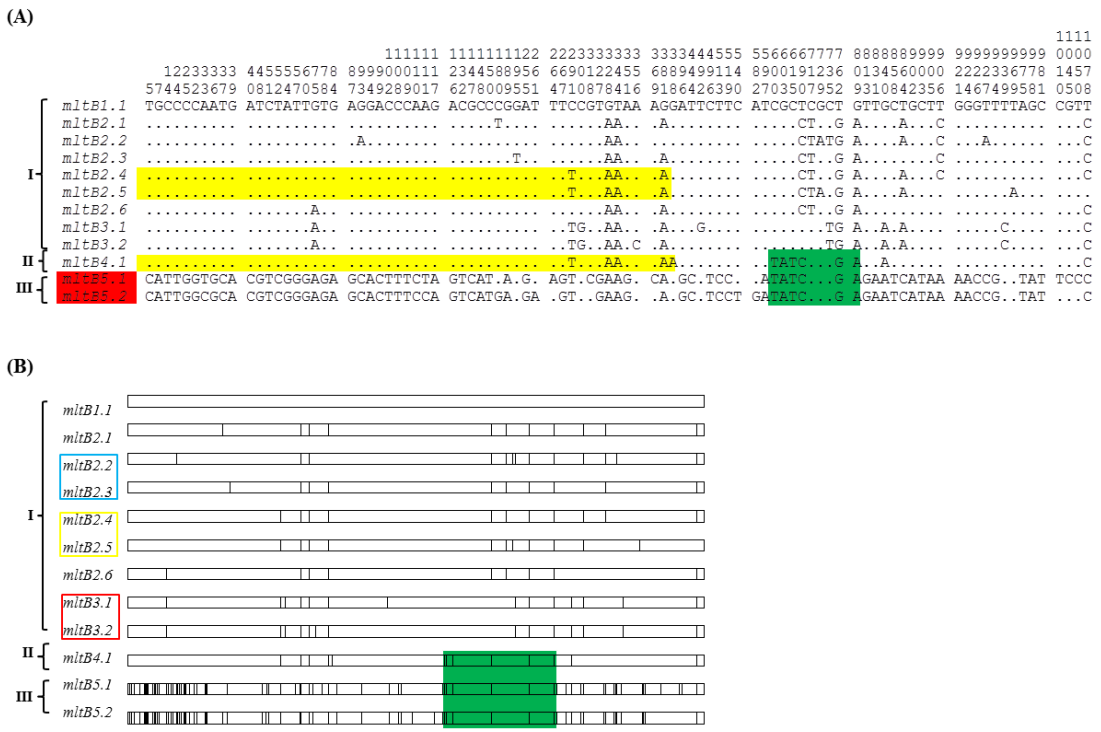

Fig. 2.6 Distribution of polymorphic nucleotide sites among the *mltB* alleles of *P. multocida*.

Allele designations are shown to the left of each sequence. Roman numerals I to III represent the phylogenetic lineages (**Fig. 2.5**). Coloured boxes highlight sequence identity and proposed recombinant segments. The vertical numbers above the sequences represent the positions of polymorphic nucleotide sites.

2.3.4.3 NlpB

NlpB is an outer membrane lipoprotein which is involved in insertion of OMPs. The complete sequence of *nlpB* is 1011 nucleotides and the encoded protein is 337 amino acids in length (Table 2.4). Total nucleotide variation among all sequences was 5% (46 polymorphic nucleotide sites) and the amino acid variation was 3% (10 variable inferred amino acid sites) (Table 2.4). The *nlpB* Neighbour-Joining phylogenetic tree identified five lineages, I to V (Fig. 2.7). Thirteen different *nlpB* nucleotide sequences were identified based upon the overall sequence similarity, each representing a distinct allele (*nlpB1.1*- to *nlpB8.2*-type alleles). The *nlpB* alleles were assigned to sub-classes (*nlpB1*- to *nlpB8*-type alleles). Lineage I included only the *nlpB1.1*-type allele and was associated with bovine pneumonia isolates PM564 and PM402 and ovine D cluster. Lineage II includes *nlpB2.1-, nlpB3.1*- and *nlpB3.2*-type alleles.

This lineage was associated with isolates from different genetic origins based on the MLST tree including isolates of capsular type A (STs 9, 15 and 26 and MLST group D), ovine isolates of capsular type A (OMP 1.1, ST 16 and MLST group B) and avian and ovine isolates of capsular type F cluster (STs 12 and 17), respectively. Lineage III was associated with *nlpB4.1*- and *nlpB4.2*-type alleles. The *nlpB4.1-type* allele was associated with bovine isolate PM490 from lineage D, whereas *nlpB4.2*-type alleles were associated with the porcine pneumonia group (capsular type A, OMPs-types 1.1, 1.2 and 6.1 and ST 10 and 7). Lineage IV included *nlpB5.1*-, *nlpB6.1*-, *nlpB6.2*-, *nlpB7.1*- and *nlpB7.2*-types alleles. The *nlpB* alleles within this lineage were associated with isolates of divergent genetic origin including avian isolate PM144 (capsular type A, OMP 1.1, ST 21 and MLST group E), porcine isolate PM382 (capsular type A, OMP 4.1, ST 13 and MLST C), isolates of the bovine pneumonia cluster (*nlpB6.1* and *nlpB6.2)* and isolates of the porcine AR cluster *nlpB7.1.* Lineage V was divergent from lineages I to IV and was represented by *nlpB8.1*- and *nlpB8.2*-type alleles (Fig. 2.7).

The *nlpB* tree showed evidence of recombination events within the *nlpB* gene of *P. multocida* because the *nlpB* phylogeny was not in agreement with the phylogeny of *P. multocida* based on the concatenated sequences of seven and fifteen housekeeping enzyme genes and on the core genome (Fig. 2.1, Fig. 2.3 & Fig. 2.4). This indicates that recombination has affected the evolution of *nlpB*.

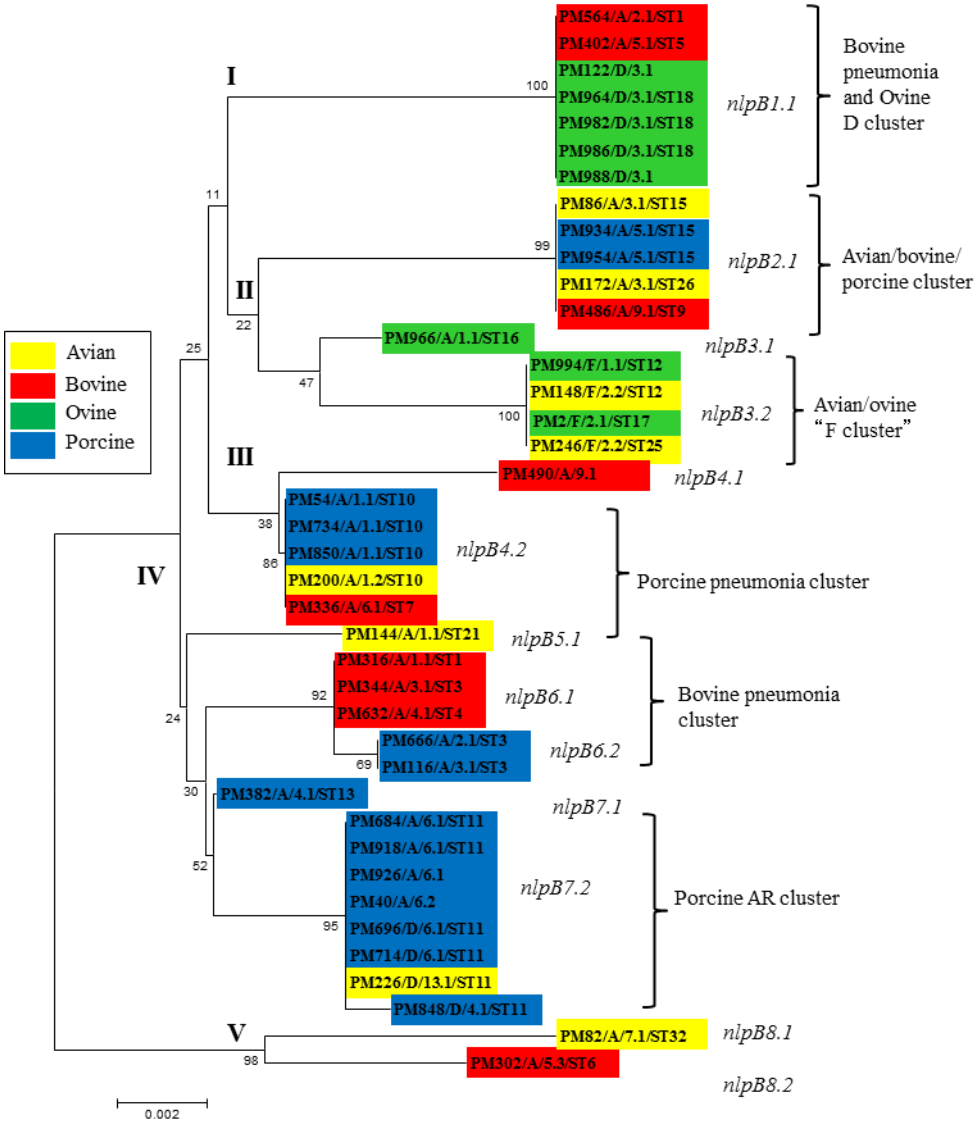

Fig. 2.7 Neighbour-Joining tree representing the phylogenetic relationships of *nlpB* alleles in 40 *P. multocida* strains.

The phylogenetic tree was constructed with Jukes-Cantor correction for nucleotide substitutions. Isolate designation, capsular type, OMP type and ST type are provided for each isolate (e.g. PM316/A/1.1/ST1). Allele designations are shown to the right (*nlpB1.1*, etc.).

For example, the *nlpB1.1*-type allele was associated with strains of two divergent lineages including PM564 from the bovine pneumonia cluster (capsular type A, OMP 2.1, ST 1 and MLST group A), bovine isolate PM402 of capsular type A (OMP-type 5.1, ST 5 and MLST group E) and isolates of the ovine serotype D cluster (OMP 3.1, ST 18 and MLST group E) (Fig. 2.7).

Pairwise differences in nucleotide and amino acid sequences between representative *nlpB* allele types ranged from 1 to 24 (0.1 to 2.4%) nucleotide sites and 0 to 4 (0.0 to 1.2%) amino acid positions. The aligned nucleotide and amino acid sequences (polymorphic sites only) of the *nlpB1.1*- to *nlpB8.2*-type alleles are shown in Fig. 2.8. Visual inspection of the nucleotide sequences of the *nlpB1.1*- to *nlpB8.2*-type alleles indicate that intragenic recombination has also occurred within the *nlpB* gene (Fig. 2.8). The *nlpB.2.1*-type allele possessed recombinant segment (grey, nucleotides 435 to 666) that was identical to the corresponding region of *nlpB3.1*-type allele (Fig. 2.8). The *nlpB.3.1*-type allele also shared segment (green, nucleotides 22 to 405) that was identical to the corresponding region of *nlpB6.1*- to *nlpB7.2*-type alleles. The *nlpB.4.1*-type allele shared segment (blue, nucleotides 192 to 744) that was identical to the corresponding region of *nlpB4.2*-type allele. The *nlpB.6.1*-type allele contained segment (red, nucleotides 22 to 741) that was identical to the corresponding region of *nlpB6.2*- to *nlpB7.2*-type alleles. The *nlpB.8.1*-type allele contained two recombinant segments (orange, nucleotides 39 to 405 and 471 to 534) that were identical to the corresponding regions of the *nlpB8.2*-type allele (Fig. 2.8). Amino acid sequence analysis (polymorphic sites only) showed less variation than nucleotide sequence analysis (Fig. 2.8C).

2.3.4.4 Outer membrane protein A (OmpA)

The heat-modifiable outer membrane protein A (OmpA) is an integral component of the outer membrane of Gram-negative bacteria and is highly conserved. OmpA was selected because of its multifunctional roles including its role in outer membrane integrity; pathogenesis and host specificity. The complete sequence of *ompA* is 1074 nucleotides and 358 amino acids in length (Table 2.4). Total nucleotides variation among all sequences was 26% (281 polymorphic nucleotide sites) and the amino acid variation was 21% (77 variable inferred amino acid sites) (Table 2.4).

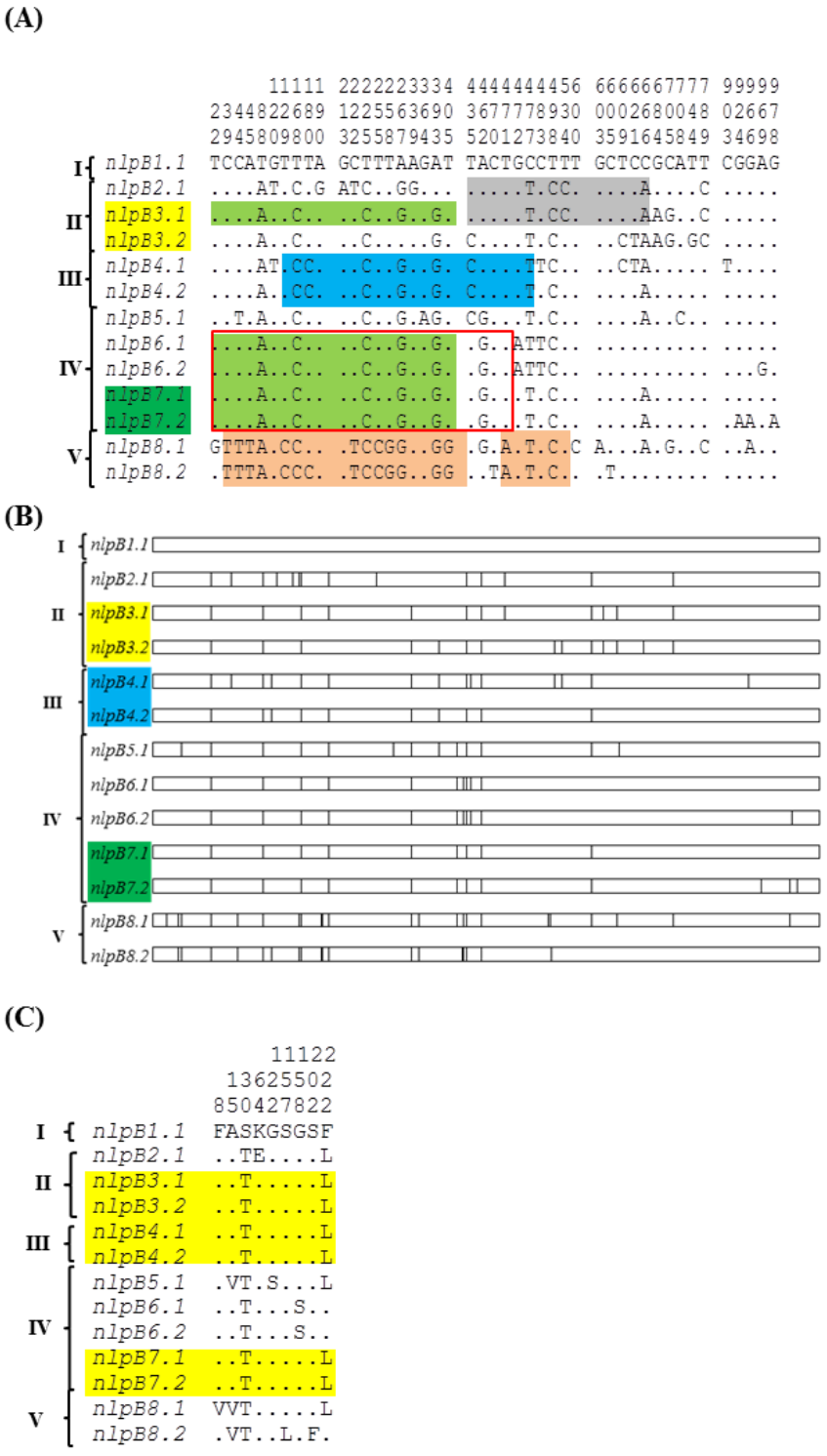

Fig. 2.8 Distribution of polymorphic nucleotides (A and B) and amino acid sites (C) among the *nlpB* alleles of *P. multocida.*

Allele designations are shown to the left of each sequence. Roman numerals I to V represent the phylogenetic lineages (**Fig. 2.7**). Coloured boxes highlight sequence identity and proposed recombinant segments. The vertical numbers above the sequences represent the positions of polymorphic nucleotide sites. Psfind and Happlot analysis were used to represent polymorphic nucleotide sites graphically and to help identify recombination events (B). The output file from Happlot was opened in Micrographic Designer software (MicrografX, Inc).

The Neighbour-Joining phylogenetic tree for *ompA* was constructed using MEGA (Fig. 2.9). Eight different lineages (I to VIII) were identified (Fig. 2.9). Fifteen different *ompA* nucleotide sequences were identified based upon the overall sequence similarity, each representing a distinct allele (*ompA1.1*- to *ompA8.1*-type alleles) and these were assigned to sub-classes (*ompA1*- to *ompA8*-type alleles). Lineage I included only *ompA1.1*- to *ompA1.5*-type alleles. Lineage II included *ompA2.1*- and *ompA2.2-t*ype alleles. Lineage III was associated with *ompA3.1*- and *ompA3.2*-type alleles. Lineage IV was associated with *ompA4.1*- and *ompA4.2*-type alleles, lineages V to VIII were each associated with a single allele type, *ompA5.1*-, *ompA6.1*-, *ompA7.1*- and *ompA8.1*-type alleles, respectively (Fig. 2.9).

The *ompA* tree revealed evidence of recombination events within the *ompA* gene of *P. multocida* because the *ompA* phylogeny was not in agreement with the phylogeny of *P. multocida* based on the concatenated sequences of seven and fifteen housekeeping enzyme genes and on the core genome (Fig. 2.1, Fig. 2.3 & Fig. 2.4). This suggests that recombination has affected the evolution of *ompA*. For example, almost identical *ompA1*-type alleles were associated with strains of three divergent lineages including bovine isolates of the bovine pneumonia cluster of MLST group A (capsular type A, OMPs 1.1 to 4.1, STs 1 to 4), and bovine strains of MLST group E (capsular type A, OMPs 5.1 and 5.2 and STs 5 and 6) and isolates of serotype D clusters of MLST group E (OMP 3.1, ST 18 and MLST group E). Similarly, almost identical *ompA* alleles were found within lineage II. Isolates associated with *ompA2.1* have previously been shown to have bovine properties and clustered with the major bovine pneumonia group (MLST group A). However, these alleles clustered in the *ompA* tree with those of major porcine pneumonia group (MLST group F) which included predominant porcine pneumonia isolates (capsular type A, OMP-type 1.1 and ST 10) but also avian isolate PM200 (capsular type A, OMP-type 1.2 and ST 10) and bovine isolate PM336 (capsular type A, OMP-type 6.1 and ST 7) to form the single *ompA* lineage II.

Pairwise difference in nucleotide and amino acid sequences between representative *ompA* alleles of *P. multocida* ranged from 2 to 164 (0.2 to 15.3%) nucleotide sites and 1 to 51 (0.2 to 14.3%) amino acid positions.

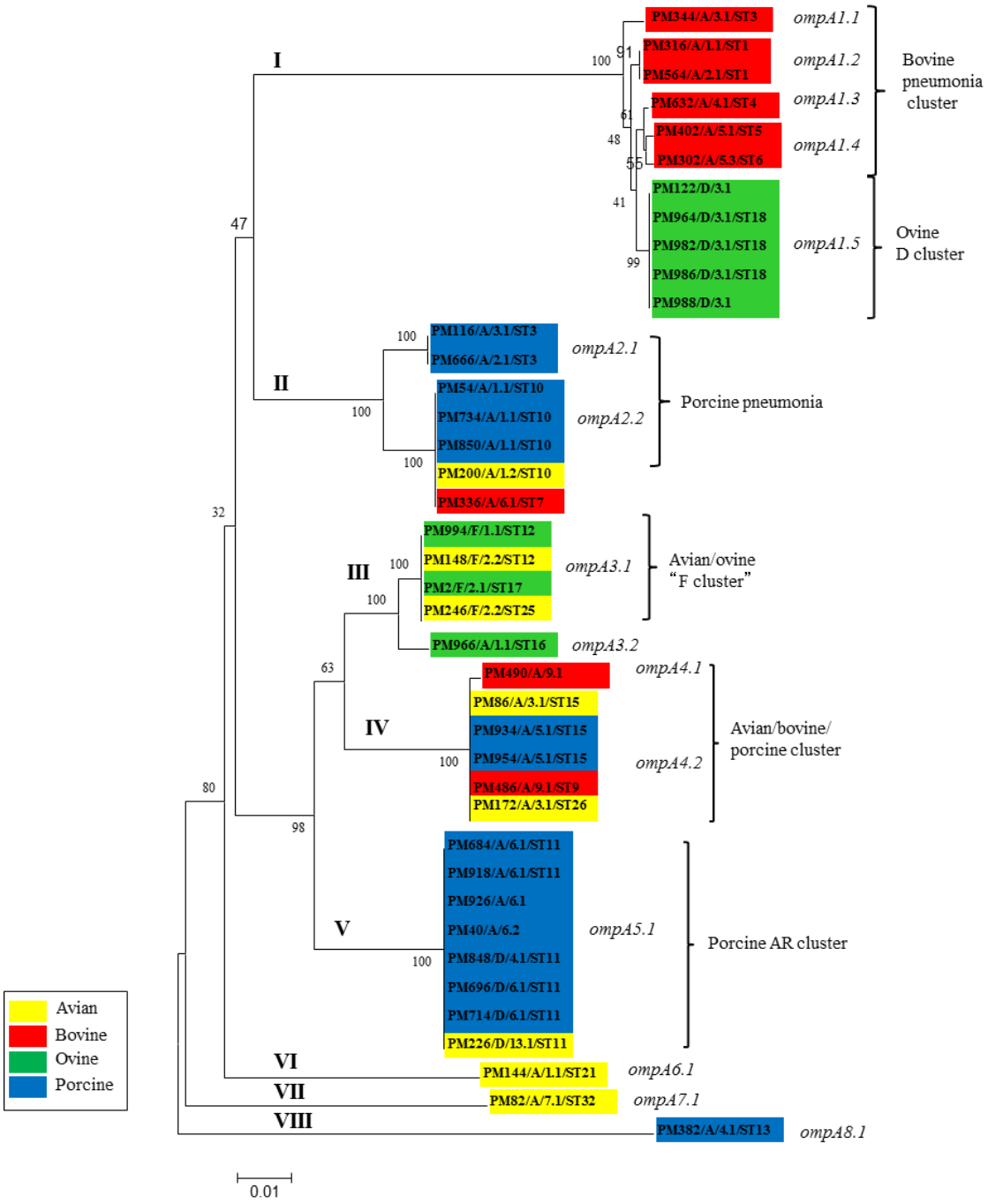

Fig. 2.9 Neighbour-Joining tree representing the phylogenetic relationships of *ompA* alleles in 40 *P. multocida* strains.

The phylogenetic tree was constructed with Jukes-Cantor correction for nucleotide substitutions. Isolate designation, capsular type, OMP type and ST type are provided for each isolate (e.g. PM316/A/1.1/ST1). Allele designations are shown to the right (*ompA1.1*, etc.).

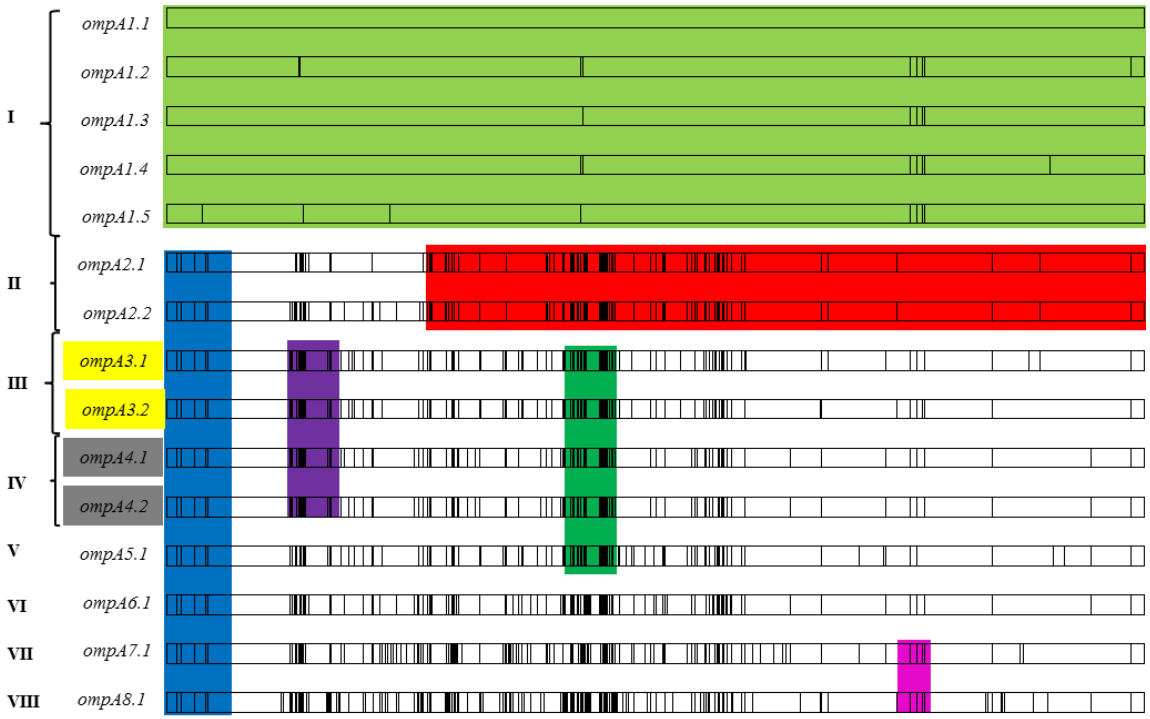

Fig. 2.10 Distribution of polymorphic nucleotide sites among the *ompA* alleles of *P. multocida*

Allele designations are shown to the left of each sequence. Roman numerals I to VIII represent the phylogenetic lineages (**Fig. 2.9**). Coloured boxes highlight sequence identity and proposed recombinant segments.

Visual inspection of the nucleotide sequences of the *ompA1.1*- to *ompA8.1*-type alleles indicated that recombination events have occurred with *ompA* gene. *OmpA1.1*- to *ompA1.5-type* alleles were almost identical and they differed only at two to nine nucleotide sites. The *ompA2.1*-type allele was also identical to *ompA2.2*-type allele and differed at only 18 nucleotide sites (Fig. 2.10). These two alleles were associated with isolates of two divergent lineages based on the MLST tree. Additionally, the *ompA2.1*- and *ompA2.2*-type alleles shared an identical segment (blue segment) with the *ompA3.1*- to *ompA8.1*-type alleles (Fig. 2.10). *The ompA3.1* and *ompA3.2* were almost identical and differed at only 10 nucleotides sites (Fig. 2.10) and these two alleles contained a segment that was identical to the corresponding region of *ompA4.1*-, *ompA4.2*- and *ompA5.1*-type alleles (dark green segment) (Fig. 2.10). The *ompA6.1*-, *ompA7.1*- and *ompA8.1*-type alleles were divergent from the others and differed at 63 to 164 nucleotide sites. The *ompA7.1*-type allele contained a small segment (pink segment) that was identical to the corresponding region of the *ompA8.1*-type allele; these two alleles were present in isolates from different lineages based the on MLST tree.

To identify OmpA domains, representative sequences of each allele were selected. The secondary structure of OmpA was elucidated based on comparison of *P. multocida* OmpA amino acid alignments with those of the closely related species *M. haemolytica* (Davies *et al.*, 2004). OmpA consists of an N-terminal transmembrane domain and a C-terminal periplasmic domain. The transmembrane domain comprises 8 transmembrane ß-sheet regions linked by short loops on the periplasmic side and four extended surface-exposed loops on the external side (Fig. 2.11). The numbers of synonymous substitutions per 100 synonymous sites (d_S) and nonsynonymous substitutions per 100 nonsynonymous sites (d_N) were estimated for the conserved and loop regions. This allowed selective constraint and diversifying selection to be examined in the *ompA* gene of *P. multocida* by calculating the d_S/d_N ratios for the various domains.

A high d_S/d_N ratio ($d_S/d_N > 1$) indicates that natural selection is acting to restrict mutations that result in amino acid alteration and replacement, i.e. selective constraint. Conversely, a low d_S/d_N ratio ($d_S/d_N < 1$) indicates that natural selection is actively driving amino acid alteration and replacement, i.e. diversifying selection. The d_S/d_N ratio for all conserved regions of the *ompA* gene

was 4.0 (Table 2.5). The data demonstrate that natural selection is acting to restrict amino acid replacement in the non-loop regions of OmpA because these parts of the molecules (the membrane-spanning and periplasmic domains) are mostly involved in maintaining outer membrane structural integrity and cannot tolerate amino acid change. The d_S/d_N ratios for the hypervariable extracellular loop domains (L1, L2, L3 and L4) were all less than 1, the ratios ranging from 0.49 to 0.8. These data provide strong evidence that natural selection is driving diversification of the hypervariable extracellular loops regions. The variation occurred exclusively in the loop regions, L1 to L4 (Fig. 2.11 & Table 2.5).

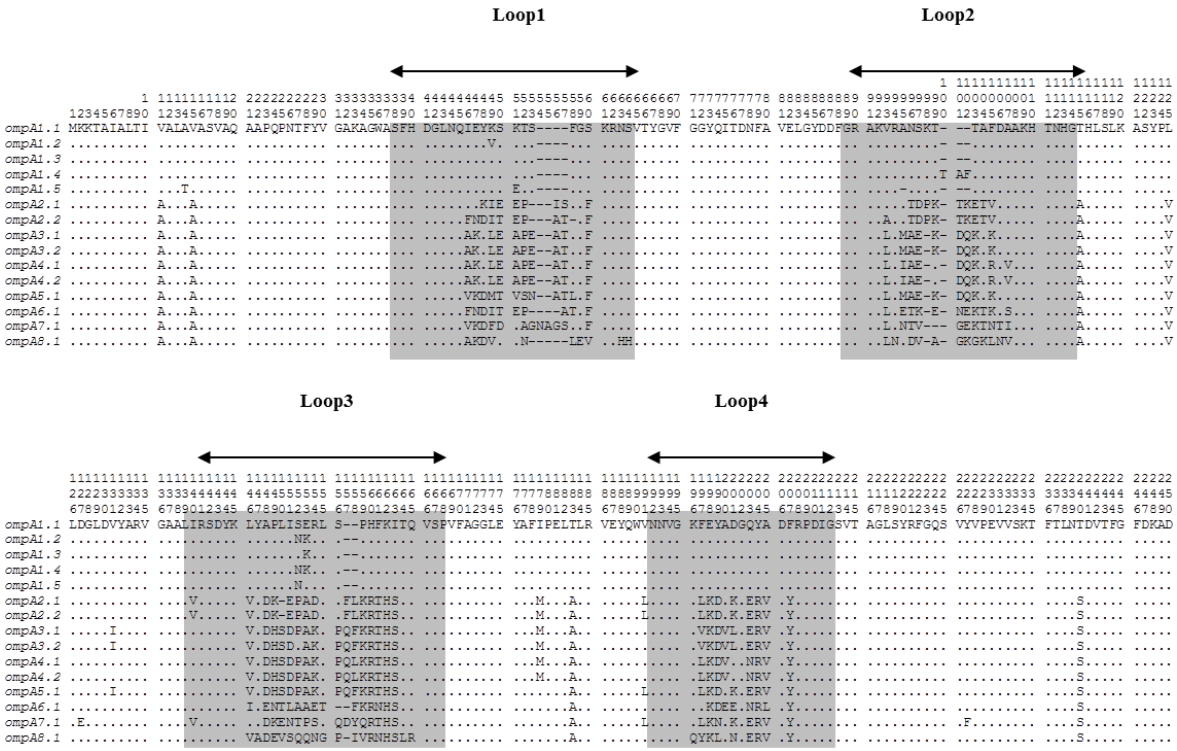

Fig. 2.11 Distribution of variable amino acid sites in the N-terminal transmembrane domains of the OmpA proteins of *P. multocida*.

Allele designations are shown to the left of each sequence. The numbers above the sequences (read vertically) represent amino acid positions. The dots represent sites where the amino acids match those of the first sequence. Gaps are indicated by dashes. HV1 to HV4 represent the hypervariable domains (highlighted in grey colour) within the surface-exposed loops 1 to 4 (highlighted in grey colour). Most of the C-terminal conserved region was excluded.

Table 2.5 Sequence diversity and substitution rates for hypervariable loop domains and conserved regions of the *ompA* genes of 40 *P. multocida* isolates.

Domains	Sequence size		Polymorphic sites		Sequence diversity %		d_s[a]	d_N[b]	d_S/d_N
	No. of nucleotides	No. of amino acids	No. of nucleotides	No. of amino acids	Nucleotides	Amino acids			
Conserved	750	250	97	14	13.0	5.6	20.781±2.461	5.284±1.375	4.0
Loop 1	84	28	44	17	52.4	60.7	3.738±0.898	7.684±1.998	0.48
Loop 2	78	26	45	15	57.6	57.6	3.025±0.736	7.152±2.205	0.42
Loop 3	99	33	68	21	68.6	63.6	9.060±1.051	11.142±2.257	0.8
Loop 4	63	21	27	10	42.8	47.6	2.432±0.782	6.046±1.729	0.4
All Loops	324	108	184	63	56.7	58.3	18.255±1.878	32.024±4.020	0.57

[a] d_S is the number of synonymous substitutions per 100 synonymous sites; d_N is the number of nonsynonymous substitutions per 100 nonsynonymous sites. Values are means ±standard deviations.

2.3.4.5 MipA

MipA is a MLT-A interacting protein that mediates assembly of enzymes involve in murein synthesising. The complete sequence of *mipA* is 771 nucleotides and the encoded protein is 257 amino acids in length (Table 2.4). Total nucleotide variation among all sequences was 13% (103 polymorphic nucleotide sites) and the amino acid variation was 18% (45 variable inferred amino acid sites). However, lineage II (see below) was very divergent and when it was excluded from the analysis the overall nucleotide and amino acids variation was reduced to only 3% (22 polymorphic nucleotide sites) and 3.5% (45 variable inferred amino acid sites), respectively. The Neighbour-Joining phylogenetic tree for *mipA* identified two distinct lineages, I and II (Fig. 2.12). Thirteen different *mipA* nucleotide sequences were identified based upon overall sequence similarity, each representing a distinct allele (*mipA1.1*- to *mipA8.2*-type alleles). The *mipA* alleles were then assigned to sub-classes (*mipA1*- to *mipA8*-type alleles). Lineage I included *mipA1.1*- to *mipA7.2*-type alleles, whereas lineage II included *mipA8.1*- and *mipA8.2*- type alleles (Fig. 2.12).

The *mipA* tree and visual inspection of the nucleotide and amino acid sequences of the *mipA* alleles (Fig. 2.12 & Fig. 2.13) indicated evidence of recombination events within *mipA* gene of *P. multocida*. The *mipA* phylogeny was not in agreement with the phylogeny of *P. multocida* based on the concatenated sequences of seven and fifteen housekeeping enzyme genes and on the core genome (Fig. 2.1, Fig. 2.3 & Fig. 2.4) and suggesting that recombination has possibly affected the evolution of *mipA*. For example, the *mipA1.1*-type allele was present in bovine and porcine isolates of the MLST group A as well as bovine isolates PM302 of the MLST group E (capsular type A, OMP-type 5.3 and ST 6). The *mipA2.1*-type allele was present in a porcine AR isolate PM40 of the capsular type A and OMP-type 6.2 as well as isolates of the major porcine pneumonia cluster. The *mipA1.1*- and *mipA2.1*-type alleles were almost identical and differed at only 4 nucleotide sites (Fig. 2.12 & Fig. 2.13A). These two alleles were associated with isolates from two divergent groups namely the bovine pneumonia and major porcine pneumonia clusters. Similarly, *mipA4.1*- and *mipA4.2*-type alleles were almost identical *mipA* alleles but were present in isolates from different lineages based on the MLST tree (MLST group C and E,

respectively). These alleles differed at only 2 nucleotide positions (Fig. 2.12 & Fig. 2.13A).

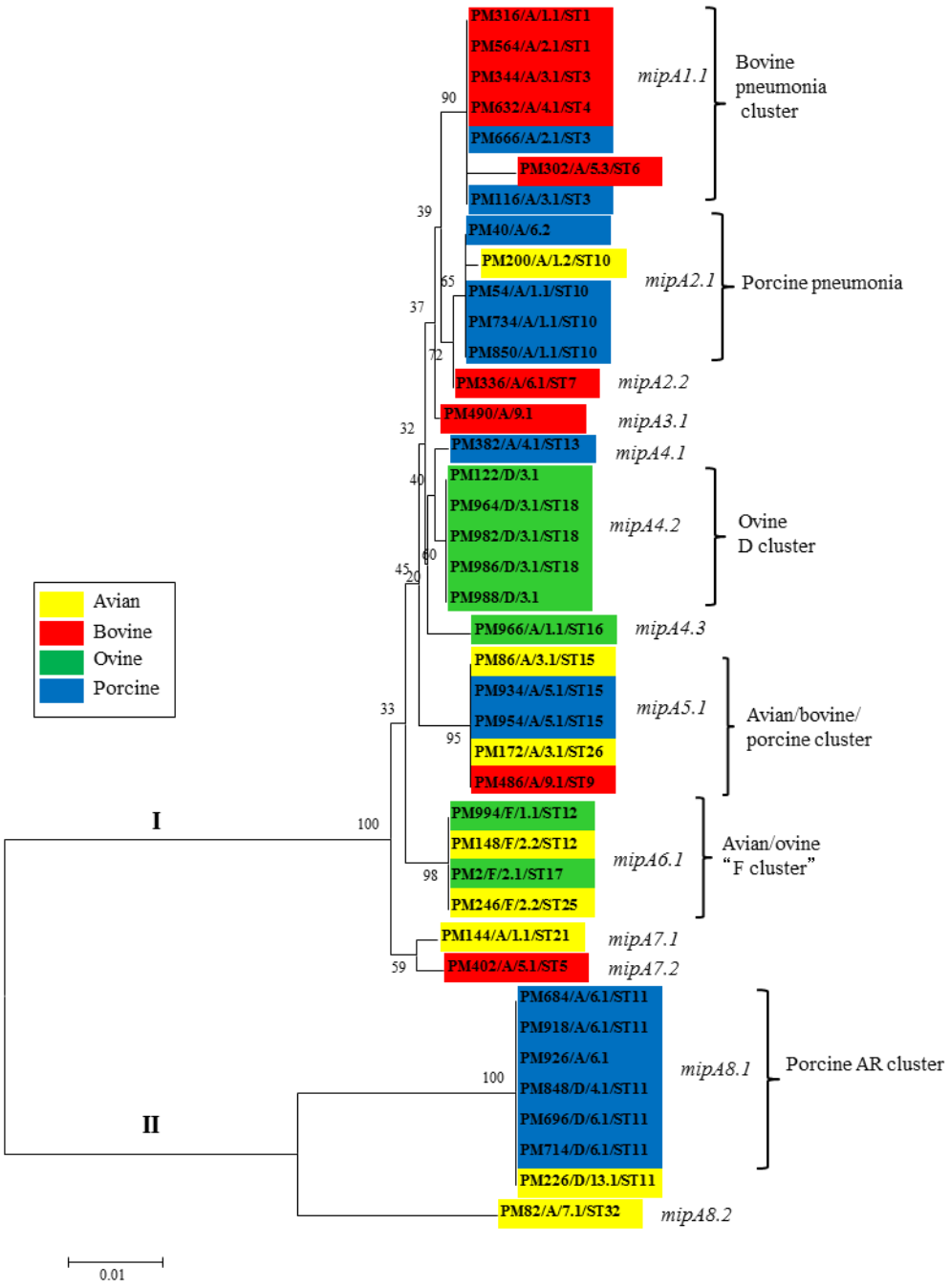

Fig. 2.12 Neighbour-Joining tree representing the phylogenetic relationships of *mipA* alleles in 40 *P. multocida* strains.

The phylogenetic tree was constructed with Jukes-Cantor correction for nucleotide substitutions. Isolate designation, capsular type, OMP type and ST type are provided for each isolate (e.g. PM316/A/1.1/ST1). Allele designations are shown to the right (*mipA1.1,* etc.).

The *mipA6.1*-type allele contained a recombinant segment (green, nucleotides 297 to 565) that was identical to the corresponding region of the *mipA7.2*-type allele, and these two alleles also differed at only 5 nucleotide sites (Fig. 2.13A). The *mipA8.1*- and *mipA8.2*-type alleles were very different from the others (Fig. 2.12 & Fig. 2.13A). *MipA8.1* was present in the porcine AR group (except isolate PM40), whereas *mipA8.2* was associated with avian isolate PM82 (capsular type A, OMP7.1, ST11 and MLST group H). The *mipA8.1*-type allele contained two different recombinant segments (pink segments) that were identical to the corresponding regions of the *mipA8.2*-type allele (Fig. 2.13A). Amino acid sequence analysis (polymorphic sites only) showed less variation than nucleotide sequence analysis but confirmed the presence of recombinant segments (Fig. 2.13B).

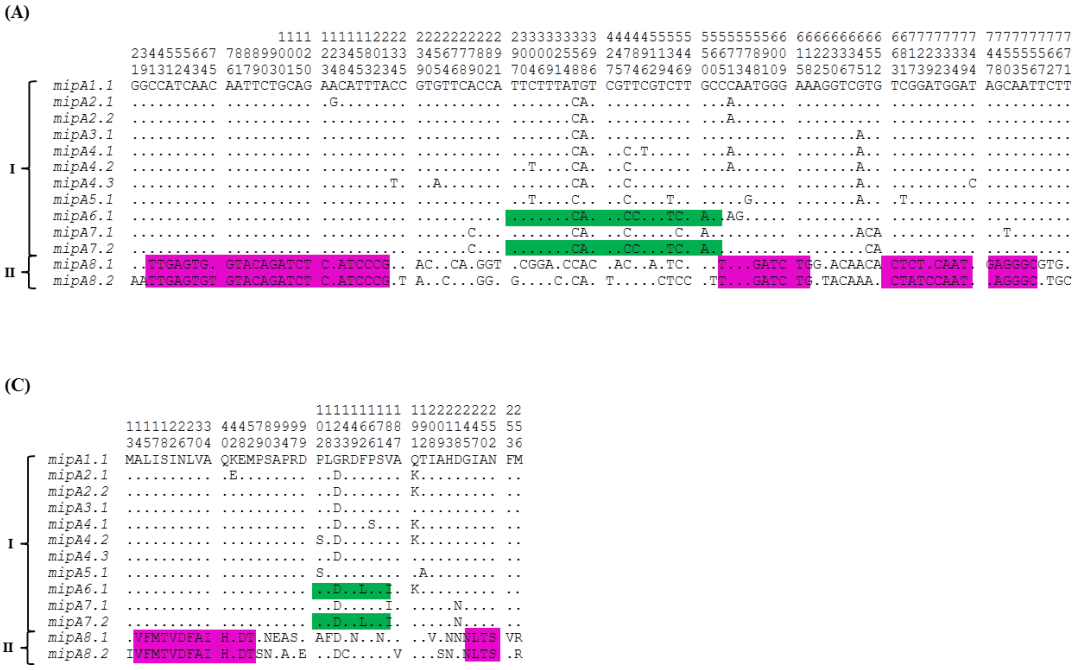

Fig. 2.13 Distribution of polymorphic nucleotide amino acids sites among the *mipA* alleles of *P. multocida*

Allele designations are shown to the left of each sequence. Roman numerals I and II represent the phylogenetic lineages (**Fig. 2.12**). Coloured boxes highlight sequence identity and proposed recombinant segments. The vertical numbers above the sequences represent the positions of polymorphic nucleotide sites.

2.3.5 Transport and receptor proteins

Twenty five OMPs were representative of this group based on the prediction tools (Table 2.3). The following proteins were selected to determine nucleotide

and amino acid variation and also to construct the phylogenetic trees, OmpW, ComL, OmpH1, PlpB, HgbA, HasR, HmbR, PfHR, LspB1, IbeB, TolC, Wza and HedX and further detail is shown in Table 2.6. The gene encoding ComL, OmpH1 and Wza were characterised in detail. The phylogenetic relatedness of the remaining genes was also examined and shown in Appendices, Fig. 8.2.

2.3.5.1 ComL

The complete sequence of *comL* is 780 nucleotides and the encoded protein is 260 amino acids in length (Table 2.6). Total nucleotide variation among all sequences was 4% (28) polymorphic nucleotide sites) and the amino acid variation was 3% (7 variable inferred amino acid sites) (Table 2.6). The *comL* Neighbour-Joining phylogenetic tree identified four lineages (I to IV) (Fig. 2.14). Twelve different *comL* nucleotide sequences were identified based upon overall sequence similarity, each representing a distinct allele (*comL1.1*- to *comL7.2*-type alleles). The *comL* alleles were assigned to sub-classes (*comL1*- to *comL7*-type alleles). The evidence of recombination within *comL* gene of *P. multocida* was found based on the *comL* phylogenetic tree because the *comL* phylogeny was not in agreement with the phylogeny of *P. multocida* based on the concatenated sequences of seven and fifteen housekeeping enzyme genes and on the core genome (Fig. 2.1, Fig. 2.3 & Fig. 2.4). This suggests that recombination has affected the evolution of *comL*.

The *comL* tree showed *comL6.1*-allele type was associated exclusively with isolates of the porcine pneumonia and AR clusters. The *comL* gene tree shows clear evidence of assortative recombination of the *comL* gene between the porcine pneumonia and AR clusters (MLST group F and G, respectively) because the two clusters possess an identical *comL* gene (Fig. 2.14). Pairwise difference in nucleotide and amino acid sequences between representative *comL* allele types of *P. multocida* was relatively low and ranged from only 2 to12 nucleotide sites and 1 to 4 amino acid positions.

Table 2.6 Details of OMPs/ genes having transport and receptor function in *P. multocida.*

Gene	Protein function	Total no. of strains	Gene size		Polymorphic sites		Sequence diversity (%)	
			No. of nucleotides	No. of amino acids	No. of nucleotides	No. of amino acids	Nucleotides	Amino acids
ompW	Transport small hydrophobic molecules	40	612	204	34	7	6	3
comL[a]	DNA uptake	40	780	260	28	7	4	3
plpB/ metQ	Amino acid transport	40	828	276	40	7	4.8	2.50
hgbA	Haemoglobin receptor & iron transport	32	2916	972	151	52	5.1	5.3
hasR	Haem receptor & transporter activities	35	2544	848	71	28	3	3
hmbR	Haemoglobin receptor and iron transport	33	2353	784	67	24	3	3
pfhR	Haemoglobin receptor & iron transport	40	2181	727	128	41	6	6
ompH1[a]	Porin/iron transport activity	40	1131	377	362	120	32	32
lspB1	Two-partner secretion/secretion of filamentous hemagglutinin	33	1449	483	61	13	4	3
ibeB	Lipid binding & transport activity	35	1389	463	44	17	3.10	3.6
tolC	Protein secretion/transporter activity	40	1365	455	84	25	6	5
wza[a]	Capsular polysaccharide transport	34	1161	387	92	15	8	4
hexD	Capsular polysaccharide transport	40	1179	393	81	16	7	4

[a]= gene/proteins analysed in further detail

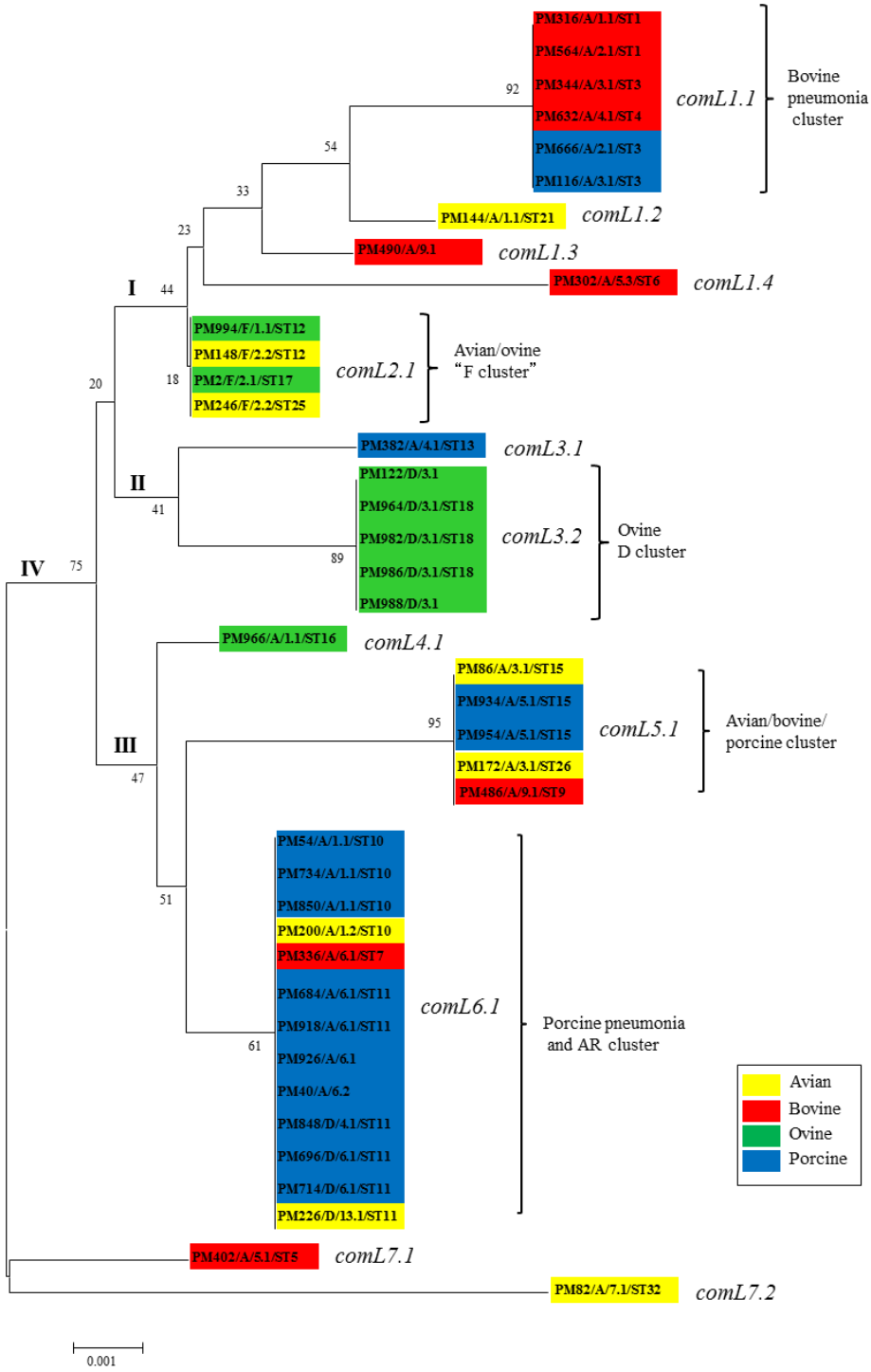

Fig. 2.14 Neighbour-Joining tree representing the phylogenetic relationships of *comL* alleles in 40 *P. multocida* strains.

The phylogenetic tree was constructed with Jukes-Cantor correction for nucleotide substitutions. Isolate designation, capsular type, OMP type and ST type are provided for each isolate (e.g. PM316/A/1.1/ST1). Allele designations are shown to the right (*comL1.1,* etc.).

The aligned nucleotide and amino acid sequences (polymorphic sites only) of *comL1.1*- to *comL7.2*- type alleles are shown in (Fig. 2.15). Visual inspection of the nucleotide sequences of the *coml1.1*- to *comL7.2*-type alleles indicated that limited recombination has occurred within the *comL* gene (Fig. 2.15). The *comL1.1 to comL2.1*-type alleles were associated with isolates from divergent lineages and differed at only 3 to 8 nucleotide positions (Fig. 2.15). Similar findings were found within lineages II to IV (Fig. 2.15).

The *comL1.3*-type allele contained a segment (nucleotides 465 to 646) that was identical to the corresponding region of the *comL1.4* -to *comL6.1*-type alleles. Amino acid sequence analysis (polymorphic sites only) showed less variation than nucleotide sequence analysis (Fig. 2.15B). The nucleotide substitutions within the recombinant segments of *P. multocida comL* were all synonymous changes and recombination does not lead to amino acids changes (Fig. 2.15B). Overall, indicating a highly conserved function there is strong selective constraint acting on the *comL* against amino acids replacement (Fig. 2.15B).

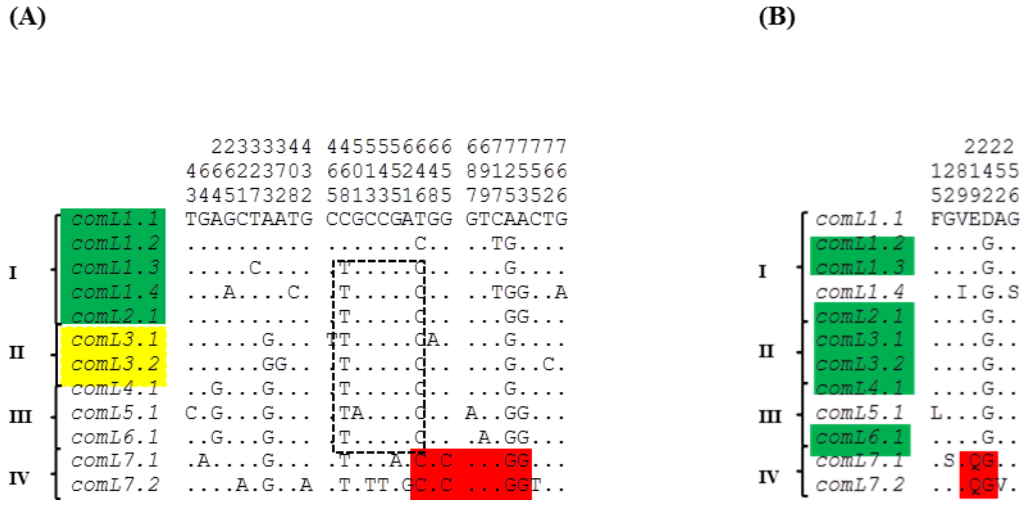

Fig. 2.15 Distribution of polymorphic nucleotide (A) and amino acid sites (B) among the *comL* alleles of *P. multocida*

Allele designations are shown to the left of each sequence. Roman numerals I to IV represent the phylogenetic lineages **(Fig. 2.14).** Coloured boxes highlight sequence identity and proposed recombinant segments. The vertical numbers above the sequences represent the positions of polymorphic nucleotide sites.

2.3.5.2 Capsular transport protein (Wza)

The *wza* gene, encoding the capsular transport protein Wza, was highly conserved. The complete sequence of *wza* was extracted using the internal BLAST tool in CLC genomics workbench form 34 isolates. The following isolates, PM402 (MLST group E), PM122, PM964, PM982, PM986 and PM988 (ovine capsular type D, OMP 3.1, ST 18 and MLST group E) were excluded from the analysis because partial sequences only were recovered. The complete sequence of *wza* is 1161 nucleotides and the encoded protein is 387 amino acids in length (Table 2.6). Total nucleotide variation among all the 34 sequences was 8% (92 polymorphic nucleotide sites) and the amino acid variation was 4% (15 variable inferred amino acid sites) (Table 2.6). The *wza* Neighbour-Joining phylogenetic tree identified four major lineages (I to IV) (Fig. 2.16).

Eleven different *wza* nucleotide sequences were identified based upon their overall sequence similarity, each representing a distinct allele (*wza1.1*- to *wza6.1*-type alleles). The *wza* alleles were assigned to sub-classes (*wza1*- to *wza6*-type alleles). The *wza* phylogenetic tree showed that *wza6.1* was highly divergent from the other alleles and it was associated only with avian isolate PM82 (Fig. 2.16).

Although *wza* is highly conserved, the *wza* phylogeny was not similar to the phylogeny of *P. multocida* based on the concatenated sequences of seven and fifteen housekeeping enzyme genes and on the core genome (Fig. 2.1, Fig. 2.3 & Fig. 2.4). Lineage I included almost identical *wza*-type alleles representing five clusters. The *wza1.1*-type allele was associated with isolates of bovine pneumonia cluster, the *wza1.2*-type allele was associated with bovine isolate PM302 (MLST group E). This lineage also inculded *wza2.1*-, *wza2.2*- and *wza2.3*-type alleles. Lineage II included four diiferent allele types (*wza3.1*- to *wza4.2*-type alleles) and which were also associted with different strain lineages (Fig. 2.16). Pairwise difference in nucleotide and amino acid sequences between representative *wza* allele types of ranged from 2 to 82 (0.2 to 7%) nucleotide sites and 1 to 15 (0.2 to 4%) amino acid positions. The aligned nucleotide and amino acid sequences (polymorphic sites only) for *wza1.1*- to *wza6.1*-type alleles are shown in (Fig. 2.17).

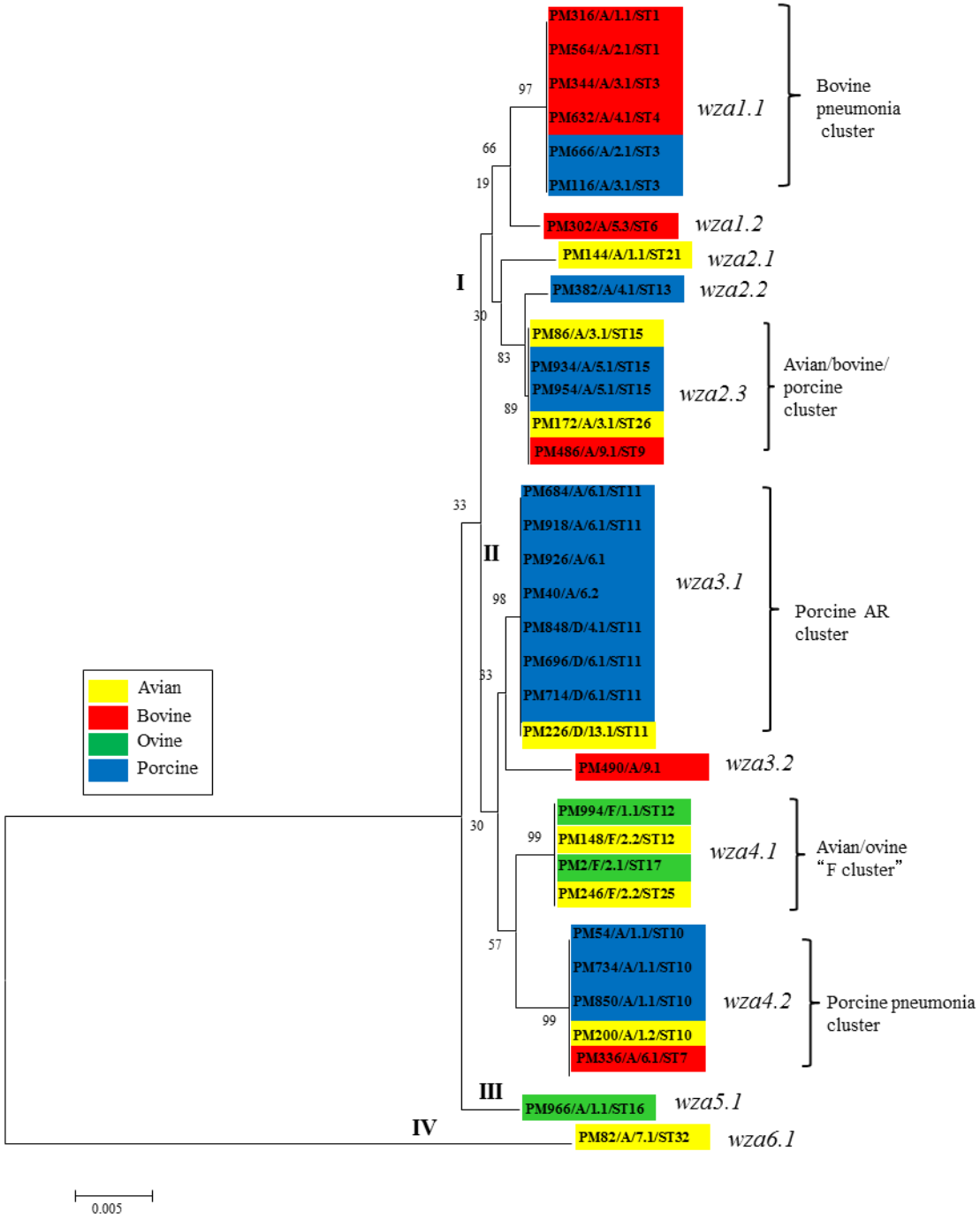

Fig. 2.16 Neighbour-Joining tree representing the phylogenetic relationships of *wza* alleles in 34 *P. multocida* strains.

The phylogenetic tree was constructed with Jukes-Cantor correction for nucleotide substitutions. Isolate designation, capsular type, OMP type and ST type are provided for each isolate (e.g. PM316/A/1.1/ST1). Allele designations are shown to the right (*wza1.1,* etc.).

The *wza1.1*-type allele differed at only 2 and 10 nucleotides sites from the *wza1.2 to wza2.3*-type (Fig. 2.17). The *wza3.1*- and *wza3.2*-type alleles contained only six different polymorphic nucleotide sites. The *wza4.1*- and *wza4.2*-type alleles differed at only seven nucleotide sites. Amino acid sequence analysis (polymorphic sites only) showed less variation than nucleotide sequence analysis (Fig. 2.17B). The *wza6.1*-type allele differed at 78 to 81 nucleotide sites from the other allele types (Fig. 2.17).

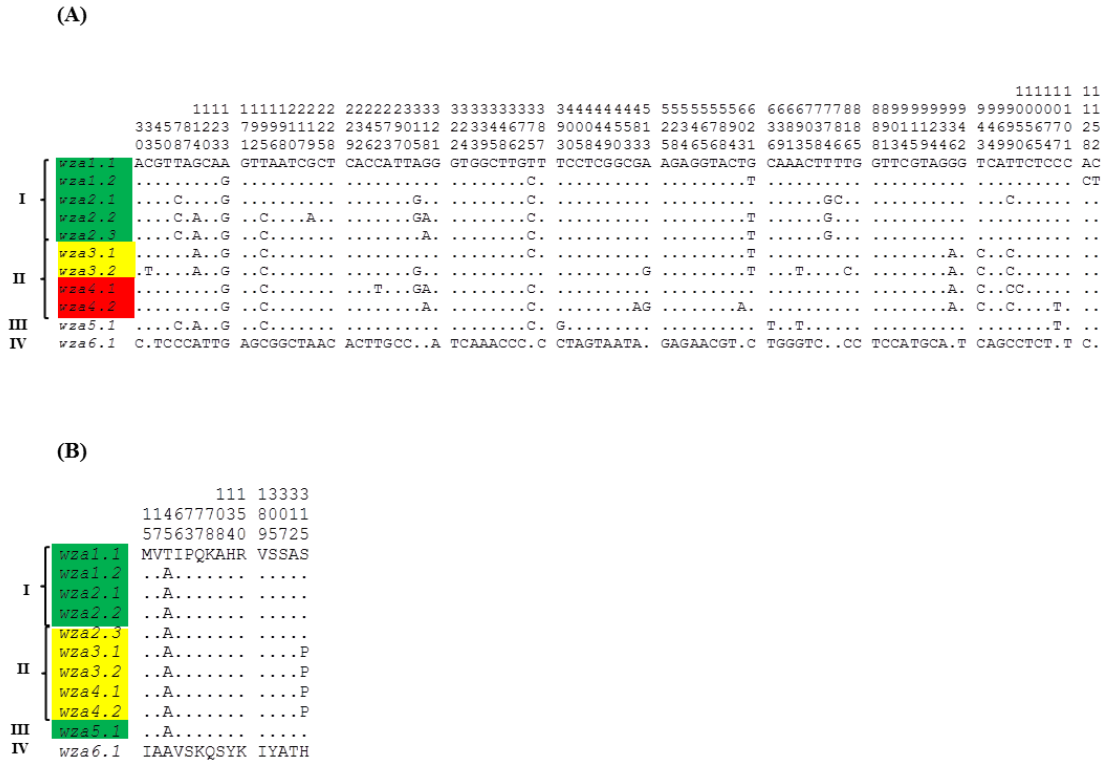

Fig. 2.17 Distribution of polymorphic nucleotide (A) and amino acid sites (B) among the *wza* alleles of *P. multocida*

Allele designations are shown to the left of each sequence. Roman numerals I to IV represent the phylogenetic lineages (**Fig. 2.16**). Coloured boxes highlight sequence identity and proposed recombinant segments. The vertical numbers above the sequences represent the positions of polymorphic nucleotide sites.

2.3.5.3 Outer membrane protein H1 (OmpH1)

The total aligned length including gaps and insertions, of the *ompH1* gene is 1131 nucleotides and the encoded protein comprises 377 amino acids. Total nucleotide variation among all sequences was 32% (362 polymorphic nucleotide sites) and the amino acid variation was 32% (120 variable inferred amino acid sites) (Table 2.6). The *ompH1* Neighbour-Joining phylogenetic tree identified VI distinct lineages (I to VI) (Fig. 2.18). Eighteen different *ompH1* nucleotide sequences were identified based upon the overall sequence similarity, each representing a distinct allele (*ompH1.1*- to *ompH8.1*-type types). The *ompH1* alleles were assigned to sub-classes (*ompH1*- to *ompH8*-type alleles).

Evidence of recombination within the *ompH1* gene of *P. multocida* was found based on the *ompH1* phylogenetic tree because the *ompH1* phylogeny was not in agreement with the phylogeny of *P. multocida* based on the concatenated sequences of seven and fifteen housekeeping enzyme genes and on the core genome (Fig. 2.1, Fig. 2.3 & Fig. 2.4). This suggests that recombination has influenced the evolution of *ompH1*. Lineage I was associated with *ompH1*-type alleles (*ompH1.1*- to *ompH1.5*-type alleles). This lineage included two isolates of the major bovine pneumonia group, PM632 (capsular type A, OMP-type 4.1 and ST 4 and PM344 (capsular type A, OMP-type 3.1 and ST 3), ovine isolates of the capsular type D cluster, bovine isolate PM490 of the MLST group D (capsular type A, and OMP-type 9.1) and bovine isolate PM302 of the MLST group E (capsular type A, OMP-type 5.3 and ST 6). The *ompH1* tree showed that the ovine capsular type D and bovine isolate PM490 had identical *ompH1* alleles (*ompH1.4*) that was similar to the *ompH1* allele gene of the major bovine pneumonia cluster. Comparison with the MLST tree (Fig. 2.1), suggests that there have been multiple HGT events of *ompH1* in bovine and ovine isolates possessing *ompH1*-type alleles (Fig. 2.16). Lineage II included only the *ompH2.1*-type allele which was associated with isolates of the porcine AR cluster. However, two other isolates of this cluster, PM848 and PM926 possessed different alleles (*ompH3.2* and *ompH3.1,* respectively*)* (Fig. 2.16). Lineage III included two alleles, *ompH3.1* and *ompH3.2* and these two alleles were associated with isolates from different genetic lineages. *OmpH3.1* included only avian isolate PM82 (capsular type A, OMP-type 7.1, ST 32 and MLST group H), whereas *ompH3.2* was associated with

porcine AR isolate PM848 (capsular type D, OMP-type 8.1. ST 11 and MLST group G) (Fig. 2.16).

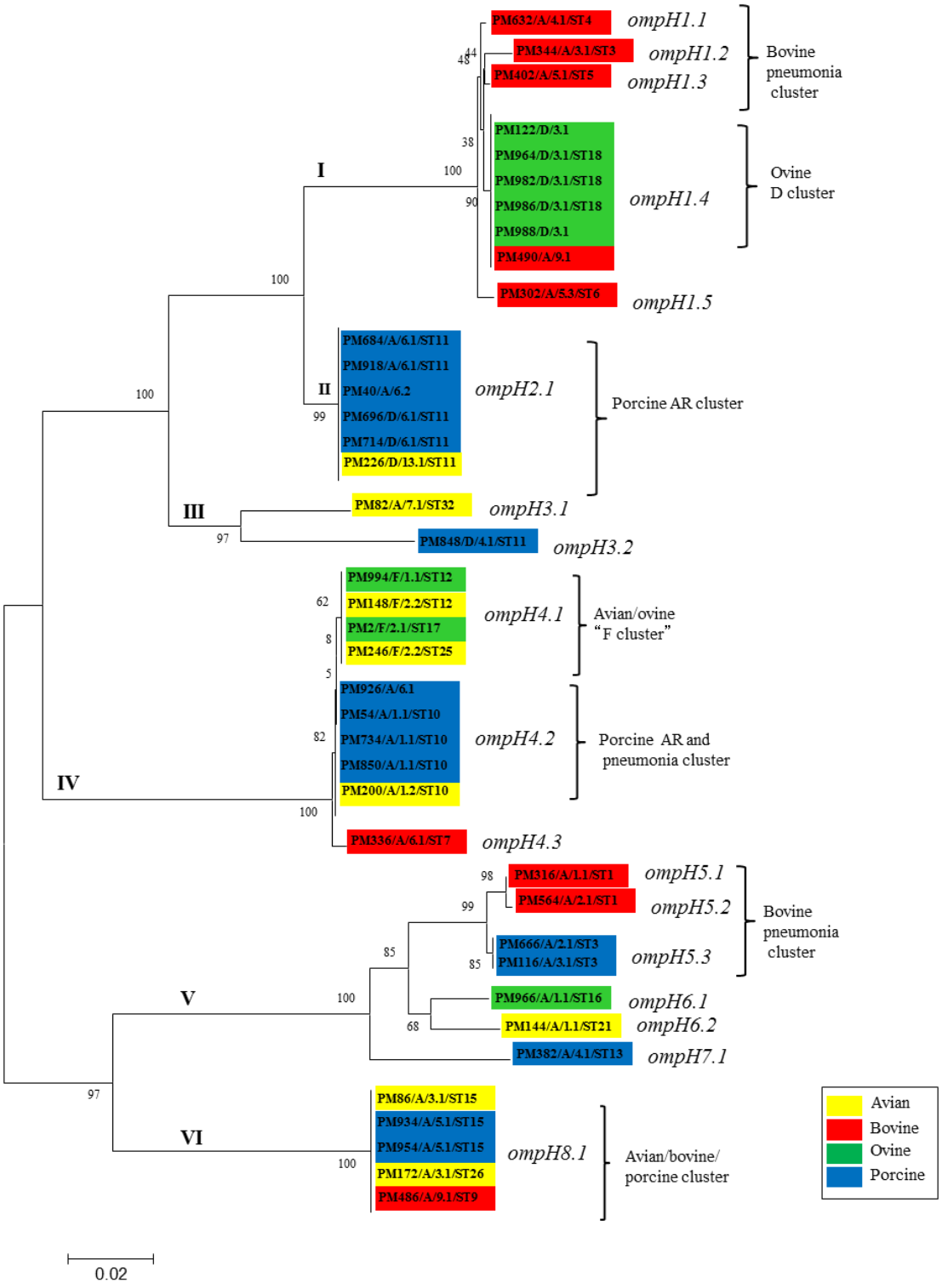

Fig. 2.18 Neighbour-Joining tree representing the phylogenetic relationships of *ompH1* alleles in 40 *P. multocida* strains.

The phylogenetic tree was constructed with Jukes-Cantor correction for nucleotide substitutions. Isolate designation, capsular type, OMP type and ST type are provided for each isolate (e.g. PM316/A/1.1/ST1). Allele designations are shown to the right (*ompH1.1*, etc.).

Evidence of recombination was also found within lineage IV. This lineage included *ompH4.1*-, *ompH4.2*- and *ompH4.3*-type alleles. The *ompH4.1*-type allele was associated with avian and ovine isolates of capsular type F*; ompH4.2* was associated with major porcine pneumonia isolates (MLST group F) as well as a single porcine AR isolate (PM926); *ompH4.3* was associated with bovine isolate PM336 which was also a representative of the major porcine pneumonia group (MLST group F) (Fig. 2.16). Lineage V included 5 different alleles (*ompH5.1*- to *ompH7.1*-type alleles). The *ompH5.1*- and *ompH5.2*- type alleles were associated with bovine isolates of the major bovine pneumonia cluster (capsular type A, OMP-types 1.1 and 2.1, ST 1 MLST group A); the ompH5.3-type allele was associated only with porcine isolates which were also representative of the major bovine pneumonia group (capsular type A, OMP-types 2.1 and 3.1, ST 3 and MLST group A); *ompH6.1-, ompH6.2*- and *ompH7.1*-type alleles were each associated with a single isolate from different genetic lineages. Finally, lineage VI consisted of a single allele, *ompH8.1* which was isolates of the MLST group D (Fig. 2.16).

Pairwise difference in nucleotide and amino acid sequences between representative *ompH1* allele types of *P. multocida* ranged from 3 to 167 (0.3 to 15.3%) nucleotide sites and 3 to 68 (0.8 to 18.6%) amino acid positions. The aligned nucleotide and amino acid sequences (polymorphic sites only) of the *ompH1.1*- to *ompH8.1*-type alleles are shown in (Fig. 2.19).

Visual inspection of the nucleotide sequences of the *ompH1.1*- to *ompH8.1*-type alleles indicated that intragenic and entire gene recombination has occurred within the *ompH1* gene (Fig. 2.19 & Fig. 2.20). The *ompH1*-type alleles within lineage I were almost identical and differed at only 3 to 11 nucleotide sites. *OmpH1.1*- to *ompH1.5*-type alleles contained four different segments (blue, nucleotides 60 to 264, 703 to 449, 450 to 546 and 839 to 925) that were identical or almost identical to the corresponding regions of the *ompH2.1*-type allele (Fig. 2.19). Allele *ompH2.1* contained two segments (light blue, nucleotides 926 to 966 and red, nucleotides 813 to 839) that were identical to the corresponding regions of the *ompH3.2*-type allele and *ompH3.1*- to *ompH8.1*-type alleles (Fig. 2.19). The putative recombinant segments were also found within *ompH3.1*- and *ompH3.2*-type alleles (green segments)

(A)

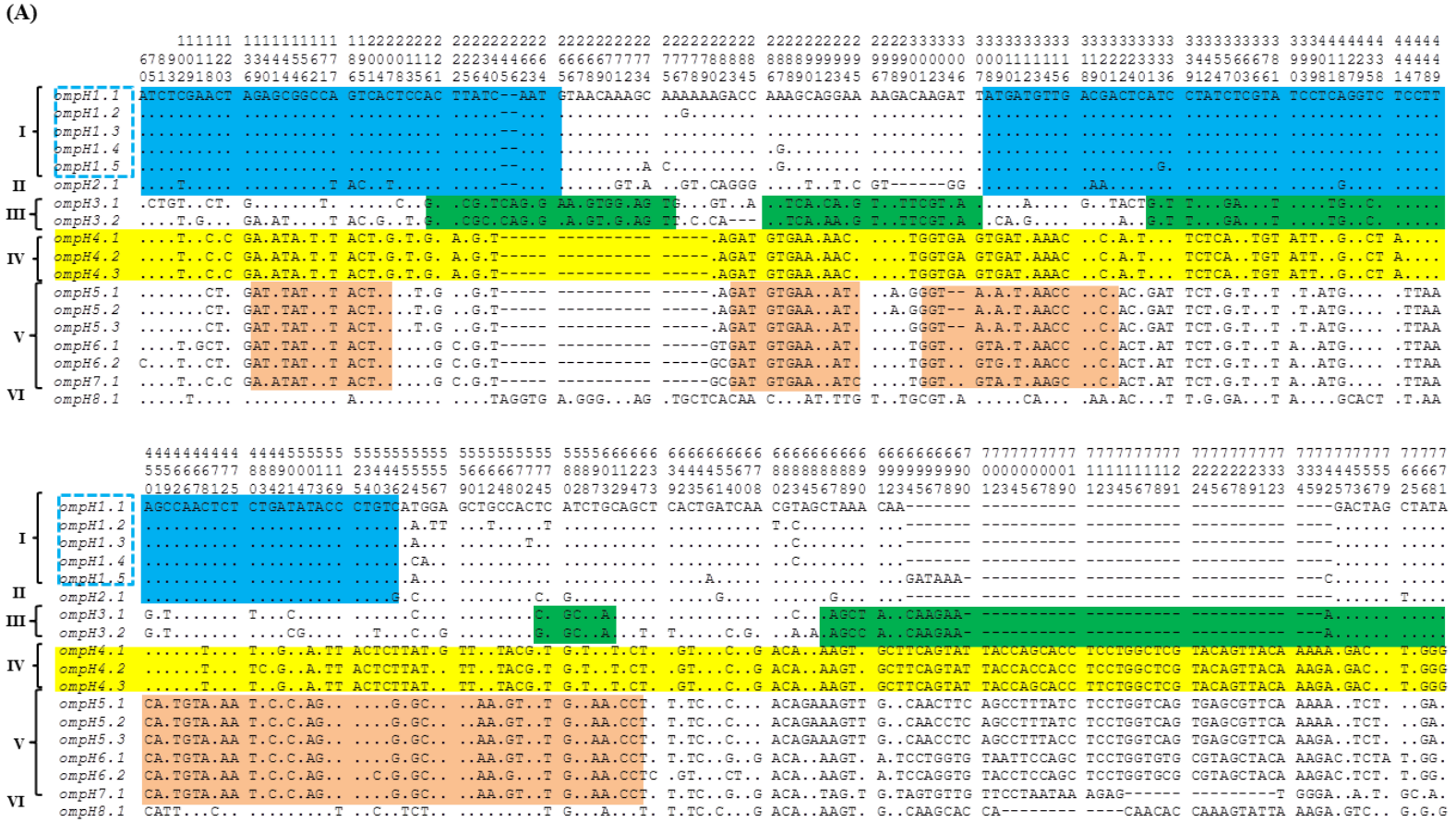

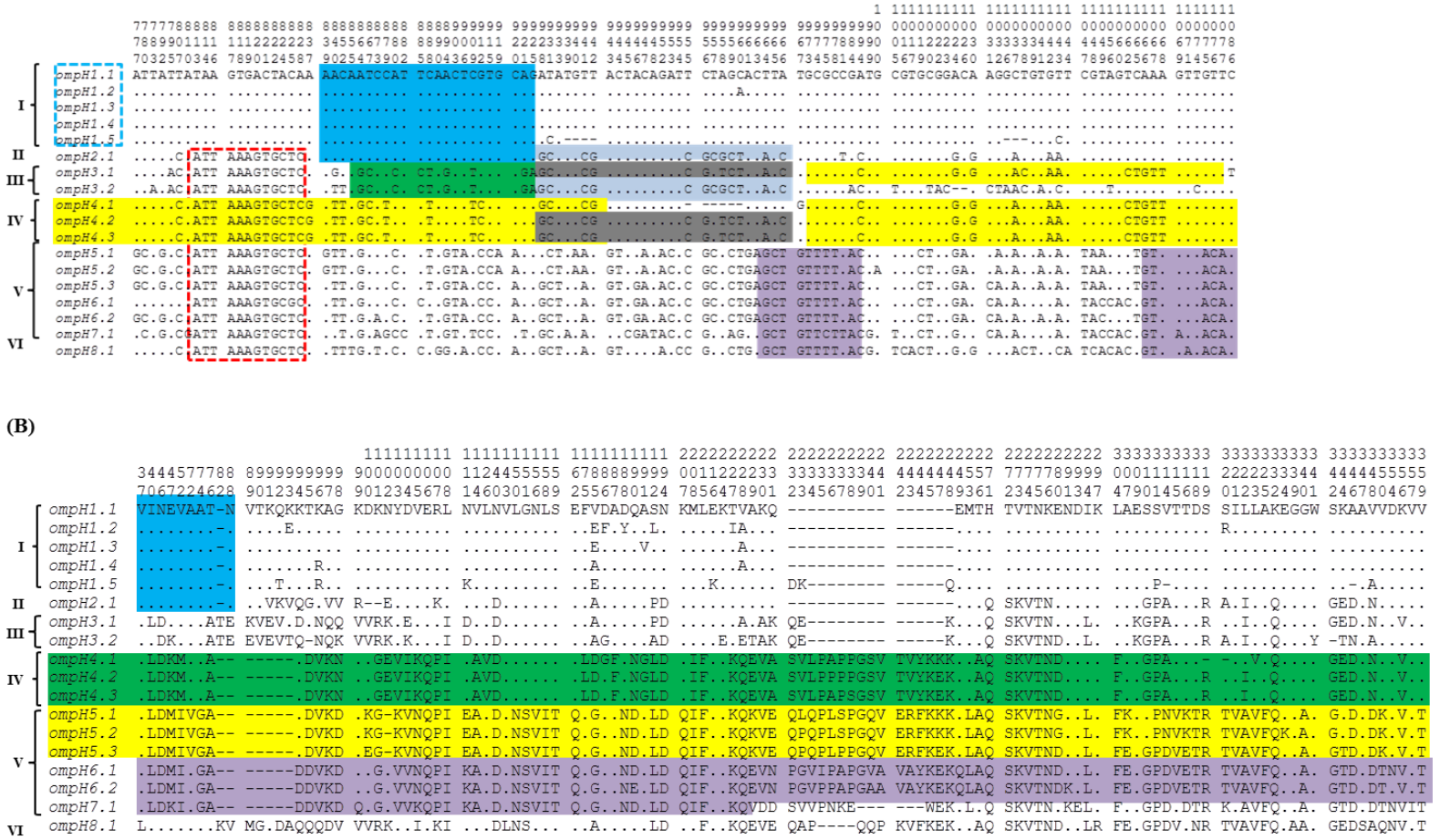

Fig. 2.19 Distribution of polymorphic nucleotide (A) and amino acid sites (B) among the 18 *ompH1* alleles of *P. multocida.*

Allele designations are shown to the left of each sequence. Roman numerals I to VI represent the phylogenetic lineages (**Fig. 2.18**). Coloured boxes highlight sequence identity and proposed recombinant segments. The vertical numbers above the sequences represent the positions of polymorphic nucleotide sites

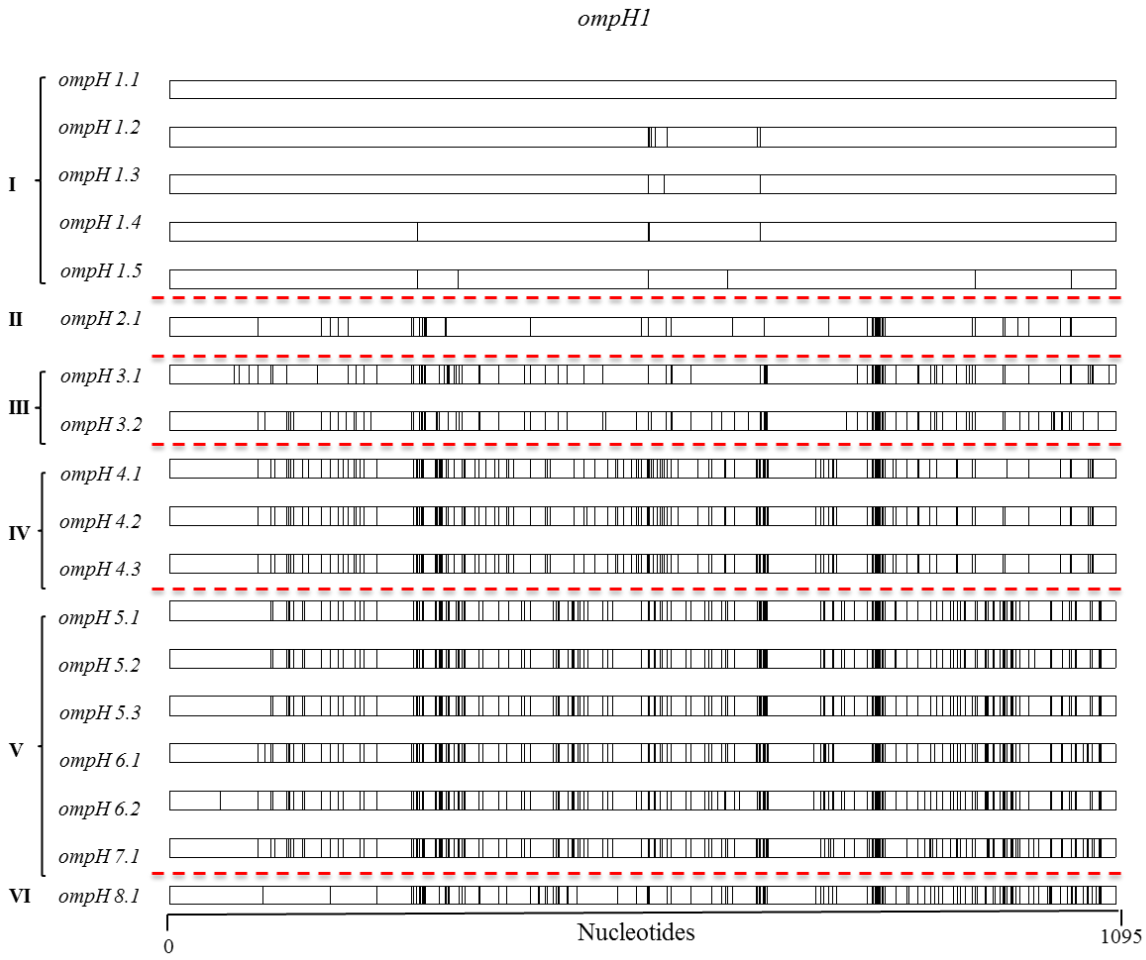

Fig. 2.20 Distribution of polymorphic nucleotide sites among the 18 *ompH1* alleles of *P. multocida* using Happlot analysis.

Allele designations are shown to the left of each sequence. Roman numerals I to VI represent the phylogenetic lineages (**Fig. 2.18**). Graph was created using Micrographic Designer.

The *ompH3.1*-type allele had a segment (grey, nucleotides 928 to 966) that was identical to the corresponding region of the *ompH4.2*- and *ompH4.3*-type alleles. The *ompH4.1*-, *ompH4.2*- and *ompH4.3*-types alleles were almost identical. Putative recombinant segments were also found within lineage V (Fig. 2.19).

To identify OmpH1 domains, representative sequences of each allele were selected. A model of OmpH1 domains and the proposed secondary structure of OmpH1 were elucidated using PRED-TMBB. The proposed secondary structure of OmpH1 in *P. multocida* consists of sixteen transmembrane ß-strands and eight extracellular loops with hypervariable regions (Fig. 2.21 & Fig. 2.22). The amino acid variation of OmpH1 occurred almost in the loop regions. However, the

variation in loop three was minimal and due to amino acids substitutions (amino acid sites 140 and 142). Some variation was also observed in transmembrane regions. The most variable loops were loops two (HV2), four (HV4), five (HV5), seven (HV7) and eight (HV8) (Fig. 2.22). In particular, variation in loops 2 and 5 consisted of insertions and/or deletions of amino acids (Fig. 2.22).

Once the domains had been identified and established, MEGA was used to calculate sequence diversity and substitution rates based on the complete alignments of the eighteen sequences. The OmpH1 protein was divided into 17 domains based on the amino acid sequence alignments (Fig. 2.22). The numbers of synonymous substitutions per 100 synonymous sites (d_S) and nonsynonymous substitutions per 100 nonsynonymous sites (d_N) were estimated for the conserved and loop regions. This allowed selective constraint and diversifying selection to be determined in the *ompH1* gene of *P. multocida* by calculating the d_S/d_N ratios for various domains (Table 2.7). A high d_S/d_N ratio ($d_S/d_N > 1$) indicates that natural selection is acting to restrict mutations that result in amino acid alteration and replacement, i.e selective constraint. Conversely, a low d_S/d_N ratio ($d_S/d_N < 1$) indicates that natural selection is actively driving amino acid alteration and replacement, i.e diversifying selection. The results indicated that selective pressures were not equal across the gene. The combined non-loop regions showed a d_S/d_N ratio of 2.00. These data demonstrate that natural selection is acting to restrict amino acid replacement in the non-loop regions of OmpH1.

However, the loops themselves had a d_S/d_N ration below 1, with the exception of loops two and three which displayed minimal variation. However, the d_S/d_N ratio for all loops combined was 0.5 (Table 2.7). These data provide strong evidence that natural selection is driving diversification of the hypervariable regions of the extracellular loops.

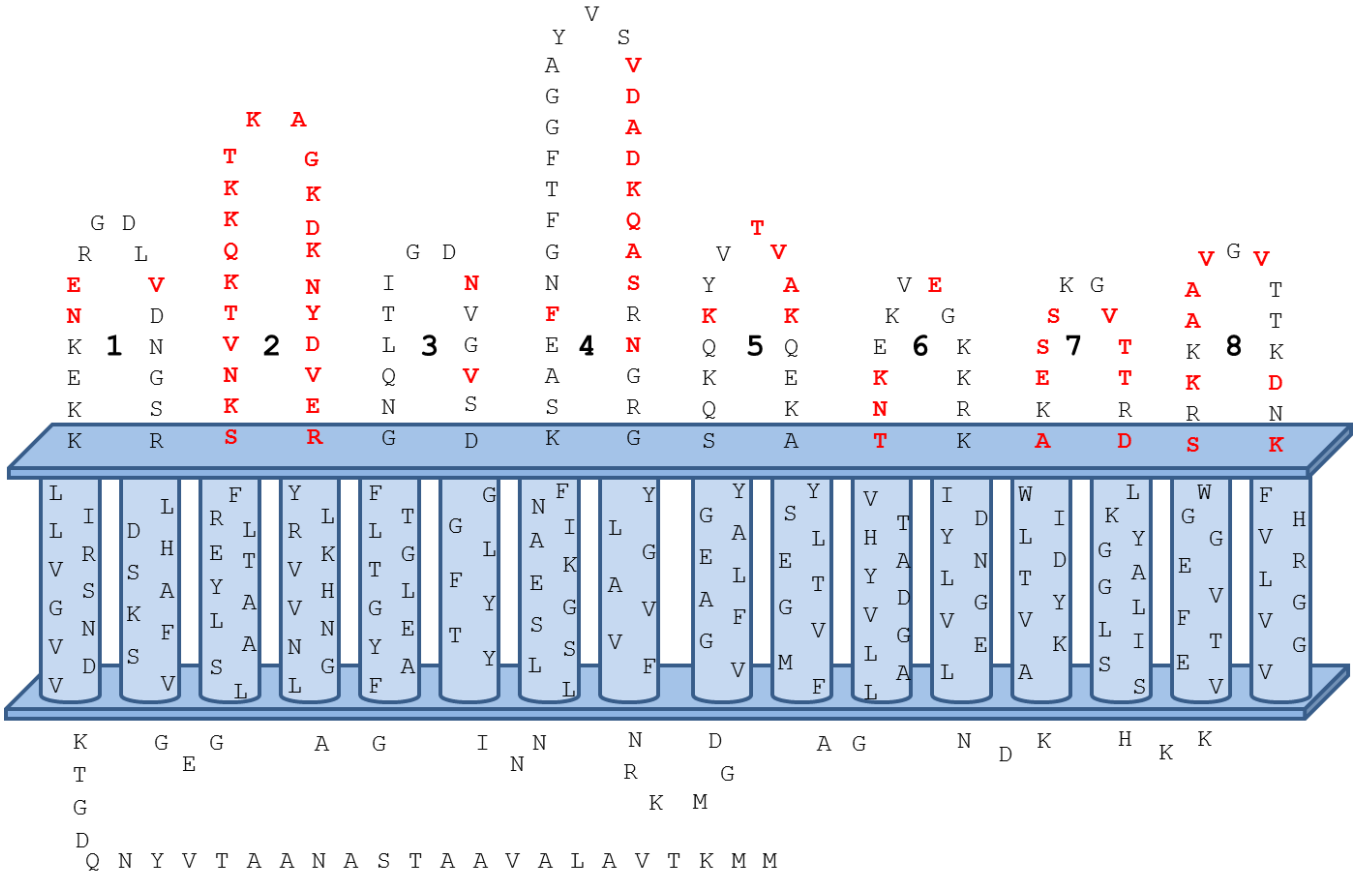

Fig. 2.21 Proposed secondary structure of the N-terminal transmembrane domain of the OmpH1 protein of *P. multocida*.

The sequence is based on OmpH1 of strain PM632. The amino acid variable positions are shown in bold red. Domains were predicted using Pred TMBB based on Hidden Markov Models.

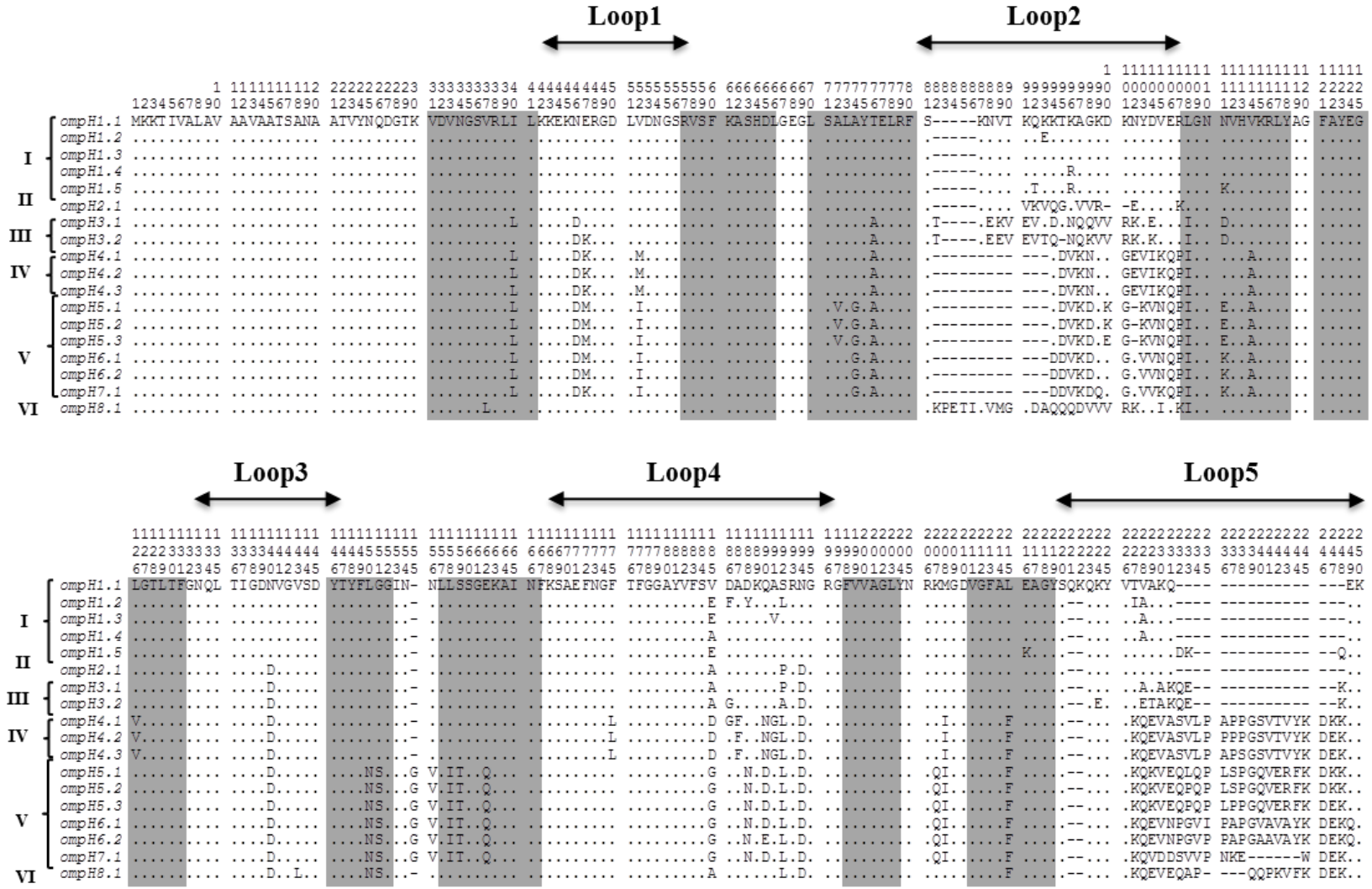
Loop1
Loop2
Loop3
Loop4
Loop5
I
II
III
IV
V
VI
ompH1.1
ompH1.2
ompH1.3
ompH1.4
ompH1.5
ompH2.1
ompH3.1
ompH3.2
ompH4.1
ompH4.2
ompH4.3
ompH5.1
ompH5.2
ompH5.3
ompH6.1
ompH6.2
ompH7.1
ompH8.1

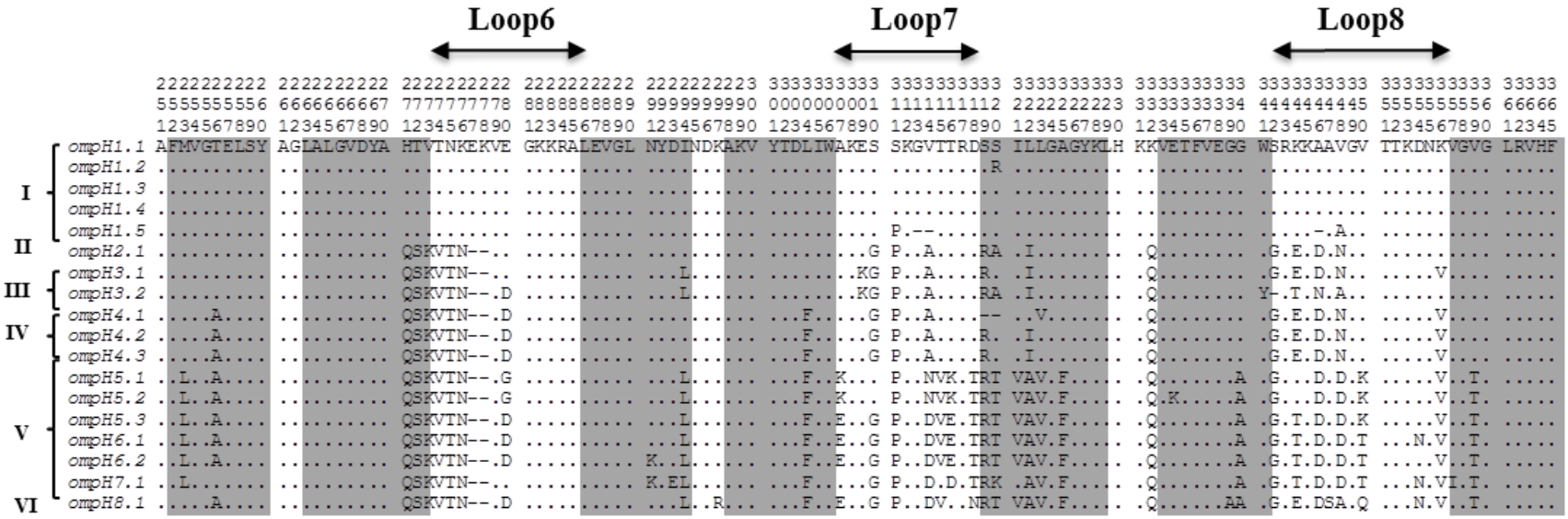

Fig. 2.22 Distribution of variable inferred amino acid sites in the N-terminal transmembrane domain of the 18 OmpH1 proteins of *P. multocida.*

Allele designations are shown to the left of each sequence. Roman numerals I to VI represent the phylogenetic lineages (**Fig. 2.18**). The numbers above the sequences (read vertically) represent amino acid positions. The dots represent sites where the amino acids match those of the first sequence. Gaps are indicated by dashes. Arrows represent the surface-exposed loops 1 to 8. Shaded regions represent predicted membrane-spanning β-strand structures.

Table 2.7 Substitution rates for the hypervariable loop domains of the *ompH1* genes of 40 *P. multocida* isolates.

Domains	d_S[a]	d_N[b]	d_S/ d_N
All Loops	1.337±0.621	2.356±1.244	0.5
Loop 1	2.315±0.466	11.005±1.361	0.2
Loop 2	1.869±0.718	0.536±0.413	3.4
Loop 3	5.856±1.187	5.516±1.772	1.0
Loop 4	2.742±0.734	5.663±1.906	0.5
Loop 5	1.847±0.613	2.466±1.011	0.7
Loop 6	1.020±0.482	4.601±1.242	0.2
Loop 7	3.190±0.771	4.608±1.727	0.7
Loop 8	1.337±0.621	2.356±1.244	0.5

[a] d_S is the number of synonymous substitutions per 100 synonymous sites; [b] d_N is the number of nonsynonymous substitutions per 100 nonsynonymous sites. Values are means ±standard deviations.

2.3.6 Adherence protein

Based on OMP prediction, *P. multocida* contain various proteins that are involved in host attachment and colonisation including ComE/PilQ, RcpA, RcpC, Hsf1, hsf2, Opa and TadD (Table 2.3). The genes encoding these proteins were obtained using the CLC genomics internal BLAST tool. ComE, RcpA and TadD were selected for further examinations. The Hsf1, Hsf2 and Opa proteins were excluded from the analysis because complete sequences were found in only a limited number of isolates. Results for RcpA were not included because they were very similar to those of the *tadD* gene. Further details are shown in Table 2.8.

Table 2.8 Properties of OMPs/ genes of *P. multocida* involved in adherence.

Gene	Protein function	Total no. of strains	Gene size		Polymorphic sites		Sequence Diversity %	
			No. of nucleotides	No. of amino acids	No. of nucleotides	No. of amino acids	Nucleotides	Amino acids
comE/pilQ[a]	Pilus assembly/protein secretion	34	1332	444	56	26	4	6
rcpA	Protein secretion/Flp pilus biogenesis	24	1410	470	112	11	8	2
tadD[a]	Assembly & transport of Flp pili	24	771	257	31	5	4	2

[a]= gene/proteins analysed in further detail

2.3.6.1 ComE/ PilQ

The gene encoding ComE (*comE*) was extracted from only 34 genomes. The *comE* gene obtained from ovine isolates of capsular type D (PM122. PM964, PM982, PM986 and PM988) and bovine isolate PM402 were excluded from the analysis because only partial sequences were obtained. The *comE* gene is 1332 nucleotides and the encoded protein comprises 444 amino acids in length. Total nucleotide variation among all sequences was 4% (54 polymorphic nucleotide sites) and the amino acid variation was 6% (26 variable inferred amino acid sites). The *comE* Neighbour-Joining phylogenetic tree identified five distinct lineages (I to V) (Fig. 2.23). Eleven different *comE* nucleotide sequences were identified based upon the overall sequence similarity, each representing a distinct allele (*comE1.1*- to *comE6.1*-type alleles). The *comE* phylogenetic tree was not similar to the phylogeny of *P. multocida* based on the concatenated sequences of seven and fifteen housekeeping enzyme genes and on the core genome (Fig. 2.1, Fig. 2.3 & Fig. 2.4). The *comE1.1*-type alleles were present in isolates PM316, PM564 and PM344 (major bovine pneumonia cluster, MLST group A) and bovine isolate PM336, the latter isolates have been shown previously to cluster with major porcine pneumonia isolates based on the concatenated sequences (3990 bp) of seven housekeeping enzyme genes (Fig. 2.1). The *comE1.2*-type alleles was associated with the bovine isolate PM632), porcine isolates PM666 and PM116 of the MLST group A (major bovine pneumonia cluster) and also with bovine isolate PM302 (capsular type A, OMP-type 5.3, ST 6 and MLST group E) (Fig. 2.23). These findings suggest that horizontal DNA transfer and recombination has occurred in the *comE* gene of *P. multocida*. The *comE*2.-type allele was associated with ovine isolate PM966 (capsular type A, PMP 1.1, S 16 and MLST group B) and bovine isolate PM490 which has been shown to cluster with isolates of the MLST group D (Fig. 2.23). Lineage II included *comE3.1*-type allele (avian and ovine F cluster), *comE3.2*-type allele (avian isolate PM144 of capsular type A, OMP-type 1.1 and ST 21) and *comE3.3*-type allele included only porcine isolate PM382 of capsular type A, OMP-type 4.1, ST 13 and MLST group C. Lineage III included only the *comE4.1*-type allele which was associated with isolates of the MLST group D. Lineage VI included only the *comE5.1*- and *comE5.2*-type allele; the *comE5.1*-type allele was associated with isolates of the major porcine pneumonia cluster, whereas the *comE5.2*-type allele was associated with isolates of the porcine AR cluster. Lineage V included only

comE6.1 which was associated with avian isolate PM82 and was highly divergent from the other lineages (Fig. 2.23). Pairwise differences in nucleotide and amino acid sequences between representative *comE* allele types were relatively low and ranged from 1 to 32 (0.1 to 2.4%) nucleotide sites and 1 to 13 (0.2 to 2.9%) inferred amino acid positions. Visual inspection of the nucleotide sequences of the *comE1.1*- to *comE6.1*-type alleles showed no evidence of intragenic recombination within the *comE* gene.

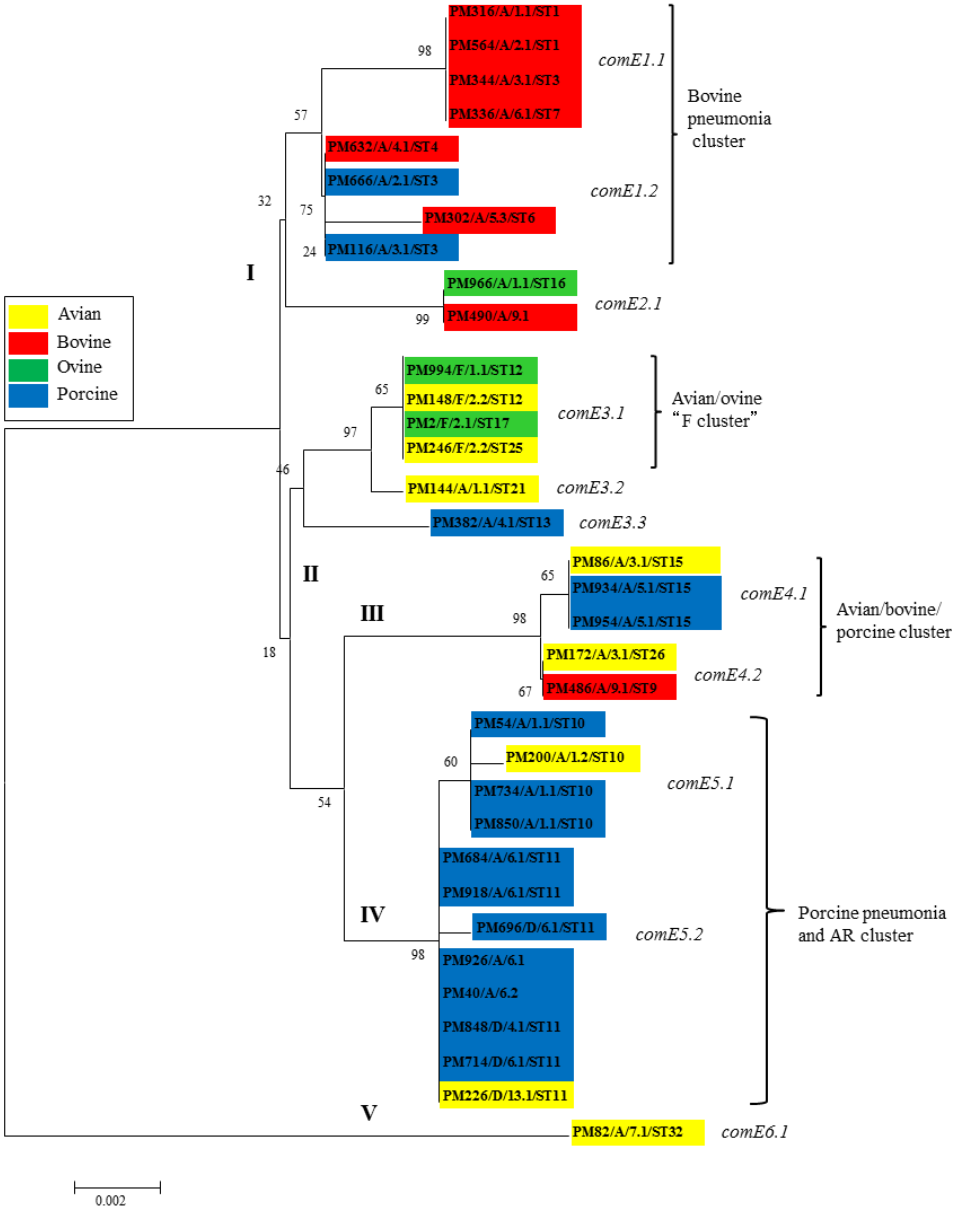

Fig. 2.23 Neighbour-Joining tree representing the phylogenetic relationships of *comE* alleles in 34 *P. multocida* strains.

The phylogenetic tree was constructed with Jukes-Cantor correction for nucleotide substitutions. Isolate designation, capsular type, OMP type and ST type are provided for each isolate (e.g. PM316/A/1.1/ST1). Allele designations are shown to the right (*comE1.1*, etc.).

2.3.6.2 TadD

The gene encoding TadD (*tadD*) was extracted from only 24 genomes. The *tadD* gene was not found in ovine isolates capsular type D (PM122. PM964, PM982, PM986 and PM988), and bovine isolates PM302 and PM402. Isolates associated with porcine atrophic rhinitis (PM684, PM918, PM926, PM848, PM696, PM714 and 200), porcine isolate PM382 and bovine isolate PM302 excluded from the analysis because only partial sequences were obtained. The *tadD* gene is 771 nucleotides and the encoded protein is 257 amino acids in length. Total nucleotide variation among all sequences was 4% (31 polymorphic nucleotide sites) and the amino acid variation was 2% (5 variable inferred amino acid sites). Pairwise difference in nucleotides and amino acids sequences between representative *tadD* allele types of *P. multocida* ranged from 3 to 26 (0.3 to 3.4%) nucleotide sites and 0 to 4 (0.0 to 1.5%) amino acid positions.

The *tadD* Neighbour-Joining phylogenetic tree identified four distinct lineages (I to IV) (Fig. 2.24). Eight different *tadD* nucleotide sequences were identified based upon their overall sequence similarity, each representing a distinct allele (*tadD1.1*- to *tadD4.2*-type alleles). The *tadD* phylogenetic tree was not in agreement with the phylogeny of *P. multocida* based on the concatenated sequences of seven and fifteen housekeeping enzyme genes and on the core genome (Fig. 2.1, Fig. 2.3 & Fig. 2.4). Lineage I included *tadD1.1*- and *tadD1.2*-type alleles. The *tadD1.1*-type allele was associated with isolates of bovine and porcine isolates of the bovine pneumonia cluster (MLST group A), bovine isolate PM336 (MLST group F) and avian and ovine isolates of capsular type F (PM2 and PM246). The *tadD1.2*-type allele was associated with avian isolate PM144. The presence of identical or almost identical alleles in isolates from different genetic lineages suggests that recombination had occurred in the *tadD* gene. The *P. multocida tadD1.1*- and *tadD1.2*-type alleles differed at only 4 nucleotide sites (Fig. 2.25). Lineage II includes *tadD2*- to *tadD2.3*-type alleles. The *tadD2.1*-type allele was associated with ovine isolate PM966 (MLST group B), *tadD2.2* was associated with major porcine pneumonia isolates (MLST group F) and *tadD2.3* included avian isolate PM200 (MLST group F). Tad2.3 differed at only 2 and 1 nucleotide sites from *tadD2.1- and tadD2.2*-type alleles, respectively (Fig. 2.25). Lineage III included only *tadD3.1* which was associated with bovine isolate PM490 (MLST group D). Lineage IV included *tadD4.1* which was associated with isolate

of the MLST group D profiles and *tadD4.2* which was associated with avian and ovine isolates of capsular type F (PM148 and PM994, ST 12 and MLST group C) (Fig. 2.24). These two alleles differed at only one nucleotide sites (Fig. 2.25). Visual inspection of the nucleotide sequences of the *tadD1.1*- to *tadD4.2*-type alleles showed no evidence of intragenic recombination within the *tadD* gene (Fig. 2.25).

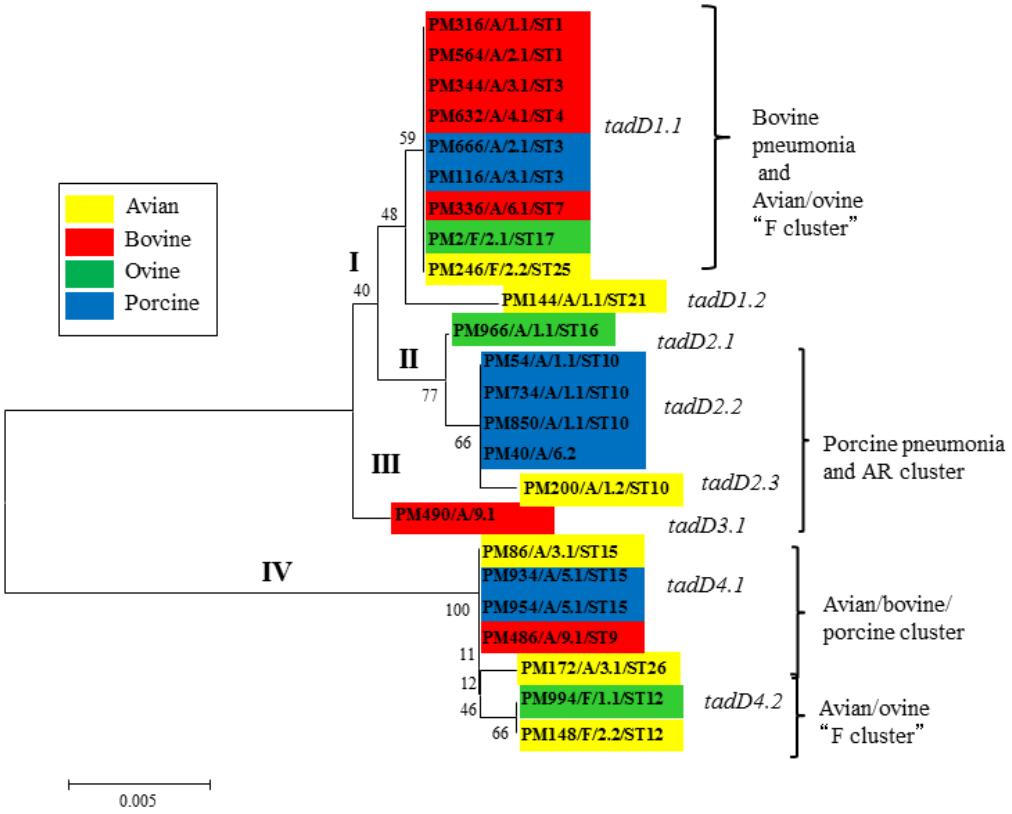

Fig. 2.24 Neighbour-Joining tree representing the phylogenetic relationships of *tadD* alleles in 24 *P. multocida* strains.

The phylogenetic tree was constructed with Jukes-Cantor correction for nucleotide substitutions. Isolate designation, capsular type, OMP type and ST type are provided for each isolate (e.g. PM316/A/1.1/ST1). Allele designations are shown to the right (*tadD1.1*, etc.).

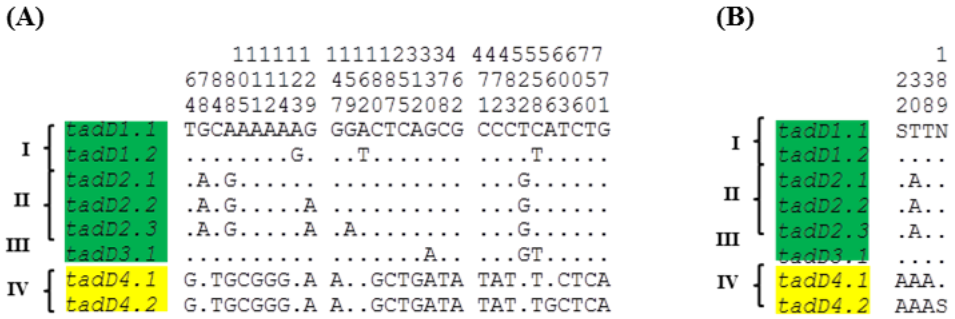

Fig. 2.25 Distribution of polymorphic nucleotide (A) and amino acid sites (B) among the *tadD* alleles of *P. multocida*

Allele designations are shown to the left of each sequence. Roman numerals I to IV represent the phylogenetic lineages (**Fig. 2.24**). Coloured boxes highlight sequence identity and proposed recombinant segment. The vertical numbers above the sequences represent the positions of polymorphic nucleotide sites.

2.3.7 Membrane-associated enzymatic activity

Proteomic prediction identified nine proteins, NlpP-like protein, Lipoprotein NlpC/P60, M48B, OmpP4, NanB, NanH, EstA, OmpLA and GlpQ (Table 2.3). Phospholipase A (OmpLA) was selected for further analysis because of its role in membrane disruption processes that occur during host cell invasion. However, the phylogenetic trees were constructed for other genes within this group and are shown in Appendices, Fig. 8.3. Further details are shown in Table 2.9.

2.3.7.1 Phospholipase A (*ompLA*)

Nucleotide sequences of the *ompLA* gene were obtained in all 40 genomes. The complete sequence of *ompLA* is 918 nucleotides and the encoded protein comprises 306 amino acids in length. Total nucleotide variation among all sequences was 5% (48 polymorphic nucleotide sites) and the amino acid variation was 7% (21 variable inferred amino acid sites). The *ompLA* tree topology identified six different lineages (I to VI). Twelve different *ompLA* nucleotide sequences were identified based upon the overall sequence similarity, each representing a distinct allele (*ompLA1.1*- to *ompLA 6.1*-type alleles). The *ompLA* alleles were assigned to sub-classes (*ompLA1*- to *ompLA A6*-type alleles) (Fig. 2.26).

Table 2.9 Details of 7 OMP genes having membrane-associated enzyme activity in *P. multocida*.

Gene	Protein function	Total no. of strains	Gene size		Polymorphic sites		Sequence Diversity (%)	
			No. of nucleotides	No. of amino acids	No. of nucleotides	No. of amino acids	Nucleotides	Amino acids
***nlpD*-like protein**	Metalloendopeptidase activity	40	1593	531	43	12	3	2
nlpC/P60	Cell-wall peptidase	40	477	159	18	3	4	2
m48B	Metalloendopeptidase activity/zinc ion biniding	40	771	257	38	9	5	4
ompP4	Acid phosphatase activity/utilization of NAD, NADP	40	816	272	39	6	5	2
estA	Lipid metabolism/hydrolase activity, acts on ester bond	40	2037	679	158	59	8	9
***ompLA*[a]**	Lipid metabolic process/maintain asymmetry of the OM	40	918	306	48	21	5	7
glpQ	Glycerol metabolic process/lipid metabolic process	33	1074	358	81	13	8	4

[a]= gene/proteins analysed in further detail

The *ompLA* phylogeny was not in agreement with the phylogeny of *P. multocida* based on the concatenated sequences of seven and fifteen housekeeping enzyme genes and on the core genome (Fig. 2.1, Fig. 2.3 & Fig. 2.4). This suggests that recombination has affected the evolution of the *ompLA* gene. Lineage I included *ompLA1.1*- and *ompLA1.2*-type alleles and these alleles were associated with isolates from different lineages. The *ompLA1.1*-type allele was associated with isolates of the bovine pneumonia cluster (MLST group A), whereas the *ompLA2.2*-type allele was associated with avian isolate PM144 of the MLST group E (Fig. 2.26). The *ompLA1.1*- to *ompLA2.2*-type alleles differed at only 4 nucleotide positions (Fig. 2.27). Lineage II included *ompLA2.1* and *ompLA2.2*; the *ompLA2.1*-type allele was associated with bovine isolate PM302 of the MLST group E; the *ompLA2.2*-type allele was associated with isolates of the MLST group E (Fig. 2.26). Lineage III included *ompLA3.1*-, *ompLA3.2*- and *ompLA3.3*-type alleles. The *ompLA3.1*-type allele was associated with bovine isolate PM490 (MLST group D); the *ompLA3.2*-type allele was associated with bovine isolate PM402 and *ompLA3.3* type was associated with ovine isolates of capsular type D cluster (Fig. 2.26). The *ompLA3.1*-, *ompLA3.2*- and *ompLA3.3*-type alleles differed at only 3 to 6 nucleotide positions (Fig. 2.27). Lineage IV included *ompLA 4.1*- and *ompLA4.2*-type alleles. The *omplA4.1*-type allele was associated only with porcine isolate PM382 (capsular type A, OMP-type 4.1. ST 13 and MLST C) and it differed at only 5 nucleotide sites compared with the *omplA4.2*-type allele. The *ompLA4.2*-type allele was associated with both major porcine pneumonia and AR isolates (Fig. 2.26). This clearly indicates that the *ompLA* gene has undone horizontal DNA transfer and assortative recombination between these two phylogenetically distinct porcine groups (Fig. 2.26).

Lineage V included *ompLA5.1*- and *ompLA5.2*-type alleles. The *ompLA5.1*-type allele was associated with ovine isolate PM966 (capsular type A, OMP-type 1.1, ST 16 and MLST group B), whereas *omplA5.1*-type allele was associated with avian and ovine isolates of capsular type F. The *ompLA5.1*- and *omplA5.2*-type alleles differed at only 5 nucleotide sites (Fig. 2.26 & Fig. 2.27). Lineage VI included *ompLA6.1*-type allele which was associated with avian isolate PM82 (capsular A, OMP-type 7.1, ST 32 and MLST group H). The *ompLA6.1*-type allele was relatively divergent from the other *ompLA*-type alleles, differed at 23 to 28 nucleotide sites (Fig. 2.26 & Fig. 2.27).

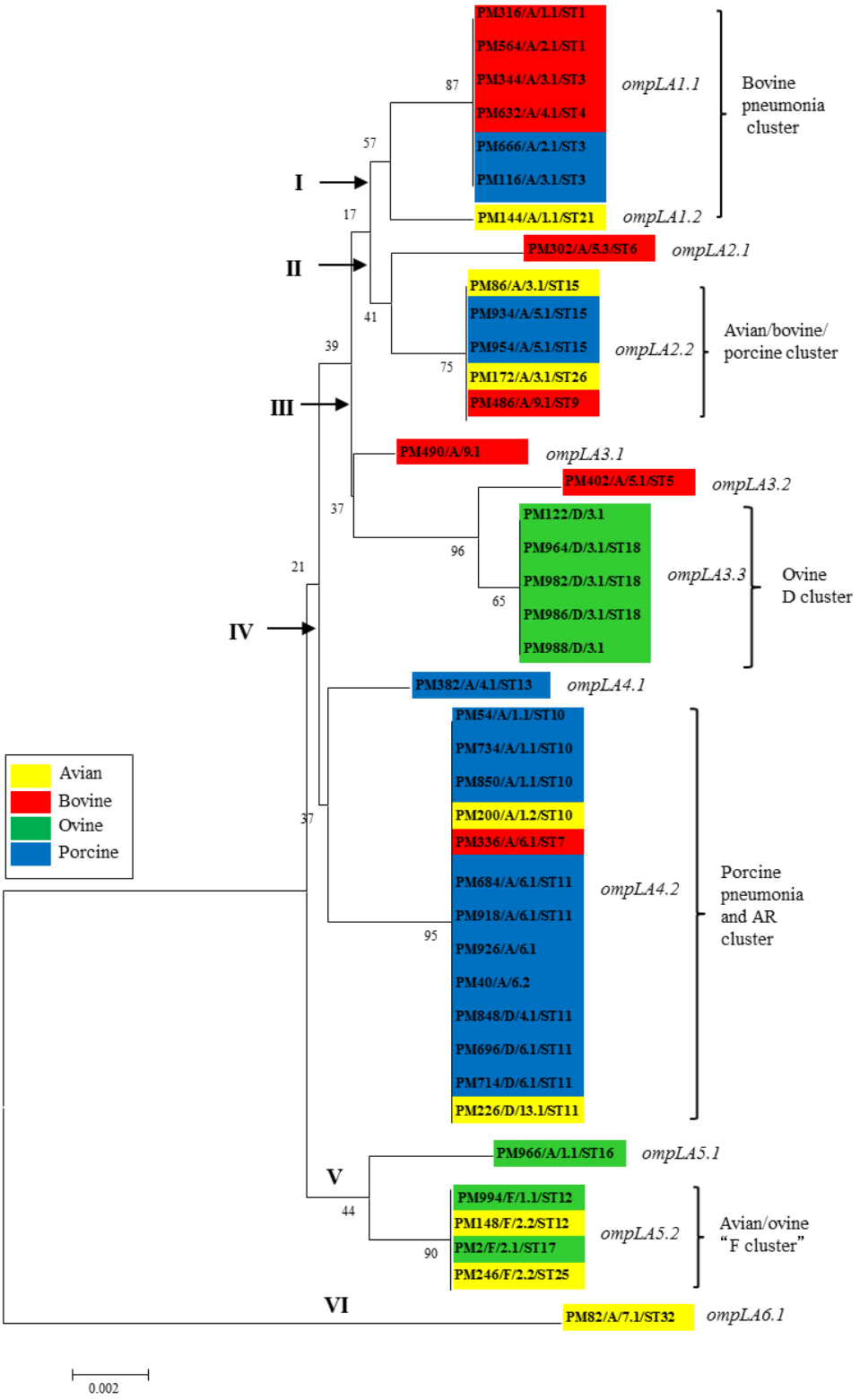

Fig. 2.26 Neighbour-Joining tree representing the phylogenetic relationships of *ompLA* alleles in 40 *P. multocida* strains.

The phylogenetic tree was constructed with Jukes-Cantor correction for nucleotide substitutions. Isolate designation, capsular type, OMP type and ST type are provided for each isolate (e.g. PM316/A/1.1/ST1). Allele designations are shown to the right (*ompLA*1.1, etc.).

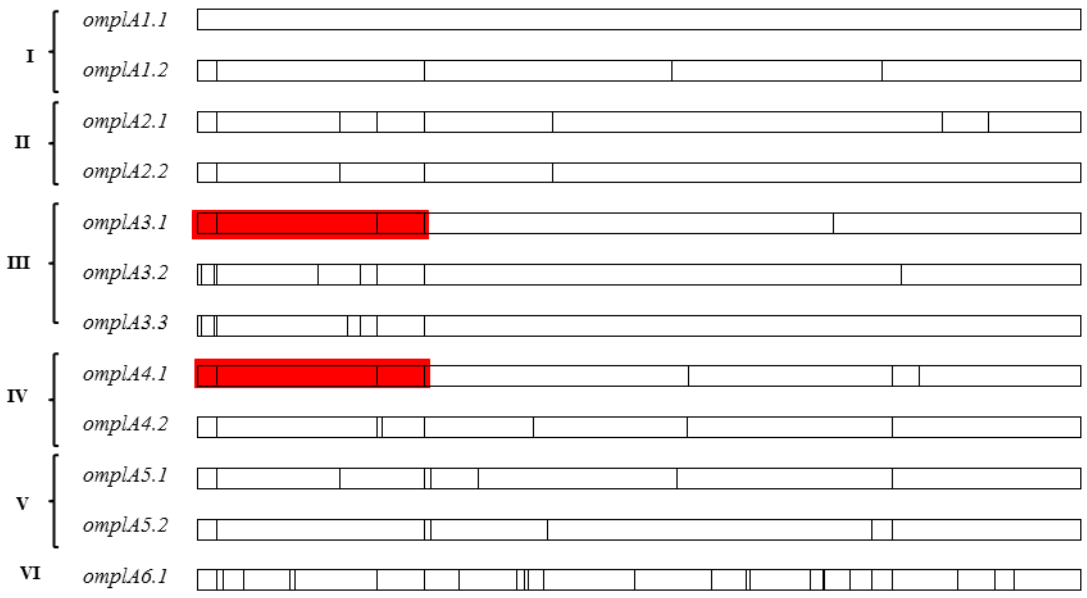

Fig. 2.27 Distribution of polymorphic nucleotide sites among the *ompLA* alleles of *P. multocida*.

Allele designations are shown to the left of each sequence. Roman numerals I to VI represent the phylogenetic lineages (**Fig. 2.26**). Coloured boxes highlight sequence identity and proposed recombinant segments. Graph was created using Micrographic Designer.

2.4 Discussion

Previous population and genetic analyses of 123 isolates of *P. multocida* based on the concatenated partial sequences (3990 bp) of seven housekeeping enzyme genes provides an evolutionary framework with which to compare the evolution of selected gene (Davies *et al.*, unpublished; http://pubmlst.org/pmultocida_multihost). Comparative nucleotide sequence analysis has been used as an effective method for understanding the diversity and evolutionary relationships among various bacterial species (Bastardo *et al.*, 2012; Chaudhuri & Henderson, 2012; Feil *et al.*, 1999; Lemée *et al.*, 2005; Maiden *et al.*, 1998; Mullins *et al.*, 2013; Naushad *et al.*, 2015). Comparative sequence analysis has shown that horizontal DNA transfer, recombination and host switching are involved in the diversification of various virulence factors including outer membrane proteins (Bart *et al.*, 1999; Davies & Lee, 2004; Evans *et al.*, 2010; Ford, 2001), transferrin iron up-take system (Lee & Davies, 2011), leukotoxin (Davies *et al.*, 2001; 2002), aureolysin gene (Sabat *et al.*, 2008), flagellar antigens (Li *et al.*, 1994; Smith *et al.*, 1990), lipopolysaccharide (D'Souza *et al.*, 2005; Reeves, 1993; Reeves *et al.*, 2013) and capsular polysaccharide (Coffey *et al.*, 1998; Wyres *et al.*, 2013).

Phylogenetic trees were constructed based on the concatenated sequences (22,731 bp) of 15 housekeeping genes and also based on the core genome alignment of 40 *P. multocida* isolates. These trees were compared with MLST tree of 123 *P. multocida* isolates associated with different diseases in different host species (cattle, sheep, pigs and poultry). Both trees were in good agreement with the phylogenetic tree based on the concatenated partial sequences of seven housekeeping genes. The phylogenetic relatedness based on seven and fifteen housekeeping enzyme genes and on the core genome, showed evidence of the association of strains with specific host species and diseases. The cluster of isolates associated with different host species could possibly be due to the transmission of *P. multocida* from one host to another and this could possibly play an important role in the generating diversity within the *P. multocida* isolates.

Many OMPs are surface-exposed proteins and, are, therefore subject to different diversification selection pressures and inter-strain heterogeneity (Davies *et al.*, 2004). Molecular mass heterogeneity of the *P. multocida* major OMPs OmpA and OmpH has been determined based on OMP profiles to compare and characterise *P. multocida* of avian, bovine, ovine and porcine origin (Davies *et al.*, 2003a; b; c; Davies, 2004; Davies *et al.*, 2004). The heterogeneity of OmpA and OmpH suggests that these proteins are subject to diversifying selection within the host and might play important roles in host–pathogen interactions (Davies *et al.*, 2004).

In the current study, comparative nucleotide sequence analyses of genes encoding OMPs of different functions were carried out in 40 isolates of *P. multocida* to investigate nucleotide sequence variation, the role horizontal DNA transfer, recombination and host switching in the evolution and diversification of *P. multocida*.

The gene encodings twelve different proteins involved in OM biogenesis and integrity were predicted (E-komon *et al.*, 2012) and these proteins were identified in all genomes (Table 2.4). The degree of nucleotide and amino acid sequence diversity were varied among the 12 genes/proteins and ranged from 2 to 26% nucleotide variation and 2 to 21% amino acid variation. The majority of proteins involved in OM biogenesis and integrity were conserved. This was not surprising and reflect important functions related to maintaining the integrity and functioning of the outer membrane (Ruiz *et al.*, 2006). The d_S/d_N rations for these proteins ranged from 0.9 to 5. A high d_S/d_N ($d_S/d_N > 1$) rations indicates that purifying selection is acting and constraining amino acid changes. No variations in molecular mass were observed with the exception of OmpA suggesting that the OmpA protein is subject to different diversification selection pressure and might play an important role in host–pathogen interactions. Molecular mass heterogeneity of OmpA has been observed in *P. multocida* of avian, bovine, ovine and porcine origin based on OMP profiles (Davies *et al.*, 2003a; b; c; Davies, 2004; Davies *et al.*, 2004). The phylogenetic trees of MltB, NlpB, and MipA showed that horizontal DNA transfer and recombination events have occurred within these genes because the phytogenic trees were not congruent with those based on the concatenated sequences of seven and fifteen housekeeping enzyme genes and on the core genome (Fig. 2.1, Fig. 2.3 & Fig.

2.4). The results showed evidence of exchange of the *mltB4.1*-type allele between isolates of the major porcine pneumonia cluster (MLST group F) and the porcine AR rhinitis cluster. Evidence of exchange of the *mltB* gene was also found in lineage III and suggested that avian and ovine isolates of capsular type F cluster could possibly derived the *mltB* gene (*mltB5*-type allele) from an avian isolate PM82 of the MLLST group H by recombinational exchanges or vice versa (Fig. 2.5).

The comparative sequences analysis of NlpB determined limited variation in both nucleotide and amino acid sequences. NlpB (Bam C) is an outer membrane-associated lipoprotein that is involved in the insertion of OMPs into the outer membrane (Kovacs-Simon *et al.*, 2011). The presence of the identical *nlpB* alleles in isolates associated within different genetic lineages suggests that the *nlpB* gene has undergone horizontal DNA transfer and assortative recombination. Identical *nlpB1.1*-type allele was found in bovine pneumonia isolates of the MLST group A, bovine isolate of the MLST group E and ovine capsular type D isolates (MLST group E). This suggests that the bovine isolate PM564 may originally have derived *nlpB* from ovine capsular type D because PM564 has previously been shown to be clustered within major pneumonia cluster (MLST group A) or vice versa. There was evidence of assortative and intergenic recombination with lineage IV. This lineage was associated with five isolates (3 bovine and 2 porcine) from the major bovine pneumonia cluster (MLST group A), porcine isolates PM382 and porcine AR isolates (MLST group G). This suggests that isolates of the major bovine pneumonia cluster could possibly exchange the *nlpB* gene with porcine isolates or vice versa (Fig. 2.7). Evidence of the *nlpB* gene exchange between bovine and avian isolates was found in lineage V. Host switching of strains from cattle to sheep and vice versa has been shown previously to contribute in the recombinational exchanges and to the emergence of new strains (Davies *et al.*, 2001; 2002; Davies & Lee, 2004; 2011).

MipA is a MLT-A-interacting protein that mediates assembly of enzymes involved in murein biosynthesis. The role of MipA in antibiotic resistance has been investigated in *E. coli* (Zhang *et al.*, 2015). Two different lineages were found and there was evidence of intragenic and assortative recombination especially in isolates associated with *mipA1.1, mipA2.1, mipA4.1* and *mipA4.2* and these alleles were associated with isolates from divergent lineages. The results showed

evidence of exchange of the *mipA2.1*-type allele between isolates of the major porcine pneumonia cluster (MLST group F) and the porcine AR rhinitis isolate PM40 (capsular type A and OMP-type 6.2) (Fig. 2.12). This suggests that PM40 may possibly have acquired its *mipA* gene from porcine pneumonia isolates. Interestingly, the divergent allele *mipA8.1* present in porcine isolates of the porcine AR cluster explained by acquisition from an avian isolate since the *mipA* closely related allele, *mipA8.2* was present in the divergent avian isolate PM82 (Fig. 2.12).

In contrast to genes described above, the *ompA* gene was highly divergent due to extensive recombinational exchanges. It has been identified that this protein is heterogeneous protein based on the OMP profiles (Davies *et al.*, 2003a; b; c; Davies, 2004; Davies *et al.*, 2004) and it has suggested that this due to selection pressure (Davies *et al.*, 2004). The presence of varied patterns of amino acid variation, suggests that these regions are under different selection pressures related to the functions and structure. It has previously been showed OmpA is under strong selective pressure (Davies & Lee, 2004; Hounsome *et al.*, 2011; Vougidou *et al.*, 2015) and is thought to play an importan role in host adaptation (Davies & Lee, 2004) and immune evasion (Joseph *et al.*, 2012). It has also been shown that OmpA is involved in adherence of *P. multocida* (Carpenter *et al.*, 2007; Dabo *et al.*, 2003).

Nucleotide sequence analysis of *ompA* identified 15 different allele types and the phylogenetic tree showed that *ompA* has undergone horizontal DNA transfer and recombinational exchanges because alleles within each lineage were associated with divergent MLST groups. The OmpA domains were identified based on a comparison of *P. multocida* OmpA amino acid alignments with those of the closely related species *M. haemolytica* (Davies *et al.*, 2004). Construction of a predicted secondary structure of OmpA based on amino acid sequence alignments showed that the variation appeared predominantly in the loops regions. The data provide strong evidence that natural selection is driving the diversification in of hypervariable extracellular loop regions because the d_S/d_N ratios for the hypervariable extracellular loop domains (L1, L2, L3 and L4) were all less than 1. Similar selection pressures and evolutionary constraints are involved in different regions of the OmpA of *M. haemolytica* (Davies & Lee, 2004) and P5 outer membrane protein of *H. influenzae* (Duim *et al.*, 1997; Webb

& Cripps, 1998). It has been shown that OmpA is involved in adherence (Carpenter *et al.*, 2007; Dabo *et al.*, 2003; Katoch *et al.*, 2014) and in other pathogenic bacteria binds to specific host cell receptors (Hill *et al.*, 2001; Dabo *et al.*, 2003; Orme *et al.*, 2006; Torres & Kaper, 2003). The location of variable sites within the four hypervariable regions at the distal ends of the surface-exposed loops of OmpA suggests that these regions of OmpA are involved in recognition and receptor binding; it is suggested that the loops are participate in the recognitions of various ligands. For example, they interact with cell-surface receptors (Carpenter *et al.*, 2007; Dabo *et al.*, 2003), colicin (Killmann *et al.*, 1995) and bacteriophage receptors (Morona *et al.*, 1985). The majority of variable sites occurred within four hypervariable regions. This has also been found in the OmpA protein of *P. multocida* isolated from bovine, ovine and porcine origin (Vougidou *et al.*, 2015), *M. haemolytica* (Davies & Lee, 2004) and the P5 outer membrane protein of *H. influenzae* (Duim *et al.,* 1997*;* Webb & Cripps, 1998). It has been suggested that the loops of OmpA confer species-specificity as identified through the use of cross absorbed antibodies (Hounsome *et al.*, 2011). The OmpA family of proteins can serve as targets of the immune system with immunogenicity related to the surface-exposed loops (Confer & Ayalew, 2013). The results here showed that greatest heterogeneity occurred among the *ompA* alleles. Furthermore, recombination has affected the evolution of the *ompA* gene of *P. multocida*. Evidence of exchange of the *ompA* gene between bovine and ovine isolates was found in lineage I. Exchange of the *ompA* gene occurred between the porcine pneumonia cluster (MLST group F) and porcine isolates of the major bovine pneumonia cluster (MLST group A). The diversity and molecular evolutionary relationships of *ompA* were further investigated in a larger selection of *P. multocida* isolates from different host species to better understand potential mechanisms of host adaptation, and to determine whether horizontal gene transfer, recombinational exchange and host-switching of isolates have been in the evolution of the *ompA* gene, and to determine the action of natural selection on amino acid diversity (Chapter 3).

Transport and receptor proteins, twenty five OMPs were identified having transport receptor functions based on the prediction analysis. The functions of these including prions, iron uptake, proteins involved in the secretion of filamentous hemagglutinin and amino acids and capsular polysaccharide

transport. Thirteen different proteins were selected for further analysis, OmpW, ComL, OmpH1, PlpB, HgbA, HasR, HmbR, PfHR, LspB1, IbeB, TolC, Wza and HedX (Table 2.6). The nucleotide and amino acid variation was generally limited. Substantial variation of both nucleotides (32%) and amino acids (32%) was identified in the major porin protein, OmpH1.

The comL gene was also conserved among the *P. multocida* isolates; again the variation was very limited. Twelve different *comL*-type alleles were identified and each allele was associated with isolates of the same genetic lineage. The results showed evidence of exchange of the *comL6.1*-type allele between isolates of the major porcine pneumonia cluster (MLST group F) and the porcine AR rhinitis cluster. This suggests that isolates of the porcine pneumonia cluster may possibly have acquired its *comL* gene from porcine AR isolates or vice versa. The ComL protein is a novel peptidoglycan-linked lipoprotein that functions in natural transformation and competence in N. gonorrhoeae (Fussenegger *et al.*, 1996). In *A. pleuropneumoniae,* ComL was also conserved across serotypes and it has been identified as a potential vaccine candidate (Oldfield *et al.*, 2008).

The *wza* gene of *P. multocida* was selected because it is involved in capsular polysaccharide transport. This gene was present in all genomes. However, only partial sequences were found in ovine capsular type D and bovine isolate PM402 and these were excluded. In *N. meningitidis* the homologous gene (*ctrA*) was found to be conserved among different meningococcal serogroups (Frosch *et al.*, 1992). Although, twelve *wza*-type alleles were identified based on nucleotide sequence comparisons, there was no clear evidence of recombinational exchange within the *wza* gene.

The OmpH1 protein is a major surface-exposed OMP of *P. multocida* and the heterogenicity of the OmpH protein has been described previously based on the OMPs profiles (Davies *et al.*, 2003a; b; c; Davies, 2004; Davies *et al.*, 2004) and it has also been shown that its heterogenicity is due to the presence of a hypervariable surface-exposed loops (Luo *et al.*, 1999). The *ompH1* gene was identified in all genomes and sequence analysis showed that the *ompH1* gene possessed substantial variation (32% in both nucleotides and amino acids). Based on the phylogenetic tree and sequence variation, 17 different *ompH* allele types were identified and each allele was associated with a specific OMP type,

capsular type and ST. Five different lineages were identified and each lineage was associated with isolates from different genetic lineages (Fig. 2.18). Each *ompH* alleles was associated with isolates of the same capsular types, OMP-types and STs. Based on amino acid sequence comparison, variation appeared almost exclusively in the loop regions of the OmpH1 protein. The presence of variation within the loop regions of the OmpH1 protein has previously been described in *P. multocida* (Luo *et al.*, 1999). All loop regions had a d_S/d_N ratio of 0.5 suggesting that natural selection is driving diversification of the hypervariable extracellular loops. The high degree of variation in the external loops for adaptation under selective pressures exerted by host immune system and other environmental conditions (Singh *et al.*, 2011). Major variation occurred in *ompH* alleles within lineages II to V. The sequence variation of OmpH1 may have functional consequences because it has been observed that the sequences variation in other OMPs may results in antigenic variation of surface-exposed loops (Singh *et al.*, 2011). In *P. multocida*, OmpH is a major antigenic and surface exposed OMP (Dabo *et al.*, 2007; Garrido *et al.*, 2008; Luo *et al.*, 1997; Okay *et al.*, 2012; Tan *et al.*, 2010). The presence of identical or almost identical *ompH1* alleles in lineage I (*ompH1.1*- to *ompH1.5*-type alleles) between bovine and ovine isolates from the divergent lineages indicating the *ompH1* has undergone horizontal DNA transfer and assortative recombination. The results suggest that bovine isolates have derived *ompH1* from the ovine isolates of the capsular type D or vice versa. Assortative recombination also occurred within lineage II. Identical *ompH4.2*-type allele was found in porcine pneumonia isolates of the MLST group F and porcine AR isolate PM926. This suggests that the porcine isolate PM926 may originally have derived *omph1* from porcine pneumonia isolates or vice versa. Evidence of exchange between avian and porcine was also occurred within lineage II. Overall, *ompH1* has undergone horizontal DNA transfer and recombination because complex mosaic structures were identified in the *ompH1* alleles within divergent lineages. Nucleotide sequence analysis of the gene encoding the porin protein of the pathogenic Neisseria species revealed that horizontal genetic exchange has resulted in the emergence of new porin classes (Derrick *et al.*, 1999).

Adherence protein, ComE/pilQ is involved in pilus formation (Boyd *et al.*, 2008). Based on phylogenetic tree assortative recombination has affected the

comE gene of *P. multocida* especially alleles within lineage III (Fig. 2.23). Exchange of the *comE* gene has occurred between isolates of different genetic lineages. The results showed evidence of exchange of the *comE.1*-type allele between isolates (PM316, PM564 and PM344) of the major bovine pneumonia cluster (MLST group A) and bovine isolate PM336 of the major porcine pneumonia cluster (MLST group F). This indicates that bovine isolate PM336 may possible have acquired its come gene from bovine pneumonia isolates. Exchange of the *comE1.2*-type allele between bovine and porcine isolates of the MLST group A and bovine isolates PM302 of the MLST E was also occurred. This suggests that bovine isolates could possible exchanges the come with porcine isolates or vice versa. Identical *comE2.1*-type allele was found in ovine isolate PM966 of the MLST group B and bovine isolate PM490 of the MLST group E. This suggests that the ovine isolate PM966 may originally have derived *comE* from bovine isolate PM490 or vice versa and this another evidence of host switching from bovine to ovine or vice versa.

Genes that were part of tad locus, *rcpA* and *tadD,* were obtained from only 24 isolates. These genes are required for assembly of adhesive Flp. The *rcpA* and *tadD* genes were not found in ovine capsular type D isolates (PM122. PM964, PM982, PM986 and PM988), bovine isolates PM302 and PM402. Isolates associated porcine atrophic rhinitis (PM684, PM918, PM926, PM848, PM696, PM714 and 200 except PM40), porcine isolate PM382 and bovine isolate PM302 (MLST group E) were also excluded from the analysis because only partial sequences were obtained. The degree of variation in both genes was very limited. It has been demonstrated that in any bacterial species tad genes have been acquired from foreign sources and have been implicated in the pathogenesis of these species (Clock *et al.*, 2008).

Phospholipase A (OmplA) was present in the genomes of all 40 isolates among all genomes. The results showed evidence of exchange of the *ompLA4.2*-type allele between isolates of the major porcine pneumonia cluster (MLST group F) and the porcine AR rhinitis cluster. This suggests that isolates of the porcine pneumonia cluster may possibly have acquired its *ompLA* gene from porcine AR isolates or vice versa. The degree of nucleotide and amino acid variation were limited. The predicted function of OmpLA is the hydrolysis of phospholipids on the outer surface of the OM (Hatfaludi *et al.*, 2010). It has also been shown to be involved

in the virulence of *Campylobacter* and *Helicobacter* strains (Koebnik *et al.*, 2000).

2.5 Conclusions

Phylogenetic trees based on the concatenated partial sequences (3990 bp) of the seven housekeeping enzyme genes, complete sequences (22,371 bp) of the fifteen housekeeping enzyme genes and on the core genome were almost identical in their topographies. They showed evidence of the association of strains with specific host species and diseases. Horizontal gene transfer and recombination (intragenic and assortative) have occurred within the genes encoding *P. multocida* OMPs. These mechanisms have contributed to the allelic diversity within each gene. Recombinational exchanges were identified based on sequence comparisons and also based on phylogenetic tree comparisons with those of the 7 and 15 housekeeping enzyme genes and core genome. High levels of nucleotide and amino acid sequence variation was found within two major surface-exposed proteins, OmpA and OmpH1. The results indicated these two proteins have undergone extensive horizontal DNA transfer, intragenic and assortative recombination. Variation in OmpA and OmpH1 occurred predominantly in the loop regions. In OmpA the variation has occurred at the tips of the loops. There was strong evidence that natural selection is driving diversification of the hypervariable extracellular loop regions in both OmpA and OmpH. Three mechanisms may contribute to the horizontal DNA transfer and recombinational exchanges in bacteria and these processes are transformation of DNA segment, transduction (bacteriophage) and conjugation (Chaguza *et al.*, 2015). These recombination events observed within the gene encoding OMPs of *P. multocida* could possibly be due to one these mechanisms. Therefore, the diversity of bacteriophages in *P. multocida* will be investigated and these phages will be analysed to determine whether they carry any virulence genes including genes encoding OMPs.

Chapter 3 Diversity and molecular evolution of *P. multocida* OmpA from different host species

3.1 Introduction

One of the major OMPs of *P. multocida* is the heat-modifiable outer membrane protein A (OmpA) which is an integral component of the outer membrane of Gram-negative bacteria (Beher *et al.*, 1980). OmpA is present at about 100,000 copies per cell (Confer & Ayalew, 2013; Koebnik *et al.*, 2000) and is a major immunogenic and antigenic OMP that is conserved, surface-exposed and expressed in vivo (Carpenter *et al.*, 2007; Dabo *et al.*, 1997; 2003; 2008). OmpA is a multifunctional protein. It is involved in the maintenance of outer membrane integrity and cell shape (Hatfaludi *et al.*, 2010; Sonntag *et al.*, 1978) because the periplasmic domain binds to the peptidoglycan layer (Pautsch & Schulz, 1998). OmpA serves as a potential secondary receptor for P22-like phage infection in *Salmonella* (Jin *et al.*, 2015), phage Sf6 in *Shigella flexneri* (Parent *et al.*, 2014; Porcek & Parent, 2015) and *E. coli* bacteriophages (Morona *et al.*, 1985). and play a role in conjugation (Klimke *et al.*, 2005; Skurray *et al.*, 1974; van Alphen *et al.*, 1977). The OmpA protein is also involved in biofilm formation (Orme *et al.*, 2006) and adherence to host tissue (Dabo *et al.*, 2003; Hill *et al.*, 2001; Torres & Kaper, 2003), acts as both an immune target and an evasin (Smith *et al.*, 2007), and stimulates pro-inflammatory cytokine production (Confer & Ayalew, 2013). It is one of the major surface antigens of Gram-negative bacteria and is therefore an important target in immune defence against many bacterial pathogens and may serve as potential vaccine candidates (Confer & Ayalew, 2013; Hounsome *et al.*, 2011; Tian *et al.*, 2011; Yan *et al.*, 2010). The 35-kDa OmpA protein has been well studied and characterised in *E. coli* and is composed of a 19 kDa (177 residues) transmembrane domain and a 16 kDa globular C-terminal domain (Arora *et al.*, 2001; Confer & Ayalew, 2013; Pautsch & Schulz, 1998; Pautsch & Schulz, 2000). Nuclear magnetic resonance (NMR) spectroscopy and X-ray crystallography were used to solve the crystal structure of the transmembrane domain of OmpA (Arora *et al.*, 2001; Pautsch & Schulz, 1998; Pautsch & Schulz, 2000). This structure consists of an eight antiparallel ß-barrel stranded and four flexible, mobile surface exposed loops (Arora *et al.*, 2001; Confer & Ayalew, 2013; Davies & Lee, 2004; Pautsch &

Schulz, 1998; Pautsch & Schulz, 2000; Smith *et al.*, 2007). It has been suggested that the loops of OmpA confer species-specificity as identified through the use of cross absorbed antibodies (Hounsome *et al.*, 2011). In *P. multocida,* OmpA has been cloned and characterised and its immunological properties have also been studied (Dabo *et al.*, 2003). It has been shown that OmpA is involved in adherence through interaction with extracellular matrix molecules (Dabo *et al.*, 2003; Carpenter *et al.*, 2007). A study by Dabo *et al.* (2008), demonstrated that recombinant OmpA has a detrimental effect on the efficacy of vaccination with OMPs in mice and targeted inactivation of *ompA* in *P. multocida* 232 represents a potential mean towards the development of an effective vaccine candidate. Horizontal transfer and recombination of DNA segments (intragenic) or entire genes (assortative) are recognised as major determinants in the evolution and diversification of bacteria (Chaguza *et al.*, 2015; Li *et al.*, 1994; Kelly *et al.*, 2009; Ochman *et al.*, 2000; Smith *et al.*, 1990). It has been shown that horizontal DNA transfer and recombination are involved in the diversification of various virulence factors in both Gram-positive and Gram-negative bacteria, including outer membrane proteins (Bart *et al.*, 1999; Davies & Lee, 2004; Evans *et al.*, 2010; Ford, 2001), transferrin iron up-take system (Lee & Davies, 2011), leukotoxin (Davies *et al.*, 2001; 2002), aureolysin gene (Sabat *et al.*, 2008), flagellar antigens (Li *et al.*, 1994; Smith *et al.*, 1990), lipopolysaccharide (D'Souza *et al.*, 2005; Reeves, 1993; Reeves *et al.*, 2013) and capsular polysaccharide (Coffey *et al.*, 1998; Wyres *et al.*, 2013). In the closely related species *M. haemolytica* OmpA is under strong selective pressure from its host (cattle or sheep) and is thought to play an important role in host adaptation (Davies & Lee, 2004). The *ompA* gene in *P. multocida* may experience similar selective pressure and undergo similar evolutionary processes resulting in increased genetic variation and diversity.

The aims of this part of the study were as follows: to investigate the diversity and molecular evolutionary relationships of *ompA* in a large selection of *P. multocida* isolates from different host species to better understand potential mechanisms of host adaptation, to determine if horizontal gene transfer, recombinational exchange and host-switching of isolates are involved in the evolution of the *ompA* gene and to determine the action of natural selection on amino acid diversity in the OmpA domains. To achieve these aims, the *ompA*

gene were sequenced in *P. multocida* strains representing various host species, diseases, capsular types, OMP types and sequence types. An established framework of evolutionary relationships among 123 isolates of *P. multocida* based on the concatenated sequences (3990 bp) of seven housekeeping enzyme genes was used to determine the role of horizontal DNA transfer and recombination in OmpA evolution

3.2 Materials and methods

3.2.1 Bacterial isolates

Seventy four *P. multocida* isolates were selected to investigate the diversity and evolution of OmpA. The isolates were recovered from different host species (cattle, sheep, pigs and poultry) and were associated with different diseases, they have been investigated in previous studies (Davies *et al.*, 2003a; b; c; Davies, 2004; Davies *et al.*, 2004). The strains represented various capsular serotypes, outer membrane protein types, 16S rRNA types, and sequence types (Davies *et al.*, unpublished; http://pubmlst.org/pmultocida_multihost). The properties of the isolates are listed in Table 2.1

3.3 Bacterial growth conditions

3.3.1 Media for bacterial growth

Both brain heart infusion agar (BHIA; Oxoid) and brain heart infusion broth (BHIB; Oxoid) were used as routine solid and liquid media, respectively, for the growth of *P. multocida*. The bacterium was cultured on blood agar (BHIA containing 5% (v/v) defibrinated sheep's blood [E & O Laboratories Limited]). BHIB was used for the preparation of overnight broth cultures. All media were sterilised by autoclaving at 120°C for 15 min.

Table 3.1 Properties of 74 *P. multocida* isolates.

Isolate [a]	ST [b]	MLST group	Host species	Clinical symptoms	Isolation site	Geographical origin	Capsular type	OMP-type [c]	16S rRNA type
PM316	1	A	Bovine	Pneumonia	Lung	Penrith	A	1.1	3
PM386	1	A	Bovine	Pneumonia	Lung	Winchester	A	1.1	1
PM564	1	A	Bovine	Pneumonia	Lung	Thirsk	A	2.1	3
PM600	1	A	Bovine	Pneumonia	Lung	Penrith	A	2.1	3
PM628	2	A	Bovine	Pneumonia	Lung	Bristol	A	2.1	3
PM344	3	A	Bovine	Pneumonia	Lung	Shrewsbury	A	3.1	1
PM384	3	A	Bovine	Pneumonia	Lung	Thirsk	A	3.1	1
PM414	3	A	Bovine	Respiratory distress	Nasal swab	Preston	A	4.1	1
PM338	4	A	Bovine	Pneumonia	Lung	Starcross	A	4.1	6
PM632	4	A	Bovine	Pneumonia	Lung	Winchester	A	4.1	1
PM430	3	A	Bovine	Pneumonia	Lung	Penrith	A	8.1	1
PM520	ND	A	Bovine	Pneumonia	Nasal swab	Carmarthen	A	8.1	ND [d]
PM666	3	A	Porcine	Pneumonia	Lung	Sutton Bonington	A	2.1	1
PM914	3	A	Porcine	Pneumonia	Lung	Winchester	A	2.1	1
PM116	3	A	Porcine	Pleuropneumonia	Lung	Sutton Bonington	A	3.1	1
PM656	3	A	Porcine	Pneumonia	Lung	Langford	A	3.1	1
PM830	3	A	Porcine	Atrophic rhinitis	Nasal swab	Thirsk	A	3.1	1
PM966	16	B	Ovine	Pneumonia	Lung	Winchester	A	1.1	1
PM974	16	B	Ovine	Pneumonia	Lung	Newcastle	A	1.1	1
PM30	44	B	Bovine	Haemorrhagic septicaemia	Nasal swab	Burma	B	ND	ND
PM1192	46	B	Bovine	Haemorrhagic septicaemia		Sri Lanka	B	ND	ND
PM1200	44	B	Bovine	Haemorrhagic septicaemia		Pakistan	B	ND	ND
PM382	13	B	Porcine	Respiratory problems	Lung	Winchester	A	4.1	2
PM706	13	C	Porcine	Pneumonia	Lung	Lincoln VIC	UT	4.1	2
PM2	17	C	Ovine	Severe peritonitis	ND	Penrith	F	2.1	4
PM8	17	C	Ovine	Asymptomatic	Vagina	Penrith	F	2.1	4
PM246	25	C	Avian	Septicaemia	Viscera	Bury St. Edmunds	F	2.2	2
PM306	8	C	Bovine	Oedema	Eyes	Sutton Bonington	F	7.1	2
PM44	12	C	Ovine	Asymptomatic	Vagina	Penrith	F	1.1	4
PM994	12	C	Ovine	Pneumonia	Lung	Penrith	F	1.1	2

Table 2.1 (continued)

Isolate [a]	ST [b]	MLST group	Host species	Clinical symptoms	Isolation site	Geographical origin	Capsular type	OMP-type [c]	16S rRNA type
PM258	12	C	Avian	Septicaemia	Viscera	Bury St. Edmunds	A	2.2	ND
PM148	12	C	Avian	Eye infection	Eye	Thirsk	F	2.2	2
PM952	12	C	Porcine	Pneumonia	Lung	Thirsk	F	3.2	2
PM210	23	C	Avian	Anorexic/depressed	Lung	Reading	A	2.1	1
PM104	28	D	Avian	Septicaemia	Liver /spleen	Aberystwyth	A	4.1	9
PM86	15	D	Avian	Fowl cholera	Pleura	Winchester	A	3.1	1
PM934	15	D	Porcine	Pneumonia	Lung	Bristol	A	5.1	1
PM954	15	D	Porcine	Pneumonia	Lung	Winchester	A	5.1	1
PM486	9	D	Bovine	Pneumonia	Lung abscess	Bristol	A	9.1	1
PM422	ND	ND	Bovine	Pneumonia	Nasal swab	Worcester	A	9.1	ND
PM62	39	E	Avian	Respiratory symptoms	Nasal swab	Thirsk	B	12.1	8
PM530	6	E	Bovine	Pneumonia	Lung	Winchester	A	5.2	ND
PM302	6	E	Bovine	Rhinitis + others	Nasal swab	Sutton Bonington	A	5.3	ND
PM548	6	E	Bovine	Vaginal discharge	Vaginal mucus	Winchester	A	5.3	7
PM528	6	E	Bovine	Pneumonia	Lung	Starcross	A	5.4	ND
PM144	21	E	Avian	Septicaemia	Lung/liver	Thirsk	A	1.1	2
PM310	21	E	Avian	Poor condition/mopey	Liver	Winchester	A	1.1	ND
PM702	14	E	Porcine	Pneumonia	Lung	Lincoln VIC	A	5.1	1
PM402	5	E	Bovine	Pneumonia	Lung	Newcastle	A	5.1	1
PM980	20	E	Ovine	Pneumonia	Lung	Sutton Bonington	D	3.2	ND
PM122	ND	ND	Ovine	Pneumonia	Lung	Sutton Bonnington	D	3.1	ND
PM982	18	E	Ovine	Pneumonia	Lung	Carmarthen	D	3.1	1
PM986	18	E	Ovine	Pneumonia	Lung	Luddington	D	3.1	1
PM54	10	F	Porcine	Pneumonia	Lung	Shrewsbury	A	1.1	1
PM734	10	F	Porcine	Pneumonia	Lung	Cambridge VIC	A	1.1	2
PM820	10	F	Porcine	Pneumonia	Lung	Thirsk	A	1.1	2
PM850	10	F	Porcine	Pneumonia	Lung	Bury St Edmunds	A	1.1	2
PM200	10	F	Avian	Pneumonia	Lung	Bristol	A	1.2	ND
PM288	10	F	Avian	Pneumonia	Lung	Bury St. Edmunds	A	1.2	2
PM336	7	F	Bovine	Pneumonia	Lung	Sutton Bonington	A	6.1	2

Table 2.1 (continued)

Isolate [a]	ST [b]	MLST group	Host species	Clinical symptoms	Isolation site	Geographical origin	Capsular type	OMP-type [c]	16S rRNA type
PM368	7	F	Bovine	Pneumonia	Lung	Sutton Bonington	A	6.1	2
PM684	11	G	Porcine	Suspect snouts	Nasal swab	Cambridge VIC	A	6.1	2
PM918	11	G	Porcine	Pneumonia	Lung	Shrewsbury	A	6.1	ND
PM716	11	G	Porcine	Toxin Assay	Nasal swab	Cambridge VIC	D	4.1	2
PM848	11	G	Porcine	Pneumonia	Lung	Starcross	D	4.1	ND
PM696	11	G	Porcine	Toxin Assay	Nasal swab	Cambridge VIC	D	6.1	ND
PM714	11	G	Porcine	Pneumonia	Lung	Thirsk	D	6.1	5
PM762	11	G	Porcine	Rhinitis	Turbinate	Worcester VIC	D	6.1	2
PM818	11	G	Porcine	Pneumonia	Lung	Bristol	D	6.1	5
PM226	11	G	Avian	Pneumonia/death	Lesion	Sutton Bonington	D	13.1	ND
PM60	36	H	Avian	Septicaemia	Heart	Thirsk	UT	10.1	17
PM82	32	H	Avian	Swollen heads3	Peritoneal	Bury St Edmunds	A	7.1	19
PM300	33	H	Avian	Septicaemia	Lung/liver	Sutton Bonington	A	7.1	ND
PM152	31	H	Avian	Swollen joints	Synovial fluid	Bury St. Edmunds	A	6.1	13

[a] isolates are arranged by order of MLST group (column 3) (Fig. 2.1); [b] ST= sequence type (Davies *et al*., unpublished http://pubmlst.org/pmultocida_multihost/); [c] OMP-types for bovine, ovine, porcine and avian are not equivalent, i.e. bovine OMP-type 1.1 is not as same as porcine OMP-type 1.1, etc. (Davies *et al.*, 2003a; b; c; Davies, 2004; Davies *et al.*, 2004); [d] ND: not determined.

3.3.2 Bacterial storage and growth conditions

P. multocida isolates were preserved in 1 ml of 50% (v/v) glycerol in BHIB at -80°C for long-term storage. Fifteen microliters of thawed stock suspensions were streaked onto blood agar plates and incubated at 37°C overnight.

3.3.3 Preparation of broth starter cultures

Liquid cultures were prepared by inoculating 3 to 4 well-isolated colonies from overnight culture plates into 10 ml volumes of BHIB in Universals and incubating at 37°C with shaking at 120 rpm.

3.4 Nucleotide sequence analysis

3.4.1 Primer design for amplification and sequencing of the *ompA* gene

The complete genome of *P. multocida* strain PM70 (accession number: NC_002663) was used as a reference genome to identify the location of the *ompA* gene. The *ompA* gene was found to be located at position 928243 to 929304 in the PM70 genome by Blast analysis. The *ompA* gene is annotated as a membrane protein (locus tag: PM_RS04060). To sequence the *ompA* gene, primers were designed in the flanking genes. The minimum region required to be sequenced was 1710 bp which includes *ompA* (1062 bp) and noncoding intergenic regions between *ompA* and PM_RS04055 (98 bp) and between *ompA* and PM_RS04065 (550 bp) (Fig. 3.1 & Fig. 3.2). The identities of *ompA* and both flanking genes were determined in *P. multocida* genomes by BLAST analysis against the National Centre for Biotechnology Information (NCBI) database (http://www.ncbi.nlm.nih.gov/genome/genomes/912).

The sequences of both flanking genes were aligned using the Lasergene Megalign (DNA star, Inc.) software. The consensus sequence of both flanking genes were used to design primers for the preliminary amplification and first stage sequencing of the *ompA* genes in the *P. multocida* isolates The computer program Primer Designer (v2.0) was used to design primers for the preliminary PCR amplification and first stage sequencing of the *ompA* gene. The primers were synthesised by Sigma-Aldrich (Sigma, United Kingdom). Two forward and

two reverse primers were designed within conserved regions of the aligned sequences of the two flanking genes for the initial PCR amplification of *ompA*. Successfully amplified bands were partially sequenced (first stage sequencing) and a second set of internal sequencing primers (nested system) were designed the within conserved region of the aligned sequences of both flanking genes. However, in specific individual strains, the same primers that were used for the preliminary amplification were also selected for the first stage sequencing. The internal sequencing primers for the second stage sequencing were designed when the data for the first stage sequencing were available. The process of (sequencing-primer design-sequencing) was continued until the entire *ompA* gene was covered (Fig. 3.2). The entire *ompA* gene was covered by two forward and three reverse reactions. All primers were designed to a length of 18 nucleotides except primer PM/OMPA/R2.1/S2 (#646: CGATGTAAGGAATTAGACTG) which contained 20 nucleotides. The primers were adjusted to 12.5 pmol μl^{-1} for PCR reactions and to 3.2 pmol μl^{-1} for sequencing reactions. The nucleotide sequences of each primer used for PCR amplification and sequencing of *ompA* fragment are showed in Fig. 3.3, Fig. 3.4 & Fig. 3.5. Details of the nucleotide sequences of the primes used for PCR amplification and sequencing are provided in Table 3.2.

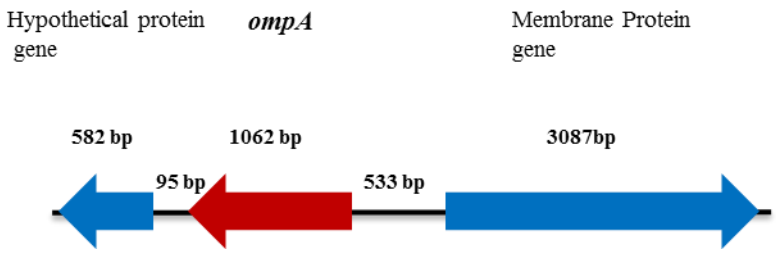

Fig. 3.1 Location of *ompA* gene within genome of avian *P. multocida* strain PM70.

The *ompA* gene was found to be located at position 928243 to 929304 within genome of avian *P. multocida* strain PM70 (accession number: NC_002663). The *ompA* gene is located downstream of the gene encoding hypothetical protein (PM_RS04055) and upstream of the gene encoding membrane protein (PM_RS04065). In order to amplify *ompA* gene, the primers need to be located in the two flanking genes. The genes are indicated by colored arrows *ompA* (red) and flanking genes (blue). The straight lines between genes (black) indicate intergenic regions. The numbers on the top represent the length of *ompA* gene, flanking genes and non-coding intergenic regions.

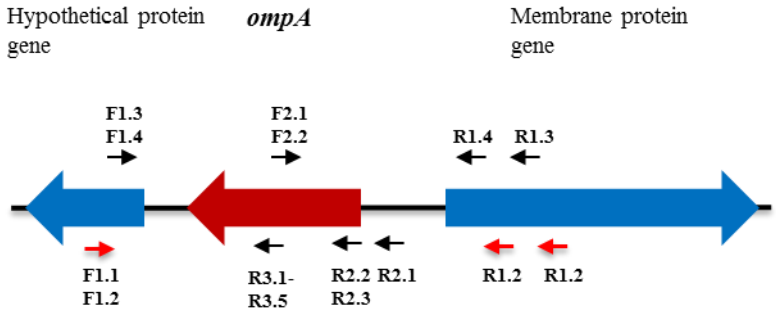

Fig. 3.2 Locations and numerical designations of PCR amplification and sequencing primers.

The positions of the primers used for sequencing are indicated by black arrows; red arrows represent position of the primers used for PCR amplification of *ompA*. The details of the primers are listed in

Table **3.2**.

Table 3.2 Details of oligonucleotide primers for sequencing of *ompA*.

Primer name [a]	Designation [b]	Primer's use [c]	Sequence (5'–3´)	Position [d]
PM/OMPA/F1.1	#626	P and S1	CGCAAGTTGTTCTTCGGA	301-318
PM/OMPA/F1.2	#627	P	TCGCGCTTCTATCACTTG	358-375
PM/OMPA/R1.1	#628	P	TTAGTGCCAGTTCCACCA	255-272
PM/OMPA/R1.2	#629	P and S1	TGCTTGTGGTAGTTGCTG	145-162
PM/OMPA/F1.3	#636	S1	CGCTCGACGTTGATAAGA	442-459
PM/OMPA/F1.4	#637	S1	AGCCACGATGATGAGAAC	550-567
PM/OMPA/R1.3	#638	S1	TGACCACATCTGCGATAC	179-196
PM/OMPA/R1.4	#639	S1	CAAGTGGTGTAAGCTGTG	26-43
PM/OMPA/F2.1	#641	S2	ACCAGCTGTTACAGAACC	424-442
PM/OMPA/F2.2	#644	S2	ACCAGCTGTTACAGAGCC	424-441
PM/OMPA/R2.1	#646	S2	CGATGTAAGGAATTAGACTG	Intergenic region
PM/OMPA/R2.2	#647	S2	CATTGACTATCGTTGCAC	1043-1025
PM/OMPA/R2.3	#648	S2	CATTGACTATCGCTGCAC	1043-1025
PM/OMPA/R3.1	#649	S3	CTCCAGTATTCGCAGGTG	575-557
PM/OMPA/R3.2	#650	S3	CTCCTGTATTCGCGGGTG	575-557
PM/OMPA/R3.3	#651	S3	CTCCAGTATTTGCAGGTG	575-557
PM/OMPA/R3.4	#652	S3	CTCCAGTATTTGCGGGTG	575-557
PM/OMPA/R3.5	#653	S3	CCCCTGTCTTTGCGGGTG	575-557

[a]PM/OMPA/F1, PM/OMPA/Forward 1; PM/OMPA/R1, PM/OMPA/Reverse 1

[b]the position of the primers are shown in Fig. 3.3, Fig. 3.4 & Fig. 3.5.

[c]P: PCR Amplification; S1: first stage of sequencing; S2: second stage of sequencing; S: third stage of sequencing.

[d]Nucleotide position corresponding to the first 5' bp of primer within hypothetical protein gene (locus tag: PM_RS04055) (Fig. 3.3), membrane protein gene (locus tag: PM_RS04065) (Fig. 3.4) and the *ompA* gene (Fig. 3.5).

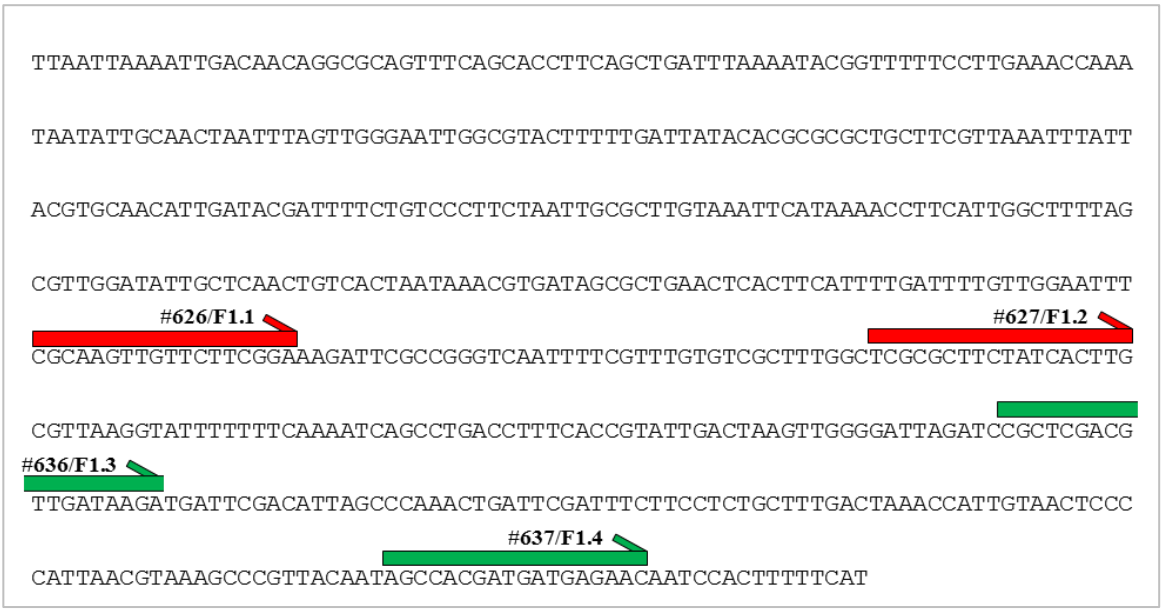

Fig. 3.3 Nucleotide sequence of flanking gene (5'—3') (hypothetical protein, PM_RS04055) of PM70.

The positions of preliminary PCR primers (red; forward 1 and forward 2) and internal primers used for the first stage sequencing (green; forward 1 and forward 2) are shown.

Fig. 3.4 Nucleotide sequence of flanking gene (membrane protein, PM_RS04065) of PM70.

The positions of preliminary PCR primers (red; reverse 1 and reverse 2) and internal primers used for the first stage sequencing (green; reverse 1 and reverse 2) are shown.

Fig. 3.5 Nucleotide sequence of *ompA* gene (PM_RS04060) of PM70.

The positions of primers used for the second and third stages of sequencing (forward primer 2 and reverse primer 2 [green] and reverse primer 3 [red] are shown

3.4.2 PCR amplification of *ompA* gene

3.4.2.1 Chromosomal DNA preparation

DNA was prepared using InstaGene matrix (Biorad, 732-6030) according to the manufacturer's instructions. From overnight plate cultures, 3 to 4 colonies were inoculated into 10 ml of BHIB. The broth cultures were incubated overnight at 37°C with shaking at 120 rpm. Bacterial cells from 1 ml of each overnight culture were harvested by centrifugation at 13,000 *x g* for 1 min. The supernatants were carefully removed and the pellets resuspended in 1 ml of autoclaved distilled water. The mixtures were vortexed for 5-10 s and centrifuged at 13,000 *x g* for 1 min. The supernatants were discarded and the pellets resuspended in 200 µl of InstaGene matrix. The suspensions were incubated at 56°C for 30 min, vortexed at high speed for 5-10 s and placed in a 100°C water bath for 8 min. The samples were vortexed at high speed for 5-10 s and centrifuged at 13,000 *x g* for 3 min, Two microliters of prepared DNA were used for PCR amplification. The prepared DNA samples were stored at –20°C.

3.4.2.2 PCR components

The *ompA* gene was amplified using a Taq DNA polymerase kit (Platinum *Pfx* DAN *Taq* polymerase, Invitrogen). PCR reactions were performed in 0.2 ml PCR tubes (Star lab), according to the manufacturer's instructions, using a total reaction volume of 50 µl. Each reaction comprised the following reagents: 29.5 µl dH_2O, 1.5 µl 50 mM $MgSO_4$, 5 µl 10x PCR buffer, 4 µl 1.25 mM dNTPs (GE Health Care), 4 µl of each forward and reverse primer (12.5 pmol µl-1), 2 µl of template DNA and 0.2 µl of Taq polymerase.

3.4.2.3 Optimisation of PCR conditions and parameters

Amplification of the *ompA* gene was first optimised in isolates PM144 (avian), PM564 (bovine), PM734 (porcine) and PM966 (ovine) using different primer pair combinations and an annealing temperature of 55°C. The following primer pair combinations were used (

Table 3.2): #626 (F1.1)/#628 (R1.1), #626 (F1.1)/#629 (R1.2), #627 (F1.2)/#628 (R1.1) and #627 (F1.2)/#629 (R1.2). Another set of internal primers for first stage sequencing (two forward and two reverse) were designed and the following

combinations were used to check the amplification of *ompA* using an annealing temperature of 55°C: #636/#638, #636/#639, #637/#638 and #637/#639. Amplification was also optimised to remove non-specific bands by using variable annealing temperatures (gradient PCR: 55, 56, 57, 58 and 59°C) with primer pair #626 and #629.

3.4.2.4 PCR amplification

PCR amplification was carried out in a Veriti 96-Well Thermo Cycler (Applied Biosystems). The following PCR parameters of 30 cycle reactions were used to for amplification of *ompA*: initial denaturation at 94°C for 2 min, denaturation at 94°C for 45 s, annealing at 59°C for 45 s, extension at 72°C for 2 min and a final extension step at 72°C for 10 min. However, for particular isolates nonspecific products were observed in agarose gels. In these cases, the PCR products were improved by varying the annealing temperature between 55°C and 61°C. The PCR products were stored at -20°C.

3.4.2.5 Agarose gel electrophoresis

Amplification of PCR products was confirmed by electrophoresis in a 1% (w/v) agarose gel prepared with 1× TAE buffer containing Syber® Safe (Invitrogen). Five microliters of each PCR product were mixed with 1 µl 10x gel loading buffer (Blue Juice: Invitrogen) and 5 µl were loaded onto wells. The size of the PCR product was indicated by loading 5 µl of 1kb DNA ladder (Sigma-Aldrich, UK) into the first and last wells. The fragment sizes were visualised and photographed under UV light.

3.4.3 Sequencing of the *ompA* gene

3.4.3.1 Purification of PCR products

The PCR products were purified using a Qiagen QIAquick DNA purification kit (Qiagen) according to the manufacturer's instructions. Two hundred and fifty microliters of buffer PB were added to 50 µl of each PCR product and mixed thoroughly. The mixtures were transferred to QIAquick spin columns. The QIAquick spin columns were centrifuged at 13,000 ***x g*** for 1 min. The columns were removed from the tubes, the supernatants discarded and the columns were

placed back into the same tube. Seven hundred and fifty microliters of buffer PE were added and the columns again centrifuged at 13,000 *x g* for 1 min. The supernatants were discarded and the columns centrifuged at 13,000 *x g* for an additional 1 min. The columns were removed and placed in clean 1.5 microfuge tubes. The DNA was eluted by adding 50 µl of sterile dH_2O, allowing to stand for 1 min and centrifuging at 13,000 *x g* for 1 min. The purity and concentration of DNA were examined using a NanoDrop 2000C spectrophotometer (Thermo Scientific). Purification of DNA was also verified by electrophoresis as described above. The concentrations of purified DNA ranged between 40 to 50 ng/µl and. DNA samples were stored at -20^{o}C for sequencing reactions.

3.4.3.2 Optimisation of sequencing reaction

Four isolates, PM144 (avian), PM564 (bovine), PM734 (porcine) and PM966 (ovine) were selected to optimise BigDye terminator dilutions. BigDye terminator was diluted: 1:4, 1:8, 1:16 and 1:32 in dilution buffer. The sequencing reactions were performed in 10 µl reaction mixes according to the BigDye Terminator Cycle Sequencing kit v3.1 instructions. Each reaction mixture consisted of 4.5 µl of purified DNA, 2 µl of forward or reverse sequencing primer (3.2 pmol/µl) and 4 µl of BigDye terminator dilutions.

3.4.3.3 Components of sequencing

Purified PCR products were sequenced with the BigDye Terminator Cycle Sequencing kit v3.1. (Applied Biosystems). The sequencing reactions were performed in 10 µl reaction mixes according to manufacturer's instructions. Each reaction consisted of 4 µl of purified DNA, 2 µl of forward or reverse sequencing primer (3.2 pmol / µl), and 4 µl of BigDye terminator mix at a dilution of 1:16. Sequencing reactions were performed in a Gene Amp PCR System 9700 Thermo Cycler (Applied Biosystems) using 0.2 ml PCR reaction tubes (Star lab). The following amplification parameters of 30 cycles were used: denaturation at 96°C for 10 s, annealing at 50°C for 5 s, and extension at 60°C for 4 min. The samples were held at 4°C. Sequence analysis was performed in an ABI 3730xl DNA Analyser (Applied Biosystems) by Source Bioscience Sequencing Service, Glasgow, UK (http://www.lifesciences.sourcebioscience.com/genomic-services/sanger-sequencing-service/).

3.4.4 Data analysis: nucleotide and amino acid sequences

The sequencing results were received as .ab1 chromatogram files. The sequence files were viewed, trimmed, edited and analysed with SeqMan (DNAstar, Inc.). The trimmed sequences were from 550 to 900 nucleotides in length. SeqMan was also used to check and correct any sequencing errors. MegAlign (DNAstar, Inc.) was used to align the sequences for each sequencing stage and, in conjugation with Primer Designer, identify the optimum location of primers for the next sequencing stage. The consensus sequence of *ompA* for each isolate was obtained with SeqMan once all five (2 x forward; 3 x reverse) reactions were obtained and confirmed to be error free. EditSeq (DNAstar, Inc.) was used to finally trim the sequences so that only the *ompA* gene was represented. The sequences of OmpA were formatted using Microsoft word document (Microsoft, 2010). The formatted files used to conduct phylogenetic and evolutionary analysis in MEGA.

Phylogenetic and evolutionary analyses were conducted with MEGA in conjunction with alignment programs written by T. S. Whittam (Michigan State University). These programs included AAseq, RealigX, Psfind and Happlot. The sequences were firstly converted to amino acid sequences using AAseq and the amino acid sequences were aligned using ClustalX (v2.0.12). The nucleotide sequences were then aligned based on the amino acid alignment using RealigX. RealigX generates an output (.meg) file which serves as an input for MEGA. MEGA was used to generate Neighbour-Joining phylogenetic trees using the Jukes-Canter correction model and also to determine sequence variation (nucleotide and amino acid polymorphisim). Boot-strap (500 replications) analysis, substitution rates and pairwise difference calculations were also conducted in MEGA. The Psfind and Happlot programs were used to represent polymorphic nucleotide sites graphically and to help identify recombination events. The output file from Happlot served as an input file to Micrographic Designer (MicrografX, Inc).

3.4.5 Secondary structure analysis

Secondary structure prediction was performed with the Psipred secondary structure prediction method (http://bioinf.cs.ucl.ac.uk/psipred/) and PRED-

TMBB (http://bioinformatics.biol.uoa.gr/PRED-TMBB/). The *ompA* gene sequences of *P. multocida* were aligned and compared with the proposed secondary structure of OmpA of the closely related species *Mannheimia haemolytica* (Davies & Lee, 2004). The domains were identified in MEGA and the d_S and d_N ratios were calculated using the Nei-Gojobori (number of differences) and boot-strap (500 replications) analysis.

3.5 Initial *ompA* sequencing

Preliminary PCR and sequencing were carried out first with nine diverse *P. multocida* isolates (PM144, PM246, PM414, PM564, PM632, PM684, PM734, PM966, and PM982). The comparative analysis of nucleotides and amino acid sequences showed obvious variation of *ompA* gene between nine isolates. Therefore, larger number of isolates, up to 74 was investigated. The isolates were selected in different batches.

3.6 Results

3.6.1 PCR Optimisation

Amplification of the *ompA* gene was first optimised in isolates PM144 (avian), PM564 (bovine), PM734 (porcine) and PM966 (ovine) by using different primer pair combinations and an annealing temperature of 55°C. Two forward (#626/F1.1 and #627/F1.2) and two reverse (#628/R1.1 and #629/R1.2) primers were designed for preliminary amplification of *ompA* (

Table 3.2). These were used in the following combination: F1.1/R1.1, F1.1/R1.2, F1.2/R1.1 and F1.2/R1.2. The *ompA* gene was amplified successfully in all isolates using an annealing temperature of 55°C with all primers pair combinations (Fig. 3.6 & Fig. 3.7). As expected, the product sizes on the agarose gels were slightly different. Thus, these primer pair combinations could be used for amplification of the *ompA* gene. However, primer pair #626 (F1.1)/#628 (R1.1) was selected for amplification of the *ompA* gene because a PCR product of the correct size (~2000 bp) was amplified. Amplification of the *ompA* gene was also optimised using different annealing temperatures by gradient PCR to remove non-specific products. Annealing temperatures of 55, 56, 57, 58 and 59°C were used with primers #626 (F1.1) and #628 (R1.2) were used. In both isolates PM144 and PM734, the *ompA* gene amplified successfully (Fig. 3.8). The product size on the agarose gels were of the correct size using annealing temperate 55, 56, 57, 58 and 59°C. Therefore, an annealing temperature of 55°C was selected as the optimum temperature for the amplification of *ompA* gene in *P. multocida*. However, the primer pairs and annealing temperature were changed when non-specific bands observed for specific isolates.

Two pairs of internal (two forward and two reverse) primers were also designed for the first stage sequencing (

Table 3.2). These primer pair combinations were tested by checking their ability to amplify the *ompA* gene. PM734 and PM966 were selected for the PCR. The following primer pair combinations were used: #636 (F1.1)/#638 (R1.1), #636 (F1.1)/#639 (R1.2), #637 (F1.2)/#638 (R1.1) and #637 (F1.2)/#639 (R1.2) at an annealing temperature of 55°C.

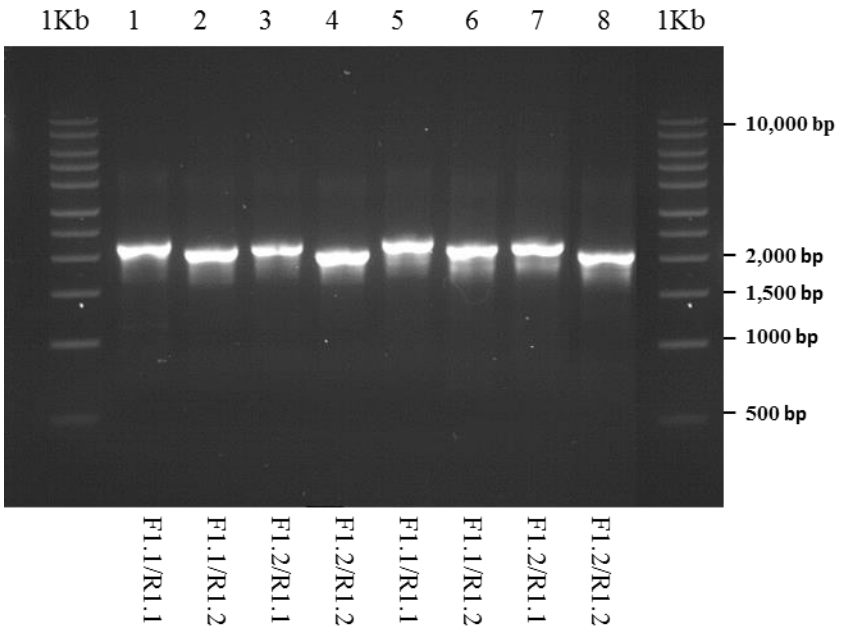

Fig. 3.6 Agarose gel electrophoresis of *ompA* PCR products in isolates PM144 and PM564.

Amplification of the *ompA* gene in isolates PM144 (lanes 1-4) and PM564 (lanes 5-8) using different primer pair combinations at an annealing temperature of 55°C. F1 = primer #626; F1.2 = primer #627; R1.1 = primer #628; R1.2 = primer #629.

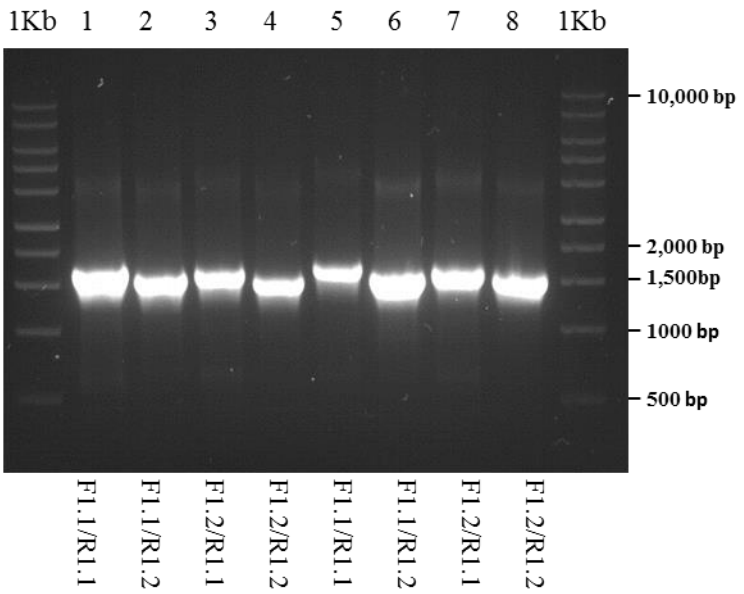

Fig. 3.7 Agarose gel electrophoresis of *ompA* PCR products in isolates PM734 and PM966.

Amplification of the *ompA* gene in isolates PM734 (lanes 1-4) and PM966 (lanes 5-8) using different primer pair combinations at an annealing temperature of 55°C. F1.1 = primer #626; F1.2 = primer #627; R1.1 = primer #628; R1.2 = primer #629.

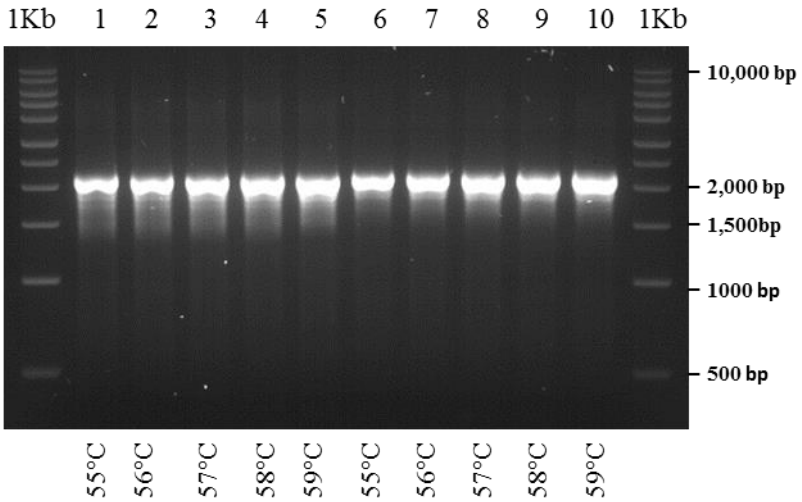

Fig. 3.8 Agarose gel electrophoresis of *ompA* PCR products in isolates PM144 and PM734.

Amplification of the *ompA* gene in isolates PM144 (lanes 1-5) and PM734 (lanes 6-10) using annealing temperatures of 55, 56, 57, 58 and 59°C with primers #626 (F1.1) and #628 (R1.1).

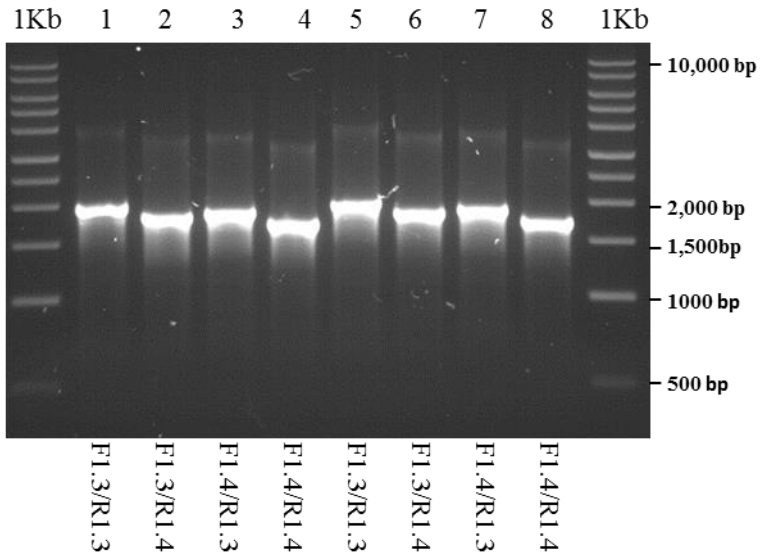

Fig. 3.9 Agarose gel electrophoresis of *ompA* PCR products in isolates PM734 and PM966.

Amplification of the *ompA* gene in isolates PM734 (lanes 1-4) and PM966 (lanes 5-8) using different primer pair combinations at an annealing temperature of 55°C. F1.3 = primer #636; F1.4 = primer #637; R1.3 = primer #638; R1.4 = primer #639.

3.6.2 Amplification of *ompA* gene in *P. multocida*

Using an annealing temperature of 55°C, the *ompA* gene was successfully amplified in all 74 *P. multocida* isolates using primer pair #626 (F1.1)/#628 (R1.1) (Fig. 3.10, Fig. 3.11 & Fig. 3.12). However, for certain isolates the amplification of *ompA* required further optimisation. In isolates PM258, PM310, PM702, PM952 and PM954 non-specific DNA bands were observed using primer pair #626 (F1.1)/#628 (R1.1) at annealing temperature of 55°C (Fig. 3.12B). The unwanted DNA band were removed by increasing the annealing temperature to 58°C using the primer pair #626 (F1.1)/#628 (R1.1) (Fig. 3.13). The primer pair #627 (F1.2) and #628 (R1.1) were used to amplify *ompA* gene in PM82, PM104 and PM344 (Fig. 3.14) because weak bands were obtained with primer pair #626/#628 (Fig. 3.12A).

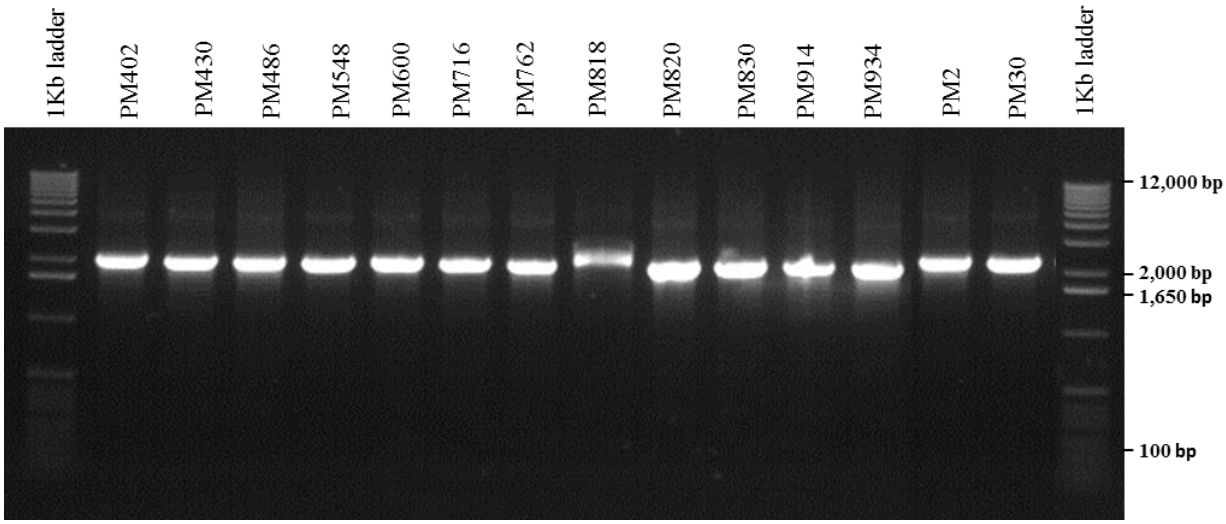

Fig. 3.10 Amplification of the *ompA* gene in 14 *P. multocida* isolates.

Primer pair #626 (F1.1)/ #628 (R1.1) with an annealing temperature of 55°C was used to amplify *ompA in P. multocida* isolates.

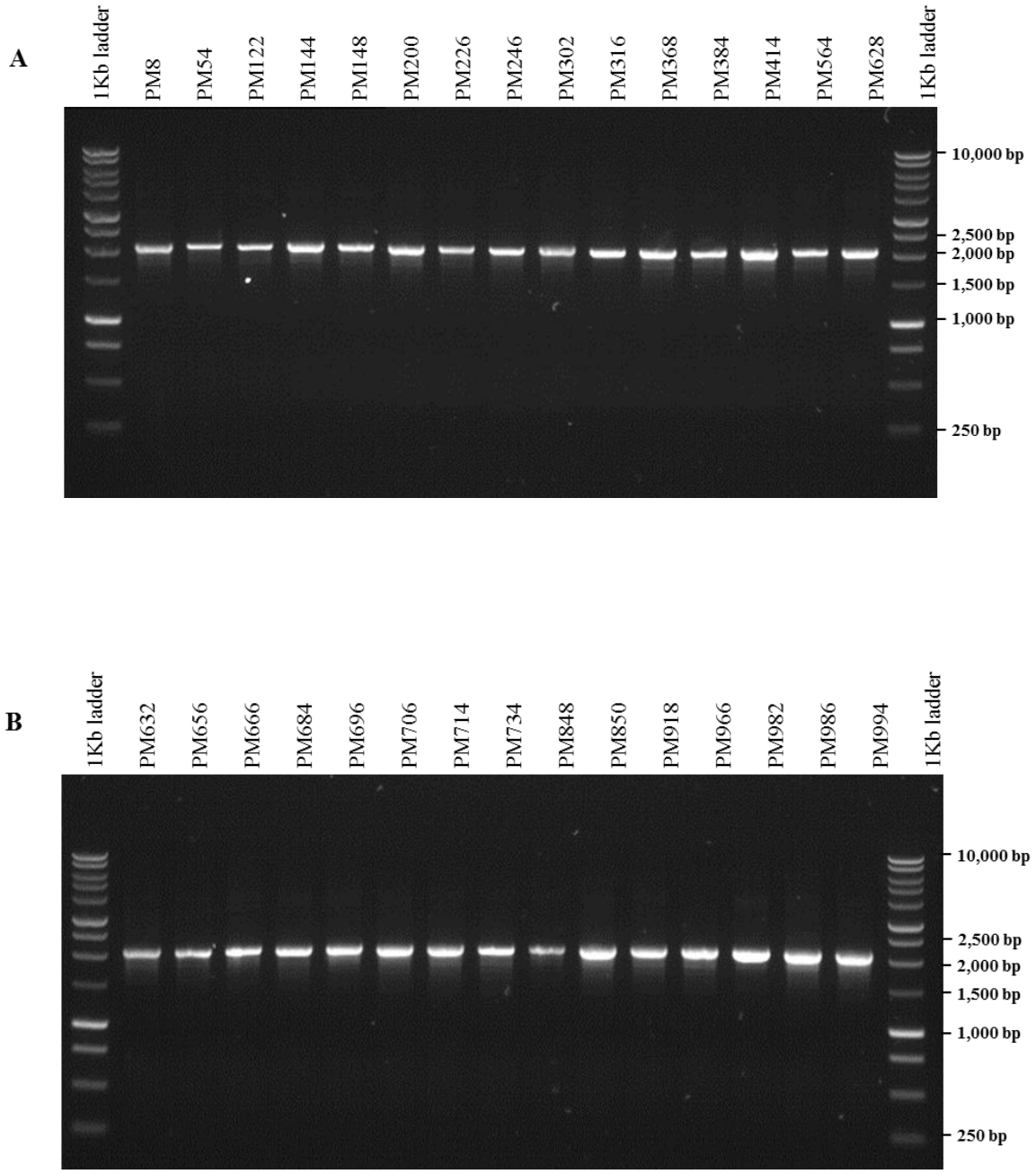

Fig. 3.11 Agarose gel electrophoresis showing the amplification of the *ompA* gene in 30 *P. multocida* isolates.

Primer pair #626 (F1.1)/ #628 (R1.1) was used to amplify *ompA* in *P. multocida* isolates using an annealing temperature of 55°C.

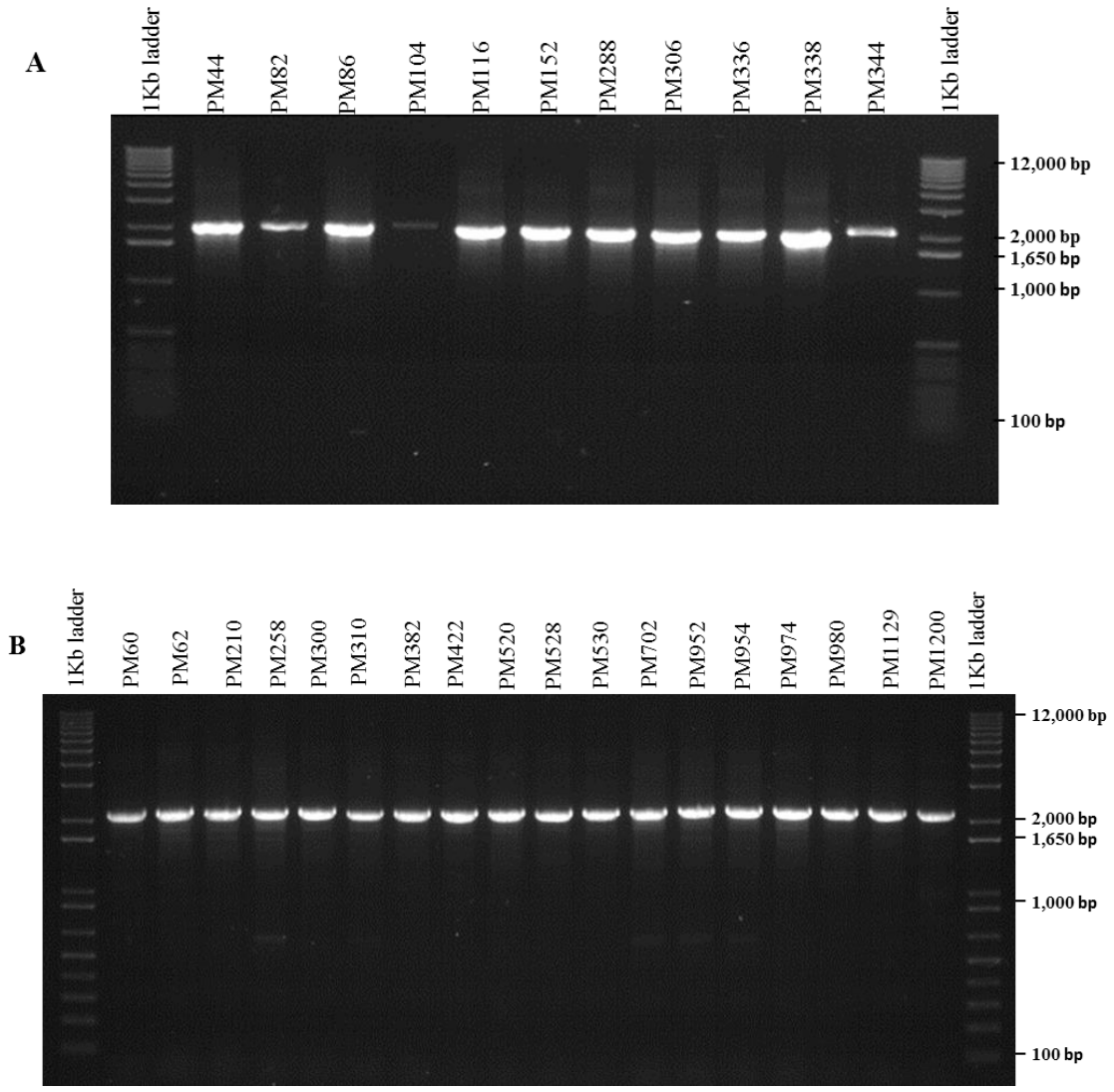

Fig. 3.12 Agarose gel electrophoresis showing the amplification of the *ompA* gene in 30 *P. multocida* isolates.

Primer pair #626 (F1.1)/ #628 (R1.1) was used to amplify *ompA* in *P. multocida* isolates using an annealing temperature of 55°C.

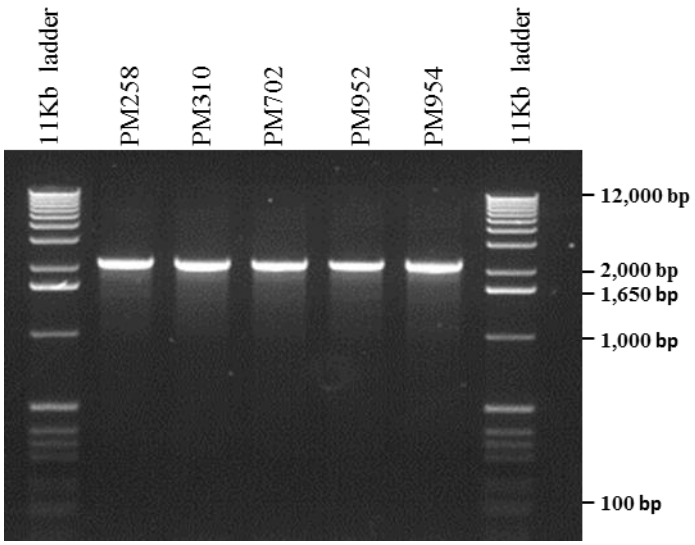

Fig. 3.13 Amplification of *ompA* in isolates PM258, PM310, PM702, PM952 and PM954.

Primer pair #626 (F1.1)/ #628 (R1.1) was used to amplify *ompA* using an annealing temperature of 58°C. Unwanted DNA bands were removed.

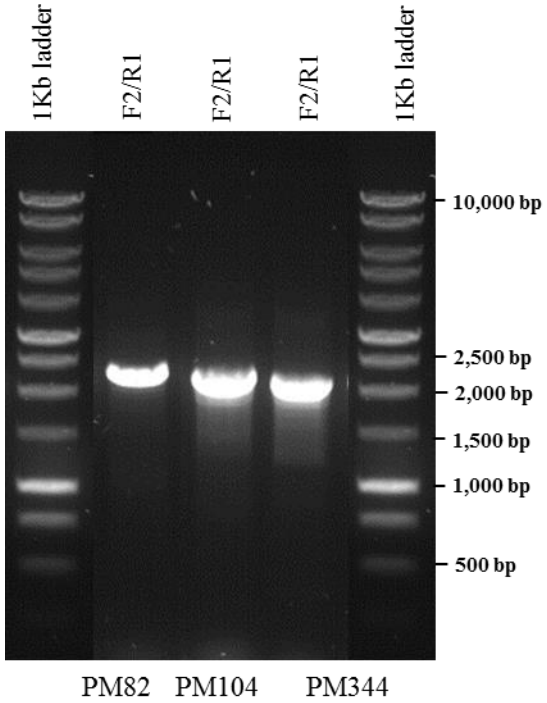

Fig. 3.14 Agarose gel electrophoresis showing the amplification of *ompA* in isolates PM82, PM104 and PM344

The *ompA* gene was amplified in isolates PM82, PM104 and PM344 using an annealing temperature of 55°C with primer pair #627 (F1.2)/ #628 (R1.1).

3.6.3 Sequencing parameters

For the preliminary partial sequencing of the *ompA* gene in *P. multocida,* isolates PM144, PM564, PM734 and PM966 were selected for optimisation of BigDye terminator using internal primers #626/F1.1 and #628/R1.1. The following dilutions of BigDye terminator were used: 1:4, 1:8, 1:16 and 1:32. Sequence analysis showed that *ompA* was partially sequenced in PM144, PM564, PM734 and PM966 with all dilutions. However, obvious differences in sequence quality were observed in both the forward and reverse reactions. With 1:4 dilutions the sequences were short (less than 400 bp). With dilutions of 1:8 and 1:32 the sequences were 500-600bp in length and the sequence quality was good. However, there was some back ground noise. Very good quality forward and reverse sequences were obtained with a dilution of 1:16 BigDye terminator. The sequence lengths were between 550-855 bp, and the peaks were high and there was no background noise (Fig. 3.15). Thus, a 1:16 dilution of BigDye terminator was selected for sequencing of the *ompA* gene in *P. multocida* isolates.

3.6.4 Sequencing reactions

The ompA gene from 74 *P. multocida (*16 avian, 25 bovine, 10 ovine and 23 porcine) isolates representing four capsular types, different OMP types (Davies *et al.*, 2003a; b; c; Davies, 2004; Davies *et al.*, 2004) and 30 sequence types (STs) (http://pubmlst.org/pmultocida_multihost/.) were sequenced (Table 3.3). The *ompA* gene was sequenced with two forward and three reverse reactions. The primers 636/F1.3 or 637/F1.4 (Fig. 3.3) and 639/R1.4 (Fig. 3.4) were used for the first stage sequencing. Internal primers for the second and third stage sequencing were designed as the sequence data became available. Primers 641/F2.1 or 644/F2.2 and 647/R2.2 or 648/R2.3 were used for the second stage sequencing (Fig. 3.5). More than one primer was designed because of sequence variation between *P. multocida* isolates. A third batch of internal primers was designed for the third stage reverse reactions. Because of variation among the aligned sequences, five reverse primers were designed: 649/R3.1, 650/R3.2, 651/R3.3, 652/R3.4 and 653/R3.5 (Fig. 3.5).

A

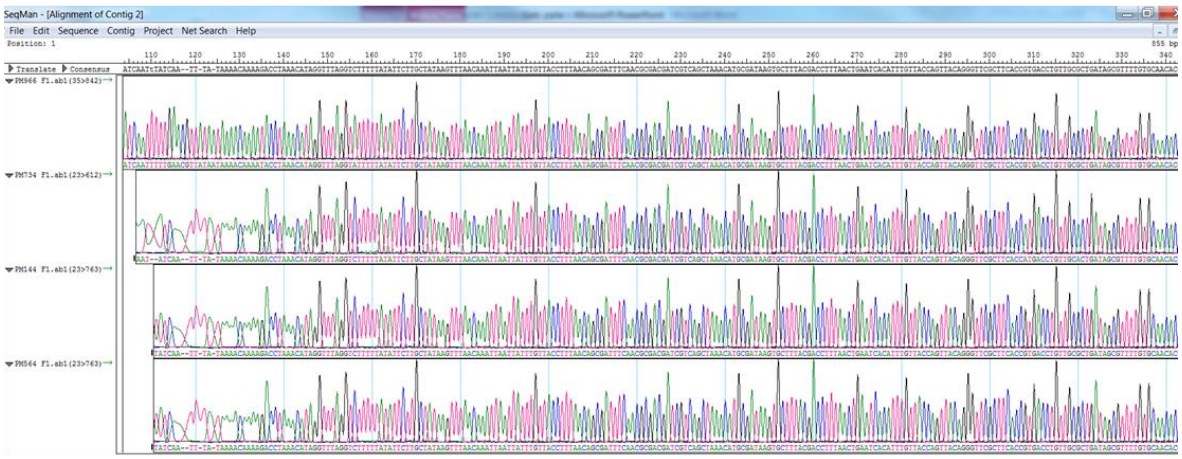

B

Fig. 3.15 Chromatogram files of forward (A) and reverse (B) sequences obtained with a dilution of 1:16 BigDye terminator.

Preliminary partial sequencing of the *ompA* gene in *P. multocida* isolates PM144, PM564, PM734 and PM966 using #626/F1.1 and #628/R1.1. Very good quality forward and reverse sequences were obtained with a dilution of 1:16 BigDye terminator. The sequence lengths were between 550-855 bp, and the peaks were high and there was no background noise.

Difficulties occurred during the sequencing of some isolates and this is may have been the result of poor DNA quality. In these cases, the PCR reactions were repeated and sequences of good quality were obtained. For each stage, the sequences ranged between 600-750 bp in length after editing and correction in SeqMan. The five individual sequences (two forward, three reverse) were assembled in SeqMan and the overlapping regions were checked for accuracy. In this way, a DNA fragment of total length 1710 bp was sequenced which included both noncoding intergenic regions (Fig. 3.2). The noncoding intergenic regions comprising 98 and 550 nucleotides were removed from the sequences. In this way, a complete *ompA* gene ranging between 1,044 and 1,077 nucleotides in length was obtained for the 74 *P. multocida* isolates (Table 3.3).

3.6.5 Phylogenetic analysis and classification of *ompA* alleles

Nucleotide sequence comparison of the 74 *ompA* gene sequences identified 26 different sequences. Each individual sequence represents a distinct allele and these were classified as described below. A Neighbour-Joining phylogenetic tree representing the *ompA* gene in *P. multocida* isolates is shown in Fig. 3.16. The tree shows the phylogenetic relationships of the different *ompA* alleles. Based upon the overall sequence similarity, the alleles were assigned to 10 different sub-classes, designated *ompA1* to *ompA10*. Alleles were designated within each sub-class as following: *ompA1* (*ompA1.1* to *ompA1.8*), *ompA2* (*ompA2.1* and *ompA2.2*), *ompA3* (*ompA3.1*), *ompA4* (*ompA4.1*), *ompA5* (*ompA5.1* and *ompA5.2*), *ompA6* (*ompA6.1* and *ompA6.2*), *ompA7* (*ompA7.1*), *ompA8* (*ompA8.1* and *ompA8.2*), *ompA9* (*ompA9.1*, *ompA9.2*, *ompA9.3*, *ompA9.4*, *ompA9.5* and *ompA9.6*) and *ompA10.1* (*ompA10.1*). The sub-classes could further be grouped into six distinct phylogenetic lineages, I to VI (Fig. 3.16). Lineage I includes only *ompA1*-type alleles, lineage II consists of *ompA2*-, *ompA3*- and *ompA4*-type alleles, lineage III includes only *ompA5*-type alleles, lineage IV consists of *ompA6*-, *ompA7*- and *ompA8*-type alleles, lineage V consists of *ompA9*- type alleles and lineage VI includes *ompA10*-type alleles.

Table 3.3 Details of *ompA* alleles among 74 *P. multocida* isolates.

Isolate [a]	Host species	ST [b]	MLST group	Capsular type	OMP-type [c]	*OmpA* allele	No. of nucleotides	No. of amino acids	Molecular mass (Da)
PM316	Bovine	1	A	A	1.1	1.1	1,047	349	37,509
PM386	Bovine	1	A	A	1.1	1.2	1,047	349	37,510
PM564	Bovine	1	A	A	2.1	1.1	1,047	349	37,509
PM600	Bovine	1	A	A	2.1	1.1	1,047	349	37,509
PM628	Bovine	2	A	A	2.1	1.1	1,047	349	37,509
PM344	Bovine	3	A	A	3.1	1.3	1,047	349	37,526
PM384	Bovine	3	A	A	3.1	1.3	1,047	349	37,525
PM414	Bovine	3	A	A	4.1	1.4	1,047	349	37,525
PM338	Bovine	4	A	A	4.1	1.4	1,047	349	37,525
PM632	Bovine	4	A	A	4.1	1.4	1,047	349	37,525
PM430	Bovine	3	A	A	8.1	3.1	1,059	353	37,888
PM520	Bovine	ND [d]	A	A	8.1	3.1	1,059	353	37,888
PM666	Porcine	3	A	A	2.1	3.1	1,059	353	37,888
PM914	Porcine	3	A	A	2.1	3.1	1,059	353	37,888
PM116	Porcine	3	A	A	3.1	3.1	1,059	353	37,888
PM656	Porcine	3	A	A	3.1	3.1	1,059	353	37,888
PM830	Porcine	3	A	A	3.1	3.1	1,059	353	37,888
PM966	Ovine	16	B	A	1.1	8.2	1,062	354	38,019
PM974	Ovine	16	B	A	1.1	8.2	1,062	354	38,019
PM30	Bovine	44	B	B	ND	9.2	1,077	359	38,326
PM1192	Bovine	46	B	B	ND	9.1	1,077	359	38,342
PM1200	Bovine	44	B	B	ND	9.1	1,077	359	38,342
PM382	Porcine	13	B	A	4.1	10.1	1,050	350	37,339
PM706	Porcine	13	C	UT	4.1	2.2	1,059	353	37,826
PM2	Ovine	17	C	F	2.1	8.1	1,071	357	38,327
PM8	Ovine	17	C	F	2.1	8.1	1,071	357	38,327
PM246	Avian	25	C	F	2.2	8.1	1,062	354	38,030
PM306	Bovine	8	C	F	7.1	8.1	1,062	354	38,030
PM44	Ovine	12	C	F	1.1	8.1	1,062	354	38,030
PM994	Ovine	12	C	F	1.1	8.1	1,062	354	38,030
PM258	Avian	12	C	A	2.2	8.1	1,062	354	38,030
PM148	Avian	12	C	F	2.2	8.1	1,062	354	38,030
PM952	Porcine	12	C	F	3.2	8.1	1,062	354	38,030
PM210	Avian	23	C	A	2.1	2.1	1,059	353	37,828
PM104	Avian	28	D	A	4.1	9.4	1,068	356	38,108
PM86	Avian	15	D	A	3.1	7.1	1,062	354	37,993
PM934	Porcine	15	D	A	5.1	7.1	1,062	354	37,993
PM954	Porcine	15	D	A	5.1	7.1	1,062	354	37,993
PM486	Bovine	9	D	A	9.1	7.1	1,062	354	37,993
PM422	Bovine	ND	ND	A	9.1	4.1	1,056	352	37,663
PM62	Avian	39	E	B	12.1	9.3	1,071	357	38,120
PM530	Bovine	6	E	A	5.2	1.6	1,056	352	37,821
PM302	Bovine	6	E	A	5.3	1.6	1,056	352	37,821
PM548	Bovine	6	E	A	5.3	1.6	1,056	352	37,821
PM528	Bovine	6	E	A	5.4	1.6	1,056	352	37,821
PM144	Avian	21	E	A	1.1	5.1	1,050	350	37,700
PM310	Avian	21	E	A	1.1	5.1	1,050	350	37,700
PM702	Porcine	14	E	A	5.1	5.2	1,050	350	37,700
PM402	Bovine	5	E	A	5.1	1.5	1,056	352	37,871
PM980	Ovine	20	E	D	3.2	1.8	1,047	349	37,527
PM122	Ovine	ND	ND	D	3.1	1.7	1,044	348	37,513
PM982	Ovine	18	E	D	3.1	1.7	1,044	348	37,513
PM986	Ovine	18	E	D	3.1	1.7	1,044	348	37,513
PM54	Porcine	10	F	A	1.1	4.1	1,056	352	37,663
PM734	Porcine	10	F	A	1.1	4.1	1,056	352	37,663

Table 3.3 (continued)

Isolate [a]	Host species	ST [b]	MLST group	Capsular type	OMP-type [c]	*OmpA* allele	No. of nucleotides	No. of amino acids	Molecular mass (Da)
PM820	Porcine	10	F	A	1.1	4.1	1,056	352	37,663
PM850	Porcine	10	F	A	1.1	4.1	1,056	352	37,663
PM200	Avian	10	F	A	1.2	4.1	1,056	352	37,663
PM288	Avian	10	F	A	1.2	4.1	1,056	352	37,663
PM336	Bovine	7	F	A	6.1	4.1	1,056	352	37,663
PM368	Bovine	7	F	A	6.1	4.1	1,056	352	37,663
PM684	Porcine	11	G	A	6.1	6.1	1,062	354	37,965
PM918	Porcine	11	G	A	6.1	6.1	1,062	354	37,965
PM716	Porcine	11	G	D	4.1	6.1	1,062	354	37,965
PM848	Porcine	11	G	D	4.1	6.1	1,062	354	37,965
PM696	Porcine	11	G	D	6.1	6.1	1,062	354	37,965
PM714	Porcine	11	G	D	6.1	6.1	1,062	354	37,965
PM762	Porcine	11	G	D	6.1	6.1	1,062	354	37,965
PM818	Porcine	11	G	D	6.1	6.1	1,062	354	37,965
PM226	Avian	11	G	D	13.1	6.1	1,062	354	37,965
PM60	Avian	36	H	UT	10.1	6.2	1,062	354	37,974
PM82	Avian	32	H	A	7.1	9.6	1,065	355	38,022
PM300	Avian	33	H	A	7.1	9.6	1,065	355	38,022
PM152	Avian	31	H	A	6.1	9.5	1,068	356	38,091

[a] isolates are arranged by order of MLST group (column 3) (Fig. 2.1); [b] ST= sequence type (Davies *et al*., unpublished http://pubmlst.org/pmultocida_multihost/); [c] OMP-types for bovine, ovine, porcine and avian are not equivalent, i.e. bovine OMP-type 1.1 is not as same as porcine OMP-type 1.1, etc. (Davies *et al.*, 2003a; b; c; Davies, 2004; Davies *et al.*, 2004); [d] ND: not determined.

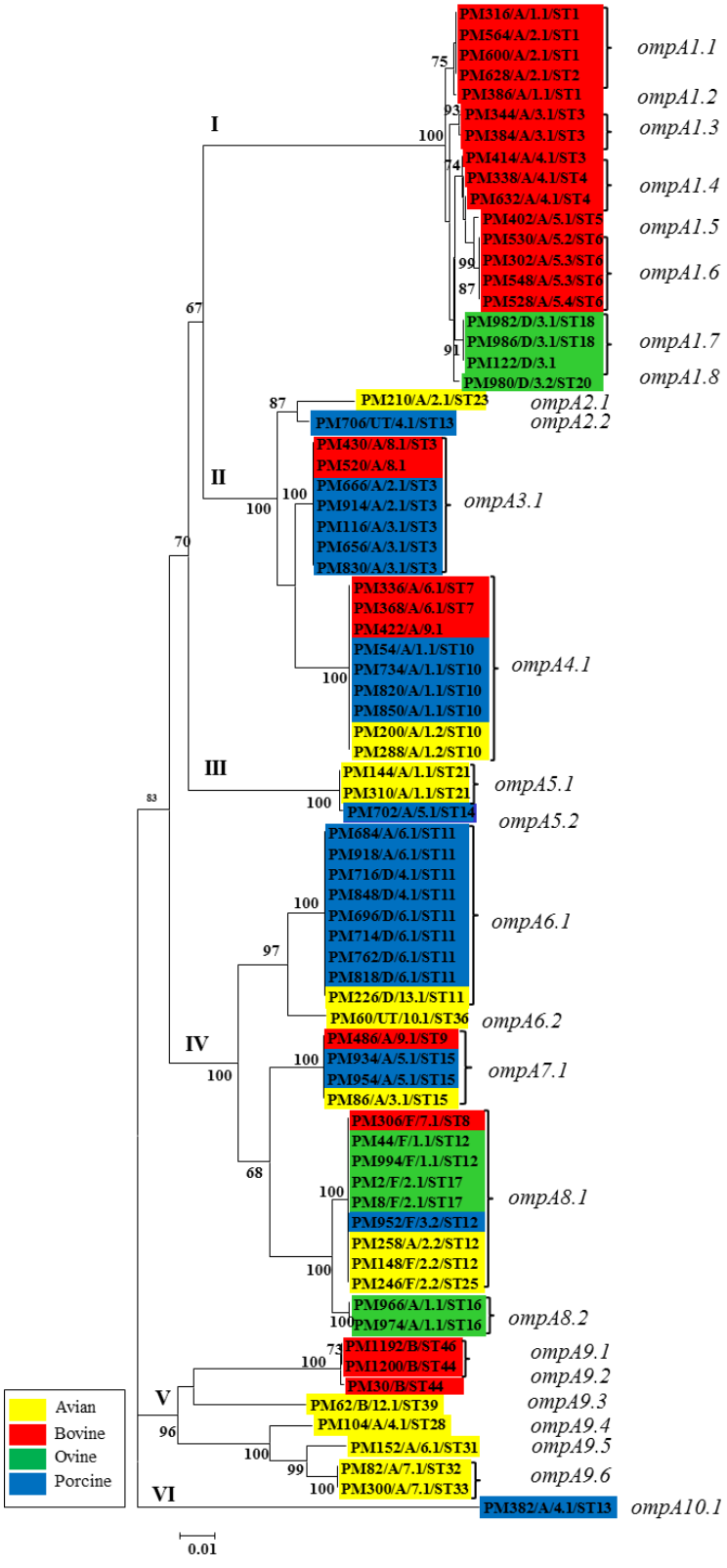

Fig. 3.16 Neighbour-Joining tree representing the phylogenetic relationships of *ompA* alleles in 74 *P. multocida* strains.

The phylogenetic tree was constructed with Jukes-Cantor correction for nucleotide substitutions and the pairwise deletion option for handling gaps. Bootstraps values (500 replications) of > 50 are only shown. Isolate designation, capsular type, OMP type and ST type are provided for each isolate (e.g. PM316/A/1.1/ST1). Allele designations are sown to the right (*ompA1.1,* etc.).

3.6.6 Comparative sequence analysis

3.6.6.1 Nucleotide and amino acid sequence analysis

Based on sequence similarity, the *ompA* alleles were assigned to 26 distinct *ompA*-types, representing six phylogenetic lineages as described in section 3.6.5. Among the *P. multocida* isolates examined, the complete sequence of *ompA* varied from 1,044 to 1,077 nucleotides in length and the length of the encoded predicted proteins varied from 348 to 359 amino acids, the molecular mass of the OmpA proteins varied from 37,513 to 38,342 Da (Table 3.3). The total aligned length of the sequences including gaps and insertions, of the *ompA* gene was 1,083 nucleotides (361 amino acids). Total nucleotide variation among all sequences was 28.1% (304 polymorphic nucleotide sites) and the amino acid variation was 22.4% (81 variable inferred amino acid sites).

3.6.6.2 OmpA domain identification

To identify the OmpA structural domains (surface-exposed loops, transmembrane domain), representative sequences of each allele were selected. The OmpA domains were identified and a proposed secondary structure of OmpA elucidated based on comparison of *P. multocida* OmpA amino acid alignments with those of the closely related species *M. haemolytica* (Davies *et al.*, 2004). Based on sequence homology, a secondary structure of OmpA was generated (Fig. 3.17). OmpA consists of an N-terminal transmembrane domain and a C-terminal periplasmic domain. The transmembrane domain comprises eight transmembrane ß-sheet regions linked by short loops on the periplasmic side and four extended surface-exposed loops on the external side (Fig. 3.17 & Fig. 3.18). The conserved regions together consist of 759 of 1,083 (70.1%) nucleotide sites, whereas the loops together comprise 324 of 1,083 (29.9%) nucleotide sites. The loops were similar in the size and ranged from 63-99 nucleotides and 21 to 33 amino acids. The C-terminal domain is the single largest conserved domain and consists of 435 of 1,082 nucleotide sites (40.2%) (Fig. 3.19). Construction of a predicted secondary structure of OmpA based on amino acid sequence alignments showed that the variation appeared predominantly in the loops regions of the protein (Fig. 3.17). Variation was observed in all loops and this led to identification of four hypervariable domains (HV1 to HV4) (Fig. 3.17). In HV1 (loop 1), HV2 (loop2) and HV3 (loop3) additional amino acids had been inserted

in isolates within lineages V and VI (*ompA9*- and *ompA10*-type alleles) (Fig. 3.17). Construction of a predicted secondary structure of OmpA showed that the hypervariable regions (HV1 to HV2) are located at the distal ends of the surface-exposed loops (Fig. 3.18).

3.6.7 Sequence diversity and substitution rates

3.6.7.1 Synonymous and nonsynonymous substitution rates

Once the domains had been identified and established (Fig. 3.19), MEGA was used to calculate sequence diversity and substitution rates based on the complete alignments of all 74 sequences. The OmpA protein was divided into 9 domains based on the amino acid sequence alignments with OmpA of *M. haemolytica* (Fig. 3.19). The numbers of synonymous substitutions per 100 synonymous sites (d_S) and nonsynonymous substitutions per 100 nonsynonymous sites (d_N) were estimated for the conserved and loop regions. This allowed selective constraint and diversifying selection to be examined in the *ompA* gene of *P. multocida* by calculating the d_S/d_N ratios for the various domains (Table 3.4). A high d_S/d_N ratio ($d_S/d_N > 1$) indicates that natural selection is acting to restrict mutations that result in amino acid alteration and replacement, i.e selective constraint. Conversely, a low d_S/d_N ratio ($d_S/d_N < 1$) indicates that natural selection is actively driving amino acid alteration and replacement, i.e diversifying selection. The results clearly indicated that the selective pressures were not equal across the gene. The d_S/d_N ratio for all conserved regions of the *ompA* gene was 4.1 (Table 3.4). The data demonstrate that natural selection is acting to restrict amino acid replacement in the non-loop regions of OmpA because these parts of the molecules (the membrane-spanning and periplasmic domains) are mostly involved in maintaining outer membrane structural integrity and cannot tolerate amino acid change. The d_S/d_N ratios for the hypervariable extracellular loop domains (L1, L2, L3 and L4) were all less than 1, the ratios ranging from 0.49 to 0.66 (Table 3.4). These data provide strong evidence that natural selection is driving diversification of the hypervariable extracellular loops regions.

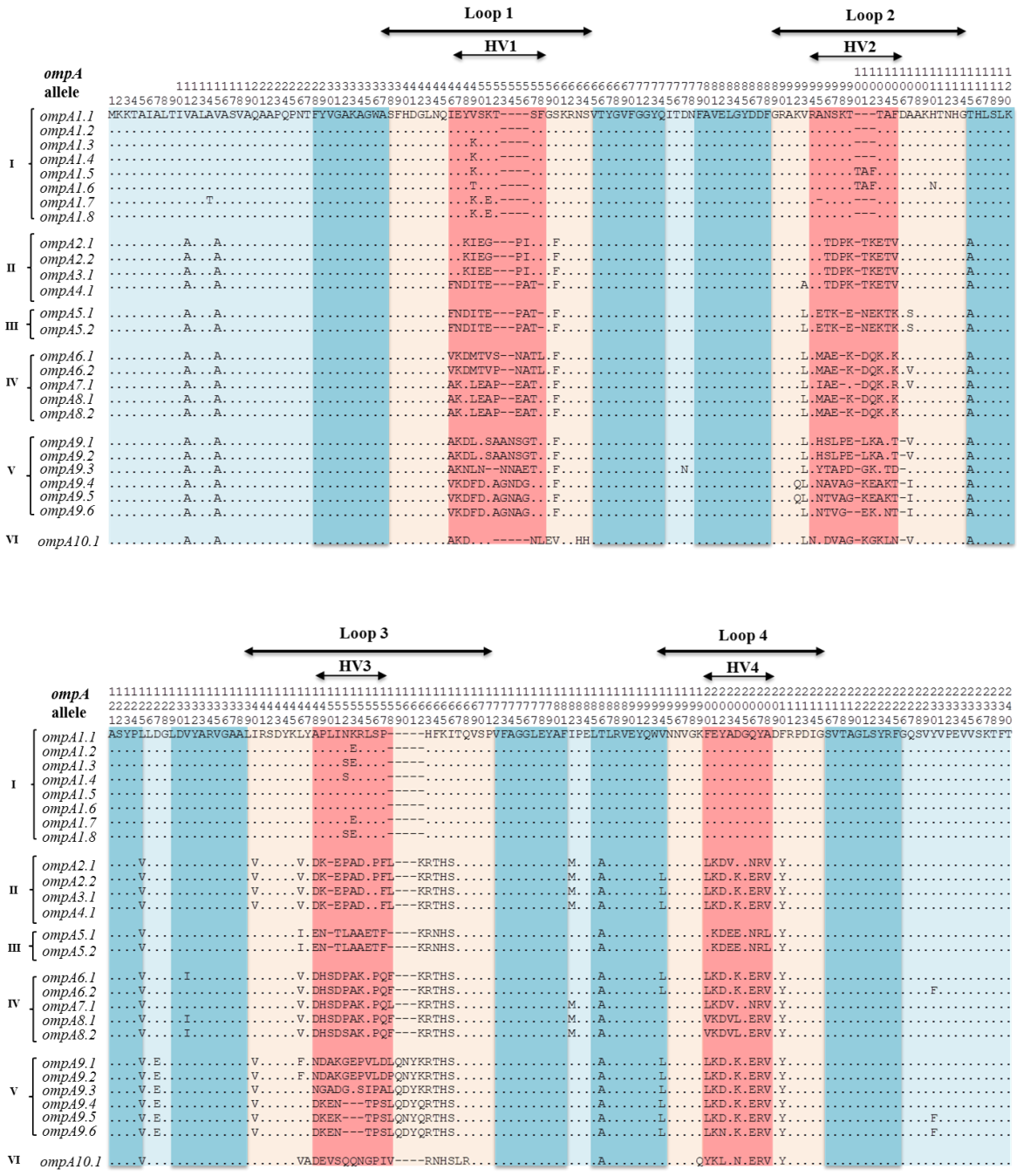

Fig. 3.17 Distribution of variable amino acid sites in the N-terminal transmembrane domain of the 26 OmpA proteins of *P. multocida*.

Allele designations are shown to the left of each sequence. Roman numerals I to IV represent the phylogenetic lineages (**Fig. 3.16**). The numbers above the sequences (read vertically) represent amino acid positions. The dots represent sites where the amino acids match those of the first sequence. Gaps are indicated by dashes. HV1 to HV4 represent the hypervariable domains (highlighted in red) within the surface-exposed loops 1 to 4 (highlighted in light brown). Dark blue regions represent predicted membrane-spanning β-strand structures. Most of the conserved C-terminal region was excluded.

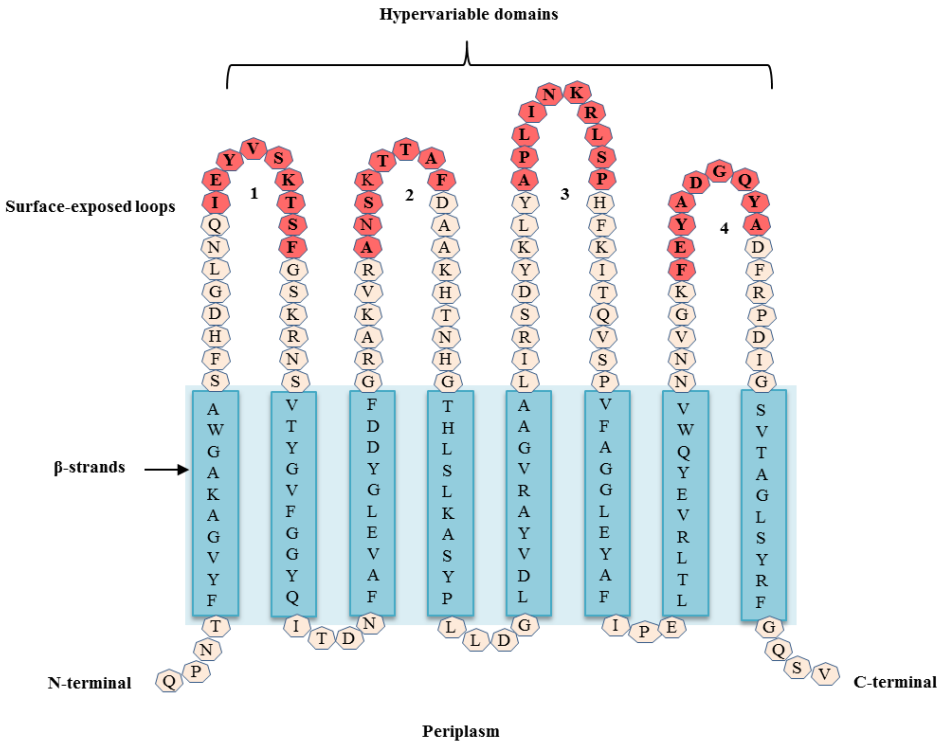

Fig. 3.18 Proposed secondary structure of N-terminal transmembrane domain of the OmpA protein of *P. multocida*.

The sequence is based on OmpA of isolate PM316 (*ompA1.1)*. The hypervariable domains are shown in red. Sequences at both N- and C-terminal are truncated.

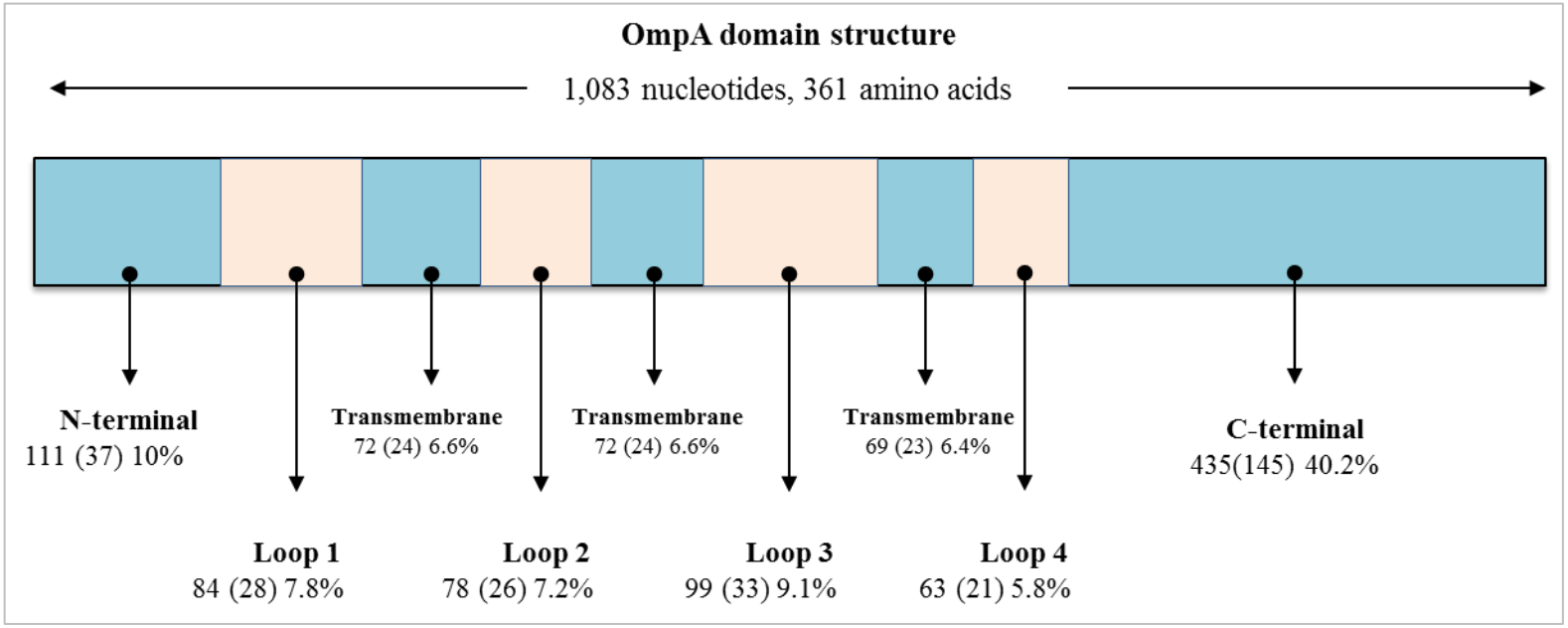

Fig. 3.19 Schematic representation of OmpA domain structure in *P. multocida* based upon the alignment of 74 *P. multocida* isolates.

The model is 1,083 nucleotides (361 amino acids) in length. The domains were assigned based on amino acid alignment with the closely related species *M. haemolytica*. Nine domains were identified and are indicated by arrows. The transmembrane domains also include periplasmic turns. Numbers represent the length of each domain in nucleotides and amino acids and the percentages indicate the overall length of that domain within the gene.

Table 3.4 Sequence diversity and substitution rates for hypervariable loop domains and conserved regions of the *ompA* genes of 74 *P. multocida* isolates.

Domains	Sequence size		Polymorphic sites		Sequence diversity %		d_S[a]	d_N[a]	d_S/d_N
	No. of nucleotides	No. of amino acids	No. of nucleotides	No. of amino acids	Nucleotides	Amino acids			
Conserved	759	253	106	15	13.9	5.9	22.073±2.473	5.412±1.285	4.10
Loop 1	84	28	47	17	54.7	60.7	3.579±00.916	7.292±2.075	0.49
Loop 2	78	26	47	15	60.2	57.6	3.287±0.616	7.012±2.110	0.46
Loop 3	99	33	74	24	74.7	72.7	8.801±0.836	13.600±2.790	0.64
Loop 4	63	21	31	10	49.2	47.6	3.753±0.859	5.686±1.639	0.66
All Loops	324	108	198	66	61.1	61.1	19.419±1.733	33.590±4.298	0.57

[a] d_S is the number of synonymous substitutions per 100 synonymous sites; d_N is the number of nonsynonymous substitutions per 100 nonsynonymous sites. Values are means ±standard deviations.

3.6.7.2 Sequence diversity

Comparative sequence analysis of the 26 *ompA* alleles showed that there were 294 (27.2%) polymorphic nucleotide sites and 78 (21.6%) variable amino acid positions. The OmpA protein of *P. multocida* contains four long surface-exposed loops and eight ß-strand regions which consist of ten amino acids. Hypervariable regions were located at the distal ends of the surface-exposed loops (Fig. 3.18). Nucleotide and amino acid sequence diversity in each domain is shown in Table 3.4. Both the N-terminal and C-terminal domains were relatively highly conserved and together contained only 106 of 759 (13.9%) polymorphic nucleotide sites and 15 of 253 (5.9%) variable amino acids. In contrast, the majority of the variable sites occurred within four hypervariable regions of the loop domains (HV1 to HV4) (Fig. 3.17 & Fig. 3.18). Together, the hypervariable domains consisted of 198 of 324 (61.1%) polymorphic nucleotide sites and 66 of 108 (61.1%) variable inferred amino acids. The degree of variation itself varied among the hypervariable domains. The HV3 domain showed the highest degree of variation and consisted of 74 of 99 (74.7%) polymorphic nucleotide sites and 24 of 33 (72.7%) variable amino acid positions, whereas the HV4 domain had the lowest degree of variation and consisted of 31 of 63 (49.2%) polymorphic nucleotide sites and 10 of 31 (47.6%) variable amino acid positions (Table 3.4). Distribution of amino acid sites within OmpA (Fig. 3.17) also showed that insertion and/or deletion of amino acids occurred within hypervariable domains 1, 2 and 3 but not 4.

3.6.7.3 Allelic variation and phylogenetic relationships

Individual sequences were assigned as distinct alleles. Eleven major groups of alleles (*ompA1* to *ompA10*) representing six phylogenetic lineages (I-VI) were identified as described in section 3.6.5. The association of *ompA* alleles with phylogenetic lineages (represented by STs), the host species of origin and OMP and capsular types of *P. multocida* are shown in (Fig. 3.16). Pairwise differences in nucleotide and amino acid sequences between representative pairs of the 10 *ompA* allele type are shown in Table 3.5. Pairwise differences ranged from 22 to 166 (2.1 to 15.3%) nucleotide sites and from 4 to 53 (1.1 to 14.7%) amino acid positions.

Table 3.5 Pairwise differences in nucleotide and amino acid sequences between representatives of the 10 *ompA* allele types of *P. multocida.*

Allele	**Pairwise differences in nucleotide and amino acid sequences (%)[a]**									
	ompA1.1	***ompA2.1***	***ompA3.1***	***ompA4.1***	***ompA5.1***	***ompA6.1***	***ompA7.1***	***ompA8.1***	***ompA9.1***	***ompA10.1***
ompA1.1		42 (11.6)	41 (11.3)	45 (12.5)	45 (12.5)	47 (13.1)	44 (12.2)	46 (12.7)	49 (13.6)	53 (14.7)
ompA2.1	101 (9.3)		7 (1.9)	14 (3.8)	32 (8.8)	32 (8.8)	25 (6.9)	28 (7.7)	36 (10)	44 (12.2)
ompA3.1	99 (9.2)	28 (2.5)		7 (1.9)	32 (8.8)	28 (7.7)	29 (8.1)	29 (8.1)	31 (8.6)	45 (12.5)
ompA4.1	111 (10.3)	50 (4.6)	22 (2.1)		26 (7.2)	23 (6.3)	28 (7.7)	28 (7.7)	29 (8.1)	43 (11.9)
ompA5.1	121 (11.2)	98 (9.1)	95 (8.7)	75 (6.9)		30 (8.3)	31 (8.6)	32 (8.8)	35 (9.7)	41 (11.3)
ompA6.1	123 (11.4)	102 (9.4)	85 (7.8)	79 (7.3)	90 (8.3)		19 (5.2)	13 (3.6)	32 (8.8)	39 (10.8)
ompA7.1	110 (10.2)	76 (7)	85 (7.8)	84 (7.7)	89 (8.2)	58 (5.3)		9 (2.5)	32 (8.8)	40 (11.1)
ompA8.1	117 (10.8)	93 (8.6)	90 (8.3)	90 (8.3)	100 (9.2)	45 (4.1)	40 (3.7)		35 (9.7)	41 (11.3)
ompA9.1	148 (13.7)	127 (11.7)	117 (10.8)	110 (10.2)	116 (10.7)	111 (10.3)	117 (10.8)	121 (11.2)		43 (11.9)
ompA10.1	166 (15.3)	136 (12.6)	147 (13.6)	140 (12.9)	135 (12.5)	140 (12.9)	136 (12.6)	143 (13.2)	138 (12.7)	

[a]Values in the upper right represent pairwise differences in amino acid sequences (number of variable amino acid sites and percentage of amino acid variation). Values in the lower left are pairwise differences in nucleotide sequences (number of polymorphic nucleotide sites and percentage of nucleotide variation).

There was a relatively high degree of variation in both nucleotides and amino acids between most of the allelic groups, *ompA1*- to *ompA10*-type alleles. For example, *ompA1.1*- and *ompA10.1*-type alleles differ from each other at 166 nucleotide sites (Fig. 3.20). However, a low degree of both nucleotide and amino acid variation was found among alleles within each group. The distribution of *ompA* alleles among the *P. multocida* isolates are shown in Fig. 3.16. *OmpA1*-type was the most prevalent group and it was represented by 19 isolates (25.6%), followed by *ompA8*- (11 isolates—14.8%), *omp4*- (9 isolates—12.2%), *ompA6*- (10 isolates 13.5%), *ompA9*- (8 isolates—10.8) and *ompA3*- (7 isolates—9.4%) type alleles. The remaining *ompA*-type alleles (*ompA2*, *ompA5*, *ompA7* and *ompA10*) were less common and were represented by one to four isolates. Lineage I represented only *ompA1*-type alleles and this group represented the most prevalent group which included 8 allele types (*ompA1.1* to *ompA1.8*). Alleles within this lineage differ from each other at only one to nine nucleotides sites (Fig. 3.20). Noticeably, alleles within this lineage were associated with capsular type A bovine isolates that were responsible for causing bovine pneumonia (OMP-types 1.1 to 4.1, ST 1 to 4 and MLST group A). This lineage also included bovine isolates of the MLST group E (capsular type A, OMP-types 5.1 to 5.4 and STs 4 and 5) and ovine isolates of the MLST group E (capsular type D ,OMP-types 3.2 and 3.2 and STs 18 and 20). Lineage II included three allele groups (*ompA2*, *ompA3* and *ompA4*); *ompA2* includes two alleles, *ompA2.1* and *ompA2.2,* which differ from each other at 21 nucleotide positions; *ompA3* includes only the *ompA3.1* type allele and was associated with bovine isolates (OMP-type 8.1 and ST 3) as well as porcine isolates of the MLST group A (capsular type A and OMP-types 2.1 and 3.1 of ST 3); *ompA4* includes only the *ompA4.1*-type allele and this group was associated with bovine, porcine and avian isolates of the major porcine pneumonia cluster (capsular type A, MLST group F). Interestingly, the majority of isolates comprising lineage II represent porcine pneumonia isolates (capsular type A) possessing *ompA3.1* and *ompA4.1* and of STs 3 and 10, respectively. The *ompA* alleles within lineage III differed at 14 to 55 nucleotide sites (Fig. 3.20). Lineage III was represented only by *ompA5.1*- and *ompA5.2*-type alleles which differed from each other at only one nucleotide position (Fig. 3.20). Allele *ompA5* was associated with avian isolates of the MLST group E (capsular type A, OMP-type 1.1 and ST 21), whereas *ompA5.2* was associated with a capsular type A porcine isolate of ST 14 (MLST

group E). Lineage IV represents a divergent group of isolates associated with different host species, capsular types, OMP types, disease types and ST types. This lineage includes *ompA6* (*ompA6.1* and *ompA6.2*), *ompA7* (*ompA7.1*), *ompA8* (*ompA8.1* and *ompA8.2*). Allele type *ompA6.1* was associated exclusively with porcine atrophic rhinitis isolates of the MLST group G (capsular A and D of OMP-types 4.1 and 6.1 and ST 11), it also included an avian isolate (capsular D) of ST 11. O*mpA6.2* was associated with an avian untypable isolate PM60 of the MLST group H (ST 36) and differs from *ompA6.1* at 23 nucleotide sites (Fig. 3.20). The *ompA7.1*-type allele group was associated with bovine, porcine and avian isolates of the MLST group D (capsular type A, STs 9 and 15). The *ompA8.1*-type allele was associated with ovine, avian, bovine and porcine of capsular type F isolates (STs 8, 12, 17 and 25 and MLST group C), whereas *ompA8.2*-type allele was associated with capsular type A ovine isolates of ST 16 and OMP-type 1.1 (MLST group B). The *ompA8.1*- and *ompA8.2*-type alleles differed from each other at ten nucleotide sites. Alleles within lineage IV differed from each other at 10 to 60 nucleotide sites (Fig. 3.20). Lineage V represented *ompA9*-type alleles (*ompA9.1* to *ompA9.6*) which differed from each other at 1 to 92 nucleotides sites (Fig. 3.20). *OmpA9.1* and *ompA9.2* represented bovine haemorrhagic septicaemia isolates of the MLST group B (capsular type B, and ST 46 and 44) which differed at only one nucleotides position, whereas *ompA9.3* to *ompA9.6* was associated with avian isolates of the MLST group H (various capsular, OMP types and ST types). Finally, lineage VI was associated with the single *ompA10.1* allele which was highly divergent from all others, differing at 135 to 166 nucleotide sites (Table 3.5).

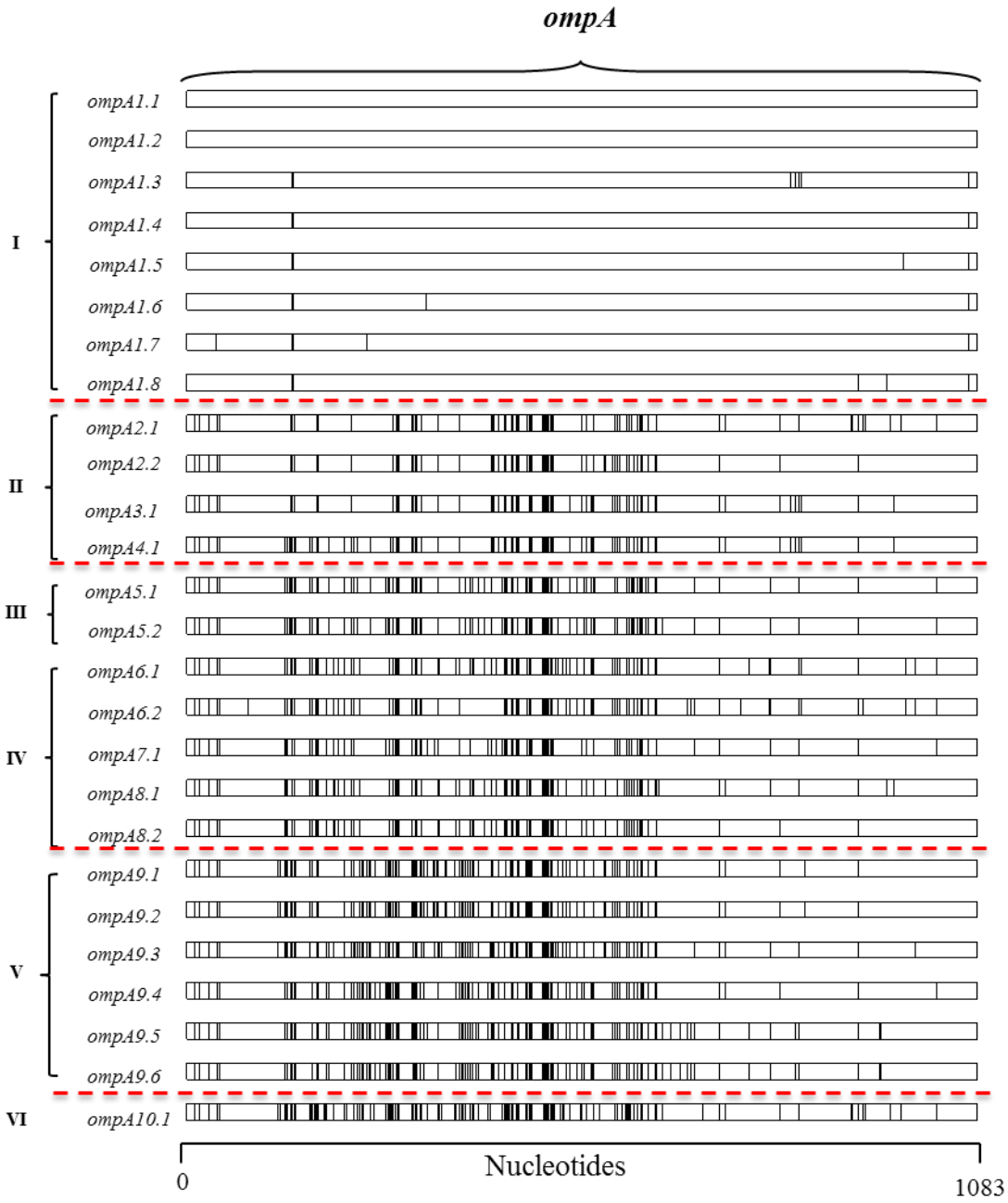

Fig. 3.20 Distribution of polymorphic nucleotide sites among the 26 *ompA* alleles of *P. multocida* using Happlot analysis.

Allele designations are shown to the left of each sequence. Roman numerals I to VI represent the phylogenetic lineages (**Fig. 3.16**). Graph was created using Micrographic Designer.

3.6.8 Assortative and intragenic recombination among *ompA* of *P. multocida*

3.6.8.1 Assortative (entire gene) recombination among *ompA* gene

The multilocus sequence typing (MLST) data were used to compare the evolutionary relationships of *P. multocida ompA* alleles with the underlying genetic relationships of the strains of origin (Davies *et al.*, unpublished; http://pubmlst.org/pmultocida_multihost). The genetic relationships of the strains of origin are shown in (Fig. 3.21B). The *ompA* phylogenetic tree was not in agreement with the phylogeny of *P. multocida* based on the concatenated sequences (3990 bp) of seven housekeeping enzyme genes. Assortative recombination has contributed to the genetic diversity of OmpA in *P. multocida*. The presence of identical, or almost identical, *ompA* alleles in genetically divergent strains representing different ST types provides evidence of horizontal gene transfer and recombinational exchanges of those alleles (Fig. 3.21B). *OmpA1-type* alleles represented by *ompA1.1* to *ompA1.8*, which differ at only one to nine nucleotide sites, and occurred in genetically diverse strains, represented by the major bovine pneumonia isolates of capsular type A, OMPS 1 to 5, STs 1 to 6 and MLST group A and ovine capsular type D isolates of STs 18 and 20 (OMP 3.1 and 3.2 and MLST group E). The MLST data (Fig 2.1) showed that the ovine isolates (PM980, PM982 and PM986) are genetically divergent from the major bovine pneumonia group. However, these isolates share clearly identical, or almost identical, *ompA* alleles (Fig. 3.20). The *P. multocida ompA2.1* and *ompA2.2* in lineage II differ from each other at only 21 nucleotide sites. The *P. multocida* isolates associated with *ompA2.1* and *ompA2.2* types have been previously shown to cluster in divergent lineages based on the concatenated sequences of the seven housekeeping genes (Fig. 3.20). The *P. multocida ompA3.1* and *ompA4.1* alleles in lineage II differ from each other at only 22 nucleotide sites. However, both alleles were present in bovine and porcine isolates that share different genetic lineages. The *P. multocida ompA3.1*-allele type was associated with bovine pneumonia isolates of capsular type A, OMP 8.1 and ST 3 and porcine pneumonia isolates of capsular type A, OMPs 1 and 2 and ST 3. The *P. multocida ompA4.1-type* allele was associated with major porcine pneumonia cluster (MLST group F) of OMP-types 6.1 and 9.1 and ST 7 and (bovine) and capsular type A, OMP-types1.1 and 1.2 and ST 10 (porcine and

avian) (Fig. 3.20). The *P. multocida* isolates of *ompA3.1*-type allele have been previously shown to cluster with the major bovine pneumonia cluster (MLST group A), whereas the *P. multocida* isolates associated with *ompA4.1* have been previously shown to cluster with the major porcine pneumonia cluster (MLST group F) (Fig. 3.20B). Another example of assortative recombination is provided by the *ompA* type in lineage IV. The *P. multocida ompA6.1* and *ompA6.2* types in lineage IV differ from each other at only 23 nucleotide sites and these two alleles were associated with isolates from two divergent lineages. The *P. multocida* isolates of *ompA6.1* type have been previously shown to cluster with the major porcine AR isolates of capsular type A and D, OMP-types 4.1, 6.1 and 13.1 and ST 11 (MLST group G), whereas the *P. multocida* isolates associated with *ompA6.2* have been previously shown to cluster with the heterogeneous avian isolates of OMP-type 10.1 and ST 36 (MLST group H) (Fig. 3.20B). Another example of assortative recombination is provided by the *ompA8.1* allele in lineage IV; this allele was associated with isolates of ST 8 (bovine), ST 12 (avian, porcine and ovine), ST 17 (ovine) and ST 25 (avian). The closely related *ompA8.2* allele was associated with ovine isolates of capsular type A, OMP-type 1.1 and ST 16. These two alleles differed from each other at only ten nucleotides sites. Furthermore, the *ompA8.1*-type and *ompA8*.1-type alleles were associated with isolates from different lineages (MLST group C and B, respectively) (Fig. 3.20).

Lineage V represents the *ompA9*-type alleles that were divided into 6 allelic subgroups, *ompA9.1*- to *ompA9.6*-type alleles, nucleotide variation ranging from 1 to 92 nucleotide sites. This group includes bovine haemorrhagic septicaemia isolates of capsular type B, STs 46 and 44 and MLST group B (PM1192, 1200 and PM30), avian isolate PM62 of capsular type B (OMP 12.1, ST 39 and MLST group D) and heterogeneous avian isolates PM104, PM152, PM82, and PM300 of STs 28, 31, 32 and 33 (MLST group H) respectively. These data provide strong evidence that the *P. multocida ompA*-type alleles have undergone horizontal gene transfer and assortative recombination.

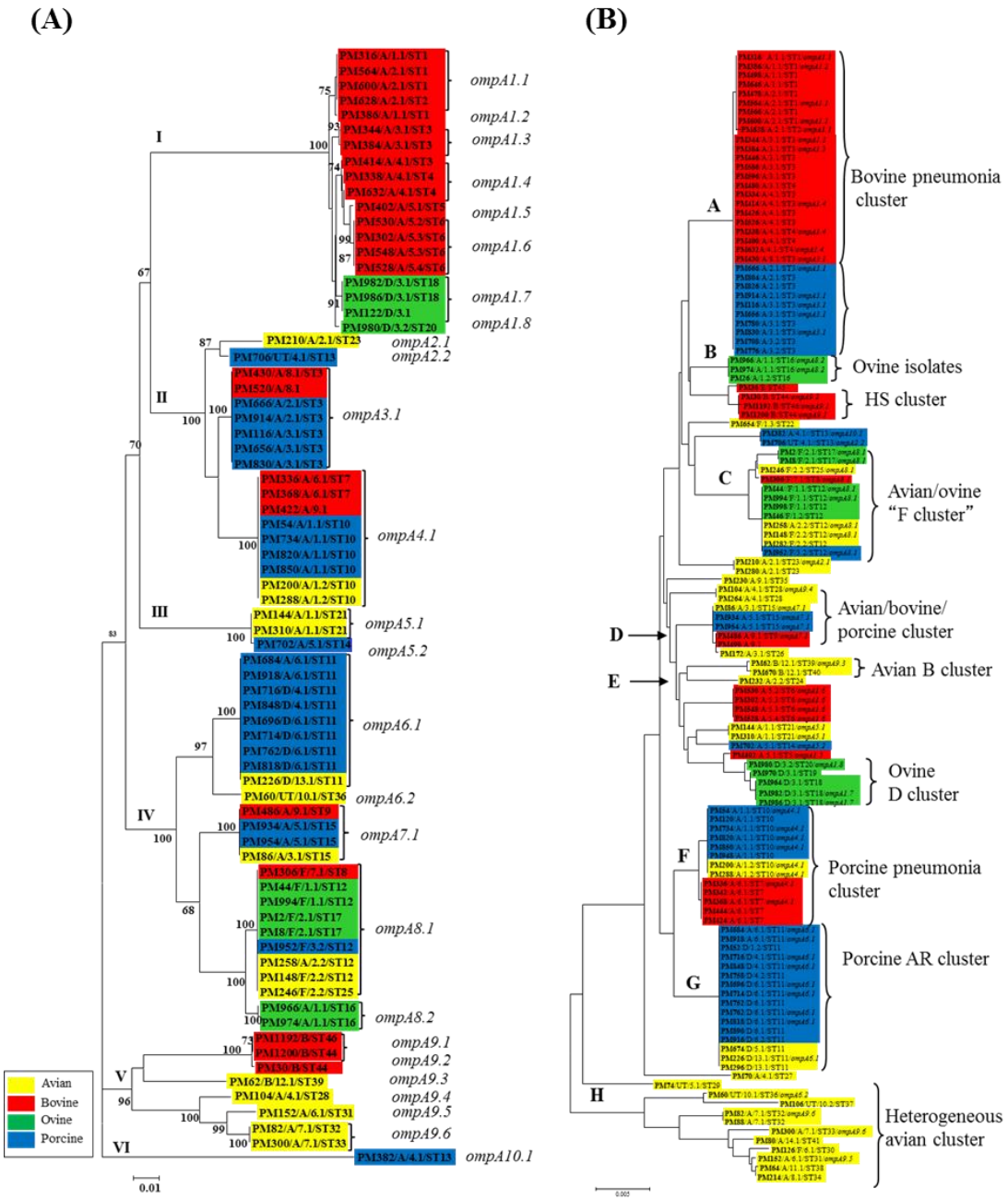

Fig. 3.21 Neighbour-Joining tree representing the phylogenetic relationships of *ompA* alleles (A) and the genetic relationships of *P. multocida* strains based on the concatenated sequences of seven housekeeping enzyme genes (MLST) (B).

Isolate designation, capsular type, OMP type and ST type are provided for each isolate (e.g. PM316/A/1.1/ST1). Allele designations are sown to the right (*ompA1.1*, etc.).

3.6.8.2 Intragenic Recombination among *ompA* Alleles

It is very important to understand the overall relationships of the *ompA* alleles among the different *P. multocida* strains where this will allow a better understanding of the molecular evolution and diversity of *ompA*. For this reason, visual inspection of polymorphic nucleotide sites in the aligned sequences of the 26 *ompA* alleles, in conjunction with graphical representation of polymorphic sites was carried out to identify regions of recombination among the *ompA* alleles (Fig. 3.22 & Fig. 3.23). Happlot analysis helps to reveal the presence of mosaic structures that result from intragenic recombination. The distribution of nucleotide polymorphic sites within lineage I showed that the *ompA* alleles were homogeneous and, with one exception, there was no evidence of intragenic recombination within the *ompA1.1* to *ompA1.8* alleles. However, *ompA1.3*-type allele contained a recombinant segment (nucleotides 825 to 909) that was identical to the corresponding region of the *P. multocida ompA3.1* and *ompA4.1* alleles (Fig. 3.22). In contrast, there was clear evidence of intragenic recombination within lineages II, III, IV, V and VI because complex mosaic structures were identified among alleles within these lineages. The proposed recombinant segments are highlighted with coloured boxes; identical or almost identical segments are coloured with same colour (Fig. 3.22). *OmpA* alleles within lineage II contained identical segment (nucleotides 12 to 44) that was identical to the corresponding region in *ompA* alleles within lineages III, IV, V and VI (Fig. 3.22). Alleles within lineage II had complex mosaic structures involving a series of recombination events with alleles of lineages III, IV, V and VI (Fig. 3.22). *A*llele *ompA2.1* had two different recombinant segments (nucleotides 580 to 642 and 726 to 1066) that were identical to the corresponding region of the *ompA7.1* and *ompA10.1* alleles, respectively. The *P. multocida ompA2.2-type* allele contained two different recombinant segments (nucleotides 727 to 1066 and 564 to 645) that were identical to the corresponding region of the *ompA8.2* allele in lineage IV and *ompA9.1*, *ompA9.2* and *ompA9.3* alleles in lineage V (Fig. 3.22). Allele *ompA3.1* contained identical recombinant segment (nucleotides 553 to 642) to the corresponding region of the *ompA4.1* allele in lineage II, *ompA6.1* and *ompA6.2* alleles in lineage IV and *ompA9.4*, *ompA9.5* and *ompA9.6* in lineage V. The *P. multocida ompA4.1*-type allele had DNA segment (nucleotides 48 to 255) that was identical to the corresponding region of the *ompA5.1* and *ompA5.2* alleles in lineage III (Fig.

3.22). Alleles within in lineage II and IV contained identical recombinant segment (nucleotides 484 to 500) (Fig. 3.22). *OmpA5.1* and *ompA5.2* shared an identical DNA segment (nucleotides 661 to 1066) to the corresponding region of *ompA7.1*. The exchange of DNA segments within lineage IV were also complex because this lineage had a segment that that was identical to the corresponding regions in lineages II, III and V as described above (Fig. 3.22). Allele *ompA9.1* shared a short identical segment (nucleotides 12 to 147) with alleles *ompA9.2* and *ompA10.1*. Recombinant segments (nucleotides 207 to 255 and 484 to 500) were common to the *ompA9.1*-, *ompA9.2*-, *ompA9.3*-, *ompA9.4*-, *ompA9.5*- and *ompA9.6*-type alleles in lineage V (Fig. 3.22). Finally, *ompA10.1* contained two different segments (nucleotides from 12 to 147 and 726 to 1066) that were identical to the corresponding region of the *ompA9.1*- and *ompA9.2*-type alleles in lineage V and *ompA2.1* allele in lineage II (Fig. 3.22).

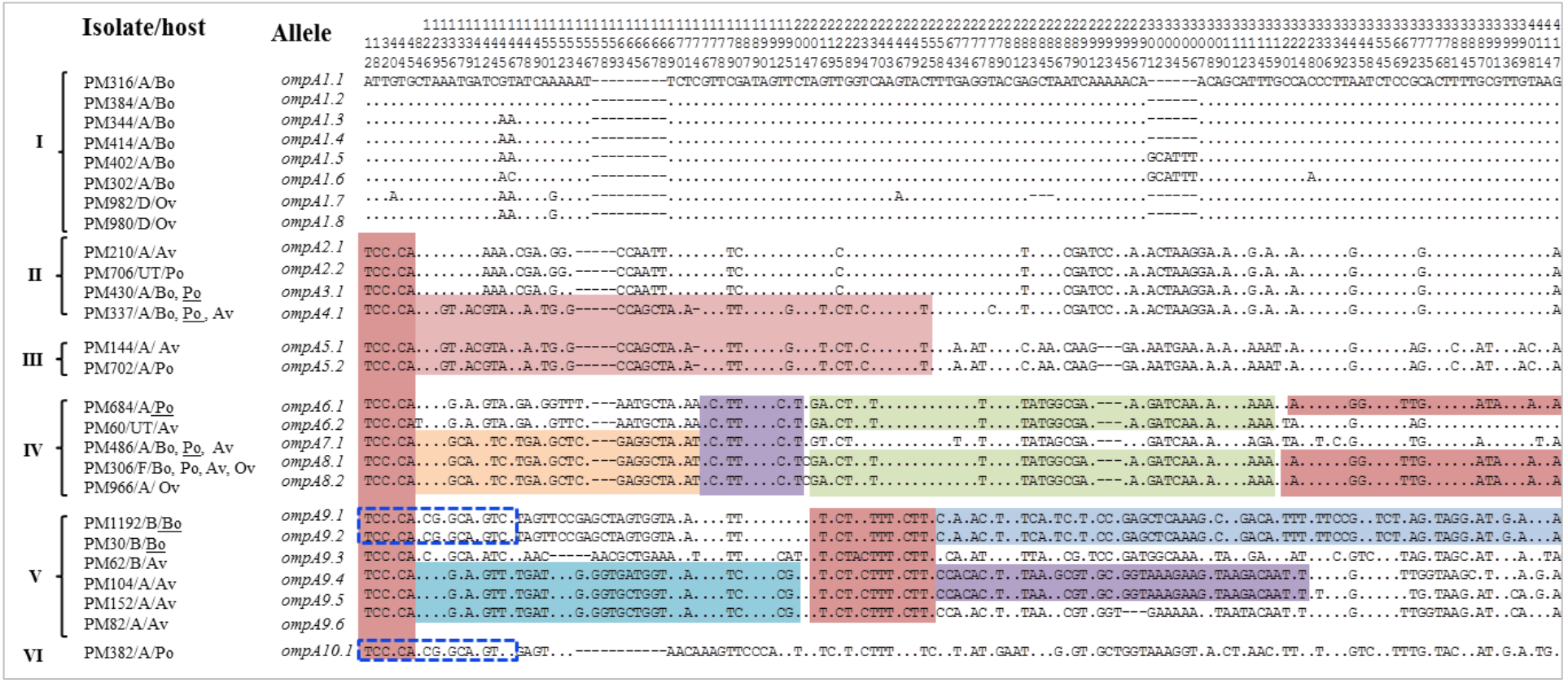
Isolate/host
Allele
I
PM316/A/Bo
PM384/A/Bo
PM344/A/Bo
PM414/A/Bo
PM402/A/Bo
PM302/A/Bo
PM982/D/Ov
PM980/D/Ov
ompA1.1
ompA1.2
ompA1.3
ompA1.4
ompA1.5
ompA1.6
ompA1.7
ompA1.8
II
PM210/A/Av
PM706/UT/Po
PM430/A/Bo, Po
PM337/A/Bo, Po, Av
ompA2.1
ompA2.2
ompA3.1
ompA4.1
III
PM144/A/ Av
PM702/A/Po
ompA5.1
ompA5.2
IV
PM684/A/Po
PM60/UT/Av
PM486/A/Bo, Po, Av
PM306/F/Bo, Po, Av, Ov
PM966/A/ Ov
ompA6.1
ompA6.2
ompA7.1
ompA8.1
ompA8.2
V
PM1192/B/Bo
PM30/B/Bo
PM62/B/Av
PM104/A/Av
PM152/A/Av
PM82/A/Av
ompA9.1
ompA9.2
ompA9.3
ompA9.4
ompA9.5
ompA9.6
VI
PM382/A/Po
ompA10.1

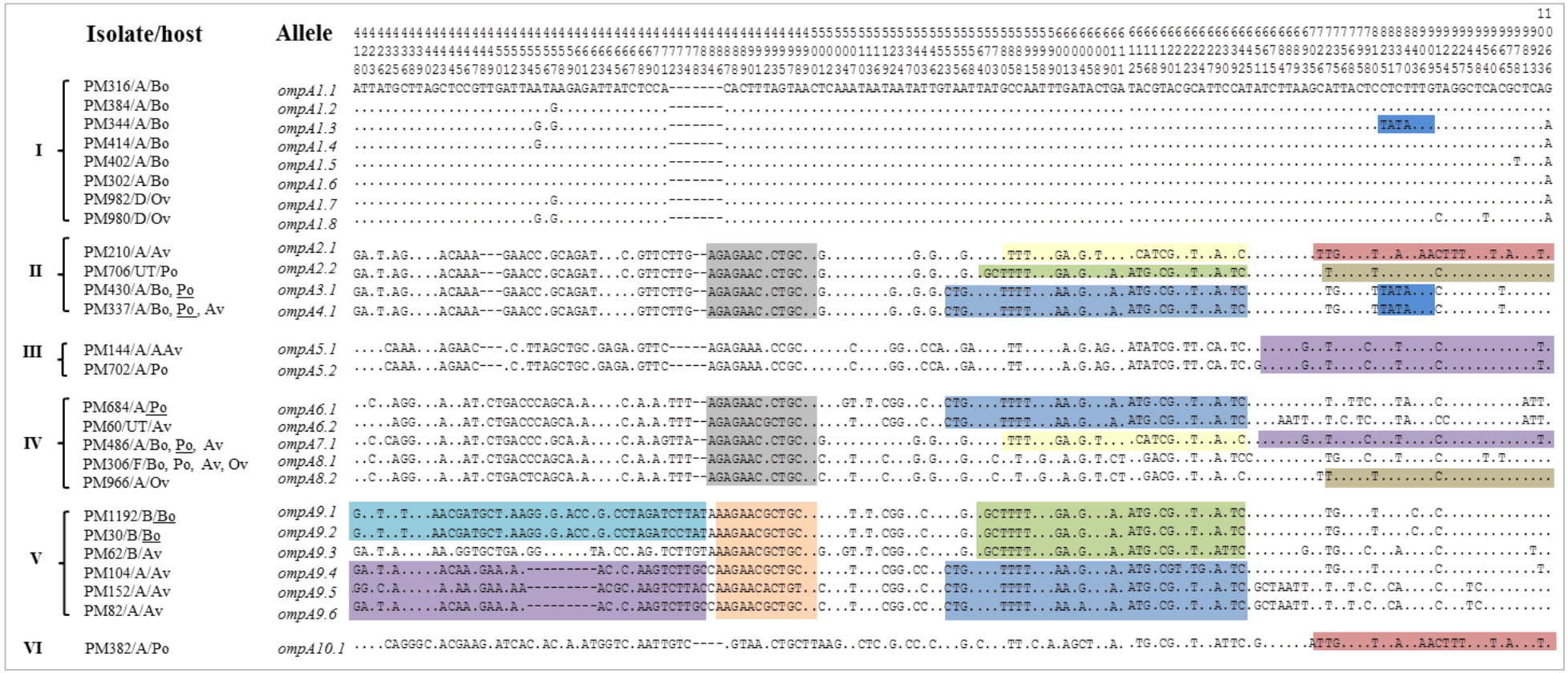

Fig. 3.22 Distribution of polymorphic nucleotide sites in the aligned sequences of the 26 *ompA* alleles of *P. multocida.*

Allele designations are shown to the left of each sequence. Roman numerals I to VI represent the phylogenetic lineages (**Fig. 3.16**). Coloured boxes highlight sequence identity and proposed recombinant segments. The vertical numbers above the sequences represent the positions of polymorphic nucleotide sites.

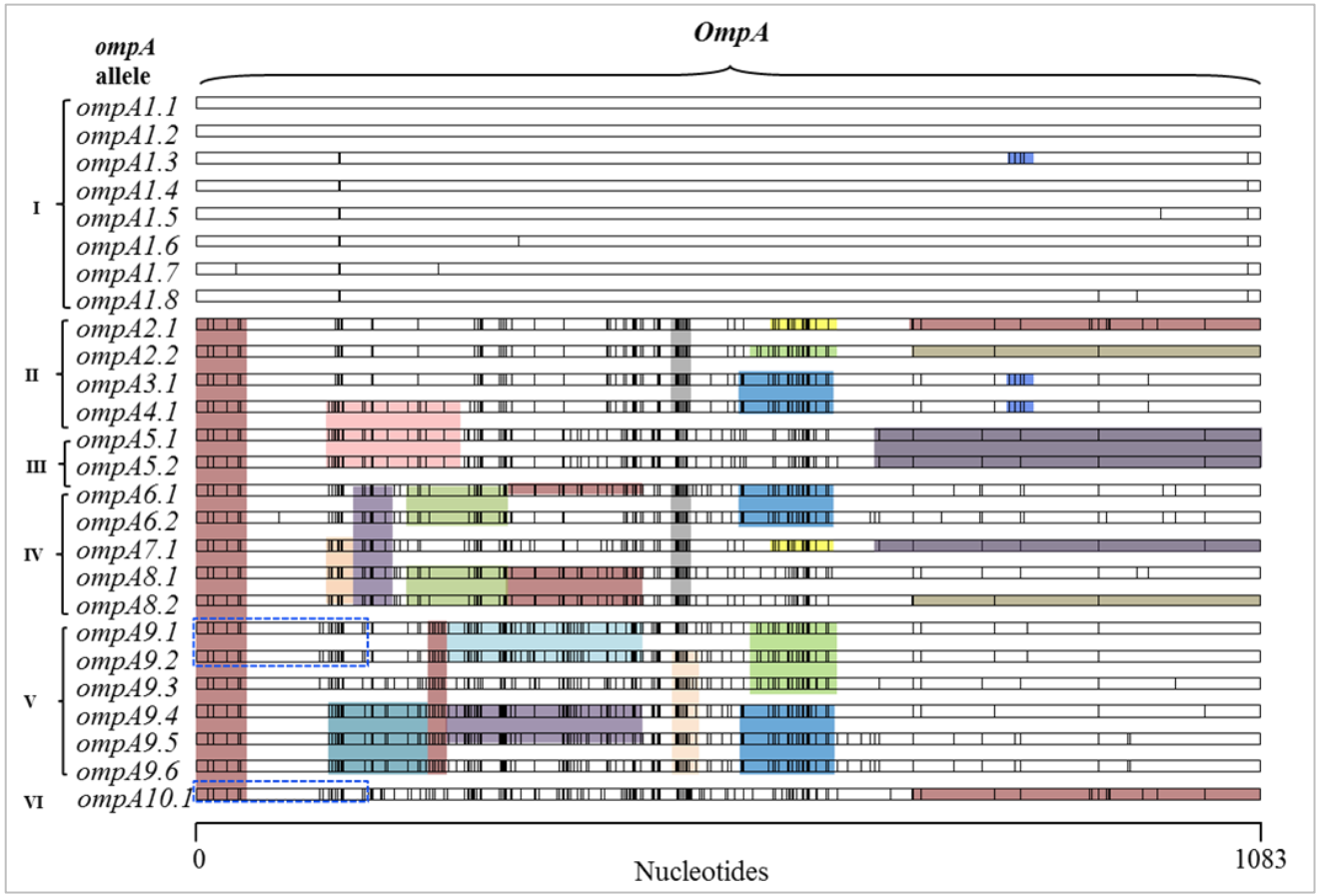

Fig. 3.23 Graphic representation of polymorphic nucleotide sites in the aligned sequences of the 26 *ompA* alleles of *P. multocida* using Happlot analysis.

Allele designations are shown to the left of each sequence. Roman numerals I to VI represent the phylogenetic lineages (**Fig. 3.16**). Coloured boxes highlight sequence identity and proposed recombinant segments. Graph was created using Micrographic Designer.

3.7 Discussion

3.7.1 Molecular evolution and diversity of OmpA in *P. multocida*

The diversity and evolution of OmpA was investigated in 74 *P. multocida* isolates representing different evolutionary lineages. The *ompA* gene of *P. multocida* is highly diverse and is represented by 26 unique alleles. Multiple subclasses of OmpA were also found among cattle, sheep and goats and swine isolates of *P. multocida* (Vougidou *et al.*, 2015) and among ovine and bovine isolates of *M. haemolytica* (Davies & Lee, 2004). The phylogenetic relationships of the *ompA* gene of *P. multocida* does not correlate with the species phylogeny based on comparative nucleotide sequence of the 16 rRNA gene (Davies, 2004) or on the concatenated partial sequences (3990 bp) of seven housekeeping enzyme genes (Davies *et al.,* unpublished; http://pubmlst.org/pmultocida_multihost) as well as based on the fifteen housekeeping enzyme genes and core genomes (Chapter 2). The present findings indicated that *ompA* has undergone horizontal DNA transfer and recombinational exchanges. Comparative nucleotide sequence of the *ompA* alleles has allowed a more complete picture of *ompA* evolution to be established. *OmpA* sequence analysis has confirmed that avian *P. multocida* isolates are more diverse than bovine, porcine and ovine isolates. These results are in agreement with previous study (Davies, 2004). The possible reasons for the diversity of avian *P. multocida* isolates were discussed in a previous study (Davies *et al.*, 2003c). The molecular mass of OmpA was heterogeneous (37.5-38.3 kDa) and this is probably due to the amino acid variation and differences in size of the hypervariable surface-exposed loops. Similar heterogeneity has been described in the OmpA protein of *P. multocida* (Vougidou *et al.*, 2015), OmpA protein of *M. haemolytica* (Davies & Lee, 2004) and P5 outer membrane protein of *H. influenzae* (Duim *et al.*, 1997).

Six different lineages, I to VI, were identified and the *ompA* alleles have very different nucleotide sequences (Fig. 3.22). Visual inspection of the distribution of polymorphic nucleotide sites among the *ompA* sequences revealed that the *P. multocida ompA*-type alleles have undergone horizontal gene transfer and recombinational exchange. The presence of identical, or almost identical, alleles in strains of divergent phylogenetic lineages indicates the occurrence of assortative (entire gene) recombination between strains., alternatively,

Intragenic recombination results in the formation of mosaic alleles in which sections of DNA in a recipient allele are replaced by DNA from one or more donor alleles (Smith, 1999). Intragenic recombination results in the formation of linked runs of nucleotides within a sequence whose ancestry is different from the other nucleotides in the same sequence (Smith, 1999). There was no evidence that intragenic recombination has occurred among the *ompA*-type alleles in lineage I. However, *ompA1.3*-type allele contained a recombinant segment that was identical to the corresponding region of the *P. multocida ompA3.1*- and *ompA4.1*- type alleles (Fig. 3.22). In contrast, there was clear evidence of intragenic recombination within lineages II, III, IV, V and VI because complex mosaic structures were identified among alleles within these lineages (Fig. 3.22). The *ompA1*-type alleles, *ompA1.1* to *ompA1.8,* in lineage I were identical, or almost identical, *ompA* alleles in genetically divergent strains provides evidence of horizontal gene transfer and entire gene recombination (Fig. 3.21). The o*mpA1*-type allele in lineage I was the most prevalent group and was present in 19 isolates. It was exclusively associated with isolates of the bovine pneumonia cluster (*ompA1.1* to *1.6*). The presence of almost identical alleles, *ompA1.7* and *ompA1.8* in divergent *P. multocida* ovine isolates of capsular type D (MLST group E) indicates evidence of exchange of the *ompA*1-type allele between isolates of the major bovine pneumonia cluster (MLST group A) and the capsular type D ovine isolates of the MLST group E. This suggests that the ovine isolates could possibly have driven *ompA1.7* and *ompA1.8* by horizontal DNA transfer and recombination from bovine isolates or vice versa. Host switching of strains from cattle to sheep, or vice versa has been shown previously to contribute in recombinational exchanges and to the emergence of new strains (Davies *et al.*, 2001; 2002; Davies & Lee, 2004; 2011). The occurrence of the *P. multocida ompA1.1*- to *ompA1.6*-type alleles within the phylogenetically divergent bovine isolates of the MLST group A (*ompA1.1*- to *ompA1.4*-type alleles) and MLST group E (*ompA1.5*- and *ompA1.6*-type alleles) (Fig. 3.16), respectively, indicate that they have a common ancestral or evolutionary origin. Assortative recombination has also occurred within lineage II. There is also evidence that *ompA2.1*- and *ompA2.2*-type alleles have undergone assortative recombination because they are associated with *P. multocida* isolates that cluster in divergent lineages based on the concatenated sequences of the seven housekeeping genes (Fig. 3.20). The *ompA2.1*-type allele was associated with

avian isolate PM210, where *ompA2.2*-type allele was associated with porcine isolates PM706 indicating the occurrence of the *ompA* gene exchange between avian and porcine isolates.

The almost identical *ompA3.1*- and *ompA4.1*-type alleles in lineage II were also associated with isolates of divergent phylogenetic lineages. The *ompA3.1*-type allele was associated with bovine pneumonia isolates of capsular type A, OMP 8.1 and ST 3 and porcine pneumonia isolates of capsular type A, OMPs 1 and 2 and ST 3 (MLST group A), whereas the *ompA4.1-type* allele was associated with isolates of the major porcine pneumonia cluster (MLST group F) (Fig. 3.20). This association suggests that bovine and porcine isolates of *ompA3.1*-type allele (MLST group A) could possibly have derived *ompA* from the major porcine pneumonia group (MLST group F) by horizontal DNA transfer and recombination, or vice versa. The identification of the *ompA3*-type allele in bovine isolates of OMP-type 8.1 and ST 3 and porcine isolates of OMP-types 2 and 3 and ST 3 indicates that these isolates have the same ancestral origin. Isolates of *ompA3.1*-type alleles have previously been shown to cluster with isolates of the *ompA1.1*- to *ompA1.4*-type alleles based on the concatenated sequences of the seven housekeeping gene (Fig. 3.21B).

The presence of divergent alleles in closely related bovine (*ompA1.1* to *ompA4.1*) and bovine and porcine (*ompA3.1*) isolates of capsular type A, OMP-types 1 to 8 and STs 1 to 6 (MLST group A) suggests a possible evolutionary origin for the strains. One possibility is that the bovine and porcine strains (*ompA3.1*) evolved from ancestral bovine pneumonia isolates (MLST group A) after transmission of *ompA* from isolates in the major porcine pneumonia group (MLST group F). The assortaitve recombination has also occurred within lineage IV particularly in *ompA6.1* and *ompA6.2* and in *ompA8.1* and *ompA8.2* and in lineage V, including in *ompA9.1* to *ompA9.2*. These data suggest that *ompA* has undergone excessive horizontal gene transfer, entire gene recombination which has contributed to the diversity of OmpA in *P. multocida*.

Visual inspection of the distribution of polymorphic nucleotide sites among the *ompA* sequences revealed that the *P. multocida ompA*-type alleles within lineages II, to VI comprises complex mosaic structures that have been formed as result of horizontal DNA transfer and intragenic recombination (Fig. 3.22). A

comparison of the *P. multocida ompA4.1*-type alleles with the *P. multocida ompA5.1*- and *ompA5.2*-type alleles suggests that *ompA5.1* and *ompA5.2* was derived from *ompA4.1* by the acquisition of identical segment (nucleotides 12 to 252) (Fig. 3.22). The results show that the P. *multocida ompA* alleles in lineages II to VI have undergone multiple horizontal DNA transfer and intragenic recombination (Fig. 3.22).

3.7.2 Structural model of OmpA and amino acid variation

The 35-kDa OmpA protein has been well studied and characterised in *E. coli* and is composed of a 19 kDa transmembrane domain and a 16 kDa globular C-terminal domain (Pautsch & Schulz, 1998; Pautsch & Schulz, 2000; Arora *et al.*, 2001; Confer & Ayalew, 2013). The structure consists of eight antiparallel ß-barrel strands, three short periplasmic turns and four flexible, mobile surface exposed loops (Confer & Ayalew, 2013; Davies & Lee, 2004; Koebnik, 1999; Smith *et al.*, 2007). In *P. multocida*, OmpA similarly consists of eight antiparallel ß-barrel strands and four flexible, mobile surfaces exposed loops (Dabo *et al.*, 2003). Amino acid sequence analysis of the *ompA* type alleles revealed that the majority of variable sites occurred within four hypervariable regions located at the distal ends of the surface-exposed loops. This has also been found in the *OmpA* protein of *P. multocida* (Dabo *et al.*, 2008; Vougidou *et al.*, 2015), *M. haemolytica* (Davies & Lee, 2004; Hounsome *et al.*, 2011) and the P5 outer membrane protein of *H. influenzae* (Duim *et al.,* 1997*;* Webb & Cripps, 1998). Sequence variation in the loop regions may reflect functional differences a mong the OmpA protein (Dabo *et al.*, 2003; Hounsome *et al.*, 2011; Koebnik, 1999a; b). The numbers of synonymous substitutions per 100 synonymous sites (d_S) and nonsynonymous substitutions per 100 nonsynonymous sites (d_N) were estimated for the conserved and loop regions The results showed that the patterns of synonymous and nonsynonymous substitution rates were not equal throughout the *ompA* gene. Different regions of OmpA are subject to different patterns of evolutionary constraint and diversification. Studies have suggested that OmpA is subject to diversifying selection within the host and might play important roles in host–pathogen interactions because the *P. multocida* OmpA had a heterogeneous molecular mass based on OMPs profiles (Davies *et al.*, 2003a; b; c; Davies, 2004; Davies *et al.*, 2004). The transmembrane domains were conserved because the number of synonymous substitutions exceeded the

number of nonsynonymous substitutions. This suggests that natural selection is acting to restrict amino acid replacement in the non-loop regions of OmpA because these parts of the molecules are mostly involved in maintaining outer membrane structural integrity by interacting with the membrane and with the peptidoglycan layer and cannot tolerate amino acid change. In contrast, the data provide strong evidence that natural selection is driving diversification of the hypervariable extracellular loop regions because the d_S/d_N ratios for the hypervariable extracellular loop domains (L1, L2, L3 and L4) were all less than 1, the ratios ranging from 0.49 to 0.66. Similar selection pressures and evolutionary constraints are involved in different regions of the OmpA of *M. haemolytica* (Davies & Lee, 2004) and the P5 outer membrane protein of *H. influenzae* (Duim *et al.*, 1997; Webb & Cripps, 1998). It has also been shown that OmpA of *Chlamydia trachomatis* is under diversifying selection for immune evasion (Joseph *et al.*, 2012). A study by Vougidou *et al.* (2015) revealed that most of the substitutions were non-synonymous outside the transmembrane domains, whereas synonymous substitutions were observed within the transmembrane domains of OmpA associated with pneumonic *P. multocida* strains. These results suggest that the loop regions of OmpA of *P. multocida* may play an important role in the pathogenesis of *P. multocida*. It has also been shown that OmpA is involved in adherence of *P. multocida* (Carpenter *et al.*, 2007; Dabo *et al.*, 2003; Katoch *et al.*, 2014) and in other pathogenic bacteria binds to specific host cell receptors (Hill *et al.*, 2001; Orme *et al.*, 2006; Torres & Kaper, 2003). In *P. multocida* recovered from the bovine nasal cavity, two *ompA* classes, *ompA* (I) and *ompA* (II) were identified (Katoch *et al.*, 2014) and their pathogenicities were studied *in vitro* and *in vivo*. The results of *in vitro* pathogenicity studies indicated that a strain with *ompA* (I) was more invasive than *P. multocida* strain with *ompA* (II). The *in vivo* studies showed that the isolates harbouring *ompA* (I) were comparatively more virulent than isolates harbouring *ompA* (II) (Katoch *et al.*, 2014). The variations in the *ompA* gene has contributed to differential virulence potential because its sequence variation resulted in differential bacterial adherence and internalisation (Katoch *et al.*, 2014). The locations of variable sites within the four hypervariable regions at the distal ends of the surface-exposed loops of OmpA suggest that these parts of OmpA are involved in recognition and receptor binding because it is suggested that the loops participate in the recognitions of various ligands. For example, they interact

with cell-surface receptors (Carpenter *et al.*, 2007; Dabo *et al.*, 2003), OmpA from *M. haemolytica* binds to cell surface fibronectin (Lo & Sorensen, 2007), colicins (Killmann *et al.*, 1995) and serve as a potential secondary receptor for P22-like phage infection in *Salmonella* (Jin *et al.*, 2015), phage Sf6 in *Shigella flexneri* (Parent *et al.*, 2014; Porcek & Parent, 2015) as a receptor for several bacteriophages in *E. coli* (Morona *et al.*, 1985). The variation in the surface-exposed loop regions between the *P. multocida ompA* alleles suggests that the OmpA protein could possibly have a role in host specificity. It has been suggested that the loops of OmpA confer species-specificity as identified through the use of cross absorbed antibodies (Hounsome *et al.*, 2011).

In conclusion, the *P. multocida* OmpA protein consists of eight antiparallel ß-barrel strands and four flexible, mobile surface-exposed loops. Amino acid sequence analysis of the *ompA* alleles revealed that the majority of variable sites occurred within four hypervariable regions located at the distal ends of the surface-exposed loops. Sequence variation in the loop regions may reflect functional differences among the OmpA protein. The data provide strong evidence that natural selection is driving diversification of the hypervariable extracellular loop regions, suggesting that the loop regions of OmpA of *P. multocida* may play an important role in the pathogenesis and immune selection of *P. multocida*. The variation in the surface-exposed loop regions between the *P. multocida ompA* alleles suggests that the OmpA protein could possibly have a role in host specificity and virulence. Sequence analysis of the 26 different *ompA*-type alleles revealed that the *P. multocida ompA* gene has undergone multiple horizontal gene transfer and recombination events. Complex mosaic structures exist which have been driven by horizontal DNA transfer and intragenic recombination between *ompA* alleles. Different mechanisms may contribute to the horizontal DNA transfer and recombinational exchanges in *P. multocida*. In particular, transduction is a likely contributor to these events because phage-related sequences are abundant in the genomes of many bacterial species. Therefore, there is a possibility that bacteriophages could be responsible for the horizontal DNA transfer and exchange of genetic material in *P. multocida*. Thus, the bacteriophages of *P. multocida* will be analysed to identify whether they might be involved in the transfer of virulence determents such as OMPs.

Chapter 4 Characterisation of temperate bacteriophages in *P. multocida*

4.1 Introduction

Bacteriophages are bacterial viruses that can normally undergo one of two types of life cycles, namely the lytic and lysogenic cycles. Unlike lytic phages, temperate bacteriophages can also enter a lysogenic cycle during which the phage genome is integrated into the bacterial chromosome to become a prophage (Feiner *et al.*, 2015). Temperate phages can achieve a state where they do not promote bacterial cell lysis but their genome is replicated along with the bacterial host chromosome by the repression of the lytic genes (Birge, 2006; Casjens, 2003; Feiner *et al.*, 2015). However, under certain circumstances, temperate bacteriophages can switch from their lysogenic state and convert to a vegetative state by the expression of the lytic genes (Birge, 2006; Oppenheim *et al.*, 2005). Temperate phages can enter the vegetative state or lytic phase either spontaneously (Dale, 1999; Oppenheim *et al.*, 2005; Waldor & Friedman, 2005) or by a process called induction caused by stressful conditions such as DNA-damaging agents (Birge, 2006; Oppenheim *et al.*, 2005). Prophage induction is brought about by the inactivation of bacteriophage repressors such as the CI repressor (Rokney *et al.*, 2008). Different DNA-damaging agents such as physical stimuli and chemical treatments have been used to switch temperate phages from their lysogenic cycle into the lytic cycle. Mitomycin C is used most frequently to induce prophages in both Gram-negative and Gram-positive bacteria. DNA damage following treatment with mitomycin C stimulates the host SOS response network, eliciting the activation of RecA as a co-protease. The activation of RecA enhances auto-cleavage of the host SOS LexA repressor (Rokney *et al.*, 2008). LexA is structurally similar to the CI repressor of bacteriophage λ. The activation of RecA also stimulates inactivation of the CI repressor promoting the lytic infection (Galkin *et al.*, 2009; Rokney *et al.*, 2008). Expression of the lytic genes promotes the excision of the phage genome, followed by DNA replication, assembly of phage particles, DNA packaging, and release of the new phage progenies through bacterial cell lysis (Feiner *et al.*, 2015). The details have been described previously in Chapter 1.

Different systems are used for the classification of bacterial viruses. They are classified based on their genetic material (single stranded or double stranded DNA or RNA viruses) and virion morphology (Ackermann, 2003; Brüssow & Hendrix, 2002). Ninety six percent of the bacterial viruses are tailed phages belonging to the order Caudovirales (Ackermann, 2001). They are grouped into three families according to tail morphology: *Siphoviridae*, with long, non-contractile, flexible tails; *Myoviridae*, with contractile tails; and *Podoviridae* with short tails (Ackermann, 2003; Ackermann, 2009; Murphy *et al.*, 2012).

Very little is known about the temperate bacteriophages of *P. multocida*. Previously, bacteriophages were described in *P. multocida* and used as typing methods in epidemiological studies (Fussing *et al.*, 1999; Nielsen & Rosdahl, 1990). In another study, the morphology of temperate phage in *P. multocida* was investigated by TEM (Ackermann & Karaivanov, 1984). A diverse group of phages belonging to the *Myoviridae*, *Siphoviridae* and *Podoviridae*-like phage were identified. Although the study showed that prophages could be induced in *P. multocida* strains, there was no indication if multiple prophages were induced from single *P. multocida* isolates. No previous studies have investigated the diversity of bacteriophages within *P. multocida* in detail. *P. multocida* represents a diverse group of Gram-negative bacteria, responsible for a variety of economically important infections in a wide range of domestic animals. Therefore, this study was designed to investigate the diversity of temperate bacteriophages within *P. multocida* and to determine if the bacteriophages are contributing to the diversity of isolates representing multiple hosts, different capsular types, OMPs and STs. The objectives of this part of the study were as follows: to determine the optimum concentration of mitomycin C for the induction of temperate phages in *P. multocida* isolates from different host species and representing different serogroups, to induce bacteriophages in 47 *P. multocida* isolates representing multiple host species, disease types, capsular serotypes, OMP-types and sequence types, to characterise phage morphology and diversity by transmission electron microscopy (TEM), to establish whether multiple prophages can be induced from single *P. multocida* isolates. Finally, to assess the host range of induced bacteriophages against a panel of indicator strains and to analyse the genetic diversity of induced phage by restriction endonuclease analysis.

4.2 Material and Methods

4.2.1 Bacterial isolates

Forty seven *P. multocida* isolates were selected to investigate the diversity and evolution of temperate bacteriophage. The isolates were well studied and characterised in previous studies (Davies *et al.*, 2003a; b; c; Davies, 2004; Davies *et al.*, 2004). The isolates were recovered from cattle, sheep, pigs and poultry and were associated with different diseases. The strains represented various capsular types, OMPs-types, 16S rRNA types, and sequence types (STs) (http://pubmlst.org/pmultocida_multihost/). The properties of the isolates are summarised in Table 4.1

4.2.2 Media for bacterial growth

Brain heart infusion agar (BHIA; Oxoid, UK) and brain heart infusion broth (BHIB; Oxoid, UK) were used as routine solid and liquid media, respectively, for the growth of *P. multocida*. *P. multocida* isolates were cultured on blood agar (BHIA containing 5% [v/v] defibrinated sheep's blood [E & O Laboratories Limited]). BHIB was used to prepare liquid starter cultures and bacterial suspensions.

4.2.3 Bacterial storage and growth conditions

P. multocida isolates were preserved in 1 ml of 50% (v/v) glycerol in BHIB at -80°C for long-term storage. Fifteen microliters of thawed stock suspensions were streaked onto blood agar plates and incubated at 37°C overnight.

4.2.4 Preparation of broth starter cultures

For optimisation of mitomycin C for bacteriophage induction, liquid cultures were prepared by inoculating 3 to 4 well-isolated colonies from overnight culture plates into 25 ml volumes of BHIB and incubating at 37°C with shaking at 120 rpm. In other experiments, such as isolation and characterisation of bacteriophages, 3 to 4 single colonies were re-suspended in 3 ml of BHIB in a bijou.

Table 4.1 Details of 47 *P. multocida* isolates.

Isolate [a]	ST [b]	MLST group	Host species	Clinical symptoms	Isolation site	Geographical origin	Capsular type	OMP-type [c]	16S rRNA type	*toxA* gene
PM316*	1	A	Bovine	Pneumonia	Lung	Penrith	A	1.1	3	ND
PM564*	1	A	Bovine	Pneumonia	Lung	Thirsk	A	2.1	3	ND [d]
PM344*	3	A	Bovine	Pneumonia	Lung	Shrewsbury	A	3.1	1	ND
PM632*	4	A	Bovine	Pneumonia	Lung	Winchester	A	4.1	1	ND
PM666*	3	A	Porcine	Pneumonia	Lung	Sutton Bonington	A	2.1	1	-
PM116*	3	A	Porcine	Pleuropneumonia	Lung	Sutton Bonington	A	3.1	1	-
PM966*	16	B	Ovine	Pneumonia	Lung	Winchester	A	1.1	1	-
PM382*	13	C	Porcine	Respiratory problems	Lung	Winchester	A	4.1	2	-
PM706	13	C	Porcine	Pneumonia	Lung	Lincoln VIC	UT	4.1	2	-
PM2*	17	C	Ovine	Severe peritonitis	-	Penrith	F	2.1	4	-
PM8	17	C	Ovine	Asymptomatic	Vagina	Penrith	F	2.1	4	-
PM246*	25	C	Avian	Septicaemia	Viscera	Bury St. Edmunds	F	2.2	2	ND
PM994*	12	C	Ovine	Pneumonia	Lung	Penrith	F	1.1	2	-
PM148*	12	C	Avian	Eye infection	Eye	Thirsk	F	2.2	2	ND
PM104	28	D	Avian	Septicaemia	Liver/spleen	Aberystwyth	A	4.1	9	ND
PM86*	15	D	Avian	Fowl cholera	Pleura	Winchester	A	3.1	1	ND
PM934*	15	D	Porcine	Pneumonia	Lung	Bristol	A	5.1	1	-
PM954*	15	D	Porcine	Pneumonia	Lung	Winchester	A	5.1	1	-
PM486*	9	D	Bovine	Pneumonia	Lung abscess	Bristol	A	9.1	1	ND
PM172*	26	D	Avian	Septicaemia	Lung	Starcross	A	3.1	ND	ND
PM302*	6	E	Bovine	Rhinitis + others	Nasal swab	Sutton Bonington	A	5.3	ND	ND
PM144*	21	E	Avian	Septicaemia	Lung/liver	Thirsk	A	1.1	2	ND
PM402*	5	E	Bovine	Pneumonia	Lung	Newcastle	A	5.1	1	ND
PM122*	ND	ND	Ovine	Pneumonia	Lung	Sutton Bonnington	D	3.1	ND	+
PM964*	18	E	Ovine	Pneumonia	Lung	Winchester	D	3.1	ND	+
PM982*	18	E	Ovine	Pneumonia	Lung	Carmarthen	D	3.1	1	+

Table 4.1 (continued)

Isolate [a]	STs [b]	MLST group	Host species	Clinical symptoms	Isolation site	Geographical origin	Capsular type	OMP-type [c]	16S rRNA type	*toxA* gene
PM986*	18	E	Ovine	Pneumonia	Lung	Luddington	D	3.1	1	+
PM988*	ND	ND	Ovine	Pasteurellosis	Lung	Winchester	D	3.1	ND	+
PM990	ND	ND	Ovine	Pneumonia	Lung	Carmarthen	D	3.1	ND	+
PM54*	10	F	Porcine	Pneumonia	Lung	Shrewsbury	A	1.1	1	-
PM734*	10	F	Porcine	Pneumonia	Lung	Cambridge VIC	A	1.1	2	-
PM820	10	F	Porcine	Pneumonia	Lung	Thirsk	A	1.1	2	-
PM850*	10	F	Porcine	Pneumonia	Lung	Cambridge VIC	A	1.1	2	-
PM200*	10	F	Avian	Pneumonia	Lung	Cambridge VIC	A	1.2	ND	ND
PM336*	7	F	Bovine	Pneumonia	Lung	Cambridge VIC	A	6.1	2	ND
PM684*	11	G	Porcine	Suspect snouts	Nasal swab	Cambridge VIC	A	6.1	2	+
PM918*	11	G	Porcine	Pneumonia	Lung	Shrewsbury	A	6.1	ND	+
PM926*	ND	ND	Porcine	Pneumonia	Lung	Bury St Edmunds	A	6.1	ND	+
PM40*	ND	ND	Porcine	-	-	NCTC	A	6.2	2	+
PM716	11	G	Porcine	Toxin Assay	Nasal swab	Cambridge VIC	D	4.1	2	+
PM848*	11	G	Porcine	Pneumonia	Lung	Starcross	D	4.1	ND	+
PM696*	11	G	Porcine	Toxin Assay	Nasal swab	Cambridge VIC	D	6.1		+
PM714*	11	G	Porcine	Pneumonia	Lung	Thirsk	D	6.1	5	-
PM762	11	G	Porcine	Rhinitis	Turbinate	Worcester VIC	D	6.1	2	+
PM890	11	G	Porcine	Toxin Assay	Nasal swab	Bury St Edmunds	D	6.1	ND	+
PM226*	11	G	Avian	Pneumonia/death	Lesion	Sutton Bonington	D	13.1	ND	-
PM82*	32	H	Avian	Swollen heads	Peritoneal	Bury St Edmunds	A	7.1	19	ND

[a] isolates are arranged by order of MLST group (column 3) (Fig. 2.1); [b] ST= sequence type (Davies *et al*., unpublished http://pubmlst.org/pmultocida_multihost/); [c] OMP-types for bovine, ovine, porcine and avian are not equivalent, i.e. bovine OMP-type 1.1 is not as same as porcine OMP-type 1.1, etc. (Davies *et al.*, 2003a; b; c; Davies, 2004; Davies *et al.*, 2004); [d] ND: not determined.

4.3 Phage induction

4.3.1 Optimisation of mitomycin C for induction of temperate bacteriophages in *P. multocida*

Eight *P. multocida* isolates were selected to determine the optimum concentration of mitomycin C for prophage induction. The strains were PM144 and PM246 (avian strains), PM564 and PM632 (bovine strains), PM684 and PM734 (porcine strains), and PM966 and PM982 (ovine strains). The details of the eight isolates are summarised in Table 4.1. For each isolate, 0.3 ml of overnight broth culture was inoculated into 30 ml BHIB in each of eight 100 ml Erlenmeyer flasks (Davies & Lee, 2006). The preparation of ON liquid cultures is described in section 2.2.2.3. The flasks were incubated at 37°C with shaking at 120 rpm and the optical densities at 600 nm (OD_{600}) were measured at 1 h intervals. When the OD_{600} values reached 0.3 or above, mitomycin C (0.1 mg/ml stock solution) was added to seven of the eight to yield eight flasks with mitomycin C concentrations of 0 (control), 0.01, 0.05, 0.1, 0.2, 0.5, 1.0 and 2.0 µg/ml. Incubation of the flasks was continued for 10 h or more and the OD_{600} at hourly intervals to monitor phage induction. Lysate induction was performed in triplicate for each isolate. Phage induction was indicated by bacterial cell lysis. The OD_{600} values of mitomycin C-treated broth cultures were compared with the OD_{600} values of control samples (same culture without mitomycin C).

4.3.2 Phage induction

Having determined the optimum concentration for the induction of temperate phages, all 47 *P. multocida* isolates were induced with an optimum mitomycin C concentration of 0.2 µg/ml. However, each experiment was repeated with the higher concentration of mitomycin C when there was no sign of induction (i.e. no visible clearing in a specific isolate). For each of the 47 *P. multocida* isolates (Table 4.1) 0.3 µl of freshly prepared bacterial suspension (section 2.2.2.3) was inoculated into 30 ml of BHIB in each of two 100 ml Erlenmeyer flasks. After inoculation, the cultures were incubated at 37°C with shaking at 120 rpm. The OD_{600} was measured at 1 h intervals in a spectrophotometer. Mitomycin C (0.1 mg/ml stock solution) was added aseptically to one of each pair of flasks to a final concentration of 0.2 µg/ml when the OD_{600} value reached 0.4. Incubation was continued for 8 h in most cases. Bacterial cell lysis or induction was

monitored by measuring the OD_{600} in a spectrophotometer for both the mitomycin C-treated and control cultures. However, for those which showed no signs of lysis after 8 h, incubation was continued for 24 h. The induction profile for each isolate was made by comparing the OD_{600} values of mitomycin C treated and control cultures from the beginning to the end of induction. Moreover, for those isolates which showed no signs of induction with 0.2 µg/ml mitomycin C, the experiment was repeated with a higher concentration of mitomycin C. Bacteriophage induction was performed in triplicate for each isolate.

4.3.3 Preparation of lysate suspension

The lysates were induced after the cultures were treated with 0.2 µg/ml or higher concentrations mitomycin C. The phage suspensions were prepared by centrifugation of the induced cultures at 4000 *x g* for 20 min at 4°C to remove unlysed bacterial cells. The resultant supernatants were carefully collected and filtered by passing through syringe filters, pore size 0.2 µm (Minisart) to remove the bacterial debris. The filtered lysate suspensions were used immediately for the study of bacteriophage host range or stored at 4°C until further characterisation and analysis.

4.4 Bacteriophages characterisation

Bacteriophages were characterised by transmission electron microscopy (TEM), determination of host range and by restriction endonuclease analysis of isolated DNA.

4.4.1 Transmission electron microscopy (TEM)

Phage particles were identified by TEM using negative staining as described below. In addition, TEM was used to assess the diversity of phage morphologies among various *P. multocida* strains (Ackermann & Karaivanov, 1984; Pullinger *et al.*, 2004).

4.4.1.1 Optimum conditions for ultracentrifugation

Two isolates PM684 (porcine strain) and PM982 (ovine strain) were selected to optimise different ultracentrifugation speeds and various time points for

negative staining. Phages were induced and filtered as described in sections 4.3.2 & 4.3.3. Ten millilitres of filtered phage suspensions were centrifuged in an Optical™ L-90K ultracentrifuge using a 70.1 TI rotor (Beckman Coulter). The following parameters were chosen to pellet the phage particles: 20,000 *x g* for 3 h at 4°C (Davies & Lee, 2006) and 20,000 *x g*, 30,000 *x g* and 40,000 *x g* for 90 min at 4°C. After centrifugation, the supernatants were carefully discarded and the sedimented particles were re-suspended gently with 0.5 ml of 0.1 M ammonium acetate (pH 7.3) (Sigma-Aldrich, UK). The re-suspended suspensions were stored overnight at 4°C for negative staining and visualisation by TEM.

4.4.1.2 Negative staining parameters

Different time points were checked to prepare the grids before visualisation under TEM (Fig. 4.1). Three hundred mesh carbon-formvar coated nickel grids were dropped gently onto 50-100 µl of phage suspension. The grids were allowed to absorb the phage suspension for 1 and 2 min. The grids were washed 3 times with dH_2O for 10 s, excess fluid was removed using Whatman filter paper and the grids placed onto a drop of negative stain (2% ammonium molybdate). Two different time points of 30 s and 1 min were used for the staining reaction (Fig. 4.1). Excess staining solution was removed with Whatman filter paper and the grids were allowed to dry at room temperature for 15 to 20 min. The grids examined by TEM (FEI Tecnai TF20) at 200kV using Gatan Microscopy Suite Software. The samples for TEM were further optimised using the following negative staining: 2% ammonium molybdate, 2% uranyl acetate and Nanovan stain.

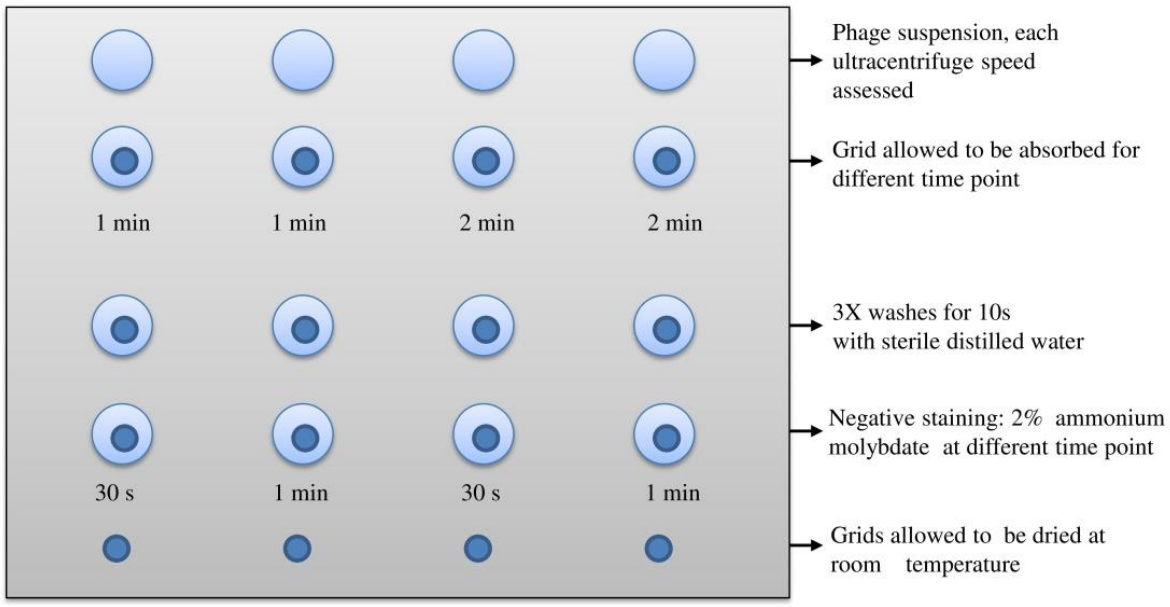

Fig. 4.1 Optimisation conditions for negative staining.

Preparation of grids for TEM using different time points for absorbtion of phage suspension and for negative staining of grids.

4.4.1.3 TEM using optimised conditions

Having determined the optimal conditions for TEM, all isolates were induced as described in sections 4.3.2 & 4.3.3. Ten millilitres of filtered phage suspensions were centrifuged at 40,000 *x g* for 90 min at 4°C. The supernatants were carefully removed and the pellets were re-suspended gently with 0.5 ml of 0.1 M ammonium acetate (pH 7.3). The suspensions were stored overnight at 4°C for negative staining and visualisation by TEM. Three hundred-mesh carbon-coated nickel grids were dropped onto 50-100 µL of phage suspension. The grids were allowed to adsorb phage for 1 min. However, the absorption time was extended to 2 min for particular isolates especially the isolates that lysed partially with mitomycin C. The grids were washed 3 times with dH_2O for 10 s, excess fluid was removed using Whatman filter paper and the grids were negatively stained with 2% ammonium molybdate for 30 s. Excess staining solution was removed with Whatman filter paper. The grids were allowed to dry at room temperature for approximately 15 to 20 min. The samples were examined by TEM (FEI Tecnai TF20) at 200kV using Gatan Microscopy Suite Software.

4.4.2 Host range of phage

The ability of induced phage to infect a range of selected indicator isolates was studied using double agar overlay plaque assay (spot test) (Clokie & Kropinski, 2009).

The host range of 29 induced phages was examined against 47 *P. multocida* isolates by plaque assay. The prophages were induced and filtered as previously described (sections 4.3.2 & 4.3.3). Indicator strains were grown overnight in BHIB at 37°C with shaking at 120 rpm. A base layer of 1% BHIA (without blood) was prepared by pouring the medium into a petri dish and allowed to set. A top layer of soft agar was made up of BHIB, 0.7% (w/v) microagar (Duchenne, London, UK) and 2 mM $CaCl_2$ (PROLABO). Both the semi-solid medium (BHIB + 0.7% microagar) and $CaCl_2$ (1 M) were prepared and autoclaved at 120°C for 15 min separately to prevent the precipitation. The semi-solid medium was cooled to 56°C and the sterile $CaCl_2$ (1 M) was added to a final concentration of 2 mM aseptically. The molten soft agar was held in the water bath at 48°C to avoid solidification of the medium. The plates were allowed to dry in the incubator for 20 min before use.

To carry out the plaque assay by the spot test three millilitres of warm molten soft were agar dispensed into bijou aseptically. Lawns of 47 *P. multocida* indicator strains were prepared by adding 50 µl of overnight both cultures into 3 ml of molten soft agar. Bacteria and agar were mixed and poured immediately onto the surface of dried base layer followed by gentle rocking. The top layers were allowed to solidify and dried at room temperature for 15 to 20 min. Ten microlitres of each filtered phage suspension were spotted onto the dried plates seeded with the indicator strains (Fig. 4.2). The plates were allowed to dry for 20-30 min before incubation at 37°C for 24 h and examined the next day for growth inhibition. The experiment was repeated in triplicate for each phage and indicator strain.

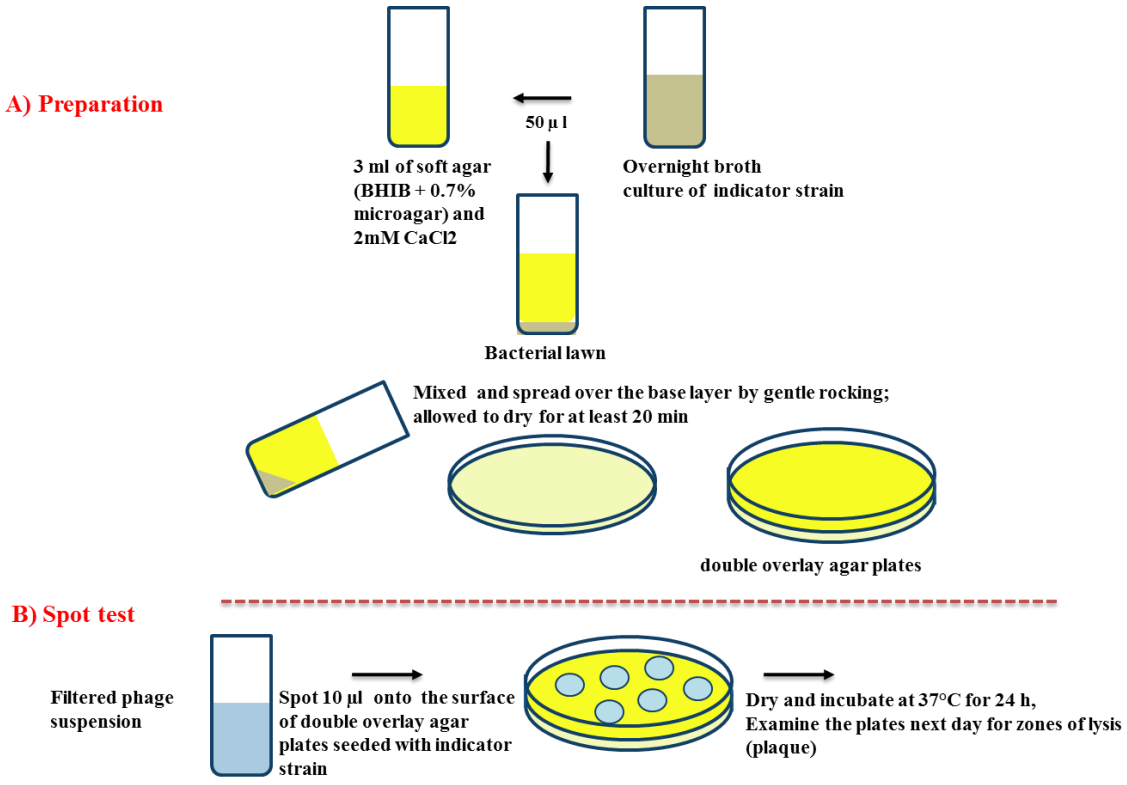

Fig. 4.2 Steps for host range analysis of lysates by spot test using double overlay agar plate.

Ten microlitres of phage suspension were spotted onto a plate seeded with indicator strain. The plates were examined next day for zones of lysis after overnight incubation at 37°C.

Serial dilutions (10 fold dilutions) of each induced phage were also used to examine the size of the zone of lysis. Different concentrations of microagar (0.6 and 0.7%) in the soft BHI overlay layer were tested. The effect of $CaCl_2$ in the overlay layer was also tested. The host range was assessed with and without adding $CaCl_2$ in the molten soft agar to evaluate if adding the salt affected the ability of phages to attach to the bacteria.

Freshly prepared phage suspensions were generally used. However, the effect of storage on phage ability to infect the indicator strains was also tested. The original phages were stored at 4°C and the experiment was repeated after 12, 24 and 48 h, as described above.

4.4.3 Phage purification using solid polyethylene glycol (PEG)

For phage purification, lysates were induced in 50 ml of BHIB in 250 ml Erlenmeyer flasks and filtered lysates prepared and stored at 4°C. Lysate purification was carried out according to the standard method by Sambrook *et al*. (1989) for purification of bacteriophage λ. Briefly, 40 ml of the filtered lysate were transferred into sterile 50 ml centrifuge tubes and allowed to reach room temperature. DNase (Sigma-Aldrich, UK) and RNase (Sigma-Aldrich, UK) (both at a final concentration of 10 µg/ ml) were added and incubated for 1 h at 37°C. Solid NaCl (Fisher Scientific, UK) was added to a final concentration of 1 M. The mixture was dissolved and left to stand for 1 h on ice allowing the separation of phage particles from the bacterial debris. The mixtures were transferred to clean centrifuge tubes and the bacterial debris removed by centrifugation at 11,000 *x g* for 10 min at 4°C (Sorvall); the supernatants were pooled into clean centrifuge tubes. The phage particles were concentrated by adding a final concentration of 10% (w/v) polyethylene glycol (PEG 8000) (Sigma-Aldrich, UK). The PEG 8000 was dissolved slowly by stirring and the treated mixture was allowed to stand on ice for 1 h or overnight instead. Precipitated bacteriophage particles were recovered by centrifugation at 11,000 *x g* for 10 to 15 min at 4°C (Sorvall). The supernatants were discarded gently and the tubes were left to dry for 10 min at room temperature. Finally, the pelleted phages were re-suspended in 200 µl phage buffer (0.1 M $MgSO_4$, 1 M $CaCl_2$, NaCl, 2.5 M Tris pH 8 and dH_2O) and stored at 4°C.

4.4.4 Phage DNA extraction

Three different methods were used to isolate DNA either from the precipitated phage particles or from broth as described below

4.4.4.1 Standard Sambrook method using phenol-chloroform-isoamyl alcohol

The phage particles were precipitated as described above (section 4.4.3). To each aliquot of re-suspended phage, 20% SDS (Sigma-Aldrich, UK) and proteinase K (20 mg/ml) (Promega) were added to the precipitated lysate and incubated at 56°C for 1 h. The digestion mixtures were allowed to reach room temperature before phenol was added. An equal volume (400 µl) of phenol-chloroform-isoamyl alcohol 25:24:1 (Sigma-Aldrich, UK) was added to each tube. The samples were mixed by inverting the tubes several times until a complete emulsion was formed. The samples were incubated at room temperature for 5 to 10 min. The DNA was recovered by centrifugation at 13,000 *x g* for 10 min. The aqueous upper phase layer was collected very gently to avoid mixing the layers and transferred to a clean Eppendorf tube (1.5 ml). The DNA was precipitated with ethanol. A 1/10 volume of 3 M sodium acetate (pH5.2) and two volumes of 100% ice-cold ethanol were added to the aqueous layer, mixed well by inverting and left for 3 h at -20°C. However, sometimes the samples were left overnight at -20°C for better DNA precipitation. The DNA was recovered by centrifugation of samples at 13,000 x g for 20 min at 4°C; the supernatant were carefully removed with a pipette without disturbing the DNA pellet. Finally, the pellets were washed with 1 ml of 70% ice-cold ethanol and centrifuged at 13,000 *x g* for 10 min at 4°C. The supernatants were discarded and the pellets allowed to air dry at room temperature. The DNA pellets were re-suspended in 50 µl TE buffer (pH 7.6) (0.1 M EDTA pH 8, 1 M Tris–HCl pH 8 and dH_2O). The DNA purity and concentration was measured using a NanoDrop 2000C spectrophotometer (Thermo Scientific). The purified phage DNA was observed by 0.7% (w/v) agarose gel electrophoresis and stored at –20°C.

4.4.4.2 Promega Wizard Clean-up Kit

Bacteriophage DNA was also isolated using a wizard DNA clean-up kit (Promega, #A7280). The phage particles were precipitated by PEG as described previously (section 4.4.3). The re-suspended particles were treated with proteinase K at a

final concentration of 100 µg/ml and incubated at 56°C for 1 h (Summer, 2009). The digestion mixtures were allowed to reach room temperature. DNA was isolated according to the manufacturer's instructions. The resin contained in the Promega kit was briefly dissolved by incubating in a water bath at 37°C for 10 min. The resin was cooled to 25–30°C before being used. DNA was isolated in three different stages: binding, washing and elution of DNA. One millilitre of wizard® DNA clean-up resin was added to a 1.5 ml micro-centrifuge tube. The digestion mixture was added to the resin and mixed well by inverting the tubes several times. The resin containing the bound DNA was taken up into a syringe and attached to a syringe barrel attached to the minicolumn provided within the kit. The syringe contents were gently pushed through the minicolumns. The mini-columns were washed with 2 ml of 80% isopropanol and centrifuged at 13,000 *x g* for 2 min. The minicolumns were transferred to a new microcentrifuge tubes and the bound DNA was eluted by adding 50 µl of prewarmed TE buffer to the minicolumns for 1 min. The phage DNA was recovered by centrifugation at 13,000 x g for 1 min at 4°C. The DNA purity and concentration were examined using a NanoDrop 2000C spectrophotometer (Thermo Scientific). The purified phage DNA was examined using 0.7% (w/v) agarose gel electrophoresis and the DNA stored at -20°C and for long-term storage at -80°C.

4.4.4.3 Norgen phage DNA isolation kit (# 46800)

A phage DNA isolation kit (Norgen Biotek Corp., Thorold, ON, Canada) was also used to extract genomic DNA directly from the lysate broth according to the manufacturer's instructions (Hsu *et al.*, 2013; Niu *et al.*, 2015). DNA was extracted from 1 ml of filtered phage suspension with the exception that the protocol was modified by increasing the volume from 1 ml to 3 ml (Basra *et al.*, 2014) (Fig. 4.3).

The filtered lysates were treated with DNase and RNase (Sigma-Aldrich, UK) (both at a final concentration of 10 µg/ ml) and incubated in a water bath for 1 h at 37°C. According to the instructions, 500 µL of lysis buffer B were added and vortexed vigorously for 10 s. Four microliters of proteinase K (20 mg/mL) were added and incubated at 55°C for 30 min to increase DNA yields. Three hundred and twenty microlitres of isopropanol were added to the lysate and vortexed to

mix. Up to 650 µL of lysate were applied to a column within a collection tube and there were centrifuged for 1 min at 6,000 *x g*. This step was repeated with remaining lysate until the entire lysate was passed through the column and each time. The columns were washed three times with 400 µL of wash solution A for 1 min at 6,000 *x g*. In order to dry the resin thoroughly, the columns were centrifuged for an additional 2 min at 14,000 *x g*. The DNA samples were eluted by placing the columns into clean 1.7 mL elution tubes and 75 µL of elution buffer B were added to each column. DNA was recovered by centrifugation for 1 min at 6,000 *x g*. DNA purity and concentration were examined using a NanoDrop 2000C spectrophotometer (Thermo Scientific). The purified phage DNA was examined by 0.7% (w/v) agarose gel electrophoresis and stored at –20 °C until needed.

4.4.1 Restriction endonuclease analysis (RE)

To analyse the genetic diversity and relatedness of the induced phages from *P. multocida*, isolated phage DNA was tested with different restriction enzymes. PsI, BamH1, Hind III, NdeI, EcoR1, XbaI (New England Biolabs Ltd, UK) were selected. According to the manufacturer's instruction, the final 20 µl reaction mixture contained DNA (1µg/µl), cut smart buffer 2 µl (1X), restriction enzyme 1 µl and nuclease-free water (Qiagen) up to a volume of 20 µl. The reactions were incubated at 37°C in a water bath for 3 to 4 h. However, in some experiments digestion was also performed overnight at 37°C. Digested phage DNA was separated by 0.7% (w/v) agarose gel electrophoresis and visualised with Syber® Safe DNA gel stain (Invitrogen). Twenty microlitres of each digested DNA sample were mixed with 2 µl 10x gel loading buffer and run on a 0.7% (w/v) agarose gel for 80 min at 80 V. The size of DNA bands was estimated using 1kb plus DNA ladder (Invitrogen).

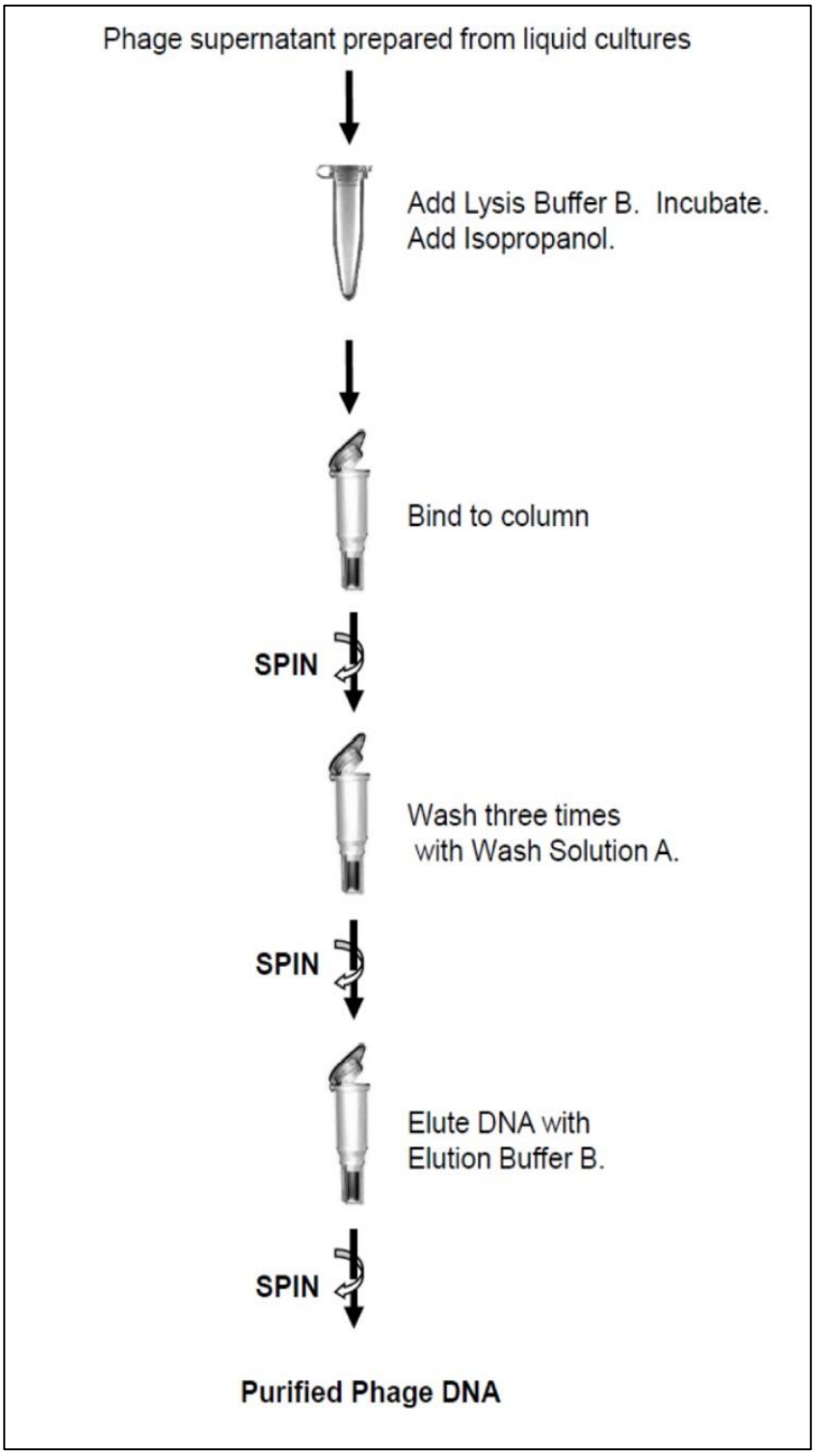

Fig. 4.3 Flow chart shows the steps to isolate the genomic DNA using Norgen's phage DNA isolation kit.

4.5 Results

4.5.1 Optimum mitomycin C concentration for prophage induction

To identify the optimum concentration of mitomycin C required to routinely induce temperate bacteriophages in *P. multocida* isolates, seven different concentrations were tested against eight strains (PM144, PM246, PM564, PM632, PM684, PM734, PM966, and PM982). The strains represented various hosts, capsular types, OMP types and STs. Properties of *P. multocida* isolates used to determine the optimum mitomycin C concentration are shown in Table 4.2. The OD_{600} was plotted against time (h) for control and seven different mitomycin C concentrations for each isolate.

Table 4.2 Properties of eight *P. multocida* isolates used in mitomycin C optimisation.

Isolate [a]	ST [b]	MLST group	Host species	Clinical symptoms	Capsular type	OMP-type [c]	*toxA* gene
PM144*	21	E	Avian	Septicaemia	A	1.1	ND
PM246*	25	C	Avian	Septicaemia	F	2.2	ND [d]
PM564*	1	A	Bovine	Pneumonia	A	2.1	ND
PM632*	4	A	Bovine	Pneumonia	A	4.1	ND
PM684*	11	G	Porcine	Suspect snouts	A	6.1	+
PM734*	10	G	Porcine	Pneumonia	A	1.1	-
PM982*	18	E	Ovine	Pneumonia	D	3.1	+
PM966*	16	B	Ovine	Pneumonia	A	1.1	-

[a] isolates are arranged by order of MLST group (column 3) (Fig. 2.1); [b] ST= sequence type (Davies *et al*., unpublished http://pubmlst.org/pmultocida_multihost/); [c] OMP-types for bovine, ovine, porcine and avian are not equivalent, i.e. bovine OMP-type 1.1 is not as same as porcine OMP-type 1.1, etc. (Davies *et al.*, 2003a; b; c; Davies, 2004; Davies *et al.*, 2004); [d] ND: not determined.

Different lysis patterns were observed for each isolate using different concentrations of mitomycin C (Fig. 4.4A-H). The patterns were complete, partial and little or no lysis after 6 to 8 h of induction with mitomycin C. The result of mitomycin C optimisation for isolates PM684 and PM892 (Fig. 4.4A & B) showed that both isolates exhibited a large amount of bacterial cell lysis compared with the other isolates. Isolates PM684 and PM982 were both highly sensitive to mitomycin C treatment. In isolates PM246, PM632, PM734 and PM966 (Fig. 4.4C, D, E & F, respectively), data showed that the isolates were sensitive to the higher concentrations rather than the lower concentrations. PM246, PM632, PM734 and PM966 were partially lysed compared to the isolates PM144 and PM564, especially with the higher concentration of mitomycin C (0.5, 1.0 and 2.0 µg /ml). The data for isolate PM144 and PM564 (Fig. 4.4G & H) indicated that both isolates were less sensitive and not induced with mitomycin C even at the higher concentration as the OD_{600} increased with time. However, isolate PM564 was partially lysed with a final concentration of 2 µg/ml (Fig. 4.4H).

The results showed that final concentrations of 0.2, 0.5, 1.0 and 2.0 µg/ml can be used for induction of temperate phages in *P. multocida*. Furthermore, incubation time for induction was increased from 8 h to 10, 12 and 24 h after being treated with the mitomycin C; the same induction profiles were obtained among the eight isolates. In this preliminary analysis, a final concentration of 0.2 µg/ml mitomycin C was selected as optimum for the induction of phages in *P. multocida* as complete and rapid bacterial cell lysis occurred in isolates PM684 (porcine) and PM982 (ovine). This suggests that PM684 and PM982 contained inducible prophages as they lysed completely 3 to 4 h after treatment with the 0.2 µg/ml. However, if there was no evidence of lysis with the 0.2 µg/ml, the higher concentrations of 0.5, 1.0 and 2.0 µg/ml of mitomycin C were used to induce prophages. Phage induction in eight isolates was further confirmed in preliminary studies by TEM and DNA extraction. For this reason, PM684 and PM982 were used subsequently as controls in phage induction and characterisation as they contained inducible phages that could be confirmed by TEM and DNA isolation.

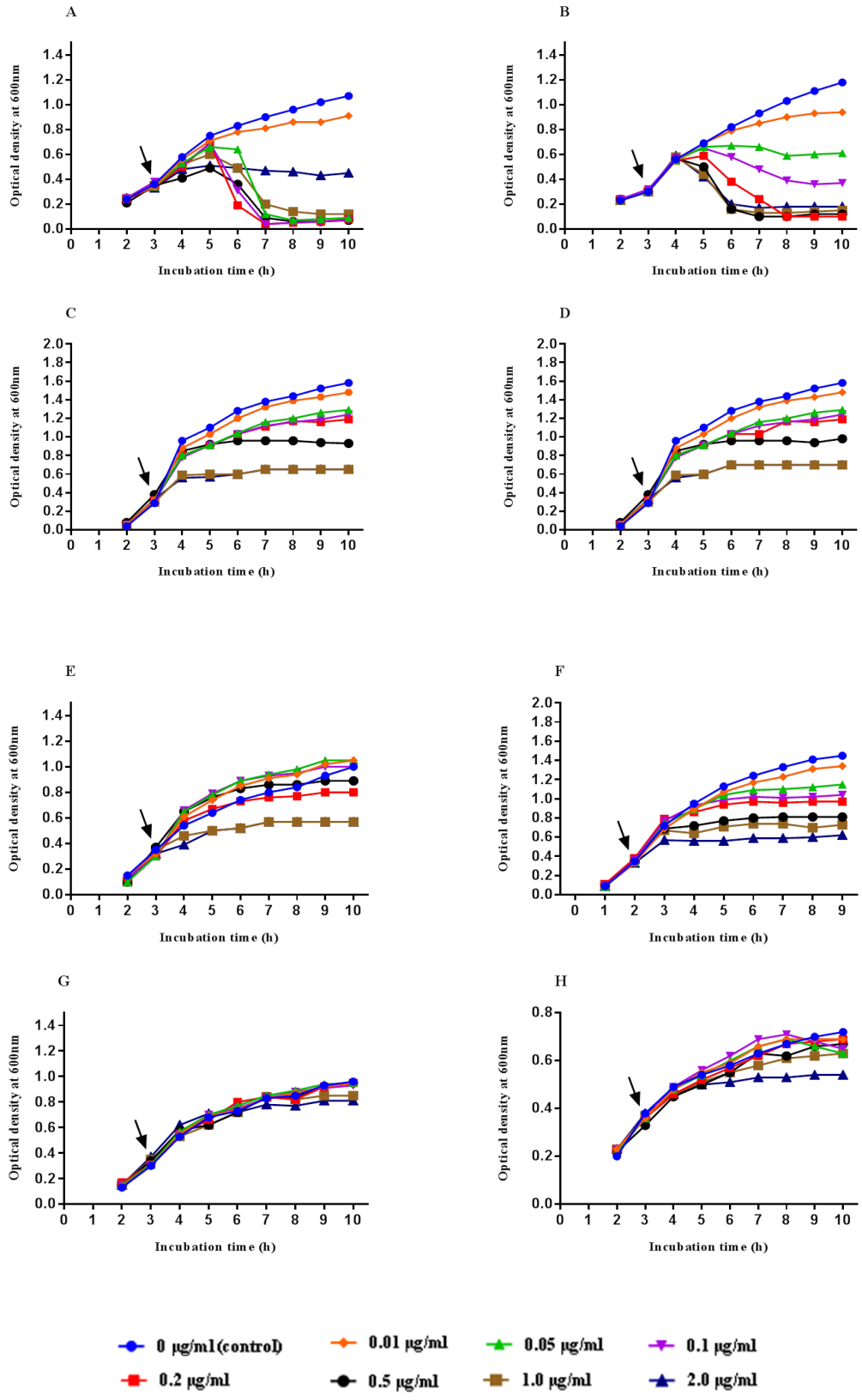

Fig. 4.4 Induction profiles comparing different mitomycin C concentrations.

Isolates PM684 (A) and PM982 (B) PM246 (C), PM632 (D), PM734 (E), PM966 (F), PM144 (G), and PM564 (H) were used to comparing different mitomycin C concentrations. The following concentrations of mitomycin C were used for each isolate: 0 (control), 0.01, 0.05, 0.1, 0.2, 0.5, 1.0 and 2.0 µg/ml. The figure shows three different patterns of lysis: complete (A & B) partial (C, D, E, & F) and no lysis (G & H). The arrow indicates the point at which the mitomycin C was added. Graphs were created using GraphPad Prism 7.

4.5.2 Induction profile for 47 *P. multocida* isolates

The induction profiles of 47 isolates of *P. multocida* from the different host species and representing various serotypes, OMPs, and STs were generated with 0.2 µg/ml mitomycin C as an optimum concentration. However, induction was repeated with higher concentrations of 0.5, 1.0 and 2.0 µg/ml mitomycin C when there was no sign of induction in a specific isolate at the lower concentration. The induction profile for each isolate was created by comparing the OD_{600} with the control (no mitomycin C) for 8 h or longer. The addition of 0.2 µg/ml mitomycin C or the higher concentrations into the *P. multocida* broth cultures identified three different patterns of lysis. The patterns are classified as complete, partial and little or no lysis as mentioned below (Fig. 4.5).

Complete lysis was indicated when the final OD_{600} was 0.4 or less (Fig. 4.5A), partial lysis when the final OD_{600} was above 0.4 (Fig. 4.5B) and no lysis when there was no reduction of the final OD_{600} and the OD_{600} values in control and mitomycin C-treated cultures remained constant after the addition of mitomycin C (Fig. 4.5C). The induction type has been generated and assigned to each isolate used in the study and they are summarised in Table 4.3. The majority of the strains were either completely or partially lysed with 0.2 µg/ml mitomycin C. A small number of isolates showed partial lysis with the higher concentration ranging from 0.5 to 2.0 µg/ml mitomycin C.

Among the 47 strains, 15 (32%) isolates exhibited complete lysis, 22 (47%) were partially lysed and 10 (21%) showed no lysis after being exposed to the mitomycin C for 8 h (Fig. 4.6). Ten isolates did not lyse with 0.2 µg/ml even when the incubation time was increased to 24 h. In these cases, the isolates were induced with higher concentrations of mitomycin C to examine if they were includible or not. Isolate PM226 was partially lysed with 0.5 µg/ml mitomycin C. Isolates PM344 and PM402 were partially lysed with 1.0 µg/ml mitomycin C, whereas isolates PM116, PM200, PM246, PM632, PM734, PM762, PM890 and PM966 were induced with 2.0 µg/ml mitomycin C (Table 4.3).

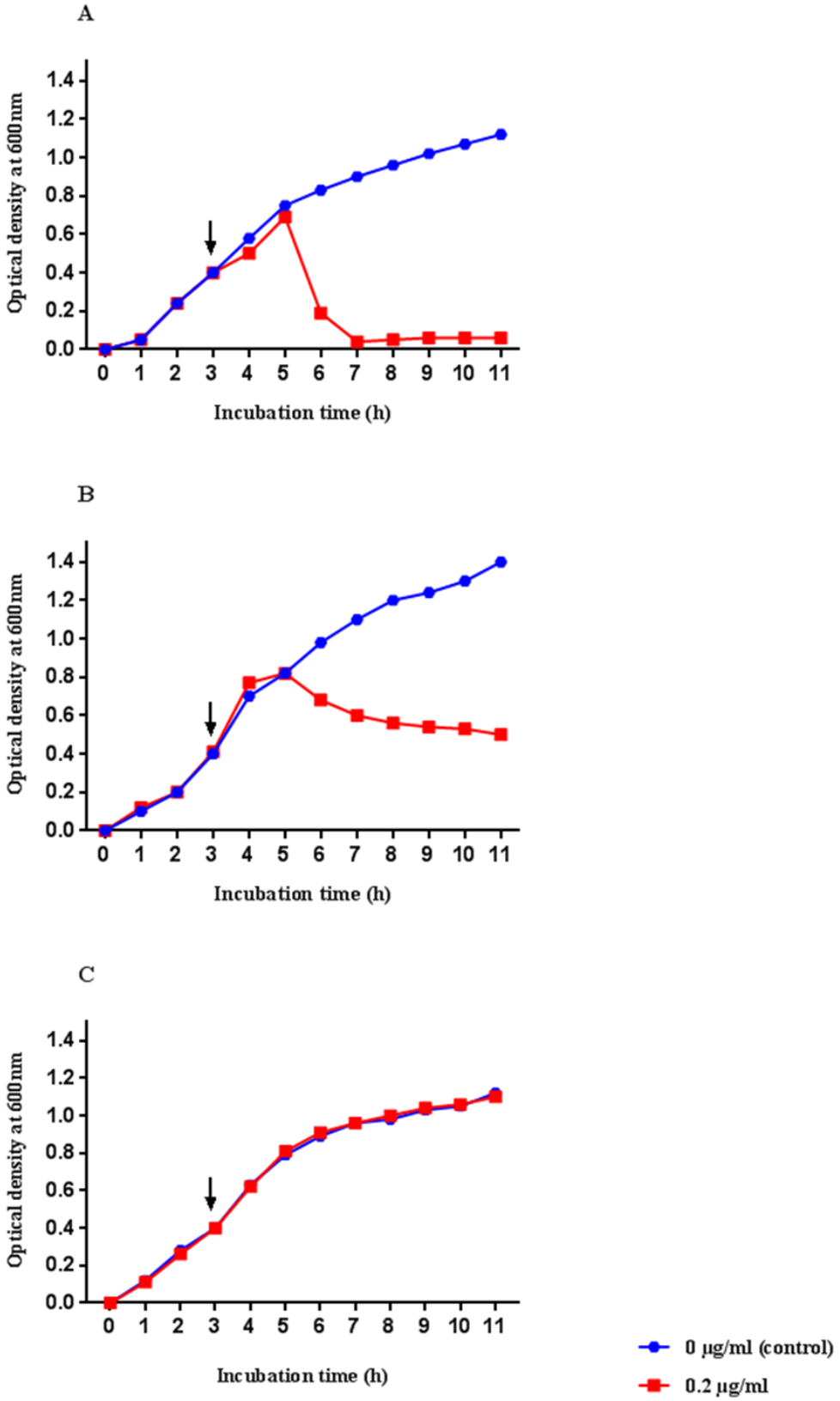

Fig. 4.5 Phage induction profiles showing (A) complete lysis, (B) partial lysis and (C) no lysis with 0.2 µg/ ml mitomycin C.

Mitomycin C was added once the OD_{600} reached 0.4 and the OD_{600} was plotted against time (h). The induction profile for each isolate was generated by comparing the OD_{600} with the control (no mitomycin C) over 11 h. The arrows indicate the points at which the mitomycin C was added. Graphs were created using GraphPad Prism 7.

Table 4.3 Induction profile in 47 *P. multocida* isolates.

Isolate [a]	ST [b]	MLST group	Host species	Capsular type	OMP-type [c]	*toxA* gene	Mitomycin C	Lysis type [d]
PM200	10	F	Avian	A	1.2	ND	2 µg/ml	Complete
PM336	7	F	Bovine	A	6.1	ND	0.2 µg/ml	Complete
PM122	ND	ND [e]	Ovine	D	3.1	+	0.2 µg/ml	Complete
PM964	18	E	Ovine	D	3.1	+	0.2 µg/ml	Complete
PM982	18	E	Ovine	D	3.1	+	0.2 µg/ml	Complete
PM986	18	E	Ovine	D	3.1	+	0.2 µg/ml	Complete
PM988	ND	ND	Ovine	D	3.1	+	0.2 µg/ml	Complete
PM382	13	C	Porcine	A	4.1	-	0.2 µg/ml	Complete
PM850	10	F	Porcine	A	1.1	-	0.2 µg/ml	Complete
PM684	11	G	Porcine	A	6.1	+	0.2 µg/ml	Complete
PM918	11	G	Porcine	A	6.1	+	0.2 µg/ml	Complete
PM926	ND	ND	Porcine	A	6.1	+	0.2 µg/ml	Complete
PM40	ND	ND	Porcine	A	6.2	+	0.2 µg/ml	Complete
PM716	11	G	Porcine	D	4.1	+	0.2 µg/ml	Complete
PM848	11	G	Porcine	D	4.1	+	0.2 µg/ml	Complete
PM246	25	C	Avian	F	2.2	ND	2 µg/ml	Partial
PM86	15	D	Avian	A	3.1	ND	0.2 µg/ml	Partial
PM172	26	D	Avian	A	3.1	ND	0.2 µg/ml	Partial
PM226	11	G	Avian	D	13.1	-	0.5 µg/ml	Partial
PM344	3	A	Bovine	A	3.1	ND	1 µg/ml	Partial
PM632	4	A	Bovine	A	4.1	ND	2 µg/ml	Partial
PM486	9	D	Bovine	A	9.1	ND	0.2 µg/ml	Partial
PM402	5	D	Bovine	A	5.1	ND	1 µg/ml	Partial
PM666	3	A	Porcine	A	2.1	-	0.2 µg/ml	Partial
PM116	3	A	Porcine	A	3.1	-	2 µg/ml	Partial
PM966	16	B	Ovine	A	1.1	-	2 µg/ml	Partial
PM990	ND	ND	Ovine	D	3.1	+	0.2 µg/ml	Partial
PM706	13	C	Porcine	UT	4.1	-	0.2 µg/ml	Partial
PM934	15	D	Porcine	A	5.1	-	0.2 µg/ml	Partial
PM954	15	D	Porcine	A	5.1	-	0.2 µg/ml	Partial
PM54	10	F	Porcine	A	1.1	-	0.2 µg/ml	Partial
PM734	10	F	Porcine	A	1.1	-	2 µg/ml	Partial
PM820	10	F	Porcine	A	1.1	-	0.2 µg/ml	Partial
PM696	11	G	Porcine	D	6.1	+	0.2 µg/ml	Partial

Table 4.3 (continued)

Isolate [a]	ST [b]	MLST group	Host species	Capsular type	OMP-type [c]	*toxA* gene	Mitomycin C	Lysis type [d]
PM714	11	G	Porcine	D	6.1	-	0.2 µg/ml	Partial
PM762	11	G	Porcine	D	6.1	+	2 µg/ml	Partial
PM890	11	G	Porcine	D	6.1	+	2 µg/ml	Partial
PM148	12	C	Avian	F	2.2	ND	0.2 µg/ml	No lysis
PM104	28	D	Avian	A	4.1	ND	0.2 µg/ml	No lysis
PM144	21	E	Avian	A	1.1	ND	0.2 µg/mL	No lysis
PM82	32	H	Avian	A	7.1	ND	0.2 µg/ml	No lysis
PM316	1	A	Bovine	A	1.1	ND	0.2 µg/ml	No lysis
PM564	1	A	Bovine	A	2.1	ND	0.2 µg/ml	No lysis
PM302	6	E	Bovine	A	5.3	ND	0.2 µg/ml	No lysis
PM2	17	C	Ovine	F	2.1	-	0.2 µg/ml	No lysis
PM8	17	C	Ovine	F	2.1	-	0.2 µg/ml	No lysis
PM994	12	C	Ovine	F	1.1	-	0.2 µg/ml	No lysis

[a] isolates are arranged by order of MLST group (column 3) (Fig. 2.1).

[b] ST: sequence types (Davies *et al.,* unpublished; http://pubmlst.org/pmultocida_multihost).

[c] OMP-types for bovine, ovine, porcine and avian are not equivalent, i.e. bovine OMP-type 1.1 is not as same as porcine OMP-type 1.1, etc. (Davies *et al.*, 2003a; b; c; Davies, 2004; Davies *et al.*, 2004).

[d] complete lysis when the final OD_{600} was 0.4 or less; partial lysis, when the OD_{600} was above 0.4; little or no lysis when the OD_{600} values in control and mitomycin C treated cultures remained constant after being treated with mitomycin C for 8 h of incubation.

[d] ND: not determined.

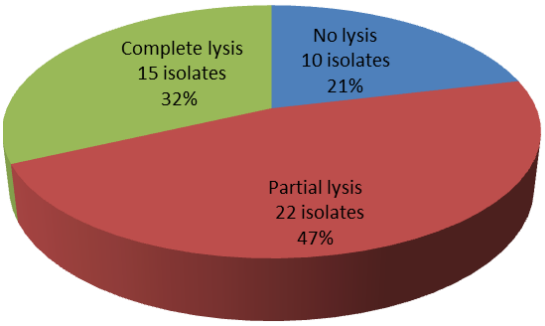

Fig. 4.6 The number and percentage of lysis patterns among 47 *P. multocida* isolates.

These finding suggest that there could be correlation between the phage and host species characteristics (capsular type, OM types and STs). The types of lysis induced by mitomycin C (i.e. complete, partial or no lysis) were exclusively associated with *P. multocida* isolates within the same, or closely related, clonal groups or lineages (STs). Notably that the *toxA* positive ovine strains of capsular type D, OMP-type 3.1 and ST 18 (PM122, PM964, PM982, PM986 and PM988) exhibited complete lysis with 0.2 µg/ml mitomycin C. Similarly, 10 isolates associated within porcine pneumonia and atrophic rhinitis groups (PM820, PM850, PM200, PM336, PM684, PM918, PM926, PM40, PM716 and PM848) were completely lysed with 0.2 µg/ml mitomycin C. Isolates PM86, PM172, PM486, PM934 and PM954 shared the same induction profiles because they were partially lysed with 0.2 µg/ml mitomycin C. Avian and ovine isolates of capsular type F including PM2, PM8, PM148, and PM994 were completely resistant to the effect of mitomycin C, although isolate PM246 (capsular type F) was partially lysed with 2 µg/ml mitomycin C. Isolates within the bovine pneumonia cluster were either completely resistant to the effect of mitomycin C (PM316 and PM564) or exhibited partial lysis at normal and higher concentrations of mitomycin C (PM344, PM632, PM666 and PM116) (Table 4.3). These strains might share similar phage or they may not contain inducible phage, especially the strains that were not lysed by mitomycin C. Therefore, the presence and identification of temperate phages will be further assessed by TEM and isolation of phage DNA.

4.5.3 Phage identification and morphology by TEM

4.5.3.1 Ultracentrifugation parameter and negative staining

As described in section 4.4.1, different parameters were tested in a preliminary study of PM684 and PM982. Centrifugation at 40,000 x g for 90 min at 4ºC was selected to pellet intact phage particles because the pellet was clearer when compared to the pellets obtained with 20,000 *x g* for 3 h, 20,000 *x g*, and 30,000 *x g* for 90 min at 4°C). Different time points including 1 and 20 min were also selected to determine the optimum time required for the phage particles to be adsorbed onto the grids. The TEM results showed that 1 min was sufficient for the grids to adsorb phage particles. However, for the isolates that were not lysed or partially lysed, 2 min was selected. Thirty seconds was chosen for negative staining with 2% ammonium molybdate.

4.5.3.2 Phage morphology

One of the objectives of this study was to induce temperate bacteriophages in selected *P. multocida* isolates and to compare their diversity. In *P. multocida* diverse group of temperate bacteriophages were characterised based on their morphologies (Ackermann & Karaivanov, 1984). TEM was used to determine whether isolates contain similar phages or have diverse phages morphologies as described by Ackermann & Karaivanov (1984). Furthermore, to demonstrate whether multiple prophages could be induced in the same *P. multocida* isolates. The induction of multiple prophages from a single host has not been confirmed in *P. multocida*.

Having determined optimal conditions for TEM, the preliminary study of isolates PM684 and PM982 revealed a diverse set of phage morphologies. The results indicated that these two strains contain temperate bacteriophages of different morphologies belonging to both *Myoviridae* and *Siphoviridae* families. In addition, phage head-like particles were present confirming that these *P. multocida* isolates contain diverse groups of bacteriophages. *Myoviridae* and *Siphoviridae*-like phages were induced in isolate PM684 indicating that the *P. multocida* genome harbours multiple prophages. TEM analysis of sedimented phage particles from *P. multocida* isolates following induction, filtration, and ultra-centrifugation revealed a diverse set of phage morphologies, as described

previously by Ackermann & Karaivanov (1984). For TEM, the incubation time for phage induction was continued to overnight particularly for the isolates that showed either partial or no lysis (Table 4.3). For example, no phage were identified in isolates PM54, PM86, PM116, PM200, PM226, PM382, PM666, PM696, PM174, PM762, PM820, PM890 and PM966 after 8 h of incubation. However, when induction was continued overnight, the phages were identified in isolates PM54, PM86, PM116, PM200, PM226, PM382, PM666, PM696, PM174, PM762, PM820, PM890 and PM966. However, no phage particles were identified in *P. multocida* isolates those resistant to 0.2 µg/ml or the higher concentration of mitomycin C even when the incubation time was increased to 24 h. Although phages were induced under the same conditions for TEM, the total numbers of phage particles were differed from one isolate to another. The number of phage particles are described as either high (+++), medium (++) or low (+), based on TEM (Table 4.4). TEM was conducted in triplicate for each isolate. Overall, phage particles were identified in 29 (61.7%) of the 47 *P. multocida* isolates (Fig. 4.7 & Table 4.4). The identified phage particles belonged to the *Siphoviridae* and *Myoviridae* families in the order *Caudovirales* based on their tail morphology. Tail-less phage particles were also identified. Among the set of 29 phage identified, a total of 18 (62%) *P. multocida* isolates carried only *Siphoviridae*-like phage. Six (20%) isolates carried only *Myoviridae*-like phage type and two (6.8%) isolates carried only tail-less phage (Table 4.4). Both *Siphoviridae* and *Myoviridae* phage types were induced from the single host in three (10%) isolates (Fig. 4.7 & Table 4.4).

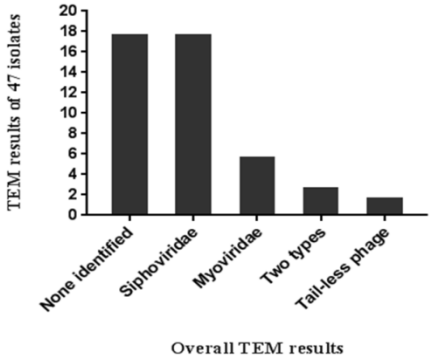

Fig. 4.7 Overall TEM results of 47 *P. multocida* isolates.

Temperate bacteriophages were identified in 29 (61.7%) of the 47 *P. multocida* isolates. Eighteen isolates carried phage belonging to only *Siphoviridae*-like phage type, six isolates carried phage belonging to only *Myoviridae*-like phage type, tail-less phage were identified in only two isolates and both *Siphoviridae* and *Myoviridae* phage types were induced in three isolates.

Table 4.4 Morphology and characteristic of temperate bacteriophages identified in 29 *P. multocida* isolates.

Isolate	ST	MLST group	Host species	Capsular type	Lysis type [a]	No of phage family	Family type [b]	Head size (nm) [c]	Tail size (nm)[d]	Semi quantitative assessment [e]
PM666*	3	A	Porcine	A	Partial	1	*Siphoviridae*	50×55	132×8	+
PM116*	3	A	Porcine	A	Partial	1	*Siphoviridae*	50×56	138×8	+
PM966*	16	B	Ovine	A	Partial	1	*Siphoviridae*	52×58	110×8	+
PM382*	13	C	Porcine	A	Complete	1	*Myoviridae*	63×55	147×16	+
PM86*	15	D	Avian	A	Partial	2	*Myoviridae* & *Siphoviridae*	38×37/63×55	190×18/138×7	+++
PM934*	15	D	Porcine	A	Partial	1	*Myoviridae*	38×37	190×18	++
PM954*	15	D	Porcine	A	Partial	1	*Myoviridae*	38×37	190×18	++
PM486*	9	D	Bovine	A	Partial	1	*Myoviridae*	38×37	190×18	+++
PM172*	26	D	Avian	A	Partial	1	*Myoviridae*	39×37	190×18	++
PM122*	ND	ND	Ovine	D	Complete	1	*Siphoviridae*	66×67	142×8	+++
PM964*	18	E	Ovine	D	Complete	1	*Siphoviridae*	62×55	141×8	+++
PM982*	18	E	Ovine	D	Complete	1	*Siphoviridae*	63×61	146×9	+++
PM986*	18	E	Ovine	D	Complete	1	*Siphoviridae*	64×60	149×8	+++
PM988*	ND	ND	Ovine	D	Complete	1	*Siphoviridae*	64×55	136×8	+++
PM54*	10	F	Porcine	A	Partial	1	*Siphoviridae*	54×54	142×9	+
PM820	10	F	Porcine	A	Partial	1	*Siphoviridae*	54×54	142×9	+
PM850*	10	F	Porcine	A	Complete	2	*Myoviridae* & *Siphoviridae*	59×51/52×59	148×16/134×8	+++
PM200*	10	F	Avian	A	Complete	1	*Siphoviridae*	63×57	138×7	+
PM336*	7	F	Bovine	A	Complete	1	*Siphoviridae*	80×59	154×7	+++
PM684*	11	G	Porcine	A	Complete	2	*Myoviridae* & *Siphoviridae*	63×52/59×57	148×15/125×8	+++
PM918*	11	G	Porcine	A	Complete	1	*Siphoviridae*	55×65	242×8	+++
PM926*	ND	ND	Porcine	A	Complete	1	*Siphoviridae*	66×56	149×8	+++

Table 4.4 (continued)

Isolate	ST	MLST group	Host species	Capsular type	Lysis type [a]	No of phage family	Family type [b]	Head size (nm) [c]	Tail size (nm)[d]	Semi quantitative assessment [e]
PM40	ND	ND	Porcine	A	Complete	1	*Myoviridae*	60×56	144×16	++
PM848	11	G	Porcine	D	Complete	1	*Siphoviridae*	63×61	143×9	++
PM696	11	G	Porcine	D	Partial	1	*Siphoviridae*	60×54	110×7	+
PM714	11	G	Porcine	D	Partial	1	*Siphoviridae*	55×56	107×6	+
PM762	11	G	Porcine	D	Partial	1	Tail-less phage	66×54	-	+
PM890	11	G	Porcine	D	Partial	1	Tail-less phage	65×60	-	+
PM226	11	G	Avian	D	Partial	1	*Siphoviridae*	54×56	126×8	+

[a] complete lysis when the final OD_{600} was 0.4 or less; partial lysis, when the OD_{600} was above 0.4; little or no lysis when the OD_{600} values in control and mitomycin C treated cultures remained constant after being treated with mitomycin C for 8 h of incubation

[b, c] and [d] based on TEM

[e] Semi quantitative assessment: quantity of phage based on TEM (+), (++, (+++) based on TEM

Siphoviridae-like phages were identified in 18 isolates. The morphology of these *Siphoviridae*-like phages differed from one isolate to another in terms of the shape and size of both the capsid and tail. These phages had either hexagonal or elongated capsids; the head size varied between 50 to 80 nm long, and 55 to 65 nm width. The capsids were connected to flexible tails of approximately 110-242 long by 8 nm diameters (Fig. 4.8 & Table 4.4). The following isolates contained only *Siphoviridae* type based on TEM: PM666, PM116, PM966, PM122, PM964, PM982, PM986, PM988, PM54, PM820, PM200, PM336, PM918, PM926, PM848, PM696, PM714, and PM226 (Table 4.4).

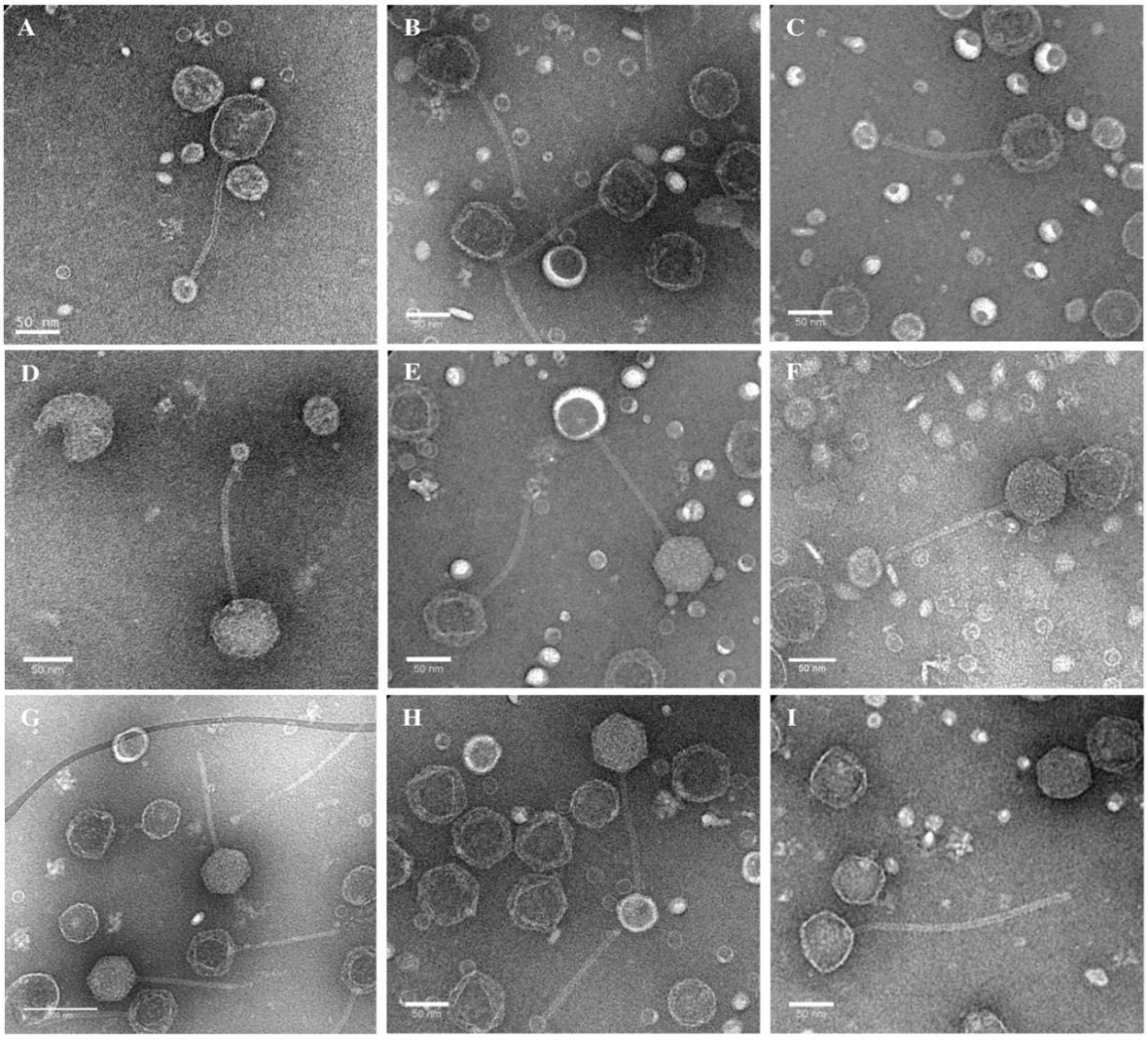

Fig. 4.8 Electron micrographs of *Siphoviridae*-like type phages induced in *P. multocida* isolates.

Differences were observed in the morphology of *Siphoviridae*-like phages in terms of capsid and tail. A, PM226 (elongated head with moderate tail); B, C, D, E , F, G, and H, phage induced from isolates PM122, PM848, PM820, PM964, PM982, PM986 and PM988, respectively and I, phage with isometric capsid and long tail induced from isolate PM918.

Myoviridae-like phages were characterised by possessing hexagonal capsids of approximately 59 to 63 nm length and 51 to 56 nm width and long contractile tails with either extended or contracted sheaths. The tails were approximately 150 nm long and 15 to 16 nm wide. Variations were also found in the tail ends: some had blunt or prominent base plates while other had short tail fibres (Fig. 4.9). Isolates PM40 and PM382 contained only *Myoviridae*-type phage.

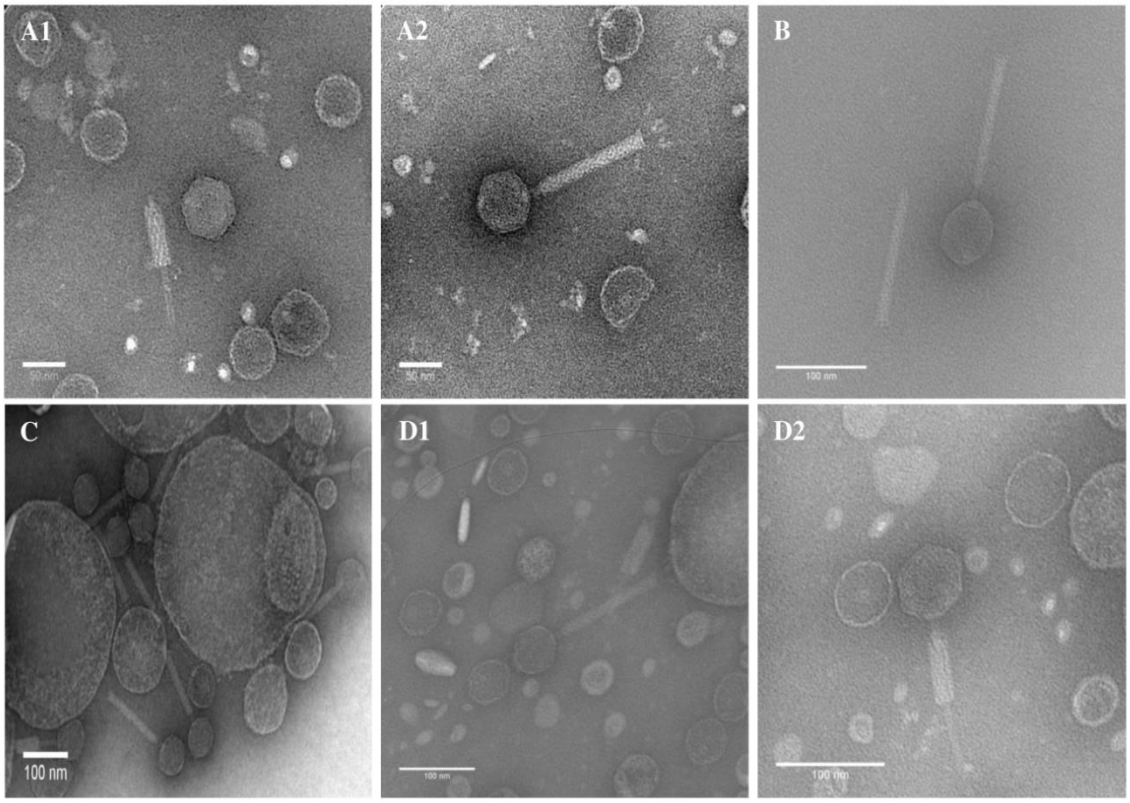

Fig. 4.9 Electron micrographs of *Myoviridae*-type phages induced in *P. multocida* isolates.

Differences were observed in the morphology of *Myoviridae* -like phages. A1, D2, phages with long contractile tails and contracted sheath and blunt tail ends were induced in isolates PM40 and PM850, respectively. B, a phage with extended sheath, prominent tail end and hexagonal capsid was induced in isolate PM382. A2, C and D1 phages with hexagonal capsids with extended sheaths and tail fibres were induced in isolate PM40, PM684 and PM850, respectively.

Interestingly, five *P. multocida* isolates PM86 (avian), PM934, PM954 (porcine), PM486 (ovine) and PM172 (avian) contained a distinct *Myoviridae*-like phage that has not been previously described in *P. multocida* (Fig. 4.10). These phage particles had a small hexagonal capsid approximately 38 to 39 nm length and 37 nm wide and a tail of approximately 190 nm long and 18 nm wide (Table 4.4). The capsid was connected to the tail by a thin structure of approximately 6-8 nm (arrow) in width (Fig. 4.10).

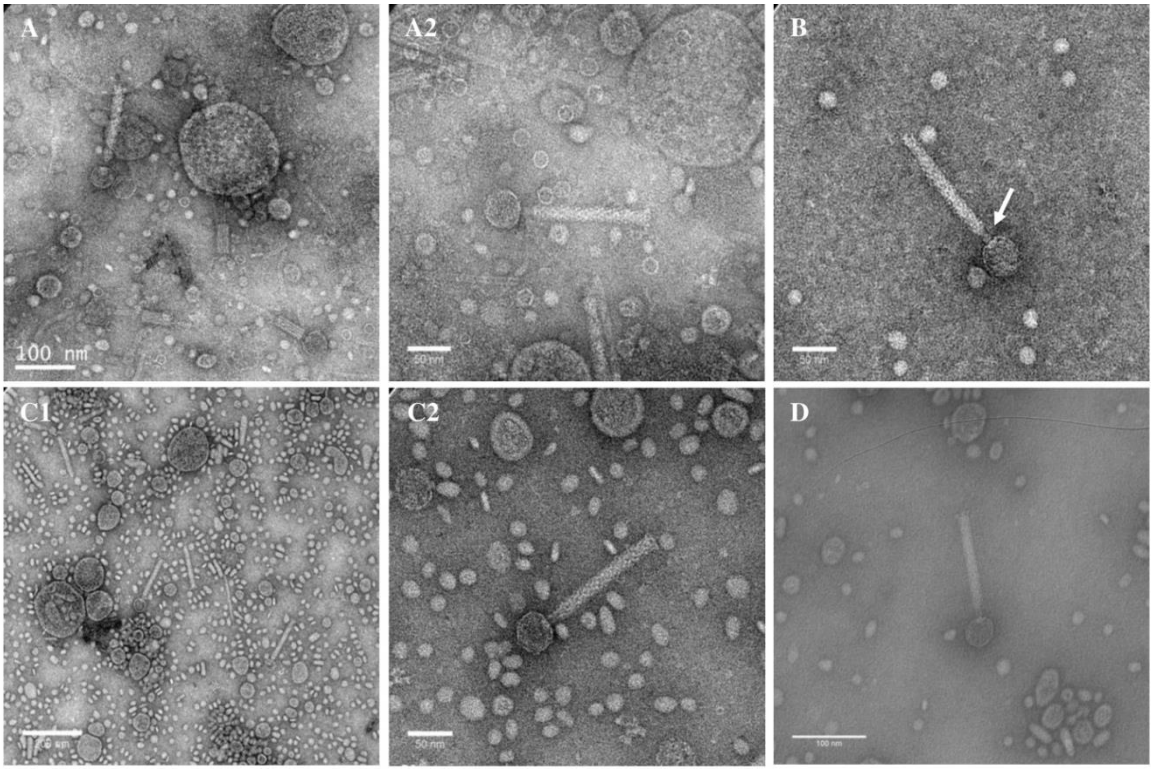

Fig. 4.10 Electron micrographs of distinct *Myoviridae*-type phages induced in *P. multocida* isolates.

Phage particles had a small hexagonal capsid of approximately 38 to 39 nm length and 37 nm width. The capsid was attached to a tail with a contracted or extended sheath of about 150 to 200 nm in length. A1 and A2, phages induced in isolate PM86; B, phage induced in isolate PM172; C1 and C2, phage induced in isolate PM486; D, phage induced in isolate PM934.

Both intact *Siphoviridae* and *Myoviridae* phage types were identified in isolates PM86, PM684 and PM850 by TEM indicating that a single host may harbour multiple prophages (Fig. 4.11). TEM was repeated to check whether more isolates contained more than one phage type, but PM86, PM684 and PM850 were the only isolates that contained two phage family types. In isolate PM86, the *Myoviridae* phage was morphologically identical to the observed in PM172, PM486, PM934 and PM954 by TEM. These details are summarised in Table 4.4.

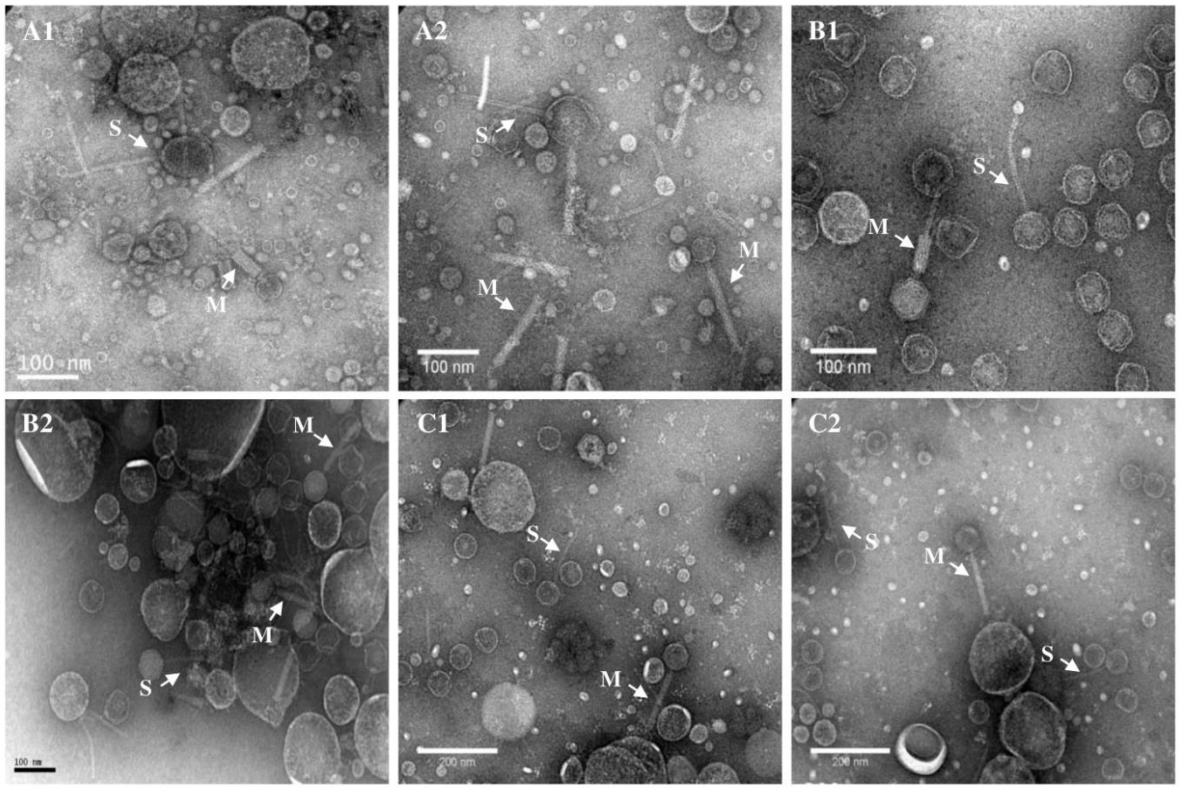

Fig. 4.11 Electron micrographs of *Siphoviridae*-type and *Myoviridae*-type phages induced in the same bacterial hosts.

PM86 (A1 and A2), PM684 (B1 and B2) and PM850 (C1 and C2) possessed multiple prophages that were identified by TEM after being induced with mitomycin C. The capsids were attached to tails with contracted or extended sheath for *Myoviridae* type phages. The capsids were attached to long non-contractile tail for the *Siphoviridae*-type phages. *Siphoviridae*-type phages are indicated by (S) while *Myoviridae*-type phages are indicated by (M).

Hexagonal capsids were observed in isolates PM762 and PM890 of approximately 65 nm diameters and without tails (Fig. 4.12). These types were classified as tail-less phages Furthermore, the tail-less phage-like particles were identified among the others isolates (Fig. 4.8, Fig. 4.9 & Fig. 4.11). However, in closely related strains such PM40, PM684, PM848, PM918 and PM926 intact phage particles were identified. The presence of only separated heads may be associated with phage replication or the heads were separated from the tail during the mixing of samples.

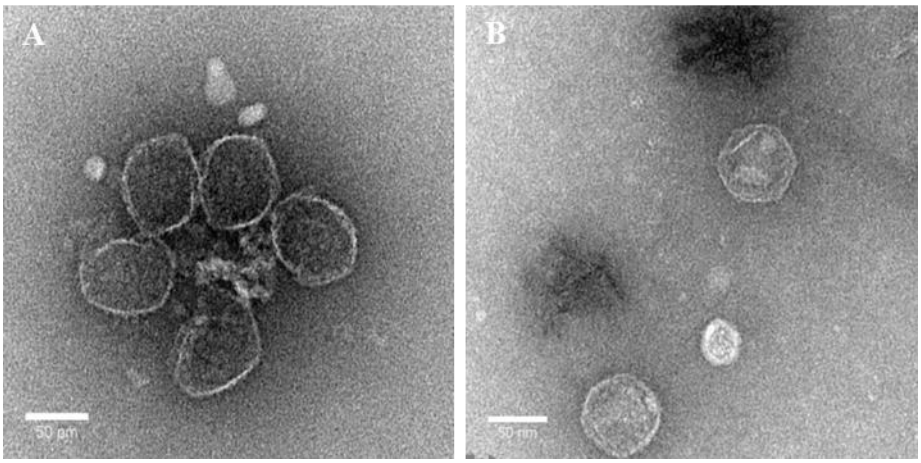

Fig. 4.12 Electron micrographs of tail-less phages induced in *P. multocida*.
Tail-less phages were induced in isolates PM762 (**A**) and PM890 (**B**) with mitomycin C.

4.5.4 Host range of temperate bacteriophages of *P. multocida*

The selected phages induced in *P. multocida* were also assessed to examine their abilities to infect indicator strains and to determine if there was any correlation between the phages and their ability to infect *P. multocida* strains. Of the 29 lysates, only 11 (38%) produced signs of infection; 18 (62%) lysates did not produce visual signs of infection on any of the indicator strains used in this study (Table 4.5). Several attempts were made to modify the protocol to determine whether there were any differences in the ability of the phage to infect the indicator strains. One of the modified factors was the use of different concentrations of microagar in the molten soft agar. The results showed that neither 0.6 nor 0.7% (w/v) agar in the top layer changed either the zone of growth inhibition or the overall results.

Furthermore, host range experiments were repeated without the addition of $CaCl_2$ to the molten soft agar to evaluate the effect of $CaCl_2$ on the ability of phages to attach to the bacteria. However, it was found that the addition of $CaCl_2$ to the BHI top layer did not significantly change the results of infection of the indicator strains. The phage suspensions were diluted but no changes were observed. Moreover, the effect of storage on phage viability was examined as described in section 4.4.2; again the overall result did not change. It was concluded that storage of the phages at 4°C for a few days did not affect their ability to infect indicator strains. Spotting 10 µl of each lysate resulted in the formation of growth inhibition (zones of lysis) on certain indicator strains. Based on their ability to lyse the indicator strains, the lysates showed both broad and narrow host range activity against *P. multocida* isolates (Table 4.5). Differences occurred in patterns of lysis produced by different phages. The lysate from isolates PM122, PM964, PM982, PM986 and PM988 showed the broadest host range. They caused lysis in 17 of 47 indicator strains and they showed the same patterns of lysis in the indicator strains (Table 4.5). They produced faint lysis zones with PM316, PM564, PM86, PM934, PM954 PM486, PM172, and PM336 and clear lysis zones with indicator strains PM344, PM632, PM666, PM116, PM302, PM684, PM918, PM926 and PM40. However, lysate from PM964 was slightly different because it caused a faint zone on isolate PM734. The lysates delivered from isolates PM684, PM918, PM926 and PM40 also showed the broadest host range. They caused lysis in 10 of 47 indicator strains.

Table 4.5 Host ranges of induced phages in 47 *P. multocida* indicator strains.

Indicator strain	STs	MLST group	Host species	Capsular type	OMP-type	Isolate of origin of lysates									
						PM122	PM986	PM982	PM988	PM964	PM850	PM336	PM684	PM918	PM926	PM40
PM316	1	A	Bovine	A	1.1	±	±	±	±	±	±	-	±	±	±	±
PM564	1	A	Bovine	A	2.1	±	±	±	±	±	+	-	±	±	±	±
PM344	3	A	Bovine	A	3.1	+	+	+	+	+	-	-	-	-	-	-
PM632	4	A	Bovine	A	4.1	+	+	+	+	+	-	-	+	+	+	+
PM666	3	A	Porcine	A	2.1	+	+	+	+	+	-	-	+	+	+	+
PM116	3	A	Porcine	A	3.1	+	+	+	+	+	-		+	+	+	+
PM966	16	B	Ovine	A	1.1	-	-	-	-	-	-	-	-	-	-	-
PM382	13	C	Porcine	A	4.1	-	-	-	-		-	-	-	-	-	-
PM706	13	C	Porcine	UT	4.1	-	-	-	-	-	-	-	-	-	-	-
PM2	17	C	Ovine	F	2.1	-	-	-	-	-	-	-	-	-	-	-
PM8	17	C	Ovine	F	2.1	-	-	-	-	-	-	-	-	-	-	-
PM246	25	C	Avian	F	2.2	-	-	-	-	-	-		-	-	-	-
PM994	12	C	Ovine	F	1.1	-	-	-	-	-	-	-	-	-	-	-
PM148	12	C	Avian	F	2.2	-	-	-	-	-	-	-	-	-	-	-
PM104	28	D	Avian	A	4.1	-	-	-	-	-	-	-	-	-	-	-
PM86	15	D	Avian	A	3.1	±	±	±	±	±	-	-	-	-	-	-
PM934	15	D	Porcine	A	5.1	±	±	±	±	±		-	-	-	-	-
PM954	15	D	Porcine	A	5.1	±	±	±	±	±	-	-	-	-	-	-
PM486	9	D	Bovine	A	9.1	±	±	±	±	±	-	-	+	-	-	-
PM172	26	D	Avian	A	3.1	±	±	±	±	±	-	-	+	-	-	-
PM302	6	E	Bovine	A	5.3	+	+	+	+	+	-	-	-	-	-	-
PM144	21	E	Avian	A	1.1	-	-	-	-	-	-	-	-	-	-	-
PM402	5	E	Bovine	A	5.1	-	-	-	-	-	-	-	-	-	-	-
PM122	ND	ND	Ovine	D	3.1	-	-	-	-	-	-	-	-	-	-	-
PM964	18	E	Ovine	D	3.1	-	-	-	-	-	-	-	-	-	-	-
PM982	18	E	Ovine	D	3.1	-	-	-	-	-	-	-	-	-	-	-
PM986	18	E	Ovine	D	3.1	-	-	-	-	-	-	-	-	-	-	-
PM988	ND	ND	Ovine	D	3.1	-	-	-	-	-	-	-	-	-	-	-
PM990	ND	ND	Ovine	D	3.1	-	-	-	-	-	-	-	-	-	-	-
PM54	10	F	Porcine	A	1.1	-	-	-	-	-	-	-	+	+	+	+
PM734	10	F	Porcine	A	1.1	-	-	-	-	±	±	-	+	±	±	+
PM820	10	F	Porcine	A	1.1	-	-	-	-	-	-	-	+	+	+	+
PM850	10	F	Porcine	A	1.1	-	-	-	-	-	-	-	+	+	+	+
PM200	10	F	Avian	A	1.2	-	-	-	-	-	-	-	-	-	-	-
PM336	7	F	Bovine	A	6.1	±	±	±	±	±	-	-	+	+	+	+
PM684	11	G	Porcine	A	6.1	+	+	+	+	+	-	-	-	-	-	-
PM918	11	G	Porcine	A	6.1	+	+	+	+	+	-	-	-	-	-	-
PM926	ND	ND	Porcine	A	6.1	+	+	+	+	+	-	-	-	-	-	-
PM40	ND	ND	Porcine	A	6.2	+	+	+	+	+	-	-	-	-	-	-
PM716	11	G	Porcine	D	4.1	-	-	-	-	-	-	-	-	-	-	
PM848	11	G	Porcine	D	4.1	-	-	-	-	-	-	-	-	-	-	-
PM696	11	G	Porcine	D	6.1	-	-	-	-	-	-	-	-	-	-	-
PM714	11	G	Porcine	D	6.1	-	-	-	-	-	-	-	-	-	-	-
PM762	11	G	Porcine	D	6.1	-	-	-	-	-	-	-	-	-	-	-
PM890	11	G	Porcine	D	6.1	-	-	-	-	-	-	-	-	-	-	-
PM226	11	G	Avian	D	13.1	-	-	-	-	-	-	+	-	-	-	-
PM82	3	H	Avian	A	7.1	-	-	-	-	-	-	-	-	-	-	-

Different lytic patterns were identified among the induced cultures with mitomycin C, (-) No lysis, (±) Faint zone of lysis, (+) Clear zone of lysis. Strains are arranged based on MLST groups. Isolates are arranged by order of MLST group (column 3) (Fig. 2.1).

They produced either clear or faint lysis zones in indicator strains PM316, PM564, PM632, PM116, PM666, PM54, PM734, PM820, PM850 and PM336. They showed the same patterns of lysis on the indicator strain. However, the phage induced from isolate PM684 also caused clear lysis in PM486 and PM172 (Table 4.5). The phage from isolate PM850 and PM336 showed very narrow host range activity against *P. multocida* indicator strains; it formed lysis zones on 3 and 1 of 47 indicator strains, respectively. A number of indicator strains such as PM316, PM564, PM666, PM116, PM486, PM172 and PM734 appeared to be more sensitive than other indicator strains in their susceptibly to phage infection (Fig. 4.13 & Table 4.5).

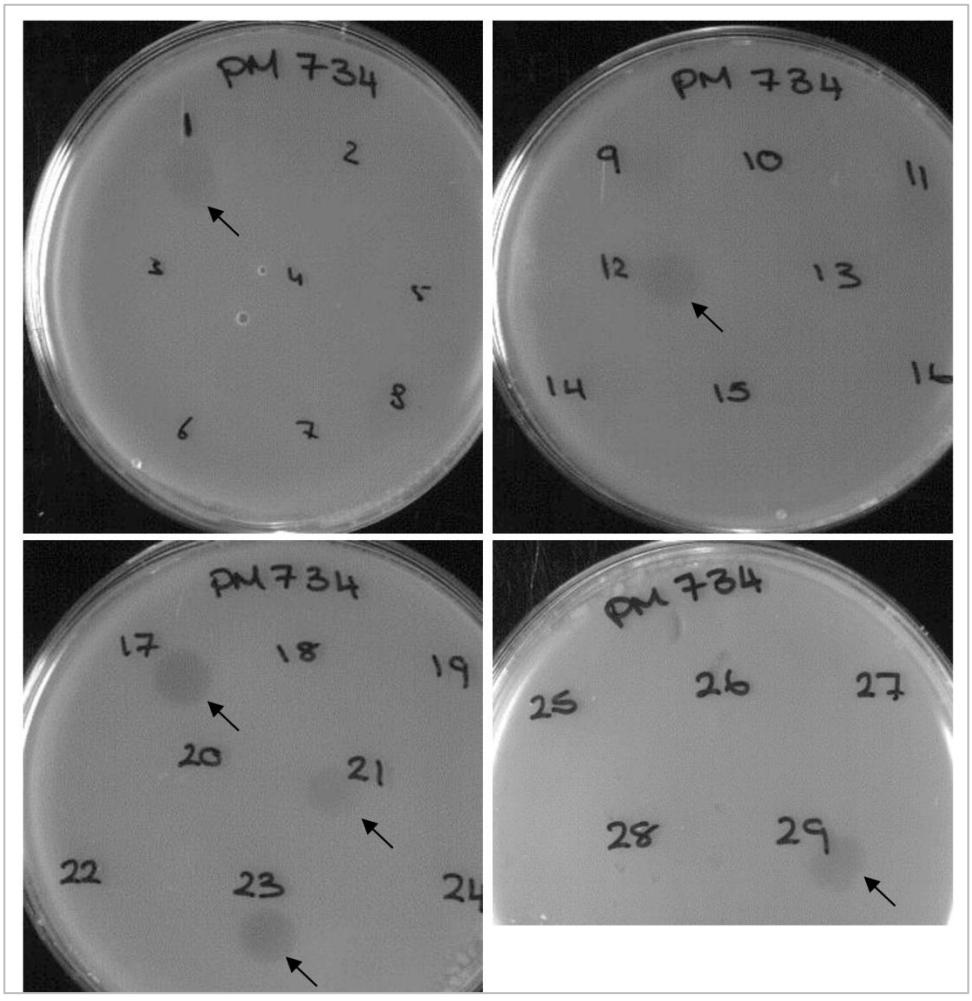

Fig. 4.13 Plaque assay showing the activities of 29 induced lysates against isolate PM734 as an indicator strain.

Faint lysis zones were produced by ΦPM850 (1), ΦPM964 (12), ΦPM918 (21) and ΦPM926 (29) (arrows), whereas ΦPM684 (17) and ΦPM40 (23) and produced clear lysis zones (arrows). The remaining lysates did not produce any signs of infection. Numbers (1 to 29) indicate phages (lysates) produced by 29 different *P. multocida* isolates. Indicator strain is labelled at the top of each plate

The results of the host range experiments showed that the indicator strain with MLST group A (bovine pneumonic group), group D, group F (porcine pneumonia group) and group G (atrophic rhinitis) were more sensitive to induced phages (Table 4.6). Different lytic patterns and the patterns were recorded based on the ability of each phage to produce infection or lysis against the indicator strains. Six different lytic patterns were identified for the phage and the patterns; named I, II, III, IV, V, and VI (Table 4.6). Lytic pattern I was found in phage from isolates PM122, PM964, PM982, PM986 and PM988, lytic pattern II was identified in ΦPM850, pattern III was associated with ΦPM336, pattern IV was observed in ΦPM684**,** the phage from isolates PM918 and PM926 showed lytic patterns V and finally pattern VI occurred in phage that induced from isolate PM40.

Table 4.6 Lytic patterns of lysates from 29 *P. multocida* isolates.

Lytic pattern	No. of phages	Phage
I	5	ΦPM122, ΦPM964, ΦPM982, ΦPM986 and ΦPM988
II	1	ΦPM850
III	1	ΦPM336
IV	1	ΦPM684
V	2	ΦPM918 and ΦPM926
VI	1	ΦPM40

4.5.5 Phage DNA isolation

DNA was isolated to examine the genetic diversity of *P. multocida* phages using restriction enzyme analysis, sequencing and identification of virulence genes. Phage DNA was isolated successfully from 18 inducible phages. These strains were lysed completely or partially with 0.2 µg/ml, or higher concentrations of mitomycin C. However, TEM identified a diverse group of phages from 29 *P. multocida* isolates (results described above). DNA was isolated from the lysates of the following *P. multocida* strains using both the standard Sambrook method and the Promega Wizard Clean-up Kit: PM40, PM86, PM122, PM172, PM336, PM382, PM486, PM684, PM848, PM850, PM918, PM926, PM934, PM954, PM964, PM982, PM986 and PM988 (Fig. 4.14 and Table 4.7). These isolates yielded large quantities of phage as observed by TEM. Two bands of different molecular sizes were identified in isolates PM86, PM172, PM486, PM934 and PM954 suggesting the presence of multiple phage. Induction of multiple temperate bacteriophages will be further confirmed by sequencing of isolated phage DNA.

Several attempts were made to improve the DNA quantity and quality because it was observed that the DNA was still contaminated with salts and solvents and the DNA yield was especially low in ØPM382, ØPM848, ØPM850, ØPM934 and ØPM954. To improve DNA quality, induction was repeated in 50 ml of BHIB overnight at 37ºC and DNA was isolated after phage particles were precipitated with PEG 8000 on ice. The precipitated DNA was washed twice with 1 ml of 70% cold ethanol. Although the phages were induced under the same conditions and the DNA extracted using the same conditions, the concentration of extracted DNA varied from one strain to another. The DNA concentrations varied from 60 to 200 ng/ µl. However, the DNA concentration obtained varied slightly from one experiment to another. Unfortunately, DNA isolation from phage using Norgen phage DNA isolation kit was unsuccessful for unknown reasons.

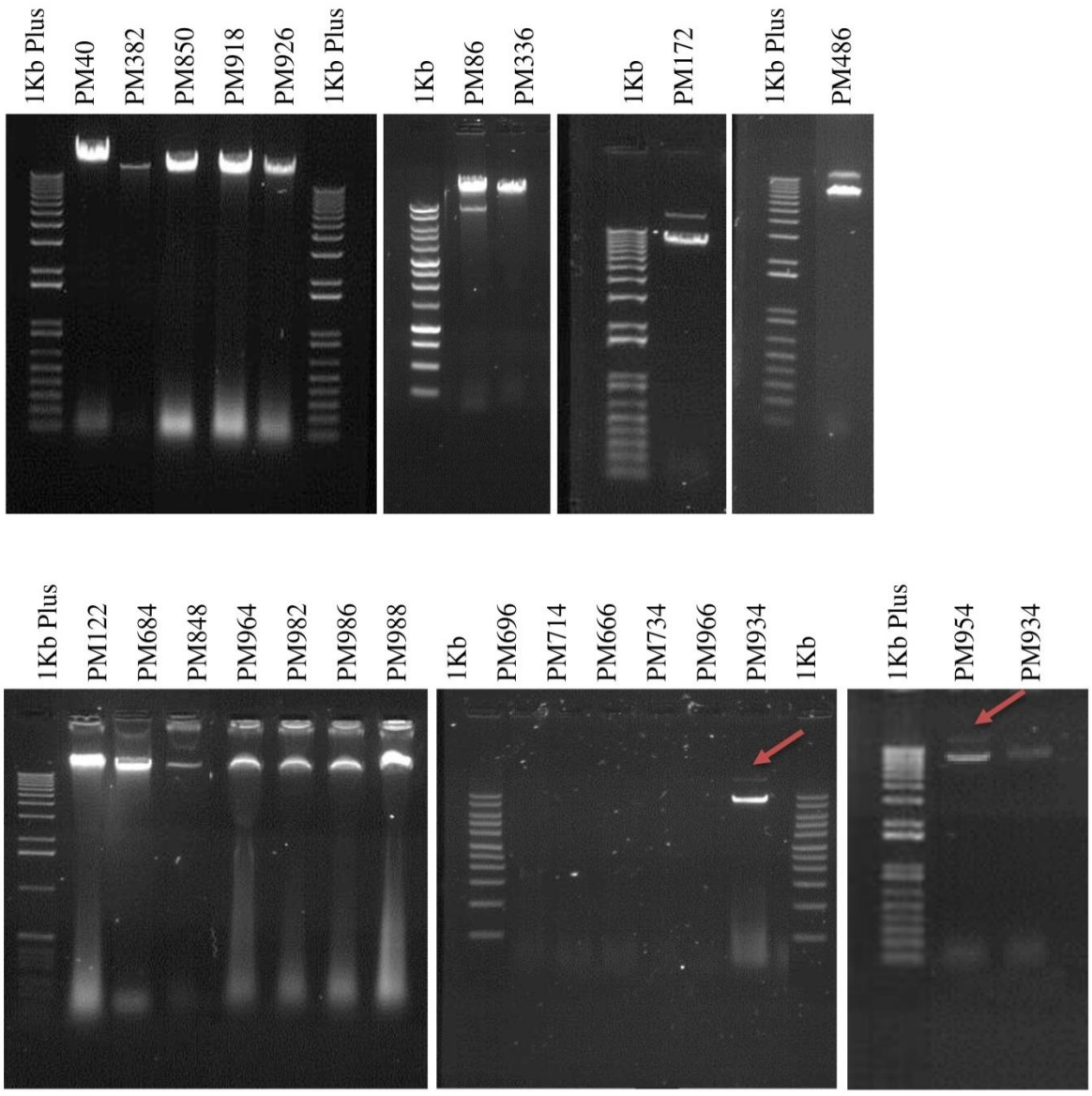

Fig. 4.14 Phage DNA from temperate bacteriophages of *P. multocida.*

The same results were obtained using either standard Sambrook method or Promega Wizard Clean-up Kit. However, the DNA concentration varied among the phage. Two bands of DNA were isolated from five *P. multocida* isolates: PM86, PM172, PM486, PM934 and PM954. However, in PM934 and PM954 a second band was faint (red arrows). This suggests that those isolates may contain more than phage. However, TEM results showed that those isolates contained only one phage type except one, PM86 which contained both *Siphoviridae* and *Myoviridae* type.

4.5.6 Restriction endonuclease analysis of phage DNA

Phage DNA was isolated from the lysates of 18 *P. multocida* isolates (see section 4.5.5). The genetic diversity of isolated DNA was assessed using different restriction enzymes (PsI, BamH1, Hind III, NdeI, EcoR1, XbaI). The restriction profiles obtained with PsI, BamH1, Hind III, NdeI, EcoR1, XbaI were poor and the DNA was not completely digested. Several attempts were made to improve the restriction digestion by improving the DNA quality. Poor restriction profiles could also be due to contamination of the DNA with salts and solvents or low DNA concentration (see section 4.5.5). The digestion reactions were incubated overnight at 37°C.

Finally, good restriction profiles were obtained with Hind III. In this case, 10 different restriction profiles were identified in 18 different phage DNA samples. The patterns were designated as A, B, C, D, E, F, G, H, I and J (Fig. 4.15). The identification of 10 different restriction endonuclease (RE) types identified that the bacteriophages in *P. multocida* are genetically diverse. The details of RE type and phage are summarised in Table 4.7.

Type A was associated with PM382 (capsular type A, ST 13). The type B profile was associated with phage from isolates PM172, PM486, PM934 and PM954 (capsular type A, ST 15, 9 and 26). The type C phages were associated with PM122, PM964, PM982, PM986 and PM988 (capsular type D and ST 18). The type D phage was associated with isolate PM850 (capsular type A and ST 10). The type E was associated with isolate PM336 (capsular type A and ST 7). The type F phage was associated with PM684 (capsular type A and ST 11). The type G phage was associated with PM918 and PM926 (capsular type A and ST 11). The type H phage was associated with PM40 (capsular type A and ST 11). The type I was associated with isolate PM848 (capsular type D and ST 11) and type J was associated with isolate PM86 (capsular type A, ST 15,). The results showed that the certain RE types such B and D were identical in phages induced from closely related *P. multocida* isolates. However, in other cases, different RE types such F, G, H, I and J were identified in closely related strains. These differences could be due to the presence of more than one phage or they may not have identical phage genomes. This needs to be confirmed by sequencing of isolated phage DNA.

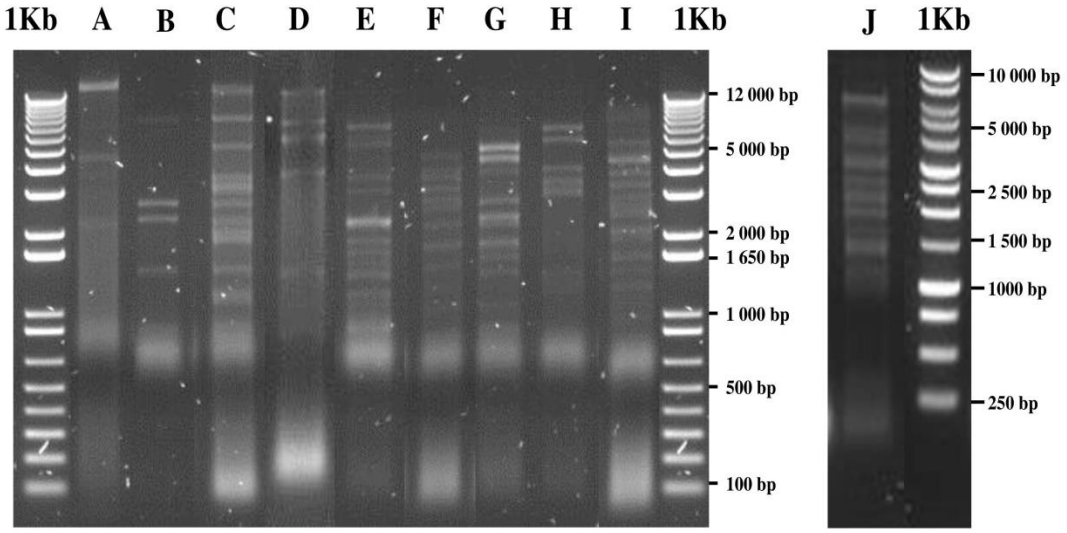

Fig. 4.15 Restriction endonuclease (RE) types of phage DNA isolated from *P. multocida*.

Ten unique RE types were identified in 18 different phage DNA samples as follows: type A (ΦPM382), type B (ΦPM172, ΦPM486, ΦPM934 and ΦPM954), type C (ΦPM122, ΦPM964, ΦPM982, ΦPM986 and ΦPM988), type D (ΦPM850), type E (ΦPM336), type F (ΦPM684), type G (ΦPM918 and ΦPM926), type H (ΦPM40), type I (ΦPM848) and type J (ΦPM86). The RE analysis was carried out with Hind III.

Table 4.7 Properties of phages induced in 29 *P. multocida* isolates.

Isolate	ST	MLST group	Host species	Capsular type	OMP-type	Lysis type	Family type by TEM	Host range patterns	Phage DNA	RE
PM666	3	A	Porcine	A	2.1	Partial	*Siphoviridae*	-	-	-
PM116	3	A	Porcine	A	3.1	Partial	*Siphoviridae*	-	-	-
PM966	16	B	Ovine	A	1.1	Partial	*Siphoviridae*	-	-	-
PM382	13	C	Porcine	A	4.1	Partial	*Myoviridae*	-	+	A
PM86	15	D	Avian	A	3.1	Partial	*Myoviridae* & *Siphoviridae*	-	+	J
PM934	15	D	Porcine	A	5.1	Partial	*Myoviridae*	-	+	B
PM954	15	D	Porcine	A	5.1	Partial	*Myoviridae*	-	+	B
PM486	9	D	Bovine	A	9.1	Partial	*Myoviridae*	-	+	B
PM172	26	D	Avian	A	3.1	Partial	*Myoviridae*	-	+	B
PM122	ND	ND	Ovine	D	3.1	Complete	*Siphoviridae*	I	+	C
PM964	18	E	Ovine	D	3.1	Complete	*Siphoviridae*	I	+	C
PM982	18	E	Ovine	D	3.1	Complete	*Siphoviridae*	I	+	C
PM986	18	E	Ovine	D	3.1	Complete	*Siphoviridae*	I	+	C
PM988	ND	ND	Ovine	D	3.1	Complete	*Siphoviridae*	I	+	C
PM54	10	F	Porcine	A	1.1	Partial	*Siphoviridae*	-	-	-
PM820	10	F	Porcine	A	1.1	Partial	*Siphoviridae*	-	-	-
PM850	10	F	Porcine	A	1.1	Partial	*Myoviridae* & *Siphoviridae*	II	+	D
PM200	10	F	Avian	A	1.2	Complete	*Siphoviridae*	-	-	-
PM336	7	F	Bovine	A	6.1	Complete	*Siphoviridae*	III	+	E
PM684	11	G	Porcine	A	6.1	Complete	*Myoviridae* & *Siphoviridae*	IV	+	F
PM918	11	G	Porcine	A	6.1	Complete	*Siphoviridae*	V	+	G
PM926	ND	ND	Porcine	A	6.1	Complete	*Siphoviridae*	V	+	G
PM40	ND	ND	Porcine	A	6.2	Complete	*Myoviridae*	VI	+	H
PM848	11	G	Porcine	D	4.1	Complete	*Siphoviridae*	-	+	I
PM696	11	G	Porcine	D	6.1	Partial	*Siphoviridae*	-	-	-
PM714	11	G	Porcine	D	6.1	Partial	*Siphoviridae*	-	-	-
PM762	11	G	Porcine	D	6.1	Partial	Tail-less phage	-	-	-
PM890	11	G	Porcine	D	6.1	Partial	Tail-less phage	-	-	-
PM226	11	G	Avian	D	13.1	Partial	*Siphoviridae*	-	-	-

4.6 Discussion

It has been shown previously that temperate bacteriophages are involved in the emergence and diversity of pathogenic bacteria via horizontal gene transfer (HGT) through the dissemination of genes encoding virulence factors such as toxins (Boyd & Brüssow, 2002; Saunders *et al.*, 2001). The aim of this study was to investigate the presence of temperate bacteriophages in *P. multocida* and to determine if they are likely to be involved in the diversity and evolution of *P. multocida* with emphasis on the OMPs of this bacterium.

Mitomycin C has been used more frequently to induce prophages in bacteria, including *P. multocida* (Campoy *et al.*, 2006; Ackermann & Karaivanov, 1984; Pullinger *et al.*, 2004). In the present study, eight different isolates (PM144, PM246, PM564, PM632, PM684, PM734, PM982 and PM966) were selected for preliminary optimisation experiments. The isolates were selected to represent different host species, disease syndromes, capsular types, OMP-types and STs. Optimisation experiments using different mitomycin C concentrations indicated that induction of temperate bacteriophages occurs in *P. multocida* after the cultures are exposed to mitomycin C for 6 to 7 h. Bacterial cell lysis was indicated by a reduction in OD_{600} of mitomycin-treated cultures when compared to the OD_{600} of control cultures (no mitomycin C). The effect of mitomycin C varied among the eight *P. multocida* isolates (section 4.5.1; Fig. 4.4). A final concentration of 0.2 µg/ml mitomycin C was selected as the optimum concentration for the induction of prophages in *P. multocida* isolates because this concentration completely lysed isolates PM684 (porcine) and PM982 (ovine) after 4 to 5 h (Fig. 4.4G, H). Thus, this concentration of mitomycin C is able to induce phages in *P. multocida*. However, higher concentrations were used for specific isolates when there was no sign of induction with 0.2 µg/ml (Table 4.3). Final concentrations of 0.2, 0.3, 0.5, 1.0 and 2.0 µg/ml mitomycin C have previously been used to induce temperate bacteriophages in many bacterial species (Davies & Lee, 2006; Highlander *et al.*, 2006; Hsu *et al.*, 2013; Muniesa *et al.*, 2003; Muniesa *et al.*, 2004; Nale *et al.*, 2012; Poblet-Icart *et al.*, 1998; Stevenson & Airdrie, 1984; Shin *et al.*, 2014; Urban-Chmiel *et al.*, 2015). The induction patterns were classified into three types: complete lysis, partial lysis and no lysis. It was noticed during lysogenic induction with mitomycin C that the degree of induction (i.e. lysis) of the bacterial cells varied depending on the

isolate. Similar findings have been described previously in *E. coli* during the induction of stx_2-converting bacteriophages with mitomycin C (Muniesa *et al.*, 2003; Muniesa *et al.*, 2004).

The majority of the 47 *P. multocida* isolates used in this study contained inducible temperate bacteriophages because 37 (79%) were sensitive to mitomycin C. The induction results revealed a possible association between mitomycin sensitivity and the genetic relatedness of the isolates. For example, isolates within MLST group D (PM86, PM172, PM486, PM934 and PM954) shared the same induction profile suggesting that these isolates may contain the same phages. Similar findings occurred within MLST groups A, B, C, E and F. Previously, it had been shown that phages are involved in the HGT of virulence genes in *P. multocida* such as the *toxA* gene in toxigenic porcine strain causing atrophic rhinitis (Pullinger *et al.*, 2004). The *toxA* gene has also been identified in ovine *P. multocida* strains (Einarsdottir *et al.*, 2016; Shayegh *et al.*, 2008; Weiser *et al.*, 2003). It was suggested that the *toxA* gene could be transferred horizontally from porcine to ovine strains. Isolates PM122, PM964, PM982, PM986 and PM988 were completely lysed (and PM990 partially lysed) after lysogenic induction with 0.2 µg/ml of mitomycin C, suggesting that the *toxA* gene might be carried by temperate bacteriophages in these isolates. This was later confirmed by sequencing of the phage DNA (discussed in Chapter 5). Induction by mitomycin C provides a preliminary indication of the presence of temperate bacteriophages. However, sometimes bacterial growth can be affected in other ways by adding mitomycin C, such as due to the induction of bacteriocins which also cause cell lysis (Bradley, 1967). For this reason, the induction of any induced phage should be confirmed either visually by TEM or by characterisation of isolated phage DNA.

Transmission electron microscopy has been used as a valuable tool in the study of phage morphology, characterisation and classification (Ackermann, 2001; Ackermann, 2003). A diverse set of temperate bacteriophage morphologies were identified in this study. Phage particles were identified in 29 (61.7%) of 47 *P. multocida* isolates (Fig. 4.7 & Table 4.4). Similar findings have previously been described in the closely related species *M. haemolytica* by TEM (Ackermann & Karaivanov, 1984; Davies & Lee, 2006; Hsu *et al.*, 2013; Urban-Chmiel *et al.*, 2015). Moreover, diverse phage morphologies have been identified in many

bacteria including *Burkholderia*, *Clostridium*, *Haemophilus*, *Lactobacillus*, Listeria, *Pseudomonas*, *Salmonella* and *Yersinia* (Denes *et al.*, 2014; Kiliç *et al.*, 2001; Moreno Switt *et al.*, 2013; Nale *et al.*, 2012; Stevenson & Airdrie, 1984; Seed & Dennis, 2005; Sepúlveda-Robles *et al.*, 2012; Sekulovic *et al.*, 2014; Williams *et al.*, 2002). Identification of temperate bacteriophages in 29 of 47 isolates suggests that temperate phages may play important and widespread roles in the generation of diversity in *P. multocida* as observed in the extensive degree of recombination in genes such as *ompA* and *ompH*. It is well established that bacteriophages play important roles in bacterial evolution via HGT (Boyd & Brüssow, 2002; Brüssow *et al.*, 2004; Canchaya *et al.*, 2003a; Masignani *et al.*, 2001).

The phage particles identified belonged to the *Siphoviridae* and *Myoviridae* phage families although tail-less phage particles were also identified. Of the 29 identified phages, the majority belonged to the family *Siphoviridae* (72%). However, three of 21 isolates also contained both *Siphoviridae* and *Myoviridae* phage types (Table 4.4). The intact *Siphoviridae* particles varied in their capsid shape, size and tail size (Fig. 4.8). Similar morphotypes were associated with isolates from the same, or closely related, lineage. For example, the same morphotype was identified in isolates PM122, PM964, PM982, PM986 and PM988. Nine of the 29 phages identified were of the *Myoviridae* type and these phages were also characterised by variation in their capsid shape and size (Table 4.4). A diverse set of temperate bacteriophages were previously identified by TEM in *P. multocida* (Ackermann & Karaivanov, 1984). However, in the present study, both *Siphoviridae* and *Myoviridae* type phages were induced from the same host for the first time (in three isolates) (Fig. 4.7 & Table 4.4). Thus, these preliminary observations suggest that a single *P. multocida* isolate may harbour multiple prophages. In addition, *Myoviridae* phages induced in isolates PM684 and PM850 were different from those induced in isolate PM86 based on TEM; phage in the latter isolate possessed an unusually small capsid; the significance of this observation will be discussed later (Chapter 5). The presence of multiple phages in a single host has not been described in *P. multocida*, although this is known to occur in other bacteria including *M. haemolytica*, *E. coli*, *Streptococcus pyogenes* and *Bacillus subtilis* (Canchaya *et al.*, 2003; Hsu *et al.*, 2013; Niu *et al.*, 2015).

Based on their morphologies as determined by TEM, five of the nine *Myoviridae*-type phages identified were very distinct in appearance and quite different from the others. These phage particles had unusually small hexagonal capsids and long tails compared to the other *Myoviridae*-type phages identified (Table 4.4). This phage type was induced only in isolates PM86, PM934, PM954, PM486 and PM172. However, these isolates notably belonged to the same genetic cluster (MLST group D) based on MLST scheme. This type of *Myoviridae*-like phage, characterised by a small capsule and long tail, has not previously been described in *P. multocida*. However, a similar phage morphology has been identified in *Clostridium difficile* 027 strains and in *Bacillus* species by TEM (Bfudley, 1965; Nale *et al.*, 2012). The particles are also known as killer particles because they possess killing properties although they were unable to multiply or replicate within indicator strains (Bfudley, 1965). However, phage particles with small capsids have been identified as components of *Staphylococcus aureus* pathogenicity islands (SaPIs) (Úbeda *et al.*, 2005). SaPIs are phage-inducible chromosomal islands (PICIs) and maintain an intimate relationship with temperate (helper) bacteriophages. Following SOS induction using antibiotics, the SaPI genome excises, replicates using its own replicon and encapsidates into special small phage heads to fit their smaller genome (Tormo *et al.*, 2008; Úbeda *et al.*, 2005). The presence of phage particles with small heads, together with the presence of two bands representing phage DNA of differing size, in isolates PM86, PM172, PM486, PM934, PM954 suggests, for the first time, the presence of PICIs in *P. multocida*. Confirmation of this was provided by sequence analysis of phage DNA and Southern blot hybridisation and is discussed in further detail below. Overall, the results showed that similar phage particles were associated with closely related isolates (i.e. within the same, or closely related, genetic lineage). For example, isolates PM122, PM964, PM982, PM986 and PM988 (ST 18) possessed similar *Siphoviridae* morphotype; isolates PM86 (ST 15), PM934 (ST 15), PM954 (ST 15), PM486 (ST 9) and PM172 (ST 26) of the MLST group D contained similar *Myoviridae*-like phage. These findings provide further support of the evolutionary relationships of *P. multocida* isolates from multiple hosts based on the MLST data.

Host range experiments were conducted to determine the presence of biologically active temperate bacteriophages and to assess the ability of these

phages to infect a range of indicator strains. The results showed that the plaque assay appeared to be less sensitive than TEM in determining the presence of phages in the lysates. Of the 29 induced phages (as determined by TEM), only 11 (38%) isolates produced signs of infection in indicator strains; 18 (62%) phages produced no visual signs of infection. In contrast, TEM identified phages in 29 (61.7%) of the 47 *P. multocida* isolates investigated. The low number of phages able to infect the indicator strains may have been due to the absence of suitable indicator strains possessing appropriate cell surface-associated phage receptors. These observations could also reflect differences in phage tail fibres, or the complete lack of tail fibres, which may affect the attachment of phages to receptors present on the bacterial cell surfaces. Attachment of phages to host cells is enhanced by the ability of phage proteins to recognise specific binding or attachment sites on the bacterial cell surface (receptors) (Lindbergl, 1973; Michael *et al.*, 2003; Rakhuba *et al.*, 2010). Receptors include OMPs (such as OmpA, porins and LamB), LPS, pili or flagella (Guttman *et al.*, 2005; Jin *et al.*, 2015; Lindbergl, 1973; Morona *et al.*, 1985; Parent *et al.*, 2014; Porcek & Parent, 2015; Randall-Hazelbauer & Schwartz, 1973; Rakhuba *et al.*, 2010). Furthermore, bacteriophages use different mechanisms to infect encapsulated bacteria and reach the bacterial cell surface because the capsule may block the access of bacteriophages to receptors localised in the cell wall (Lindbergl, 1973; Rakhuba *et al.*, 2010). In these cases, phages produce an enzyme called capsular depolymerase that causes degradation of the capsular layer and allows the phage to reach the bacterial cell wall (Lindbergl, 1973). However, it is not known which receptors in the *P. multocida* cell wall enhance attachment of phages to the host cells. Therefore, further studies are required to identify the bacterial receptors of *P. multocida* phages in more detail.

Overall, the results showed that *P. multocida* phages have a limited host range since they produced zones of lysis in strains within specific groups. Eighteen of the phages (ΦPM666, ΦPM116, ΦPM966, ΦPM382, ΦPM86, ΦPM934, ΦPM954, ΦPM172, ΦPM486, ΦPM54, ΦPM820, ΦPM200, ΦPM848, ΦPM696, ΦPM714, ΦPM762, ΦPM890 and ΦPM226) identified by TEM were unable to infect any indicator strains. This suggests that the indicator strains lack appropriate receptors for phage attachment or the phages may be defective and unable to infect any indicator strains. It has been shown that temperate bacteriophages

induced from *E. coli* (STEC) were not detectable directly by the spot test although these phages were detectable by hybridisation using specific phage probes (Muniesa *et al.*, 2004). It is possible that some of the phages caused infection in *P. multocida* indicator strains but this was not visible to the naked eye. Another reason why induced phages are unable to produce zones of lysis is that the lysogenic bacteria may be affected by another phage. Prophages may confer immunity by repressor proteins. It has been found the ability of phage to produce faint plaques, could probably be due to lysogenisation of some bacterial cells within the plaques (Guttman *et al.*, 2005; Hsu *et al.*, 2013). Lytic types I, IV, V and VI showed the broadest host range and caused zones of lysis on indicator strains within the same, or closely related lineages (Table 4.5). In contrast, lytic types II and III caused zones of lysis on a small number of specific isolates. Interestingly, some phages from isolates of the same genetic lineage and with the same RE types had similar host ranges. Thus, phage induced in ovine isolates PM122, PM964, PM982, PM986 and PM988 (capsular type D, OMP-type 3.1, ST 18 and MLST group D) were of RE type C and had the same lytic pattern (type I). Therefore, it is likely that these closely-related isolates also contain identical phages. There were differences in the ability of the same phage to infect indicator strains of the same clonal group or lineage. As discussed above, differences in the ability of phages to infect indicator strains could be due to difference in cell-surface receptors present on the indicator strains (Kiliç *et al.*, 2001). However, these findings also suggest that OMPs may act as phage receptor because some phage caused infection of indicator strains having the same OMPs (Table 4.5). Further work will be required to identify the bacterial receptors of *P. multocida* phages.

Although phage particles were identified by TEM in 29 *P. multocida* lysates, phage DNA was isolated from only 18 lysates. However, the concentration of DNA differed from one strain to another (Fig. 4.14). The variation in DNA concentration suggests that some isolates have a higher rate of phage production than others (phage replication and release), although all lysates were induced under the same conditions. The results showed the isolates having lower optical densities after induction with mitomycin C (i.e. complete lysis) produced higher concentrations of DNA. In contrast, low or medium phage DNA concentrations were typical of those isolates exhibiting higher optical densities due to less

extensive lysis after addition of mitomycin C. From a 50 ml culture, the DNA concentrations varied from 50 to 200 ng/µl. However, the DNA concentration obtained varied slightly from one experiment to another. Similar findings have been described in *E. coli* (Muniesa *et al.*, 2003; Muniesa *et al.*, 2004). Two phage DNA bands appeared to be common to certain strains within the MLST group D (PM86, PM172, PM486, PM934 and PM954). The presence of two bands of different size strongly suggests the presence of more than one phage in the genome. Furthermore, TEM identified the presence of unusual small capsids of *Myoviridae*–type phages in lysates induced from these isolates. Therefore, the TEM results, together with the presence of two DNA bands, suggest the presence and induction of PICIs in *P. multocida*. This represents the first description of PICIs in *P. multocida*. Phage particles with small capsids, but of the *Siphoviridae* family, have been identified in *S. aureus* as pathogenicity island (SaPIs) (Úbeda *et al.*, 2005). The presence of PICIs in *P. multocida* strains was confirmed by Southern blot analysis and sequencing (discussed in Chapter 5).

Restriction endonuclease analysis has been used to assess the genetic diversity of induced phages in a wide-range of bacteria (Davies & Lee, 2006; Hsu *et al.*, 2013; Jakhetia & Verma, 2015 Muniesa *et al.*, 2004; Pullinger *et al.*, 2003; Sepúlveda-Robles *et al.*, 2012; Sekulovic *et al.*, 2014; Urban-Chmiel *et al.*, 2015). Phage DNA was digested with different restriction enzymes but optimum digestion patterns were obtained with Hind III. Ten different RE patterns were identified among the 18 DNA samples (Fig. 4.15). The identification of 10 different RE types in only 18 samples suggests that *P. multocida* bacteriophages are relatively diverse and may be genetically different. RE analysis has been used to study the genetic relatedness of induced phages because classification of bacteriophages based on phage morphology alone has limitations and does not provide such information (Lawrence *et al.*, 2002). Phages of RE types B, C and G had identical morphologies (Table 4.7). Thus, these findings revealed an association between RE type and phage morphology. RE type B was associated with the *Myoviridae*-type phages having the unusually small capsids, whereas RE types C and G were associated with *Siphoviridae*-type phages. The presence of multiple RE types among phages having the same morphologies clearly suggests that phages of similar morphotypes may be genetically different and have different genomes. Furthermore, phages of RE types B, C and G were each

associated with isolates of the same genetic lineage (MLST). Similar findings have been described in the closely-related species *M. haemolytica* (Davies & Lee, 2006). However, restriction endonuclease analysis demonstrated that isolates of the same clonal group or lineage may be associated with more than one RE type. For example, RE types D, E, F, G, H and I. The presence of more than one RE profile in phages of isolates within the same lineage could be due to the presence of different or multiple phages which have not been identified by TEM. Therefore, further analysis will be required to address the presence of different or multiple phages in isolates within closely related lineages by sequencing of phage DNA (Chapter 5).

4.7 Conclusion

The majority (79%) of *P. multocida* isolates were sensitive to mitomycin C indicating that these isolates contain temperate bacteriophages. TEM identified a diverse set of phages in 29 induced cultures. The phage particles were morphologically diverse and represented both the *Siphoviridae* and *Myoviridae* families. Both *Siphoviridae*- and *Myoviridae*-type phage were induced in certain isolates indicating that a single host may harbour multiple prophages. Moreover, a distinct *Myoviridae* phage type with an unusually small capsid was identified in certain isolates by TEM. Plaque assays were less sensitive than TEM for detection of temperate bacteriophages. Only 11 (38%) isolates produced signs of infection against indicator strains. The identification of seven different lytic patterns on indicator strains and 10 different RE profile provided further evidence that temperate bacteriophages in *P. multocida* are diverse. There was an association between phage type and *P. multocida* isolates within the same or closely related lineages (capsular type, OMPs, and STs). These findings further support the evolutionary relationships of *P. multocida* based on MLST data.

Chapter 5 Genomic characterisation of temperate bacteriophages from *P. multocida*

5.1 Introduction

Bacteriophages as bacterial viruses are able to infect and replicate inside bacterial cells. Temperate bacteriophages switch between lytic and lysogenic cycles after infecting host cells. In the lysogenic cycle, temperate bacteriophages integrate their genome into the host chromosome and remain in a dormant stage as prophage where they replicate with the host chromosome, until the induction (Bobay *et al.*, 2014; Weinbauer, 2004). Integrated prophages are major contributors to bacterial diversity and drive bacterial evolution (Brüssow *et al.*, 2004; Canchaya *et al.*, 2004). It has been shown that prophages play a role in host survival (Brüssow *et al.*, 2004) and they can confer upon their bacterial host enhanced fitness (Bobay *et al.*, 2014; Fortier & Sekulovic, 2013).

Temperate bacteriophages, especially those carrying bacteriophage-encoded virulence genes, have also been demonstrated to contribute to bacterial pathogenesis (Boyd & Brüssow, 2002; Boyd, 2012; Penades *et al.*, 2015). Bacteriophage-encoded virulence determinants can transform their host from a commensal to a pathogen or virulent strain by a process known as lysogenic conversion (Allison, 2007; Boyd & Brüssow, 2002; Boyd, 2012; Veses-Garcia *et al.*, 2015). In lysogenic conversion bacteriophage-encoded virulence genes provide mechanisms that enable attachment, invasion, survival and damage to the host and/ or host cells bacterial cell (Boyd & Brüssow, 2002; Boyd, 2012). In Gram-negative and Gram-positive bacteria, common bacteriophage-encoded virulence factors include well-studied toxins and effector proteins (Allison, 2007; Boyd, 2012; Brüssow *et al.*, 2004; Cheetham & Katz, 1995; Pullinger *et al.*, 2003; Saunders *et al.*, 2001; Smith *et al.*, 2012; Volponi *et al.*, 2012). Bacteriophages can transfer fragments of chromosomal DNA or virulence genes horizontally by a process called transduction. This process can drive the evolution of bacterial pathogens resulting in the emergence of novel pathogens (Penadés & Christie, 2015; Penadés *et al.*, 2015). For example, the *E. coli* O157 Sakai genome contains approximately 18 prophages which account for 50% of its site-specific genomic DNA sequences (Weinbauer & Rassoulzadegan, 2004). This indicates that bacteriophages mediate HGT through transduction resulting in the

emergence of new *E. coli* strains, contributing to the genetic diversity of the *E. coli* species (Weinbauer & Rassoulzadegan, 2004). These virulence factors are normally encoded by diverse group of bacteriophages including members of the *Siphoviridae*, *Myoviridae*, *Podoviridae* and *Inoviridae* families (Brüssow *et al.*, 2004). The virulence genes transferred by a family of mobile pathogenicity islands are referred to as pathogenicity-inducible chromosomal islands (PICIs) (Penadés & Christie, 2015). Pathogenicity-inducible chromosomal islands are satellite phages that have an intimate relationship with temperate (helper) bacteriophages (Penadés & Christie, 2015). For examples, *Staphylococcus aureus* pathogenicity islands (SaPIs) are a well-studied PICI (Novick *et al.*, 2010; Penadés & Christie, 2015; Tormo *et al.*, 2008; Úbeda *et al.*, 2005). Following infection by helper phage or induction of helper phage with antibiotics, PICIs are able to excise from the genome, replicate using their own replicon and encapsidate themselves into special small phage heads to fit their smaller genome (Tormo *et al.*, 2008; Úbeda *et al.*, 2005).

Prophage integration is normally mediated by a site-specific tyrosine or serine recombinase (Bobay *et al.*, 2013). However, other temperate bacteriophages such as Mu-like phages integrate into the host chromosome using transposase where they integrate randomly at any location into the host chromosome via transposition (Faelen & Toussaint, 1976). Random integration may lead to mutations in the host by interrupting bacterial transcription at the site of insertion or integration (Faelen & Toussaint, 1976; Jakhetia & Verma, 2015; Zehr *et al.*, 2012). However, transposase-encoding genes have also been identified in the genome of P2-like phages of *Burkholderia cepacia* (Lynch *et al.*, 2010) and P2-like and λ-like phages of *M. haemolytica* (Niu *et al.*, 2015). It has been suggested that the presence of transposase in P2-like and λ-like phages may be involved in the acquisition of foreign genes from other bacteria or phages (Niu *et al.*, 2015).

Very little is known about the role of temperate bacteriophages of *P. multocida* with regards to evolution and genetic diversity. Bacteriophages were described as typing methods in epidemiological studies (Fussing *et al.*, 1999; Nielsen & Rosdahl, 1990). To date, only one temperate bacteriophage genome, named F108, has been sequenced (Campoy *et al.*, 2006a). F108 belongs to the family *Myoviridae* and was isolated from a serogroup A strain; its genome is composed

of 30,505 bp double-stranded DNA. The F108 genome showed the highest homology with *H. influenzae* HP1 and HP2 phages. Comparative genome analysis of F108 showed that no virulence genes were encoded and it was also able to perform generalised transduction using chromosomal markers. The absence of any virulence genes and the ability to perform generalised transduction makes F108 a valuable tool for genetic manipulation in *P. multocida* (Campoy *et al.*, 2006a). Sequence analysis of the DNA flanking *toxA* in *P. multocida* revealed the presence of genes homologous to bacteriophage tail protein genes and a bacteriophage antirepressor, suggesting that the *toxA* gene resides within a bacteriophage (Pullinger *et al.*, 2004). Previously, *toxA* has been identified in ovine *P. multocida* strains (Einarsdottir *et al.*, 2016; Shayegh *et al.*, 2008; Weiser *et al.*, 2003). The presence of *toxA* in non-toxigenic strains of *P. multocida* indicates that the gene has been horizontally transferred from toxigenic porcine strain to the ovine stains where bacteriophages could possibly play a role in the acquisition of *toxA*.

As described previously in Chapter 4, a diverse group of temperate bacteriophages belonging to the *Siphoviridae* and *Myoviridae* families has been identified by TEM using mitomycin C. Restriction endonuclease analysis was performed and the results identified 10 different RE types, suggesting that *P. multocida* phages are genetically diverse. TEM also identified phages with unusually small capsids in isolates PM86, PM172, PM486, PM934 and PM954. Two bands of phage DNA were also identified in these isolates when analysing the phage DNA by agarose gel electrophoresis. These results suggested that another phage, or PICIs, may be induced in these *P. multocida* strains. To date, the presence of PICIs has not been described in *P. multocida* and no study has been conducted to analyse the comparative genomics of temperate bacteriophages in *P. multocida*. Little is known about whether *P. multocida* carries bacteriophage-encoded virulence genes or about the role of bacteriophages in the evolution and pathogenesis of this bacterium. The whole genomes of 18 phage DNA samples and the complete genome sequences of 40 *P. multocida* isolates were determined using the Illumina Mi-Seq platform. The aims of this part of the study were as follow: To classify the temperate bacteriophages of *P. multocida* using comparative genomic sequence analysis of 40 *P. multocida* isolates representing multiple host species, disease types, capsular serotypes, OMP-types

and sequence types, to demonstrate whether functional temperate bacteriophages in *P. multocida* encode any virulence genes. Finally, to evaluate the role of temperate bacteriophages in the evolution of *P. multocida* and host adaptation by comparing functional phages with the intact (non-inducible) prophage pool in a panel of *P. multocida* genomes.

5.2 Materials and methods

5.2.1 Preparation of phage DNA

Single induced phage preparations were used to carry out TEM analysis, RE analysis and to prepare phage genomic DNA. For phage DNA extraction, *P. multocida* broth cultures were induced in 50 ml of BHIB with mitomycin C as previously described in Chapter 4 (Materials and methods). Phage DNA was isolated from the induced preparations after bacterial contaminants were removed from the prepared lysates using DNase and RNase (both at a final concentration of 10 µg/ ml) (Sigma-Aldrich, UK). Phage particles were pelleted and concentrated using polyethylene glycol (PEG 8000) (Sigma-Aldrich, UK). Phage genomic DNA was purified and extracted using phenol-chloroform-isoamyl alcohol 25:24:1 (Sigma-Aldrich, UK) and 70% ethanol (section 4.4.4). The prepared phage DNA samples were used for whole bacteriophage DNA sequencing.

5.2.2 Preparation of bacterial DNA for PCR reactions

For PCR reactions, chromosomal DNA was prepared using InstaGene matrix (Biorad, 732-6030) according to the manufacturer's instructions as described previously in Chapter 3 (Materials and methods, section 3.4.2.1).

5.2.3 Phage genome sequencing

DNA sequencing was carried out by Glasgow polyomics using the Illumina Mi-Seq platform, employing 300bp paired-end sequencing. The reads were trimmed of Illumina adapter sequences and low quality bases, then de novo assembled and scaffolded using the CLC Genomics Workbench (v7.5.1, Qiagen). Assembled scaffolds were annotated using the Rapid Annotation using Subsystem Technology (RAST) resource (Aziz *et al.*, 2008; Overbeek *et al.*, 2014).

5.2.4 Identification of prophages within the bacterial genomes

Whole genome sequences of *P. multocida* isolates were used to confirm the assembly of induced phage genomes and to identify other prophages that were present within the *P. multocida* genomes. PHAge Search Tool (PHAST) analysis was used for the rapid detection of intact prophages sequences within bacterial genomes (Zhou *et al.*, 2011). CLC genomics workbench (v7.5.1, Qiagen) was used to visualise the presence of prophages within both bacterial and sequenced phage genomes, to identify the open reading frames (ORFs) of each phage and inspect the phage genome sequences for the presence of any potential virulence genes. CLC genomics workbench was also used to locate the integration sites of intact prophages within the bacterial genomes. An internal BLAST database was created in CLC genomics workbench to identify genes within the 40 *P. multocida* genomes of the present study. The properties of the isolates are listed previously in Table 2.1 (Chapter 2).

5.2.5 Primer design

Primer-BLAST (http://www.ncbi.nlm.nih.gov/tools/primer-blast/) was used to design primers. The primers were synthesised by Sigma-Aldrich (Sigma, United Kingdom).

5.2.5.1 Southern blot analysis

Bacteriophage DNA from isolates PM86, PM172, PM486, PM934 and PM954 showed the presence of two bands of different molecular size. Viewing bacterial genomes in CLC genomics workbench showed that these isolates contained two phage sequences (a Mu-like phage and a short phage sequence). Both phage genomes were induced and sequenced successfully. Primer pair (#654/#655) was designed to amplify 560 bp of terminase gene belonging to the Mu-like phage. Primer pair (#656/#657) was designed to amplify 593 bp of the small phage sequence. The primers were used to differentiate between the two bands using Southern blot hybridisation and also to examine the presence of the same phages among other phage DNA samples (PM40, PM864 and PM926) using PCR. Details of the oligonucleotide primers are provided in Table 5.1.

Table 5.1 Details of oligonucleotide primers used for Southern blot hybridisation.

Primer name	Designation	Sequence (5'—3´)	Length
ϕPM86.1/F1	#654	CAGAATGGTCACGTCATACCG	21
ϕPM86.1/R1	#655	GCCTTGGGGGATACGAATTTG	21
ϕPM86.2/F1	#656	TATACCCGTTCAACATAACCC	21
ϕPM86.2/R1	#657	CTGCGACGTATGGAACACAGC	21

5.2.5.2 Identification of attachment sites and spontaneous induction in *P. multocida* bacteriophages

Sets of primers were designed to identify attachment sites and also to examine whether the prophages of *P. multocida* are spontaneously induced from broth cultures (no mitomycin C). ϕPM982.1 was selected for this purpose. Primer pairs F1/R1 and F2/R1 were designed to confirm the attachment sites as shown in Fig. 5.1; primer pair F1/R2 was used to examine whether the phages were excised and spontaneously induced. Details of the nucleotide sequences of the primers are provided in Table 5.2.

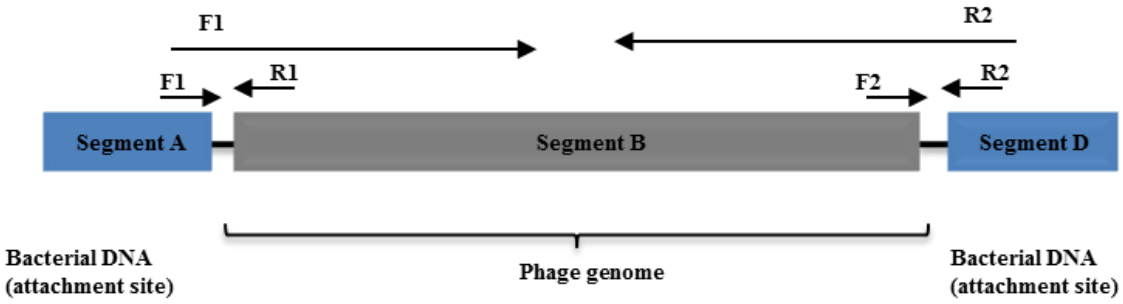

Fig. 5.1 Details of primers used for identification of attachment sites and spontaneous induction in *P. multocida* isolates.

Primer pairs F1/R1 and F2/R2 were designed to identify attachment sites; primers pair F1/R3 was used to check whether ϕPM982.1 induced spontaneously. Phage genome is shown in grey box (segment B); bacterial genomic DNA is shown in blue boxes (segments A and D). Small arrows indicate the positions of the primers used for PCR.

Table 5.2 Details of primers used for identification of attachment sites and spontaneous induction.

Primers name	Designation	Sequence (5'—3´)	Length
ϕPM982.1/F1	#678	TGTACCACATCCTCTGCC	18
ϕPM982.1/R1	#679	CTGACTTTGCCTGAACCA	18
ϕPM982.1/F2	#680	CCCACGCATTAGCTTCTG	18
ϕPM982.1/R2	#681	GGTTCTGTTGGGTCAGGT	18

5.2.5.3 Completion of phage genome sequences

Sets of forward and reverse primers were designed to amplify the gaps between the phage sequences contigs in order to close the bacteriophage genomes in certain isolates. In PM850, ϕPM850.3 was induced and the phage genome was located in contigs C3 and C6. BLAST analysis of each contig against the whole bacterial genome using CLC genomics workbench showed that the phage genome was located in contigs C2 and C12. To close the gaps and determine the size of the DNA fragment between C2 and C12 (C3 and C6 in the phage genome), primer pair F2/R2 was designed from C2 and C12 (Fig. 5.2). To identify the integration sites, BLASTn analysis of the integrase gene along with the NCBI database was used to identify an identical integrase gene (100%) in *P. multocida* strain HN06. The flaking genes were identified in the PM850 genome using internal BLASTn analysis (CLC genomics workbench). Primer pairs F1/R1 and F3/R3 were designed to close the gaps between the phage genome and flanking genes. Primer pair F2/R2 was designed to close the gaps within the phage genome. Primer pair F1/R3 was used to examine whether the ϕPM850.1 phage has been spontaneously induced (Fig. 5.2). A similar, although more complex, strategy was used for to close the gaps in ϕPM848.2 so as to obtain the single complete genome of ϕPM848.2. Different sets of primers were used for ϕPM848.2 (Fig. 5.3). Details of the nucleotide sequences of the primers are provided in Table 5.3.

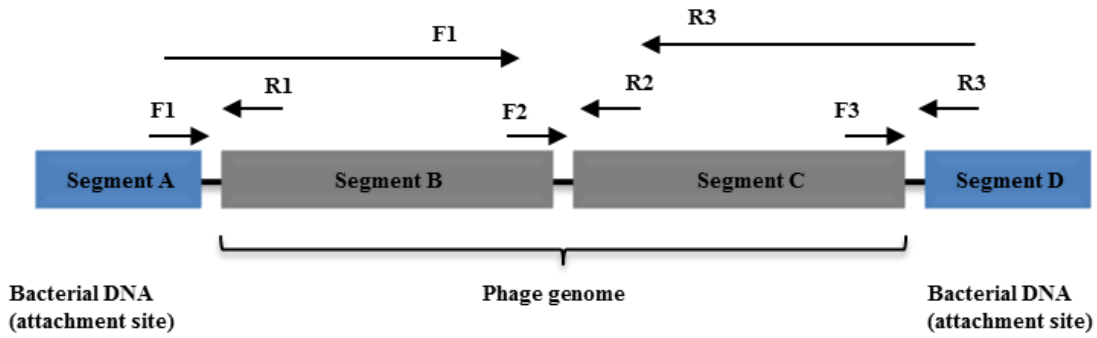

Fig. 5.2 Details of primers used to complete the phage genome sequence of ϕPM850.3.

Primer pairs (F1/R1 and F3/R3) were used to identify integration sites; primer pair F1/R3 was used to check whether ϕPM850.3 induced spontaneously in isolate PM850. Phage genome is shown in grey boxes (segment B and C); bacterial genomic DNA is shown in blue boxes (segments A and D). Small arrows indicate the positions of primers used for PCR. Primer pair F2/R2 was designed to close the gaps within the phage genome.

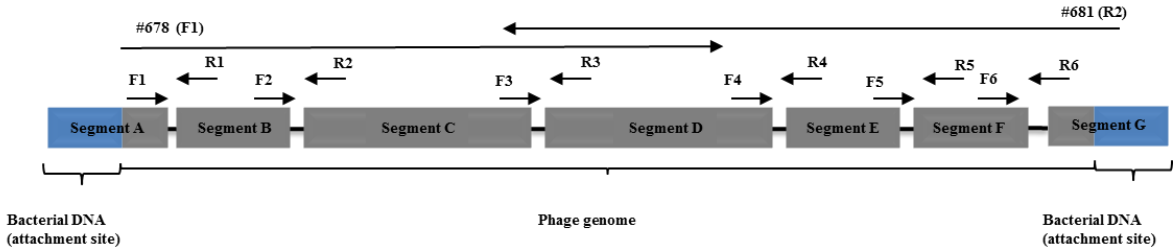

Fig. 5.3 Details of primers used to complete the phage genome sequence of ϕPM848.2.

Primer pairs (F1/R1 and F3/R3) were used to identify attachment sites; primer pair ≠678 (F1)/≠681 (R2) (**Table 5.2)** was used to check whether ϕPM848.2 induced spontaneously in isolate PM848. Phage genome is shown in grey boxes; bacterial genomic DNA is shown in blue boxes (segments A and G). Small arrows indicate the positions of primers used for PCR.

Table 5.3 Details of oligonucleotide primers used to complete the phage genome sequences of ϕPM850.3 and ϕPM848.2.

Primer's name	Designation	Sequence (5'–3´)	Length
ϕPM850.3/F1	#682	CCCATCGCTTTCAGTTGT	18
ϕPM850.3/R1	#683	CAACGATAGCATAGGAGG	18
ϕPM850.3/F2	#684	CTCAAGTGCCTTGCAAAG	18
ϕPM850.3/R2	#685	CGGTGGTATCGTAGGTTC	18
ϕPM850.3/F3	#686	ATCCCGTCGATCGATATG	18
ϕPM850.3/R3	#687	GGCAGCTCAAAACCAGTG	18
ϕPM848.2/F1	#698	CACGAGAGATCGTTTCCATC	20
ϕPM848.2/R1	#699	GGGGAGGATGTCAATATGAG	20
ϕPM848.2/F2	#700	GCTGATACTGGATGACAACC	20
ϕPM848.2/R2	#701	AACGGAACCCATAGCAACTC	20
ϕPM848.2/F3	#702	GTTCCGTTGGTCGACAACTG	20
ϕPM848.2/R3	#703	GTCACAATCCTTGCTGCTGC	20
ϕPM848.2/F4	#704	CACGCGCTGAACAAATCAAG	20
ϕPM848.2/R4	#705	GCGCTGTGATTGTGCTATTC	20
ϕPM848.2/F5	#706	GACCGTGATGGTGACAGAAC	20
ϕPM848.2/R5	#707	GAACTGGGAGATAGACTGCC	20
ϕPM848.2/F6	#708	CAATGATCGAGAGTGCGAGG	20
ϕPM848.2/R6	#709	AGGCTTCTTGTACCACATCC	20

5.2.6 PCR reactions

PCR reactions were conducted using one of the Taq DNA polymerase kits (Platinum *Pfx* DNA *Taq* polymerase, Invitrogen or Go Taq G2 DNA polymerase, Promega). PCR reactions were performed in 0.2 ml PCR tubes (Star lab) according to the manufacturer's instructions with a total reaction volume of 50 µl. Each reaction comprised the following reagents: 29.5 µl dH_2O, 1.5 µl 50 mM $MgSO_4$, 5 µl 10x PCR buffer, 4 µl 1.25 mM dNTPs, 4 µl of each forward and reverse primer (12.5 pmol), 2 µl of template DNA and 0.2 µl of Platinum *Pfx* DAN *Taq* polymerase. For Go Taq G2 DNA polymerase, the reactions consisted of 23 µl dH_2O, 3 µl 25 mM $MgCl_2$, 10 µl 10x PCR buffer, 4 µl 1.25 mM dNTPs, 4 µl of each forward and reverse primer (12.5 pmol), 2 µl of template DNA and 0.2 µl of Go Taq G2 DNA polymerase. PCR amplification was carried out in Veriti 96 Well Thermo Cycler (Applied Biosystems). The following PCR parameters of 30 reaction cycles were used for PCR amplification: initial denaturation at 94°C for 2 min, denaturation at 94°C for 45 s, annealing at 59°C for 45 s, extension at 72°C for 2 min and a final extension step at 72°C for 10 min. However, certain PCR reactions were carried out with annealing temperatures between 55°C and 61°C. The PCR products were stored at -20°C. Amplification of PCR products was confirmed by electrophoresis in a 1% (w/v) agarose gel prepared with 1× TAE buffer.

5.2.7 Purification of PCR product

For Southern blot hybridisation and Sanger sequencing, the PCR products were purified using a Qiagen QIAquick DNA purification kit (Qiagen) according to the manufacturer's instructions as described previously in Chapter 3 (Materials and methods, section 3.4.3.1). The purity and concentration of DNA were examined using a NanoDrop 2000C spectrophotometer (Thermo Scientific). Purification of DNA was also verified by electrophoresis as described above.

5.2.8 Southern blot hybridisation

For Southern blot hybridisation, bacterial DNA was purified as described in section 5.2.2. Phage DNA was separated by agarose gel electrophoresis and DNA was transferred to nylon membranes (0.45 mm Hybond-N pore diameter; Amersham Life Science) using standard methods (Ausubel *et al.*, 1990; Sambrook

et al., 1989). Two labelled probes were prepared from chromosomal DNA obtained from isolate PM86 using labelled dNTPs and the primers shown in Table 5.1. Hybridisation was carried out according to the protocol provided by the DNA Labelling Kit and PCR DIG-chemiluminescence detection (Roche).

5.2.9 Sanger sequencing

Conventional Sanger sequencing was used to close the gaps between the various contigs and to determine the full size of the phage genomes. Purified PCR products were sequenced with the BigDye Terminator Cycle Sequencing kit V3.1. (Applied Biosystems) as described previously in Chapter 3 (Materials and methods, section 3.4.3.3). The sequencing reaction were analysed with SeqMan, EditSeq and MegAlign module of Lasergene (DNAstar, Inc.) as described in Chapter 3 (Materials and methods, section 3.4.4).

5.2.10 Whole phage genome sequence analysis

The ORFs of each phage genome were identified using CLC genomics workbench. The phage genomes were annotated automatically using RAST. An internal BLAST database was created using the CLC genomics workbench. The genome visualisation program SnapGene (http://www.snapgene.com/) was used to generate the maps of each phage and to visualise the ORFs of sequenced phages. Whole genome sequence alignments were conducted with progressive Mauve alignment (Darling *et al.*, 2004). Easyfig was also used to construct genomic maps and to determine the level of both nucleotide and amino acid identify using sequence BLAST comparisons (Sullivan *et al.*, 2011). BLAST algorithms were used for the similarity searches in the NCBI database (http://www.ncbi.nlm.nih.gov). Phylogenetic trees were constructed with Geneious Tree Builder (Neighbor-Joining method) using the Jukes-Cantor model in Geneious v9.1.40 (http://www.geneious.com, Kearse *et al.*, 2012). Pairwise nucleotide sequence alignment identity was calculated by EMBOSS Stretcher analysis (http://www.ebi.ac.uk/Tools/psa/) and ClustalW alignment in Geneious.

5.3 Results

5.3.1 Phage genomic results

Phage DNA was isolated from 18 induced strains as described previously in Chapter 4 (Results, section 4.5.5). Details relating to the phage genomes are shown in Table 5.4. The sequencing results revealed that Mu-like (*Myoviridae*) phages λ-like (*Siphoviridae*) phages and phages of short sequences were induced in the 18 *P. multocida* isolates. The TEM results showed that three isolates (PM86, PM850 and PM684) contained functional phages of both *Myoviridae* and *Siphoviridae* phage types. However, apart from these three isolates PM86, PM850, and PM684 sequencing of the phage DNA confirmed that isolates PM918, PM926 and PM40 also possessed functional phages belonging to the *Myoviridae* and *Siphoviridae* phage types (Table 5.4) Furthermore, isolates PM86, PM934, PM954, PM486 and PM172 contained functional phages of *Myoviridae* and small phage type (PICIs) (Table 5.4).

In addition to the induction of phages belonging to different families, the genomic results also showed the some isolates (PM850, PM684, PM40 and PM848) contained more than one functional phage belonging to the same family type (Table 5.4). The Mu-like phage types were obtained from single fragment of purified genomic phage DNA. However, a few λ-like phages were found to be distributed between different contigs, these phages were ϕPM850.3, ϕPM684.3 and ϕPM848.2. In these cases, single complete genomes were obtained by targeted PCR as described in section 5.3.1.4. The ORFs of each phage were identified manually using CLC genomics workbench and the Genbank file for each phage was obtained and annotated automatically using RAST. Annotation of the sequenced phages resulted in five different Mu-like, one short phage type (PICI) and seven λ-like phages. Assembly of sequenced phage genomes was confirmed by comparing with the genome sequences of *P. multocida* isolates.

5.3.1.1 Mu-like phages

Mu-like phages were induced in isolates PM382, PM86, PM934, PM954, PM486, PM172, PM850, PM684, PM918, PM92 and PM40 (Table 5.4). The genomes were annotated and assembled and the %GC content ranged from 39.5 to 41.7%. These phages were between 32,417 and 37,392 bp in length and encoded 44 to51 CDCs

(Table 5.4). Phylogenetic tree of the whole phage genomes identified five different Mu-like phages; PMMu1, PMMu2, PMMu3, PMMu4 and PMMu5 (Fig. 5.4). PMMu1 includes ϕPM86.1, ϕPM934.1, ϕPM945.1, ϕPM486.1 and ϕPM172.1; PMMu2 includes ϕPM684.1, ϕPM918.1, ϕPM926.1 and ϕPM40.1; PMMu3 and PMMu4 include ϕPM850.2 and ϕPM850.1, respectively; PMMu5 includes only ϕPM382.1. The analysis also revealed that isolates within the same, or closely related, lineages as determined by MLST (Fig. 2.1) had similar Mu-like phages (Fig. 5.4). With the exception of PMMu1, the Mu-like phages were all associated with porcine isolates. Nucleotide sequence analysis revealed that the Mu-like phage genome sequences revealed that the phages were highly homogeneous, except for ϕPM850.1 (PMMu4) and ϕPM382.1 (PMMu5) (Fig. 5.5).

Pairwise sequence similarity showed that the PMMu1, PMMu2, PMMu3 phages were the most genomically similar. PMMu1 has a pairwise sequence identity of 81.9% and 81.7% to PMMu2 and PMMu3, respectively; PMMu2 has 85.5% similarity to PMMu3. Pairwise nucleotide sequence similarity showed that PMMu4 and PMMu5 phages were significantly different from the PMMu1, PMMu2, PMMu3 phages and they had low sequence identity of 47 to 48%. Phage PMMu5 had low pairwise sequence similarities of 57.2, 59.9 and 58.7% to phages PMMu1, PMMu2 and PMMu3, respectively. The similarities were highest in common Mu-like genes particularly those involve in regulation, transposition and head and tail morphogenesis. The terminase-large unit gene shared no similarity among the five Mu-like phages. The genome PMMu4 diverged from the other PMMu-like phages and BLASTn analysis of the whole genomes showed no similarities (Fig. 5.5).

Table 5.4 Genomic characteristics of the temperate phages induced in *P. multocida*.

Isolate [a]	ST	MLST group [b]	Host species	Capsular type	OMP-type [c]	Type of lysis	Family type identified by TEM	No. of phages induced	Phage designation	Phage-type	Phage family	Size (bp)	GC content (%)	CDCs
PM382	13	C	Porcine	A	4.1	Complete	*Myoviridae*	1	ϕPM382.1	Mu-like	*Myoviridae*	34,026	41.70	51
PM86	15	D	Avian	A	3.1	Partial	*Myoviridae* & *Siphoviridae*	3	ϕPM86.1	Mu-like	*Myoviridae*	33,388	39.5	48
									ϕPM86.2	PICI		7,830	38.7	9
									ϕPM86.3	λ-like	*Siphoviridae*	56,050	38.5	92
PM934	15	D	Porcine	A	5.1	Partial	*Myoviridae*	2	ϕPM934.1	Mu-like	*Myoviridae*	33,388	39.5	48
									ϕPM934.2	PICI		7,830	38.7	9
PM954	15	D	Porcine	A	5.1	Partial	*Myoviridae*	2	ϕPM954.1	Mu-like	*Myoviridae*	33,388	39.5	48
									ϕPM954.2	PICI		7,830	38.7	9
PM486	9	D	Bovine	A	9.1	Partial	*Myoviridae*	2	ϕPM486.1	Mu-like	*Myoviridae*	33,388	39.5	48
									ϕPM486.2	PICI		7,830	38.7	9
PM172	26	D	Avian	A	3.1	Partial	*Myoviridae*	2	ϕPM172.1	Mu-like	*Myoviridae*	33,388	39.5	48
									ϕPM172.2	PICI		7,830	38.7	9
PM122	ND	E	Ovine	D	3.1	Complete	*Siphoviridae*	1	ϕPM122.1	λ-like	*Siphoviridae*	45,131	37.90	67
PM964	18	E	Ovine	D	3.1	Complete	*Siphoviridae*	1	ϕPM964.1	λ-like	*Siphoviridae*	45,131	37.90	67
PM982	18	E	Ovine	D	3.1	Complete	*Siphoviridae*	1	ϕPM982.1	λ-like	*Siphoviridae*	45,131	37.90	67
PM986	18	E	Ovine	D	3.1	Complete	*Siphoviridae*	1	ϕPM986.1	λ-like	*Siphoviridae*	45,131	37.90	67
PM988	ND	ND [d]	Ovine	D	3.1	Complete	*Siphoviridae*	1	ϕPM988.1	λ-like	*Siphoviridae*	45,131	37.90	67
PM850	10	F	Porcine	A	1.1	Complete	*Myoviridae* & *Siphoviridae*	3	ϕPM850.1	Mu-like	*Myoviridae*	37,392	41	51
									ϕPM850.2	Mu-like	*Myoviridae*	32,417	39.8	44
									ϕPM850.3	λ-like	*Siphoviridae*	48,455	38.0	69
PM336	7	F	Bovine	A	6.1	Complete	*Siphoviridae*	1	ϕPM336.1	λ-like	*Siphoviridae*	49,821	38.20	73
PM684	11	G	Porcine	A	6.1	Complete	*Myoviridae* & *Siphoviridae*	3	ϕPM684.1	Mu-like	*Myoviridae*	33,288	39.5	40
									ϕPM684.2	λ-like	*Siphoviridae*	42,490	38.8	65
									ϕPM684.3	λ-like	*Siphoviridae*	54,876	36.7	71
PM918	11	G	Porcine	A	6.1	Complete	*Siphoviridae*	2	ϕPM918.1	Mu-like	*Myoviridae*	33,288	39.5	40
									ϕPM918.3	λ-like	*Siphoviridae*	42,490	38.8	65
PM926	ND	ND	Porcine	A	6.1	Complete	*Siphoviridae*	2	ϕPM926.1	Mu-like	*Myoviridae*	33,288	39.5	40
									ϕPM926.2	λ-like	*Siphoviridae*	42,490	38.8	65

Table 5.4 (continued)

Isolate [a]	ST	MLST group [b]	Host species	Capsular type	OMP-type [c]	Type of lysis	Family type identified by TEM	No. of phages induced	Phage designation	Phage-type	Phage family	Size (bp)	GC content (%)	CDCs
PM40	ND	ND	Porcine	A	6.2	Complete	*Myoviridae*	3	ϕPM40.1	Mu-like	*Myoviridae*	33,288	39.5	40
									ϕPM40.2	λ-like	*Siphoviridae*	42,490	38.8	65
									ϕPM40.3	λ-like	*Siphoviridae*	43,385	38.6	68
PM848	11	G	Porcine	D	4.1	Complete	*Siphoviridae*	2	ϕPM848.1	λ-like	*Siphoviridae*	42,490	38.8	65
									ϕPM848.2	λ-like	*Siphoviridae*	54,876	36.7	71

[a] isolates are arranged by order of MLST group (column 3) (Fig. 2.1); [b] ST= sequence type (Davies *et al*., unpublished http://pubmlst.org/pmultocida_multihost/); [c] OMP-types for bovine, ovine, porcine and avian are not equivalent, i.e. bovine OMP-type 1.1 is not as same as porcine OMP-type 1.1, etc. (Davies *et al.*, 2003a; b; c; Davies, 2004; Davies *et al.*, 2004); [d] ND: not determined.

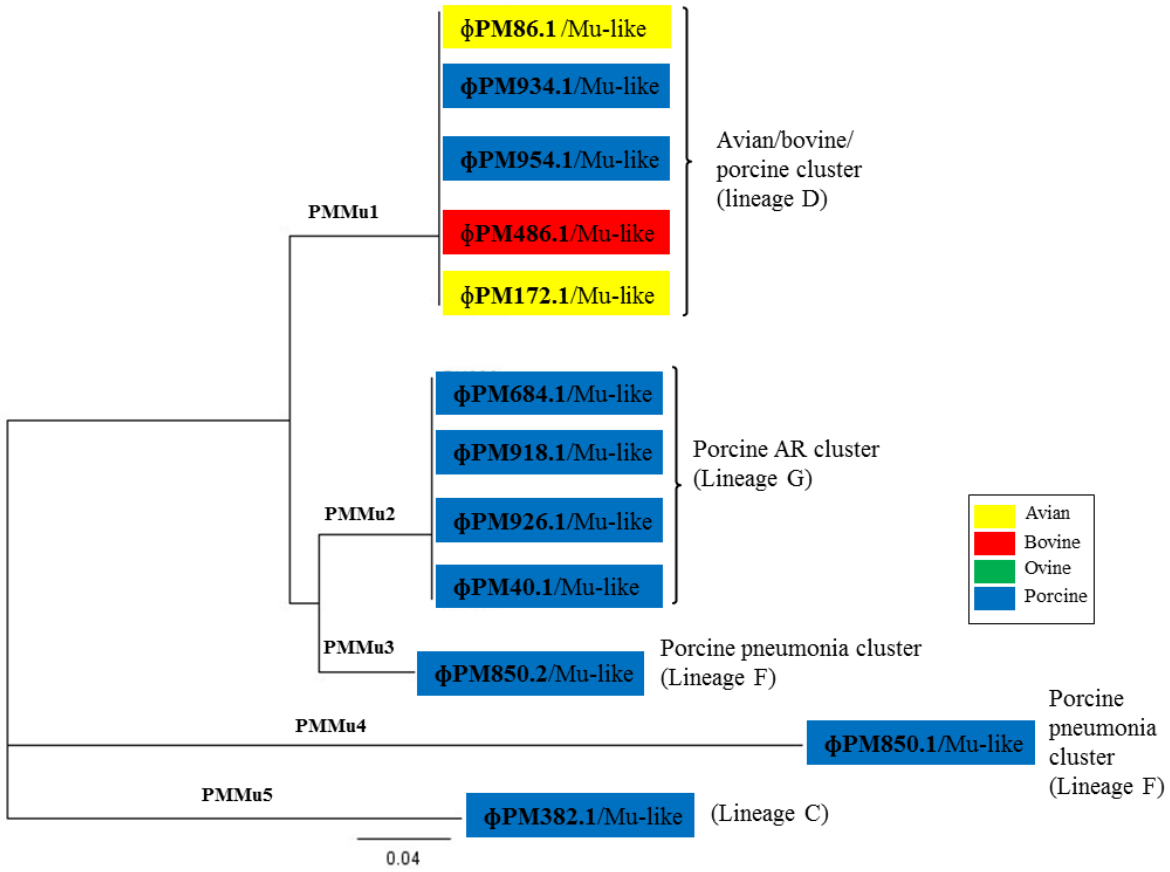

Fig. 5.4 Neighbour-Joining tree representing the phylogenetic relationships of Mu-like phages induced in *P. multocida* isolates.

The results showed the presence of five different Mu-like phages which were associated with distinct genetic lineage. However, PMMu1 and PMMu2 phages were each associated with closely-related *P. multocida* isolates (representing lineages D and G, respectively-see Fig. 2.1). The phylogenetic tree was constructed with Jukes-Cantor correction using Geneious (v. 9.1.4). Each phage is abbreviated with the phage designation followed by the phage type.

Nucleotide and amino acid comparison using either Mauve or BLAST algorithms in Easyfig showed that isolates PM86, PM934, PM954, PM486 and PM172 possessed identical Mu-like phages (PMMu1 phage). Notably, these isolates are of the same genetic lineage (MLST group D, Fig 2.1). These phages were designated as ϕPM86.1, ϕPM934.1, ϕPM954.1, ϕPM486.1 and ϕPM172.1, respectively. Their genomes have a GC content of 39.5% and were 33,388 bp in length, encoding 48 CDCs. Isolates PM684, PM918, PM926 and PM40 are associated with porcine atrophic rhinitis (capsular type A, OMP-types 6.1.and 6.2 of ST 11) and also had identical Mu-like phages (PMMu2 phage). These phages were designated as ϕPM684.1, ϕPM918.1, ϕPM926.1 and ϕPM40.1, respectively (Fig. 5.6). Their genomes have a GC content of 39.5% and were of 33,288 bp in length; encoding 46 CDCs. The four genomes shared 100% identical nucleotide and amino acid sequences (Fig. 5.6). Two different Mu-like phage, PMMu3 (ϕPM850.2) and PMMu4 (ϕPM850.1) were induced in isolate PM850. PMMu3 and PMMu4 have GC content of 41 and 39.8% and were 37,392 and 32,417 bp in length, and encoded 51 and 44 CDCs, respectively.

Genome comparison showed that PMMu3 and PMMu4 were very different from each other (Fig. 5.4 & Fig. 5.5). The genomic maps of PMMu3 and PMMu4 are shown in (Fig. 5.7). Phage PMMu5 includes only ϕPM382.1 and was only induced in PM382. This phage was different from the Mu-like phages induced in the other strains. PMMu5 had a GC content of 41.7%, was 34,026 bp in length and encoded 51 CDCs (Fig. 5.7). The presence of Mu-like phages was also indicated by BLASTp of phage proteins. BLASTp analysis revealed homologies of known features of Mu bacteriophage such as SuMu, SfMu, BcepMu and PaeS_PM105. Based on the similarities, possible functions were assigned to 24 to 26 ORFs and the remaining ORFs were associated with proteins of unknown functions. BLASTp analysis of the *P. multocida* Mu-like phages (PMMu1 to PMMu5) showed that these phages contained genes encoding transcriptional regulator (*c* and *ner*), phage transposases which are involved in integration and transposition, host-nuclease inhibitor Gam protein, transcriptional regulator of Mor, DNA packaging, capsid and tail morphogenesis (Table 5.5, Table 5.6 & Supplementary Tables 8.1 to 8.3).

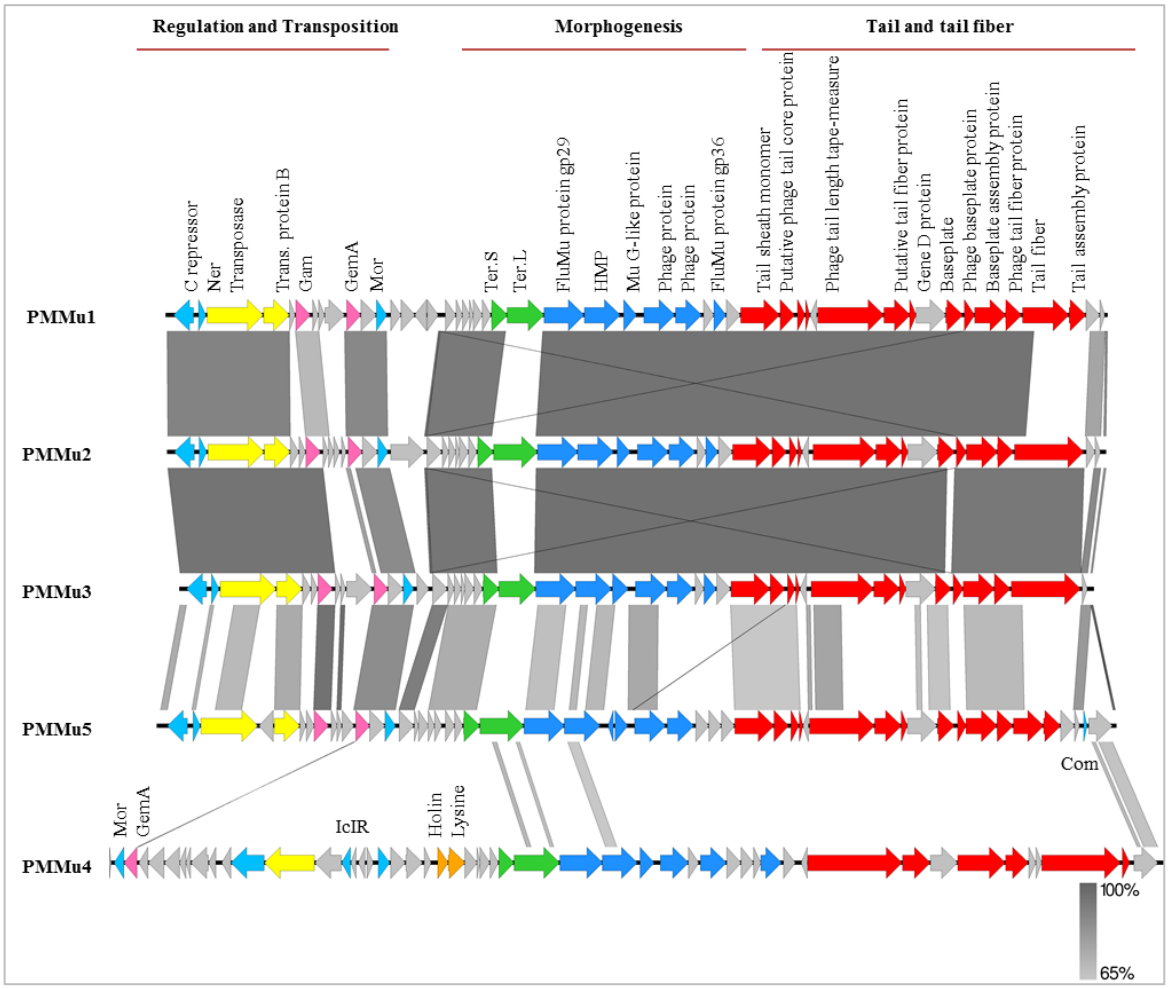

Fig. 5.5 Whole genome sequence comparisons of the five Mu-like phage types (PMMu1 to PMMu5) induced in *P. multocida* strains.

The sequence alignments were carried out using the BLASTn algorithm in Easyfig. The degree of sequence similarity is indicated by the intensity of the grey shading (darker grey indicates the highest sequence similarity). The position of genes within each genome is indicated by arrows.

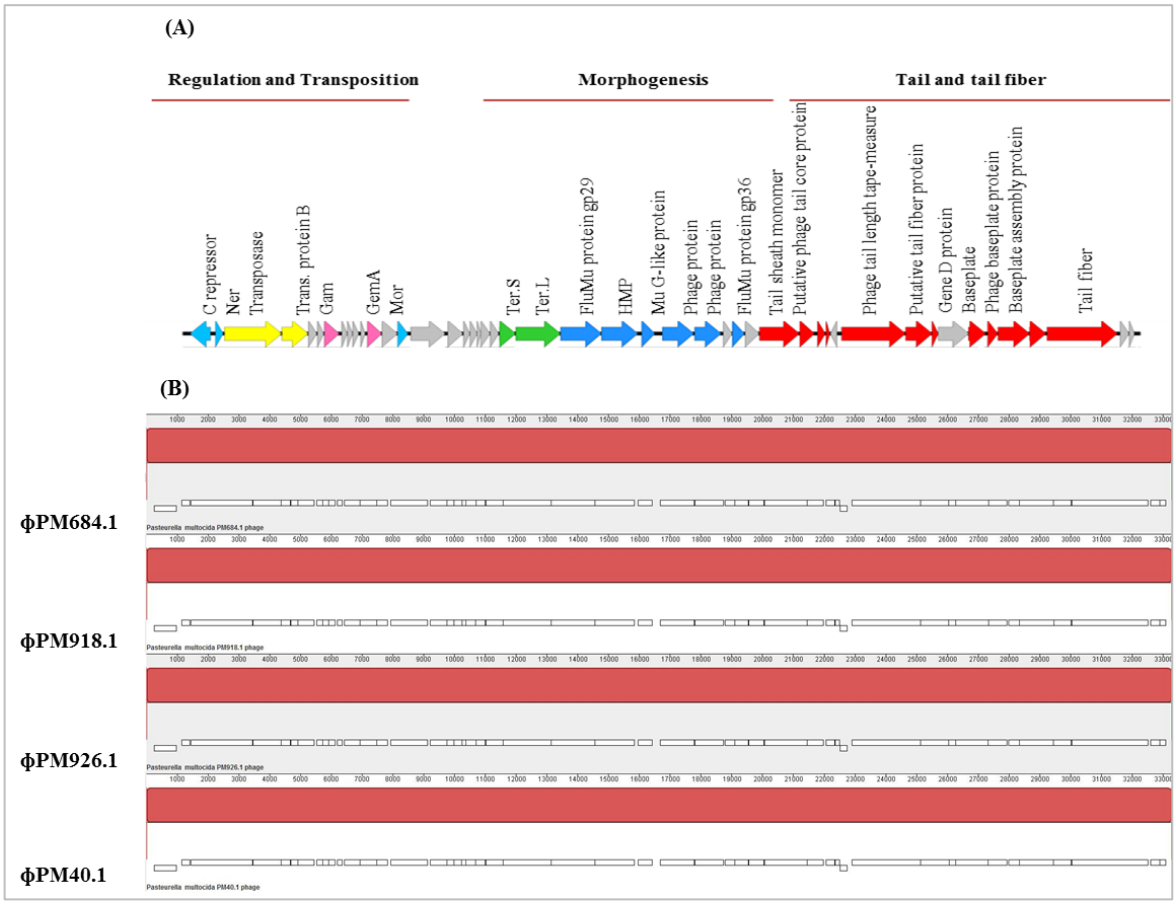

Fig. 5.6 Genomic structure (A) and nucleotide sequence comparison (B) of *P. multocida* PMMu2 phages.

The genomic map was created using Easyfig. The four genomes were aligned using a progressive MAUVE alignment.

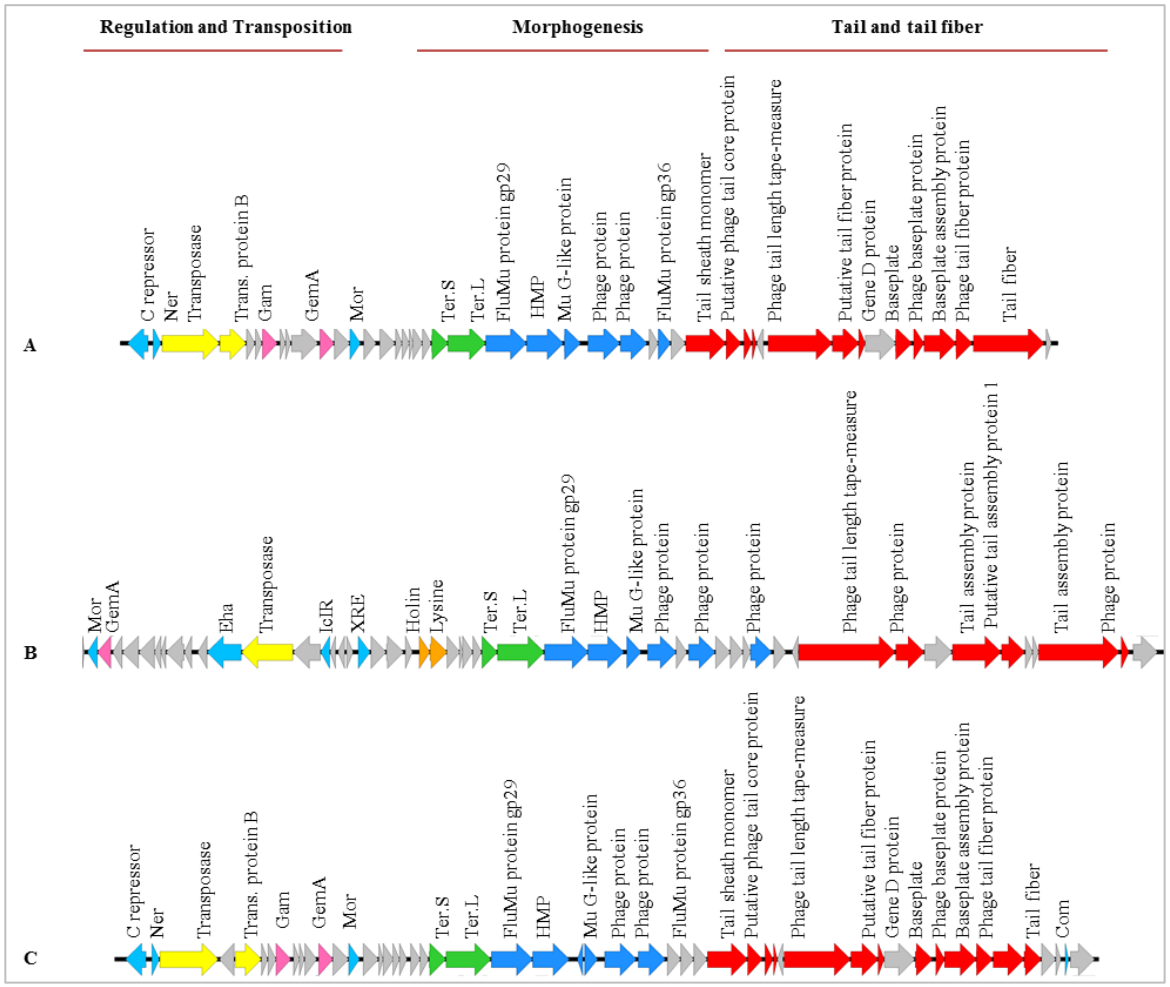

Fig. 5.7 Genomic structure (A) PMMu3 (B) PMMu4 and (C) PMMu5.

The genomic maps were generated using Easyfig.

Table 5.5 PHAST analysis of PMMu1 against phage genome database.

Orfs	Protein product	Size (bp/aa)	BLAST_hit	E-value
Orf1	Prophage MuSo2, transcriptional regulator, Cro/CI family	708/235	PHAGE_Haemop_SuMu: transcription regulator	2e-54
Orf2	DNA-binding protein	267/89	PHAGE_Haemop_SuMu: Mu-like prophage FluMu DNA-binding protein Ner	6e-21
Orf3	Transposase	1989/662	PHAGE_Vibrio_12B12: transposase	1e-161
Orf4	DNA transposition protein #protein B	918/306	PHAGE_Haemop_SuMu: phage transposase	4e-28
Orf5	Hypothetical protein	204/67	Hypothetical protein	0.0
Orf6	DNA recombination nuclease inhibitor Gam (ACLAME 731)	519/172	PHAGE_Entero_SfMu: host nuclease inhibitor protein	3e-55
Orf7	Hypothetical protein	192/63	PHAGE_Haemop_SuMu: hypothetical protein	2e-06
Orf8	Hypothetical protein	216/71	Hypothetical protein	0.0
Orf9	Hypothetical protein	702/233	PHAGE_Pseudo_B3: hypothetical protein	9e-22
Orf10	Mu-like prophage protein gp16	507/168	PHAGE_Burkho_BcepMu: gp02	1e-13
Orf11	Hypothetical protein	546/181	PHAGE_Mannhe_vB_MhM_3927AP2: hypothetical protein	7e-42
Orf12	Probable bacteriophage transcriptional regulator	375/125	PHAGE_Burkho_BcepMu: gp01	2e-25
Orf13	Transcriptional regulator, Xre family	366/121	Transcriptional regulator, Xre family	0.0
Orf14	Hypothetical protein	495/164	Hypothetical protein	0.0
Orf15	Hypothetical protein	426/141	Hypothetical protein	0.0
Orf16	Hypothetical protein	390/130	Hypothetical protein	0.0
Orf17	Negative regulator of beta-lactamase expression	372/123	PHAGE_Haemop_SuMu: putative N-acetylmuramoyl-L-alanine amidase	6e-55
Orf18	Hypothetical protein	228/75	PHAGE_Haemop_SuMu: hypothetical protein	2e-22
Orf19	Hypothetical protein	261/86	Hypothetical protein	0.0
Orf20	Hypothetical protein	132/43	PHAGE_Haemop_SuMu: hypothetical protein	9e-06
Orf21	Mu-like phage gp25	330/109	PHAGE_Entero_SfMu: hypothetical protein	8e-07
Orf22	Phage protein	303/101	PHAGE_Entero_SfMu: hypothetical protein	4e-27
Orf23	Phage terminase, small subunit	573/190	PHAGE_Vibrio_12B12: hypothetical protein	6e-39
Orf24	Phage terminase, large subunit	1308/435	PHAGE_Burkho_BcepMu: gp28	2e-28
Orf25	Mu-like prophage FluMu protein gp29	1422/474	PHAGE_Burkho_BcepMu: gp29	8e-116

Table 5.5 (continued)

Orfs	Protein product	Size (bp/aa)	BLAST_hit	E-value
Orf26	Phage (Mu-like) virion morphogenesis protein	1272/424	PHAGE_Pseudo_vB_PaeS_PM105putative head morphogenesis protein	7e-41
Orf27	possible bacteriophage Mu G-like protein	465/154	PHAGE_Rhizob_RR1_B: virion morphogenesis protein	4e-18
Orf28	Phage protein	1104/367	PHAGE_Burkho_BcepMu: gp32	7e-84
Orf29	Phage protein	927/308	PHAGE_Burkho_BcepMu: gp34	2e-74
Orf30	Hypothetical protein	369/122	PHAGE_Saimir_herpesvirus_2: unnamed protein product	1e-09
Orf31	Hypothetical protein	435/145	PHAGE_Burkho_BcepMu: gp36	4e-21
Orf32	Hypothetical protein	498/165	PHAGE_Burkho_BcepMu: gp37	1e-21
Orf33	Phage tail sheath monomer	1386/461	PHAGE_Burkho_BcepMu: gp39	4e-99
Orf34	Putative phage tail core protein	519/173	PHAGE_Burkho_BcepMu: gp40	1e-38
Orf35	Hypothetical protein	276/91	PHAGE_Burkho_BcepMu: gp41	3e-07
Orf36	Hypothetical protein	141/47	hypothetical protein	0.0
Orf37	Hypothetical protein	234/78	Hypothetical protein	0.0
Orf38	Phage tail length tape-measure protein	2349/782	PHAGE_Burkho_BcepMu: gp44	1e-62
Orf39	Putative methyl-accepting chemotaxis protein	933/311	PHAGE_Burkho_BcepMu: gp45	1e-22
Orf40	putative bacteriophage tail fibre protein	219/72	PHAGE_Burkho_BcepMu: gp46	3e-14
Orf41	Gene D protein	1065/354	PHAGE_Burkho_BcepMu: gp47	6e-69
Orf42	Baseplate	609/203	PHAGE_Burkho_BcepMu: gp48	2e-22
Orf43	Phage baseplate protein	366/122	PHAGE_Burkho_BcepMu: gp49	5e-15
Orf44	Phage-related baseplate assembly protein	1107/368	PHAGE_Burkho_BcepMu: gp50	2e-62
Orf45	Phage tail fibre protein	570/190	PHAGE_Burkho_BcepMu: gp51	5e-40
Orf46	Putative tail fibre	1641/546	PHAGE_Haemop_HP2: tail fibres	6e-77
Orf47	Phage tail assembly protein	597/199	PHAGE_Haemop_HP2: tail collar	5e-63
Orf48	Putative cytoplasmic protein	495/164	PHAGE_Haemop_SuMu: enoyl-CoA hydratase/carnithine racemase-like protein	7e-55

Table 5.6 PHAST analysis of PMMu2 against phage genome database.

Orfs	Protein product	Size (bp/aa)	BLAST_hit	E-value
Orf1	Transcriptional regulatory protein	711/237	PHAGE_Haemop_SuMu: Transcription regulator	2e-53
Orf2	DNA-binding protein	267/88	PHAGE_Haemop_SuMu: Mu-like prophage FluMu DNA-binding protein Ner	6e-21
Orf3	Transposase	1989/663	PHAGE_Entero_SfMu: Transposase	9e-161
Orf4	DNA transposition protein B	918/305	PHAGE_Haemop_SuMu: Phage transposase	4e-28
Orf5	Hypothetical protein	297/99	PHAGE_Haemop_SuMu: hypothetical protein	1e-06
Orf6	Hypothetical protein	228/75	Hypothetical protein	0.0
Orf7	DNA recombination nuclease inhibitor Gam	522/174	PHAGE_Haemop_SuMu: Host-nuclease inhibitor protein	5e-49
Orf8	Hypothetical protein	195/64	PHAGE_Haemop_SuMu: hypothetical protein	2e-07
Orf9	Hypothetical protein	186/62	Hypothetical protein	0.0
Orf10	Hypothetical protein	210/69	Hypothetical protein	0.0
Orf11	Hypothetical protein	159/52	Hypothetical protein	0.0
Orf12	Mu-like prophage protein gp16	507/168	PHAGE_Burkho_BcepMu: gp02	2e-14
Orf13	Hypothetical protein	546/181	PHAGE_Mannhe_vB_MhM_3927AP2: hypothetical protein	9e-39
Orf14	Probable bacteriophage transcriptional regulator	363/121	PHAGE_Burkho_BcepMu: gp01	1e-26
Orf15	Hypothetical protein	1197/399	Hypothetical protein	0.0
Orf16	Negative regulator of beta-lactamase expression	537/178	PHAGE_Haemop_SuMu: putative N-acetylmuramoyl-L-alanine amidase	2e-74
Orf17	Hypothetical protein	228/76	PHAGE_Haemop_SuMu: hypothetical protein	3e-22
Orf18	Hypothetical protein	261/86	Hypothetical protein	0.0
Orf19	Hypothetical protein	132/44	PHAGE_Haemop_SuMu: hypothetical protein	4e-06
Orf20	Mu-like phage gp25	330/109	PHAGE_Entero_SfMu: hypothetical protein	8e-07
Orf21	Phage protein	303/100	PHAGE_Entero_SfMu: hypothetical protein	4e-27
Orf22	Phage terminase, small subunit	567/188	PHAGE_Vibrio_12B12: hypothetical protein	4e-41
Orf23	Phage terminase, large subunit	1554/517	PHAGE_Burkho_BcepMu: gp28	5e-146
Orf24	Mu-like prophage FluMu protein gp29	1431/476	PHAGE_Burkho_BcepMu: gp29	2e-114
Orf25	Phage (Mu-like) virion morphogenesis protein	1272/424	PHAGE_Pseudo_vB_PaeS_PM105: Putative head morphogenesis protein	2e-41

Table 5.6 (continued)

Orfs	Protein product	Size (bp/aa)	BLAST_hit	E-value
Orf26	Possible bacteriophage Mu G-like protein	564/187	PHAGE_Rhizob_RR1_B: virion morphogenesis protein	4e-18
Orf27	Phage protein	1104/368	PHAGE_Burkho_BcepMu: gp32	7e-82
Orf28	Phage protein	927/309	PHAGE_Burkho_BcepMu: gp34	3e-76
Orf29	Hypothetical protein	318/105	PHAGE_Parame_bursaria_Chlorella_virus_1: hypothetical protein	3e-07
Orf30	Mu-like prophage FluMu protein gp36	435/144	PHAGE_Burkho_BcepMu: gp36	1e-20
Orf31	Hypothetical protein	498/166	PHAGE_Burkho_BcepMu: gp37	1e-22
Orf32	Phage tail sheath monomer	1386/462	PHAGE_Burkho_BcepMu: gp39	8e-97
Orf33	Putative phage tail core protein	519/172	PHAGE_Burkho_BcepMu: gp40	1e-38
Orf34	Hypothetical protein	276/91	PHAGE_Burkho_BcepMu: gp41	3e-07
Orf35	Hypothetical protein	135/44	Hypothetical protein	0.0
Orf36	Hypothetical protein	234/77	Hypothetical protein	0.0
Orf37	Phage tail length tape-measure protein	2223/740	PHAGE_Burkho_BcepMu: gp44	4e-61
Orf38	Putative methyl-accepting chemotaxis protein	933/310	PHAGE_Burkho_BcepMu: gp45	1e-22
Orf39	Putative bacteriophage tail fibre protein	231/76	PHAGE_Burkho_BcepMu: gp46	5e-14
Orf40	Gene D protein	1065/355	PHAGE_Burkho_BcepMu: gp47	2e-68
Orf41	Baseplate	609/202	PHAGE_Burkho_BcepMu: gp48	8e-23
Orf42	BASEPLATE	366/121	PHAGE_Burkho_BcepMu: gp49	1e-14
Orf43	Phage-related baseplate assembly protein	1107/369	PHAGE_Burkho_BcepMu: gp50	1e-63
Orf44	Phage tail fibre protein	570/189	PHAGE_Burkho_BcepMu: gp51	1e-40
Orf45	Phage protein	2457/818	PHAGE_Mannhe_vB_MhM_3927AP2: defective tail fibre protein	1e-32
Orf46	Putative cytoplasmic protein	312/103	PHAGE_Haemop_SuMu: enoyl-CoA hydratase/carnithine racemase-like protein	8e-37

5.3.1.2 Sequencing of the small phage type

DNA analysis identified the presence of two bands of two different molecular sizes in isolates PM86, PM934, PM954, PM486 and PM172 as previously described in Chapter 4 (Fig. 4.14). This observation suggested the presence of two phage types. Furthermore, distinct *Myoviridae*-type phage with unusually small capsids and long tails was identified in these isolates by TEM as described in Chapter 4 (Fig. 4.10). PCR analysis of the phage DNA was used to identify whether these phage types were present in other DNA samples. Primer pair #656 (F1)/#657 (R1) and an annealing temperature of 59°C for 45 s were used. The results showed that these phage types were induced only in isolates PM86, PM934, PM954, PM486 and PM172 (Fig. 5.8). Sequencing of phage DNA identified temperate bacteriophages and short sequences in isolates PM86, PM934, PM954, PM486 and PM172. These phages were assigned as ϕPM86.2, ϕPM934.2, ϕPM954.2, ϕPM486.2 and ϕPM172.2 (Table 5.4). The genomic map is shown in (Fig. 5.9A). The genomes were annotated and assembled; the genomes had a GC content of 38.72%. These sequences consisted of 7,830 bp and encoded 9 CDCs and were 100% identical (Fig. 5.9B). To integrate into the host chromosome, this phage type used typical integrase-encoding genes (*int)* at the left end (ORF1) (Fig. 5.9A). Two genes adjacent to the integrase-encoding genes encode homologues to HTH (Xis protein) and STKc (ORF2 and ORF3), respectively. The genomes also contained gene encoding DNA primase (ORF5) which enhance replication, followed by the transcriptional regulator Mor (ORF6) (Fig. 5.9A). This type of phage lacks the genes encoding proteins which are involved in head morphogenesis and also genes encoding tail morphogenesis.

The isolates PM86, PM934, PM954, PM486 and PM172 also contained additional functional Mu-like phages of 33,388 bp and DNA isolation showed the presence of two bands of different sizes. These results, together with the identification of small capsids by TEM, suggest that these elements belong to the phage-inducible chromosomal islands (PICIs) in the *P. multocida* isolates PM86, PM934, PM954, PM486 and PM172, because the PICIs use helper phage for their propagation and they produce small capsids to fit their smaller genomes (Fig. 5.10A). PICIs are satellite phages that have an intimate relationship with temperate (helper) bacteriophages (Penadés & Christie, 2015).

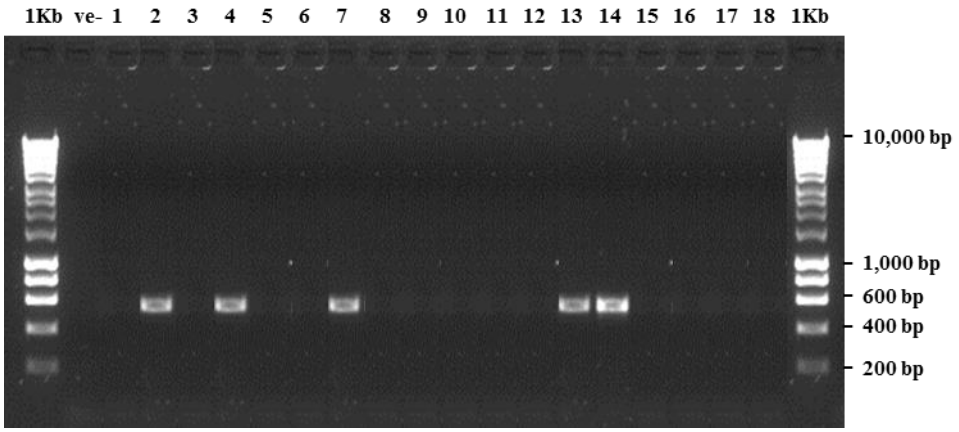

Fig. 5.8 Induction of short phage type in isolates PM86, PM172, PM486, PM934 and PM954.

The results indicated the presence of short phage type only in isolates PM86 (L2), PM172 (L4), PM486 (L7), PM934 (14) and PM954 (L14). However, they were not induced in isolates PM40 (L1), PM122 (L3), PM336 (L5), PM382 (L6), PM684 (L8), PM848 (L9), PM850 (L10), PM918 (L11), PM926 (12), PM964 (L15), PM982 (L16), PM986 (L17), PM988 (L18) and negative control (ve-). PCR reactions were conducted using primer pair #656 (F1)/#657 (R1) (**Table 5.1**).and an annealing temperature of 59°C.

Fig. 5.9 Genomic structure (A) and nucleotide sequence comparison (B) of *P. multocida* short phage types.

The genomic map was constructed using Easyfig. The five genomes were aligned using a progressive MAUVE alignment.

Southern blot hybridisation was carried out using two labelled probes to differentiate the two elements: phage and PICI, to examine whether both types are present in other isolates, to differentiate between two bands, and to examine whether PICI can be packaged in small capsids. When the DNA of the PICI has been packaged in small capsids the size of the band will be smaller than the one from the phage. Southern blot hybridisation confirmed the induction of Mu-like phages (Fig. 5.10A) and PICIs (Fig. 5.10B) only in isolates PM86, PM934, PM954, PM486 and PM172. A labelled probe based on the gene encoding phage terminase using primer pair #654 (F1)/#655(R1) showed that the Mu-like phages were packaged in large- and small-sized capsids (Fig. 5.10A). However, a labelled probe based one the gene encoding short sequence using primer pair #656 (F1)/#657 (R1) showed that the PICIs were identified only in isolates PM86, PM172, PM486, PM934 and PM954 and were all packaged in small capsids only (Fig. 5.10B). Details of the nucleotide sequences of the primers are listed in Table 5.2

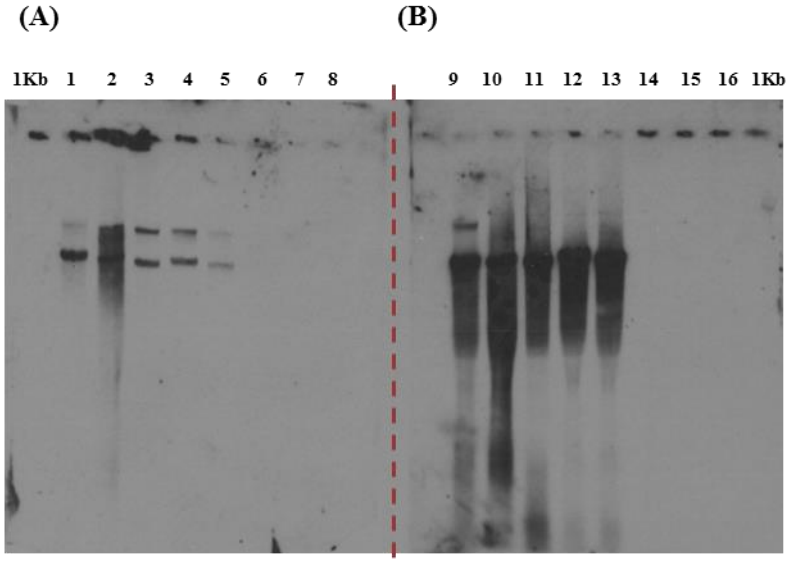

Fig. 5.10 Southern blot hybridisation showing the packaging of helper phage and PICI in small and large capsids.

The Southern blot hybridisation confirmed the induction of both Mu-like (A) and PICI (B) only in isolates PM86 (L1 & L9), PM172 (L2 & L10), PM486 (L3 & L11), PM934 (L4 & 12) and PM954 (L5 & L13). However, they were not found in isolates PM40 (L6 & L14), PM684 (L7 & L15) and PM926 (L8 & L16). Labelled probe based on the gene encoding Mu-like phage terminase using primer pair #654 (F1)/#655 (R1) showed that the Mu-like phages were packaged in large and small size capsids (A). However, a labelled probe based one the gene encoding short sequence using Primer pair #656 (F1)/#657 (R1) showed that the PICIs were identified only in isolates PM86, PM172, PM486, PM934 and PM954 and were all packaged in small capsids only (B).

5.3.1.3 Lambda-like phages

Lambda-like (λ-like) phages were the only *Siphoviridae* phages induced in this study. The λ-like phages were induced in isolates PM86 (avian isolate), PM122, PM964, PM982, PM986 and PM988 (ovine isolates), PM336 (bovine isolate), PM850, PM684, PM918, PM926, PM40 and PM848 (porcine isolates) (Table 5.4). The complete bacterial genome sequences were also used to confirm the presence and assembly of the λ-like phages. The sequencing results confirmed induction of more than one λ-like phage in isolates PM684, PM40 and PM848; Mu-like phages were also induced in isolate PM684 and PM40. Unlike the Mu-like phages, a few λ-like phages were found to be distributed between different contigs, these phages were ϕPM850.3, ϕPM684.3 and ϕPM848.2. In these cases, single complete genomes were obtained by targeted PCR as described in section 5.3.1.4.

5.3.1.4 Completion of single bacteriophage genome and identification of attachment sites

In isolate PM850, ϕPM850.3 was distributed between two contigs (Fig. 5.2). An approximate size of the un-sequenced gap between C12 and C2 was first indicated by a positive PCR amplification using primer pair #684 (F2)/#685 (R2) (Fig. 5.11). PCR products were sequenced successfully and the consensus sequence was aligned with C12 and C2 resulting a single sequence of representing ϕPM850.3. Chromosomal flanking genes for this phage were identified by BLAST analysis with *P. multocida* from the NCBI database. BLASTn identified an identical integrase (1089 bp) gene with 100% similarity in *Pasteurella multocida* subsp. *multocida* str. HN06. In HN06, the prophage was found to have inserted into the genome in a tRNA-trp downstream gene encoding D,D-heptose 1,7-bisphosphate phosphatase (PMCN06_2045) and upstream is a gene encoding the protein VisC (PMCN06_2120). These two genes were identified in PM850, and primer pairs F1/R1 and F3/R3 were designed and used to identify flanking genes within isolate PM850 (Fig. 5.2). Both attachment sites *attL* and *attR* within the bacterial genome was identified by BLAST analysis of ϕPM850.3 and also by aligning the sequences from the ends of the phage genome (C12 and C2). Analysis identified two identical short sequences (54 bp) at the ends of C12 and C2. The identical 54 bp nucleotides at both ends were proposed as the *attL*

and *attR* (Fig. 5.12). After assembly and identification of the attachment sites, a single ϕPM850.3 genome totalling 48,455 bp was obtained.

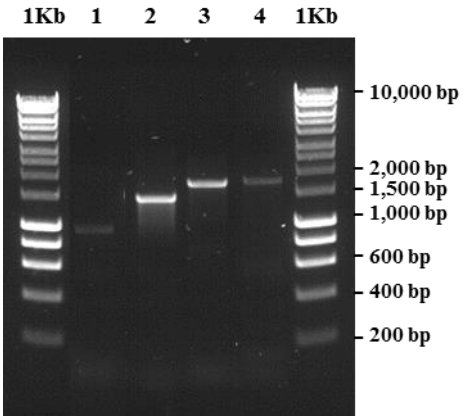

Fig. 5.11 PCR products in isolate PM850 used to complete genome sequence of ϕPM850.3.

Primer pairs F1/R1 (L1) and F3/R3 (L3) were used to identify attachment sites; primer pair F2/R2 (L2) was used to close the gap between C12 and C2; primer pair F1/R3 (L4) was used to examine the spontaneous induction of ϕPM850.3 in PM850 in broth culture without exposure to mitomycin C.

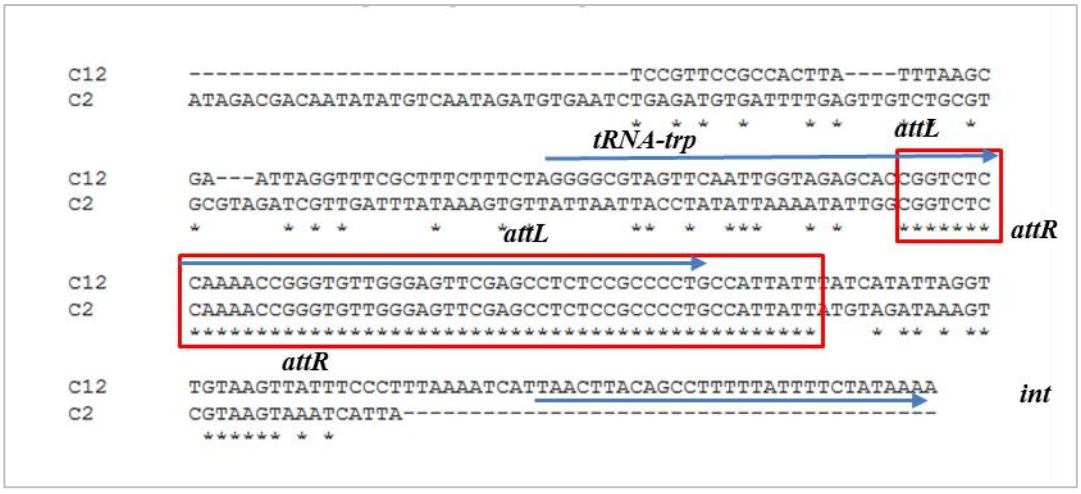

Fig. 5.12 Comparison of the nucleotide sequences of contigs C12 and C2 of isolate PM850 to identify attachment sites (*attL* and *attR*) for ϕPM850.3.

The proposed *attL* and *attR* sites at the end of C12 and C2 are shown in red boxes, respectively. The asterisks indicate the identity of nucleotides in C12 and C2. The blue arrows indicate the *tRNA*-trp gene and the start (5' end) of the phage integrase (*int*) gene.

A single continuous λ-like phage with a closely related integrase was found in isolates PM86, PM122, PM336, PM964, PM982, PM986 and PM988. Similar phages were also found in isolates PM684 and PM848, but they were found to be distributed between different contigs. BLASTn analysis of the integrase (990 bp) showed no similarities with the *P. multocida* database and other bacterial species. Bacterial genome analysis of isolate PM982 showed that the integrase gene was located upstream of the gene encoding SecG. BLASTn of the gene encoding SecG showed that this gene is upstream to RNA polymerase sigma-70 factor. The tRNA-leu gene was located between both genes. As described in Fig. 5.1, primer pair #678 (F1)/#679(R1) and primer pair #680 (F2)/#681 (R2) were designed from the flanking genes in the host chromosome and both ends of the phage genome. Positive PCR amplification confirmed these phages were found to have inserted into the genomes in a tRNA-leu gene which is located downstream of the gene encoding SecG and upstream of RNA polymerase sigma-70 factor. Attachment sites were identified by BLASTn of whole phage and flanking genes against online databases. A short sequence of 19 identical nucleotides was found at both ends which probably represent the *attR* and *attL* attachment sites. Similar phages were found in isolates PM86, PM122, PM336, PM684, PM848, PM964, PM986 and PM988. (Fig. 5.13). These phages were designated ϕPM86.3, ϕPM122.1, ϕPM336.1, ϕPM684.3, ϕPM848.2, ϕPM964.1, ϕPM982.1, ϕPM986.1 and ϕPM988.1 (Fig. 5.13).

Furthermore, ϕPM848.2 was found to be distributed between 7 contigs (Fig. 5.3). Gaps were closed by targeted PCR as described previously (Fig. 5.3). The size of unsequenced regions was indicated first by a positive PCR amplification (Fig. 5.14). PCR products were sequenced successfully and the consensus sequence of each reaction was aligned with the phage genome. After assembly and identification of the attachment sites, a single ϕPM848.2 genome totalling 54,876 bp was obtained. The same primers that used to obtain ϕPM848.2 were used for ϕPM684.3. Both phages had identical attachment sites to ϕPM982.1 and they were able to excise spontaneously (Fig. 5.13).

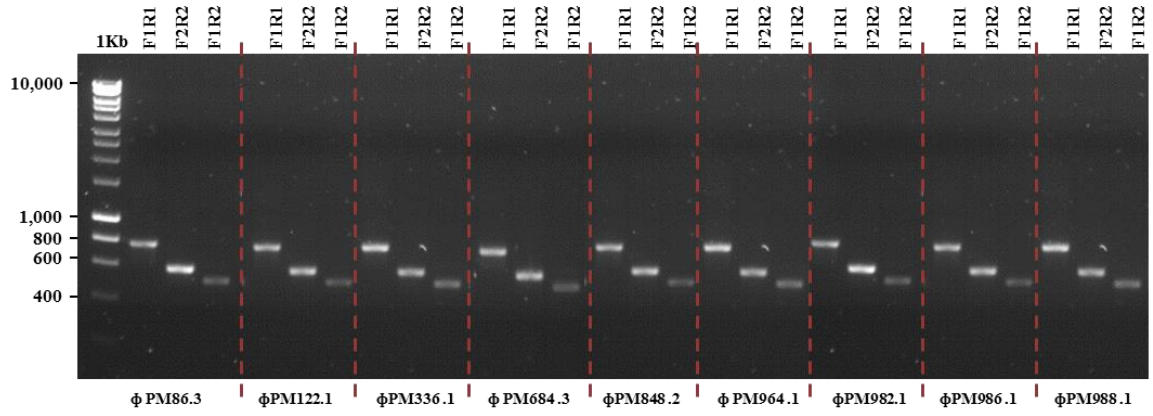

Fig. 5.13 Identification and examination of attachment sites and spontaneous induction.

The following phages were used: ϕPM86.3, ϕPM122.1, ϕPM336.1, ϕPM684.3, ϕPM848.2, ϕPM964.1, ϕPM982.1, ϕPM986.1 and ϕPM988.1. The results show the presence of the same attachment sites and these phages were induced spontaneously. Primer pairs F1/R1 (L1) and F2/R2 (L2) were used to identify both flanking genes; primer pair F1/R2 (L3) to) was used to examine the spontaneous induction of these phages in bacterial broth cultures without exposure to mitomycin C. F1 = primer #678, R1 = primer #679, F2 = primer #680 and R2 = primer #681.

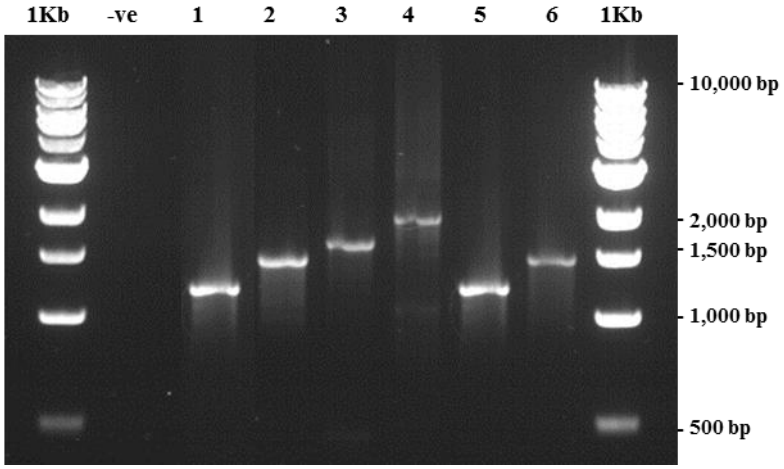

Fig. 5.14 PCR products in isolate PM848 used to complete genome sequence of ϕPM848.2.

The gaps were closed successfully using primer pairs F1/R1 (L1), F2/R2 (L2), F3/R3 (L3), F4/R4 (L4), F5/R5 (L5) and F6/R6 (L6) with an annealing temperature of 59°C. Details of the nucleotide sequences of the primers are listed in **Table 5.3.**

5.3.1.5 Spontaneous induction

ϕPM850.3 was examined to determine whether this phage was able to induce and excise spontaneously from the bacterial genome without exposure to mitomycin (Fig. 5.11). Spontaneous induction was confirmed by targeted PCR using primers designed from the chromosomal flanking genes (F1/R3) as shown in Fig. 5.2. ϕPM86.3, ϕPM122.1, ϕPM336.3, ϕPM684.3, ϕPM848.2, ϕPM964.1, ϕPM982.1, ϕPM986.1 and ϕPM988.1 were also able to induce and excise spontaneously from their host chromosome (Fig. 5.13). The excision of phages was confirmed by a positive PCR amplification of 522 bp using primer pair #678 (F1)/#681 (R2) (Fig. 5.13).

5.3.1.6 Types of λ-like phages induced in *P. multocida*

The complete genome sequences of the λ-like phages were obtained and annotated automatically using the RAST server. The annotation of each phage was compared with the prophage sequence within the bacterial genomes by manual inspection using CLC genomics workbench. The phages were designated as ϕPM86.3, ϕPM122.1, ϕPM964.1, ϕPM982.1, ϕPM986.1, ϕPM988.1, ϕPM336.1, ϕPM850.3, ϕPM684.2, ϕPM684.3, ϕPM918.2, ϕPM926.2, ϕPM40.2, ϕPM40.3, ϕPM848.1 and ϕPM848.2. The genomic features of each phage are shown in Table 5.4.

Phylogenetic analysis of the complete genome sequences identified seven different λ-like phages among the induced phages (PMλ1-like to PMλ7-like) phages (Fig. 5.15). PMλ1-like phages were induced in ovine isolates including PM122, PM964, PM982, PM986 and PM988, the phage were designated as ϕPM122.1, ϕPM964.1, ϕPM982.1, ϕPM986.1, ϕPM988.1, respectively. PMλ2-like phages were induced in porcine isolates PM684 and PM848 and designated ϕPM684.3 and ϕPM848.2. PMλ3-like phages were induced in isolate PM850 and designated as ϕPM850.3. PMλ4-like phages were induced in isolates PM684, PM918, PM926, PM40 and PM848 and designated as ϕPM684.2, ϕPM918.2, ϕPM926.2, ϕPM40.2 and ϕPM848.2, respectively. PMλ5-like phages designated as ϕPM40.3 which was induced from porcine isolate PM40. PMλ6-like phages were induced only in isolate PM86 and designated as ϕPM86.3. PMλ7-like phages were induced only in isolate PM336 and designated as ϕPM336.1.

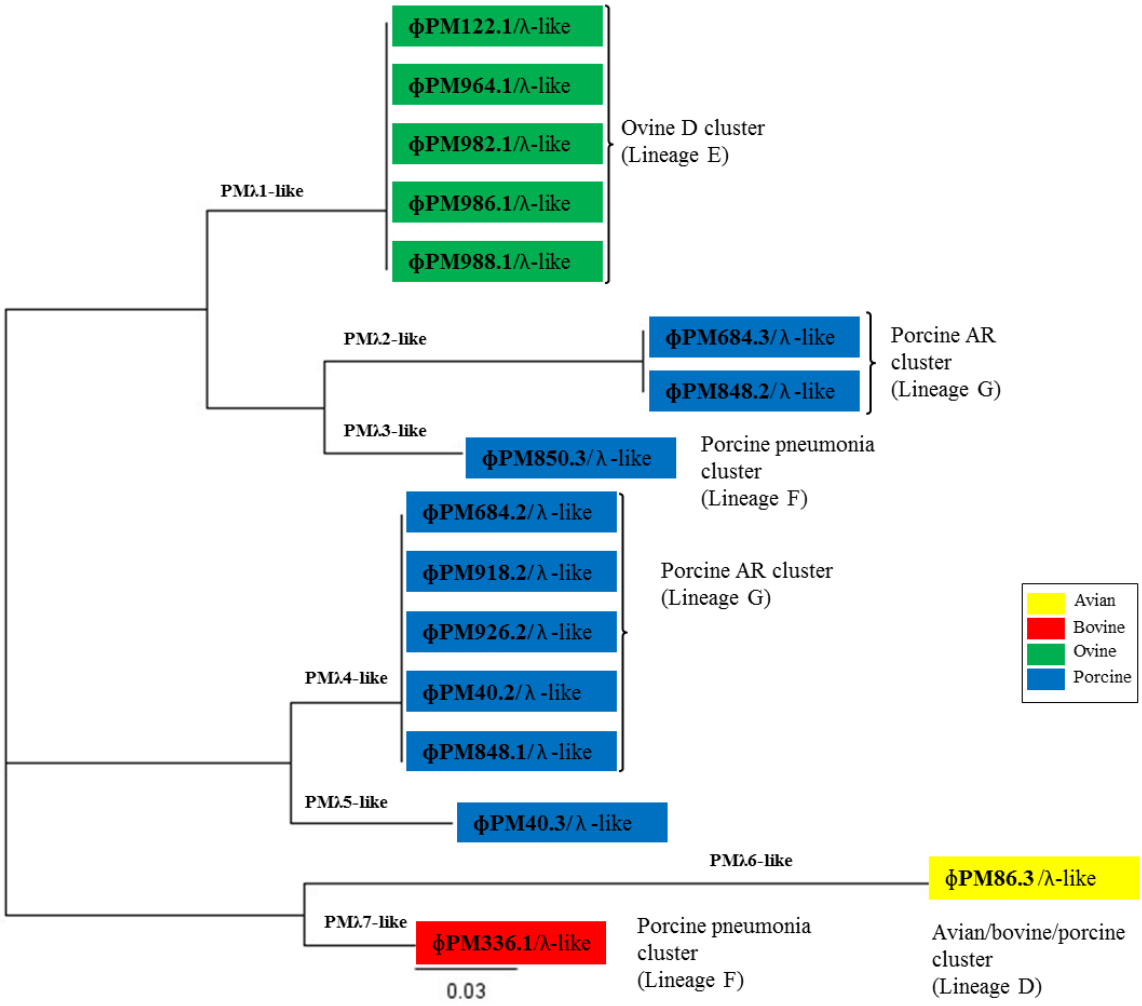

Fig. 5.15 Neighbour-Joining tree represents the phylogenetic relationships of λ-like phages (PMλ1-like to PMλ7-like) induced in *P. multocida* isolates.

The phylogenetic tree was constructed with the Jukes-Cantor correction model using Geneious (v. 9.1.4). Each phage is abbreviated with the phage designation, followed by the phage type. The results showed the identification of seven different PMλ-like phages.

One phage from each group (ϕPM982.1, ϕPM848.2, ϕPM850.3, ϕPM684.2, ϕPM40.3, ϕPM86.3 and ϕPM336.1) was selected and analysed in detail. The complete genomes of these phages consist of 45,131 bp, 54, 876 bp, 48,455 bp, 42,90 bp, 43,385 bp, 56,050 bp and 49, 821 bp and GC contents of 37.9%, 38.8%, 38.0%, 38.8%, 38.6%, 38.5% and 38.2%, respectively; the genomes encode for 69, 74, 69, 65, 68, 92 and 73 CDCs, respectively (Table 5.4). Additionally, 1 tRNA, 4 tRNAs and 3 tRNAs were found in the genomes of ϕPM848.2, ϕPM86.3 and ϕPM336.1, respectively. Predictions of the functions of each gene within the genomes were carried out by comparison of the gene products with other phage sequences using PHAST analysis and BLAST analysis against the NCBI database. The genomic organisation of the PMλ-like phages is shown in Fig. 5.16

The λ-like phages induced in *P. multocida* were diverse and different from each other (Fig. 5.15). The genome sequences were aligned using BLASTn algorithm in Easyfig and degree of similarities are shown in (Fig. 5.17). Pairwise analysis showed that ϕPM684.2 and ϕPM40.3 were closely related and showed 83% pairwise nucleotide sequence similarity (Fig. 5.17 & Table 5.7). ϕPM982.1 showed sequences similarity of 75% to ϕPM850.3 and ϕPM848.2 (Fig. 5.17 & Table 5.7).

Table 5.7 Pairwise nucleotide sequence similarity of induced λ-like phages in *P. multocida* isolates.

	ϕPM982.1	ϕPM848.2	ϕPM850.3	ϕPM684.2	ϕPM40.3	ϕPM86.3	ϕPM336.1
ϕPM982.1							
ϕPM848.2							
ϕPM850.3							
ϕPM684.2							
ϕPM40.3							
ϕPM86.3							
ϕPM336.1							

Pairwise nucleotide sequence similarities were calculated using ClustalW and EMBOSS Stretcher analysis. Different colours indicate difference in sequence similarity, green= 80-89%, red= 70-79%, blue= 60-69%, yellow= 50-49%, and grey= 40-49%.

The PHAST and BLAST analysis showed that the λ-like phages induced in *P.* multocida exhibit similarity with the λ-like phages in the closely related species *M. haemolytica* (1152AP2, 587AP2 and 535AP2). In particular, genes encoding integrase, methyltransferase, pyruvate kinase, exonuclease, recombinase, antitermination protein Q, replication proteins O, genes encoding lysis, regulation and immunity, DNA packaging, head morphogenesis, tail morphogenesis including genes coding for tail length tape measure protein, minor tail proteins M, L and K, tail assembly protein I, host specificity protein (phage tail fibre) J were similar (Table 5.8 to

Table 5.12 & Supplementary Tables 8.4 & 8.5). The results showed that 33 to 39 of the annotated ORFs were assigned essential functions of λ-like phage, whereas the remaining ORFs were encoded hypothetical proteins and genes of other functions. The genomes contained genes responsible for major functions of λ-like phage, including integration, DNA metabolism and recombination, regulation, DNA replication immunity, DNA packaging and capsid morphogenesis, tail morphogenesis and host cell lysis (Table 5.8 to

Table 5.12 & Supplementary Tables 8.4 & 8.5).

The genomic organisation of ϕPM86.3, ϕPM982.1, ϕPM336.1, ϕPM850.3 and ϕPM848.2 are similar, with the integrase gene (*int*) at the beginning. However, in ϕPM684.2 and ϕPM40.3, *int* was found in the middle of the genomes. All λ-like phages induced in this study used *int* to integrate into the host chromosomes. The λ-like phages possess genes that are responsible for switching between the lytic and the lysogenic cycles; these genes, *cI* and *cro,* were found in all λ-like phages induced in this study (they were transcribed in opposite directions) (Fig. 5.16). The λ-like phages also contain genes involved in lysis of host cell, including holin, endolysin and RZ.1. Genes encoding the HicB-like antitoxin were identified only in ϕPM982.1, ϕPM850.3 and ϕPM848.2. ϕPM850.3 and ϕPM848.2 contained identical transposase-encoding genes (100%). Transposase genes were identified immediately downstream of the genes coding host cell lysis (Fig. 5.16). The presence of a gene encoding transposase in ϕPM850.3 and ϕPM848.2, suggests that the transposase may play a role in the acquisition of foreign genes either from other bacteriophages or other bacteria. Genomic analysis of the induced λ-like phages identified a number of virulence encoding genes.

Interestingly, the gene encoding the *Pasteurella multocida* toxin (PMT) was identified within the genomes of the PMλ2–like phages ϕPM684.3 and ϕPM848.2. These phages are functional λ–like phages induced in isolates PM684 (capsular type A, OMP-type 6.1, ST 11 and MLST group G) and PM848, (capsular type D, OMP-type 4.1, ST11 and MLST group G). Both isolates are toxigenic strains which cause atrophic rhinitis in pigs. Phage-encoded PMT was found to be located downstream of the phage tail fibre genes that are involved in host recognition (Fig. 5.16). The presence of PMT encoded by temperate bacteriophages of the *Siphoviridae* family suggests that the phages may play an important role in pathogenesis and HGT in *P. multocida*.

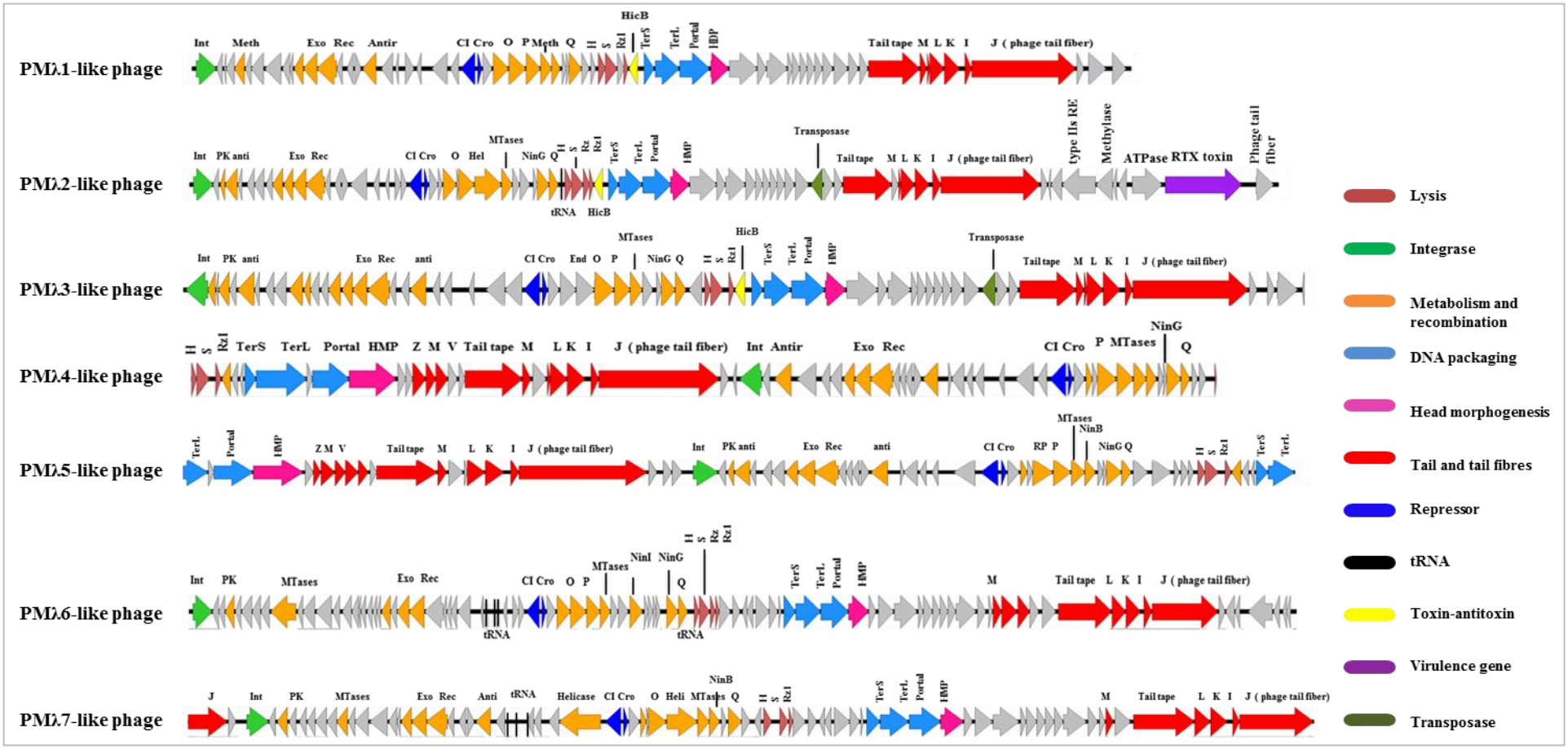

Fig. 5.16 Genomic organisation of the seven λ–like phage types (PMλ1-like to PMλ7-like) induced in *P. multocida* isolates.

The genomic maps were constructed using Easyfig. Further detail of protein products is provided in Table 5.8 to Table **5.12**.

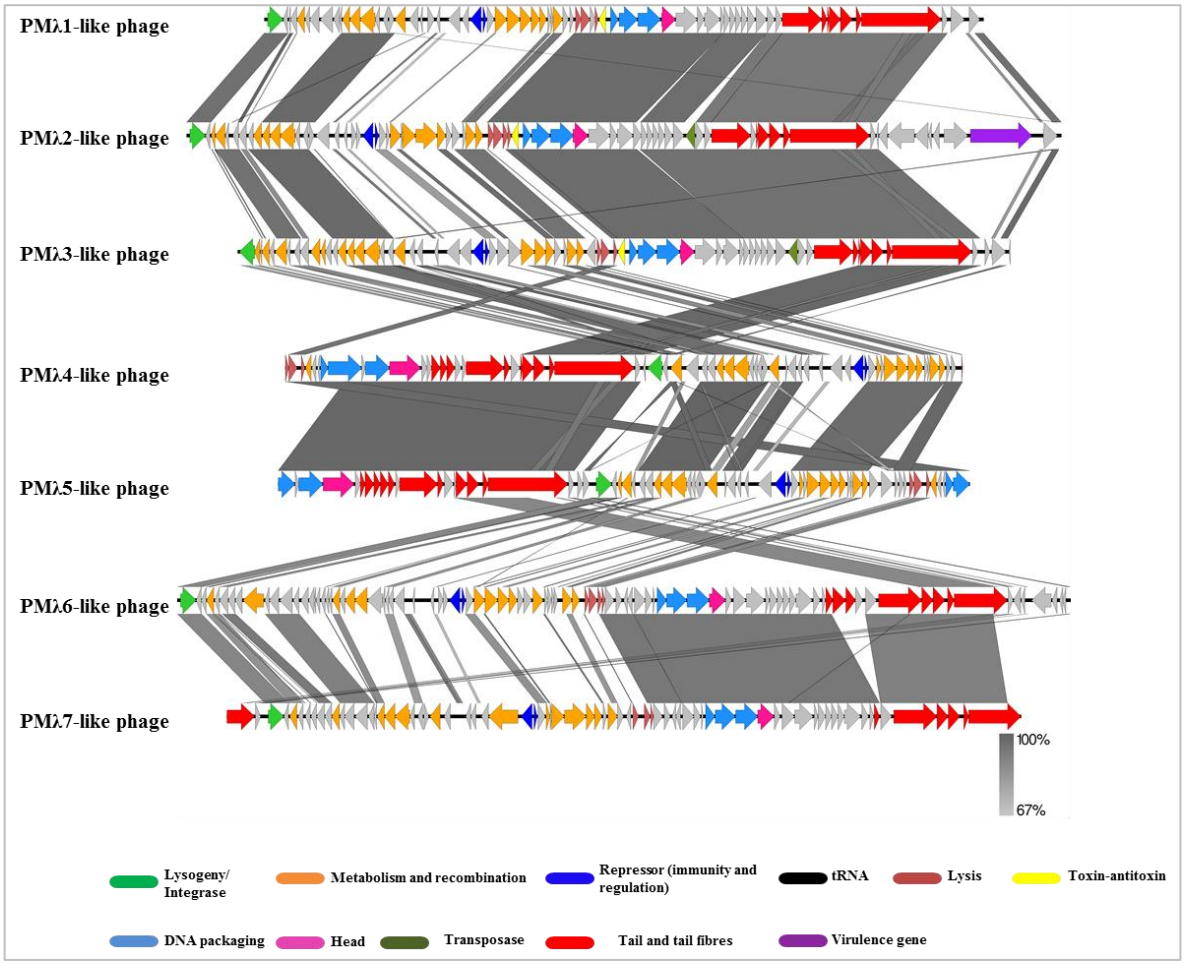

Fig. 5.17 Whole genome comparisons of the seven λ-like phage types (PMλ1-like to PMλ7-like) induced and sequenced in *P. multocida* strains.

The sequence alignments were carried out using the BLASTn algorithm in Easyfig. The degree of sequence similarity is indicated by the intensity of the grey shading (darker grey indicates the highest sequence similarity). The position of genes within each genome is indicated by arrows.

Table 5.8 Major protein products of ϕPM982.1 (PMλ1–like phage) using PHAST and BLAST analysis.

Orfs	Protein product	Size (bp/aa)	BLAST_HIT	E-value
Orf1	Phage integrase, site-specific tyrosine recombination	990/329	PHAGE_Mannhe_vB_MhS_535AP2: integrase	2e-99
Orf5	Putative methyltransferase	486/161	PHAGE_Mannhe_vB_MhS_535AP2: methyltransferase	5e-64
Orf7	COG1896: Predicted hydrolases of HD superfamily	600/200	PHAGE_Salmon_ST64B: hypothetical protein sb35	5e-25
Orf11	Single-stranded DNA-binding protein	453/151	PHAGE_Vibrio_VvAW1: single-stranded DNA-binding protein	2e-41
Orf12	Hypothetical protein	660/219	PHAGE_Mannhe_vB_MhS_587AP2: exonuclease	3e-98
Orf13	Recombinational DNA repair protein RecT	954/318	PHAGE_Mannhe_vB_MhS_587AP2: recombinase	6e-127
Orf17	Putative antirepressor protein	648/216	PHAGE_Haemop_Aaphi23: putative antirepressor protein Ant	2e-38
Orf24	Putative phage repressor	684/227	PHAGE_Pseudo_vB_PaeS_PAO1_Ab30: putative c repressor	1e-20
Orf25	Hypothetical protein	201/67	PHAGE_Salmon_ST160: Cro	6e-11
Orf27	Hypothetical protein	753/251	PHAGE_Pseudo_F10: Putative DNA-binding protein (Roi))	4e-35
Orf28	Primosomal protein I	834/277	PHAGE_Entero_Sf101: replication protein O	4e-20
Orf29	Replication protein P	690/229	PHAGE_Mannhe_vB_MhS_587AP2: replication protein P	2e-23
Orf30	Putative DNA methylase	537/178	PHAGE_Mannhe_vB_MhS_587AP2: DNA N-6-adenine-methyltransferase	1e-54
Orf31	Phage NinB DNA recombination protein	426/141	PHAGE_Aggreg_S1249: putative recombination protein NinB	5e-45
Orf34	Phage NinG rap recombination	603/200	PHAGE_Salmon_SPN3UB_: NinG	1e-43
Orf35	Hypothetical protein	366/121	PHAGE_Mannhe_vB_MhS_587AP2: antitermination protein Q	2e-10
Orf37	Hypothetical protein	366/121	PHAGE_Mannhe_vB_MhS_587AP2: holin	4e-06
Orf38	Phage endolysin	585/195	PHAGE_Mannhe_vB_MhS_587AP2: endolysin	1e-55
Orf40	Uncharacterised protein HI1413	207/69	PHAGE_Mannhe_vB_MhS_587AP2: lytic protein Rz1	2e-11
Orf41	DNA-binding protein, CopG family, HicB_like antitoxin	435/145	PHAGE_Haemop_HP2: hypothetical protein HP2p14	1e-13
Orf42	Phage terminase, small subunit	498/166	PHAGE_Pseudo_vB_PaeP_Tr60_Ab31: Putative terminase small subunit	4e-36
Orf43	Phage terminase, large subunit	1170/389	PHAGE_Mannhe_vB_MhS_587AP2: terminase large subunit	0.0
Orf44	Hypothetical protein	1446/482	PHAGE_Mannhe_vB_MhS_587AP2: portal protein	1e-148
Orf45	Phage head decoration protein	888/295	PHAGE_Mannhe_vB_MhS_587AP2: head morphogenesis protein	9e-53
Orf58	Phage tail length tape-measure protein 1	2475/824	PHAGE_Mannhe_vB_MhS_587AP2: tail length tape measure protein	0.0
Orf59	Hypothetical protein	330/109	PHAGE_Mannhe_vB_MhS_587AP2: minor tail protein M	7e-22
Orf60	Phage tail length tape-measure protein 1	114/37	Phage tail length tape-measure protein 1	0.0
Orf61	Phage minor tail protein	705/235	PHAGE_Mannhe_vB_MhS_587AP2: minor tail protein L	1e-82
Orf62	Phage tail assembly protein	744/247	PHAGE_Mannhe_vB_MhS_587AP2: minor tail protein K	1e-84
Orf63	Phage tail assembly protein I	327/109	PHAGE_Mannhe_vB_MhS_587AP2: tail assembly protein I	4e-20
Orf64	Phage tail fibre protein	5007/1669	PHAGE_Mannhe_vB_MhS_587AP2: host specificity protein J	0.0
Orf67	Phage Rha protein	666/222	PHAGE_Shigel_SfII_NC_021857: KliA-N domain protein	1e-21

Table 5.9 Major protein products of ϕPM848.2 (PMλ2–like phage) using PHAST and BLAST analysis.

Orfs	Protein product	Size (bp/aa)	BLAST_HIT	E-value
Orf1	Phage integrase, site-specific tyrosine recombination	990/330	PHAGE_Mannhe_vB_MhS_535AP2: integrase	5e-99
Orf3	Single-stranded DNA-binding protein	237/78	PHAGE_Mannhe_vB_MhS_535AP2: pyruvate kinase	6e-11
Orf4	Putative antirepressor	624/207	Phage antirepressor protein	3e-38
Orf9	Phage DNA binding protein	522/173	PHAGE_Mannhe_vB_MhS_535AP2: hypothetical protein	6e-20
Orf10	Single-stranded DNA-binding protein	453/150	Putative single-strand DNA binding protein	2e-39
Orf11	Hypothetical protein	660/119	PHAGE_Mannhe_vB_MhS_587AP2: exonuclease	3e-98
Orf12	Recombinational DNA repair protein RecT	954/317	PHAGE_Mannhe_vB_MhS_587AP2: recombinase	6e-127
Orf21	putative prophage repressor CI	657/218	PHAGE_Mannhe_vB_MhS_535AP2: CI repressor	9e-69
Orf22	Cro repressor-like protein	207/68	PHAGE_Mannhe_vB_MhS_535AP2: Cro repressor	9e-22
Orf25	Putative DNA-binding protein Roi of bacteriophage	684/227	*P*asteurella *multocida*: antirepressor	1e-166
Orf27	Phage replication protein O	819/272	PHAGE_Haemop_Aaphi23: putative DNA replication protein O	7e-80
Orf28	DNA helicase	1365/454	PHAGE_Mannhe_vB_MhS_535AP2: helicase	2e-129
Orf29	MunI-like protein	540/179	PHAGE_Mannhe_vB_MhS_535AP2: methyltransferase	1e-89
Orf31	Gifsy-2 prophage protein	507/168	PHAGE_Mannhe_vB_MhS_535AP2: hypothetical protein	6e-82
Orf33	Phage NinG rap recombination	603/200	PHAGE_Salmon_SPN3UB_NC_019545: NinG	8e-45
Orf34	Hypothetical protein	462/153	PHAGE_Mannhe_vB_MhS_535AP2: antitermination protein Q	6e-15
Orf36	Hypothetical protein	366/121	PHAGE_Aeromo_phiO18P_NC_009542: putative holin	1e-06
Orf37	Phage endolysin	585/194	PHAGE_Haemop_Aaphi23_NC_004827: putative Lys protein	2e-59
Orf39	Uncharacterised protein HI1413	207/68	PHAGE_Mannhe_vB_MhS_535AP2: lytic protein Rz1	3e-09
Orf40	DNA-binding protein, CopG family	435/144	*Pasteurella multocida* :CopG family	0.0
Orf41	Phage DNA binding protein	498/165	PHAGE_Pseudo_vB_PaeP_Tr60_Ab31: Putative terminase small subunit	4e-36
Orf42	Phage terminase, large subunit	1170/389	PHAGE_Mannhe_vB_MhS_535AP2: terminase large subunit	0.0
Orf44	Phage head decoration protein	972/323	PHAGE_Mannhe_vB_MhS_535AP2: head morphogenesis protein	7e-59
Orf53	Phage neck whiskers	483/160	PHAGE_Mannhe_vB_MhS_535AP2: major tail protein	8e-48
Orf55	Mobile element protein	588/195	PROPHAGE_Neisse_MC58: IS1016C2 transposase	3e-71
Orf58	Phage tail length tape-measure protein 1	2445/814	PHAGE_Mannhe_vB_MhS_535AP2: tail length tape measure protein	0.0
Orf59	Hypothetical protein	330/109	PHAGE_Mannhe_vB_MhS_535AP2: minor tail protein M	2e-22
Orf60	Phage tail length tape-measure protein 1	114/37	Phage tail length tape-measure protein 1	0.0
Orf61	Phage minor tail protein	705/234	PHAGE_Mannhe_vB_MhS_535AP2: minor tail protein L	3e-81
Orf62	Phage tail assembly protein	735/224	PHAGE_Mannhe_vB_MhS_535AP2: minor tail protein K	3e-87
Orf63	Phage tail assembly protein I	408/135	PHAGE_Mannhe_vB_MhS_535AP2: tail assembly protein I	4e-32
Orf64	Phage tail fibre protein	5004/1667	PHAGE_Mannhe_vB_MhS_535AP2: host specificity protein J	0.0
Orf66	Hypothetical protein	132/43	*P. multocida*: integrase	0.0

Table 5.9 (continued)

Orfs	Protein product	Size (bp/aa)	BLAST_HIT	E-value
Orf67	Conserved domain protein	555/184	*P. multocida*: hypothetical protein	1e-07
Orf68	Type IIs restriction endonuclease	1686/561	*P. multocida*: AlwI restriction endonuclease; This family includes the AlwI (recognises GGATC)	0.0
Orf69	Methyl-directed repair DNA adenine methylase	852/283	*P. multocida*: putative adenine methyltransferase	0.0
Orf70	Hypothetical protein	207/68	Multi-species and *Streptococcus pneumonia:* transcriptional regulator	2e-42, 8e-15
Orf71	Hypothetical protein	408/135	*P. multocida*: transcriptional regulator	5e-97
Orf72	Chromosome segregation ATPase	1497/498	*P. multocida* and *Haemophilus parasuis*: chromosome segregation ATPase	0.0, 0.0
Orf73	RTX toxin determinant A	3858/1285	*P. multocida*: dermonecrotic toxin	0.0
Orf74	Phage tail fibres	885/294	*P. multocida* and *Haemophilus parasuis:* putative antirepressor	0.0, 8e-103

Table 5.10 Major protein products of ϕPM850.3 (PMλ3–like phage) using PHAST and BLAST analysis.

Orfs	Protein product	Size (bp/aa)	BLAST_hit	E-value
Orf1	Single-stranded DNA-binding protein	966/322	Integrase	1e-51
Orf4	Single-stranded DNA-binding protein	471/157	PHAGE_Mannhe_vB_MhS_535AP2: pyruvate kinase	4e-24
Orf6	Putative antirepressor	723/240	Phage antirepressor protein	1e-37
Orf10	DNA recombination-dependent growth factor C	567/189	DNA recombination-dependent growth factor C	2e-37
Orf11	DNA recombination-dependent growth factor C	276/92	PHAGE_Vibrio_12A4: recombination-associated protein RdgC	7e-11
Orf14	Phage DNA binding protein	522/173	PHAGE_Mannhe_vB_MhS_535AP2: hypothetical protein	6e-20
Orf15	Single-stranded DNA-binding protein	453/150	PHAGE_Vibrio_VvAW1: single-stranded DNA-binding protein	1e-39
Orf16	Hypothetical protein	675/225	PHAGE_Mannhe_vB_MhS_587AP2: exonuclease	2e-94
Orf17	Recombinational DNA repair protein RecT	954/317	PHAGE_Mannhe_vB_MhS_587AP2: recombinase	6e-127
Orf20	Phage Rha protein	693/231	PHAGE_Haemop_Aaphi23: putative antirepressor protein Ant	4e-38
Orf26	Transcriptional regulator	687/228	PHAGE_Haemop_Aaphi23: putative CI protein	1e-72
Orf27	Cro repressor-like protein	210/69	PHAGE_Mannhe_vB_MhS_535AP2: Cro repressor	4e-13
Orf29	Uncharacterised phage-encoded protein	702/234	PHAGE_Aggreg_S1249: uncharacterized phage-encoded protein	3e-32
Orf31	Primosomal protein I	861/287	PHAGE_Stx2_vB_EcoP_24B: O	2e-34
Orf32	Replication protein P	696/231	Possible bacteriophage replication protein P	2e-33
Orf33	MunI-like protein	531/177	PHAGE_Mannhe_vB_MhS_535AP2: methyltransferase	5e-89
Orf36	Phage NinG rap recombination	603/201	PHAGE_Salmon_SPN3UB: NinG	8e-45
Orf37	Hypothetical protein	462/154	PHAGE_Mannhe_vB_MhS_535AP2: antitermination protein Q	6e-15
Orf39	Haemophilus-specific protein, uncharacterised	255/84	PHAGE_Mannhe_vB_MhS_535AP2: holin	1e-11
Orf40	phage lysin, putative phage lysozyme or muramidase	531/176	PHAGE_Mannhe_vB_MhS_535AP2: endolysin	8e-42
Orf41	Uncharacterised protein HI1413	231/76	PHAGE_Mannhe_vB_MhS_535AP2: lytic protein Rz1	3e-09
Orf42	DNA-binding protein, CopG family, HicB_like antitoxin	435/144	*Pasteurella multocida*: CopG family	0.0
Orf43	Phage terminase, small subunit	498/165	PHAGE_Pseudo_vB_PaeP_Tr60_Ab31: Putative terminase small subunit	3e-36
Orf44	Phage terminase, large subunit	1170/389	PHAGE_Mannhe_vB_MhS_535AP2: terminase large subunit	0.0
Orf45	Hypothetical protein	1446/481	PHAGE_Mannhe_vB_MhS_535AP2: portal protein	4e-149
Orf46	Phage head decoration protein	909/302	PHAGE_Mannhe_vB_MhS_535AP2: head morphogenesis protein	6e-54
Orf55	Phage neck whiskers	483/160	PHAGE_Mannhe_vB_MhS_535AP2: major tail protein	8e-48
Orf57	Mobile element protein	588/196	PROPHAGE_Neisse_MC58: IS1016C2 transposase	3e-71
Orf60	Phage tail length tape-measure protein 1	2445/815	PHAGE_Mannhe_vB_MhS_535AP2: tail length tape measure protein	0.0
Orf61	Hypothetical protein	330/109	PHAGE_Mannhe_vB_MhS_535AP2: minor tail protein M	2e-22
Orf63	Phage minor tail protein	705/234	PHAGE_Mannhe_vB_MhS_535AP2: minor tail protein L	4e-83
Orf64	Phage tail assembly protein	741/247	PHAGE_Mannhe_vB_MhS_535AP2: minor tail protein K	2e-84
Orf65	Phage tail assembly protein I	318/105	PHAGE_Mannhe_vB_MhS_535AP2: tail assembly protein I	1e-21
Orf66	Phage tail fibre protein	5004/1667	PHAGE_Mannhe_vB_MhS_535AP2: host specificity protein J	0.0
Orf69	Phage Rha protein	882/293	PHAGE_Shigel_SfII_NC_021857: KliA-N domain protein	2e-17

Table 5.11 Major protein products of ϕPM684.2 (PMλ4–like phage) using PHAST and BLAST analysis.

Orfs	Protein product	Size (bp/aa)	BLAST_hit	E-value
Orf1	Hypothetical protein	222/73	PHAGE_Mannhe_vB_MhS_1152AP2: holin	1e-07
Orf2	Putative phage lysozyme	531/177	PHAGE_Mannhe_vB_MhM_587AP1: endolysin	7e-46
Orf3	Hypothetical protein	231/77	PHAGE_Mannhe_vB_MhS_587AP2: lytic protein Rz1	6e-11
Orf4	Putative regulatory protein	369/123	Putative regulatory protein	0.0
Orf7	Hypothetical protein	474/158	PHAGE_Entero_c_: terminase small subunit	2e-43
Orf8	Phage terminase/large subunit	2109/703	PHAGE_Gifsy_2: bacteriophage DNA packaging protein; terminase/ large subunit	0.0
Orf10	Phage portal protein	1539/512	PHAGE_Gifsy_2: bacteriophage portal protein	6e-164
Orf11	Prophage Clp protease-like protein	1950/649	PHAGE_Gifsy_2: bacteriophage Clp protease involved in capsid processing	0.0
Orf14	Phage tail completion protein	552/183	PHAGE_Entero_mEp237: minor tail protein Z	3e-38
Orf15	Phage minor tail protein	408/135	PHAGE_Entero_mEp460: minor tail protein	2e-11
Orf16	Phage tail fibre protein	507/169	PHAGE_Entero_HK225: major tail protein V	3e-43
Orf19	Phage tail length tape-measure protein 1	2394/797	PHAGE_Idioma_Phi1M2_2: putative tail tape measure protein	6e-40
Orf20	Phage minor tail protein	351/116	PHAGE_Salmon_vB_SosS_Oslo: minor tail protein	7e-17
Orf23	Phage minor tail protein	705/235	PHAGE_Mannhe_vB_MhS_587AP2: minor tail protein L	7e-83
Orf24	Phage tail assembly protein	744/247	PHAGE_Mannhe_vB_MhS_587AP2: minor tail protein K	4e-84
Orf25	Phage tail assembly protein I	327/109	PHAGE_Mannhe_vB_MhS_587AP2: tail assembly protein I	1e-19
Orf26	Phage tail fibre protein	5004/1668	PHAGE_Mannhe_vB_MhS_587AP2: host specificity protein J	0.0
Orf29	Phage integrase family protein	918/306	Putative integrase	6e-51
Orf31	Phage Rha protein	687/228	Phage antirepressor	1e-24
Orf35	Single-stranded DNA-binding protein	453/151	PHAGE_Vibrio_VvAW1: single-stranded DNA-binding protein	1e-39
Orf36	Hypothetical protein	675/224	PHAGE_Mannhe_vB_MhS_587AP2: exonuclease	1e-99
Orf37	Recombinational DNA repair protein RecT (prophage associated)	954/318	PHAGE_Mannhe_vB_MhS_587AP2: recombinase	6e-127
Orf42	Phage antirepressor protein	621/207	PHAGE_Mannhe_vB_MhS_587AP2: antirepressor	9e-44
Orf50	Hypothetical protein	660/220	PHAGE_Mannhe_vB_MhS_1152AP2: CI repressor	1e-36
Orf51	Phage repressor protein	189/62	PHAGE_Salmon_vB_SemP_Emek_: Cro	1e-11
Orf53	Putative DNA-binding protein Roi of bacteriophage BP-933W	261/86	*P*asteurella *multocida*: antirepressor	1e-166
Orf55	Primosomal protein I	813/271	PHAGE_Aggreg_S1249: replication protein	3e-61
Orf56	Replication protein P	690/229	PHAGE_Mannhe_vB_MhS_587AP2: replication protein P	6e-23
Orf57	Putative DNA methylase	537/178	PHAGE_Mannhe_vB_MhS_587AP2: DNA N-6-adenine-methyltransferase	1e-55
Orf58	Phage NinB DNA recombination	426/142	PHAGE_Aggreg_S1249: putative recombination protein NinB	1e-44
Orf61	Phage NinG rap recombination	603/201	PHAGE_Salmon_SPN3UB: NinG	6e-45
Orf62	Hypothetical protein	366/121	PHAGE_Mannhe_vB_MhS_587AP2: antitermination protein Q	4e-10
Orf65	Haemophilus-specific protein/uncharacterised	66/21	PHAGE_Mannhe_vB_MhS_1152AP2: holin	9e-05

Table 5.12 Major protein products of ϕPM86.3 (PMλ6–like phage using PHAST and BLAST analysis.

Orfs	Protein product	Size (bp/aa)	BLAST_hit	E-value
Orf1	Phage integrase,	990/330	PHAGE_Mannhe_vB_MhS_535AP2: integrase	1e-99
Orf4	Single-stranded DNA-binding protein	459/153	PHAGE_Mannhe_vB_MhS_1152AP2: pyruvate kinase	8e-21
Orf9	DNA-cytosine methyltransferase	1293/430	PHAGE_Vibrio_vB_VchM_138: putative methylase	5e-82
Orf11	COG1896: Predicted hydrolases of HD superfamily	600/199	PHAGE_Salmon_ST64B: hypothetical protein sb35	1e-24
Orf21	Single-stranded DNA-binding protein	453/151	PHAGE_Vibrio_VvAW1: single-stranded DNA-binding protein	2e-39
Orf23	Phage-related exonuclease	615/204	PHAGE_Mannhe_vB_MhS_1152AP2: exonuclease	3e-88
Orf24	Phage recombination Beta protein	783/260	PHAGE_Mannhe_vB_MhS_1152AP2: recombinase	1e-83
Orf34	Putative prophage repressor CI	657/218	PHAGE_Mannhe_vB_MhS_1152AP2: CI repressor	2e-68
Orf35	Cro repressor-like protein	207/69	PHAGE_Mannhe_vB_MhS_1152AP2: Cro repressor	3e-20
Orf37	Uncharacterised phage-encoded protein	693/230	*Pasteurella multocida*: antirepressor protein	3e-175
Orf38	Primosomal protein I	813/271	PHAGE_Entero_mEpX1: DNA replication protein O	2e-13
Orf39	Replication protein P	699/232	Replicationprotein P	1e-25
Orf40	MunI-like protein	531/177	PHAGE_Mannhe_vB_MhS_1152AP2: methyltransferase	8e-90
Orf43	Serine/threonine protein phosphatase	641/216	PHAGE_Entero_HK630: NinI protein	9e-64
Orf48	Phage NinG rap recombination	597/198	PHAGE_Mannhe_vB_MhS_1152AP2: NinG protein	3e-37
Orf49	Hypothetical protein	462/153	PHAGE_Mannhe_vB_MhS_1152AP2: antitermination protein Q	5e-15
Orf50	Haemophilus-specific protein, uncharacterised	261/85	PHAGE_Mannhe_vB_MhS_1152AP2: holin	1e-11
Orf51	Putative phage lysozyme, lysin	531/176	PHAGE_Mannhe_vB_MhS_1152AP2: endolysin	3e-42
Orf52	Hypothetical protein	324/107	PHAGE_Mannhe_vB_MhS_1152AP2: lytic protein Rz	3e-06
Orf53	Uncharacterised protein HI1413	180/59	PHAGE_Mannhe_vB_MhS_1152AP2: lytic protein Rz1	5e-09
Orf61	Phage terminase, small subunit	591/196	PHAGE_Entero_phiEf11: phage terminase A domain protein	2e-08
Orf62	Phage terminase, large subunit	1272/424	Putative large terminase;	5e-117
Orf63	62kDa structural protein	1404/468	PHAGE_Mannhe_vB_MhS_1152AP2: portal protein	9e-154
Orf64	Hypothetical protein	1035/344	PHAGE_Mannhe_vB_MhS_1152AP2: head morphogenesis protein	1e-106
Orf66	Hypothetical protein	786/261	PHAGE_Xantho_Xp15: putative phage structural protein	2e-14
Orf67	Hypothetical protein	1158/385	PHAGE_Rhizob_vB_RglS_P106B: putative coat protein	4e-75
Orf76	Phage minor tail protein	441/145	PHAGE_Mannhe_vB_MhS_1152AP2: minor tail protein M	1e-26
Orf78	Phage tail assembly protein	603/201	PHAGE_Haemop_HP2: tail collar	2e-79
Orf81	Phage tail tape measure protein	2715/904	PHAGE_Mannhe_vB_MhS_1152AP2: tail length tape measure protein	0.0
Orf82	Phage minor tail protein	705/235	PHAGE_Mannhe_vB_MhS_1152AP2: minor tail protein L	2e-83
Orf83	Phage tail assembly protein	744/248	PHAGE_Mannhe_vB_MhS_1152AP2: minor tail protein K	2e-85
Orf84	Phage tail assembly protein I	406/135	PHAGE_Mannhe_vB_MhS_1152AP2: tail assembly protein I	1e-42
Orf85	Phage tail fibre protein	3342/1113	PHAGE_Mannhe_vB_MhS_1152AP2: host specificity protein J	0.0

5.3.2 Bacterial genome (intact prophages)

5.3.2.1 *Myoviridae* phages

PHAST analysis and CLC genomics workbench were used to investigate whether additional intact prophages belonging to the *Myoviridae* family type could be identified in the *P. multocida* genomes isolates. As described previously in Chapter 4, a diverse set of bacteriophages were identified by TEM in 29 isolates. However, phage DNA was only isolated from 18 isolates. Therefore, forty *P. multocida* genomes representing different hosts, capsular types, OMP types and ST types were selected to investigate whether the genomes contain intact prophages belonging to *Myoviridae* family and also to examine whether the isolates containing inducible Mu-like phages also possess additional non-inducible prophages. Viewing the bacterial genomes of the isolates using CLC genomics workbench identified multiple intact prophages. The prophages belonged either to the *Siphoviridae* or *to Myoviridae* families. The results showed that Mu-like phages were the common *Myoviridae* phage within the *P. multocida* genomes. Among the isolates containing Mu-like phages, two isolates, PM40 and PM486, contained additional non-inducible Mu-like phages. These phages designated as ϕPM40.4 and ϕPM486.3, respectively. The complete genomes of these Mu-like phages were obtained, annotated and analysed. However, certain isolates such as PM632 and PM344 contained more than two Mu-like phages but because the genomes were of poor quality, the Mu-like phages were distributed between different contigs. Therefore, only those Mu-like phages that could be obtained from a single contig were analysed (Table 5.13).

Phylogenetic analysis of annotated intact inducible and non-inducible Mu-like phages identified additional PMMu-like phages (Fig. 5.18). The phylogenetic tree showed that PMMu1 and PMMu2 were associated with isolates of the same lineage (section 5.3.1.1). PMMu1 was present only in avian, bovine and porcine isolates of lineage D and they used the same insertion site to integrate into the bacterial chromosome. However, this group was found to have a different insertion point site compared to the other PMMu-like phages.

Table 5.13 Genomic characterisation of 40 *P. multocida* isolates showing induced temperate bacteriophages and non-inducible prophages.

Isolate [a]	ST [b]	MLST group	Host species	Capsular type	OMP-type [c]	Type of lysis	Family type by TEM	No. of induced phage	Phage genome	Bacterial genome	Phage type	Phage family	*toxA* positive phage
PM316	1	A	Bovine	A	1.1	No lysis	None identified	-	None	None identified	None identified	None identified	-
PM564	1	A	Bovine	A	2.1	No lysis	None identified	-	None	None identified	None identified	None identified	-
PM344	3	A	Bovine	A	3.1	Partial	None identified	-	None	ϕPM344.1	Mu-like	*Myoviridae*	
										ϕPM344.2	F108-like	*Myoviridae*	
										ϕPM344.3	P2-like	*Myoviridae*	
										ϕPM344.4	λ-like	*Siphoviridae*	-
PM632	4	A	Bovine	A	4.1	Partial	None identified	-	None	ϕPM632.1	Mu-like	*Myoviridae*	
										ϕPM632.2	Mu-like	*Myoviridae*	
										ϕPM632.3	λ-like	*Siphoviridae*	-
										ϕPM632.4	λ-like	*Siphoviridae*	-
PM666	3	A	Porcine	A	2.1	Partial	*Siphoviridae*	-	None	ϕPM666.1	Mu-like	*Myoviridae*	
										ϕPM666.2	λ-like	*Siphoviridae*	-
PM116	3	A	Porcine	A	3.1	Partial	*Siphoviridae*	-	None	ϕPM116.1	Mu-like	*Myoviridae*	
										ϕPM116.2	Mu-like	*Myoviridae*	
										ϕPM116.3	λ-like	*Siphoviridae*	-
PM966	16	B	Ovine	A	1.1	Partial	*Siphoviridae*	-	None	ϕPM966.1	P2-like	*Myoviridae*	
PM382	13	C	Porcine	A	4.1	Complete	*Myoviridae*	+		ϕPM382.1	Mu-like	*Myoviridae*	
PM2	17	C	Ovine	F	2.1	No lysis	None identified	-	None	None identified	None identified	None identified	
PM246	25	C	Avian	F	2.2	Partial	None identified	-	None	None identified	None identified	None identified	
PM994	12	C	Ovine	F	1.1	No lysis	None identified	-	None	None identified	None identified	None identified	
PM148	12	C	Avian	F	2.2	No lysis	None identified	-	None	None identified	None identified	None identified	
PM86	15	D	Avian	A	3.1	Partial	*Myoviridae* & *Siphoviridae*	+	ϕPM86.1	ϕPM86.1	Mu-like	*Myoviridae*	
									ϕPM86.2	ϕPM86.2	PICI		
									ϕPM86.3	ϕPM86.3	λ-like	*Siphoviridae*	-
PM934	15	D	Porcine	A	5.1	Partial	*Myoviridae*	+	ϕPM934.1	ϕPM934.1	Mu-like	*Myoviridae*	
									ϕPM934.2	ϕPM934.2	PICI		
PM954	15	D	Porcine	A	5.1	Partial	*Myoviridae*	+	ϕPM954.1	ϕPM954.1	Mu-like	*Myoviridae*	
									ϕPM954.2	ϕPM954.2	PICI		

Table 5.13 (continued)

Isolate [a]	ST [b]	MLST group	Host species	Capsular type	OMP-type [c]	Type of lysis	Family type by TEM	No. of induced phage	Phage genome	Bacterial genome	Phage type	Phage family	*toxA* positive phage
PM486	9	D	Bovine	A	9.1	Partial	*Myoviridae*	+	ϕPM486.1	ϕPM486.1	Mu-like	*Myoviridae*	
									ϕPM486.2	ϕPM486.2	PICI		
										ϕPM486.3	Mu-like	*Myoviridae*	
										ϕPM486.4	λ-like	*Siphoviridae*	-
PM490	ND	ND	Bovine	A	9.1	ND	ND	ND	ND	ϕPM490.1	Mu-like	*Myoviridae*	
PM172	26	D	Avian	A	3.1	Partial	*Myoviridae*	+	ϕPM172.1	ϕPM172.1	Mu-like	*Myoviridae*	
									ϕPM172.2	ϕPM172.2	PICI		
PM302	6	E	Bovine	A	5.3	No lysis	None identified	-	None	ϕPM302.1	Mu-like	*Myoviridae*	
										ϕPM302.2	P2-like	*Myoviridae*	
										ϕPM302.3	F108-like	*Myoviridae*	
										ϕPM302.4	λ-like	*Siphoviridae*	-
PM144	21	E	Avian	A	1.1	No lysis	None identified	-	None	None identified	None identified	None identified	
PM402	5	E	Bovine	A	5.1	Partial	None identified	-	None	ϕPM402.1	λ-like	*Siphoviridae*	-
PM122	ND [d]	E	Ovine	D	3.1	Complete	*Siphoviridae*	+	ϕPM122.1	ϕPM122.1	λ-like	*Siphoviridae*	-
										ϕPM122.2	λ-like	*Siphoviridae*	+
PM964	18	E	Ovine	D	3.1	Complete	*Siphoviridae*	+	ϕPM964.1	ϕPM964.1	λ-like	*Siphoviridae*	-
										ϕPM964.2	λ-like	*Siphoviridae*	+
PM982	18	E	Ovine	D	3.1	Complete	*Siphoviridae*	+	ϕPM982.1	ϕPM982.1	λ-like	*Siphoviridae*	-
										ϕPM982.2	λ-like	*Siphoviridae*	+
PM986	18	E	Ovine	D	3.1	Complete	*Siphoviridae*	+	ϕPM986.1	ϕPM986.1	λ-like	*Siphoviridae*	-
										ϕPM986.2	λ-like	*Siphoviridae*	+
PM988	ND	ND	Ovine	D	3.1	Complete	*Siphoviridae*	+	ϕPM988.1	ϕPM988.1	λ-like	*Siphoviridae*	-
										ϕPM988.2	λ-like	*Siphoviridae*	+
PM54	10	F	Porcine	A	1.1	Partial	*Siphoviridae*	-	None	ϕPM54.1	Mu-like	*Myoviridae*	
										ϕPM54.2	Mu-like	*Myoviridae*	
										ϕPM54.3	λ-like	*Siphoviridae*	-
PM734	10	F	Porcine	A	1.1	Partial	None identified	-	None	ϕPM734.1	Mu-like	*Myoviridae*	
										ϕPM734.2	λ-like	*Siphoviridae*	-
PM850	10	F	Porcine	A	1.1	Complete	*Myoviridae* & *Siphoviridae*	+	ϕPM850.1	ϕPM850.1	Mu-like	*Myoviridae*	
									ϕPM850.2	ϕPM850.2	Mu-like	*Myoviridae*	
									ϕPM850.3	ϕPM850.3	λ-like	*Siphoviridae*	-
PM200	10	F	Avian	A	1.2	Complete	*Siphoviridae*	-	None	ϕPM200.1	Mu-like	*Myoviridae*	
										ϕPM200.2	Mu-like	*Myoviridae*	
										ϕPM200.3	F108-like	*Myoviridae*	
										ϕPM200.4	λ-like	*Siphoviridae*	-

Table 5.13 (continued)

Isolate [a]	ST [b]	MLST group	Host species	Capsular type	OMP-type [c]	Type of lysis	Family type by TEM	No. of induced phage	Phage genome	Bacterial genome	Phage type	Phage family	*toxA* positive phage
PM200										ϕPM200.5	λ-like	*Siphoviridae*	-
PM336	7	F	Bovine	A	6.1	Complete	*Siphoviridae*	+	ϕPM336.1	ϕPM336.1	λ-like	*Siphoviridae*	-
PM684	11	G	Porcine	A	6.1	Complete	*Myoviridae* &	+	ϕPM684.1	ϕPM684.1	Mu-like	*Myoviridae*	
							Siphoviridae		ϕPM684.2	ϕPM684.2	λ-like	*Siphoviridae*	-
									ϕPM684.3	ϕPM684.3	λ-like	*Siphoviridae*	+
PM918	11	G	Porcine	A	6.1	Complete	*Siphoviridae*	+	ϕPM918.1	ϕPM918.1	Mu-like	*Myoviridae*	
									ϕPM918.2	ϕPM918.2	λ-like	*Siphoviridae*	-
										ϕPM918 .3	λ-like	*Siphoviridae*	+
PM926	ND	ND	Porcine	A	6.1	Complete	*Siphoviridae*	+	ϕPM926.1	ϕPM926.1	Mu-like	*Myoviridae*	
									ϕPM926.2	ϕPM926.2	λ-like	*Siphoviridae*	-
										ϕPM926.3	λ-like	*Siphoviridae*	+
PM40	ND	ND	Porcine	A	6.2	Complete	*Myoviridae*	+	ϕPM40.1	ϕPM40.1	Mu-like	*Myoviridae*	
									ϕPM40.2	ϕPM40.2	λ-like	*Siphoviridae*	-
									ϕPM40.3	ϕPM40.3	λ-like	*Siphoviridae*	-
										ϕPM40.4	Mu-like	*Myoviridae*	
										ϕPM40.5	λ-like	*Siphoviridae*	+
PM848	11	G	Porcine	D	4.1	Complete	*Siphoviridae*	+	ϕPM848.1	ϕPM848.1	λ-like	*Siphoviridae*	-
									ϕPM848.2	ϕPM848.2	λ-like	*Siphoviridae*	+
PM696	11	G	Porcine	D	6.1	Partial	*Siphoviridae*	-	None	ϕPM696.1	λ-like	*Siphoviridae*	+
										ϕPM696.2	λ-like	*Siphoviridae*	-
PM714	11	G	Porcine	D	6.1	Partial	*Siphoviridae*	-	None	ϕPM714.1	λ-like	*Siphoviridae*	-
										ϕPM714.2	λ-like	*Siphoviridae*	-
PM226	11	G	Avian	D	13.1	Partial	*Siphoviridae*	-	None	ϕPM226.1	λ-like	*Siphoviridae*	-
										ϕPM226.2	λ-like	*Siphoviridae*	-
										ϕPM226.3	λ-like	*Siphoviridae*	-
PM82	32	H	Avian	A	7.1	No lysis	None identified	-	None	ϕPM82.1	λ-like	*Siphoviridae*	-

[a] isolates are arranged by order of MLST group (column 3) (Fig. 2.1); [b] ST= sequence type (Davies *et al*., unpublished http://pubmlst.org/pmultocida_multihost/); [c] OMP-types for bovine, ovine, porcine and avian are not equivalent, i.e. bovine OMP-type 1.1 is not as same as porcine OMP-type 1.1, etc. (Davies *et al.*, 2003a; b; c; Davies, 2004; Davies *et al.*, 2004); [d] ND: not determined.

PMMu2 included Mu-like phages induced only in porcine atrophic rhinitis isolates of MLST group G and of capsular type A, OMP-type 6.1 or 6.2, and ST 11 Interestingly, Mu2-like phages were not found in porcine atrophic rhinitis isolates PM848, PM696 and PM714 of capsular type D and in avian isolate PM226. PMMu2-type phages used the same insertion site to integrate into the bacterial chromosome. However, this group was found to have a different insertion point site compared to the other PMMu-like phages.

The PMMu3 phage group includes inducible phage ϕPM850.2, together with non-inducible phages ϕPM54.2 and ϕPM116.2; these were found in the genomes of porcine isolates PM850, PM54 and PM116, respectively (Table 5.13). PMMu3-type phage, were associated with porcine pneumonia isolates from two divergent phylogenetic lineages (MLST group A and F) (Fig. 5.18). Although these phages were identical, they integrated at different insertion points. ϕPM116.2 inserted at a different insertion points compared with ϕPM54.2 and ϕPM850.2. ϕPM850.2 was found to be inserted within type the II/IV secretion system, tadA subfamily gene. ϕPM54.2 was found to be inserted within type the DcaA gene.

PMMu4 includes inducible phage ϕPM850.1 as mentioned previously (section 5.3.1.1). This group also includes identical intact prophages from porcine isolates PM666 (ϕPM666.1) and PM116 (ϕPM116.1) from the bovine pneumonia lineage (OMP-types 1.2 and 3.1, ST 3 and MLST group A), from isolates PM54 (ϕPM54.1), PM734 (ϕPM734.1) and PM200 (ϕPM200.1) associated with porcine pneumonia group (OMP-types 1.1 and 1.2, ST 10 and MLST group F) and porcine isolate PM40 (ϕPM40.4) associated with atrophic rhinitis (capsular type A, OMP-type 6.2). A similar phage with 85% pairwise sequence similarity was also found in the genome of isolate PM486 (ϕPM486.3) (Fig. 5.18). ϕPM666.1 and ϕPM116.1 used a methyltransferase protein for integration, whereas, ϕPM54.1, ϕPM734.1, ϕPM850.1 and ϕPM40.4 integrated into the host chromosomes at a putative large exoprotein involved in haem utilization (belonging to the FhaA family). However, ϕPM486.3 inserted in the middle of a λ-like phage. Genome analysis showed that these phages were identical (100%) to the prophage remnant from *P. multocida* strain 3480 in NCBI database.

PMMu5 included two related phages, ϕPM382.1 and ϕPM302.1. ϕPM382.1 was induced in porcine isolate PM382 of capsular type A, OMP-type 4.1 and ST 13 (MLST group C) while ϕPM302.1 was obtained from the genome of bovine isolate PM302 of capsular type A, OMP-type 5.3 and ST 6 (MLST group E). These two phages used different integration points to insert into the host chromosome (Fig. 5.18 & Table 5.13). PMMu6 includes the two related non-inducible Mu-like phages ϕPM344.1 and ϕPM200.2. These phages were obtained from isolates of two different genetic lineages. Similarly, their insertions were different from each other and also from the other Mu-like phages. ϕPM344.1 obtained from the genome of bovine pneumonia isolate PM344 (capsular type A, OMP-type 3.1 and ST 3 (MLST group A), whereas, ϕPM200.2 was obtained from the avian isolate PM200 of capsular type A, OMP-type 1.2 and ST 10 (MLST group F). PMMu7 includes ϕPM632.1 obtained from bovine isolate PM632 of capsular type A, OMP-type 4.1 and ST 4 (MLST group A) (Fig. 5.18 & Table 5.13).

Pairwise nucleotide sequence similarities are shown in Table 5.14. From Fig. 5.18 it be seen that the inducible and non-inducible Mu-like phages were mostly associated with porcine isolates. However, bovine isolates PM344, PM632, PM302 and PM486 and avian isolates PM86, PM172 and PM200 contained Mu-like phages. Interestingly, neither inducible nor non-inducible Mu-like phages were found in any of the ovine isolates. The complete genome sequences of Mu-like phages representing each group were compared using progressive Mauve alignment (Fig. 5.19). The results showed that the Mu-like phages were very similar except for PMMu4 and PMMu7 which were different from the others.

To date only one *P. multocida* phage genome, named F108 has been published online yet. BlAST analysis identified a phage similar to F108 in isolates PM344, PM200 and PM302 and the phages were designated as ϕPM344.2, ϕPM200.3 and ϕPM302.3. P2-like phage was also identified in isolates from different genetic lineages and these isolates were PM344 (bovine), PM966 (ovine) and PM302 (bovine). These phages were designated as ϕPM344.3, ϕPM966.1 and ϕPM302.2. PHAST analysis showed that these phages showed similarity with the P2-like phages in *M. haemolytica,* especially phage 587AP1 (NC_028898). They have a GC content of 39% and consisted of 33,186 bp in length and encode 46 CDCs.

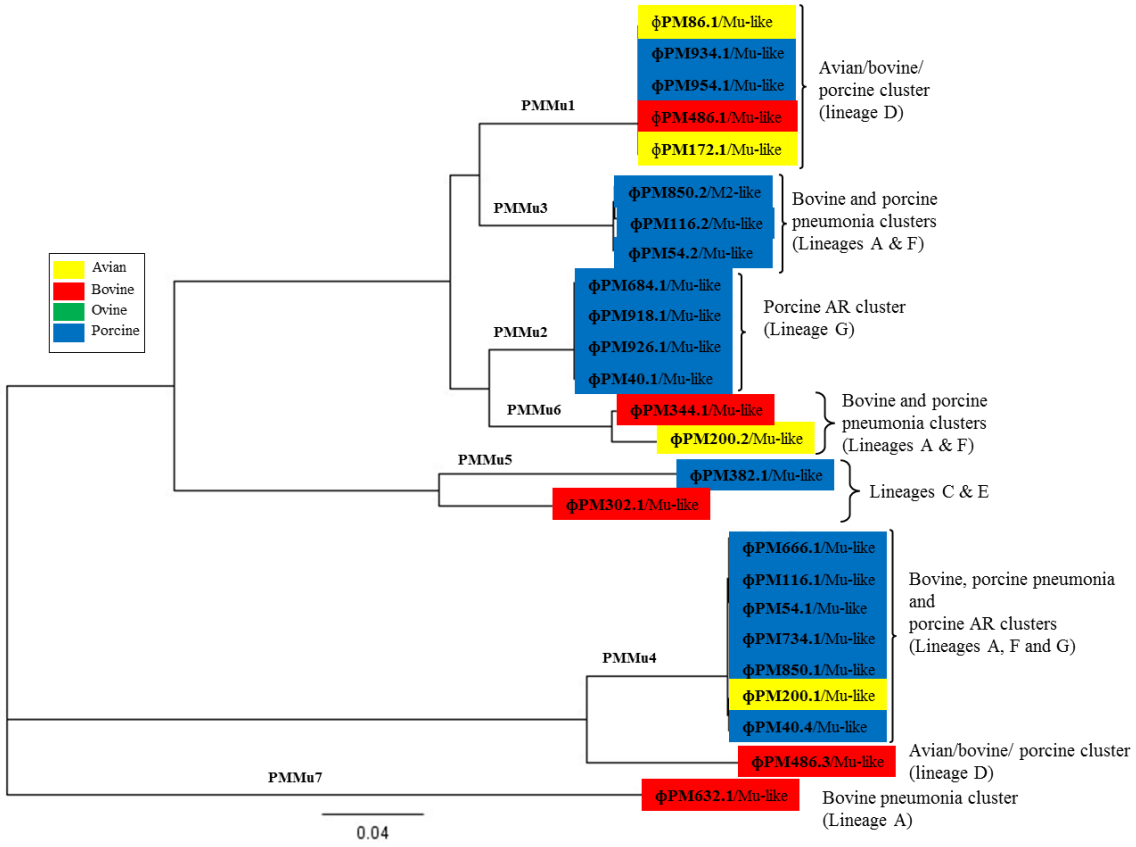

Fig. 5.18 Neighbour-Joining tree representing the phylogenetic relationships of inducible and non-inducible Mu-like phages in *P. multocida* isolates.

The phylogenetic tree was constructed with Jukes-Cantor correction using Geneious (v9.1.4). Each phage is abbreviated with the phage designation, followed by phage type.

Table 5.14 Pairwise nucleotide sequence similarity between inducible and non-inducible Mu-like phages of *P. multocida* isolates.

	PMMu1/ ϕPM86.3	PMMu2/ ϕPM684.1	PMMu3/ ϕPM850.2	PMMu4/ ϕPM850.1	PMMu4/ ϕPM486.3	PMMu5/ ϕPM382.1	PMMu5/ ϕPM302.1	PMMu6/ ϕPM344.1	PMMu6/ ϕPM200.2	PMMu7/ ϕPM632.1
PMMu1/ϕPM86.3										
PMMu2/ϕPM684.1										
PMMu3/ϕPM850.2										
PMMu4/ϕPM850.1										
PMMu4/ϕPM486.3										
PMMu5/ϕPM382.1										
PMMu5/ϕPM302.1										
PMMu6/ϕPM344.1										
PMMu6/ϕPM200.2										
PMMu7/ϕPM632.1										

Pairwise nucleotide sequence similarities were calculated using ClustalW alignment and EMBOSS Stretcher analysis. Different colours indicate difference in sequence similarity. Purple= 90%, green= 80-89%, red= 70-79%, blue= 60-69%, yellow= 50-49%, and grey= 40-49% sequence similarity.

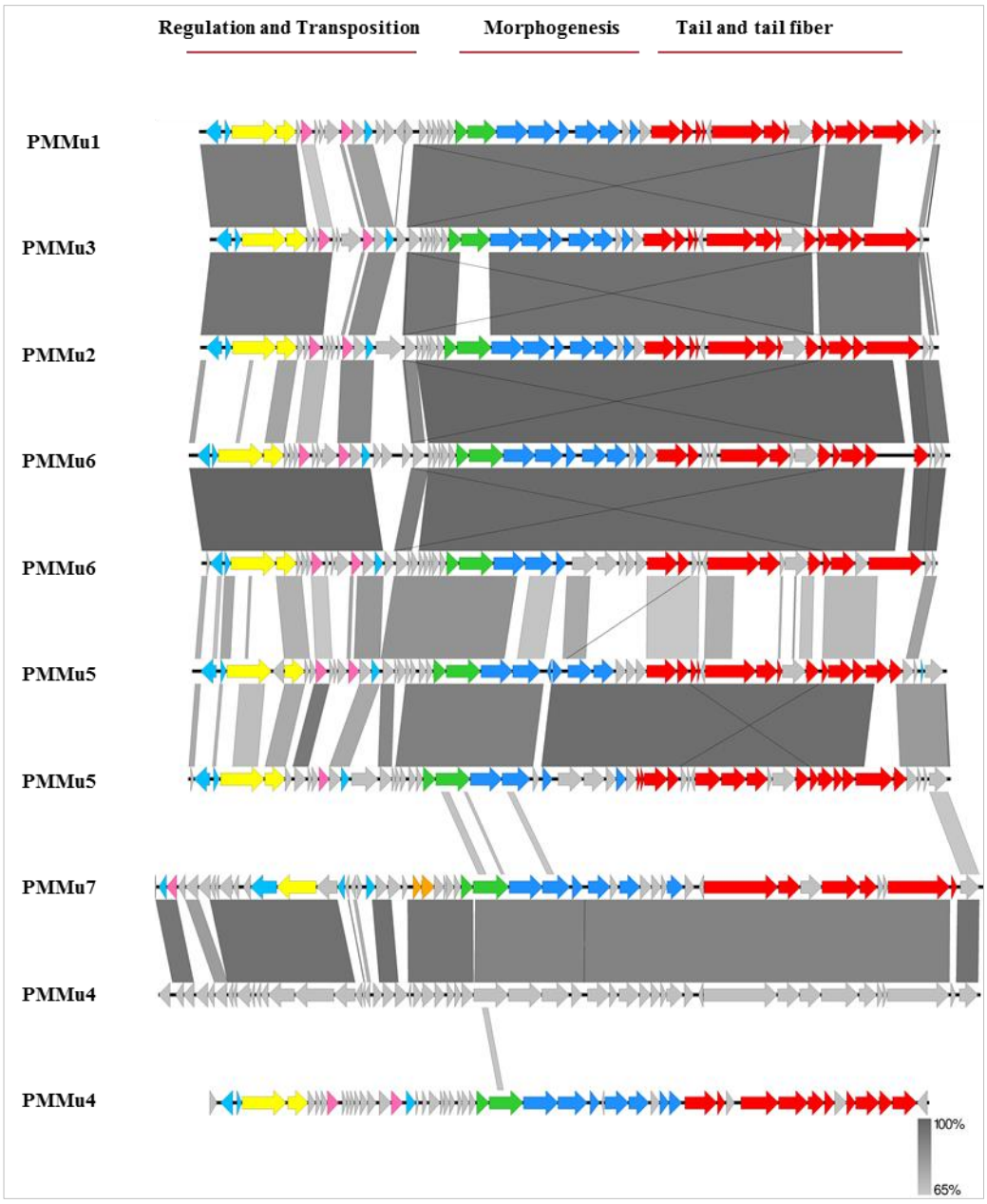

Fig. 5.19 Whole genome comparisons of the inducible and non-inducible Mu-like phages (PMMu1 to PMMu7) of *P. multocida.*

The sequence alignments were carried out using the BLASTn algorithm in Easyfig. The degree of sequence similarity is indicated by the intensity of the grey shading (darker grey indicates the highest sequence similarity). The position of genes within each genome is indicated by arrows

5.3.2.2 Non-inducible λ-like phages

PHAST analysis together with manual inspection using CLC genomics workbench identified additional intact non-inducible λ-like prophages alongside the inducible phage identified in 18 *P. multocida* isolates. The overall results of genome analysis are shown in Table 5.13. Isolates PM486 contained a λ-like phage which was designated ϕPM486.4. Two porcine atrophic rhinitis strains of capsular type A, PM918 and PM926 contained additional λ-like phage within their genomes and these phages were designated as ϕPM918.3 and ϕPM926.3. The complete genome alignment of ϕPM918.3 and ϕPM926.3 showed that these phages were 100% identical to phages ϕPM684.3 and ϕPM848.2 (PMλ2-like phage) where were also associated with porcine isolates (Fig. 5.20). Phages ϕPM918.3 and ϕPM926.3 also contained the gene encoding PMT (Fig. 5.20).

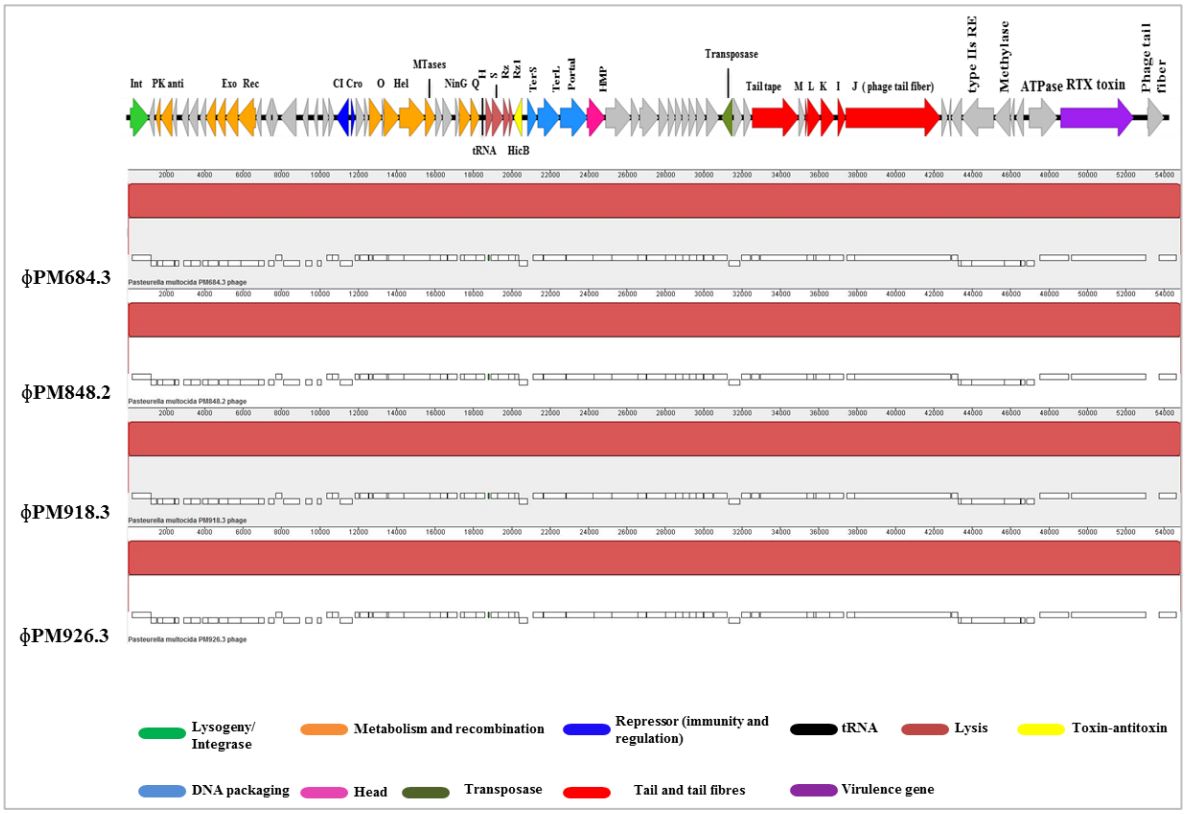

Fig. 5.20 Genomic structure and multiple nucleotide sequence alignment of *P. multocida toxA* positive λ-like phages ϕPM684.3, ϕPM848.2, ϕPM918.3 and ϕPM926.3.

The complete genome alignment of non-inducible phages ϕPM918.3 and ϕPM926.3 showed that these phages were 100% identical to the inducible phages ϕPM684.3 and ϕPM848.2 (PMλ2-like phage). In addition, they also carry PMT within their genomes. The genomic maps were constructed using Easyfig. The four genomes were aligned using a progressive MAUVE alignment.

Two porcine atrophic rhinitis strains of capsular type A, PM918 and PM926 contained additional λ-like phage within their genomes and these phages were designated as ϕPM918.3 and ϕPM926.3. The complete genome alignment of ϕPM918.3 and ϕPM926.3 showed that these phages were 100% identical to phages ϕPM684.3 and ϕPM848.2 (PMλ2-like phage)

The genomic analysis of *P. multocida* isolates PM40 and PM696 identified another λ-like phage carrying gene encoding PMT and these phage designated as ϕPM40.5 and ϕPM696.1. Phage ϕPM40.5 and ϕPM696.1 were 100% identical.

The genomes of ovine capsular types D isolates PM122, PM964, PM982, PM986 and PM988 are also *toxA* positive. The presence of the *toxA* gene in these ovine isolates suggests that the gene may have been transferred horizontally from the porcine strains to the ovine through mobile elements such as bacteriophages. The sequencing of the inducible phage genomes showed the presence of only one λ-like phage and the analysis of these phage genomes showed that the phage ϕPM122.1, ϕPM964.1, ϕPM982.1, ϕPM986.1 and ϕPM988.1 did not contain the *toxA* gene encoding PMT. Analysis of the whole bacterial genome revealed the presence of another integrase and mapping to the HN06 genome revealed the presence of the *toxA* gene within the phage genes (section 5.3.3). However, the genomes of isolates PM122, PM964, PM982, PM986 and PM988 were, unfortunately of poor quality. Therefore, complete phage genomes containing *toxA* were not obtained and the data is not shown.

Bovine isolate PM302 contained a λ-like phage, ϕPM302.4 which was similar to ϕPM982.1. Porcine isolate PM734 contained a prophage, ϕPM734.2 that was identical to ϕPM850. Phage ϕPM734.2 was distributed between two different contigs. The contigs were closed by targeted PCR and sequencing using the same primers used for completing ϕPM850.3 as explained in Fig. 5.2 & Table 5.3.

Avian isolate PM200 (MLST group F) also contained two additional λ-like prophages, ϕPM200.4 and ϕPM200.5; these were identical to ϕPM54.3 and ϕPM850.3, respectively. Isolates PM54, PM116 and PM666 also contained intact λ-like prophages which were similar to some extent; and this type phage was not induced among the *P. multocida* isolates. The phages shared the same genomic organisation and attachment sites and were designated as ϕPM54.3, ϕPM116.3

and ϕPM666.2. BLAST analysis of the integrase-encoding gene showed 100% similarity with the integrase-encoding gene of intact prophages within the genomes of *P. multocida* on the NCBI database, especially *P. multocida* strains 3480 and HN06. Overall, the results showed that the majority of *P. multocida* isolates carry λ-like prophages and the phages within strain in the same genetic lineage (as determined by MLST) were similar to each other. Isolate PM714 carried two prophages, ϕPM714.1 and ϕPM714.2. Phage ϕPM714.1 was similar to ϕPM848, whereas ϕPM714.2 was similar ϕPM696.2 and ϕPM226.3. Isolate PM226 contained three different λ-like prophages. These phages were designated as ϕPM226.1, ϕPM226.2 and ϕPM226.3 and they were similar to ϕPM200.4, ϕPM696.1 and ϕPM696.2, respectively. PM82 carried only a single λ-like phage which was similar to phage ϕPM696.2, ϕPM714.2 and ϕPM226.3.

Variation between strains within the bovine pneumonia lineage (MLST group A) was also found (Table 5.13). Surprisingly, no prophages were identified within the genomes of isolates PM316 and PM564. Both PM316 and PM564 are bovine isolates associated with bovine pneumonia. These isolates are of capsular type A, OMP-type 1.1 and 2.1 and ST 1 (MLST group A). However, prophages were identified within the genome of isolates PM344, PM632, PM666 and PM116. These isolates are also associated with the bovine pneumonia cluster (MLST group A), but they are of OMP-types 2.1 to 4.1 and STs 3 and 4. Furthermore, no prophages were identified within the genomes of avian and ovine capsular type F, isolates PM2, PM246, PM994, PM148 (OMP-types 1 and 2, STs 17, 25 and 12 and MLST group C). These details are described in Table 5.13.

5.3.3 Bacteriophages-encoded virulence genes

Complete genome analysis of induced phages (λ-like and Mu-like) revealed the induction of bacteriophage-encoding virulence determinants. Bacteriophage-encoding virulence factors in *P. multocida* were found to be associated with λ-like phages but not with Mu-like phages. Genomic analysis identified two functional phages, ϕPM684.3 and ϕPM848.2 belonging to the lambdoid family which carry the *Pasteurella multocida* toxin (PMT) gene. These two phages were distributed between different contigs and the complete genomes were obtained by targeted PCR and sequencing (section 5.3.1.4). They were induced spontaneously and shared 100% genome identity. The complete genomes of

ϕPM684.3 and ϕPM848.2 consist of 54 bp, a GC content of 38.9%, encoded 74 CDCs and have one tRNA site (Fig. 5.20 &Table 5.9).

Both PM684 and PM848 are toxigenic porcine isolates associated atrophic rhinitis; this group also includes other toxigenic strains including PM918, PM926, PM40 and PM696. However, genomic analysis of phage DNA from PM918, PM926 and PM40 showed that the phage-encoded PMT gene was not induced. The reasons why toxin-encoded phages were not induced is unclear. It could be due to the method of induction or the existence of multiple prophages within the bacterial genomes which may develop competitive interaction of prophages during induction; they could also be non-functional. However, genomic analysis of isolates PM918, PM926, PM40 and PM696 identified PMT-encoded bacteriophages within the genomes. These phages were designated as ϕPM918.3 ϕPM926.3, ϕPM40.5 and ϕPM696.1. BLASTn analysis showed that ϕPM918.3 and ϕPM926.3 were identical to ϕPM684.3 and ϕPM848.2 and they possessed the same attachment site. They were also found to be distributed between different contigs and the gaps were closed (section 5.3.1.4). ϕPM684.3 and ϕPM848.2 were found to have inserted into the genomes in a tRNA-leu gene which was located downstream to gene encoding SecG and upstream to RNA polymerase sigma-70 factor. The following phages shared the same attachment sites, ϕPM86.3, ϕPM122.1, ϕPM336.1, ϕPM964.1, ϕPM982.1, ϕPM986.1 and ϕPM988.1.

However, different PMT-encoding bacteriophages were found in isolates PM40 and PM696. Phages ϕPM40.5 and ϕPM696.1 were different and used different attachment sites to integrate into the host chromosomes when compared with ϕPM684.3 and ϕPM848.2. These phages were identified by mapping to the reference genome HN06 on NCBI database (GeneBank: NC_017027). *Pasteurella multocida* strain HN06 is a porcine toxigenic strain of serogroup D containing prophage-encoded PMT gene (*toxA*). ϕPM40.5 and ϕPM696.1 shared the same integrase, identical attachment sites and same genomic organisation with the HN06. Phages ϕPM40.5 and ϕPM696.1 were found to have inserted into the genomes in a tRNA-trp gene, the same as ϕPM850.3 (section 5.3.1.4). They had 77.1% and 64% pairwise sequences similarity with HN06 and ϕPM848.2.

The PMT-encoding gene (*toxA*) was also found in the genomes of other isolates using CLC genomics workbench and an internal BLAST tool. These included the

ovine capsular type D, isolates PM122, PM964, PM982, PM986 and PM988. Only one functional phage, ϕPM122.1, ϕPM964.1, ϕPM982.1, ϕPM986.1 and ϕPM988.1 was induced in each of these ovine isolates. Genomic analysis showed that these phages were not carrying the PMT-toxin gene, although these phages shared the same ϕPM684.3 and ϕPM848.2 attachment sites and they were induced spontaneously. In addition, they exhibited 74% pairwise similarities with ϕPM684.3 and ϕPM848.2. However, genome analysis of isolates PM122, PM964, PM982, PM986 and PM988 revealed that the PMT-encoded gene was found to be part of a different bacteriophage. Internal BLAST of the integrase gene identified a similar integrase in porcine isolates PM54, PM116, and PM666 and also in the reference genomes HN06 and 3480. The prophages in these genomes do not encode the PMT gene. The prophages in isolates PM122, PM964, PM982, PM986 and PM988 shared identical attachment site to the intact prophages PM54, PM116, and PM666 and also to the reference genomes HN06 and 3480. These phages were found to have inserted into the genomes in a tRNA-Ala gene at the region between genes encoding glutamyl-tRNA synthetase and polynucleotide phosphorylase. However, we were unable to construct the complete genome of these phages because the genomes were of poor quality even when mapped to the reference genome. Another reason for that could be that these phages are incomplete phages in the genomes of PM122, PM964, PM982, PM986 and PM988.

5.4 Discussion

As described previously in Chapter 4, temperate bacteriophages were induced with mitomycin C in a panel of *P. multocida* strains representing multiple host species, clinical symptoms, capsular types, OMP-types and ST types. Phage morphology was assessed using electron microscopy, host ranges were determined and genetic relatedness examined by restriction endonuclease enzymes. The results showed the presence of a diverse range of phage morphologies belonging either to the *Siphoviridae* or *Myoviridae* families. The results indicated that *P. multocida* bacteriophages are relatively diverse and may be genetically different, because 10 different RE types were identified in only 18 phage DNA samples. Therefore, 18 phage DNA samples and the whole genome of 40 *P. multocida* isolates were sequenced using the Illumina Mi-Seq platform to conduct the comparative genome analysis of induced bacteriophages from *P. multocida* strains and to identify the presence of intact prophages within the *P. multocida* genomes.

Induction of multiple prophages in certain isolates indicates that a single host harbours multiple prophages (Canchaya *et al.*, 2003; Hsu *et al.*, 2013; Niu *et al.*, 2015). So far, the induction of multiples phage types from a single *P. multocida* strain has not been described. *P. multocida* genome analysis identified multiple Mu-like and λ-like phages within the genome. Although, in isolates PM916, PM926 and PM40, one phage type belonging to either the *Siphoviridae or Myoviridae* families was identified by TEM, sequencing of phage DNA revealed that both Mu-like (*Myoviridae*) and λ-like (*Siphoviridae*) phages co-existed in the genomes of isolates PM918, PM926 and PM40. The reason why additional phage types were not found by TEM was unclear. It could possibly indicate that the quantity of one phage type was higher than the others, although the same induced preparations were used both TEM and DNA extraction. The induction of multiple phages in a single host was common in closely related *M. haemolytica* strains (Hsu *et al.*, 2013; Niu *et al.*, 2015) and in other bacteria such as in the *E. coli*, *Streptococcus pyogenes* and *Bacillus subtilis* genomes (Canchaya *et al.*, 2003). Genomic analysis identified additional intact prophages within the bacterial genomes of 40 isolates. The results identified from one to five intact prophages and prophage-like elements within the genomes of *P. multocida* strains. These findings suggest that the presence of multiple phages within one genome may

play a role in the genetic diversity of *P. multocida*, and in transferring virulence genes and other genetic material between strains. Comparative genomics analysis of bacterial genomes have revealed that prophages are common in bacterial genomes (Canchaya *et al.*, 2003; Casjens, 2003; Fortier & Sekulovic, 2013). Studies have shown that prophages are one of the main sources of genetic diversity and strain variation associated with the virulence of many bacterial pathogens including *E. coli* (Ohnishi *et al.*, 2001; Weinbauer & Rassoulzadegan, 2004), *S. enterica* (Cooke *et al.*, 2007), *S. aureus* (Rahimi *et al.*, 2012); and *S. pyogenes* (Aziz *et al.*, 2005). In *E. coli* strain O157 Sakai, bacteriophages were shown to be major contributors to the genetic diversity of the species due to the acquisition of new DNA though transduction (Weinbauer & Rassoulzadegan, 2004). The genome of *E. coli* strain O157 Sakai contains 18 prophages and prophage-like elements accounting for approximately 50% of site-specific genomic DNA sequences, suggesting that phages contribute to the emergence of new strains (Weinbauer & Rassoulzadegan, 2004).

P2-like phages were identified among the induced phage. PHAST analysis of *P. multocida* genomes showed that P2-like phages were not common in the genomes and were identified in only three of 40 genomes (PM344, PM996 and PM302). PHAST analysis and BLAST analysis demonstrated similarities of 46% with *M. haemolytica* P2-like phages, particularly 587AP1 (Niu *et al.*, 2015). Thus, P2-like phages are not common in *P. multocida*. However, P2-like phages have been induced and sequenced from the *Pasteurellaceae* family. The genomes of *H. influenzae* phages HP1 and HP2, have been sequenced and both are P2-like phage (Esposito *et al.*, 1996; Williams *et al.*, 2002). Likewise, the genomes of five *M. haemolytica,* phage, ϕMhaA1-PHL101, vB_MhM_1152AP, 535AP1, 587AP1 1127AP1 and 2256AP1, have been sequenced and all are of P2-like phages (Highlander *et al.*, 2006; Hsu *et al.*, 2013; Niu *et al.*, 2015).

The findings of temperate bacteriophage characterisation using TEM and DNA extraction suggested the presence of PICIs in isolates PM86, PM172, PM486, PM934 and PM954. These isolates are associated with avian, bovine and porcine isolates of capsular type A, OMP-types 3, 5 and STs 9, 26 and 15 (MLST group D). In order to confirm this, we carried out Southern blot hybridisation using prepared labelled probes. The results showed that Mu-like phages were packaged in a large capsid and also in small-sized capsids. PICIs use helper phage

for their propagation, which produce small capsids to fit their smaller genomes. PICIs are satellite phages that have an intimate relationship with temperate (helper) bacteriophages (Penadés & Christie, 2015). *S. aureus* pathogenicity islands (SaPIs) are a well-studied PICI (Novick *et al.*, 2010; Penadés & Christie, 2015; Tormo *et al.*, 2008; Úbeda *et al.*, 2005). Following infection by the helper phage or induction of the helper phage with antibiotics, the PICI genomes are able to excise, replicate using its own replicon and encapsidate into special small phage heads to fit their smaller genome (Tormo *et al.*, 2008; Úbeda *et al.*, 2005). This is the first description of PICIs in *P. multocida*.

Induction of Mu-like phages was more common among the *P. multocida* porcine strains of different capsular, OMP and ST types. This suggests that Mu-like phages may contribute to virulence of *P. multocida* porcine strains. It has been shown previously in the closely related species *H. parasuis,* a Mu-like bacteriophage SuMu portal gene was found to be present in 90% of virulent porcine strains, suggesting the SuMu phage may contribute to virulence of *H. parasuis* (Zehr & Tabatabai, 2011; Zehr *et al.*, 2012). Functional Mu-like phages have also been isolated and sequenced in many bacterial species. These phages are *Haemophilus* phage SuMu (NC_019455) (Zehr *et al.*, 2012), *Mannheimia* phage vB_MhM (3927AP2) (Niu *et al.*, 2015), *Burkholderia* phage BcepMu (NC_005882) (Summer *et al.*, 2004), *Pseudomonas* phage vB_PaeS_PM105 (NC_028667) (Pourcel *et al.*, 2016), and *Enterobacteria* phage SfMu (NC_027382) (Jakhetia & Verma, 2015). Mu-like phages induced in this study showed the same genomic organisation of other Mu-like bacteriophages particularly SuMu, 3927AP2, PaeS_PM105, BcepMu and SfMu phages by BLAST analysis. They exhibited 40-47% pairwise sequences similarity. Comparative studies have confirmed that members of the Mu-related family of phage genomes are genetic mosaics with respect to each other (Morgan *et al.*, 2002). Mu-like phage of *P. multocida*, particularly PMMu1, PMMu2, PMMu3 and PMMu6 were similar to the prophages in the genomes of *H. influenzae* 2019, *H. influenzae* F3031 and the *H. influenzae* biotype *aegyptius*. This suggests that the *P. multocida* Mu-like phages are closely related to these of the genus *Haemophilus*.

Seven different Mu-like phages were identified in *P. multocida* and identical phages were identified in isolates within the same phylogenetic lineage, although there were some exceptions. These findings support the evolutionary

relationships of *P. multocida* isolates from multiple hosts based on MLST data. It also suggests that identical Mu-like phages are adapted to isolates of the same, or closely related genetic lineage. Interestingly, no Mu-like phages were found within the ovine strains or within porcine atrophic rhinitis strains of capsular type D, OMP-types 4.1, 6.1 and 13.1 and ST 11. Genome analysis showed that intact Mu-like prophages were common in the *P. multocida* genome. Mu-like prophages have also been identified in the genomes of *H. influenzae* (FluMu), *N. meningitidis* (PmM1), *Deinococcus radiodurans* R1 (RadMu) (Morgan *et al.*, 2002) and *E. coli* O157 Satai (Sp10) (Hayashi *et al.*, 2001).

One of the characteristics features of Mu-like phages is that they integrate randomly at any location in the host chromosome via transposition (Faelen & Toussaint, 1976). Random integration may lead to mutation of genes by transcription at the site of insertion or integration (Zehr *et al.*, 2012). *P. multocida* Mu-like phages use a transposase to integrate into the bacterial chromosome where they integrate at random locations. Although, some Mu-like phages were identical, they use different random points to insert although phages from the same lineage use the same insertion point to integrate into the host chromosome. Mu-like phages also package some chromosomal DNA which may lead to the transduction of host DNA (Faelen & Toussaint, 1976). Transposase-encoding genes have also been found within the λ–like phage genomes induced in *P. multocida* and their presence may contribute to the acquisition of new foreign genes. Similar finding have been identified in P2-like phages of *Burkholderia cepacia* (Lynch *et al.*, 2010) and P2-like and λ–like phage genomes induced in *M. haemolytica* (Niu *et al.*, 2015).

Seven different λ-like phages were induced in *P. multocida* isolates. Phages with identical genomes were associated with isolates of the same genetic lineage. Sequencing of seven different λ-like phages indicates the genetic diversity of λ-like phages in *P. multocida*. To date, the complete genome sequence of temperate phage Aaphi23 of *A. actinomycetemcomitans* (Resch *et al.*, 2004) and 535AP2, 587AP2, 1152AP2 and 3927AP1 (Niu *et al.*, 2015) have been published from the *Pasteurellaceae* family. BLAST analysis showed very low (39-405) sequence similarity with the *A. actinomycetemcomitans*. However, PHAST analysis showed similar hits with the genomes of closely related *M. haemolytica* phages particularly 1152AP2, 535AP2 and 587AP2 (Niu *et al.*, 2015), although

pairwise nucleotide sequence similarities were only 40-48%. Likewise, the degree of amino acid similarity for each gene was relatively low, indicating the highly mosaic nature of lambdoid phage genomes. Identical λ-like phages were induced in strains of the same genetic lineages, supporting the evolutionary relationships among *P. multocida* isolates from multiple hosts based on MLST data. For example, ϕPM684.2, ϕPM918.2, ϕPM926.2, ϕPM40.2 and ϕPM848.1 were found only in isolates of the porcine atrophic rhinitis group and they did not carry the gene encoding PMT. These phages were closely related to intact prophage remnants from the genome of porcine strain HN06 in NCBI and showed 94.7% pairwise nucleotide similarity. The gene encoding methyltransferase was identified in all induced λ-like phages. The function of methyltransferase in phages is still unclear and there is no publication on the role of methyltransferase in phage conversion but it may play a role in regulation of the phage life cycle (Bochow *et al.*, 2012). Further analysis will be required to investigate the role of methyltransferase within the phage genomes.

PHAST analysis detected additional intact prophages in the genome of *P. multocida* isolates and it was not clear why some phages were not induced. It has been suggested that this could be due to the occurrence of the competitive interactions between phages during induction (Niu *et al.*, 2015), or this could be due to the method of induction the phage may be no longer active. However, in *Clostridium difficile* 027 strains the capacity of two antibiotics mitomycin C and norfloxacin to induce temperate bacteriophages was compared (Nale *et al.*, 2012) and the results revealed that two antibiotics induced specific bacteriophages from *Clostridium difficile* 027 strains (Nale *et al.*, 2012). Likewise, it has been shown that prophages Lp1 and Lp2 (two are about 40 kb long) as members of Sfi11-like, *Siphoviridae* in *Lactobacillus plantarum* strain WCFS1 were non-inducible using mitomycin C (Ventura *et al.*, 2003).

Temperate bacteriophages, especially those encoding virulence genes, have been shown to play an important role in bacterial pathogenesis (Boyd & Brüssow, 2002; Boyd, 2012; Fortier & Sekulovic, 2013; Penades *et al.*, 2015). Bacteriophage-encoded virulence determinants can transform their host from a commensal to a pathogen or virulent strain by lysogenic conversion (Allison, 2007; Boyd & Brüssow, 2002; Boyd, 2012; Veses-Garcia *et a*l., 2015). Such bacteriophage-encoded virulence genes provide mechanisms that enable

attachment, invasion, survival and damage to host cells (Boyd & Brüssow, 2002; Boyd, 2012). A variety of toxins expressed by pathogenic bacteria represent phage-encoded virulence factors. Examples of well-studied phage-encoded toxins include diphtheria toxin, botulinum toxin, exfoliative toxin, Shiga-like toxin, cytotoxin and cholera toxin (Boyd, 2012; Brüssow *et al.*, 2004; Cheetham & Katz, 1995; Saunders *et al.*, 2001). It is well known that λ-like phage encode virulence genes and this contributes to the emergence of new pathogenic strains (Allison, 2007). In *P. multocida*, it has been suggested that PMT is encoded within temperate bacteriophages in porcine strains (Pullinger *et al.*, 2004). In the present study, sequence analysis revealed that two identical functional λ-like phages, ϕPM684.3 and ϕPM848.2, carried the PMT-encoded gene. These phages showed 70% pairwise similarity with a prophage remnant encoding PMT from the genome of porcine strain HN06. However, comparative analysis of phage genomes from toxigenic porcine isolates PM918, PM926 and PM40 showed that bacteriophage-encoded PMT was not induced. Genome analysis identified bacteriophages encoding PMT in PM918, PM926, PM40 and PM696.

It has been mentioned that *toxA* may have been horizontally transferred to ovine strains (Einarsdottir *et al.*, 2016; Shayegh *et al.*, 2008; Weiser *et al.*, 2003). Using CLC genomic workbench internal BLAST tool, the PMT-encoding gene was identified in ovine isolates PM122, PM964, PM982, PM986 and PM988, suggesting that *toxA* could be transferred by bacteriophages. TEM results revealed the presence of only *Siphoviridae*-type phages and phage genome analysis also revealed the presence of only one λ-like phage (ϕPM122, ϕPM964, ϕPM982, ϕPM986 and ϕPM988). Comparative genome analysis showed that these phages did not carry the *toxA* gene. However, genome analysis of these isolates and mapping to the reference genome showed that PMT is encoded by another phage, although it was not possible to obtain the complete genome sequence because they were in complete. To date, no study has confirmed the presence of the *toxA* gene within the genome of bacteriophages from ovine isolates. Bacteriophages-encoded PMT were associated with a different integrase and they used different attachment sites. Likewise, heterogeneity in integrase genes amongst *stx* phages was observed in LEE-negative Shiga toxin-producing *E. coli* (Steyert *et al.*, 2012).

In conclusion, nucleotide sequence analysis of phage genomic DNA from the *P. multocida* isolates revealed induction of Mu-like, λ-like phage and PICIs. The results also demonstrated that both λ-phage and Mu-like phages are induced in the same isolates of *P. multocida*. The results also confirmed the presence of PICIs in *P. multocida* isolates PM86, PM172, PM486, PM934 and PM954. This is the first description of PICIs in *P. multocida*. The results also revealed that more than one λ- and Mu-like phages were induced in the majority of isolates. Nucleotide sequence analysis of λ-phage genomes induced in toxigenic porcine strains of capsular types A and D demonstrated the presence of the *toxA* gene.

Chapter 6 General discussion and conclusion

Pasteurella multocida is a Gram-negative commensal bacterium which resides in the upper respiratory tract of mammals and birds. The organism is responsible for a variety of economically important diseases in a wide range of domestic animal species. It causes fowl cholera of poultry, haemorrhagic septicaemia of cattle and water buffalo, atrophic rhinitis of pigs, and pneumonia of cattle, sheep and pigs. The aim of this study was to use comparative genomic approaches to investigate the molecular evolution of genes encoding the predicted outer membrane proteome in selected isolates recovered from these different host species. In particular, a major objective was to assess the role of horizontal DNA transfer and recombination (intragenic and assortative) in the evolution of these genes. Since previous studies have demonstrated that *ompA* is a highly diverse gene, and plays an important role in pathogenesis, this gene was sequenced in an expanded collection (74) of isolates to further examine the roles of horizontal DNA transfer and recombination in its evolution.

Since bacteriophages are known to mediate horizontal gene transfer events, another goal was to characterise the temperate bacteriophages of *P. multocida* with the aim of determining whether they carry any virulence genes, especially OMP- and toxin-encoding genes. In this study, *P. multocida* isolates were selected based on an established framework of evolutionary relationships among 123 isolates of *P. multocida* based on the concatenated partial sequences (3990 bp) of seven housekeeping enzyme genes (Davies *et al.*, unpublished; http://pubmlst.org/pmultocida_multihost). The isolates were recovered from different host species (cattle, sheep, pigs and poultry) and were associated with different disease syndromes they have been characterised in previous studies (Davies *et al.*, 2003a; b; c; Davies, 2004; Davies *et al.*, 2004). The isolates represented various capsular serotypes, OMP-types, 16S rRNA types, and sequence types. Comparative nucleotide sequence analysis has been used as an effective method for understanding the diversity and evolutionary relationships among various bacterial species (Bastardo *et al.*, 2012; Chaudhuri & Henderson, 2012; Feil *et al.*, 1999; Lemée *et al.*, 2005; Maiden *et al.*, 1998; Mullins *et al.*, 2013; Naushad *et al.*, 2015). It has shown that horizontal DNA transfer and recombination are involved in the diversification of various virulence factors

including OMPs (Bart *et al.*, 1999; Davies & Lee, 2004; Lee & , 2011 ; Evans *et al.*, 2010; Ford, 2001),

Phylogenetic trees were constructed based on the concatenated sequences (22,731 bp) of 15 housekeeping genes and on the core genome for 40 *P. multocida* isolates. These trees were compared with the MLST tree for 123 *P. multocida* isolates associated with different diseases in different host species (cattle, sheep, pigs and poultry). Both trees were almost identical to the phylogenetic tree based on the concatenated partial sequences of seven housekeeping genes. The phylogenetic relatedness based on seven and fifteen housekeeping enzyme genes, and on the core genome, showed a correlation between phylogenetic cluster and association with specific hosts and disease types. The clustering of isolates associated with different host species suggests that certain lineages have evolved with/become adapted to specific hosts. Exceptions include the bovine and porcine strains within the bovine pneumonia cluster (MLST group A). This cluster is represented by the majority of the bovine pneumonia isolates of capsular type A, OMP-type 2.1, 3.1 and 3.2 and ST 3 but also includes certain porcine isolates of capsular type A and ST 3 (OMPS-types 2.1, 3.1 and 3.2). These findings clearly indicate that the bovine and porcine isolates of cluster A have a common ancestral origin. It is possible that the porcine isolates have been derived from bovine isolates but have cross the species barrier (by host-switching) and have subsequently become adapted to pigs by acquisition of specific genes from resident pig strains. Another example is that of the single bovine isolates PM306 of capsular type F (OMP-type 7.1 and ST 8) which clustered with avian and ovine serotype F isolates (MLST group C). Isolate PM306 was isolated from infected calves that were kept in the cattle shed that poultry had been previously housed (Jones *et al.*, 1988). This suggests that isolates PM306 may have had an avian origin.

In the current study, comparative nucleotide sequence analysis of genes encoding predicted OMPs of different functions was carried out in 40 isolates of *P. multocida* to the roles horizontal DNA transfer, recombination and host switching in the evolution and diversification of *P. multocida*. Many OMPs are surface-exposed proteins and are, therefore, subject to different diversification selection pressure and inter-strain heterogeneity (Davies *et al.*, 2004). Molecular mass heterogeneity of the *P. multocida* major OMPs OmpA and OmpH was

identified based on OMP profiles of *P. multocida* isolates of avian, bovine, ovine and porcine origin (Davies *et al.*, 2003a; b; c; Davies, 2004; Davies *et al.*, 2004). The heterogeneity of OmpA and OmpH suggests that these proteins are subject to diversifying selection within the host and may play important roles in host–pathogen interactions (Davies *et al.*, 2004). The genes encoding twelve proteins involved in OM biogenesis and integrity were predicted (E-komon *et al.*, 2012) and these proteins were identified in all genomes. The majority of proteins involved in OM biogenesis and integrity were conserved with the exception of OmpA. This was not surprising and reflect important functions related to maintaining the integrity and functioning of the outer membrane (Ruiz *et al.*, 2006).

Twenty five OMPs were identified as having transport and receptor functions based on the prediction analysis. Thirteen different proteins were selected for further analysis. The nucleotide and amino acid variation of these genes/proteins was generally limited. However, substantial variation of both nucleotides (32%) and amino acids (32%) was identified in the major porin protein, OmpH1. The amino acid variation of OmpH1 occurred almost in the loop regions, as previously shown (Luo *et al.*, 1999). The high degree of variation in the external loops is likely due to selective pressures exerted by the host immune system and other environmental conditions (Singh *et al.*, 2011). The result showed strong evidence that natural selection is driving diversification of the hypervariable regions of the extracellular loops. The sequence variation of OmpH1 may have functional consequences (Singh *et al.*, 2011). There was clear evidence of *ompH1* exchange between different strains of *P. multocida*. The *ompH1* gene has undergone horizontal DNA transfer and recombination because complex mosaic structures were identified in the *ompH1* alleles within divergent lineages. Nucleotide sequence analysis of the gene encoding the porin protein of the pathogenic *Neisseria* species revealed that horizontal genetic exchange has resulted in the emergence of new porin classes (Derrick *et al.*, 1999). Limited levels of nucleotide and amino acid sequence variation was found within genes encoding the predicted outer membrane proteins having adherence and membrane-associated enzyme activity.

The diversity and evolution of OmpA was investigated in 74 *P. multocida* isolates representing different evolutionary lineages. The *ompA* gene of *P. multocida* is

highly diverse and is represented by 26 unique alleles. Multiple subclasses of OmpA were also found among cattle, sheep, goat and swine isolates of *P. multocida* (Vougidou *et al.*, 2015) and among ovine and bovine isolates of *M. haemolytica* (Davies & Lee, 2004). The present findings indicated that *ompA* has undergone horizontal DNA transfer and recombinational exchanges. Comparative nucleotide sequence comparison of the *ompA* alleles has allowed a more complete picture of *ompA* evolution to be established. The results confirm that *ompA* in avian *P. multocida* isolates are more diverse than bovine, porcine and ovine isolates (Davies, 2004). The molecular mass of OmpA was previously shown to be heterogeneous (37.5- 38.3 kDa) and this is probably due to the amino acid variation and differences in size of the hypervariable surface-exposed loops. Similar heterogeneity has been described in the OmpA protein of *P. multocida* (Vougidou *et al.*, 2015), OmpA protein of *M. haemolytica* (Davies & Lee, 2004) and P5 outer membrane protein of *H. influenzae* (Duim *et al.*, 1997). Visual inspection of the distribution of polymorphic nucleotide sites among the *ompA* sequences revealed that the *P. multocida ompA* alleles have undergone horizontal DNA transfer and intragenic recombinational exchange. The presence of identical, or almost identical, alleles in strains of divergent phylogenetic lineages also indicates the occurrence of assortative (entire gene) recombination between strains. Evidence for *ompA* gene exchange between isolates from different host species and isolates of divergent lineages was found. Analysis of inferred amino acid sequences revealed that the majority of variable sites occurred within four hypervariable regions located at the distal ends of the surface-exposed loops. This has also been found in the *OmpA* protein of *P. multocida* (Dabo *et al.*, 2008; Vougidou *et al.*, 2015), *M. haemolytica* (Davies & Lee, 2004; Hounsome *et al.*, 2011) and the P5 outer membrane protein of *H. influenzae* (Duim *et al.*, 1997; Webb & Cripps, 1998). Sequence variation in the loop regions may reflect functional differences among the OmpA protein (Dabo *et al.*, 2003; Hounsome *et al.*, 2011; Koebnik, 1999a; b). The data provide strong evidence that natural selection is driving diversification of the hypervariable extracellular loop regions. These results suggest that the loop regions of OmpA of *P. multocida* may play an important role in the pathogenesis of *P. multocida*. It has also been shown that OmpA is involved in adherence of *P. multocida* (Carpenter *et al.*, 2007; Dabo *et al.*, 2003; Katoch *et al.*, 2014). The locations of variable sites within the four hypervariable regions at the distal ends of the

surface-exposed loops of OmpA suggest that these parts of OmpA are involved in recognition and receptor binding because it is suggested they interact with cell-surface receptors (Carpenter *et al.*, 2007; Dabo *et al.*, 2003). OmpA of *M. haemolytica* binds to cell-surface fibronectin (Lo & Sorensen, 2007), colicins (Killmann *et al.*, 1995) and serves as a receptor for several bacteriophages (Jin *et al.*, 2015; Morona *et al.*, 1985; Parent *et al.*, 2014; Porcek & Parent, 2015). Variation in the surface-exposed loop regions suggests that the OmpA protein may also have a role in host specificity. It has been suggested that the loops of OmpA confer species-specificity as identified through the use of cross absorbed antibodies (Davies & Lee, 2004). However, further analysis is required to confirm these functions.

It has previously been shown that temperate bacteriophages are involved in the emergence and diversity of pathogenic bacteria via HGT through the dissemination of genes encoding virulence factors such as toxins (Boyd & Brüssow, 2002; Saunders *et al.*, 2001). This study was designed to investigate the presence of temperate bacteriophage in *P. multocida* and to determine if they are likely to be involved in the diversity and evolution of *P. multocida*. The induction patterns were classified into three types: complete lysis, partial lysis and no lysis. Different induction profiles were obtained and were varied from one isolate to another. Similar findings were found in *E. coli* during the induction of *stx*$_2$-converting bacteriophages (Muniesa *et al.*, 2003; Muniesa *et al.*, 2004). The identical induction profiles were found among isolates of the same genetic lineage based on the MLST suggesting that these isolates may contain the same phages. Transmission electron microscopy has been used as a valuable tool in the study of phage morphology, characterisation and classification (Ackermann, 2001; Ackermann, 2003). A diverse set of temperate bacteriophage morphologies were identified in this study. Diverse phage morphologies have been identified in many bacterial species (Davies & Lee, 2006; Denes *et al.*, 2014; Hsu *et al.*, 2013; Kiliç *et al.*, 2001; Moreno Switt *et al.*, 2013; Nale *et al.*, 2012; Stevenson & Airdrie, 1984; Seed & Dennis, 2005; Sepúlveda-Robles *et al.*, 2012; Sekulovic *et al.*, 2014; Urban-Chmiel *et al.*, 2015; Urban-Chmiel *et al.*, 2015; Williams *et al.*, 2002). Identification of temperate bacteriophages in 29 of 47 isolates suggests that these phages may play roles in generating diversity within *P. multocida* and the observed recombination events observed in some genes such as *ompA* and

ompH1. It is well established that bacteriophages play important roles in bacterial evolution via HGT (Boyd & Brüssow, 2002; Brüssow *et al.*, 2004; Canchaya *et al.*, 2003a; Masignani *et al.*, 2001). The phage particles were morphologically diverse and represented both the *Siphoviridae* and *Myoviridae* families. Generally, phage particles were similar in closely related isolates or isolates within the same genetic lineage. However, distinct *Myoviridae*-like phage types with unusually small hexagonal capsids and long tails were also identified in a specific group of isolates (PM86, PM934, PM954, PM486 and PM172) that were of the same genetic lineage (MLST group D) based on the MLST scheme. Similar phage particles having small capsids have been identified in *S. aureus* and designated as *S. aureus* pathogenicity island (SaPIs) (Úbeda *et al.*, 2005). Overall, the findings support the evolutionary relationships among *P. multocida* isolates from multiple hosts based on MLST data.

Host range experiments were conducted to assess the presence of temperate bacteriophages and to examine the ability of these phages to infect a range of indicator strains. The results showed that the plaque assay appeared to be less sensitive than TEM. The low number of phages able to infect the indicator strains may have been due to the absence of suitable indicator strains possessing appropriate phage receptors because certain receptors on the cell wall of bacterial cells could be responsible for determining phage host range. (Lindbergl, 1973; Michael *et al.*, 2003; Rakhuba *et al.*, 2010). Receptors can be either OMPs LPS, pili or flagella (Guttman *et al.*, 2005; Jin *et al.*, 2015; Lindbergl, 1973; Morona *et al.*, 1985; Parent *et al.*, 2014; Porcek & Parent, 2015; Randall-Hazelbauer & Schwartz, 1973; Rakhuba *et al.*, 2010). However, it is not known which receptors in the *P. multocida* cell wall enhance attachment of phages to the host cells. Therefore, further studies are required to identify the bacterial receptors of *P. multocida* phages in more detail.

Phage DNA was isolated from only 18 lysates. However, the concentration of DNA differed from one strain to another. The variation in DNA concentration indicated that some isolates had a higher rate of phage production (phage replication and release), although all lysates were induced under the same conditions. Similar findings have been described in *E. coli* (Muniesa *et al.*, 2003; Muniesa *et al.*, 2004). Two phage DNA bands appeared to be common in certain strains within the same genetic lineage (PM86, PM172, PM486, PM934 and

PM954). The presence of two bands of different sizes indicates the presence of more than one phage in the corresponding genomes. Furthermore, TEM identified the presence of unusually small capsids belonging to the *Myoviridae* family in lysates induced from isolates PM86, PM172, PM486, PM934 and PM954. Taken together, the TEM results and the presence of two DNA bands (and especially the low molecular mass band corresponding to approximately 8,000 bps) suggests the induction of phage-inducible chromosomal islands (PICIs) in *P. multocida*. The presence of PICIs has not previously been described in *P. multocida*.

Restriction endonuclease analysis has been widely used to assess genetic diversity of induced phages (Davies & Lee, 2006; Hsu *et al.*, 2013; Jakhetia & Verma, 2015 Muniesa *et al.*, 2004; Pullinger *et al.*, 2003; Sepúlveda-Robles *et al.*, 2012; Sekulovic *et al.*, 2014; Urban-Chmiel *et al.*, 2015). The identification of 10 different RE types in only 18 samples suggests that *P. multocida* bacteriophages are relatively diverse. RE analysis has been used to study the genetic relatedness of induced phages because classification of bacteriophages based on phage morphology does not provide information about their genetic relatedness and diversity (Lawrence *et al.*, 2002). The results demonstrated an association between phage type and *P. multocida* isolates within the same or closely related lineages (capsular type, OMPs, and STs). The findings support the evolutionary relationship of *P. multocida* based on MLST data.

Induction of multiple prophages in bacterial isolates indicates that a single host harbours multiple prophages (Canchaya *et al.*, 2003; Hsu *et al.*, 2013; Niu *et al.*, 2015). The induction of multiples phage types from a single strain has not previously been described in *P. multocida*. Analysis of 40 *P. multocida* genomes identified multiple Mu-like and λ-like phages within the same genome. Although only a single phage type belonging to either the *Siphoviridae or Myoviridae* families was identified by TEM in isolates PM916, PM926 and PM40, sequencing of phage DNA revealed that both Mu-like (*Myoviridae*) and λ-like (*Siphoviridae*) phages were actually induced in these isolates. The reason why additional phage types were not found by TEM was unclear. It could indicate that the quantity of one phage type was higher than the other, although identical induced protocols were used for both TEM and DNA extraction. Genomic analysis identified further intact prophages within the genomes of 40 isolates. From one to five intact

prophages and prophage-like elements were identified within the genomes of *P. multocida* strains. The findings suggest that the presence of multiple phages within a single genome is likely to play a role in the genetic diversity of *P. multocida* and, possibly, in transferring virulence genes and other genetic material between strains. Comparative genomic analysis of bacterial genomes has revealed that prophages are common in bacterial genomes (Canchaya *et al.*, 2003; Casjens, 2003; Fortier & Sekulovic, 2013). Studies have shown that prophages are one of the main sources of genetic diversity and strain variation associated with the virulence of many bacterial pathogens including *E. coli* (Ohnishi *et al.*, 2001; Weinbauer & Rassoulzadegan, 2004), *S. enterica* (Cooke *et al.*, 2007), *S. aureus* (Rahimi *et al.*, 2012); and *S. pyogenes* (Aziz *et al.*, 2005). The presence of two bands of different molecular size representing phage DNA from a cluster (MLST group D) of closely related isolates (PM86, PM172, PM486, PM934 and PM954), together with the identification of small capsids by TEM, suggest that these elements possibly represent PICIs. These PICIs were associated with avian, bovine and porcine isolates of capsular type A, OMP-types 3, 5 and and STs 9, 26 and 15. Southern blot hybridisation showed that Mu-like phages were packaged in a large capsid and also in small-sized capsids. This is the first description of PICIs in *P. multocida*.

Induction of Mu-like phages was more common among the *P. multocida* porcine strains of different capsular, OMP and ST types. In the closely related species *H. parasuis,* a Mu-like bacteriophage SuMu portal gene was found to be present in 90% of virulent porcine strains, suggesting that the SuMu phage may contribute to virulence of *H. parasuis* (Zehr & Tabatabai, 2011; Zehr *et al.*, 2012). Functional Mu-like phages have also been isolated and sequenced in many other bacterial species. These phages include *Haemophilus* phage SuMu (NC_019455) (Zehr *et al.*, 2012), *Mannheimia* phage vB_MhM (3927AP2) (Niu *et al.*, 2015), *Burkholderia* phage BcepMu (NC_005882) (Summer *et al.*, 2004), *Pseudomonas* phage vB_PaeS_PM105 (NC_028667) (Pourcel *et al.*, 2016), and *Enterobacteria* phage SfMu (NC_027382) (Jakhetia & Verma, 2015). Seven different Mu-like phages were identified in *P. multocida* and identical phages were identified in isolates within the same phylogenetic lineage, although there were some exceptions. These findings again support the evolutionary relationships of *P. multocida* isolates from multiple hosts based on MLST data. It also suggests that

identical Mu-like phages are adapted to isolates of the same, or closely related genetic lineage. Interestingly, no Mu-like phages were found within the ovine strains or within porcine atrophic rhinitis strains of capsular type D, OMP-types 4.1, 6.1 and 13.1 and ST 11. Therefore, they cannot be involved in and transfer between or to and from these groups of isolates. *P. multocida* Mu-like phages use a transposase to integrate into random locations within the bacterial chromosome. Random integration may lead to mutation of genes at the site of insertion (Zehr *et al.*, 2012).

Seven different λ-like phages were induced in *P. multocida* isolates. Phages with identical genomes were associated with isolates of the same genetic lineage, further supporting the evolutionary relationships among *P. multocida* isolates from multiple hosts based on MLST data. PHAST analysis detected additional intact prophages in the genomes of *P. multocida* isolates although it was unclear why some phages were not induced. It has been suggested that this could be due to the occurrence of competitive interactions between phages during induction (Niu *et al.*, 2015), or due to the method of induction or the phage may no longer be active. Temperate bacteriophages, especially those encoding virulence genes, have been shown to play an important role in bacterial pathogenesis (Boyd & Brüssow, 2002; Boyd, 2012; Fortier & Sekulovic, 2013; Penades *et al.*, 2015). Bacteriophage-encoded virulence determinants can transform their host from a commensal to a pathogenic or virulent strain by lysogenic conversion (Allison, 2007; Boyd & Brüssow, 2002; Boyd, 2012; Veses-Garcia *et a*l., 2015). Such bacteriophage-encoded virulence genes provide mechanisms that enable attachment, invasion, survival and damage to host cells (Boyd & Brüssow, 2002; Boyd, 2012). In the present study, sequence analysis revealed that two identical functional λ-like phage were induced in porcine AR rhinitis isolates (ϕPM684.3 and ϕPM848.2) which carried the PMT-encoded gene. However, comparative analysis of phage genomes from toxigenic porcine isolates PM918, PM926 and PM40 showed that bacteriophage-encoded PMT was not induced. Genome analysis identified bacteriophages encoding PMT in PM918, PM926, PM40 and PM696. It has been mentioned that *toxA* may have been horizontally transferred to ovine strains (Einarsdottir *et al.*, 2016; Shayegh *et al.*, 2008; Weiser *et al.*, 2003). Comparative genome analyses identified bacteriophages encoding PMT in ovine isolates PM122, PM964, PM982, PM986 and PM988, suggesting that *toxA*

could be transferred by bacteriophages. To date, no study has confirmed the presence of the *toxA* gene within the genomes of bacteriophages from ovine isolates.

General conclusions and future work

There was evidence of transmission of *P. multocida* from one host to another and this could possibly play an important role in generating genetic diversity in *P. multocida*. This was based on the concatenated partial sequences (3990 bp) of seven housekeeping enzyme genes, complete sequences (22,371 bp) of fifteen housekeeping enzyme genes and on the core genome. Comparative nucleotide sequence analysis of genes encoding different functional classes of OMPs indicates that each has varying degree of nucleotide and amino acid sequence diversity; there was also evidence of varying degrees of intragenic and assortative recombination affecting these genes. High levels of nucleotide and amino acid sequence variation was found within two major surface-exposed proteins, OmpA and OmpH1. The results indicated that these two proteins have undergone multiple horizontal DNA transfer and intragenic and assortative recombination events. Variation in OmpA and OmpH1 occurred predominantly in the loop regions. In OmpA the variation occurred at the tips of the loops. There was strong evidence that natural selection is driving diversification of the hypervariable extracellular loop regions in both OmpA and OmpH1. Further structural and functional studies will be required to confirm and understand the role of these proteins in virulence and host specificity. Antigenic variation of these proteins will also be relevant to their potential use in vaccination. Bacteriophages were abundant in the genomes of *P. multocida* and the presence of identical bacteriophages in closely related lineages supports the evolutionary relationships among *P. multocida* isolates based on the MLST. No OMP-encoding genes were identified within the genome of any of the bacteriophages. However, the phage genomes carried a number of hypothetical proteins. Further analysis will be required to determine the role of these hypothetical proteins in the biology of *P. multocida*. The *P. multocida toxA* gene was the only virulence gene identified within any of the phage genomes; it was identified in phages associated exclusively with porcine AR rhinitis isolates and ovine isolates of capsular type D. Finally, for the first time in this study PICIs were identified in *P. multocida*.

Chapter 7 References

Ackermann, H. W. & Karaivanov, L. (1984). Morphology of *Pasteurella multocida* bacteriophages. *Can J Microbiol* **30**, 1141–8.

Ackermann, H. (2001). Bacteriophages : Tailed. *Encycl Life Sci* 1–7.

Ackermann, H. (2009). Phage classification and characterization. In *Bacteriophages Methods Protoc*, Methods in Molecular Biology, pp. 127–140. Edited by M. R. J. Clokie & A. M. Kropinski. Totowa, NJ: Humana Press.

Ackermann, H. (2011). Bacteriophage taxonomy. *Microbiol* 90–94.

Ackermann, H.-W. (2003). Bacteriophage observations and evolution. *Res Microbiol* **154**, 245–51.

Ackermann, H.-W. (2007). 5500 Phages examined in the electron microscope. *Arch virol* **152**, 227–43.

Adlam, C. & Rutter, J. M. (1989). *Pasteurella and Pasteurellosis*. UK: Academic press Limited.

Adler, B., Bulach, D., Chung, J., Doughty, S., Hunt, M., Rajakumar, K., Serrano, M., Van Zanden, A., Zhang, Y. & Ruffolo, C. (1999). Candidate vaccine antigens and genes in *Pasteurella multocida*. *J Biotechnol* **73**, 83–90.

Alexander, C. & Rietschel, E. T. (2001). Invited review: Bacterial lipopolysaccharides and innate immunity. *J Endotoxin Res* **7**, 167–202.

Allison, G. E. & Verma, N. K. (2000). Serotype-converting bacteriophages and O-antigen modification in *Shigella flexneri*. *Trends Microbiol* **8**, 17–23.

Allison, H. E. (2007). Stx-phages : drivers and mediators of the evolution of STEC and STEC-like pathogens. *Futur Microbiol* **2**, 165–174.

van Alphen, L., Havekes, L. & Lugtenberg., B. (1977). Major outer membrane protein d of *E. coli* K12. Purification and in vitro activity on bacteriophage K3 and F-pilus mediated conjugation. *FEBS Lett* 285–290.

Armentrout, R. W. & Rutberg, L. (1971). Heat induction of prophage phi 105 in *Bacillus subtilis*: replication of the bacterial and bacteriophage genomes. *J Virol* **8**, 455–68.

Arora, a, Abildgaard, F., Bushweller, J. H. & Tamm, L. K. (2001). Structure of outer membrane protein A transmembrane domain by NMR spectroscopy. *Natu Struc Biol* **8**, 334–338.

Ausubel, F. M., Brent, R., Kingston, R. E., Moore, D. D., Seidman, J. G., Smith, J. A. & Struhl, K. (1990). *Current protocols in molecular biology*. New York, N.Y: John Wiley & Sons.

Aziz, R. K., Bartels, D., Best, A. A., DeJongh, M., Disz, T., Edwards, R. A., Formsma, K., Gerdes, S., Glass, E. M. & other authors. (2008). The RAST Server: rapid annotations using subsystems technology. *BMC Genomics* **9**, 75.

Aziz, R. K., Edwards, R. A., Taylor, W. W., Low, D. E., McGeer, A. & Kotb, M. (2005). Mosaic prophages with horizontally acquired genes account for the emergence and diversification of the globally disseminated M1t1 clone of *Streptococcus pyogenes*. *J Bacteriol* **187**, 3311–3318.

Barksdale, L. & Arden, S. B. (1974). Persisting bacteriophage infections, lysogeny, and phage conversions. *Annu Rev Microbiol* **28**, 265–299.

Barondess, J. J. & Beckwith, J. (1990). A bacterial virulence determinant encoded by lysozenic coliphage lambda. *Nature* **346**, 871–874.

Bart, A., Dankert, J. & Van Der Ende, A. (1999). Antigenic variation of the class I outer membrane protein in hyperendemic *Neisseria meningitidis* strains in The Netherlands. *Infec Immun* **67**, 3842–3846.

Basra, S., Anany, H., Brovko, L., Kropinski, A. M. & Griffiths, M. W. (2014). Isolation and characterization of a novel bacteriophage against *Mycobacterium avium* subspecies *paratuberculosis*. *Arch Virol* **159**, 2659–2674.

Bastardo, A., Ravelo, C. & Romalde, J. L. (2012). Multilocus sequence typing reveals high genetic diversity and epidemic population structure for the fish pathogen *Yersinia ruckeri*. *Env Microbiol* **14**, 1888–1897.

Beher, M. G., Schnaitman, C. a. & Pugsley, a. P. (1980). Major heat-modifiable outer membrane protein in gram-negative bacteria: comparison with the OmpA protein of *Escherichia coli*. *J Bacteriol* **143**, 906–913.

Bfudley, B. Y. D. E. (1965). The isolation and morphology of some new bacteriophages specific for *Bacillus* and *Acetobacter* species. *J Gen Microbiol* **41**, 233–241.

Birge, E. A. (2006). *Bacterial and Bacteriophage Genetics*, 5th edn. USA: Springer Science+ Business Media, Inc.

Birtles, A., Virgincar, N., Sheppard, C. L., Walker, R. a, Johnson, A. P., Warner, M., Edwards-Jones, V. & George, R. C. (2004). Antimicrobial resistance of invasive *Streptococcus pneumoniae* isolates in a British district general hospital: the international connection. *J Med Microbiol* **53**, 1241–6.

Birtles, A., Hardy, K., Gray, S. J., Kaczmarski, E. B., Edwards-jones, V., Fox, A. J. & Handford, S. (2005). Multilocus sequence typing of *Neisseria meningitidis* Directly from clinical samples and application of the method to the investigation of meningococcal disease case clusters. *J Clin Microbiol* **43**, 6007–6014.

Blackall, P. J. & Miflin, J. K. (2000). Identification and typing of *Pasteurella multocida* : A review Identification and typing of *Pasteurella multocida*: a review 37–41.

Bobay, L. M., Rocha, E. P. C. & Touchon, M. (2013). The adaptation of temperate bacteriophages to their host genomes. *Mol Biol Evol* **30**, 737–751.

Bobay, L.-M., Touchon, M. & Rocha, E. P. C. (2014). Pervasive domestication of defective prophages by bacteria. *Natl Acad Sci U S A* **111**, 12127–32.

Bochow, S., Elliman, J. & Owens, L. (2012). Bacteriophage adenine methyltransferase: A life cycle regulator? Modelled using Vibrio harveyi myovirus like. *J App Microbiol* **113**, 1001–1013.

Bos, M. P. & Tommassen, J. (2004). Biogenesis of the Gram-negative bacterial outer membrane. *Curr Opin Microbiol* **7**, 610–6.

Bos, M. P., Robert, V. & Tommassen, J. (2007). Biogenesis of the gram-negative bacterial outer membrane. *Annu Rev Microbiol* **61**, 191–214.

Boyce, J. D. & Adler, B. (2000). The capsule is a virulence determinant in the pathogenesis of *Pasteurella multocida* M1404 (B:2). *Infec Immun* **68**, 3463–3468.

Boyce, J. D., Chung, J. Y. & Adler, B. (2000). *Pasteurella multocida* capsule: Composition,

function and genetics. *J Bacteriol* **83**, 153–160.

Boyd, E. F. & Brüssow, H. (2002). Common themes among bacteriophage-encoded virulence factors and diversity among the bacteriophages involved. *Trends Microbiol* **10**, 521–9.

Boyd, E. F. (2012). Bacteriophage-encoded bacterial virulence factors and phage-pathogenicity island interactions. *Adv Virus Res* **82**, 91–118. Elsevier Inc.

Boyd, J. M., Dacanay, A., Knickle, L. C., Touhami, A., Brown, L. L., Jericho, M. H., Johnson, S. C. & Reith, M. (2008). Contribution of type IV pili to the virulence of Aeromonas salmonicida subsp. *salmonicida* in Atlantic salmon (Salmo salar L.). *Infec Immun* **76**, 1445–1455.

Bradley, D. E. (1967). Ultrastructure of bacteriophage and bacteriocins. *Bacteriol Rev* **31**, 230–314.

Brüssow, H. & Hendrix, R. W. (2002). Phage genomics: small is beautiful. *Cell* **108**, 13–6.

Brüssow, H., Canchaya, C. & Hardt, W. (2004). Phages and the evolution of bacterial pathogens: from genomic rearrangements to lysogenic conversion. *Micr Mol Bio Rev* **68**, 560–602.

Burke, J., Schneider, D. & Westpheling, J. (2001). Generalized transduction in *Streptomyces coelicolor*. *Proc Natl Acad Sci USA* **98**, 6289–94.

Byl, C. Vander & Kropinski, A. M. (2000). Sequence of the genome of *Salmonella* bacteriophage P22. *J Bacteriol* **182**, 6472–6481.

Campoy, S., Aranda, J., Àlvarez, G., Barbé, J. & Llagostera, M. (2006a). Isolation and sequencing of a temperate transducing phage for *Pasteurella multocida*. *Appl Env Microbiol* **72**, 3154–3160.

Campoy, S., Hervàs, A., Busquets, N., Erill, I., Teixidó, L. & Barbé, J. (2006b). Induction of the SOS response by bacteriophage lytic development in *Salmonella enterica*. *Virol* **351**, 360–367.

Canchaya, C., Fournous, G., Chibani-Chennoufi, S., Dillmann, M.-L. & Brüssow, H. (2003a). Phage as agents of lateral gene transfer. *Curr Opin Microbiol* **6**, 417–424.

Canchaya, C., Proux, C., Fournous, G., Bruttin, A. & Brüssow, H. (2003b). Prophage genomics. *Microbiol Mol Biol Rev* **67**, 238–276.

Canchaya, C., Fournous, G. & Brüssow, H. (2004). The impact of prophages on bacterial chromosomes. *Mol Microbiol* **53**, 9–18.

Capitini, C. M., Herrero, I., Patel, R., Ishitani, M. B. & Boyce, T. G. (2002). Wound infection with *Neisseria weaveri* and a novel subspecies of *Pasteurella multocida* in a child who sustained a tiger bite. *Clin iInfec Dises* **34**, E74–6.

Cardoso-Toset, F., G??mez-Laguna, J., Callejo, M., Vela, A. I., Carrasco, L., Fern??ndez-Garayz??bal, J. F., Maldonado, A. & Luque, I. (2013). Septicaemic pasteurellosis in free-range pigs associated with an unusual biovar 13 of *Pasteurella multocida*. *Vet Microbio* **167**, 690–694.

Carpenter, T., Khalid, S. & Sansom, M. S. P. (2007). A multidomain outer membrane protein from *Pasteurella multocida*: modelling and simulation studies of PmOmpA. *Biochim Biophys Acta* **1768**, 2831–40.

Carter, G. R. (1955). Studies on *Pasteurella multocida*. I. A hemagglutination test for the

identification of serological types. *Amer J Vet Res* **16**, :481–484.

Carter, G. R. & De Alwis, M. C. L. (1989). Haemorrhagic Septicaemia. In *Pasteurella and Pasteurellosis*, pp. 131– 160. Edited by C. Adlam & J. M. Rutter. UK: Academic press Limited.

Casjens, S. (2003). Prophages and bacterial genomics: what have we learned so far? *Mol Microbiol* **49**, 277–300.

Castillo-ramirez, S., Corander, J., Marttinen, P., Aldeljawi, M., Hanage, W. P., Westh, H., Boye, K., Gulay, Z., Bentley, S. D. & other authors. (2012). Phylogeographic variation in recombination rates within a global clone of Methicillin-Resistant *Staphylococcus aureus* (MRSA). *Genome Biol* **13**, R126.

Catry, B., Chiers, K., Schwarz, S., Kehrenberg, C., Decostere, A. & Kruif, A. De. (2005). Fatal peritonitis caused by *Pasteurella multocida* capsular type F in calves. *J Clin Microbiol* **43**, 1480–1483.

Ch'ng, S. L., Octavia, S., Xia, Q., Duong, A., Tanaka, M. M., Fukushima, H. & Lan, R. (2011). Population structure and evolution of pathogenicity of *Yersinia pseudotuberculosis*. *Appl Env Microbiol* **77**, 768–75.

Chaguza, C., Cornick, J. E. & Everett, D. B. (2015). Mechanisms and impact of genetic recombination in the evolution of *Streptococcus pneumoniae*. *Comp Struc Biotechnol J* **13**, 241–247. Elsevier B.V.

Chalker, V. J., Waller, A., Webb, K., Spearing, E., Crosse, P., Brownlie, J. & Erles, K. (2012). Genetic diversity of *Streptococcus equi* subsp. *zooepidemicus* and doxycycline resistance in kennelled dogs. *J Clin Microbiol* **50**, 2134–6.

Chanter, N. & Rutter, J. M. (1989). Pasteurellosis in Pigs and the Determinants of virulence of Toxigenic *Pasteurella multocida*. In *Pasteurella and Pasteurellosis*, pp. 161– 195. Edited by C. A. & J. M. Rutter. UK: Academic press Limited.

Chaudhuri, R. R. & Henderson, I. R. (2012). The evolution of the *E. coli* phylogeny. *Infect Gen Evol* **12**, 214–226. Elsevier B.V.

Cheetham, B. F. & Katz, M. E. (1995). A role for bacteriophages in the evolution and transfer of bacterial virulence determinants. *Mol Microbiol* **18**, 201–8.

Christensen, H. & Bisgaard, M. (2008). Taxonomy and biodiversity of members of *Pasteurellaceae*. In *Pasteurellaceae Biol Genomic Mol Asp*, pp. 1–26. Edited by P. Kuhnerst & H. Christensen. Norfolk, UK: Caister Academic Press.

Christensen, H. & Bisgaard, M. (2006). The Genus *Pasteurella*. *Prokaryotes* **6**, 1062–1090.

Christensen, H., Bertelsen, M. F., Bojesen, A. M. & Bisgaard, M. (2012). Classification of *Pasteurella* species B as *Pasteurella oralis* sp. nov. *Inter J Sys Evol Microbiol* **62**, 1396–1401.

Chung, J. Y., Zhang, Y. & Adler, B. (1998). The capsule biosynthetic locus of *Pasteurella multocida* A:1. *FEMS microbiol lett* **166**, 289–296.

Clark, C. A., Beltrame, J. & Manning, P. A. (1991). The oac gene encoding a lipopolysaccharide O-antigen acetylase maps adjacent to the integrase-encoding gene on the genome of *Shigella flexneri* bacteriophage Sf6. *Gene* **107**, 43–52.

Clock, S. A., Planet, P. J., Perez, B. A. & Figurski, D. H. (2008). Outer membrane components

of the tad (tight adherence) secreton of *Aggregatibacter actinomycetemcomitans*. *J Bacteriol* **190**, 980–990.

Clokie, M. R. J. & Kropinski, A. M. (2009). *Bacteriophages: Methods and Protocols; Isolation, Characterization, and Interactions*, 1st edn. New York, USA: Humana Press.

Coffey, T. J., Enright, M. C., Daniels, M., Morona, J. K., Morona, R., Hryniewicz, W., Paton, J. C. & Spratt, B. G. (1998). Recombinational exchanges at the capsular polysaccharide biosynthetic locus lead to frequent serotype changes among natural isolates of *Streptococcus pneumoniae*. *Mol Microbiol* **27**, 73–83.

Confer, A. W. & Ayalew, S. (2013). The OmpA family of proteins: Roles in bacterial pathogenesis and immunity. *Vet Microbiol* **163**, 207–222. Elsevier B.V.

Cooke, F. J., Wain, J., Fookes, M., Ivens, A., Thomson, N., Brown, D. J., Threlfall, E. J., Gunn, G., Foster, G. & Dougan, G. (2007). Prophage sequences defining hot spots of genome variation in *Salmonella enterica* serovar *Typhimurium* can be used to discriminate between field isolates. *J Clin Microbiol* **45**, 2590–2598.

Cowan, S. W., Schirmer, T., Rummel, G., Steiert, M., Ghosh, R., Pauptit†, R. A., Jansonius, J. N. & Rosenbusch, J. P. (1992). Crystal structures explain functional properties of two *E. coli* porins. *Nature* **358**, 727 – 733.

Craig, N. L. (1988). The mechanism of conservative site-specific recombination. *Annu Rev Genet* **22**, 77–105.

Croucher, N. J., Finkelstein, J. A., Pelton, S. I., Mitchell, P. K., Lee, G. M., Parkhill, J., Bentley, S. D., Hanage, W. P. & Lipsitch, M. (2013). Population genomics of post-vaccine changes in pneumococcal epidemiology. *Nat Genet* **45**, 656–63. Nature Publishing Group.

Croucher, N. J., Page, A. J., Connor, T. R., Delaney, A. J., Keane, J. A., Bentley, S. D., Parkhill, J. & Harris, S. R. (2015). Rapid phylogenetic analysis of large samples of recombinant bacterial whole genome sequences using Gubbins. *Nucleic Acids Res* **43**, e15.

Crowl, R. M., Boyce, R. P. & Echol, H. (1981). Repressor cleavage as a prophage of a mutant induction mechanism. *J Mol Biol* 815–819.

Cuervo, A. & Carrascosa, J. L. (2012). Bacteriophages: Structure. *eLS*.

D'Souza, J. M., Samuel, G. N. & Reeves, P. R. (2005). Evolutionary origins and sequence of the *Escherichia coli* O4 O-antigen gene cluster. *FEMS Microbiol Lett* **244**, 27–32.

Dabo, S. M., Confer, a W. & Murphy, G. L. (1997). Outer membrane proteins of bovine *Pasteurella multocida* serogroup A isolates. *Vet Microbio* **54**, 167–83.

Dabo, S. M., Taylor, J. D. & Confer, a W. (2007). *Pasteurella multocida* and bovine respiratory disease. *Anim Heal Res Rev* **8**, 129–50.

Dabo, S. M., Confer, A., Montelongo, M., York, P. & Wyckoff, J. H. (2008). Vaccination with *Pasteurella multocida* recombinant OmpA induces strong but non-protective and deleterious Th2-type immune response in mice. *Vaccine* **26**, 4345–4351.

Dabo, S. M., Confer, A. W. & Quijano-Blas, R. a. (2003). Molecular and immunological characterization of *Pasteurella multocida* serotype A:3 OmpA: evidence of its role in *P. multocida* interaction with extracellular matrix molecules. *Microb Pathog* **35**, 147–157.

Dale, J. W. (1999). *Molecular Genetics of Bacteria*, 3rd edn. John Wiley & Sons LtD, England.

Darling, A. C. E., Mau, B., Blattner, F. R. & Perna, N. T. (2004). Mauve: Multiple alignment of

conserved genomic sequence with rearrangements. *Genome Res* **14**, 1394–1403.

Datta, D. B., Arden, B. & Henning., U. (1977). Major proteins of the *Escherichia coli* outer cell envelope membrane as bacteriophage receptors. *J Bacteriol* **131**, 821–829.

Davies, R. L., Watson, J. & Caffrey, B. (2003a). Comparative analyses of *Pasteurella multocida* strains associated with the ovine respiratory and vaginal tracts. *Vet Rec* **152**, 7–10.

Davies, R. L., Campbell, S. & Whittam, T. S. (2002). Mosaic structure and molecular evolution of the leukotoxin operon (*lktCABD*) in *Mannheimia* (*Pasteurella*) *haemolytica*, *Mannheimia glucosida*, and *Pasteurella trehalosi*. *J Bacteriol* **184**, 266–277.

Davies, R. L., MacCorquodale, R., Baillie, S. & Caffrey, B. (2003b). Characterization and comparison of *Pasteurella multocida* strains associated with porcine pneumonia and atrophic rhinitis. *J Med Microbiol* **52**, 59–67.

Davies, R. L. (2004). Genetic diversity among *Pasteurella multocida* strains of avian, bovine, ovine and porcine origin from England and Wales by comparative sequence analysis of the 16S rRNA gene. *Microbiol* **150**, 4199–210.

Davies, R. L. & Lee, I. (2004). Sequence diversity and molecular evolution of the heat-modifiable outer membrane protein gene (*ompA*) of *Mannhemia* (*pasteurella*) *haemolytica*, *Mannheimia glucosida*, and *Pasteurella trehalosi*. *J Bacteriol*.

Davies, R. L. & Lee, I. (2006). Diversity of temperate bacteriophages induced in bovine and ovine *Mannheimia haemolytica* isolates and identification of a new P2-like phage. *FEMS Microbiol Lett* **260**, 162–70.

Davies, R. L., Whittam, T. S. & Selander, R. K. (2001). Sequence diversity and molecular evolution of the leukotoxin (*lktA*) gene in bovine and ovine strains of *Mannheimia* (*Pasteurella*) *haemolytica*. *J Bacteriol* **183**, 1394–1404.

Davies, R. L., MacCorquodale, R. & Caffrey, B. (2003c). Diversity of avian *Pasteurella multocida* strains based on capsular PCR typing and variation of the OmpA and OmpH outer membrane proteins. *Vet Microbiol* **91**, 169–82.

Davies, R. L., MacCorquodale, R. & Reilly, S. (2004). Characterisation of bovine strains of *Pasteurella multocida* and comparison with isolates of avian, ovine and porcine origin. *Vet Microbiol* **99**, 145–58.

Denes, T., Vongkamjan, K., Ackermann, H. W., Moreno Switt, A. I., Wiedmann, M. & den Bakker, H. C. (2014). Comparative genomic and morphological analyses of *Listeria* phages isolated from farm environments. *Appl Env Microbiol* **80**, 4616–4625.

Derrick, J. P., Urwin, R., Suker, J., Feavers, I. M. & Maiden, M. C. J. (1999). Structural and evolutionary inference from molecular variation in *Neisseria* porins. *Infec Immun* **67**, 2406–2413.

Dewhirst, F. E., Paster, B. J., Olsen, I. & Fraser, G. J. (1992). Phylogeny of 54 representative strains of species in the family *Pasteurellaceae* as determined by comparison of 16S rRNA sequences. *J Bacteriol* **174**, 2002–13.

Dodd, I. B., Shearwin, K. E. & Egan, J. B. (2005). Revisited gene regulation in bacteriophage ?? *Curr Opin Genet Dev* **15**, 145–152.

Dziva, F., Muhairwa, A. P., Bisgaard, M. & Christensen, H. (2008). Diagnostic and typing options for investigating diseases associated with *Pasteurella multocida*. *Vet Microbiol* **128**,

1–22.

Einarsdottir, T., Gunnarsson, E., Sigurdardottir, O. G., Jorundsson, E., Fridriksdottir, V., Thorarinsdottir, G. . E. & Hjartardottir, S. (2016). Variability of *Pasteurella multocida* isolated from Icelandic sheep and detection of the *toxA* gene. *J Med Microbiol* **press**.

E-komon, T., Burchmore, R., Herzyk, P. & Davies, R. (2012). Predicting the outer membrane proteome of *Pasteurella multocida* based on consensus prediction enhanced by results integration and manual confirmation. *BMC Boinformatics* **13**, 63. BioMed Central Ltd.

Elbreki, M., Ross, R. P., Hill, C., O'Mahony, J., McAuliffe, O. & Coffey, A. (2014). Bacteriophages and their derivatives as biotherapeutic agents in disease prevention and treatment. *J Viruses* 1–20.

Esposito, D., Fitzmaurice, W. P., Benjamin, R. C., Goodman, S. D., Waldman, A. S. & Scocca, J. J. (1996). The complete nucleotide sequence of bacteriophage HP1 DNA. *Nucleic Acids Res* **24**, 2360–2368.

Evans, N. J., Harrison, O. B., Clow, K., Derrick, J. P., Feavers, I. M. & Maiden, M. C. J. (2010). Variation and molecular evolution of HmbR, the *Neisseria meningitidis* haemoglobin receptor. *Microbiol* **156**, 1384–1393.

Facey, S. J. & Kuhn, A. (2010). Biogenesis of bacterial inner-membrane proteins. *CMLS* **67**, 2343–62.

Faelen, M. & Toussaint, A. (1976). Bacteriophage Mu-1: A tool to transpose and to localize bacterial genes. *J Mol Biol* **104**, 525–539.

Feil, E. J., Maiden, M. C., Achtman, M. & Spratt, B. G. (1999). The relative contributions of recombination and mutation to the divergence of clones of *Neisseria meningitidis*. *Mol Biol Evol* **16**, 1496–502.

Feil, E. J., Smith, J. M., Enright, M. C. & Spratt, B. G. (2000). Estimating recombinational parameters in *Streptococcus pneumoniae* from multilocus sequence typing data. *Genetics* **154**, 1439–50.

Feiner, R., Argov, T., Rabinovich, L., Sigal, N., Borovok, I. & Herskovits, A. A. (2015). A new perspective on lysogeny: prophages as active regulatory switches of bacteria. *Natu Rev Microbiol* **13**, 641–650. Nature Publishing Group.

Figueroa-Bossi, N., Uzzau, S., Maloriol, D. & Bossi, L. (2001). Variable assortment of prophages provides a transferable repertoire of pathogenic determinants in *Salmonella*. *Mol Microbiol* **39**, 260–271.

Ford, M. J. (2001). Molecular evolution of transferrin: evidence for positive selection in salmonids. *Mol Biol Evol* **18**, 639–647.

Forde, T., Biek, R., Zadocks, R., Workentine, M. L., De Buck, J., Kutz, S., Opriessnig, T., Trewby, H., van der Meer, F. & Orsel, K. (2016). Genomic analysis of the multi-host pathogen *Erysipelothrix rhusiopathiae* reveals extensive recombination as well as the existence of three generalist clades with wide geographic distribution. *BMC Genomics* **17**, 461. BMC Genomics.

Fortier, L.-C. & Sekulovic, O. (2013). Importance of prophages to evolution and virulence of bacterial pathogens. *Virulence* **4**, 354–65.

Frank, G. J. (1989). Pasteurellosis of Cattle. In *Pasteurella and Pasteurellosis*, pp. 197– 222.

Edited by C. A. & J. M. Rutter. UK: Academic press Limited.

Frederiksen, W. (1989). Pasteurellosis of Man. In *Pasteurella and Pasteurellosis*, pp. 303– 320. Edited by C. A. & J. M. Rutter. UK: Academic press Limited.

Freeman, V. J. (1951). Studies on the virulence of bacteriophage-infected strains of *Corynebacterium diptheriae*. *J Bacteriol* **61**, 675–688.

Freshwater, a. (2008). Why your housecat's trite little bite could cause you quite a fright: a study of domestic felines on the occurrence and antibiotic susceptibility of *Pasteurella multocida*. *Zoonoses Public Heal* **55**, 507–13.

Frosch, M., Müller, D., Bousset, K. & Müller, A. (1992). Conserved outer membrane protein of *Neisseria meningitidis* involved in capsule expression. *Infect Immun* **60**, 798–803.

Furian, T., Ka, B., Rm, P., Vp, N., Ctp, S. & Hl, M. (2014). Identification of the capsule type of *Pasteurella multocida* isolates from cases of fowl cholera by Multiplex PCR and comparison with phenotypic methods. *J Poutl Sci*.

Fussenegger, M., Facius, D., Meier, J. & Meyer, T. F. (1996). A novel peptidoglycan-linked lipoprotein (ComL) that functions in natural transformation competence of *Neisseria gonorrhoeae*. *Mol Microbiol* **19**, 1095–1105.

Fussing, V., Nielsen, J. P., Bisgaard, M. & Meyling, A. (1999). Development of a typing system for epidemiological studies of porcine toxin-producing *Pasteurella multocida* ssp. *multocida* in Denmark. *Vet Microbio* **65**, 61–74.

Galdiero, M., Folgore, A., Nuzzo, I. & Galdiero, E. (2000). Neutrophil adhesion and transmigration through bovine endothelial cells in vitro by protein H and LPS of *Pasteurella multocida*. *Immunobiol* **202**, 226–38.

Galkin, V. E., Yu, X., Bielnicki, J., Ndjonka, D., Bell, C. E. & Egelman, E. H. (2009). Cleavage of Bacteriophage λ cI Repressor Involves the RecA C-Terminal Domain. *J Mol Biol* **385**, 779–787. Elsevier Ltd.

García-Alvarez, A., Chaves, F., Fernández, A., Sanz, C., Borobia, M. & Cid, D. (2015). An ST11 clone of *Pasteurella multocida*, widely spread among farmed rabbits in the Iberian Peninsula, demonstrates respiratory niche association. *Infect Gen Evol* **34**, 81–87.

Garrido, M. E., Bigas, A., Badiola, I. & Barbé, J. (2008). Heterologous protective immunization elicited in mice by *Pasteurella multocida fur ompH*. *Inter Microbiol* 17–24.

Goerke, C., Koller, J. & Wolz, C. (2006). Ciprofloxacin and trimethoprim cause phage induction and virulence modulation in *Staphylococcus aureus*. *Antimic Agents Chemoth* **50**, 171–177.

Grant, J. R. & Stothard, P. (2008). The CGView Server: a comparative genomics tool for circular genomes. *Nucleic Acids Res* **36**, 181–184.

Grindley, N. D. F., Whiteson, K. L. & Rice, P. A. (2006). Mechanisms of site-specific recombination. *Annu Rev Bioch* **75**, 567–605.

Groth, A. C. & Calos, M. P. (2004). Phage integrases: Biology and applications. *J Mol Biol* **335**, 667–678.

Guttman, B., Raya, R. & Kutter, E. (2005). Basic phage biology. In *Bacteriophages Biol Appl*, pp. 28–66. Edited by A. Kutter, E. and Sulakvelidze. Boca Raton, FL ; London: CRC Press.

de Haan, C. P. a, Kivistö, R. I., Hakkinen, M., Corander, J. & Hänninen, M.-L. (2010). Multilocus sequence types of Finnish bovine *Campylobacter jejuni* isolates and their

attribution to human infections. *BMC Microbiol* **10**, 200.

Hall, M., Chattaway, M. a., Reuter, S., Savin, C., Strauch, E., Carniel, E., Connor, T., Van Damme, I., Rajakaruna, L. & other authors. (2015). Use of whole-genus genome sequence data to develop a multilocus sequence typing tool that accurately identifies *Yersinia* isolates to the species and subspecies levels. *J Clin Microbiol* **53**, 35–42.

Hanage, W. P., Fraser, C., Tang, J., Connor, T. R. & Corander, J. (2009). Hyper-recombination, diversity, and antibiotic resistance in *Pneumococcus*. *Science (80-)* **324**, 1454–1457.

Harper, M., Cox, A. D., St. Michael, F., Wilkie, I. W., Boyce, J. D. & Adler, B. (2004). A heptosyltransferase mutant of *Pasteurella multocida* produces a truncated lipopolysaccharide structure and is attenuated in virulence. *Infec Immun* **72**, 3436–3443.

Harper, M., Boyce, J. D. & Adler, B. (2006). *Pasteurella multocida* pathogenesis: 125 years after Pasteur. *FEMS microbiol lett* **265**, 1–10.

Harper, M., Boyce, J. D., Cox, A. D., St. Michael, F., Wilkie, I. W., Blackall, P. J. & Adler, B. (2007). *Pasteurella multocida* expresses two lipopolysaccharide glycoforms simultaneously, but only a single form is required for virulence: Identification of two acceptor-specific heptosyl I transferases. *Infec Immun* **75**, 3885–3893.

Harper, M., St. Michael, F., John, M., Vinogradov, E., Adler, B., Boyce, J. D. & Cox, A. D. (2011). *Pasteurella multocida* Heddleston serovars 1 and 14 express different lipopolysaccharide structures but share the same lipopolysaccharide biosynthesis outer core locus. *Vet Microbio* **150**, 289–296.

Harper, M., St. Michael, F., Vinogradov, E., John, M., Boyce, J. D., Adler, B. & Cox, A. D. (2012). Characterization of the lipopolysaccharide from *Pasteurella multocida* Heddleston serovar 9: Identification of a proposed bi-functional dTDP-3-acetamido-3,6-dideoxy-??-D-glucose biosynthesis enzyme. *Glycobiol* **22**, 332–344.

Harper, M., St.Michael, F., John, M., Vinogradov, E., Steen, J. A., van Dorsten, L., Steen, J. A., Turni, C., Blackall, P. J. & other authors. (2013a). *Pasteurella multocida* heddleston serovar 3 and 4 strains share a common lipopolysaccharide biosynthesis locus but display both inter- and intrastrain lipopolysaccharide heterogeneity. *J Bacteriol* **195**, 4854–4864.

Harper, M., Michael, F. S., Vinogradov, E., John, M., Steen, J. A., Van Dorsten, L., Boyce, J. D., Adler, B. & Cox, A. D. (2013b). Structure and biosynthetic locus of the lipopolysaccharide outer core produced by *Pasteurella multocida* serovars 8 and 13 and the identification of a novel phospho-glycero moiety. *Glycobiol* **23**, 286–294.

Harper, M., St. Michael, F., John, M., Steen, J., Van Dorsten, L., Parnas, H., Vinogradov, E., Adler, B., Cox, A. D. & Boyce, J. D. (2014). Structural analysis of lipopolysaccharide produced by Heddleston serovars 10, 11, 12 and 15 and the identification of a new *Pasteurella multocida* lipopolysaccharide outer core biosynthesis locus, L6. *Glycobiol* **24**, 649–659.

Hatfaludi, T., Al-Hasani, K., Boyce, J. D. & Adler, B. (2010). Outer membrane proteins of *Pasteurella multocida*. *Vet Microbio* **144**, 1–17.

Hatfull, G. F. (2008). Bacteriophage genomics. *Curr Opin Microbiol* **11**, 447–453.

Hatfull, G. F. & Hendrix, R. W. (2012). Bacteriophage and thier genomics. *Curr Opin Microbiol*

1, 298–303.

Hava, D. L. & Camilli, A. (2001). Isolation and characterization of a temperature-sensitive generalized transducing bacteriophage for *Vibrio cholerae*. *J Microbiol Meth* **46**, 217–225.

Hayashi, T., Makino, K., Ohnishi, M., Kurokawa, K., Ishii, K., Yokoyama, K., Han, C. G., Ohtsubo, E., Nakayama, K. & other authors. (2001). Complete genome sequence of enterohemorrhagic *Escherichia coli* O157 : H7 and genomic comparison with a laboratory strain K-12. *DNA Res* **8**, 11–22.

Hendrix, R. W. (2002). Bacteriophages: evolution of the majority. *Theor Popul Biol* **61**, 471–480.

Highlander, S. K., Weissenberger, S., Alvarez, L. E., Weinstock, G. M. & Berget, P. B. (2006). Complete nucleotide sequence of a P2 family lysogenic bacteriophage, varphiMhaA1-PHL101, from *Mannheimia haemolytica* serotype A1. *Virol* **350**, 79–89.

Hill, D. J., Toleman, M. A., Evans, D. J., Villullas, S., Alphen, L. Van & Virji, M. (2001). The variable P5 proteins of typeable and non-typeable *Haemophilus influenzae* target human CAECAM1. *Mol Microbiol* **39**, 850–862.

Hodgson, D. A. (2000). Generalized transduction of serotype 1/2 and serotype 4b strains of *Listeria monocytogenes*. *Mol Microbiol* **35**, 312–323.

Hoegy, F., Celia, H., Mislin, G. L., Vincent, M., Gallay, J. & Schalk, I. J. (2005). Binding of iron-free siderophore, a common feature of siderophore outer membrane transporters of *Escherichia coli* and *Pseudomonas aeruginosa*. *J Biol Chem* **280**, 20222–30.

Horadagoda, N. U., Hodgson, J. C., Moon, G. M., Wijewardana, T. G. & Eckersall, P. D. (2002). Development of a clinical syndrome resembling haemorrhagic septicaemia in the buffalo following intravenous inoculation of *Pasteurella multocida* serotype B:2 endotoxin and the role of tumour necrosis factor-?? *Res Vet Sci* **72**, 194–200.

Horiguchi, Y. (2012). Swine atrophic rhinitis caused by *Pasteurella multocida* toxin and *Bordetella* dermonecrotic toxin. *Curr Top Microbiol Immunol* **361**, 113–129.

Hotchkiss, E. J., Hodgson, J. C., Lainson, F. A. & Zadoks, R. N. (2011). Multilocus sequence typing of a global collection of *Pasteurella multocida* isolates from cattle and other host species demonstrates niche association. *BMC Microbiol* **11**, 115. BioMed Central Ltd.

Hounsome, J. D. a, Baillie, S., Noofeli, M., Riboldi-Tunnicliffe, A., Burchmore, R. J. S., Isaacs, N. W. & Davies, R. L. (2011). Outer membrane protein a of bovine and ovine isolates of *Mannheimia haemolytica* is surface exposed and contains host Species-Specific Epitopes. *Infec Immun* **79**, 4332–4341.

Hsu, Y.-H., Cook, S. R., Alexander, T. W., Klima, C. L., Niu, Y. D., Selinger, L. B. & McAllister, T. a. (2013). Investigation of *Mannheimia haemolytica* bacteriophages relative to host diversity. *J App Microbiol* **114**, 1592–603.

Ingrey, K. T., Ren, J. & Prescott, J. F. (2003). A fluoroquinolone induces a novel mitogen-encoding bacteriophage in *Streptococcus canis*. *Infec Immun* **71**, 3028–3033.

Inouye, M., Conway, T. C., Zobel, J. & Holt, K. E. (2012). Short read sequence typing (SRST): multi-locus sequence types from short reads. *BMC Genomics* **13**, 338. ???

Jacobson, M. J., Lin, G., Whittam, T. S. & Johnson, E. A. (2009). Phylogenetic Analysis of *Clostridium botulinum* Type A by Multi- Locus Sequence Typing. *Microbiol* **154**, 2408–2415.

Jakhetia, R. & Verma, N. K. (2015). Identification and Molecular Characterisation of a Novel

Mu-Like Bacteriophage, SfMu, of *Shigella flexneri*. *PLoS One* **10**, e0124053.

Jin, Y., Sdao, S. M., Dover, J. A., Porcek, N. B., Knobler, C. M., Gelbart, W. M. & Parent, K. N. (2015). Bacteriophage P22 ejects all of its internal proteins before its genome. *Virology* **485**, 128–134. Elsevier.

Jolley, K. a, Chan, M.-S. & Maiden, M. C. J. (2004). mlstdbNet - distributed multi-locus sequence typing (MLST) databases. *BMC Bioinformatics* **5**, 86.

Jones, T. O., Minns, M. & Rimler, R. B. (1988). Isolation of *P. multocida* F-3,4 from a calf in the UK. *Vet Rec* **123**, 354.

Joseph, S. J., Didelot, X., Rothschild, J., De Vries, H. J. C., Morré, S. A., Read, T. D. & Dean, D. (2012). Population genomics of chlamydia trachomatis: Insights on drift, selection, recombination, and population structure. *Mol Biol Evol* **29**, 3933–3946.

Katoch, S., Sharma, M., Patil, R. D., Kumar, S. & Verma, S. (2014). *In vitro* and *in vivo* pathogenicity studies of *Pasteurella multocida* strains harbouring different *ompA*. *Vet Res Commun* **38**, 183–191.

Kearse, M., Moir, R., Wilson, A., Stones-Havas, S., Cheung, M., Sturrock, S., Buxton, S., Cooper, A., Markowitz, S. & other authors. (2012). Geneious Basic: An integrated and extendable desktop software platform for the organization and analysis of sequence data. *Bioinformatics* **28**, 1647–1649.

Kelly, B. G., Vespermann, A. & Bolton, D. J. (2009). The role of horizontal gene transfer in the evolution of selected foodborne bacterial pathogens. *Food Chem Toxicol* **47**, 951–68. Elsevier Ltd.

Kiliç, a O., Pavlova, S. I., Alpay, S., Kiliç, S. S. & Tao, L. (2001). Comparative study of vaginal *Lactobacillus* phages isolated from women in the United States and Turkey: prevalence, morphology, host range, and DNA homology. *Clin diagn lab immunol* **8**, 31–9.

Klimke, W., Rypien, C., Klinger, B., Kennedy, R., Rodriguez-Maillard, J. & Frost, L. (2005). The mating pair stabilization protein, TraN, of the F plasmid is an outer-membrane protein with two regions that are important for its function in conjugation. *Microbiol* **151**, 3527–40.

Kloos, B., Chakraborty, S., Lindner, S. G., Noack, K., Harre, U., Schett, G., Krämer, O. H. & Kubatzky, K. F. (2015). *Pasteurella multocida* toxin- induced osteoclastogenesis requires mTOR activation. *Cell Commun Signal* **1**, 1–13. Cell Communication and Signaling.

Knirel, Y. A. & Valvano, M. A. (2011). *Bacterial Lipopolysaccharides*. Wein, New York: Springer.

Koebnik, R. (1999a). Structural and functional roles of the surface-exposed loops of the beta-barrel membrane protein OmpA from *Escherichia coli*. *J Bacteriol* **181**, 3688–3694.

Koebnik, R. (1999b). Membrane assembly of the *Escherichia coli* outer membrane protein OmpA: exploring sequence constraints on transmembrane beta-strands. *J Mol Biol* **285**, 1801–1810.

Koebnik, R., Locher, K. P. & Van Gelder, P. (2000). Structure and function of bacterial outer membrane proteins: barrels in a nutshell. *Mol Microbiol* **37**, 239–53.

Kovacs-Simon, A., Titball, R. W. & Michell, S. L. (2011). Lipoproteins of bacterial pathogens. *Infec Immun* **79**, 548–561.

Krewulak, K. D. & Vogel, H. J. (2008). Structural biology of bacterial iron uptake. *Biochim Biophys Acta* **1778**, 1781–804.

Krupovič, M. & Bamford, D. H. (2008). Holin of bacteriophage lambda: Structural insights into a membrane lesion. *Mol Microbiol* **69**, 781–783.

Kuhn, S. P., Lampel, J. S. & Strohl, W. R. (1987). Isolation and characterization of a temperate bacteriophage from *Streptomyces galilaeus*. *Appl Env Microbiol* **53**, 2708–13.

Kuhnert, P., Boerlin, P., Emler, S., Krawinkler, M. & Frey, J. (2000). Phylogenetic analysis of *Pasteurella multocida* subspecies and molecular identification of feline *P. multocida* subsp. *septica* by 16S rRNA gene sequencing. *Inter J Med Microbiolo* **290**, 599–604.

Kuhnert, P. & Christensen, H. (2008). *Pasteurellaceae: Biology, Genomics and Molecular Aspects*. Norfolk, UK: Caister Academic Press.

Kuhnert, P. & Korczak, B. M. (2006). Prediction of whole-genome DNA-DNA similarity, determination of G+C content and phylogenetic analysis within the family *Pasteurellaceae* by multilocus sequence analysis (MLSA). *Microbiol* **152**, 2537–48.

Kutter, E. & Alexander, S. (2005). *Bacteriophages : biology and applications*. CRC Press.

Laukkanen-Ninios, R., Didelot, X., Jolley, K. a, Morelli, G., Sangal, V., Kristo, P., Brehony, C., Imori, P. F. M., Fukushima, H. & other authors. (2011). Population structure of the *Yersinia pseudotuberculosis* complex according to multilocus sequence typing. *Env Microbiol* **13**, 3114–27.

Lawrence, J. G., Hatfull, G. F. & Hendrix, R. W. (2002). Imbroglios of viral taxonomy: genetic exchange and failings of phenetic approaches. *J Bacteriol* **184**, 4891–4905.

Lee, I. & Davies, R. L. (2011). Evidence for a common gene pool and frequent recombinational exchange of the *tbpBA* operon in *Mannheimia haemolytica*, *Mannheimia glucosidal* and *Bibersteinia trehalosi*. *Microbiol* **157**, 123–135.

Lee, J., Kim, Y. B. & Kwon, M. (2007). Outer membrane protein H for protective immunity against *Pasteurella multocida*. *J Microbiol* **45**, 179–84.

Lemée, L., Bourgeois, I., Ruffin, E., Collignon, A., Lemeland, J.-F. & Pons, J.-L. (2005). Multilocus sequence analysis and comparative evolution of virulence-associated genes and housekeeping genes of *Clostridium difficile*. *Microbiol* **151**, 3171–80.

De Ley, J., Mannheim, W., Mutters, R., Piechulla, K., Tytgat, R., Segers, P., Bisgaard, M., Frederiksen, W., Hinz, K. H. & Vanhoucke, M. (1990). Inter- and intrafamilial similarities of rRNA cistrons of the *Pasteurellaceae*. *Inter J Syst Bacteriol* **40**, 126–37.

Li, J., Nelson, K., McWhorter, a C., Whittam, T. S. & Selander, R. K. (1994). Recombinational basis of serovar diversity in *Salmonella enterica*. *Proc Natl Acad Sci USA* **91**, 2552–2556.

Li, M., Wang, X., Gao, Q. & Lu, Y. (2009). Molecular characterization of *Staphylococcus epidermidis* strains isolated from a teaching hospital in Shanghai, China. *J Med Microbiol* **58**, 456–61.

Lin, J., Huang, S. & Zhang, Q. (2002). Outer membrane proteins: key players for bacterial adaptation\rin host niches. *Microbes Infect* **4**, 325–331.

Lindbergl, A. A. (1973). Bacteriophage receptors. *Annu Rev Microbiol* **27**, 205–241.

Lo, R. Y. C. & Sorensen, L. S. (2007). The Outer membrane protein OmpA of *Mannheimia haemolytica* A1 is involved in the binding of fibronectin. *FEMS Microbiol lett* **274**, 226–231.

Luo, Y., Glisson, J. R., Jackwood, M. W., Hancock, R. E., Bains, M., Cheng, I. H. & Wang, C. (1997). Cloning and characterization of the major outer membrane protein gene (*ompH*) of

Pasteurella multocida X-73. *J Bacteriol* **179**, 7856–64.

Luo, Y., Zeng, Q., Glisson, J. R., Jackwood, M. W., Cheng, I. H. & Wang, C. (1999). Sequence analysis of *Pasteurella multocida* major outer membrane protein (OmpH) and application of synthetic peptides in vaccination of chickens against homologous strain challenge. *Vaccine* **17**, 821–31.

Lynch, K. H., Stothard, P. & Dennis, J. J. (2010). Genomic analysis and relatedness of P2-like phages of the *Burkholderia cepacia* complex. *BMC Genomics* **11**, 599.

Macdonald, T. E., Helma, C. H., Shou, Y., Valdez, Y. E., Ticknor, L. O., Foley, B. T., Davis, S. W., Hannett, G. E., Kelly-Cirino, C. D. & other authors. (2011). Analysis of *Clostridium botulinum* serotype E strains by using multilocus sequence typing, amplified fragment length polymorphism, variable-number tandem-repeat analysis, and botulinum neurotoxin gene sequencing. *Appli Env Microbiol* **77**, 8625–34.

Maiden, M. C. J. (2006). Multilocus sequence typing of bacteria. *Annu Rev Microbiol* **60**, 561–88.

Maiden, M. C. J., Bygraves, J. A., Feil, E., Morelli, G., Russell, J. E., Urwin, R., Zhang, Q., Zhou, J., Zurth, K. & other authors. (1998). Multilocus sequence typing- A portable approach to the identification of clones within populations of clones within populations of pathogenic microorganisms. *Microbiol* **95**, 3140–3145.

Manning, P. J., DiGiacomo, R. F. & DeLong, D. (1989). Pasteurellosis in Laboratory Animals. In *Pasteurella and Pasteurellosis*, pp. 264– 302. Edited by C. Adlam & J. M. Rutter. UK: Academic press Limited.

Masignani, V., Giuliani, M. M., Tettelin, H., Comanducci, M., Rappuoli, R. & Scarlato, V. (2001). Mu-like prophage in serogroup B *Neisseria meningitidis* coding for surface-exposed antigens. *Infec Immun* **69**, 2580–2588.

Matsuura, M. (2013). Structural modifications of bacterial lipopolysaccharide that facilitate gram-negative bacteria evasion of host innate immunity. *Front Immun* **4**, 1–9.

Mccarter, J. D., Stephens, D., Shoemaker, K., Rosenberg, S., Kirsch, J. F., Georgiou, G. & Acteriol, J. B. (2004). Substrate specificity of the *Escherichia coli* Outer membrane protease OmpT. *J Bacteriol* **186**, 5919–5925.

Mell, J. C. & Redfield, R. J. (2014). Natural competence and the evolution of DNA uptake specificity. *J Bacteriol* **196**, 1471–1483.

St. Michael, F., Harper, M., Parnas, H., John, M., Stupak, J., Vinogradov, E., Adler, B., Boyce, J. D. & Cox, A. D. (2009). Structural and genetic basis for the serological differentiation of *Pasteurella multocida* Heddleston serotypes 2 and 5. *J Bacteriol* **191**, 6950–6959.

Michael, T., Martinko, J. M. & Parker, J. M. (2003). *Brock Biology of Microorganisms*, 10th edn. Pearson Education LTD., London.

Michel, B. (2005). After 30 years of study, the bacterial SOS response still surprises us. *PLoS Biol* **3**, 1174–1176.

Miller, C., Thomsen, L. E., Gaggero, C., Mosseri, R., Ingmer, H. & Cohen, S. N. (2004). SOS response induction by beta-lactams and bacterial defense against antibiotic lethality. *Science (80-)* **305**, 1629–31.

Miller, W. G., Englen, M. D., Kathariou, S., Wesley, I. V, Wang, G., Pittenger-Alley, L., Siletz,

R. M., Muraoka, W., Fedorka-Cray, P. J. & Mandrell, R. E. (2006). Identification of host-associated alleles by multilocus sequence typing of *Campylobacter coli* strains from food animals. *Microbiol* **152**, 245–55.

Mirold, S., Rabsch, W., Rohde, M., Stender, S., Tschäpe, H., Rüssmann, H., Igwe, E. & Hardt, W. D. (1999). Isolation of a temperate bacteriophage encoding the type III effector protein SopE from an epidemic *Salmonella typhimurium* strain. *Proc Natl Acad Sci* **96**, 9845–50.

Mohamed, M. a, Mohamed, M.-W. a, Ahmed, A. I., Ibrahim, A. a & Ahmed, M. S. (2012). *Pasteurella multocida* in backyard chickens in Upper Egypt: incidence with polymerase chain reaction analysis for capsule type, virulence in chicken embryos and antimicrobial resistance. *Vet Ital* **48**, 77–86.

Moreno Switt, A. I., Orsi, R. H., den Bakker, H. C., Vongkamjan, K., Altier, C. & Wiedmann, M. (2013). Genomic characterization provides new insight into *Salmonella* phage diversity. *BMC Genomics* **14**, 481.

Morgan, G. J., Hatfull, G. F., Casjens, S. & Hendrix, R. W. (2002). Bacteriophage Mu genome sequence: analysis and comparison with Mu-like prophages in *Haemophilus*, *Neisseria* and *Deinococcus*. *J Mol Biol* **317**, 337–359.

Morona, R., Kramer, C. & Henning, U. L. F. (1985). Bacteriophage Receptor Area of Outer Membrane Protein OmpA of *Escherichia coli* K-12. *J Bacteriol* **164**, 539–543.

Moustafa, A. M., Bennett, M. D., Edwards, J., Azim, K., Mesaik, M. a, Choudhary, M. I., Pathanasophon, P., Worarach, A., Ali, Q. & other authors. (2013). Molecular typing of haemorrhagic septicaemia-associated *Pasteurella multocida* isolates from Pakistan and Thailand using multilocus sequence typing and pulsed-field gel electrophoresis. *Res Vet Sci* **95**, 986–90. Elsevier Ltd.

Muhldorfer, K., Speck, S. & Wibbelt, G. (2014). Proposal of *Vespertiliibacter pulmonis* gen. nov., sp. nov. and two genomospecies as new members of the family *Pasteurellaceae* isolated from European bats. *Inter J Syst Evol Microbiol* **64**, 2424–2430.

Mullins, M. A., Register, K. B., Brunelle, B. W., Aragon, V., Galofr??-Mila, N., Bayles, D. O. & Jolley, K. A. (2013). A curated public database for multilocus sequence typing (MLST) and analysis of *Haemophilus parasuis* based on an optimized typing scheme. *Vet Microbiol* **162**, 899–906.

Muniesa, M., Simon, M. De, Prats, G., Ferrer, D., Pañella, H. & Jofre, J. (2003). Shiga toxin 2-converting bacteriophages associated with clonal variability in *Escherichia coli* O157 : H7 strains of human origin isolated from a single outbreak. *Infec Immun* **71**, 4554–4562.

Muniesa, M., Blanco, J. E., De Simón, M., Serra-Moreno, R., Blanch, A. R. & Jofre, J. (2004). Diversity of stx2 converting bacteriophages induced from Shiga-toxin-producing *Escherichia coli* strains isolated from cattle. *Microbiol* **150**, 2959–71.

Murphy, F. a, Kingsbury, D. W., Fields, B. N. & Knipe, D. M. (2012). Classification and nomenclature of viruses: ninth report of the international committee on taxonomy of viruses. In *Virus Taxon*. San Diego: Elsevier Inc.

Mutters, R., Ihm, P., Pohl, S., Frederiksen, W. & Mannheim, W. (1985). Reclassification of the genus *Pasteurella trevisan* 1887 on the basis of deoxyribonucleic acid homology , with proposals for the new species *Pasteurella dagmatis* , *Pasteurella canis* , *Pasteurella* 309–

322.

Nagai, S., Someno, S. & Yagihashi, T. (1994). Differentiation of toxigenic from nontoxigenic isolates of *Pasteurella multocida* by PCR. *J Clin Microbiol* **32**, 1004–10.

Nakayama, K., Kanaya, S., Ohnishi, M., Terawaki, Y. & Hayashi, T. (1999). The complete nucleotide sequence of phi CTX, a cytotoxin-converting phage of *Pseudomonas aeruginosa*: implications for phage evolution and horizontal gene transfer via bacteriophages. *Mol Microbiol* **31**, 399–419.

Nale, J. Y., Shan, J., Hickenbotham, P. T., Fawley, W. N., Wilcox, M. H. & Clokie, M. R. J. (2012). Diverse temperate bacteriophage carriage in *Clostridium difficile* 027 strains. *PLoS One* **7**, e37263.

Naushad, S., Adeolu, M., Goel, N., Khadka, B., Al-Dahwi, A., Gupta, R. S., Naushad, S., Adeolu, M., Goel, N. & other authors. (2015). Phylogenomic and molecular demarcation of the core members of the polyphyletic *Pasteurellaceae* genera *Actinobacillus*, *Haemophilus*, and *Pasteurella*. *Inter J Genom* **2015**, 1–15.

Nelson, D. (2004). Phage taxonomy : we agree to disagree. *J Bacteriol* **186**.

Nielsen, J. P. & Rosdahl, V. T. (1990). Development and epidemiological applications of a bacteriophage typing system for typing *Pasteurella multocida*. *J Clin Microbiol* **28**, 103–7.

Nikaido, H. (2003). Molecular basis of bacterial outer membrane permeability revisited **67**.

Niu, Y. D., Cook, S. R., Hsu, Y., Kropinski, A. M. & Mcallister, T. a. (2013). Comparative genomic analysis of multiple inducible bacteriophages from *Mannheimia haemolytica*. *Mol Genet Bact Phage Meet*. BMC Microbiology.

Niu, Y. D., Cook, S. R., Wang, J., Klima, C. L., Hsu, Y., Kropinski, A. M., Turner, D. & McAllister, T. A. (2015). Comparative analysis of multiple inducible phages from *Mannheimia haemolytica*. *BMC Microbiol* **15**, 175. BMC Microbiology.

Novick, R. P., Christie, G. E. & Penadés, J. R. (2010). The phage-related chromosomal islands of Gram-positive bacteria. *Nat Rev Microbiol* **8**, 541–51.

Ochman, H., Lawrence, J. G. & Groisman, E. a. (2000). Lateral gene transfer and the nature of bacterial innovation. *Nature* **405**, 299–304.

Oehler, R. L., Velez, A. P., Mizrachi, M., Lamarche, J. & Gompf, S. (2009). Bite-related and septic syndromes caused by cats and dogs. *Lancet Infec Dise* **9**, 439–447.

Ohnishi, M., Kurokawa, K. & Hayashi, T. (2001). Diversification of *Escherichia coli* genomes: Are bacteriophages the major contributors? *Tren Microbiol* **9**, 481–485.

Okay, S., Özcengiz, E., Gürsel, I. & Özcengiz, G. (2012). Immunogenicity and protective efficacy of the recombinant *Pasteurella* lipoprotein E and outer membrane protein H from *Pasteurella multocida* A:3 in mice. *Res Vet Sci* **93**, 1261–1265.

Oldfield, N. J., Donovan, E. A., Worrall, K. E., Wooldridge, K. G., Langford, P. R., Rycroft, A. N. & Ala'Aldeen, D. A. A. (2008). Identification and characterization of novel antigenic vaccine candidates of *Actinobacillus pleuropneumoniae*. *Vaccine* **26**, 1942–1954.

Olvera, A., Cerdà-Cuéllar, M. & Aragon, V. (2006). Study of the population structure of *Haemophilus parasuis* by multilocus sequence typing. *Microbiol* **152**, 3683–90.

Oppenheim, A. B., Kobiler, O., Stavans, J., Court, D. L. & Adhya, S. (2005). Switches in bacteriophage lambda development. *Annu Rev Genet* **39**, 409–429.

Orlova, E. V. (2012). Bacteriophages and their structural organisation. *Bacteriophages* 3–30.

Orme, R., Douglas, C. W. I., Rimmer, S. & Webb, M. (2006). Proteomic analysis of *Escherichia coli* biofilms reveals the overexpression of the outer membrane protein OmpA. *Proteomics* **6**, 4269–4277.

Orth, J. H. C. & Aktories, K. (2010). *Pasteurella multocida* toxin activates various heterotrimeric G proteins by deamidation. *Toxins (Basel)* **2**, 205–214.

Overbeek, R., Olson, R., Pusch, G. D., Olsen, G. J., Davis, J. J., Disz, T., Edwards, R. A., Gerdes, S., Parrello, B. & other authors. (2014). The SEED and the Rapid Annotation of microbial genomes using Subsystems Technology (RAST). *Nucleic Acids Res* **42**, 206–214.

Pan, X., Yang, Y. & Zhang, J.-R. (2014). Molecular basis of host specificity in human pathogenic bacteria. *Emerg Microbes Infect* **3**, e23.

Parent, K. N., Erb, M. L., Cardone, G., Nguyen, K., Gilcrease, E. B., Porcek, N. B., Pogliano, J., Baker, T. S. & Casjens, S. R. (2014). OmpA and OmpC are critical host factors for bacteriophage Sf6 entry in *Shigella*. *Mol Microbiol* **92**, 47–60.

Parija, S. C. (2009). *Textbook of Microbiology & Immunolog*. Elsevier, A division of Reed Elsevier India Pvt.Ltd.

Pautsch, a & Schulz, G. E. (1998). Structure of the outer membrane protein A transmembrane domain. *Nat Struc Biol* **5**, 1013–1017.

Pautsch, a & Schulz, G. E. (2000). High-resolution structure of the OmpA membrane domain. *J Mol Biol* **298**, 273–282.

Penadés, J. R. & Christie, G. E. (2015). The Phage-Inducible Chromosomal Islands: A Family of Highly Evolved Molecular Parasites. *Annu Rev Virol* **2**, 181–201.

Penadés, J. R., Chen, J., Quiles-Puchalt, N., Carpena, N. & Novick, R. P. (2015). Bacteriophage-mediated spread of bacterial virulence genes. *Curr Opin Microbiol* **23**, 171–178.

Petersen, A., Bisgaard, M., Townsend, K. & Christensen, H. (2014). MLST typing of *Pasteurella multocida* associated with haemorrhagic septicaemia and development of a real-time PCR specific for haemorrhagic septicaemia associated isolates. *Vet Microbio* **170**, 335–341. Elsevier B.V.

Piddock, L. J. V. (2006). Multidrug-resistance efflux pumps - not just for resistance. *Natu Rev Microbiol* **4**, 629–636.

Poblet-Icart, M., Bordons, A. & Lonvaud-Funel, A. (1998). Lysogeny of *Oenococcus oeni* (syn. *Leuconostoc oenos*) and study of their induced bacteriophages. *Curr Microbiol* **36**, 365–9.

Polissi, A. & Sperandeo, P. (2014). The lipopolysaccharide export pathway in *Escherichia coli*: Structure, organization and regulated assembly of the Lpt machinery. *Mar Drugs* **12**, 1023–1042.

Porcek, N. B. & Parent, K. N. (2015). Key residues of *S. flexneri* OmpA mediate infection by bacteriophage Sf6. *Mol Biol* **427**, 1964–1976. Elsevier Ltd.

Pourcel, C., Midoux, C., Bourkaltseva, M. & Pleteneva, E. (2016). Complete Genome Sequence of PM105 , a New *Pseudomonas aeruginosa* B3-Like Transposable Phage. *Amer Soc Microbiol* **4**, 2015–2016.

Prasannavadhana, A., Kumar, S., Thomas, P., Sarangi, L. N., Gupta, S. K., Priyadarshini, A.,

Nagaleekar, V. K. & Singh, V. P. (2014). Outer membrane proteome analysis of indian strain of *Pasteurella multocida* serotype B:2 by MALDI-TOF/MS analysis. *Scien World J* **2014**.

Pullinger, G. D., Bevir, T. & Lax, A. J. (2004). The *Pasteurella multocida* toxin is encoded within a lysogenic bacteriophage. *Mol Microbiol* **51**, 255–269.

Rahimi, F., Bouzari, M., Katouli, M. & Pourshafie, M. R. (2012). Prophage and antibiotic resistance profiles of methicillin-resistant *Staphylococcus aureus* strains in Iran. *Arch virol* **157**, 1807–1811.

Rakhuba, D. V, Kolomiets, E. I., Dey, E. S. & Novik, G. I. (2010). Bacteriophage receptors, mechanisms of phage adsorption and penetration into host cell. *Pol J Microbiol* **59**, 145–55.

Randall-Hazelbauer, L. & Schwartz, M. (1973). Isolation of the bacteriophage lambda receptor from *Escherichia coli*. *J Bacteriol* **116**, 1436–1446.

Reeves, P. (1993). Evolution of *Salmonella* O antigen variation by interspecific gene transfer on a large scale. *Tren Genet* **9**, 17–22.

Reeves, P. R., Cunneen, M. M., Liu, B. & Wang, L. (2013). Genetics and evolution of the *Salmonella* galactose-initiated set of O antigens. *PLoS One* **8**, 1–22.

Reid, S. D., Herbelin, C. J., Bumbaugh, a C., Selander, R. K. & Whittam, T. S. (2000). Parallel evolution of virulence in pathogenic *Escherichia coli*. *Nature* **406**, 64–7.

Resch, G., Kulik, E. M., Dietrich, F. S. & Meyer, J. (2004). Complete genomic nucleotide sequence of the temperate bacteriophage Aaphi23 of *Actinobacillus actinomycetemcomitans*. *J Bacteriol* **186**, 5523–5528.

Richards, A., Renshaw, H. & Sneed, L. (1985). *Pasteurella haemolytica* bacteriophage : identification , partial characterization , and relationship of temperate bacteriophages from isolates of *Pasteurella haemolytica* (biotype A , serotype 1). *Am J Vet Res* **46**, 1215–20.

Rimler, R. B. & Rhoades, K. R. (1989). *Pasteurella multocida*. In *Pasteurella and Pasteurellosis*, pp. 37–73. Edited by C. Adlam & J. M. Rutter. UK: Academic press Limited.

Roberts, I. S. (1996). The biochemistry and genetics of capsular polysaccharide production in bacteria. *Annu Rev Microbiol* **50**, 285–315.

Rogers, S. O. (2012). *Integrated Molecular Evolution*. Boca Raton, London & NewYork: CRC Press.

Rohwer, F. & Edwards, R. (2002). The phage proteomic tree : a genome-based taxonomy for phage. *J Bacteriol* **184**.

Rokney, A., Kobiler, O., Amir, A., Court, D. L., Stavans, J., Adhya, S. & Oppenheim, A. B. (2008). Host responses influence on the induction of lambda prophage. *Mol Microbiol* **68**, 29–36.

Rollauer, S. E., Sooreshjani, M. A., Noinaj, N., Buchanan, S. K. & Buchanan, S. K. (2015). Outer membrane protein biogenesis in Gram-negative bacteria. *R Soci*.

Ruffolo, C. G., Tennent, J. M., Michalski, W. P. & Adler, B. (1997). Identification, purification, and characterization of the type 4 fimbriae of *Pasteurella multocida*. *Infec Immun* **65**, 339–343.

Ruiz, N., Kahne, D. & Silhavy, T. J. (2006). Advances in understanding bacterial outer-

membrane biogenesis. *Nat Rev Microbiol* **4**, 57–66.

Sabat, A. J., Wladyka, B., Kosowska-Shick, K., Grundmann, H., van Dijl, J. M., Kowal, J., Appelbaum, P. C., Dubin, A. & Hryniewicz, W. (2008). Polymorphism, genetic exchange and intragenic recombination of the aureolysin gene among *Staphylococcus aureus* strains. *BMC Microbiol* **8**, 129.

Sadowski, P. (1986). Site-specific recombinases: changing partners and doing the twist. *J Bacteriol* **165**, 341–347.

Saif, Y. M. (2008). *Diseases of poultry*. Wiley-Blackwell,Ames.

Salmond, G. P. C. & Fineran, P. C. (2015). A century of the phage: past, present and future. *Nat Rev Microbiol* **13**, 777–786. Nature Publishing Group.

Sambrook, J., Fristch, E. F. & Maniatis, T. (1989). *Molecular cloning, a laboratory manual*, 2nd edn. Cold Spring Harbor, New York: Cold Spring Harbor Laboratory Press.

Sandt, C. H., Hopper, J. E. & Hill, C. W. (2002). Activation of Prophage eib Genes for Immunoglobulin-Binding Proteins by Genes from the IbrAB Genetic Island of *Escherichia coli* ECOR-9. *J Bacteriol* 3640–3648.

Saunders, J. R., Allison, H., James, C. E., McCarthy, A. J. & Sharp, R. (2001). Phage-mediated transfer of virulence genes. *J Chem Technol Biotechnol* **76**, 662–666.

Schicklmaier, P. & Schmieger, H. (1995). Frequency of generalized transducing phages in natural isolates of the *Salmonella typhimurium* complex. *Appl Env Microbiol* **61**, 1637–1640.

Schicklmaier, P., Moser, E., Wieland, T., Rabsch, W. & Schmieger, H. (1998). A comparative study on the frequency of prophages among natural isolates of *Salmonella* and *Escherichia coli* with emphasis on generalized transducers. *Antonie van Leeuwenhoek,* **73**, 49–54.

Seed, K. D. & Dennis, J. J. (2005). Isolation and characterization of bacteriophages of the *Burkholderia cepacia* complex. *FEMS Microbiol Lett* **251**, 273–280.

Sekulovic, O., Garneau, J. R., Neron, A. & Fortier, L. C. (2014). Characterization of temperate phages infecting *Clostridium difficile* isolates of human and animal origins. *Appl Env Microbiol* **80**, 2555–2563.

Sellyei, B., Banyai, K. & Magyar, T. (2010). Characterization of the *ptfA* gene of avian *Pasteurella multocida* strains by allele-specific polymerase chain reaction. *J Vet Diagn Inves* **22**, 607–610.

Sepúlveda-Robles, O., Kameyama, L. & Guarneros, G. (2012). High diversity and novel species of *Pseudomonas aeruginosa* bacteriophages. *Appl Env Microbiol* **78**, 4510–4515.

Shayegh, J., Atashpaz, S. & Hejazi, M. S. (2008). Virulence Genes Profile and Typing of Ovine 380 *Pasteurella multocida*. *Asian J Anim Vet Adv* **3**, 206–213.

Shin, H., Lee, J.-H., Yoon, H., Kang, D.-H. & Ryu, S. (2014). Genomic investigation of lysogen formation and host lysis systems of the *Salmonella* temperate bacteriophage SPN9CC. *Appl Env Microbiol* **80**, 374–84.

Shinagawa, H., Mizuuchi, K. & Emmerson, P. T. (1977). Induction of prophage lambda by X-rays, mitomycin C and tif; Repressor cleavage studied by immunoprecipitation. *Mol Gen Genet* **155**, 87–91.

Silhavy, T. J., Kahne, D. & Walker, S. (2010). The bacterial cell envelope. *Cold Spring Harb Perspect Biol* **2**, 1–16.

Silva, G. F. R., Brandão, L. N. S., Paula, D. A. J., Pescador, C. A. P., Chitarra, C. S., Carvalho, R. C. T., Nakazato, L. & Dutra, V. (2012). Characterization using multilocus sequence typing and virulence factor of *Pasteurella multocida* from pigs with pneumonia in States of Mato Grosso and Mato Grosso Do Sul-Brazil. *Vet Sci Res* **3**, 55–59.

Singh, R., Tewari, K., Packiriswamy, N., Marla, S. & Rao, V. D. P. (2011). Molecular characterization and computational analysis of the major outer membrane protein (*ompH*) gene of *Pasteurella multocida* P52. *Vet Arh* **81**, 211–222.

Skurray, R. A., Hancock, R. E. W. & P. Reeves. (1974). Con- mutants: class of mutants in *Escherichia coli* K-12 lacking a major cell wall protein and defective in conjugation and adsorption of a bacteriophage. *J Bacteriol* **119**, 726–735.

Smith, D. L., Rooks, D. J., Fogg, P. C., Darby, A. C., Thomson, N. R., McCarthy, A. J. & Allison, H. E. (2012). Comparative genomics of Shiga toxin encoding bacteriophages. *BMC Genomics* **13**, 311.

Smith, N. H., Beltran, P. & Selander, R. K. (1990). Recombination of *Salmonella* phase 1 flagellin genes generates new serovars. *J Bacteriol* **172**, 2209–2216.

Smith, S. G. J., Mahon, V., Lambert, M. a & Fagan, R. P. (2007). A molecular Swiss army knife: OmpA structure, function and expression. *FEMS microbiol lett* **273**, 1–11.

Sonntag, I., Schwarz, H. & Hirota, Y. (1978). Cell envelope and shape of *Escherichia coli* : multiple mutants missing the outer membrane lipoprotein and other major outer membrane proteins. *J Bacteriol* **136**, 280–285.

Spratt, B. G. (1999). Multilocus sequence typing: molecular typing of bacterial pathogens in an era of rapid DNA sequencing and the internet. *Curr Opin Microbiol* **2**, 312–6.

St Michael, F., Vinogradov, E., Li, J. & Cox, A. D. (2005). Structural analysis of the lipopolysaccharide from *Pasteurella multocida* genome strain Pm70 and identification of the putative lipopolysaccharide glycosyltransferases. *Glycobiol* **15**, 323–33.

Stevenson, R. M. & Airdrie, D. W. (1984). Isolation of *Yersinia ruckeri* bacteriophages. *Appl Env Microbiol* **47**, 1201–5.

Steyert, S. R., Sahl, J. W., Fraser, C. M., Teel, L. D., Scheutz, F. & Rasko, D. A. (2012). Comparative genomics and stx phage characterization of LEE-negative Shiga toxin-producing *Escherichia coli*. *Front Cell Infect Microbiol* **2**, 133.

Strauch, E., Schaudinn, C. & Beutin, L. (2004). First-time isolation and characterization of a bacteriophage encoding the shiga toxin 2c variant , which is globally spread in strains of *Escherichia coli* O157. *Infec Immun*.

Strockbine, N. A., Jackson, M. P., Sung, L. M., Holmes, R. K. & O'Brien, A. D. (1988). Cloning and sequencing of the genes for Shiga toxin from *Shigella dysenteriae* type 1. *J Bacteriol* **173**, 1116–1122.

Subaaharan, S., Blackall, L. L. & Blackall, P. J. (2010). Development of a multi-locus sequence typing scheme for avian isolates of *Pasteurella multocida*. *Vet Microbiol* **141**, 354–61. Elsevier B.V.

Sullivan, M. J., Petty, N. K. & Beatson, S. A. (2011). Easyfig: a genome comparison visualizer. - PubMed - NCBI. *Bioinformatics* **27**, 1009–1010.

Summer, E. J. (2009). Preparation of a phage DNA fragment library for whole genome shotgun

sequencing. *Meth Mol Biol* **502**, 27–46.

Summer, E. J., Gonzalez, C. F., Carlisle, T., Mebane, L. M., Cass, A. M., Savva, C. G., LiPuma, J. & Young, R. (2004). *Burkholderia cenocepacia* Phage BcepMu and a Family of Mu-like Phages Encoding Potential Pathogenesis Factors. *J Mol Biol* **340**, 49–65.

Tamm, L. K., Hong, H. & Liang, B. (2004). Folding and assembly of beta-barrel membrane proteins. *Biochim Biophys Acta* **1666**, 250–63.

Tamura, K., Dudley, J., Nei, M. & Kumar, S. (2007). Molecular Evolutionary Genetics Analysis (MEGA) software version 4.0. *Mol Biol Evol* **24**, 1596–1599.

Tan, H. Y., Nagoor, N. H. & Sekaran, S. D. (2010). Cloning, expression and protective capacity of 37 kDa outer membrane protein gene (*ompH*) of *Pasteurella multocida* serotype B:2. *Trop Biomed* **27**, 430–41.

Tang, X., Zhao, Z., Hu, J., Wu, B., Cai, X., He, Q. & Chen, H. (2009). Isolation, antimicrobial resistance, and virulence genes of *Pasteurella multocida* strains from swine in China. *J Clin Microbiol* **47**, 951–958.

Tian, H., Fu, F., Li, X., Chen, X., Wang, W., Lang, Y., Cong, F., Liu, C., Tong, G. & Li, X. (2011). Identification of the immunogenic outer membrane protein A antigen of *Haemophilus parasuis* by a proteomics approach and passive immunization with monoclonal antibodies in mice. *Clin Vaccine Immunol* **18**, 1695–1701.

Tomich, M., Planet, P. J. & Figurski, D. H. (2007). The tad locus: postcards from the widespread colonization island. *Natu Rev Microbiol* **5**, 363–75.

Tommassen, J. (2010). Assembly of outer-membrane proteins in bacteria and mitochondria. *Microbiol* **156**, 2587–2596.

Tormo, M. Á., Ferrer, M. D., Maiques, E., Úbeda, C., Selva, L., Lasa, Í., Calvete, J. J., Novick, R. P. & Penadés, J. R. (2008). *Staphylococcus aureus* pathogenicity island DNA is packaged in particles composed of phage proteins. *J Bacteriol* **190**, 2434–2440.

Torres, A. G. & Kaper, J. B. (2003). Multiple elements controlling adherence of enterohemorrhagic *Escherichia coli* O157 : H7 to heLa cells. *Infec Immun* **71**, 4985–4995.

Treangen, T. J., Ondov, B. D., Koren, S. & Phillippy, A. M. (2014). Rapid core-genome alignment and visualization for thousands of microbial genomes. *Genome Biol*.

Turner, S. M., Chaudhuri, R. R., Jiang, Z.-D., DuPont, H., Gyles, C., Penn, C. W., Pallen, M. J. & Henderson, I. R. (2006). Phylogenetic comparisons reveal multiple acquisitions of the toxin genes by enterotoxigenic *Escherichia coli* strains of different evolutionary lineages. *J Clin Microbiol* **44**, 4528–36.

Ubeda, C., Olivarez, N. P., Barry, P., Wang, H., Kong, X., Matthews, A., Tallent, S. M., Christie, G. E. & Novick, R. P. (2009). Specificity of *Staphylococcal* phage and SaPI DNA packaging as revealed by integrase and terminase mutations. *Mol Microbiol* **72**, 98–108.

Úbeda, C., Maiques, E., Knecht, E., Lasa, Í., Novick, R. P. & Penadés, J. R. (2005). Antibiotic-induced SOS response promotes horizontal dissemination of pathogenicity island-encoded virulence factors in *Staphylococci*. *Mol Microbiol* **56**, 836–844.

Uchiyama, J., Takemura-Uchiyama, I., Sakaguchi, Y., Gamoh, K., Kato, S.-I., Daibata, M., Ujihara, T., Misawa, N. & Matsuzaki, S. (2014). Intragenus generalized transduction in *Staphylococcus* spp. by a novel giant phage. *ISME J* **8**, 1–4. Nature Publishing Group.

Urban-Chmiel, R., Wernicki, A., Stęgierska, D., Dec, M., Dudzic, A. & Puchalski, A. (2015). Isolation and characterization of lytic properties of bacteriophages specific for *M. haemolytica* strains. *PLoS One* **10**, e0140140.

Urwin, R. & Maiden, M. C. J. (2003). Multi-locus sequence typing-a tool for global epidemiology. *Tren Microbiol* **11**, 479–487.

Varga, Z., Volokhov, D. V., Stipkovits, L., Thuma, Á., Sellyei, B. & Magyar, T. (2013). Characterization of *Pasteurella multocida* strains isolated from geese. *Vet Microbio* **163**, 149–156.

Ventura, M., Canchaya, C., Kleerebezem, M., De Vos, W. M., Siezen, R. J. & Brüssow, H. (2003). The prophage sequences of *Lactobacillus plantarum* strain WCFS1. *Virology* **316**, 245–255.

Veses-Garcia, M., Liu, X., Rigden, D. J., Kenny, J. G., McCarthy, A. J. & Allison, H. E. (2015). Transcriptomic analysis of shiga-toxigenic bacteriophage carriage reveals a profound regulatory effect on acid resistance in *Escherichia coli*. *Appl Env Microbiol* **81**, 8118–8125.

Volponi, G., Rooks, D. J., Smith, D. L., Picozzi, C., Allison, H. E., Vigentini, I., Foschino, R. & McCarthy, a J. (2012). Short communication: Characterization of Shiga toxin 2-carrying bacteriophages induced from Shiga-toxigenic *Escherichia coli* isolated from Italian dairy products. *J dairy Sci* **95**, 6949–56. Elsevier.

Vougidou, C., Sandalakis, V., Psaroulaki, A., Siarkou, V., Petridou, E. & Ekateriniadou, L. (2015). Distribution of the *ompA*-types among ruminant and swine pneumonic strains of *Pasteurella multocida* exhibiting various *cap*-locus and *toxA* patterns. *Microbiol Res* **174**, 1–8. Elsevier GmbH.

Waldor, M. K. & Mekalanos, J. J. (1996). Lysogenic conversion by a filamentous phage encoding cholera toxin. *Science (80-)* 1910–1914.

Waldor, M. K. & Friedman, D. I. (2005). Phage regulatory circuits and virulence gene expression. *Curr Opin Microbiol* **8**, 459–465.

Walker, G. C. (1984). Mutagenesis and inducible responses to deoxyribonucleic acid damage in *Escherichia coli*. *Microbiol Rev* **48**, 60–93.

Walther, D. M., Rapaport, D. & Tommassen, J. (2009). Biogenesis of beta-barrel membrane proteins in bacteria and eukaryotes: evolutionary conservation and divergence. *CMLS* **66**, 2789–804.

Weeks, .R. & Ferretti, J. J. (1984). The gene for type A streptococcal exotoxin (erythrogenic toxin) is located in bacteriophage T12. *Infect Immun* **46**, 531–536.

Weinbauer, M. G. (2004). Ecology of prokaryotic viruses. *FEMS Microbioll Rev* **28**, 127–181.

Weinbauer, M. G. & Rassoulzadegan, F. (2004). Are viruses driving microbial diversification and diversity? *Enviro Microbiol* **6**, 1–11.

Weiser, G. C., DeLong, W. J., Paz, J. L., Shafii, B., Price, W. J. & Ward, A. C. (2003). Characterization of *Pasteurella multocida* associated with pneumonia in bighorn sheep. *J Wildl dise* **39**, 536–544.

Wilkie, I. W., Harper, M., Boyce, J. D. & Adler, B. (2012). Diseases and Pathogenesis. In *Pasteurella multocida*, pp. 1–22. Edited by K. Aktories, J. H. C. Orth & B. Alder. Springer Berlin Heidelberg.

Williams, B. J., Golomb, M., Phillips, T., Brownlee, J., Olson, M. V & Smith, A. L. (2002). Bacteriophage HP2 of *Haemophilus influenzae*. *J Bacteriol* **184**, 6893–6905.

Wu, J. R., Shien, J. H., Shieh, H. K., Chen, C. F. & Chang, P. C. (2007). Protective immunity conferred by recombinant *Pasteurella multocida* lipoprotein E (PlpE). *Vaccine* **25**, 4140–4148. Elsevier Ltd.

Wyres, K. L., Lambertsen, L. M., Croucher, N. J., McGee, L., Von Gottberg, A., Liñares, J., Jacobs, M. R., Kristinsson, K. G., Beall, B. W. & other authors. (2013). Pneumococcal capsular switching: A historical perspective. *J Infect Dis* **207**, 439–449.

Yamaguchi, T., Hayashi, T., Takami, H., Nakasone, K., Ohnishi, M., Nakayama, K., Yamada, S., Komatsuzawa, H. & Sugai, M. (2000). Phage conversion of exfoliative toxin A production in *Staphylococcus aureus*. *Mol Microbiol* **38**, 694–705.

Yan, W., Faisal, S. M., McDonough, S. P., Chang, C. F., Pan, M. J., Akey, B. & Chang, Y. F. (2010). Identification and characterization of OmpA-like proteins as novel vaccine candidates for Leptospirosis. *Vaccine* **28**, 2277–2283. Elsevier Ltd.

Zehr, E. S. & Tabatabai, L. B. (2011). Detection of a bacteriophage gene encoding a Mu-like portal protein in *Haemophilus parasuis*. *J Vet Diagn Invest* **23**, 538–42.

Zehr, E. S., Tabatabai, L. B. & Bayles, D. O. (2012). Genomic and proteomic characterization of SuMu, a Mu-like bacteriophage infecting *Haemophilus parasuis*. *BMC Genomics* **13**, 331.

Zhang, D. feng, Li, H., Lin, X. min & Peng, X. xian. (2015). Outer membrane proteomics of kanamycin-resistant *Escherichia coli* identified MipA as a novel antibiotic resistance-related protein. *FEMS microbiol lett* **362**, 1–8.

Zhou, Y., Liang, Y., Lynch, K. H., Dennis, J. J. & Wishart, D. S. (2011). PHAST: A Fast Phage Search Tool. *Nucleic Acids Res* **39**, 1–6.

Chapter 8 Appendices

Table 8.1 PHAST analysis of PMMu3 (ϕPM850.2) against phage genome database.

Orfs	Protein product	Size (bp/aa)	BLAST_hit	E-value
Orf1	Probable transcription regulator	711/236	PHAGE_Haemop_SuMu_NC_019455: transcription regulator	2e-53
Orf2	DNA-binding protein	267/89	PHAGE_Haemop_SuMu_NC_019455: Mu-like prophage FluMu DNA-binding protein Ner	6e-21
Orf3	Transposase	1986/661	PHAGE_Vibrio_12B12_NC_021070: transposase	1e-161
Orf4	DNA transposition protein #protein B	918/306	PHAGE_Haemop_SuMu_NC_019455: phage transposase	4e-28
Orf5	Hypothetical protein	297/98	PHAGE_Haemop_SuMu_NC_019455: hypothetical protein	2e-06
Orf6	Hypothetical protein	228/76	Hypothetical protein	0.0
Orf7	DNA recombination nuclease inhibitor Gam (ACLAME 731)	522/173	PHAGE_Haemop_SuMu_NC_019455: host-nuclease inhibitor protein	7e-49
Orf8	Hypothetical protein	189/63	PHAGE_Haemop_SuMu_NC_019455: hypothetical protein	5e-05
Orf9	Hypothetical protein	168/55	Hypothetical protein	0.0
Orf10	Hypothetical protein	915/305	Hypothetical protein	0.0
Orf11	Mu-like prophage protein gp16, GamA	501/167	PHAGE_Burkho_BcepMu_NC_005882: gp02	3e-12
Orf12	Hypothetical protein	543/180	PHAGE_Mannhe_vB_MhM_3927AP2_NC_028766: hypothetical protein	1e-41
Orf13	Putative bacteriophage transcriptional regulator, Mor	363/120	PHAGE_Burkho_BcepMu_NC_005882: gp01	1e-26
Orf14	Hypothetical protein	423/140	Hypothetical protein	0.0
Orf15	Negative regulator of beta-lactamase expression	537/179	PHAGE_Haemop_SuMu_NC_019455: putative N-acetylmuramoyl-L-alanine amidase	7e-75
Orf16	Hypothetical protein	228/75	PHAGE_Haemop_SuMu_NC_019455: hypothetical protein	4e-22
Orf17	Hypothetical protein	261/87	Hypothetical protein	0.0
Orf18	Hypothetical protein	132/43	PHAGE_Haemop_SuMu_NC_019455: hypothetical protein	4e-06
Orf19	Mu-like phage gp25	330/110	PHAGE_Entero_SfMu_NC_027382: hypothetical protein	8e-07
Orf20	Phage protein	303/100	PHAGE_Entero_SfMu_NC_027382: hypothetical protein	4e-27
Orf21	Phage terminase, small subunit	573/191	PHAGE_Vibrio_12B12_NC_021070: hypothetical protein	6e-39
Orf22	Phage terminase, large subunit	1233/441	PHAGE_Burkho_BcepMu_NC_005882: gp28	3e-29
Orf23	Mu-like prophage FluMu protein gp29	1416/435	PHAGE_Burkho_BcepMu_NC_005882: gp29	3e-115
Orf24	Phage (Mu-like) virion morphogenesis protein	1272/423	PHAGE_Pseudo_vB_PaeS_PM105_NC_028667: putative head morphogenesis protein	3e-41
Orf25	Possible bacteriophage Mu G-like protein	564/187	PHAGE_Burkho_BcepMu_NC_005882: gp31	4e-12

Table 8.1 (continued)

Orfs	Protein product	Size (bp/aa)	BLAST_hit	E-value
Orf26	Phage protein	1104/367	PHAGE_Burkho_BcepMu_NC_005882: gp32	2e-81
Orf27	Phage protein (ACLAME 413)	927/308	PHAGE_Burkho_BcepMu_NC_005882: gp34	1e-75
Orf28	Hypothetical protein	318/105	PHAGE_Saimir_herpesvirus_2_NC_001350: unnamed protein product	8e-07
Orf29	Hypothetical protein	435/145	PHAGE_Burkho_BcepMu_NC_005882: gp36	5e-21
Orf30	Hypothetical protein	498/165	PHAGE_Burkho_BcepMu_NC_005882: gp37	1e-22
Orf31	Phage tail sheath monomer	1386/461	PHAGE_Burkho_BcepMu_NC_005882: gp39	3e-98
Orf32	Putative phage tail core protein	519/173	PHAGE_Burkho_BcepMu_NC_005882: gp40	6e-39
Orf33	Hypothetical protein	270/89	PHAGE_Burkho_BcepMu_NC_005882: gp41	3e-08
Orf34	Hypothetical protein	135/44	FIG00697479: hypothetical protein	0.0
Orf35	Hypothetical protein	234/77	Hypothetical protein	0.0
Orf36	Phage tail length tape-measure protein	2223/740	PHAGE_Burkho_BcepMu_NC_005882: gp44	9e-61
Orf37	Putative methyl-accepting chemotaxis protein	933/310	PHAGE_Burkho_BcepMu_NC_005882: gp45	2e-22
Orf38	Putative bacteriophage tail fibre protein	219/72	PHAGE_Burkho_BcepMu_NC_005882: gp46	5e-14
Orf39	Gene D protein	1065/355	PHAGE_Burkho_BcepMu_NC_005882: gp47	3e-69
Orf40	Baseplate	570/189	PHAGE_Burkho_BcepMu_NC_005882: gp48	7e-16
Orf41	Phage baseplate protein	366/121	PHAGE_Burkho_BcepMu_NC_005882: gp49	9e-14
Orf42	Phage-related baseplate assembly protein	1107/369	PHAGE_Burkho_BcepMu_NC_005882: gp50	2e-63
Orf43	Phage tail fibre protein	570/189	PHAGE_Burkho_BcepMu_NC_005882: gp51	2e-40
Orf44	Phage protein	2457/818	PHAGE_Mannhe_vB_MhM_3927AP2_NC_028766: defective tail fibre protein	5e-33

Table 8.2 PHAST analysis of PMMu4 (ϕPM850.1) against phage genome database.

Orfs	Protein product	Size (bp/aa)	BLAST_hit	E-value
Orf1	Phage-related putative DNA-binding protein	348/115	PHAGE_Burkho_BcepMu: gp01	4e-12
Orf2	Protein gp16	462/154	PHAGE_Burkho_phiE255: gp33	2e-22
Orf3	Hypothetical protein	324/107	Hypothetical protein	0.0
Orf4	Hypothetical protein	561/186	PHAGE_Mannhe_vB_MhM_3927AP2: hypothetical protein	1e-19
Orf5	Hypothetical protein	546/181	Hypothetical protein	0.0
Orf6	Hypothetical protein	228/76	Hypothetical protein	0.0
Orf7	Hypothetical protein	168/56	Hypothetical protein	0.0
Orf8	Phage protein	621/206	PHAGE_Mannhe_vB_MhM_3927AP2: hypothetical protein	1e-68
Orf9	Hypothetical protein	255/84	Hypothetical protein	0.0
Orf10	Hypothetical protein	222/74		
Orf11	Hypothetical protein	324/108	Hypothetical protein	0.0
Orf12	Eha protein	1179/392	PHAGE_Peruvi_horse_sickness_virus_: VP5	4e-05
Orf13	Phage transposase	1770/589	PHAGE_Pseudo_B3_NC_006548: putative transposase A subunit	4e-137
Orf14	Hypothetical protein	945/315	PHAGE_Burkho_phiE255: gp41	4e-26
Orf15	Transcriptional regulator, IclR family	315/104	PHAGE_Pseudo_B3_NC_006548: hypothetical protein B3ORF14	1e-15
Orf16	Hypothetical protein	186/61	Hypothetical protein	0.0
Orf17	Hypothetical protein	237/78	PHAGE_Pseudo_B3_NC_006548: hypothetical protein B3ORF17	2e-05
Orf18	Hypothetical protein	228/76	Hypothetical protein	0.0
Orf19	Putative transcriptional regulator, XRE	411/136	PHAGE_Burkho_BcepMu: gp17	1e-15
Orf20	Hypothetical protein	528/175	Hypothetical protein	0.0
Orf21	Hypothetical protein	591/196	Hypothetical protein	0.0
Orf22	Hypothetical protein	240/79	Hypothetical protein	0.0
Orf23	Phage protein/holin	372/124	PHAGE_Pseudo_vB_PaeS_PM105: putative holin protein	5e-10
Orf24	Phage lysin	600/199	PHAGE_Pseudo_vB_PaeS_PM105: putative transglycosylase SLT domain protein	2e-60
Orf25	Hypothetical protein	447/149	PHAGE_Pseudo_MP48_NC_024782: hypothetical protein MP48_0022	7e-08

Table 8.2 (continued)

Orfs	Protein product	Size (bp/aa)	BLAST_hit	E-value
Orf26	Hypothetical protein	114/37	Hypothetical protein	0.0
Orf27	Hypothetical protein	351/117	PHAGE_Burkho_BcepMu: gp25	1e-10
Orf28	Hypothetical protein	306/101	PHAGE_Pseudo_B3_NC_006548: hypothetical protein B3ORF29	1e-22
Orf29	Phage terminase, small subunit	540/180	PHAGE_Burkho_phiE255: gp1	1e-50
Orf30	Phage terminase, large subunit	1617/538	PHAGE_Vibrio_12B12: portal protein	7e-118
Orf31	Mu-like prophage FluMu protein gp29	1524/507	PHAGE_Pseudo_B3_NC_006548: portal protein	3e-150
Orf32	Phage (Mu-like) virion morphogenesis protein	1239/412	PHAGE_Rhizob_RR1_B_NC_021557: head morphogenesis protein	4e-69
Orf33	Phage virion morphogenesis/head protein	501/167	PHAGE_Pseudo_vB_PaeS_PM105: putative virion morphogenesis protein	7e-26
Orf34	Phage protein	1002/333	PHAGE_Pseudo_B3_NC_006548: protease	6e-45
Orf35	Hypothetical protein	366/122	PHAGE_Pseudo_vB_PaeS_PM105: hypothetical protein	1e-19
Orf36	Phage protein	924/308	PHAGE_Pseudo_vB_PaeS_PM105: putative capsid protein	2e-103
Orf37	Hypothetical protein	507/169	PHAGE_Pseudo_B3: hypothetical protein B3ORF40	2e-30
Orf38	Hypothetical protein	447/148	PHAGE_Pseudo_vB_PaeS_PM105: hypothetical protein	5e-16
Orf39	Hypothetical protein	261/86	Hypothetical protein	0.0
Orf40	Hypothetical protein	747/248	PHAGE_Pseudo_H70_: virion structural protein	3e-36
Orf41	Phage protein	426/141	PHAGE_Pseudo_vB_PaeS_PAO1_Ab30_NC_026601: hypothetical protein	9e-20
Orf42	Hypothetical protein	216/71	Hypothetical protein	0.0
Orf43	Phage tail tape measure protein	3348/1115	PHAGE_Pseudo_MP42_NC_018274: putative tail component protein	3e-74
Orf44	Phage protein	993/330	PHAGE_Pseudo_B3_NC_006548: hypothetical protein B3ORF50	4e-33
Orf45	Phage protein	963/320	PHAGE_Pseudo_H70_: virion structural protein	2e-28
Orf46	Hypothetical protein	1680/560	PHAGE_Pseudo_H70_: virion structural protein	5e-91
Orf47	Phage FAD/FMN-containing dehydrogenase	810/269	PHAGE_Staphy_SA1_: conserved tail assembly protein	7e-48
Orf48	Hypothetical protein	252/83	PHAGE_Proteu_pPM_01: putative tail assembly protein 1	1e-13
Orf49	Hypothetical protein	201/66	PHAGE_Pseudo_PaMx74_: hypothetical protein	2e-09
Orf50	Phage protein	2790/929	PHAGE_Burkho_BcepNazgul: conserved tail assembly protein	3e-119
Orf51	Phage protein	261/87	PHAGE_Haemop_SuMu: hypothetical protein	3e-21
Orf52	Hypothetical protein	846/281	PHAGE_Haemop_SuMu: hypothetical protein	8e-103

Table 8.3 PHAST analysis of PMMu5 (ϕPM382.1) against phage genome database.

Orfs	Protein product	Size (bp/aa)	BLAST_hit	E-value
Orf1	Probable transcription regulator	714/238	PHAGE_Haemop_SuMu: transcription regulator	1e-44
Orf2	Putative DNA-binding protein	264/88	PHAGE_Haemop_SuMu: Mu-like prophage FluMu DNA-binding protein Ner	3e-31
Orf3	Transposase	2022/673	PHAGE_Vibrio_12B12: transposase	4e-144
Orf4	Hypothetical protein	507/168	Hypothetical protein	0.0
Orf5	DNA transposition protein B	918/305	PHAGE_Haemop_SuMu: phage transposase	2e-23
Orf6	Hypothetical protein	204/67	Hypothetical protein	0.0
Orf7	Hypothetical protein	282/94	Hypothetical protein	0.0
Orf8	DNA recombination nuclease inhibitor, Gam	522/173	PHAGE_Haemop_SuMu: host-nuclease inhibitor protein	5e-49
Orf9	Hypothetical protein	210/69	PHAGE_Haemop_SuMu: Hypothetical protein	9e-09
Orf10	Hypothetical protein	174/57	Hypothetical protein	0.0
Orf11	Hypothetical protein	408/135	Hypothetical protein	0.0
Orf12	Hypothetical protein	501/166	PHAGE_Burkho_BcepMu: gp02	3e-12
Orf13	Hypothetical protein	546/182	PHAGE_Mannhe_vB_MhM: Hypothetical protein	6e-40
Orf14	Probable bacteriophage transcriptional regulator, MOR	378/125	PHAGE_Burkho_BcepMu: gp01	2e-25
Orf15	Negative regulator of beta-lactamase expression	537/179	PHAGE_Haemop_SuMu: putative N-acetylmuramoyl-L-alanine amidase	2e-73
Orf16	Hypothetical protein	144/47	Hypothetical protein	0.0
Orf17	Hypothetical protein	360/119	Hypothetical protein	0.0
Orf18	Hypothetical protein	231/76	PHAGE_Haemop_SuMu: Hypothetical protein	1e-20
Orf19	Hypothetical protein	258/85	PHAGE_Haemop_SuMu: Hypothetical protein	6e-05
Orf20	Mu-like phage gp25	330/109	PHAGE_Vibrio_12B12_NC_021070: Hypothetical protein	2e-07
Orf21	Phage protein	291/96	PHAGE_Vibrio_12B12_NC_021070: Hypothetical protein	2e-28
Orf22	Phage terminase, small subunit	582/193	PHAGE_Burkho_BcepMu: gp27	2e-10
Orf23	Mu-like prophage FluMu protein gp28	1557/518	PHAGE_Burkho_BcepMu: gp28	2e-146
Orf24	Mu-like prophage FluMu protein gp29	1437/478	PHAGE_Burkho_BcepMu: gp29	5e-118
Orf25	Phage (Mu-like) virion morphogenesis protein	1275/425	PHAGE_Pseudo_vB_PaeS_PM105: putative head morphogenesis protein	5e-56

Table 5.5 (continued)

Orfs	Protein product	Size (bp/aa)	BLAST_hit	E-value
Orf26	Hypothetical protein	186/61	Hypothetical protein	0.0
Orf27	Phage virion morphogenesis/head protein	456/151	PHAGE_Pseudo_vB_PaeS_PM105: putative virion morphogenesis protein	5e-14
Orf28	Phage protein	1101/367	PHAGE_Burkho_BcepMu: gp32	3e-80
Orf29	Hypothetical protein	942/314	PHAGE_Burkho_BcepMu: gp34	2e-55
Orf30	Hypothetical protein	459/152	PHAGE_Pseudo_DL68_NC_028971: Hypothetical protein	5e-07
Orf31	Hypothetical protein	450/149	PHAGE_Burkho_BcepMu: gp36	2e-21
Orf32	Hypothetical protein	468/156	PHAGE_Burkho_BcepMu: gp37	2e-15
Orf33	Major tail sheath protein	1392/464	PHAGE_Burkho_BcepMu: gp39	9e-109
Orf34	Phage tail tube protein FII	516/171	PHAGE_Burkho_BcepMu: gp40	7e-41
Orf35	Hypothetical protein	279/93	PHAGE_Burkho_BcepMu: gp41	2e-06
Orf36	Hypothetical protein	135/44	Hypothetical protein	0.0
Orf37	Hypothetical protein	192/63	Hypothetical protein	0.0
Orf38	Phage tail length tape-measure protein	2304/768	PHAGE_Escher_vB_EcoM_ECO1230_10: putative phage tail protein	2e-68
Orf39	putative methyl-accepting chemotaxis protein	951/316	PHAGE_Burkho_BcepMu: gp45	5e-27
Orf40	Putative inner membrane protein	222/74	PHAGE_Burkho_BcepMu: gp46	7e-12
Orf41	Gene D protein	1053/350	PHAGE_Burkho_BcepMu: gp47	3e-65
Orf42	Baseplate	600/199	PHAGE_Burkho_BcepMu: gp48	4e-15
Orf43	putative phage baseplate protein	306/101	PHAGE_Burkho_BcepMu: gp49	2e-13
Orf44	Phage-related baseplate assembly protein	1113/371	PHAGE_Burkho_BcepMu: gp50	2e-57
Orf45	Phage tail fibre protein	567/188	PHAGE_Burkho_BcepMu: gp51	8e-43
Orf46	Phage tail fibre protein	1071/357	PHAGE_Haemop_Aaphi23: putative tail fibre protein	2e-28
Orf47	Phage tail fibre assembly protein	606/202	PHAGE_Haemop_Hypothetical protein: tail collar	1e-53
Orf48	Putative cytoplasmic protein	495/164	PHAGE_Haemop_SuMu: enoyl-CoA hydratase/carnithine racemase-like protein	2e-56
Orf49	Hypothetical protein	174/57	Hypothetical protein	0.0
Orf50	Hypothetical protein	120/39	PHAGE_Haemop_SuMu: Mu-like prophage protein Com	4e-08
Orf51	Hypothetical protein	840/280	PHAGE_Haemop_SuMu: Hypothetical protein	1e-108

Table 8.4 Major protein products of ϕPM40.3 (PMλ5–like phage) using PHAST and BLAST analysis.

Orfs	Protein product	Size (bp/aa)	BLAST_hit	E-value
Orf1	Phage terminase, large subunit	1071/356	PHAGE_Gifsy_2bacteriophage DNA packaging protein; terminase, large subunit	1e-128
Orf3	Phage portal protein	1539/513	PHAGE_Gifsy_2: bacteriophage portal protein	6e-164
Orf4	Prophage Clp protease-like protein	1950/649	PHAGE_Gifsy_2: bacteriophage Clp protease involved in capsid processing	0.0
Orf7	Phage tail completion protein	552/183	PHAGE_Entero_mEp237: minor tail protein Z	3e-38
Orf8	Phage minor tail protein	408/136	PHAGE_Entero_mEp460: minor tail protein	2e-11
Orf9	Phage tail fibre protein	507/168	PHAGE_Entero_HK225: major tail protein V	3e-43
Orf12	Phage tail length tape-measure protein 1	2394/797	PHAGE_Idioma_Phi1M2_2: putative tail tape measure protein	6e-40
Orf13	Phage minor tail protein	351/117	PHAGE_Salmon_vB_SosS_Oslo: minor tail protein	7e-17
Orf16	Phage minor tail protein	705/234	PHAGE_Mannhe_vB_MhS_587AP2: minor tail protein L	9e-83
Orf17	Phage tail assembly protein	744/248	PHAGE_Mannhe_vB_MhS_587AP2: minor tail protein K	4e-84
Orf18	Phage tail assembly protein I	327/108	PHAGE_Mannhe_vB_MhS_587AP2: tail assembly protein I	1e-19
Orf19	Phage tail fibre protein	5004/1667	PHAGE_Mannhe_vB_MhS_587AP2: host specificity protein J	0.0
Orf22	Phage Rha protein	381/126	Phage Rha protein	0.0
Orf23	Phage integrase	990/329	PHAGE_Mannhe_vB_MhS_535AP2: integrase	5e-99
Orf25	Single-stranded DNA-binding protein	237/78	PHAGE_Mannhe_vB_MhS_587AP2: pyruvate kinase	3e-10
Orf26	Putative antirepressor	624/207	PHAGE_Cronob_ENT47670: phage antirepressor protein	3e-38
Orf30	Single-stranded DNA-binding protein	453/150	PHAGE_Vibrio_VvAW1: single-stranded DNA-binding protein	1e-39
Orf31	Hypothetical protein	675/224	PHAGE_Mannhe_vB_MhS_587AP2: exonuclease	1e-99
Orf32	Recombinational DNA repair protein RecT (prophage associated)	954/317	PHAGE_Mannhe_vB_MhS_587AP2: recombinase	6e-127
Orf37	Phage Rha protein	669/222	PHAGE_Mannhe_vB_MhS_587AP2: antirepressor	7e-45
Orf43	Putative phage repressor	684/227	PHAGE_Pseudo_vB_PaeS_PAO1_Ab30: putative c repressor	1e-20
Orf44	Hypothetical protein	201/66	PHAGE_Salmon_ST160: Cro	6e-11
Orf46	Putative DNA-binding protein Roi of bacteriophage BP-933W	261/87	PHAGE_Aggreg_S1249: uncharacterised phage-encoded protein	3e-21
Orf48	Primosomal protein I	813/271	PHAGE_Aggreg_S1249: replication protein	3e-61
Orf49	Replication protein P	690/229	PHAGE_Mannhe_vB_MhS_587AP2: replication protein P	2e-23

Table 8.4 (continued)

Orfs	Protein product	Size (bp/aa)	BLAST_hit	E-value
Orf50	Putative DNA methylase	537/179	PHAGE_Mannhe_vB_MhS_587AP2: DNA N-6-adenine-methyltransferase	1e-55
Orf51	Phage NinB DNA recombination	426/142	PHAGE_Aggreg_S1249: putative recombination protein NinB	1e-44
Orf54	Phage NinG rap recombination	603/201	PHAGE_Salmon_SPN3UB: NinG	6e-45
Orf55	Hypothetical protein	366/121	PHAGE_Mannhe_vB_MhS_587AP2: antitermination protein Q	2e-10
Orf57	Phage tail fibres	741/246	PHAGE_Shigel_SfII: KliA-N domain protein)	2e-15
Orf61	Haemophilus-specific protein, uncharacterised	291/96	PHAGE_Mannhe_vB_MhS_1152AP2: holin; -; phage(gi971760557)	8e-20
Orf62	Putative phage lysozyme	531/177	PHAGE_Mannhe_vB_MhM_587AP1: endolysin	5e-46
Orf63	Uncharacterised protein HI1413	231/77	PHAGE_Mannhe_vB_MhS_587AP2: lytic protein Rz1	7e-12
Orf64	Putative regulatory protein	369/122	Putative regulatory protein	0.0
Orf67	Hypothetical protein	474/157	PHAGE_Entero_c_1: terminase small subunit	2e-43
Orf68	Phage terminase, large subunit	1035/344	PHAGE_Entero_c_1: terminase large subunit	1e-156

Table 8.5 Major protein products of ϕPM336.1 (PMλ7–like phage) using PHAST and BLAST analysis.

Orfs	Protein product	Size (bp/aa)	BLAST_hit	E-value
Orf1	Phage tail fibre protein	1743/580	PHAGE_Mannhe_vB_MhS_587AP2: host specificity protein J	4e-41
Orf3	Phage integrase, site-specific tyrosine recombination	990/330	PHAGE_Mannhe_vB_MhS_535AP2: integrase	5e-99
Orf5	Single-stranded DNA-binding protein	456/151	PHAGE_Mannhe_vB_MhS_1152AP2: pyruvate kinase	1e-22
Orf11	Putative methyltransferase	486/162	PHAGE_Mannhe_vB_MhS_535AP2: methyltransferase	5e-64
Orf13	COG1896: Predicted hydrolases of HD superfamily	600/199	PHAGE_Salmon_ST64B: hypothetical protein sb35	5e-25
Orf17	Single-stranded DNA-binding protein	453/150	PHAGE_Vibrio_VvAW1: single-stranded DNA-binding protein	2e-41
Orf18	Hypothetical protein	660/219	PHAGE_Mannhe_vB_MhS_587AP2: exonuclease	3e-98
Orf19	Recombinational DNA repair protein RecT	954/317	PHAGE_Mannhe_vB_MhS_587AP2: recombinase	6e-127
Orf23	Putative antirepressor protein	657/218	PHAGE_Haemop_Aaphi23: putative antirepressor protein Ant	1e-41
Orf28	Hypothetical protein	1845/614	PHAGE_Strept_YMC_2011: Helicase	2e-15
Orf29	Transcriptional regulator	687/228	PHAGE_Haemop_Aaphi23: putative CI protein	4e-70
Orf30	Hypothetical protein	201/66	PHAGE_Shigel_SfIV: Cro	4e-07
Orf32	Putative DNA-binding protein Roi of bacteriophage	261/86	PHAGE_Aggreg_S1249: uncharacterised phage-encoded protein	2e-20
Orf34	Phage replication protein O	819/272	PHAGE_Haemop_Aaphi23: putative DNA replication protein O	7e-80
Orf35	DNA helicase	1365/454	PHAGE_Mannhe_vB_MhS_1152AP2: helicase	2e-129
Orf36	Putative DNA methylase	537/179	PHAGE_Mannhe_vB_MhS_587AP2: DNA N-6-adenine-methyltransferase	5e-55
Orf37	Phage NinB DNA recombination protein	459/152	PHAGE_Aggreg_S1249: putative recombination protein NinB	1e-40
Orf39	Phage NinG rap recombination	603/200	PHAGE_Salmon_SPN3UB: NinG	2e-44
Orf40	Hypothetical protein	366/121	PHAGE_Mannhe_vB_MhS_587AP2: antitermination protein Q	2e-10
Orf42	Hypothetical protein	363/120	PHAGE_Aeromo_phiO18P: putative holin	1e-06
Orf43	Hypothetical protein	381/127	hypothetical protein	0.0
Orf44	Uncharacterised protein HI1413	174/57	PHAGE_Mannhe_vB_MhS_1152AP2: lytic protein Rz1	5e-09
Orf48	Hypothetical protein	297/98	PHAGE_Sinorh_phiN3: putative YahA protein	3e-16
Orf52	Phage terminase, small subunit	594/197	PHAGE_Entero_phiEf11: phage terminase A domain protein	1e-07
Orf53	Phage terminase, large subunit	1272/424	PHAGE_Pseudo_H105/1: phage terminase large subunit	4e-117
Orf54	Putative structural protein	1404/468	PHAGE_Mannhe_vB_MhS_1152AP2: portal protein	2e-154
Orf55	Hypothetical protein	1035/344	PHAGE_Mannhe_vB_MhS_1152AP2: head morphogenesis protein	3e-107
Orf57	Hypothetical protein	786/261	PHAGE_Xantho_Xp15: putative phage structural protein	4e-15
Orf58	Hypothetical protein	1158/385	PHAGE_Rhizob_vB_RglS_P106B: putative coat protein	6e-76
Orf67	Phage minor tail protein	330/110	PHAGE_Mannhe_vB_MhS_1152AP2: minor tail protein M	2e-28

Table 8.5 (continued)

Orfs	Protein product	Size (bp/aa)	BLAST_hit	E-value
Orf69	Phage tail tape measure protein	2715/904	PHAGE_Mannhe_vB_MhS_1152AP2: tail length tape measure protein	0.0
Orf70	Phage minor tail protein	705/235	PHAGE_Mannhe_vB_MhS_1152AP2: minor tail protein L	1e-83
Orf71	Phage tail assembly protein	741/246	PHAGE_Mannhe_vB_MhS_1152AP2: minor tail protein K	2e-84
Orf72	Phage tail assembly protein I	375/124	PHAGE_Mannhe_vB_MhS_1152AP2: tail assembly protein I	2e-20
Orf73	Phage tail fibre protein	3291/1096	PHAGE_Mannhe_vB_MhS_587AP2: host specificity protein J	0.0

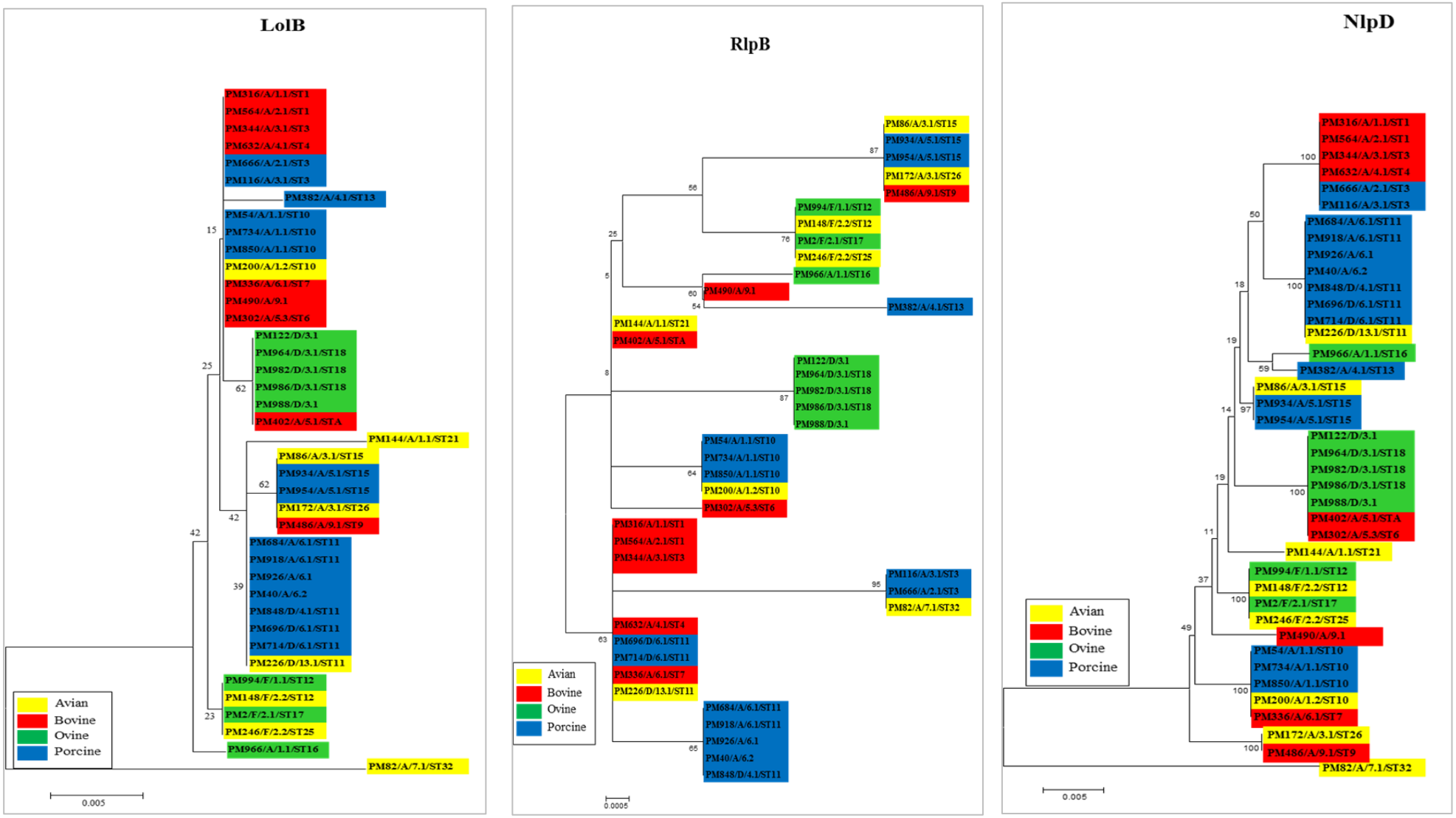
LolB
PM316/A/1.1/ST1
PM564/A/2.1/ST1
PM344/A/3.1/ST3
PM632/A/4.1/ST4
PM666/A/2.1/ST3
PM116/A/3.1/ST3
PM382/A/4.1/ST13
PM54/A/1.1/ST10
PM734/A/1.1/ST10
PM850/A/1.1/ST10
PM200/A/1.2/ST10
PM336/A/6.1/ST7
PM490/A/9.1
PM302/A/5.3/ST6
PM122/D/3.1
PM964/D/3.1/ST18
PM982/D/3.1/ST18
PM986/D/3.1/ST18
PM988/D/3.1
PM402/A/5.1/STA
PM144/A/1.1/ST21
PM86/A/3.1/ST15
PM934/A/5.1/ST15
PM954/A/5.1/ST15
PM172/A/3.1/ST26
PM486/A/9.1/ST9
PM684/A/6.1/ST11
PM918/A/6.1/ST11
PM926/A/6.1
PM40/A/6.2
PM848/D/4.1/ST11
PM696/D/6.1/ST11
PM714/D/6.1/ST11
PM226/D/13.1/ST11
PM994/F/1.1/ST12
PM148/F/2.2/ST12
PM2/F/2.1/ST17
PM246/F/2.2/ST25
PM966/A/1.1/ST16
PM82/A/7.1/ST32
Avian
Bovine
Ovine
Porcine
0.005
RlpB
PM86/A/3.1/ST15
PM934/A/5.1/ST15
PM954/A/5.1/ST15
PM172/A/3.1/ST26
PM486/A/9.1/ST9
PM994/F/1.1/ST12
PM148/F/2.2/ST12
PM2/F/2.1/ST17
PM246/F/2.2/ST25
PM966/A/1.1/ST16
PM490/A/9.1
PM382/A/4.1/ST13
PM144/A/1.1/ST21
PM402/A/5.1/STA
PM122/D/3.1
PM964/D/3.1/ST18
PM982/D/3.1/ST18
PM986/D/3.1/ST18
PM988/D/3.1
PM54/A/1.1/ST10
PM734/A/1.1/ST10
PM850/A/1.1/ST10
PM200/A/1.2/ST10
PM302/A/5.3/ST6
PM316/A/1.1/ST1
PM564/A/2.1/ST1
PM344/A/3.1/ST3
PM116/A/3.1/ST3
PM666/A/2.1/ST3
PM82/A/7.1/ST32
PM632/A/4.1/ST4
PM696/D/6.1/ST11
PM714/D/6.1/ST11
PM336/A/6.1/ST7
PM226/D/13.1/ST11
PM684/A/6.1/ST11
PM918/A/6.1/ST11
PM926/A/6.1
PM40/A/6.2
PM848/D/4.1/ST11
Avian
Bovine
Ovine
Porcine
0.0005
NlpD
PM316/A/1.1/ST1
PM564/A/2.1/ST1
PM344/A/3.1/ST3
PM632/A/4.1/ST4
PM666/A/2.1/ST3
PM116/A/3.1/ST3
PM684/A/6.1/ST11
PM918/A/6.1/ST11
PM926/A/6.1
PM40/A/6.2
PM848/D/4.1/ST11
PM696/D/6.1/ST11
PM714/D/6.1/ST11
PM226/D/13.1/ST11
PM966/A/1.1/ST16
PM382/A/4.1/ST13
PM86/A/3.1/ST15
PM934/A/5.1/ST15
PM954/A/5.1/ST15
PM122/D/3.1
PM964/D/3.1/ST18
PM982/D/3.1/ST18
PM986/D/3.1/ST18
PM988/D/3.1
PM402/A/5.1/STA
PM302/A/5.3/ST6
PM144/A/1.1/ST21
PM994/F/1.1/ST12
PM148/F/2.2/ST12
PM2/F/2.1/ST17
PM246/F/2.2/ST25
PM490/A/9.1
PM54/A/1.1/ST10
PM734/A/1.1/ST10
PM850/A/1.1/ST10
PM200/A/1.2/ST10
PM336/A/6.1/ST7
PM172/A/3.1/ST26
PM486/A/9.1/ST9
PM82/A/7.1/ST32
Avian
Bovine
Ovine
Porcine
0.005

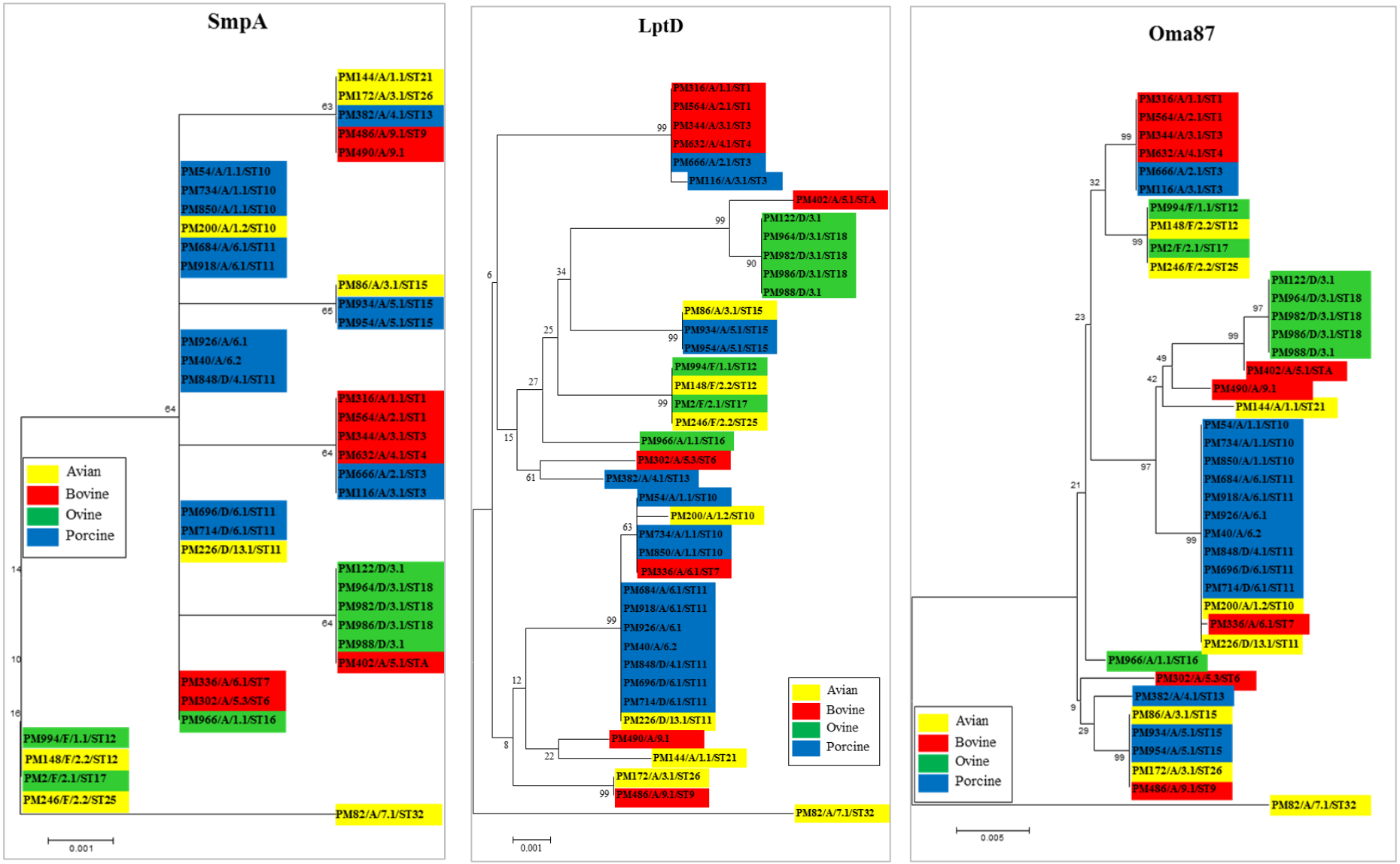
SmpA
PM144/A/1.1/ST21
PM172/A/3.1/ST26
PM382/A/4.1/ST13
PM486/A/9.1/ST9
PM490/A/9.1
PM54/A/1.1/ST10
PM734/A/1.1/ST10
PM850/A/1.1/ST10
PM200/A/1.2/ST10
PM684/A/6.1/ST11
PM918/A/6.1/ST11
PM86/A/3.1/ST15
PM934/A/5.1/ST15
PM954/A/5.1/ST15
PM926/A/6.1
PM40/A/6.2
PM848/D/4.1/ST11
PM316/A/1.1/ST1
PM564/A/2.1/ST1
PM344/A/3.1/ST3
PM632/A/4.1/ST4
PM666/A/2.1/ST3
PM116/A/3.1/ST3
PM696/D/6.1/ST11
PM714/D/6.1/ST11
PM226/D/13.1/ST11
PM122/D/3.1
PM964/D/3.1/ST18
PM982/D/3.1/ST18
PM986/D/3.1/ST18
PM988/D/3.1
PM402/A/5.1/STA
PM336/A/6.1/ST7
PM302/A/5.3/ST6
PM966/A/1.1/ST16
PM994/F/1.1/ST12
PM148/F/2.2/ST12
PM2/F/2.1/ST17
PM246/F/2.2/ST25
PM82/A/7.1/ST32
Avian
Bovine
Ovine
Porcine
0.001
LptD
PM316/A/1.1/ST1
PM564/A/2.1/ST1
PM344/A/3.1/ST3
PM632/A/4.1/ST4
PM666/A/2.1/ST3
PM116/A/3.1/ST3
PM402/A/5.1/STA
PM122/D/3.1
PM964/D/3.1/ST18
PM982/D/3.1/ST18
PM986/D/3.1/ST18
PM988/D/3.1
PM86/A/3.1/ST15
PM934/A/5.1/ST15
PM954/A/5.1/ST15
PM994/F/1.1/ST12
PM148/F/2.2/ST12
PM2/F/2.1/ST17
PM246/F/2.2/ST25
PM966/A/1.1/ST16
PM302/A/5.3/ST6
PM382/A/4.1/ST13
PM54/A/1.1/ST10
PM200/A/1.2/ST10
PM734/A/1.1/ST10
PM850/A/1.1/ST10
PM336/A/6.1/ST7
PM684/A/6.1/ST11
PM918/A/6.1/ST11
PM926/A/6.1
PM40/A/6.2
PM848/D/4.1/ST11
PM696/D/6.1/ST11
PM714/D/6.1/ST11
PM226/D/13.1/ST11
PM490/A/9.1
PM144/A/1.1/ST21
PM172/A/3.1/ST26
PM486/A/9.1/ST9
PM82/A/7.1/ST32
Avian
Bovine
Ovine
Porcine
0.001
Oma87
PM316/A/1.1/ST1
PM564/A/2.1/ST1
PM344/A/3.1/ST3
PM632/A/4.1/ST4
PM666/A/2.1/ST3
PM116/A/3.1/ST3
PM994/F/1.1/ST12
PM148/F/2.2/ST12
PM2/F/2.1/ST17
PM246/F/2.2/ST25
PM122/D/3.1
PM964/D/3.1/ST18
PM982/D/3.1/ST18
PM986/D/3.1/ST18
PM988/D/3.1
PM402/A/5.1/STA
PM490/A/9.1
PM144/A/1.1/ST21
PM54/A/1.1/ST10
PM734/A/1.1/ST10
PM850/A/1.1/ST10
PM684/A/6.1/ST11
PM918/A/6.1/ST11
PM926/A/6.1
PM40/A/6.2
PM848/D/4.1/ST11
PM696/D/6.1/ST11
PM714/D/6.1/ST11
PM200/A/1.2/ST10
PM336/A/6.1/ST7
PM226/D/13.1/ST11
PM966/A/1.1/ST16
PM302/A/5.3/ST6
PM382/A/4.1/ST13
PM86/A/3.1/ST15
PM934/A/5.1/ST15
PM954/A/5.1/ST15
PM172/A/3.1/ST26
PM486/A/9.1/ST9
PM82/A/7.1/ST32
Avian
Bovine
Ovine
Porcine
0.005

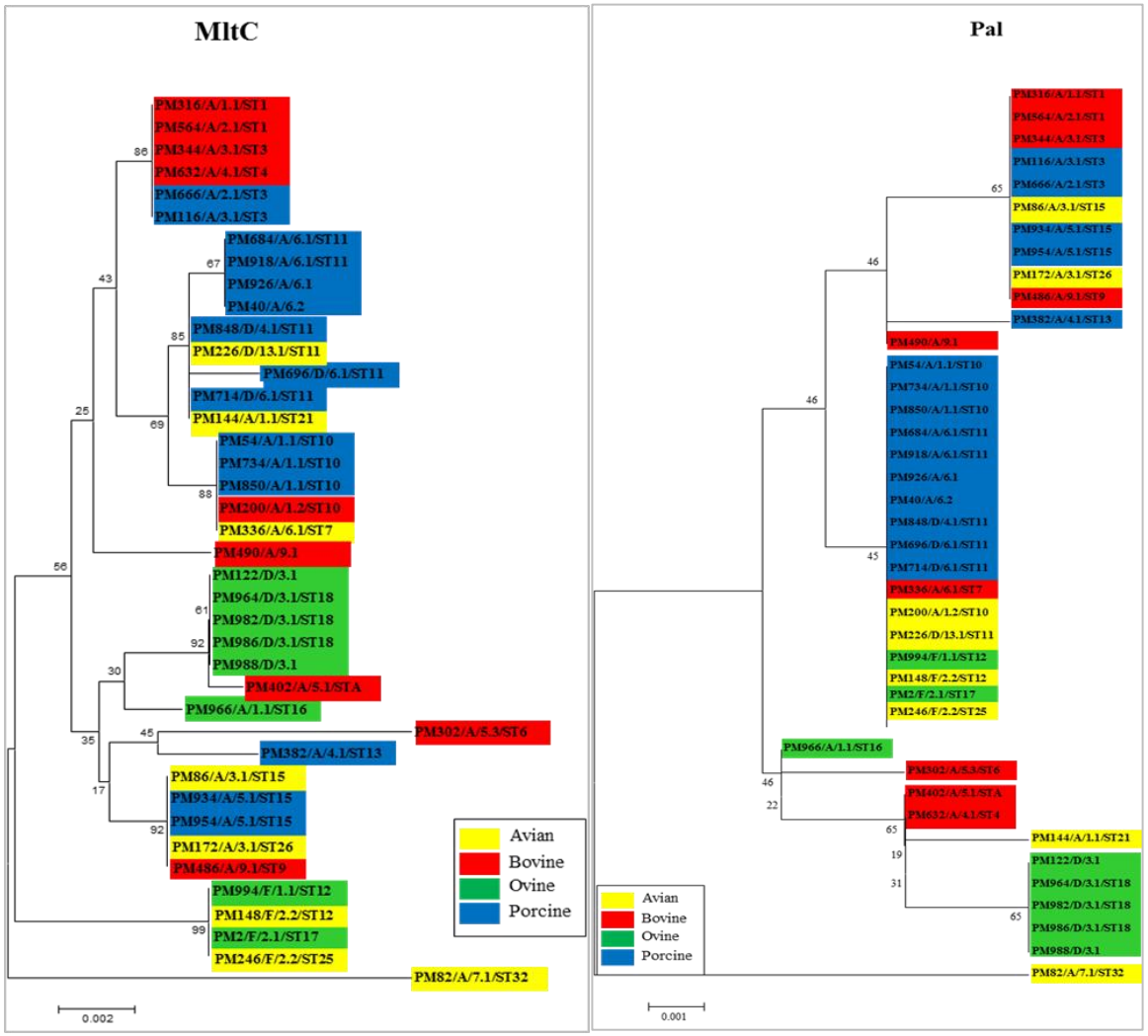

Fig. 8.1 Neighbour-Joining tree of eight OMPs/ genes of *P. multocida* involved in outer membrane biogenesis and integrity.

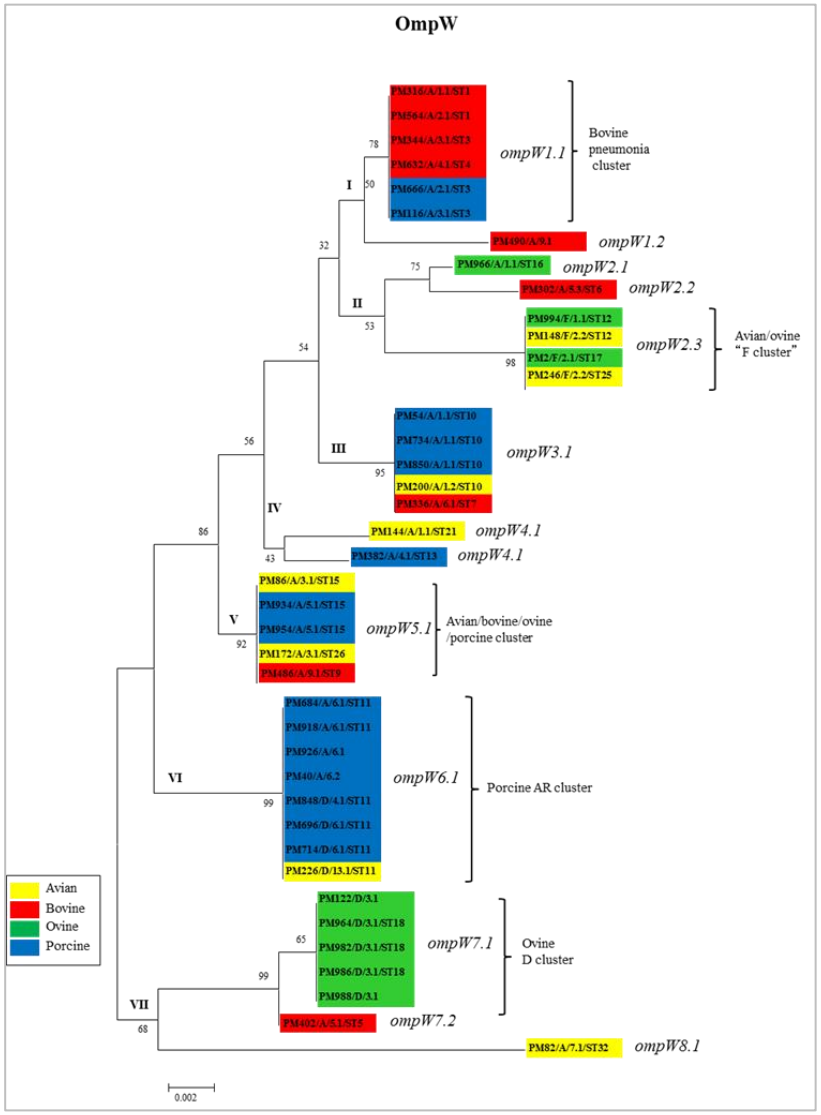
OmpW
PM318/A/1.1/ST1
PM564/A/2.1/ST1
PM344/A/3.1/ST3
PM632/A/4.1/ST4
PM666/A/2.1/ST3
PM116/A/3.1/ST3
ompW1.1
Bovine pneumonia cluster
PM490/A/9.1
ompW1.2
PM966/A/1.1/ST16
ompW2.1
PM302/A/5.3/ST6
ompW2.2
PM994/F/1.1/ST12
PM148/F/2.2/ST12
PM2/F/2.1/ST17
PM246/F/2.2/ST25
ompW2.3
Avian/ovine "F cluster"
PM54/A/1.1/ST10
PM734/A/1.1/ST10
PM850/A/1.1/ST10
PM200/A/1.2/ST10
PM336/A/6.1/ST7
ompW3.1
PM144/A/1.1/ST21
ompW4.1
PM382/A/4.1/ST13
ompW4.1
PM86/A/3.1/ST15
PM934/A/5.1/ST15
PM954/A/5.1/ST15
PM172/A/3.1/ST26
PM486/A/9.1/ST9
ompW5.1
Avian/bovine/ovine /porcine cluster
PM684/A/6.1/ST11
PM918/A/6.1/ST11
PM926/A/6.1
PM40/A/6.2
PM848/D/4.1/ST11
PM696/D/6.1/ST11
PM714/D/6.1/ST11
PM226/D/13.1/ST11
ompW6.1
Porcine AR cluster
PM122/D/3.1
PM964/D/3.1/ST18
PM982/D/3.1/ST18
PM986/D/3.1/ST18
PM988/D/3.1
ompW7.1
Ovine D cluster
PM402/A/5.1/ST5
ompW7.2
PM82/A/7.1/ST32
ompW8.1
I
II
III
IV
V
VI
VII
Avian
Bovine
Ovine
Porcine
0.002

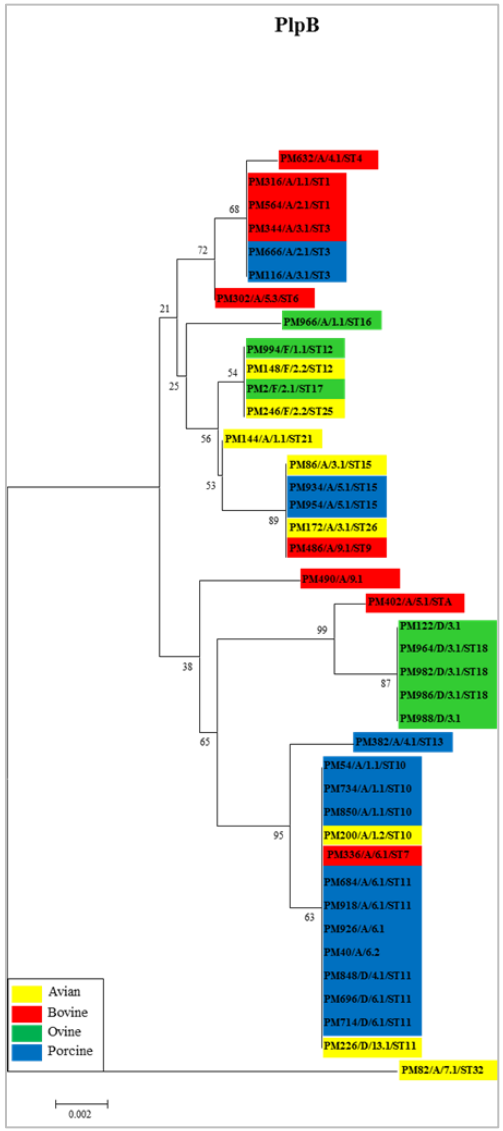
PlpB
PM632/A/4.1/ST4
PM316/A/1.1/ST1
PM564/A/2.1/ST1
PM344/A/3.1/ST3
PM666/A/2.1/ST3
PM116/A/3.1/ST3
PM302/A/5.3/ST6
PM966/A/1.1/ST16
PM994/F/1.1/ST12
PM148/F/2.2/ST12
PM2/F/2.1/ST17
PM246/F/2.2/ST25
PM144/A/1.1/ST21
PM86/A/3.1/ST15
PM934/A/5.1/ST15
PM954/A/5.1/ST15
PM172/A/3.1/ST26
PM486/A/9.1/ST9
PM490/A/9.1
PM402/A/5.1/STA
PM122/D/3.1
PM964/D/3.1/ST18
PM982/D/3.1/ST18
PM986/D/3.1/ST18
PM988/D/3.1
PM382/A/4.1/ST13
PM54/A/1.1/ST10
PM734/A/1.1/ST10
PM850/A/1.1/ST10
PM200/A/1.2/ST10
PM336/A/6.1/ST7
PM684/A/6.1/ST11
PM918/A/6.1/ST11
PM926/A/6.1
PM40/A/6.2
PM848/D/4.1/ST11
PM696/D/6.1/ST11
PM714/D/6.1/ST11
PM226/D/13.1/ST11
PM82/A/7.1/ST32
Avian
Bovine
Ovine
Porcine
0.002

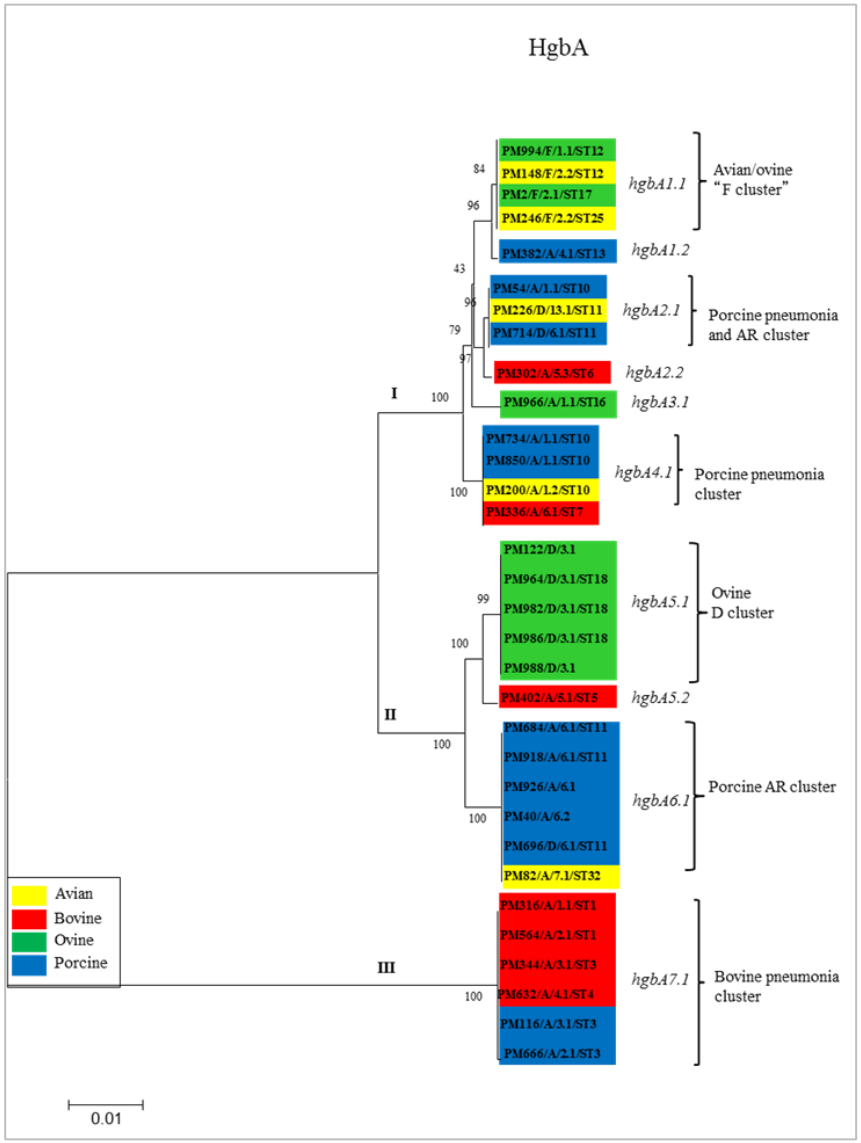
HgbA
PM994/F/1.1/ST12
PM148/F/2.2/ST12
PM2/F/2.1/ST17
PM246/F/2.2/ST25
hgbA1.1
Avian/ovine "F cluster"
PM382/A/4.1/ST13
hgbA1.2
PM54/A/1.1/ST10
PM226/D/13.1/ST11
hgbA2.1
Porcine pneumonia and AR cluster
PM714/D/6.1/ST11
PM302/A/5.3/ST6
hgbA2.2
PM966/A/1.1/ST16
hgbA3.1
PM734/A/1.1/ST10
PM850/A/1.1/ST10
PM200/A/1.2/ST10
PM336/A/6.1/ST7
hgbA4.1
Porcine pneumonia cluster
PM122/D/3.1
PM964/D/3.1/ST18
PM982/D/3.1/ST18
PM986/D/3.1/ST18
PM988/D/3.1
hgbA5.1
Ovine D cluster
PM402/A/5.1/ST5
hgbA5.2
PM684/A/6.1/ST11
PM918/A/6.1/ST11
PM926/A/6.1
PM40/A/6.2
PM696/D/6.1/ST11
PM82/A/7.1/ST32
hgbA6.1
Porcine AR cluster
PM316/A/1.1/ST1
PM564/A/2.1/ST1
PM344/A/3.1/ST3
PM632/A/4.1/ST4
PM116/A/3.1/ST3
PM666/A/2.1/ST3
hgbA7.1
Bovine pneumonia cluster
I
II
III
Avian
Bovine
Ovine
Porcine
0.01

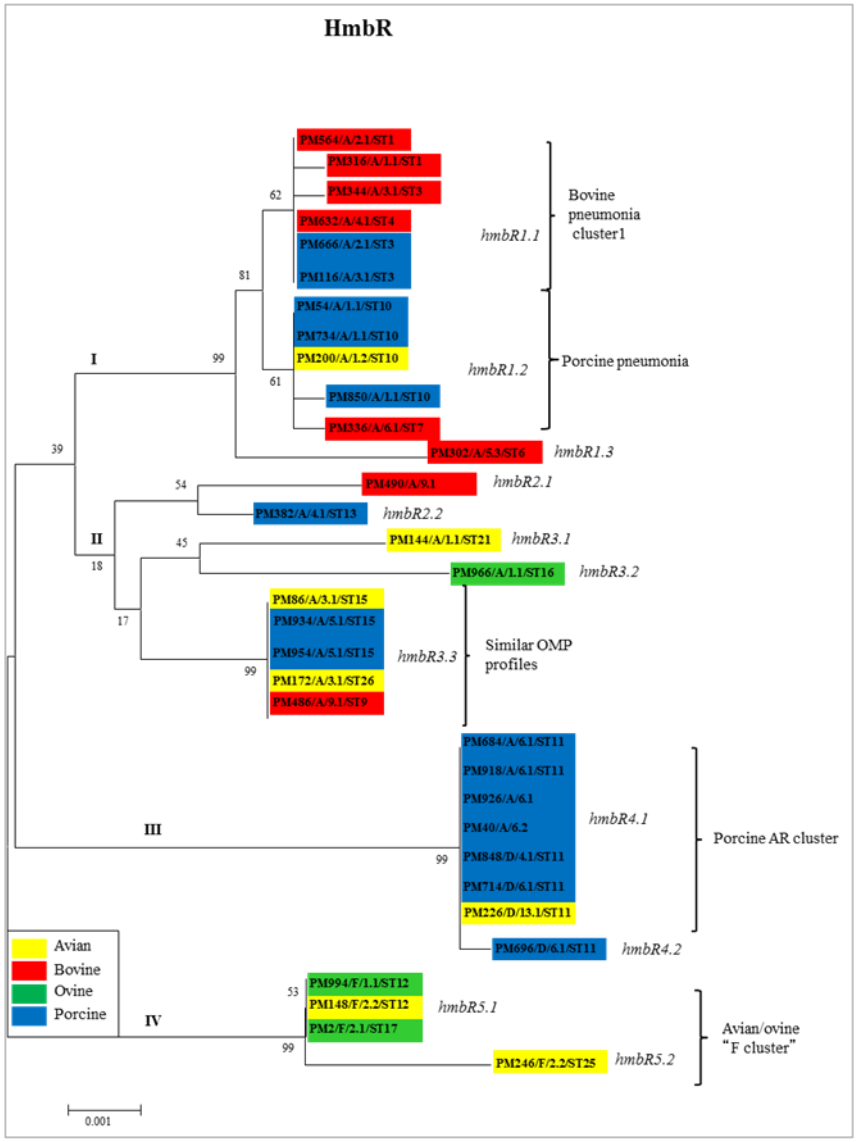
HmbR
PM564/A/2.1/ST1
PM316/A/1.1/ST1
PM344/A/3.1/ST3
PM632/A/4.1/ST4
PM666/A/2.1/ST3
PM116/A/3.1/ST3
hmbR1.1
Bovine pneumonia cluster1
PM54/A/1.1/ST10
PM734/A/1.1/ST10
PM200/A/1.2/ST10
hmbR1.2
Porcine pneumonia
PM850/A/1.1/ST10
PM336/A/6.1/ST7
PM302/A/5.3/ST6
hmbR1.3
PM490/A/9.1
hmbR2.1
PM382/A/4.1/ST13
hmbR2.2
PM144/A/1.1/ST21
hmbR3.1
PM966/A/1.1/ST16
hmbR3.2
PM86/A/3.1/ST15
PM934/A/5.1/ST15
PM954/A/5.1/ST15
PM172/A/3.1/ST26
PM486/A/9.1/ST9
hmbR3.3
Similar OMP profiles
PM684/A/6.1/ST11
PM918/A/6.1/ST11
PM926/A/6.1
PM40/A/6.2
PM848/D/4.1/ST11
PM714/D/6.1/ST11
PM226/D/13.1/ST11
hmbR4.1
Porcine AR cluster
PM696/D/6.1/ST11
hmbR4.2
PM994/F/1.1/ST12
PM148/F/2.2/ST12
PM2/F/2.1/ST17
hmbR5.1
PM246/F/2.2/ST25
hmbR5.2
Avian/ovine "F cluster"
I
II
III
IV
Avian
Bovine
Ovine
Porcine
0.001

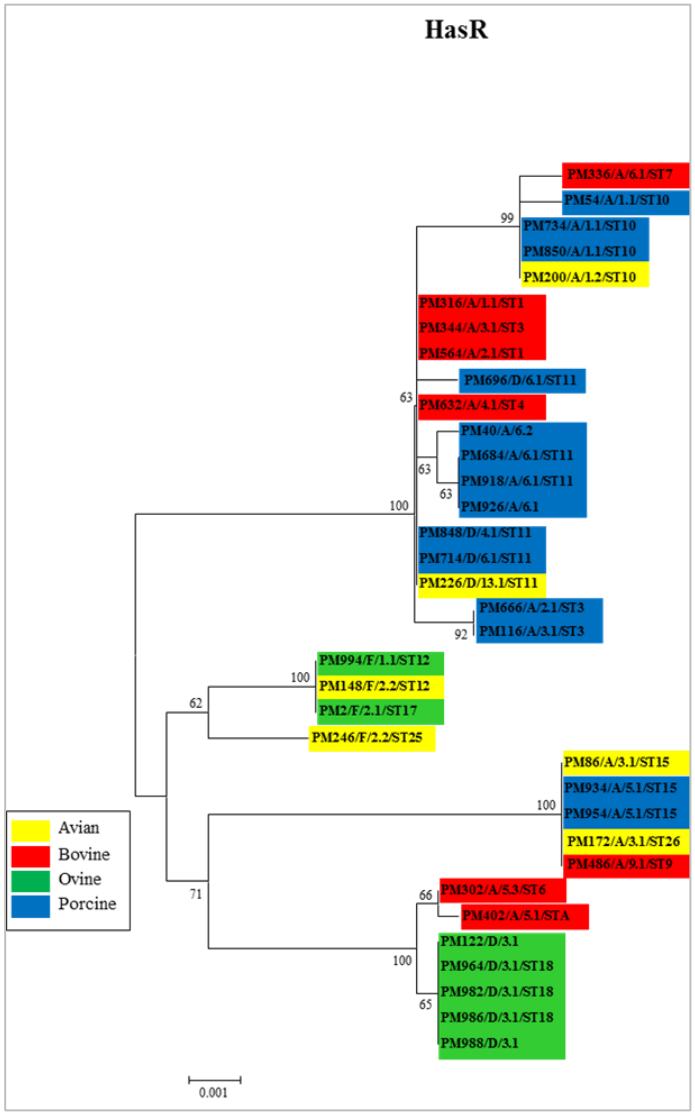
HasR
PM336/A/6.1/ST7
PM54/A/1.1/ST10
PM734/A/1.1/ST10
PM850/A/1.1/ST10
PM200/A/1.2/ST10
PM316/A/1.1/ST1
PM344/A/3.1/ST3
PM564/A/2.1/ST1
PM696/D/6.1/ST11
PM632/A/4.1/ST4
PM40/A/6.2
PM684/A/6.1/ST11
PM918/A/6.1/ST11
PM926/A/6.1
PM848/D/4.1/ST11
PM714/D/6.1/ST11
PM226/D/13.1/ST11
PM666/A/2.1/ST3
PM116/A/3.1/ST3
PM994/F/1.1/ST12
PM148/F/2.2/ST12
PM2/F/2.1/ST17
PM246/F/2.2/ST25
PM86/A/3.1/ST15
PM934/A/5.1/ST15
PM954/A/5.1/ST15
PM172/A/3.1/ST26
PM486/A/9.1/ST9
PM302/A/5.3/ST6
PM402/A/5.1/STA
PM122/D/3.1
PM964/D/3.1/ST18
PM982/D/3.1/ST18
PM986/D/3.1/ST18
PM988/D/3.1
Avian
Bovine
Ovine
Porcine
0.001

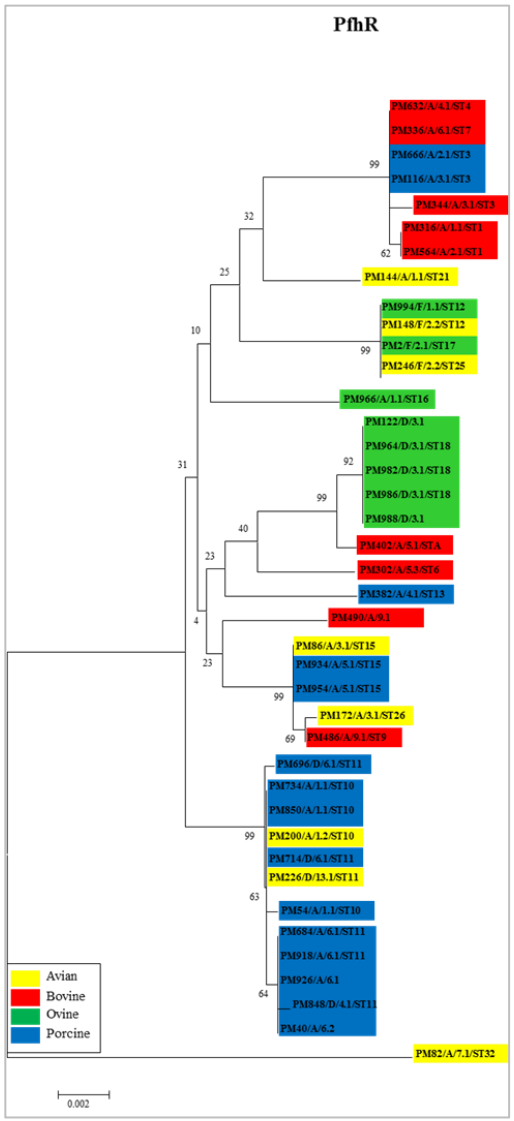
PfhR
PM632/A/4.1/ST4
PM336/A/6.1/ST7
PM666/A/2.1/ST3
PM116/A/3.1/ST3
PM344/A/3.1/ST3
PM316/A/1.1/ST1
PM564/A/2.1/ST1
PM144/A/1.1/ST21
PM994/F/1.1/ST12
PM148/F/2.2/ST12
PM2/F/2.1/ST17
PM246/F/2.2/ST25
PM966/A/1.1/ST16
PM122/D/3.1
PM964/D/3.1/ST18
PM982/D/3.1/ST18
PM986/D/3.1/ST18
PM988/D/3.1
PM402/A/5.1/STA
PM302/A/5.3/ST6
PM382/A/4.1/ST13
PM490/A/9.1
PM86/A/3.1/ST15
PM934/A/5.1/ST15
PM954/A/5.1/ST15
PM172/A/3.1/ST26
PM486/A/9.1/ST9
PM696/D/6.1/ST11
PM734/A/1.1/ST10
PM850/A/1.1/ST10
PM200/A/1.2/ST10
PM714/D/6.1/ST11
PM226/D/13.1/ST11
PM54/A/1.1/ST10
PM684/A/6.1/ST11
PM918/A/6.1/ST11
PM926/A/6.1
PM848/D/4.1/ST11
PM40/A/6.2
PM82/A/7.1/ST32
Avian
Bovine
Ovine
Porcine
0.002

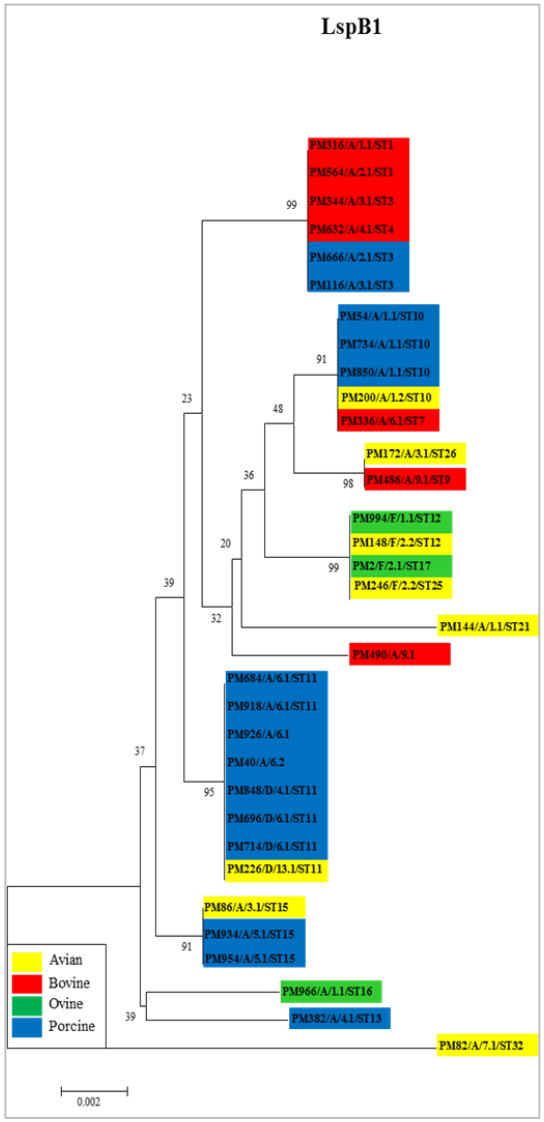
LspB1
PM316/A/1.1/ST1
PM564/A/2.1/ST1
PM344/A/3.1/ST3
PM632/A/4.1/ST4
PM666/A/2.1/ST3
PM116/A/3.1/ST3
PM54/A/1.1/ST10
PM734/A/1.1/ST10
PM850/A/1.1/ST10
PM200/A/1.2/ST10
PM336/A/6.1/ST7
PM172/A/3.1/ST26
PM486/A/9.1/ST9
PM994/F/1.1/ST12
PM148/F/2.2/ST12
PM2/F/2.1/ST17
PM246/F/2.2/ST25
PM144/A/1.1/ST21
PM490/A/9.1
PM684/A/6.1/ST11
PM918/A/6.1/ST11
PM926/A/6.1
PM40/A/6.2
PM848/D/4.1/ST11
PM696/D/6.1/ST11
PM714/D/6.1/ST11
PM226/D/13.1/ST11
PM86/A/3.1/ST15
PM934/A/5.1/ST15
PM954/A/5.1/ST15
PM966/A/1.1/ST16
PM382/A/4.1/ST13
PM82/A/7.1/ST32
Avian
Bovine
Ovine
Porcine
0.002

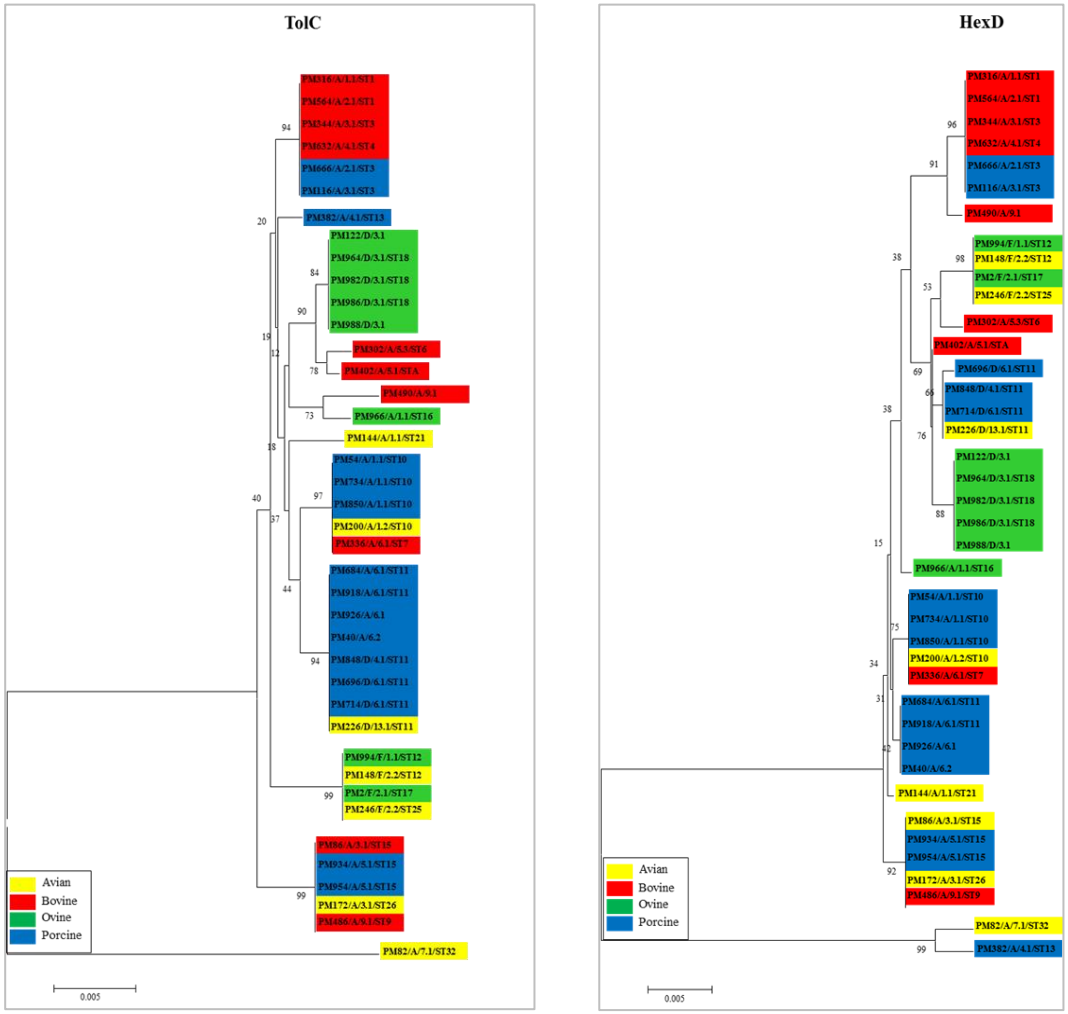

Fig. 8.2 Neighbour-Joining tree of nine OMPs/ genes having transport and receptor function in *P. multocida.*

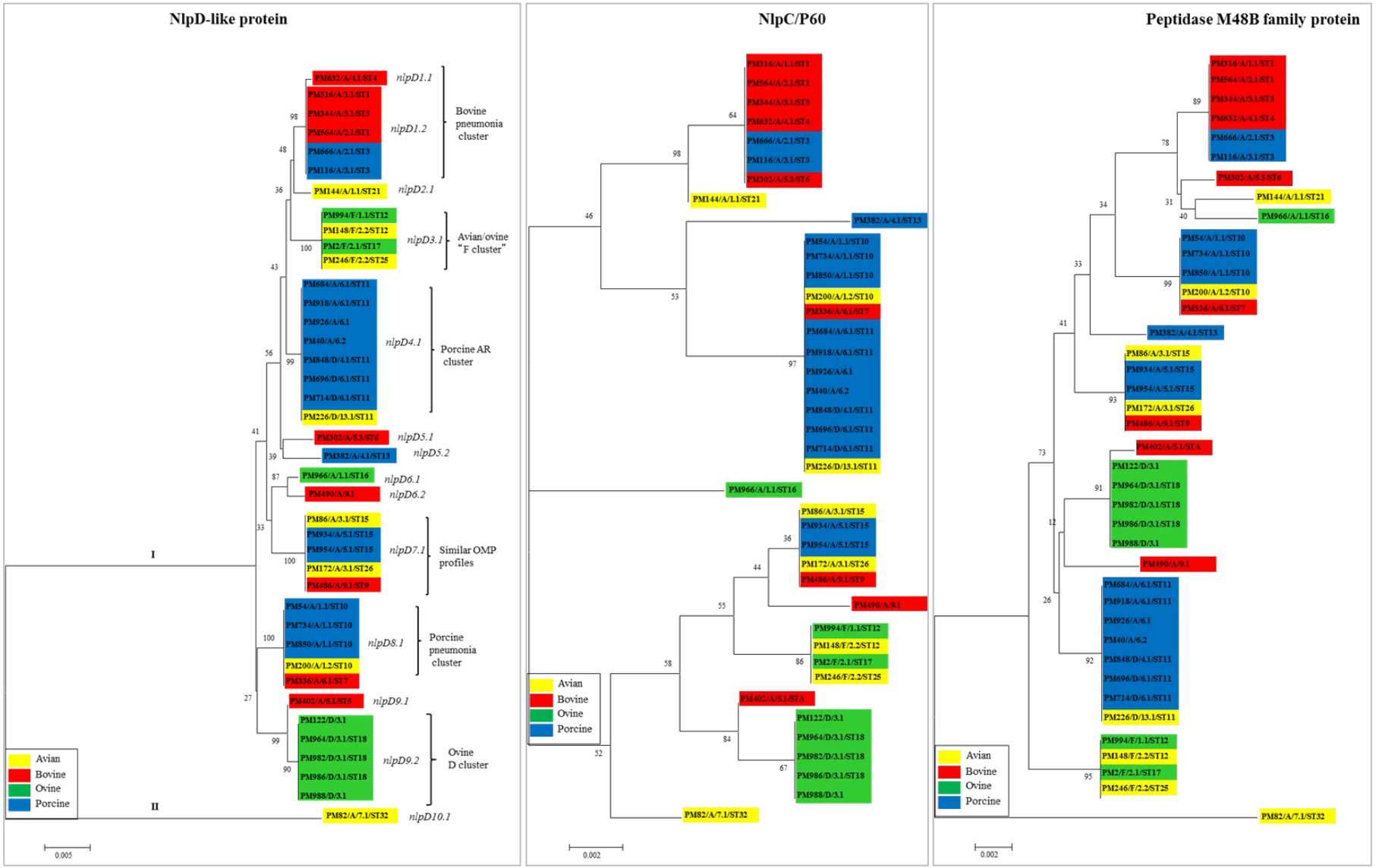
NlpD-like protein
PM632/A/4.1/ST4
PM316/A/1.1/ST1
PM344/A/3.1/ST3
PM564/A/2.1/ST1
PM666/A/2.1/ST3
PM116/A/3.1/ST3
PM144/A/1.1/ST21
PM994/F/1.1/ST12
PM148/F/2.2/ST12
PM2/F/2.1/ST17
PM246/F/2.2/ST25
PM684/A/6.1/ST11
PM918/A/6.1/ST11
PM926/A/6.1
PM40/A/6.2
PM848/D/4.1/ST11
PM696/D/6.1/ST11
PM714/D/6.1/ST11
PM226/D/13.1/ST11
PM302/A/5.3/ST6
PM382/A/4.1/ST13
PM966/A/1.1/ST16
PM490/A/9.1
PM86/A/3.1/ST15
PM934/A/5.1/ST15
PM954/A/5.1/ST15
PM172/A/3.1/ST26
PM486/A/9.1/ST9
PM54/A/1.1/ST10
PM734/A/1.1/ST10
PM850/A/1.1/ST10
PM200/A/1.2/ST10
PM336/A/6.1/ST7
PM402/A/5.1/ST5
PM122/D/3.1
PM964/D/3.1/ST18
PM982/D/3.1/ST18
PM986/D/3.1/ST18
PM988/D/3.1
PM82/A/7.1/ST32
nlpD1.1
nlpD1.2
nlpD2.1
nlpD3.1
nlpD4.1
nlpD5.1
nlpD5.2
nlpD6.1
nlpD6.2
nlpD7.1
nlpD8.1
nlpD9.1
nlpD9.2
nlpD10.1
Bovine pneumonia cluster
Avian/ovine "F cluster"
Porcine AR cluster
Similar OMP profiles
Porcine pneumonia cluster
Ovine D cluster
I
II
Avian
Bovine
Ovine
Porcine
0.005
NlpC/P60
0.002
Peptidase M48B family protein
0.002

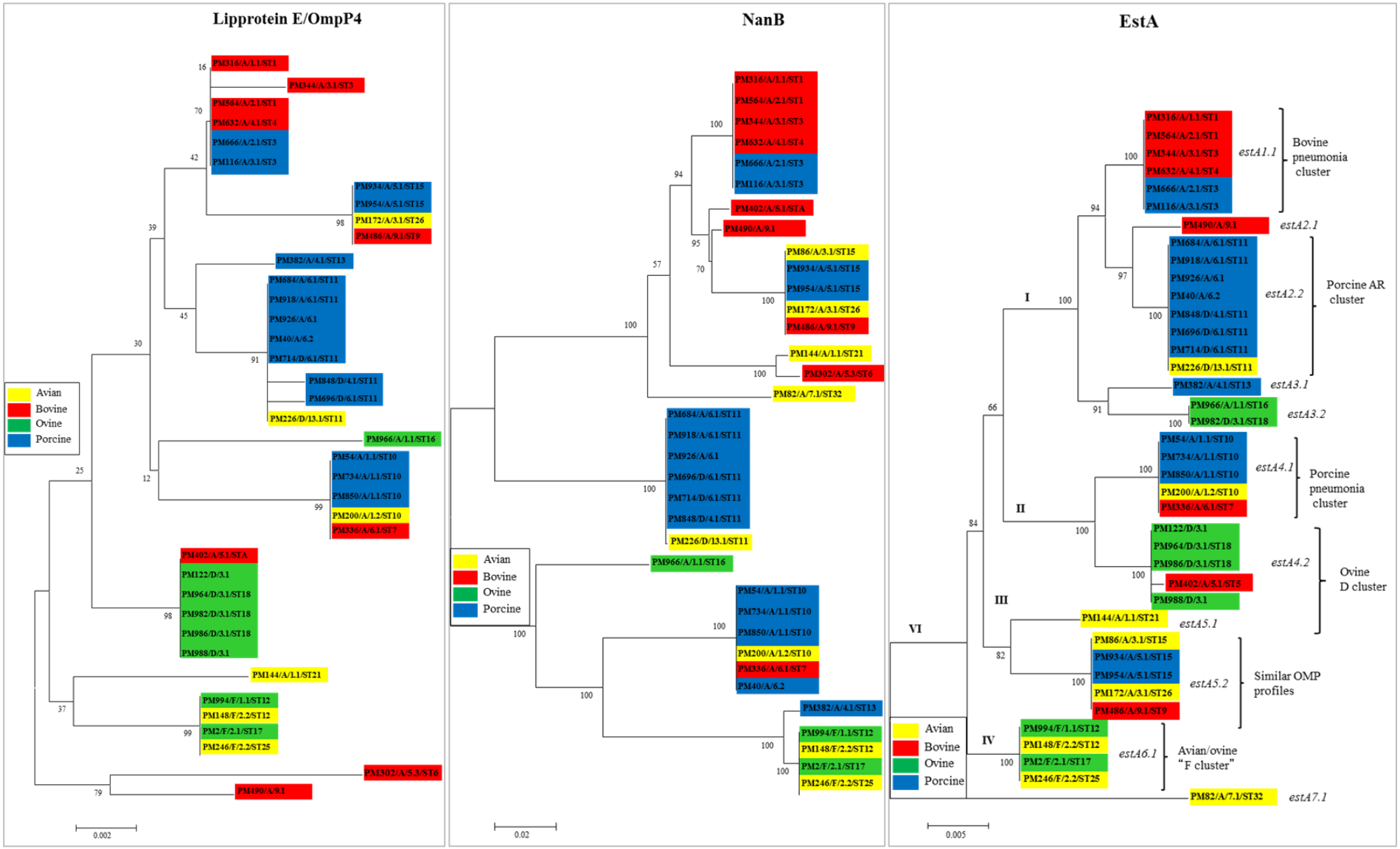
Lipprotein E/OmpP4
PM316/A/1.1/ST1
PM344/A/3.1/ST3
PM564/A/2.1/ST1
PM632/A/4.1/ST4
PM666/A/2.1/ST3
PM116/A/3.1/ST3
PM934/A/5.1/ST15
PM954/A/5.1/ST15
PM172/A/3.1/ST26
PM486/A/9.1/ST9
PM382/A/4.1/ST13
PM684/A/6.1/ST11
PM918/A/6.1/ST11
PM926/A/6.1
PM40/A/6.2
PM714/D/6.1/ST11
PM848/D/4.1/ST11
PM696/D/6.1/ST11
PM226/D/13.1/ST11
PM966/A/1.1/ST16
PM54/A/1.1/ST10
PM734/A/1.1/ST10
PM850/A/1.1/ST10
PM200/A/1.2/ST10
PM336/A/6.1/ST7
PM402/A/5.1/STA
PM122/D/3.1
PM964/D/3.1/ST18
PM982/D/3.1/ST18
PM986/D/3.1/ST18
PM988/D/3.1
PM144/A/1.1/ST21
PM994/F/1.1/ST12
PM148/F/2.2/ST12
PM2/F/2.1/ST17
PM246/F/2.2/ST25
PM302/A/5.3/ST6
PM490/A/9.1
Avian
Bovine
Ovine
Porcine
0.002
NanB
PM316/A/1.1/ST1
PM564/A/2.1/ST1
PM344/A/3.1/ST3
PM632/A/4.1/ST4
PM666/A/2.1/ST3
PM116/A/3.1/ST3
PM402/A/5.1/STA
PM490/A/9.1
PM86/A/3.1/ST15
PM934/A/5.1/ST15
PM954/A/5.1/ST15
PM172/A/3.1/ST26
PM486/A/9.1/ST9
PM144/A/1.1/ST21
PM302/A/5.3/ST6
PM82/A/7.1/ST32
PM684/A/6.1/ST11
PM918/A/6.1/ST11
PM926/A/6.1
PM696/D/6.1/ST11
PM714/D/6.1/ST11
PM848/D/4.1/ST11
PM226/D/13.1/ST11
PM966/A/1.1/ST16
PM54/A/1.1/ST10
PM734/A/1.1/ST10
PM850/A/1.1/ST10
PM200/A/1.2/ST10
PM336/A/6.1/ST7
PM40/A/6.2
PM382/A/4.1/ST13
PM994/F/1.1/ST12
PM148/F/2.2/ST12
PM2/F/2.1/ST17
PM246/F/2.2/ST25
Avian
Bovine
Ovine
Porcine
0.02
EstA
PM316/A/1.1/ST1
PM564/A/2.1/ST1
PM344/A/3.1/ST3
PM632/A/4.1/ST4
PM666/A/2.1/ST3
PM116/A/3.1/ST3
estA1.1
Bovine pneumonia cluster
PM490/A/9.1
estA2.1
PM684/A/6.1/ST11
PM918/A/6.1/ST11
PM926/A/6.1
PM40/A/6.2
PM848/D/4.1/ST11
PM696/D/6.1/ST11
PM714/D/6.1/ST11
PM226/D/13.1/ST11
estA2.2
Porcine AR cluster
PM382/A/4.1/ST13
estA3.1
PM966/A/1.1/ST16
PM982/D/3.1/ST18
estA3.2
PM54/A/1.1/ST10
PM734/A/1.1/ST10
PM850/A/1.1/ST10
PM200/A/1.2/ST10
PM336/A/6.1/ST7
estA4.1
Porcine pneumonia cluster
PM122/D/3.1
PM964/D/3.1/ST18
PM986/D/3.1/ST18
PM402/A/5.1/ST5
PM988/D/3.1
estA4.2
Ovine D cluster
PM144/A/1.1/ST21
estA5.1
PM86/A/3.1/ST15
PM934/A/5.1/ST15
PM954/A/5.1/ST15
PM172/A/3.1/ST26
PM486/A/9.1/ST9
estA5.2
Similar OMP profiles
PM994/F/1.1/ST12
PM148/F/2.2/ST12
PM2/F/2.1/ST17
PM246/F/2.2/ST25
estA6.1
Avian/ovine "F cluster"
PM82/A/7.1/ST32
estA7.1
I
II
III
IV
VI
Avian
Bovine
Ovine
Porcine
0.005

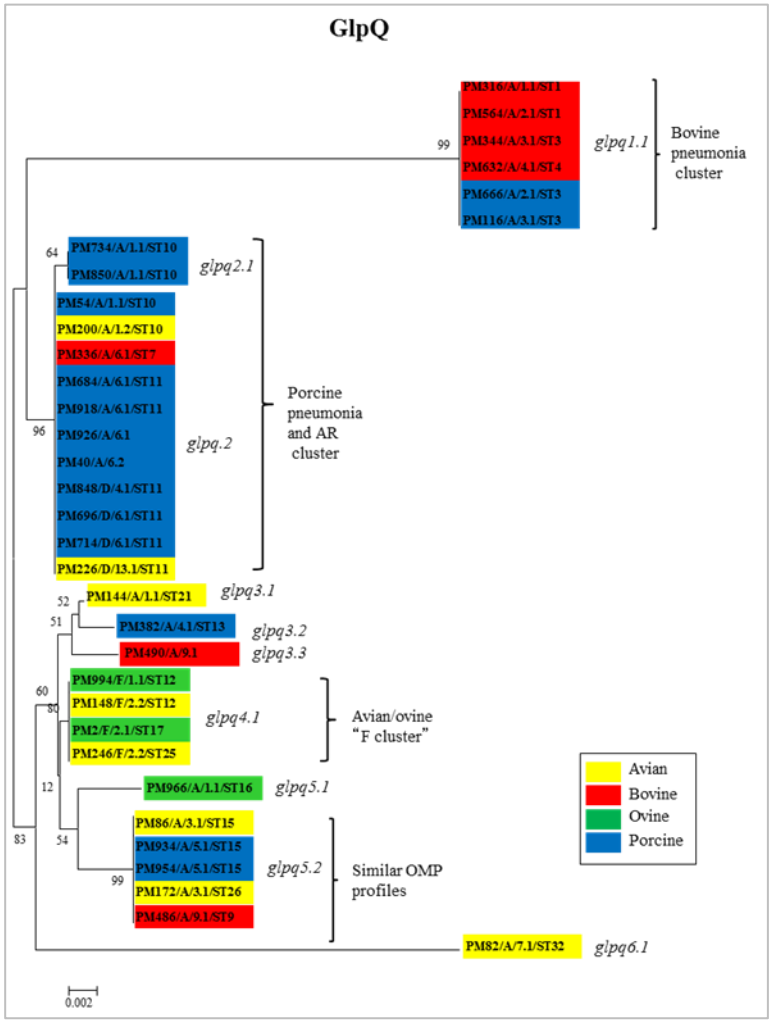

Fig. 8.3 Neighbour-Joining tree of seven OMPs/ genes membrane-associated enzyme activity in *P. multocida.*